



# Technetium-99m Radiopharmaceuticals: Status and Trends

# **IAEA RADIOISOTOPES AND RADIOPHARMACEUTICALS SERIES PUBLICATIONS**

One of the main objectives of the IAEA Radioisotope Production and Radiation Technology programme is to enhance the expertise and capability of IAEA Member States in deploying emerging radioisotope products and generators for medical and industrial applications in order to meet national needs as well as to assimilate new developments in radiopharmaceuticals for diagnostic and therapeutic applications. This will ensure local availability of these applications within a framework of quality assurance.

Publications in the IAEA Radioisotopes and Radiopharmaceuticals Series provide information in the areas of: reactor and accelerator produced radioisotopes, generators and sealed sources development/production for medical and industrial uses; radiopharmaceutical sciences, including radiochemistry, radiotracer development, production methods and quality assurance/quality control (QA/QC). The publications have a broad readership and are aimed at meeting the needs of scientists, engineers, researchers, teachers and students, laboratory professionals, and instructors. International experts assist the IAEA Secretariat in drafting and reviewing these publications. Some of the publications in this series may also be endorsed or co-sponsored by international organizations and professional societies active in the relevant fields.

There are two categories of publications: the **IAEA Radioisotopes and Radiopharmaceuticals Series** and **IAEA Radioisotopes and Radiopharmaceuticals Reports**.

## **IAEA RADIOISOTOPES AND RADIOPHARMACEUTICALS SERIES**

Publications in this category present guidance information or methodologies and analyses of long term validity, for example protocols, guidelines, codes, standards, quality assurance manuals, best practices and high level technological and educational material.

## **IAEA RADIOISOTOPES AND RADIOPHARMACEUTICALS REPORTS**

In this category, publications complement information published in the IAEA Radioisotopes and Radiopharmaceuticals Series in areas of the: development and production of radioisotopes and generators for medical and industrial applications; and development, production and QA/QC of diagnostic and therapeutic radiopharmaceuticals. These publications include reports on current issues and activities such as technical meetings, the results of IAEA coordinated research projects, interim reports on IAEA projects, and educational material compiled for IAEA training courses dealing with radioisotope and radiopharmaceutical related subjects. In some cases, these reports may provide supporting material relating to publications issued in the IAEA Radioisotopes and Radiopharmaceuticals Series.

All of these publications can be downloaded cost free from the IAEA web site:

<http://www.iaea.org/Publications/index.html>

Further information is available from:

Sales and Distribution Unit  
International Atomic Energy Agency  
Vienna International Centre  
PO Box 100  
1400 Vienna, Austria

Readers are invited to provide feedback to the IAEA on these publications. Information may be provided through the IAEA web site, by mail at the address given above, or by email to:

Official.Mail@iaea.org

TECHNETIUM-99m  
RADIOPHARMACEUTICALS:  
STATUS AND TRENDS

The following States are Members of the International Atomic Energy Agency:

AFGHANISTAN	GHANA	NORWAY
ALBANIA	GREECE	OMAN
ALGERIA	GUATEMALA	PAKISTAN
ANGOLA	HAITI	PALAU
ARGENTINA	HOLY SEE	PANAMA
ARMENIA	HONDURAS	PARAGUAY
AUSTRALIA	HUNGARY	PERU
AUSTRIA	ICELAND	PHILIPPINES
AZERBAIJAN	INDIA	POLAND
BAHRAIN	INDONESIA	PORTUGAL
BANGLADESH	IRAN, ISLAMIC REPUBLIC OF	QATAR
BELARUS	IRAQ	REPUBLIC OF MOLDOVA
BELGIUM	IRELAND	ROMANIA
BELIZE	ISRAEL	RUSSIAN FEDERATION
BENIN	ITALY	SAUDI ARABIA
BOLIVIA	JAMAICA	SENEGAL
BOSNIA AND HERZEGOVINA	JAPAN	SERBIA
BOTSWANA	JORDAN	SEYCHELLES
BRAZIL	KAZAKHSTAN	SIERRA LEONE
BULGARIA	KENYA	SINGAPORE
BURKINA FASO	KOREA, REPUBLIC OF	SLOVAKIA
BURUNDI	KUWAIT	SLOVENIA
CAMBODIA	KYRGYZSTAN	SOUTH AFRICA
CAMEROON	LATVIA	SPAIN
CANADA	LEBANON	SRI LANKA
CENTRAL AFRICAN REPUBLIC	LESOTHO	SUDAN
CHAD	LIBERIA	SWEDEN
CHILE	LIBYAN ARAB JAMAHIRIYA	SWITZERLAND
CHINA	LIECHTENSTEIN	SYRIAN ARAB REPUBLIC
COLOMBIA	LITHUANIA	TAJIKISTAN
CONGO	LUXEMBOURG	THAILAND
COSTA RICA	MADAGASCAR	THE FORMER YUGOSLAV REPUBLIC OF MACEDONIA
CÔTE D'IVOIRE	MALAWI	TUNISIA
CROATIA	MALAYSIA	TURKEY
CUBA	MALI	UGANDA
CYPRUS	MALTA	UKRAINE
CZECH REPUBLIC	MARSHALL ISLANDS	UNITED ARAB EMIRATES
DEMOCRATIC REPUBLIC OF THE CONGO	MAURITANIA	UNITED KINGDOM OF GREAT BRITAIN AND NORTHERN IRELAND
DENMARK	MAURITIUS	UNITED REPUBLIC OF TANZANIA
DOMINICAN REPUBLIC	MEXICO	UNITED STATES OF AMERICA
ECUADOR	MONACO	URUGUAY
EGYPT	MONGOLIA	UZBEKISTAN
EL SALVADOR	MONTENEGRO	VENEZUELA
ERITREA	MOROCCO	VIETNAM
ESTONIA	MOZAMBIQUE	YEMEN
ETHIOPIA	MYANMAR	ZAMBIA
FINLAND	NAMIBIA	ZIMBABWE
FRANCE	NEPAL	
GABON	NETHERLANDS	
GEORGIA	NEW ZEALAND	
GERMANY	NICARAGUA	
	NIGER	
	NIGERIA	

The Agency's Statute was approved on 23 October 1956 by the Conference on the Statute of the IAEA held at United Nations Headquarters, New York; it entered into force on 29 July 1957. The Headquarters of the Agency are situated in Vienna. Its principal objective is "to accelerate and enlarge the contribution of atomic energy to peace, health and prosperity throughout the world".

IAEA RADIOISOTOPES AND RADIOPHARMACEUTICALS SERIES No. 1

TECHNETIUM-99m  
RADIOPHARMACEUTICALS:  
STATUS AND TRENDS

INTERNATIONAL ATOMIC ENERGY AGENCY  
VIENNA, 2009

## COPYRIGHT NOTICE

All IAEA scientific and technical publications are protected by the terms of the Universal Copyright Convention as adopted in 1952 (Berne) and as revised in 1972 (Paris). The copyright has since been extended by the World Intellectual Property Organization (Geneva) to include electronic and virtual intellectual property. Permission to use whole or parts of texts contained in IAEA publications in printed or electronic form must be obtained and is usually subject to royalty agreements. Proposals for non-commercial reproductions and translations are welcomed and considered on a case-by-case basis. Enquiries should be addressed to the IAEA Publishing Section at:

Sales and Promotion, Publishing Section  
International Atomic Energy Agency  
Vienna International Centre  
PO Box 100  
1400 Vienna, Austria  
fax: +43 1 2600 29302  
tel.: +43 1 2600 22417  
email: sales.publications@iaea.org  
<http://www.iaea.org/books>

© IAEA, 2009

Printed by the IAEA in Austria  
December 2009  
STI/PUB/1405

### IAEA Library Cataloguing in Publication Data

Technetium-99m radiopharmaceuticals : status and trends. — Vienna : International Atomic Energy Agency, 2009.

p. ; 24 cm. — (IAEA radioisotopes and radiopharmaceuticals series,  
ISSN 2077-6462 ; no. 1)

STI/PUB/1405

ISBN 978-92-0-103509-7

Includes bibliographical references.

1. Technetium — Isotopes — Diagnostic use. 2. Radiopharmaceuticals.

I. International Atomic Energy Agency. II. Series.

## **FOREWORD**

Technetium-99m radiopharmaceuticals are applied in morphological and dynamic imaging of many organs in the body, to diagnose various diseases. It is estimated that about 25 million diagnostic investigations are performed annually using this single isotope. It is expected that current applications using <sup>99m</sup>Tc radiopharmaceuticals in renal, hepatic, hepatobiliary, bone, cardiac and oncological disease, as well as in other well entrenched pathologies, will continue to be depended on for successful patient management. The IAEA recently published Technical Reports Series No. 466, Technetium-99m Radiopharmaceuticals: Manufacture of Kits, that gives the details of manufacturing kits for formulation of 23 different <sup>99m</sup>Tc radiopharmaceuticals that are in wide use.

The development of successful <sup>99m</sup>Tc based radiopharmaceuticals, and introducing them into clinical practice, are challenges to be overcome to make nuclear medicine available to a large cross-section of the developing world. Advances in technetium chemistry over the last 15 years have facilitated the development of new radiopharmaceuticals with greatly improved clinical potential. However, many of the new products are not commercially exploited due to the high cost involved in complying with regulatory standards, which include requirements for detailed toxicity data and approved clinical studies. It is broadly accepted that the regulatory burden needs to be ameliorated.

A technical meeting on the current status and future trends in <sup>99m</sup>Tc radiopharmaceuticals, organized by the IAEA, identified oncology, cardiology, neurology and infection/inflammation imaging as areas in which <sup>99m</sup>Tc radiopharmaceuticals could make substantial contributions in the future. This publication is a compilation of papers dealing with the development of radiopharmaceuticals for the areas identified above. The chapters were written by scientists who have extensive experience in the development of <sup>99m</sup>Tc radiopharmaceuticals in the respective fields.

The IAEA thanks the authors who contributed to this publication. The invaluable peer reviews by several experts as well as the contributions of: L. Wiebe, of the University of Alberta, Canada; R. Alberto, of the University of Zurich, Switzerland; and S. Liu, of Purdue University, United States of America, for their help in editing the articles are also acknowledged. The valuable assistance of A. Duatti, of the University of Ferrara, Italy, in coordinating with the authors, and compiling and editing the book is gratefully recorded. The IAEA officer responsible for this publication was M.R.A. Pillai of the Division of Physical and Chemical Sciences.

#### *EDITORIAL NOTE*

*The papers in this publication have been edited by the editorial staff of the IAEA to the extent considered necessary for the reader's assistance. The views expressed remain, however, the responsibility of the named authors or participants. In addition, the views are not necessarily those of the governments of the nominating Member States or of the nominating organizations.*

*Although great care has been taken to maintain the accuracy of information contained in this publication, neither the IAEA nor its Member States assume any responsibility for consequences which may arise from its use.*

*The use of particular designations of countries or territories does not imply any judgement by the publisher, the IAEA, as to the legal status of such countries or territories, of their authorities and institutions or of the delimitation of their boundaries.*

*The mention of names of specific companies or products (whether or not indicated as registered) does not imply any intention to infringe proprietary rights, nor should it be construed as an endorsement or recommendation on the part of the IAEA.*

*The authors are responsible for having obtained the necessary permission for the IAEA to reproduce, translate or use material from sources already protected by copyrights.*

*Material prepared by authors who are in contractual relation with governments is copyrighted by the IAEA, as publisher, only to the extent permitted by the appropriate national regulations.*

## CONTENTS

INTRODUCTION AND SUMMARY .....	1
Background .....	1
Scope .....	2
Structure .....	3
CHAPTER 1. ROLE OF $^{99m}\text{Tc}$ IN DIAGNOSTIC IMAGING .....	7
<i>A. Duatti</i>	
1.1. Preface .....	7
1.2. The dawn of molecular imaging .....	8
1.3. The tracer principle .....	9
1.4. Advent of $^{99m}\text{Tc}$ small molecule tracers .....	10
1.5. The age of molecular imaging .....	12
1.6. Epilogue .....	14
References to Chapter 1 .....	17
CHAPTER 2. OVERVIEW OF CURRENT LABELLING METHODS .....	19
<i>R. Alberto</i>	
2.1. Introduction .....	19
2.2. Requirements for labelling targeting molecules .....	21
2.3. Labelling methods: State of the art .....	23
2.4. Summary and conclusions .....	34
References to Chapter 2 .....	34
CHAPTER 3. APPLICATION OF CLICK CHEMISTRY TO THE DESIGN OF LIGAND SYSTEMS AND FUNCTIONALIZATION OF BIOMOLECULES SUITABLE FOR RADIOLABELLING WITH THE TECHNETIUM AND RHENIUM TRICARBONYL CORE .....	41
<i>T.L. Mindt, H. Struthers, R. Schibli</i>	
3.1. Introduction .....	41
3.2. Design of click chelators for the $^{99m}\text{Tc}$ tricarbonyl core .....	43
3.3. Structural diversity of click chelating systems .....	45

3.4. One-pot protocols . . . . .	47
3.5. In vivo assessment of click chelators and comparison with non-clicked analogues . . . . .	50
3.6. Further examples of the ‘click-to-chelate’ approach . . . . .	50
3.7. Conclusions . . . . .	52
References to Chapter 3 . . . . .	53
 CHAPTER 4. ADVANCES IN SPECT INSTRUMENTATION (INCLUDING SMALL ANIMAL SCANNERS) . . . . .	
<i>G. Di Domenico, G. Zavattini</i>	
4.1. Introduction . . . . .	57
4.2. SPECT imaging system . . . . .	58
4.3. Clinical systems . . . . .	77
4.4. Small animal SPECT . . . . .	81
4.5. Conclusion . . . . .	87
References to Chapter 4 . . . . .	87
 CHAPTER 5. CATIONIC $^{99m}\text{Tc}$ COMPLEXES AS RADIOTRACERS FOR MYOCARDIAL PERFUSION IMAGING . . . . .	
<i>S. Liu, A. Duatti</i>	
5.1. Introduction . . . . .	92
5.2. New cationic $^{99m}\text{Tc}$ radiotracers for myocardial perfusion imaging . . . . .	94
5.3. Factors influencing heart uptake and liver clearance . . . . .	101
5.4. Future direction . . . . .	103
5.5. Conclusions . . . . .	104
References to Chapter 5 . . . . .	105
 CHAPTER 6. TECHNETIUM-99m RADIOPHARMACEUTICALS IN NEUROLOGY . . . . .	
<i>I. Pirmettis, H.-J. Pietzsch</i>	
6.1. Introduction . . . . .	111
6.2. Designing a CNS receptor based on $^{99m}\text{Tc}$ radiopharmaceuticals . . . . .	114
6.3. Technetium-99m complexes for the dopamine transporter . . . . .	119
6.4. Technetium-99m complexes for the 5-HT <sub>1A</sub> receptor . . . . .	122

6.5. Technetium-99m complexes for amyloid plaques . . . . .	125
6.6. Perspectives and conclusions . . . . .	126
References to Chapter 6 . . . . .	128

**CHAPTER 7. TECHNETIUM-99m LABELLED INFECTION IMAGING AGENTS . . . . . 137**

*M. Welling, G. Ferro-Flores, I. Pirmettis*

7.1. Introduction . . . . .	137
7.2. Pathophysiology of infection . . . . .	138
7.3. Diagnosis of infection . . . . .	139
7.4. Radiopharmaceuticals for the imaging of infection . . . . .	140
7.5. Antibiotics . . . . .	141
7.6. Antimicrobial peptides . . . . .	143
7.7. Technetium labelling techniques . . . . .	146
7.8. Pharmacokinetics . . . . .	149
7.9. Conclusions . . . . .	150
7.10. Fundamental questions . . . . .	150
References to Chapter 7 . . . . .	152

**CHAPTER 8. GENE AND MOLECULAR IMAGING USING  $^{99\text{m}}\text{Tc}$  LABELLED RADIOPHARMACEUTICALS . . . . . 157**

*L.I. Wiebe*

8.1. Introduction . . . . .	157
8.2. Definitions . . . . .	158
8.3. Gene transfer and gene therapy imaging: a brief history . . . . .	159
8.4. Technetium-99m labelled DNA/RNA products for imaging complementary mRNA . . . . .	176
References to Chapter 8 . . . . .	181
Bibliography . . . . .	196

**CHAPTER 9. TECHNETIUM-99m LABELLED RGD PEPTIDES AS INTEGRIN  $\alpha_5\beta_3$ -TARGETED RADIOTRACERS FOR TUMOUR IMAGING . . . . . 197**

*S. Liu*

9.1. Introduction . . . . .	197
9.2. Radiopharmaceutical design . . . . .	198

9.3. Technetium-99m labelled RGD peptides as radiotracers for imaging tumour angiogenesis . . . . .	206
9.4. Conclusions . . . . .	213
References to Chapter 9 . . . . .	214

**CHAPTER 10. TECHNETIUM-99m LABELLED REGULATORY  
PEPTIDE FOR TUMOUR IMAGING . . . . . 221**

*C. Decristoforo*

10.1. Introduction: Regulatory peptides and human cancer . . . . .	221
10.2. Pharmacokinetics and pharmacodynamics . . . . .	222
10.3. Technetium-99m labelled somatostatin analogues . . . . .	228
10.4. Other <sup>99m</sup> Tc labelled peptides targeting regulatory receptors . . . . .	231
10.5. Summary and conclusion . . . . .	235
References to Chapter 10 . . . . .	236

**CHAPTER 11. TECHNETIUM-99m ANNEXIN-A5 FOR  
APOPTOSIS IMAGING . . . . . 241**

*Y. Kuge*

11.1. Introduction . . . . .	241
11.2. Principle of apoptosis imaging with annexin-A5 . . . . .	242
11.3. Technetium-99m labelled annexin-A5 by use of bifunctional chelating agents . . . . .	243
11.4. Technetium-99m labelled annexin-A5 mutants with endogenous chelation sites . . . . .	248
11.5. Other approaches to improve biodistribution profiles of labelled compounds . . . . .	248
11.6. Annexin-A5 labelled with other radionuclides . . . . .	249
11.7. Conclusion . . . . .	250
References to Chapter 11 . . . . .	250

**CHAPTER 12. TECHNETIUM-99m RADIOPHARMACEUTICALS  
FOR MONITORING DRUG RESISTANCE . . . . . 255**

*H. Akizawa, T. Uehara, Y. Arano*

12.1. Introduction . . . . .	255
12.2. Technetium-99m-MIBI . . . . .	256
12.3. Technetium-99m-tetrofosmin . . . . .	259
12.4. Other compounds . . . . .	260

12.5. Conclusions .....	263
References to Chapter 12 .....	264
 CHAPTER 13. TECHNETIUM-99m RADIOPHARMACEUTICALS FOR LYMPHOSCINTIGRAPHY .....	
<i>T. Uehara, H. Akizawa, Y. Arano</i>	269
13.1. Introduction .....	269
13.2. Technetium-99m labelled colloidal particles .....	271
13.3. Technetium-99m labelled non-colloidal particles .....	273
13.4. Conclusions .....	276
References to Chapter 13 .....	277
 CHAPTER 14. RADIOPHARMACEUTICALS FOR BONE METASTASIS IMAGING .....	
<i>K. Ogawa</i>	281
14.1. Introduction .....	281
14.2. Technetium-99m-bisphosphine complexes (polynuclear) .....	282
14.3. Mononuclear $^{99\text{m}}\text{Tc}$ labelled bisphosphonate compounds ( $^{99\text{m}}\text{Tc}$ complex conjugated bisphosphonate compounds) .....	285
14.4. Technetium-99m-complex conjugated oligopeptides .....	287
14.5. Technetium-99m-DMSA .....	288
14.6. Conclusion .....	289
References to Chapter 14 .....	290
 CHAPTER 15. TECHNETIUM-99m LABELLED MOLECULES FOR HYPOXIA IMAGING .....	
<i>M.B. Mallia, S. Banerjee, M. Venkatesh</i>	295
15.1. Introduction .....	295
15.2. Hypoxia .....	296
15.3. Methods for detecting tumour hypoxia .....	300
15.4. Conclusion .....	311
References to Chapter 15 .....	312

CHAPTER 16. ROLE OF $^{99m}\text{Tc}$ IN THE DEVELOPMENT OF RHENIUM RADIOPHARMACEUTICALS . . . . .	317
<i>R.T.M. De Rosales, P. Blower</i>	
16.1. Introduction . . . . .	317
16.2. Radiological properties and radiobiology . . . . .	318
16.3. Review of currently investigated rhenium radiopharmaceuticals . . . . .	323
16.4. Summary . . . . .	337
References to Chapter 16 . . . . .	338
CHAPTER 17. FUTURE TRENDS IN THE DEVELOPMENT OF TECHNETIUM RADIOPHARMACEUTICALS . . . . .	347
<i>R. Alberto</i>	
17.1. Introduction . . . . .	347
17.2. Chemistry . . . . .	348
17.3. Targets . . . . .	351
17.4. Targeting molecules and complexes . . . . .	354
References to Chapter 17 . . . . .	357
CONTRIBUTORS TO DRAFTING AND REVIEW . . . . .	359

## INTRODUCTION AND SUMMARY

### BACKGROUND

The growth and wide application of diagnostic nuclear medicine have been mainly driven by the easy availability (through the transportable  $^{99}\text{Mo}/^{99\text{m}}\text{Tc}$  generator system) and almost ideal nuclear properties of the gamma emitting radionuclide  $^{99\text{m}}\text{Tc}$ , and by the introduction of clinically useful  $^{99\text{m}}\text{Tc}$  radiopharmaceuticals for imaging different tissues. Even today, over 70% of diagnostic investigations are still performed with this single isotope. However, the recent surge in the use of radiopharmaceuticals labelled with positron emitters is challenging the field of single photon emission computed tomography (SPECT) tracers and, in particular, raises the question about the role of  $^{99\text{m}}\text{Tc}$  imaging agents in future diagnostic nuclear medicine. Although there have been significant improvements in  $^{99\text{m}}\text{Tc}$  labelling methods, no new products have been commercially exploited in the last decade. The inferior sensitivity, and temporal and spatial resolution of SPECT as compared to positron emission tomography (PET), conjoined with the complex, inorganic and encumbering chemistry of this radiometal are key problems in the development of new  $^{99\text{m}}\text{Tc}$  agents for imaging more specific molecular targets. Another major concern with the introduction of new SPECT agents into clinical use is the high cost involved in complying with regulatory requirements, toxicity and preliminary clinical studies together with a limited return on investment.

The IAEA organized a technical meeting on the current status and future trends in  $^{99\text{m}}\text{Tc}$  radiopharmaceuticals to review the trends in  $^{99\text{m}}\text{Tc}$  radiopharmaceuticals development. The focus of the meeting was to identify areas in which  $^{99\text{m}}\text{Tc}$  radiopharmaceuticals could make substantial contributions in the future and the means to identify strategies for the development of useful agents in those areas in order to enhance the current applications using  $^{99\text{m}}\text{Tc}$  radiopharmaceuticals.

The technical meeting addressed some key issues on the current utility and future needs of using  $^{99\text{m}}\text{Tc}$  radiopharmaceuticals in the new age of molecular medicine. The analysis first focused on the evaluation of the current status of nuclear medicine procedures using both SPECT and PET modalities, with the aim of identifying those key factors that should always be met to ensure the success of a particular nuclear imaging procedure.

As a fundamental requirement, it was recognized that the major factor in determining the diagnostic utility of an imaging agent lies in its biodistribution characteristics and, in particular, in its ability to achieve a sharp contrast between the target and the surrounding tissues. Hence, the quality of the

radiopharmaceutical is the key issue, with the superiority of the instrumentation technique playing a secondary role. This also explains the overwhelming success of PET as essentially being due to the superiority of fluoro-18 fluorodeoxyglucose ( $^{18}\text{FDG}$ ) as a proliferation specific tracer.

The current PET–CT images are inherently superior to the SPECT images. However, recent advances in detector technologies and reconstruction algorithms clearly showed that spatial resolution in SPECT is approaching that of PET without a concomitant decrease in sensitivity. Detector technology does not appear to have reached its physical limits, thus suggesting that spatial resolution in SPECT may go well below the sub-millimetre scale, particularly because there is no intrinsic physical limitation to the detection mechanism as, conversely, there always is in PET as a result of the annihilation process.

The versatile chemistry of  $^{99\text{m}}\text{Tc}$  due to its multi-oxidation states and, consequently, the ability to produce a variety of complexes with particular desired characteristics are the major advantages of  $^{99\text{m}}\text{Tc}$  as a radionuclide for radiopharmaceutical development. Labelling methods with  $^{99\text{m}}\text{Tc}$  have attained an extremely high degree of efficiency and sophistication. High specific activities needed for targeting low concentration targets are easily achievable through advanced chemical procedures employing the novel  $^{99\text{m}}\text{Tc}$ -carbonyl,  $^{99\text{m}}\text{Tc}$ -nitrido and  $^{99\text{m}}\text{Tc}(\text{III})$  cores. It is worth emphasizing that no other labelling methods based on different radionuclides have achieved such a high level of chemical development. Hence, further advancements are still possible and these may prove extremely useful for the solution of problems related to the design of new  $^{99\text{m}}\text{Tc}$  imaging agents.

The above considerations lead to the conclusion that  $^{99\text{m}}\text{Tc}$  radiopharmaceuticals still have an important role in nuclear medicine if some fundamental issues are satisfactorily addressed. These are mostly related to the possibility of designing and preparing, in high specific activity, novel categories of  $^{99\text{m}}\text{Tc}$  imaging agents showing an almost optimal target:counts/min background ratio and affinity for specific biomolecular targets.

## SCOPE

This publication is intended to provide a broad overview of the current status and future prospects of  $^{99\text{m}}\text{Tc}$  radiopharmaceuticals, including a description of the most advanced chemical techniques for labelling biomolecules and synthesizing suitable multifunctional ligands, along with a review of the most recent applications of  $^{99\text{m}}\text{Tc}$  agents for monitoring different biological processes. Various subfields of clinical relevance have been identified where  $^{99\text{m}}\text{Tc}$  radiopharmaceuticals will surely continue to have a significant impact on nuclear

medicine, such as: (1) cardiology; (2) oncology; (3) neurology; (4) infection/inflammation; and (5) gene expression.

## STRUCTURE

This publication comprises 17 chapters, each illustrating a specific topic in the broad field of  $^{99m}\text{Tc}$  radiopharmaceuticals, as outlined below.

Chapter 1 offers a critical review of the role played by  $^{99m}\text{Tc}$  radiopharmaceuticals in the development of nuclear imaging, which follows both a historical and scientific analysis, and aims at envisaging some future perspectives.

Chapter 2 discusses the most advanced developments in the chemistry of the new  $^{99m}\text{Tc}$  cores and synthons, and their application to the high specific labelling of biomolecules.

Chapter 3 describes the application of click chemistry, a new versatile method in organic chemistry for linking different functional groups on the same ligand, to the design and production of new categories of  $^{99m}\text{Tc}$  radiopharmaceuticals.

Chapter 4 offers an overview of the most recent advances in SPECT detector technology and of the progress in the attempt to increase the sensitivity and spatial resolution of conventional gamma cameras.

Chapter 5 discusses the most recent development in cationic  $^{99m}\text{Tc}$  myocardial perfusion radiotracers. It focuses on the use of ether and crown ether groups to improve the liver clearance of cationic  $^{99m}\text{Tc}$  complexes. The main objective of this review is to illustrate that coordination chemistry continues to play a pivotal role in the development of new cationic  $^{99m}\text{Tc}$  radiotracers. The ultimate goal is to develop new radiotracers that will satisfy unmet medical needs and serve a large population of patients with known or suspected coronary artery disease.

Chapter 6 discusses the problem associated with the development of  $^{99m}\text{Tc}$  tracers for the imaging of the central nervous system, with particular emphasis on challenges imposed by the concomitant requirements of crossing the blood-brain barrier and targeting specific receptor sites.

Chapter 7 provides an overview of current approaches for imaging infection and inflammation, including labelled antibiotics, peptides and large proteins.

Chapter 8 looks at areas such as gene therapy, multidrug resistance (MDR) and pathology specific gene expression as a target for  $^{99m}\text{Tc}$  radiopharmaceuticals. A review of the progress in the development of  $^{99m}\text{Tc}$  labelled oligonucleotides (antisense, aptamers) concludes this chapter.

Chapter 9 focuses on  $^{99m}\text{Tc}$  labelled RGD (arginine-glycine-aspartate) peptides as SPECT radiotracers for imaging integrin  $\alpha_v\beta_3$  expression in tumours of different origin. Despite the wide availability of PET isotopes (such as  $^{18}\text{F}$ ,  $^{62/64}\text{Cu}$  and  $^{68}\text{Ga}$ ) in developed countries,  $^{99m}\text{Tc}$  remains the radionuclide of choice for development of diagnostic radiotracers in most developing countries. Technetium-99m radiotracers offer significant advantages over their corresponding  $^{18}\text{F}$  analogues with respect to cost, availability and ease of routine radiotracer preparation.

Chapter 10 discusses the most recent developments in  $^{99m}\text{Tc}$  labelled highly selective regulatory peptides, which target somatostatin receptors, neuropeptides, the gastrin-releasing peptide receptor, gastrin and cholecystokinins receptors, neuropeptide Y receptors, and vasoactive intestinal peptide receptors.

Chapter 11 offers an overview of attempts to develop a  $^{99m}\text{Tc}$  radiopharmaceutical for in vivo targeting of apoptotic tissues and of results obtained with  $^{99m}\text{Tc}$ -annexin(V), the most successful  $^{99m}\text{Tc}$  agent in this field.

Chapter 12 discusses the application of  $^{99m}\text{Tc}$  radiopharmaceuticals for monitoring MDR. It is very important to note that a deficit of  $^{99m}\text{Tc}$ -MIBI (methoxy isobutyl isonitrile) activity within tumour cells can be related to several contradictory biological phenomena: poor accessibility to the tumour, decreased viability and electrical gradients in ‘over-aged’ and hypoxic cells, loss of influx in cells at an early stage of apoptosis owing to a decrease in their electrical gradient, lack of retention in resistant cells mediated by multidrug resistant proteins and/or overexpression of the anti-apoptotic protein Bcl-2, thus preventing any mitochondrial accumulation.

Chapter 13 illustrates the principles of lymphoscintigraphy and its widespread application to sentinel node detection. The various agents including  $^{99m}\text{Tc}$  labelled colloids and new dextran based macromolecular compounds are also discussed.

Chapter 14 reviews the currently available bone seeking  $^{99m}\text{Tc}$  radiopharmaceuticals, and recent efforts towards the development of new radiopharmaceuticals for imaging bone metastasis.

Chapter 15 discusses the most important challenges still facing the development of a  $^{99m}\text{Tc}$  agent for monitoring hypoxic tissues, which constitutes one of the most interesting targets in different diseases.

Chapter 16 reports examples of the close interplay that exists between  $^{99m}\text{Tc}$  and  $^{188/186}\text{Re}$  radiopharmaceuticals employed for diagnostic and therapeutic purposes, respectively. An extensive discussion of the ‘matching pair’ concept as applied to  $^{99m}\text{Tc}$  and  $^{188}\text{Re}$  agents is also given.

Chapter 17 attempts to draw some general conclusions from the large amount of work that has been done so far and, thus, to offer some new perspectives for the future development of  $^{99m}\text{Tc}$  imaging agents, specifically designed for *in vivo* visualization of selected molecular targets.



# Chapter 1

## ROLE OF $^{99m}\text{Tc}$ IN DIAGNOSTIC IMAGING

A. DUATTI

Laboratory of Nuclear Medicine, Department of Radiological Sciences,  
University of Ferrara, Ferrara, Italy

### Abstract

A short overview of the most relevant steps towards the discovery of useful  $^{99m}\text{Tc}$  diagnostic agents is outlined. Emphasis is placed mostly on the evolution of concepts and methods that have been devised for the design of new classes of  $^{99m}\text{Tc}$  tracers targeting specific biological processes and substrates. This evolution can be divided into different periods, each corresponding to a characteristic conceptual approach employed for the development of  $^{99m}\text{Tc}$  radiopharmaceuticals. The analysis of these distinctive traits reveals the fundamental role played by  $^{99m}\text{Tc}$  imaging agents in favouring the continuous growth of nuclear medicine, and may allow envisaging future outlooks of the possible use of  $^{99m}\text{Tc}$  complexes in the age of molecular imaging.

### 1.1. PREFACE

Has  $^{99m}\text{Tc}$  already become an old story? This question is currently plaguing scientists still involved in the study of technetium chemistry and of new categories of  $^{99m}\text{Tc}$  radiopharmaceuticals. Indeed, after the advent of positron emission tomography (PET) and of the cyclotron produced short lived positron emitting radionuclides  $^{18}\text{F}$  and  $^{11}\text{C}$ , the main interest of radiopharmaceutical chemists has progressively shifted towards the investigation of an increasing number of PET tracers, thus leaving the task of further exploring the field of  $^{99m}\text{Tc}$  radiopharmaceuticals to a restricted group of surviving experts. In spite of this, the introduction of new labelling methods based on  $^{99m}\text{Tc}$  has also grown continuously over the last few years, indicating that the field is still alive. However, the number of new  $^{99m}\text{Tc}$  agents recently introduced to the market is practically zero. This is usually attributed to the rise of molecular medicine as well as the closely related field of molecular imaging. If molecular imaging is defined as a method for investigating *in vivo* biological processes at the molecular level, it is usually maintained that  $^{99m}\text{Tc}$  tracers are less suitable for this application as  $^{99m}\text{Tc}$  labelling always involves the use of sterically encumbering chelating moieties to incorporate this metallic radionuclide into the final radiocompound. Conversely, labelling methods based on  $^{18}\text{F}$  and  $^{11}\text{C}$  seem to

induce only a small perturbation on the resulting radiocompound and, therefore, may appear to be more appropriate for functioning as *in vivo* molecular probes. Obviously, this situation does not hold for other PET radionuclides, such as  $^{68}\text{Ga}$ , for which similar problems as with  $^{99\text{m}}\text{Tc}$  are always encountered.

Although this interpretation may help to explain the difficulty in developing  $^{99\text{m}}\text{Tc}$  agents for, for example, imaging the central nervous system (CNS), it does not appear completely appropriate for other molecular targets outside the brain. Evidently, a new paradigm for  $^{99\text{m}}\text{Tc}$  radiopharmaceuticals must be found if this category of diagnostic agents is to maintain its relevancy in the age of molecular medicine. To accomplish this task, it may prove helpful to briefly analyse how the role of  $^{99\text{m}}\text{Tc}$  radiopharmaceuticals has changed over the last few decades since they were introduced. Ultimately, this analysis may lead to a better understanding of the factors that made  $^{99\text{m}}\text{Tc}$  radiopharmaceuticals so successful in diagnostic nuclear medicine in the past and, particularly, in nuclear cardiology. Thus, in this first chapter, a critical overview of the historical development of  $^{99\text{m}}\text{Tc}$  imaging agents is presented. Although this overview should not be considered to be fully exhaustive, and could easily be replaced by other more consistent critical approaches, it aims to identify some fundamental traits of the above mentioned hypothetical new paradigm and to suggest novel future trends.

## 1.2. THE DAWN OF MOLECULAR IMAGING

It is generally accepted that a key advantage of using  $^{99\text{m}}\text{Tc}$  radiopharmaceuticals is, essentially, related to the ease of production of this radionuclide through the transportable  $^{99}\text{Mo}/^{99\text{m}}\text{Tc}$  generator. This constitutes a very efficient and reliable source of high specific activity, and still remains a unique and unrepeated example of a truly useful generator system. However, the existence of an efficient production system of a certain radionuclide is not sufficient for determining its success in clinical applications, as this advantage should be complemented by the availability of labelled compounds exhibiting biodistribution properties that could be conveniently employed for diagnostic purposes. The most stable form of the radionuclide  $^{99\text{m}}\text{Tc}$  in water is the tetraoxo pertechnetate anion  $[^{99\text{m}}\text{TcO}_4]^-$ . It is well known that this species accumulates in the thyroid gland as it mimics the behaviour of the iodide anion  $\text{I}^-$ . As usually occurs in biological interactions, the key factors determining a specific biodistribution behaviour of a compound do not depend on the particular chemical nature of the elements composing it, but rather on its bulky properties such as lipophilicity, molecular dimensions and reactivity. Specifically,  $[^{99\text{m}}\text{TcO}_4]^-$  is recognized as a surrogate of  $\text{I}^-$  because it almost has the same ionic size and identical negative charge [1.1]. More precisely,  $[^{99\text{m}}\text{TcO}_4]^-$  has a slightly

smaller ionic volume than  $I^-$  and, interestingly, is transported more efficiently by the sodium/iodide symporter, the protein responsible for iodide transport, than  $I^-$ . Paradoxically, the observed surrogate behaviour of the iodide ion by the simplest  $^{99m}Tc$  compound can be considered as a forerunner example of a molecular imaging approach. In fact, although  $[^{99m}TcO_4]^-$  is an unnatural compound that does not play a role in biological processes, it is capable of mimicking the behaviour of a true biological substrate as a result of its intrinsic physicochemical characteristics. As mentioned before, molecular imaging can be thought of as a method for *in vivo* monitoring of biological processes at the molecular level. For pursuing this effort, nuclear imaging makes use of very small objects formed by single radiolabelled molecules. These radiocompounds act as molecular probes by transferring information to the outside through their interaction with a target substrate. As a consequence, nuclear imaging is an intrinsic molecular technology, and this can be considered to be its most characteristic trait. The affinity of the pertechnetate anion for the iodide transporter provides an excellent example of a molecular probe, i.e. of a single structurally characterized molecule interacting with a biological substrate through a well established mechanism. The existence of a molecular interaction is essential for extracting information from the signals arising from the radioactive probe. In particular, with  $[^{99m}TcO_4]^-$ , the underlying molecular information is closely connected to the activity of the sodium/iodide symporter that, ultimately, can be interpreted to be a true molecular target. The inherent molecular character of the imaging approach based on  $[^{99m}TcO_4]^-$  as a radioactive probe is clearly evidenced by the recent surge of interest in this compound as an agent for monitoring gene expression.

### 1.3. THE TRACER PRINCIPLE

Despite early applications of the  $^{99m}Tc$  compound being associated with a molecular imaging attitude, subsequent approaches to the design of  $^{99m}Tc$  radiopharmaceuticals have mostly been based on a straightforward interpretation of the tracer principle first formulated by De Hevesey in 1957. This principle simply states that the path and concentration in particular areas of a definite quantity of radiolabelled substance introduced into a biological or mechanical system can be followed by measuring its radioactivity. It is apparent that this principle focuses on the determination of the spatial distribution of radioactivity within an organism. Therefore, the type of information that can be drawn from this approach is entirely within a three dimensional Euclidean space. Scintigraphic images are essentially interpreted as reflecting localization in space, without having to worry about the underlying biomolecular machinery. As a result, there is no need to elucidate the molecular nature of the carrier of

radioactivity, but rather only sticking the radionuclide onto the substrate and tracking its path by seeking the radioactive emission. This lack of interest in the details of the molecular structure incorporating the radionuclide nicely explains the type of labelling techniques employed at the beginning of the age of  $^{99m}\text{Tc}$  radiopharmaceuticals. Since the goal was only to follow the journey of a compound within the body, labelling was accomplished simply by appending a radioactive tag to the molecule without requesting a specific control of the tagged site. This technique has been largely employed for  $^{99m}\text{Tc}$  labelling of large nanostructures (colloids, macroaggregates) accumulating in the target location simply through a non-specific mechanism. The observed distribution of activity is almost perfectly superimposable on that of the unlabelled substrate itself, thus offering a remarkable example of the application of De Hevesey's tracer principle.

A similar situation was implicitly assumed in the labelling of small molecules (e.g. bis-phosphonates, dimercaptosuccinic acid (DMSA) and polycarboxylates) with  $^{99m}\text{Tc}$ . The influence of the labelling procedure on the biological behaviour of the native compound was largely underestimated or even neglected. It should not come as a surprise, therefore, that only a limited number of first generation  $^{99m}\text{Tc}$  radiopharmaceuticals has been structurally characterized. In fact,  $^{99m}\text{Tc}$  bis-phosphonates, belonging to the most successful category of first generation  $^{99m}\text{Tc}$  agents, do not correspond to a single molecular entity, but are rather formed by a mixture of different compounds of unknown chemical composition. Thus, it may sound incredible that, over a period of almost thirty years, these compounds have revealed a great clinical utility as bone seeking agents.

#### 1.4. ADVENT OF $^{99m}\text{Tc}$ SMALL MOLECULE TRACERS [1.2–1.10]

The possibility of finding a useful imaging agent (sometimes called serendipity) was not, however, frequently encountered when dealing with tracers with a reduced molecular size. Something more precise would have to be added to the characterization of a  $^{99m}\text{Tc}$  radiopharmaceutical for there to be a chance of being able to target other tissues such as heart and brain. This additional information was exactly contained in its molecular structure. In fact, it became gradually evident that the specific structural features of a radiopharmaceutical are essential for determining whether it can undergo a biomolecular process. Under ideal conditions, when precise knowledge of the structural features of a selected biological target is available, designing the most suitable radioactive targeting molecule could theoretically be possible. In this case, emphasis is mainly placed on the radiolabelled molecule itself, considered as a whole, and on its interactions

with the surrounding biological environment. The observed biodistribution does not, therefore, merely represent the simple tracing of the radioactivity in the organism, but also incorporates hints of the underlying biomolecular interaction responsible for the localization mechanism. It is clear that this new approach further paved the way towards achieving full molecular interpretation of scintigraphic images.

The development of  $^{99m}\text{Tc}$  cardiac imaging agents is the first example of the design of a new class of  $^{99m}\text{Tc}$  compounds starting from a precise molecular requirement. The key molecular feature that was assumed to impart a specific biological behaviour on the resulting radiopharmaceuticals was that they should carry a monopositive charge. Originally, the idea that a monocationic  $^{99m}\text{Tc}$  complex might interact selectively with the myocardial tissue was derived from the experimental observation that monocationic ions, such as  $\text{Na}^+$  and  $\text{K}^+$ , are avidly taken up by myocytes by the Na/K pump. Similarly, the first radiopharmaceutical employed for heart imaging was the monocationic ion  $^{201}\text{TI}^+$ . Thus, the ‘monocationic hypothesis’ provided very precise molecular information for tailoring the design of a potential  $^{99m}\text{Tc}$  myocardial imaging agent. This approach proved to be highly successful and transformed nuclear cardiology into a mature scientific field. Although subsequent studies showed that the biological behaviour of monocationic  $^{99m}\text{Tc}$  complexes does not mimic that of simpler monocationic ions, and that the role of the positive charge was only in determining their trapping by the negative gradient on the inner mitochondrial membrane, the great impact of the introduction of monocationic tracers in cardiac nuclear imaging undoubtedly demonstrated the effectiveness of the molecular approach for investigating new generations of  $^{99m}\text{Tc}$  imaging agents.

It, therefore, seems reasonable to conclude that the golden era of  $^{99m}\text{Tc}$  radiopharmaceuticals lasted until the end of the last century, and that the development of a significant number of small-molecule  $^{99m}\text{Tc}$  agents for imaging different organs and the CNS, was promoted and sustained by a more efficient approach based on a deeper molecular representation of the targeting process associated with a precise characterization of the molecular structure of a radiopharmaceutical. With this approach, it was apparent that the biological behaviour of a small-molecule  $^{99m}\text{Tc}$  tracer results from the chemical and structural features of the complex as a whole and cannot be attributed to a specific part of it.

## 1.5. THE AGE OF MOLECULAR IMAGING [1.11–1.13]

It is worth noting here that the advent of a full molecular picture in diagnostic imaging did not come from an acquainted and clear discussion of the inherent molecular traits always present in nuclear imaging methods, but rather stemmed from a completely different field related to genomics. Indeed, the view emerging from genetic studies was an obvious molecular representation of living systems as a complicated network of chemical interactions (systems biology). According to this, disease onset always originates by some error in the chain of transmission of chemical information from genes to proteins. This led to the discovery that there is a new world between the genotype and the phenotype of an individual, and that this is formed by the chemotype, the complex machinery of chemical reactions that occur inside an organism. In addition, it soon became clear that the huge amount of biochemical data collected from studies on isolated cells and tissues was not sufficient to obtain the whole picture, as it turned out that the behaviour of a living system does not seem to correspond simply to the sum of its parts. On the contrary, when the various pieces are put together, something new always emerges as a consequence of the interactions between all the parts. Therefore, to gain full comprehension of the behaviour of a living system, addressing the problem of the description and measurement of the strength of these interactions cannot be avoided. However, since these effects are obviously suppressed in isolated tissues, they can only be studied on an integrated living organism where the resulting network of interactions is turned on.

The new paradigm had a dramatic impact on imaging methods as, evidently, these techniques were immediately viewed as being important tools for investigating *in vivo* fundamental biological mechanisms on an unperturbed living system. In this context, imaging agents are more conveniently considered to be true molecular probes capable of selectively interacting *in vivo* with a specific biomolecular target and, consequently, to convey information about the underlying biological process.

The most challenging problem in trying to develop a true molecular probe is how to design it. As no clear strategy exists for this, the most common approach is to label a selected chemical species that is known in advance to possess particular biological properties. This could be a molecule of biological origin, such as a protein or a bioactive peptide, or a synthetic drug. Through this approach, the resulting imaging agent can be thought to be composed of essentially two parts, one containing the radionuclide and the other including the bioactive group. Usually, these two sections of the molecule are connected by a suitable chain of bridging atoms (linker). Evidently, this strategy, that is commonly dubbed the ‘bifunctional approach’, strongly deviates from the design of  $^{99m}\text{Tc}$  small-molecule tracers where biological behaviour was considered to

arise from the overall properties of the radiocompound and not from a subsection of it.

In appending a radioactive label to this molecule, it is always assumed that the labelling procedure should not alter its indigenous biological behaviour. According to this, radionuclides having a low sterical hindrance are preferred. For instance, the  $\beta^+$  emitting radionuclides  $^{18}\text{F}$  and  $^{11}\text{C}$  are usually considered to impart only a negligible perturbation when introduced into a molecule, a fact that easily explains their relevant role in molecular imaging. Conversely, metallic radionuclides are thought to occupy a larger molecular volume, particularly because they usually require a convenient chelating system to be appended to a molecule.

In spite of this, many bioactive molecules have been successfully labelled with  $^{99\text{m}}\text{Tc}$  without losing their biological activity. In particular, various bioactive peptides and proteins have been used as starting substrates for yielding new categories of  $^{99\text{m}}\text{Tc}$  radiopharmaceuticals targeting specific receptors. As expected, these successful achievements have mostly been promoted by significant advancements in  $^{99\text{m}}\text{Tc}$  chemistry that have led to the discovery of novel cores ( $^{99\text{m}}\text{Tc}$ -nitrido,  $^{99\text{m}}\text{Tc}$ -hynic) and reactive metallic fragments ( $^{99\text{m}}\text{Tc}$ -tricarbonyl,  $^{99\text{m}}\text{Tc}$ -4+1,  $^{99\text{m}}\text{Tc}$ -N-PNP) [1.2]. In this respect, the approach based on reactive metallic fragments proved to be particularly successful. This method is based on the chemical properties of certain types of substitution-labile technetium complexes that show a marked reactivity only towards ligands that have a specific set of coordinating atoms. In these complexes, a few coordination positions are occupied by a set of ligands that is tightly bound to the metal centre. The resulting strong ligand field allows significant stabilization of the metal oxidation state, preventing the complex from undergoing oxidation-reduction reactions. The remaining positions of the coordination arrangement are usually spanned by weakly bound ligands that could be easily replaced by another incoming ligand carrying a specific set of donor atoms. As a result, the reaction between the precursor complex and the hypothetical incoming ligand is expected to be kinetically favoured and should afford the final substituted complex at very high yield. This behaviour can be efficiently exploited for tethering a stable  $^{99\text{m}}\text{Tc}$  fragment to a biomolecule with the appropriate set of coordinating atoms. A high affinity of the precursor metal fragment for the specific donor set on the bioactive ligand would ensure the perfect fit of these two molecular building blocks in forming the final conjugated complex.

Using the various metallic  $^{99\text{m}}\text{Tc}$  synthons, it has been possible to label biologically active molecules at very high specific activity and, therefore, to obtain radioactive probes for molecular imaging based on  $^{99\text{m}}\text{Tc}$ . When employed for labelling substrates with a molecular size comparable to that of the metallic fragment, such as short peptide sequences, these methods were found to be

capable of fully preserving their starting biological properties. Conversely, the labelling of small biomolecules always constitutes a great challenge because of the possibility of causing a large perturbation in the molecular structure of the labelled substrate.

## 1.6. EPILOGUE

Approximately 70% of nuclear medicine procedures around the world are still based on  $^{99m}\text{Tc}$  radiopharmaceuticals. In particular, nuclear imaging in cardiology, which covers a significant part of all diagnostic procedures, is almost completely carried out using  $^{99m}\text{Tc}$  perfusion tracers. However, over the last two decades, only two new  $^{99m}\text{Tc}$  radiopharmaceuticals have been introduced into clinical practice. Thus, a few important questions are currently challenging the field and these are mostly related to the role that might be envisaged for  $^{99m}\text{Tc}$  radiopharmaceuticals in nuclear medicine in the future. More precisely, could  $^{99m}\text{Tc}$  still be considered a useful radionuclide for the next generation of radiopharmaceuticals? The answer to this question is not as simple as it may first appear since many factors are involved in this analysis, including potential advances in basic sciences and in imaging technology, and market trends. However, some considerations might help in attempting to figure out the new scenario.

PET radionuclides, such as  $^{11}\text{C}$  and  $^{18}\text{F}$ , apparently, seem to possess chemical properties that could facilitate the development of useful molecular probes for *in vivo* imaging of fundamental biological processes. This appears even more plausible if the labelling of biologically active species remains the most common route for designing new molecular agents. Yet, a useful tracer for molecular imaging does not necessarily mean that this same compound could also be useful for normal diagnostic applications. An essential outcome of a diagnostic procedure is that it should provide a clear answer to the clinical question and, eventually, indicate the most appropriate treatment for the patient. Moreover, when the underlying technology is relatively easy to use in clinical practice, this adds a further key advantage. These concepts nicely explain the persistent and dominant role of  $^{99m}\text{Tc}$  perfusion imaging agents over PET tracers in cardiology. In fact, although PET compounds allow *in vivo* monitoring of some basic metabolic processes in the myocardium, they do not add a significant improvement to the diagnostic outcome when compared to  $^{99m}\text{Tc}$  agents. Thus, when also considering the complex apparatus required for preparing PET tracers,  $^{99m}\text{Tc}$  cardiac agents still remain the most convenient diagnostic tool. Presumably, only a sharp improvement in chemical methods employed in the production of

current PET cardiac tracers would justify their routine application in nuclear cardiology (see Chapter 16 for further discussion).

In turn, however, these arguments may also apply to the development of novel  $^{99m}\text{Tc}$  radiopharmaceuticals. Whether they will continue to play a useful role in diagnostic nuclear medicine is very much dependent on whether they will be able to offer a real advantage over existing and new radiopharmaceuticals. In particular, the biological properties of the new  $^{99m}\text{Tc}$  tracers should approach, as closely as possible, those of an ideal imaging agent. More precisely, the target:background ratio should be almost optimal ( $>3$ ) as this will ensure that the final image quality always allows a clear diagnostic outcome to be reached. This fact, coupled with the ongoing technological improvements in SPECT scanners, may contribute to greatly decreasing the gap between PET and SPECT.

Obviously, a critical question still remains to be answered. How should the next generation of  $^{99m}\text{Tc}$  tracers be designed? Presumably, the field of small-molecule  $^{99m}\text{Tc}$  agents is still open and may yield a number of unexpected results. Yet, it is very difficult to clearly indicate which way to go, and it is likely that unprecedented chemical methods may help to find the most efficient strategy. It should be noted, however, that even PET is often plagued by the poor biological behaviour of its small-molecule tracers. Labelling a bioactive molecule without causing any perturbation of its biological properties by no means implies that the resulting tracer will definitely exhibit a useful *in vivo* behaviour. After administration, a single molecule has a difficult journey inside the body where it has to interact with a number of chemical species and cross different barriers that may impair its ability to reach the target. A key problem with a small-molecule tracer is usually determined by the requirement that this single entity should perform different molecular functions for successfully approaching the target. For example, a receptor imaging agent for the CNS should possess the ability to cross the blood-brain barrier, but concomitantly should also be able to interact with the receptor site with high affinity and specificity [1.14, 1.15]. Recently, a single molecule trifunctional approach was proposed [1.16]. The neuropeptide bombesin (BBN) and a highly fluorescent acridine derivative have been combined and linked to each other through a  $[\text{M}(\text{CO})_3]^+$  ( $\text{M} = {^{99m}\text{Tc}}$ , Re) moiety, which represents the third functionality. This new concept was successfully employed for developing trifunctional metal complexes for cell specific nuclear targeting. However, it is not always feasible to incorporate these multiple functions into a single molecular entity with dimensions smaller than a nanometre.

Conversely, to address the demand for a multifunctional agent, it would be more convenient to consider molecular entities as being sufficiently large for hosting a number of different functional groups carrying out various biological functions. Indeed, in nature, there is widespread use of this type of bulky

biological species. From a general point of view, all reactions in a living system occur at a nanoscale level under non-equilibrium conditions. Even if small molecules are always involved in the process, these usually have to be supported by a larger entity (e.g. a protein) with nano-sized dimensions. The large size of these structures may allow them to exhibit a variety of biological functions, all contributing to achieving a final specific goal. In principle, the same approach might be applied to the design of a multifunctional  $^{99m}\text{Tc}$  agent. Therefore, a potential new generation of  $^{99m}\text{Tc}$  radiopharmaceuticals might be thought of as being composed of radiolabelled macromolecular entities with dimensions greater than 10 nm, and exhibiting a specific biological activity. This property should arise from the combined action of different functional groups located in selected positions of the macromolecule. These nanostructures could be conveniently pictured as chemical machines performing a molecular function inside the cell [1.17–1.24]. Evidently, the incorporation of a  $^{99m}\text{Tc}$  chelate within the structure of these large molecular objects would only have a limited impact on their biological behaviour.

To illustrate this concept further, it would be useful to introduce the notion of a ‘multifunctional ligand’. As mentioned previously, a bifunctional ligand is, usually, designed to perform two basic functions, namely to bind the metallic group and to impart specific biological properties to the final  $^{99m}\text{Tc}$  radiopharmaceutical. In principle, however, the number of functional motifs does not have to be limited to just two functions. This suggests going beyond the notion of a bifunctional ligand and including the broader concept of a ‘multifunctional ligand’. According to this, a multifunctional ligand is commonly depicted as a macromolecular scaffold, sufficiently large in size to accommodate a number of different functional groups. Obviously, these functional moieties may play various chemical and biological roles, but preliminary studies indicate that even when identical bioactive groups are appended to the same macromolecular structure, it is usually expected that the resulting multifunctional conjugate would exhibit an enhanced biological behaviour as compared to the corresponding bifunctional analogue.

It is not simple to predict whether the transition from small-molecule radiotracers to radiolabelled multifunctional nanomachines will really provide an alternative approach for developing the next generation of  $^{99m}\text{Tc}$  radiopharmaceuticals (Fig. 1.1). However, if a potentially useful compound results from this new category of molecular systems, it seems reasonable to expect that the ‘ideal’ physical properties of the ‘old’ radionuclide  $^{99m}\text{Tc}$  will make the difference.

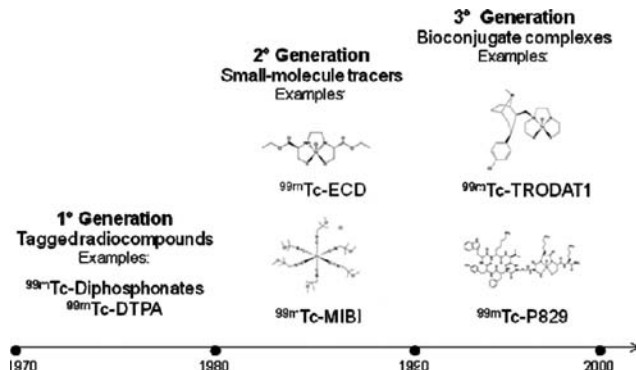


FIG. 1.1. The various generations of  $^{99m}\text{Tc}$  radiopharmaceuticals.

## REFERENCES TO CHAPTER 1

- [1.1] LEE, W.W., et al., Imaging of adenovirus-mediated expression of human sodium iodide symporter gene by  $^{99m}\text{TcO}_4$  scintigraphy in mice, *Nucl. Med. Biol.* **31** (2004) 31–40.
- [1.2] INTERNATIONAL ATOMIC ENERGY AGENCY, Labelling of Small Biomolecules Using Novel Technetium-99m Cores, Technical Reports Series No. 459, IAEA, Vienna (2007).
- [1.3] BANDOLI, G., TISATO, F., DOLMELLA, A., AGOSTINI, S., Structural overview of technetium compounds (2000–2004), *Coord. Chem. Rev.* **250** (2006) 561–573.
- [1.4] ARANO, Y., Recent advances in  $^{99m}\text{Tc}$  radiopharmaceuticals, *Ann. Nucl. Med.* **16** (2002) 79–93.
- [1.5] BANERJEE, S.R., et al., New directions in the coordination chemistry of  $^{99m}\text{Tc}$ : a reflection on technetium core structures and a strategy for new chelate design, *J. Nucl. Med. Biol.* **32** (2005) 1–20.
- [1.6] JURISSON, S.S., LYDON, J.D., Potential technetium small molecule radiopharmaceuticals, *Chem. Rev.* **99** (1999) 2205–2218.
- [1.7] BOSCHI, A., DUATTI, A., UCCELLI, L., Development of technetium-99m and rhenium-188 radiopharmaceuticals containing a terminal metal-nitrido multiple bond for diagnosis and therapy, *Top. Curr. Chem.* **252** (2005) 85–101.
- [1.8] SCHIBLI, R., SCHUBIGER, P.A., Current use and future potential of organometallic radiopharmaceuticals, *Eur. J. Nucl. Med. Mol. Imaging* **29** (2002) 1529–1542.
- [1.9] ALBERTO, R., Technetium, in *Comprehensive Coordination Chemistry II*, McCLEVERTY, J.A., MEYER, T.J. (Eds), Vol. 5, Elsevier, New York (2004) p. 127.
- [1.10] ALBERTO, R., SCHIBLI, R., WAIBEL, R., ABRAM, U., SCHUBIGER, A.P., Basic aqueous chemistry of  $[\text{M}(\text{OH}_2)_3(\text{CO})_3]^+$  ( $\text{M} = \text{Re}, \text{Tc}$ ) directed towards radiopharmaceutical application, *Coord. Chem. Rev.* **190–192** (1999) 901–919.
- [1.11] LEVIN, C.S., Primer on molecular imaging technology, *Eur. J. Nucl. Med. Mol. Imaging* **35** (2005) S325–S345.

- [1.12] DZIRK-JURASZ, A.S.K., Molecular imaging in vivo: an introduction, *Br. J. Radiol.* **76** (2003) S98–S109.
- [1.13] HERSCHEMAN, H.R., Molecular imaging: looking at problems, seeing solutions, *Science* **302** (2003) 605–608.
- [1.14] WONG, D.F., POMPER, M.G., Predicting the success of a radiopharmaceutical for in vivo imaging of central nervous system neuroreceptor systems, *Mol. Imag. Biol.* **5** (2003) 350–362.
- [1.15] JOHANNSEN, B., PIETZSCH, H.-J., Development of technetium-99m-based CNS receptor ligands: have there been any advances? *Eur. J. Nucl. Med.* **29** (2002) 263–275.
- [1.16] AGORASTOS, N., et al., Cell-specific and nuclear targeting with  $[M(CO)_3]^+$  ( $M = {}^{99m}\text{Tc}$ , Re)-based complexes conjugated to acridine orange and bombesin, *Chemistry* **13** (2007) 3842–3852.
- [1.17] CUI, Y., WEI, Q., PARK, H., LIEBER, C.M., Nanowire nanosensors for highly sensitive and selective detection of biological and chemical species, *Science* **293** (2001) 1289–1292.
- [1.18] VO-DINH, T., (Ed.), *Nanotechnology in Biology and Medicine: Methods, Devices, and Applications*, CRC Press, Taylor & Francis Group, Boca Raton, FL (2007).
- [1.19] EBBESEN, M., JENSEN, T.J., Nanomedicine: techniques, potentials, and ethical implications, *J. Biomed Biotechnol.* **2006** (2006) 1–11.
- [1.20] EMERICH, D.F., THANOS, C.G., Nanotechnology and medicine, *Expert Opin. Biol. Ther.* **3** (2003) 655–663.
- [1.21] EMERICH, D.F., THANOS, C.G., The pinpoint promise of nanoparticle-based drug delivery and molecular diagnosis, *Biomol. Eng.* **23** (2006) 171–184.
- [1.22] EMERICH, D.F., THANOS, C.G., Targeted nanoparticle-based drug delivery and diagnosis, *J. Drug Target.* **15** (2007) 163–183.
- [1.23] LIU, Y., MIYOSHI, H., NAKAMURA, M., Nanomedicine for drug delivery and imaging: a promising avenue for cancer therapy and diagnosis using targeted functional nanoparticles, *Int. J. Cancer* **120** (2007) 2527–2537.
- [1.24] CARUTHERS, S.D., WICKLINE, S.A., LANZA, G.M., Nanotechnological applications in medicine, *Curr. Opin. Biotechnol.* **18** (2007) 26–30.

## Chapter 2

# OVERVIEW OF CURRENT LABELLING METHODS

R. ALBERTO

Institute of Inorganic Chemistry, University of Zurich,  
Zurich, Switzerland

### Abstract

The conjugation of  $^{99m}\text{Tc}$  complexes or complex fragments to targeting vectors is the core science of labelling chemistry. The first sections of the chapter outline the non-chemical constraints to be considered for successful biomolecule labelling and for a chance of becoming introduced to the market. Without taking these constraints into account, even the best radiopharmaceutical will not gain access to the market. Labelling methods, which either fulfil these constraints completely or, at least, to a significant extent, will then be emphasized. Besides the old cores, such as  $[\text{Tc}=\text{O}]^{3+}$ , the novel cores  $[\text{Tc}]^{3+}$ ,  $[\text{Tc}=\text{N}]^{2+}$  and  $[\text{Tc}(\text{CO})_3]^+$  as well as the intensive research based on these cores are discussed in detail. Recent examples towards novel  $^{99m}\text{Tc}$  based radiopharmaceuticals are described. Based on the current methods for the labelling of biomolecules, the objective of the chapter is to guide towards potential novel approaches in radiopharmaceutical chemistry.

### 2.1. INTRODUCTION

Modern radiopharmaceutical chemistry aims at combining targeting molecules with radionuclides, in general, and technetium complexes in particular. The conjugation of a metal complex to a biologically active molecule is referred to as the labelling step. The nature of the biologically active molecules is diverse. They could be composed of a few amino acids (peptides) or a large number of amino acids (proteins), designed for binding to particular receptors overexpressed on, for example, cancer cells [2.1]. They could be composed of nucleobases in the form of DNAs or PNAs for, for example, antisense imaging or gene expression imaging [2.2–2.4]. Besides these relatively large targeting molecules, smaller ones such as steroid hormones, central nervous system (CNS) receptor binding molecules, molecules involved in metabolism, such as carbohydrates or amino acids, but also normal pharmaceuticals, such as tamoxifen [2.5, 2.6], are of major importance for labelling, for the diagnosis and therapy of a very broad variety of socially relevant diseases. This list can be extended and the search for new targets in clinical imaging will certainly lead to an involvement of more molecules, and especially of more diverse molecules. Despite its great importance, the impact and the introduction of new radiopharmaceuticals has, thus far, been modest.

When selecting a particular biomolecule for targeting a clinically relevant disease, the method of labelling is the immediate question and sometimes the challenge. Labelling can substantially influence biological behaviour and, therefore, ultimately the quality of the image and the success of the diagnosis. The question about the core to be selected is, therefore, crucial but is still not routine. In contrast to labelling with the typical positron emission tomography (PET) radionuclides,  $^{11}\text{C}$ ,  $^{18}\text{F}$  and  $^{123}\text{I}$ , the label in single photon emission computed tomography (SPECT) is a multi-component system, consisting of the transition metal centre and some inherently connected groups. These functionalities make up the ‘core’. To complete the label, a ligand, which should bind the core tightly and irreversibly, is bound to the targeting molecule [2.7].

Under the prerequisite that the complex is stable, variation of the ligand enables the tuning and sometimes the fine tuning of the biological behaviour. Radiopharmaceutical literature in the distant and recent past establishes that even minor chemical alterations in the transition metal label imposes different biological distributions or target accumulations. It is to be expected that completely altering the label will cause even more dramatic effects. However, systematic studies with the same biomolecules but different metal complexes are very scarce. In general, research groups are familiar with a particular labelling method and, thus, do not apply another one, but rather rely on only varying the ligand. This specialization is reasonable since  $^{99\text{m}}\text{Tc}$  labelling is not a completely routine task. It demands partly complicated synthesis of new ligands, coupling to the biomolecule and labelling under very different conditions. It is, therefore, of great importance that organizations such as the IAEA coordinate research with the same biomolecule but with different labels, as recently done.

This section does not intend to summarize the labelling methods for biomolecules as this is beyond the scope of this chapter. For a comprehensive literature overview, the reader is referred to a number of excellent reviews which appeared recently and which are quoted throughout this article. Instead, labelling methods are summarized from a chemical point of view and the references should encourage the radiopharmaceutical researcher to explore alternative methods as well, rather than simply varying the ligand of one particular core.

In current technetium chemistry, a number of very well explored and developed labelling methods exist which will be described below. Novel cores have been and are still being introduced with the objective of facilitating and generalizing labelling, while having the smallest possible effect on the targeting molecule. Among this realm of possibilities, there are certainly more appropriate labelling methods for a particular biomolecule. The sections should, thus, help the reader to identify and chemically realize the labelling methods that hold greatest promise for the attempted targets. This concerns new and yet to be developed targets but, even more so, also old targets for which there has not yet been success.

## 2.2. REQUIREMENTS FOR LABELLING TARGETING MOLECULES

Research towards labelling targeting molecules (or technetium essential radiopharmaceuticals) must consider scientific requirements, which will be discussed below, and a number of non-scientific points that are of equal importance and which are not necessarily under the control of the researchers. When selecting a targeting molecule and, thus, a particular labelling method, the question of the relevance of the radiopharmaceutical for public health care arises. A thorough market study about potential demand and feasibility provides a reliable basis for ongoing development. Radiopharmaceuticals that act as good targeting molecules often fail to be introduced to the market and, consequently, the benefit for public health care is not realized. Sometimes, the market is not large enough or the costs are too high. In any case, market introduction is not the ultimate objective in radiopharmaceutical chemistry, especially for technetium or rhenium. Scientific results justify research at the academic level and are strategically more important. The contributions of labelled compounds to the fundamental understanding of biological mechanisms or the *in vivo* behaviour of drugs or targeting agents are as important as market introduction. Nevertheless, one must admit that the possibility of finding a new product is the real driving force behind technetium chemistry. Potential applicability is also becoming more and more important for non-commercial funding.

Competition from other rapidly growing diagnostic tools is a further issue. It does not make much sense to develop a radiopharmaceutical for a target that can be better imaged by ultrasound, MRI or even X rays. The major advantages of technetium radiopharmaceuticals are still their cost and availability. However, if their significance is minor compared to one of the aforementioned methods, those will remain the tools of choice.

Last but not least, the educational aspects of labelling chemistry should not be forgotten. Labelling chemistry is a strongly interdisciplinary field, ranging from the synthesis of chelators, via the coupling to partly sensitive biomolecules, to inorganic complex formation reactions. Stability or affinity assays close the circle. It is, thus, an important requirement to involve people with broad knowledge and expertise or to give them appropriate training in order to perform suitable and versatile research in labelling chemistry.

### 2.2.1. From a scientific point of view

Labelling chemistry, as presented in the following sections, has to consider a number of scientific requirements in order to be successful, either for gaining important scientific knowledge or for producing a routinely applicable

radiopharmaceutical. The following points are crucial prerequisites for these purposes:

- Labelling yield must be close to quantitative but better than 95%;
- Labelling chemistry may not include purification processes;
- Labelling chemistry must be highly efficient at low biomolecule concentration;
- Potentially toxic or unstable ingredients are not desirable;
- No bio-incompatible organic solvents may be used;
- The complex label must be well defined, if possible not only by high performance liquid chromatography (HPLC) but also by classical chemical analysis;
- No unspecific labelling of the biomolecule should occur;
- Transfer of the process to rhenium (for therapy) is desirable;
- In vivo stability is required.

These requirements are compulsory and the labelling chemistry discussed below was selected since these approaches fulfil the demands to a reasonable extent. Biological factors and requirements are not discussed, since the focus of this chapter is labelling chemistry. The objective is to present labelling methods that can be used, without substantial difficulties, to label a particular biomolecule of choice.

### **2.2.2. From routine application**

For research purposes, many biomolecules can be labelled and studied without fulfilling the criteria outlined in Section 2.2.1. However, if a new radiopharmaceutical is to find wide application in clinical practice, a number of additional points should be considered, ideally right from the beginning of the studies. An approach for which these points cannot be addressed will remain limited to pure research labs. Some of the important additional requirements are listed below:

- The procedure should be concentrated in an instant kit formulation;
- The kits are lyophilized, thus, the ingredients should not be volatile or decomposed during this process;
- After labelling, the radiopharmaceutical should be ready to administer;
- Very precise labelling conditions (e.g. 12.56 min at 94.3°C) are not desirable;
- A reasonable radiochemical purity test should be feasible in a short time.

These are some mandatory points. A more detailed discussion about further requirements can be found in Ref. [2.8].

## 2.3. LABELLING METHODS: STATE OF THE ART

### 2.3.1. Labelling with the $[Tc=O]^{3+}$ core

The technetium core most widely applied in radiopharmaceutical chemistry is the  $[Tc=O]^{3+}$  moiety, in which technetium is in the oxidation state +V. For many years, technetium essential radiopharmaceuticals were essentially based on this core. Accordingly, labelling of biomolecules followed a similar approach.  $[TcO_4]^-$  is reduced by two electrons coming from  $Sn^{2+}$  or other two electron reducing agents. The chemistry and radiopharmacy of the  $[Tc=O]^{3+}$  core has been extensively reviewed [2.9–2.14]. The core is stabilized with tetradeinate pure N mixed NS or NO ligands. Several of these ligands are depicted in Fig. 2.1.

Despite the fact that an enormous variety of ligands has been prepared and studied, the field is still open for further development. With respect to targeting, the most prominent example from this series is certainly TRODAT, an agent that crosses the blood–brain barrier and binds to the DAT receptor [2.15–2.19]. Of further interest is Technescan® (MAG3) which has found widespread application as a renal clearing imaging agent [2.20].

One typical example from the recent literature describing peptide labelling with pendent MAG3 ligand is described here in more detail, since it allows quick and clean labelling of peptides and fulfils the requirements outlined above. It should be emphasized that this is not the only example but that it represents very well the state of the art of labelling with MAG3 based ligands.

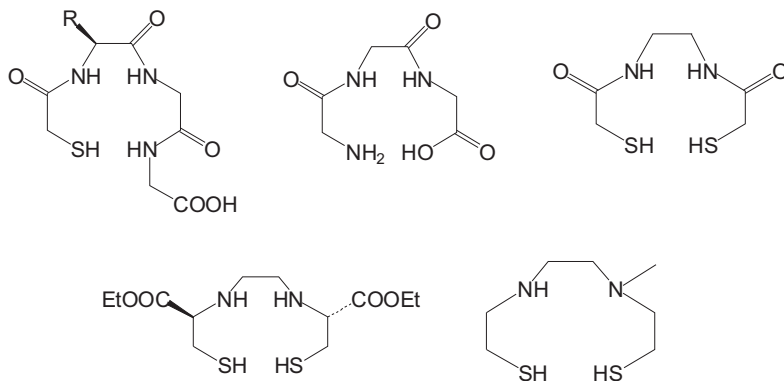


FIG. 2.1. Commonly used tetradeinate ligands for stabilizing the  $[Tc=O]^{3+}$  core.

*Example.* In this work, a MAG3 chelating agent was introduced in the last step of the solid phase peptide synthesis as a simple elongation applying the Fmoc strategy [2.21]. The selected peptide was a bombesin (BBN) fragment with an aminohexanoic spacer. To introduce the N<sub>2</sub>S chelators, the BBN analogue sequence was N-terminally elongated by respective couplings with Fmoc-Ahx-OH, three times with Fmoc-gly-OH and finally with an acetyl S-protected mercapto-acetyl group [2.22]. The structure is depicted in Fig. 2.2.

Whereas the mercapto-acetyl terminus is usually protected by a benzoyl group requiring boiling for deprotection, the acetyl protecting group can be removed at room temperature. This is a significant advantage with respect to application. After removal of the protecting group, radiolabelling can then be achieved at room temperature with a good yield with the following protocol. A total of 10 µL of a peptide solution (10 mg/mL) was mixed with a total of 8 µL of a SnF<sub>2</sub>/NaBH<sub>4</sub> solution and 200 µL of generator eluate. Keeping the reaction mixture for 1 h at room temperature gives an essentially quantitative labelling yield. However, due to the relatively high peptide concentration ( $\approx$ 300 µM), separation from the cold peptide is required. Alternative labelling procedures are performed under similar conditions [2.23–2.25]. Labelling at room temperature with thiol containing ligands sometimes has the drawback that a kinetic intermediate is formed rather than the thermodynamically favoured product. The high nucleophilicity of the thiolato group might initially form a compound in which four thiolato groups bind around the [Tc=O]<sup>3+</sup> core, leading to a {TcO(pep)<sub>4</sub>} intermediate [2.26]. Rearrangement leads to a 2:1 compound which converts under slightly basic conditions to the final 1:1 product. In this example, and in many other papers, the application of a ligand with two terminal mercapto groups bypasses this problem and only one product is formed. The N<sub>2</sub>S<sub>2</sub> ligands have the drawback of having substantially higher lipophilicity as compared to the anionic N<sub>2</sub>S MAG3 like systems.

The example discussed above exemplifies rather clearly the problems but also the versatility encountered with the [Tc=O]<sup>3+</sup> approach. Mercapto groups are always tricky since they tend to be oxidized and to form disulphides, even under

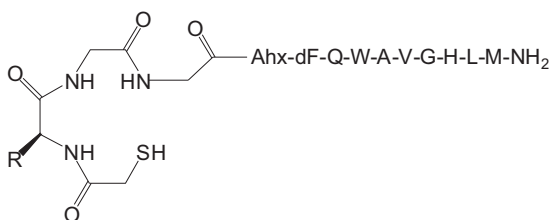


FIG. 2.2. MAG3 ligand conjugated to a bombesin derivative.

completely anaerobic conditions. Protection and deprotection is a more or less mandatory step. NS like ligands have been applied to more or less all sorts of targeting agents and technetium essential radiopharmaceuticals. The complexes can be neutral and of high lipophilicity as required for CNS receptor imaging agents or they can be hydrophilic as required for peptide labelling. Changing their authenticity is not easy. The introduction of tuning groups into the carbon backbone will inevitably lead to stereochemically active centres. The tetradentate ligand scaffold is more or less fixed and fine tuning is, therefore, almost impossible or, at least, requires lengthy organic synthesis. Since the building blocks of the ligand are natural or artificial amino acids, it is possible to synthesize the ligand directly according to solid phase synthetic strategies. However, additional side chains in the building block, in general, impair the labelling efficiency.

The approach cannot be readily adapted to corresponding rhenium chemistry for therapeutic purposes. On the one hand,  $[ReO_4]^-$  is much more difficult to reduce than  $[TcO_4]^-$  and, on the other hand, the corresponding Re analogues are much more easily reoxidized to  $[ReO_4]^-$ . Nevertheless, labelling of peptides has been studied with success but, for the reasons mentioned above, there is less research activity than with  $^{99m}Tc$  [2.27, 2.28].

Molecular imaging is a research field, which is becoming a focus of new radiopharmaceutical developments. The targeting agents in this context are, among others, PNAs, mRNAs and antisense oligonucleotides [2.3, 2.29–2.31]. The approach of labelling antisense oligodeoxynucleotides (ODN) with NS type ligands is reported to underline the flexibility of this method [2.32, 2.33]. Labelling followed the usual strategy; the MAG3 ligand on the ODN was benzoyl protected and, therefore, heating for deprotection and concomitant labelling was required. To achieve high radiochemical purity, a relatively large concentration of MAG3-ODN is necessary; this necessitates purification. Despite these side issues, ODNs can be neatly labelled with the  $[Tc=O]^{3+}$  moiety. Another approach was undertaken to label antisense ODNs for molecular imaging of atherosclerotic plaques. Similarly, relatively high concentrations of biomolecule are required for high radiochemical purity [2.34].

In summary, although the  $[Tc=O]^{3+}$  approach with various tetradentate ligands is the least recent but the most established approach, it has developed over the past decade to such an extent that it can be applied to essentially all kinds of targeting molecules for molecular imaging. The approach has comparably limited flexibility with respect to the ligand, as such, but it tolerates a relatively broad range of labelling conditions. Most importantly, the complexes are well characterized and the authenticity of the labels is, in most cases, unambiguously known. In some rare examples, the biomolecule labelled with cold rhenium has been directly characterized by 2D NMR spectroscopy, proving the identity with

the  $^{99m}\text{Tc}$  complex not only by comparing the HPLC retention times but characterizing the coordination sphere by spectroscopic methods [2.35]. Such efforts to characterize the authenticity makes market introduction easier.

### 2.3.2. Labelling with the $[\text{Tc}\equiv\text{N}]^{2+}$ core

The  $[\text{Tc}\equiv\text{N}]^{2+}$  core is a moiety in which technetium is also in the oxidation state +V. Although known as a building block for rather a long time, its extended potential for radiopharmaceutical application has only recently been recognized and studied [2.36, 2.37]. In contrast to the  $[\text{Tc}=\text{O}]^{3+}$  core, the reduced charge and the  $\pi$ -loading induced by the nitrido ligand renders the technetium centre much more b type. As the  $[\text{Tc}=\text{O}]^{3+}$  building block,  $[\text{Tc}\equiv\text{N}]^{2+}$  also does not exist in free or hydrated form but has to be stabilized by additional ligands. These are then replaced via trans-metallation to the bifunctional chelator conjugated to the targeting molecule or remaining part of it [2.38]. The second option, especially, leads to a variety of new building blocks in which the chelator bound to the targeting molecule remains constant and the auxiliary ligand is altered. This methodology has been developed recently and shows great potential as a very useful method for preparing either novel radiolabelled targeting biomolecules or technetium essential radiopharmaceuticals such as  $[\text{TcN}(\text{NOEt})_2]$ . Although this compound is an excellent myocardial imaging agent, it was not introduced to the market for one of the reasons discussed in the requirements section [2.39].

Of particular success, in this respect, is the asymmetrical  $[\text{Tc}\equiv\text{N}]^{2+}$  approach recently developed by Duatti et al. [2.40–2.44] (Fig. 2.3).

*Example.* As a representative example of how the  $[\text{Tc}\equiv\text{N}]^{2+}$  moiety can be used in asymmetrical labelling of biomolecules, the reaction with derivatives of a benzodiazepine receptor binding molecule is introduced (Fig. 2.4) [2.45].

In a first step, the nitrido precursor is generated from  $[^{99m}\text{TcO}_4]^-$  in the presence of the nitrido source succinic dihydrazide and a reducing agent at room temperature. The generation of this immediate precursor is available in a kit formulation, which makes the application of the nitrido technology very

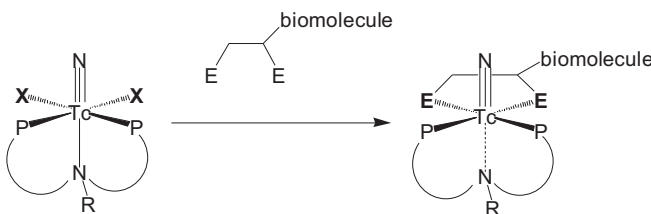


FIG. 2.3. The mixed ligand approach with the  $[\text{Tc}\equiv\text{N}]^{2+}$  core for labelling targeting biomolecules.

convenient. In a second step, the asymmetric ligand PXP (with X = O, S, N) and the derivatized biomolecules are added to afford the labelling of the benzodiazepine derivative. The structure of the benzodiazepine derivative is shown on the left side in Fig. 2.4. Heating to 98°C gives the product in perfect radiochemical purity and yield. As an important proof for the authenticity of the compound, analogues with  $^{99}\text{Tc}$  or Re have been prepared and characterized by normal spectroscopic methods and, for some examples, by X ray structure analyses as well [2.38].

This method has been applied to a wide variety of biomolecules, including peptides and ODNs, but to small CNS receptor binding molecules in particular [2.46–2.50]. The nitrido approach fulfils all the requirements necessary for routine application. The basic building block  $[\text{TcN}(\text{PXP})]^{2+}$  can be regarded as a true synthon. The labelling procedure is facile and complex alteration without changing the central core is possible. The ligands conjugated to the biomolecules are not complicated and are commercially available. A disadvantage is the presence of air sensitive and potentially toxic phosphines. However, this is a technical problem which can probably be solved by searching for alternative PXP like ligands. The approach is also compatible with  $^{188}\text{Re}$  although different reaction conditions apply.

### 2.3.3. Hynic labelling

Hynic (hydrazinonicotinamide) is the method of labelling preferentially used in the context of peptides. It is probably the most widely used approach for labelling peptides and proteins. It has been reviewed many times recently and there is no need to review the literature at this point [2.10, 2.51–2.54]. The compounds likely to be formed with hynic and some additional coligands are depicted in Fig. 2.5.

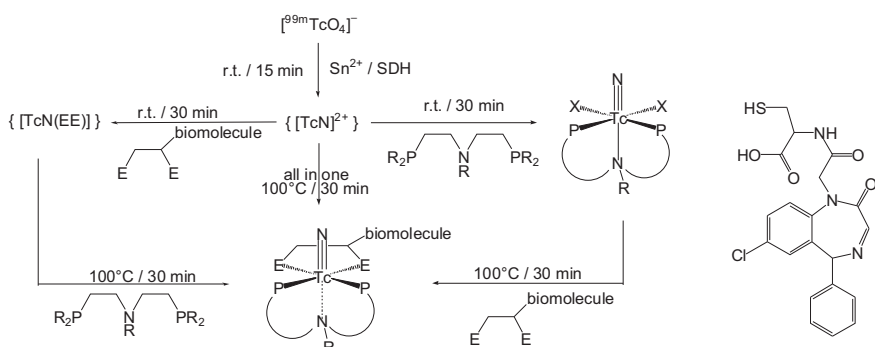


FIG. 2.4. Flow chart for the asymmetrical labelling of benzodiazepine.

The labelling method is exemplified with a study performed for the labelling of salmon calcitonin and showing how a hynic building block can conveniently be used in solid phase peptide synthesis. In general, the NHS activated carboxylic acid of hynic is mixed with the peptide or protein and covalently bound via amide formation to the vector. This is convenient if there are not multiple binding sites (as in proteins) but one single amine group only to which hynic is then coupled. Otherwise, the coupling method is unspecific and statistical distribution of numbers and sites is found. For proteins, this is not of major importance but it is decisive for peptides. The different products have to be separated or synthetic techniques applied which ensure binding to one site only.

*Example.* Such a generally applicable synthetic technique has been described by applying an Fmoc-N- $\epsilon$ -(hynic-Boc)-lysine building block for solid phase synthesis of peptide radiopharmaceuticals [2.55]. This building block is of the utmost importance and can be subjected to any Fmoc based solid phase synthesis of peptides. It can be incorporated site specifically in any sequence and be deprotected prior to the labelling step. The labelling procedure essentially follows the pathway that has been described for hynic in the literature. It shall be presented in detail here to give the reader an idea about the synthetic possibilities. The deprotection of the hynic group, diluted TFA for 2.5 h at room temperature, precedes the labelling and can conveniently be monitored by RP-HPLC/ESI-MS. The solution contains about 270  $\mu$ g of peptide per mL, which results in a concentration of about 0.2 mM. A 50  $\mu$ L portion of the coligand tricine (100 mg/mL) was added to 7 mL of the peptide solution, followed by  $\text{SnCl}_2$  and generator eluate  $[^{99\text{m}}\text{TcO}_4]^-$ , resulting in a final peptide concentration of about 10  $\mu$ M. Incubation at room temperature for 60 min gives a quantitative yield (Fig. 2.6). The amount of peptide is probably small enough so that no further purification is required. Binding affinity is

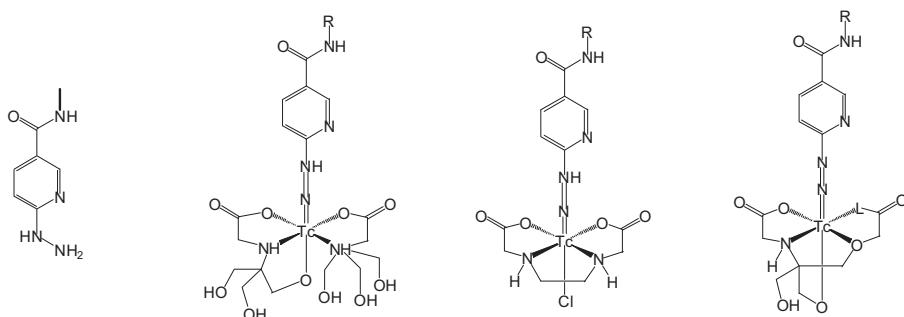
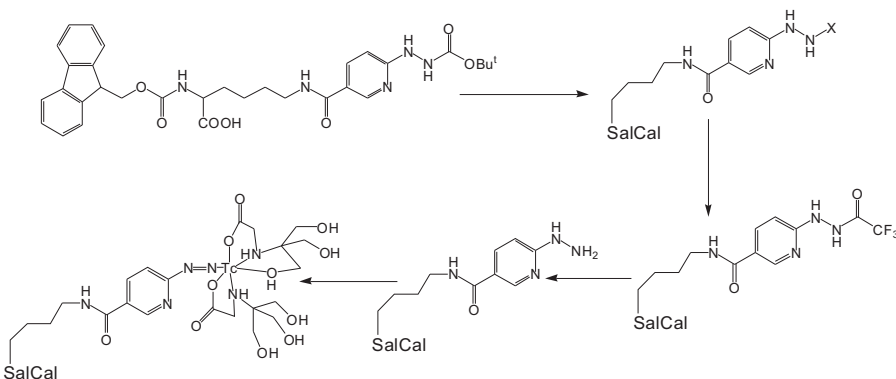


FIG. 2.5. Assumed structures of  $^{99\text{m}}\text{Tc}$  hynic complexes with different coligands.



*FIG. 2.6. Introduction of hynic to a peptide.*

retained, but since the biological behaviour is not of importance in this chapter, it is not discussed.

This very typical protocol is a good example of what can be achieved with hynic labelling. There are many alterations in the literature. It is possible to accelerate the labelling process at higher temperatures [2.56] or to alter the coligand, which represents the relatively ill defined part in the process [2.57–2.61]. The advantage of the hynic approach is, certainly, the well described protocols which can be performed for peptides and antibodies. The approach does, however, have some disadvantages which are, in particular, the unknown structure of the label and the difficulty or impossibility of transferring the conditions to labelling with  $^{188}\text{Re}$ . The former of these two points is especially problematic if a drug is to be introduced to the market, since the authorities normally require the exact composition and structure of the radiopharmaceutical, although this might be strange considering the minute quantities of compound administered to patients. Furthermore, the hynic labels can hardly be applied to targeting molecules other than peptides, proteins or nucleic acids. Smaller targeting molecules such as CNS receptor binders and pharmaceuticals, or small molecules such as amino acids or carbohydrates are hardly feasible due to the large complex size and/or its hydrophilicity.

In summary, the hynic approach represents an excellent strategy for amino acid or nucleic acid based macromolecules. Its protocol can readily be adapted to selected targeting vectors and is probably the method of choice for molecular imaging of gene expression. Its spectrum of application is narrow but excellent within this spectrum. The technique requires some skill in organic synthesis and precautions due to the sensitivity of the compounds. Labelling can be performed at high biomolecule dilution and might often not even require purification or separation from the cold peptide.

### 2.3.4. Labelling with ‘umbrella’-type Tc(III) cores

Complexes with technetium in the oxidation state +III are the focus of a more recent approach. The chemistry of technetium in this valency is relatively well developed but it has scarcely been used for the labelling of biomolecules [2.62]. As most of the other synthons, there is no aqua-ion available for technetium, but it was speculated that Tc(III) is the only form in which an aqua-ion might exist. This has not been confirmed so far, but it is still a challenge to prove or disprove its existence.

Correspondingly, if technetium is reduced to the oxidation state +III, it must be intermediately stabilized by a ligand prior to trans-metallation to the targeting molecule or the final complex. For stabilization, a tetradeinate ‘umbrella’ type  $\text{NS}_3$  ligand is typically used, which yields a synthon with one position available for conjugation to the biomolecule or to an additional ligand for technetium essential radiopharmaceuticals. The method is also referred to as the ‘4+1’ approach and its principle is outlined in Fig. 2.7 [2.63].

As in the sections before, one typical example is discussed in detail to give representative labelling conditions useful for potential applications. It should be noted at this point that the final radiolabels are relatively lipophilic and, correspondingly, the approach is convenient for, for example, CNS receptor ligands or fatty acids. A recent paper describes the labelling of this latter class of biomolecules. Fatty acids are important in the context of myocardial imaging via fatty acid metabolism [2.64]. One of the most convenient monodentate ligands for the ‘4+1’ approach are isocyanides although others such as phosphines or thioethers have been introduced as well. Since isocyanides tend to be volatile and air sensitive, they are best stabilized via coordination to a metal centre such as Cu(I). This method has been employed for a long time in the Cardiolite® kit. In the example that follows, this method has been applied as well.

*Example.* A typical labelling procedure is as follows. As a direct precursor, the Tc(III)-EDTA complex is prepared by incubating 500  $\mu\text{l}$  of generator eluate with  $\text{SnCl}_2$  in the presence of 1 mg of EDTA for 20 min at 37°C. This reconstitutes the Tc(III)-EDTA complex quantitatively. For the preparation of the

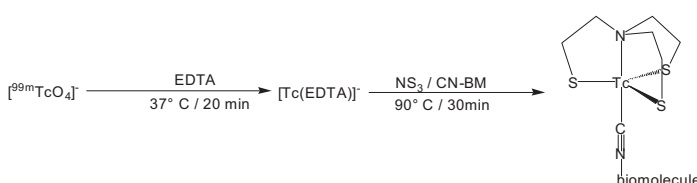


FIG. 2.7. Synthetic scheme for the preparation of Tc(III) ‘umbrella’-type complexes.

final complex, 300 µg of the NS<sub>3</sub> umbrella ligand in water and 50 µg of the Cu(I) complex of the fatty acid isocyanide complex in *n*-propanol is added and the mixture kept at 90°C for 30 min. Further steps follow but are biomolecule specific and do not need to be considered here. Purification is required since yields range from 50 to 80%. The complex was structurally characterized as its rhenium analogue. The stability of the fatty acid radioconjugate showed no decomposition over 12 h.

This protocol is a good example of the application of the ‘4+1’ principle. As outlined earlier, the complexes are rather lipophilic and the major range of application is CNS receptor ligands. A number of corresponding papers appeared in the literature together with thorough structural and chemical characterizations of the compounds [2.65–2.67].

The ‘4+1’ radiolabelling strategy has potential for alterations. The biomolecule, for instance, (here the fatty acid) can be pendent to the monodentate or to the tetridentate ligand, although the introduction in the latter case might generate a chiral carbon. The donors can be varied as well, although phosphines have the problem of sometimes being rather bulky co-substituents. A strong point in favour of the ‘4+1’ approach is definitely the characterization of the radiolabel. Disadvantages are lipophilicity, the sensitivity of the NS<sub>3</sub> trithiol ligand and, sometimes, solubility concerns. The building block is relatively small in size, which predestines its application in combination with smaller biomolecules. The organic syntheses are rather demanding, and the isocyanide generation and chemistry not routine. However, once in the field, the approach represents a very useful strategy for radiopharmaceutical chemistry and also has the potential for in depth fundamental investigations. Last but not least, the chemistry can be adapted with minor changes to <sup>188</sup>Re, a most important point if cancer therapy with radionuclides is in mind [2.68, 2.69].

### 2.3.5. Labelling with the [Tc(CO)<sub>3</sub>]<sup>+</sup> core

The last of the novel building blocks is the organometallic [<sup>99m</sup>Tc(CO)<sub>3</sub>]<sup>+</sup> core. It represents a building block for the labelling of biomolecules since it contains three fixed CO ligands, comparable to the ‘O’ in [Tc=O]<sup>3+</sup> or the ‘N’ in [Tc≡N]<sup>2+</sup> invariant coligands. In addition, three water molecules are bound to the remaining coordination sites which, can be exchanged by other biomolecule attached chelators for labelling targeting molecules, or by simple ligands for the preparation of technetium essential radiopharmaceuticals. The immediate precursor [<sup>99m</sup>Tc(OH<sub>2</sub>)<sub>3</sub>(CO)<sub>3</sub>]<sup>+</sup> can be prepared by homemade kits or is available commercially [2.70–2.72]. Several reviews have discussed the methodology comprehensively [2.12, 2.13, 2.73, 2.74]. The approach is of broad applicability and many biomolecules have been labelled with the [<sup>99m</sup>Tc(CO)<sub>3</sub>]<sup>+</sup> core. Among

these are peptides [2.75–2.77], antibodies [2.78], glucose [2.79–2.81], CNS receptor ligands [2.82] and many small molecules [2.83, 2.84]. Since some of the complexes are knowingly fluorescent, a combination of both fluorescence and radiodetection is possible [2.85]. The principle of the precursor preparation is given in Fig. 2.8 and is discussed below.

*Example.* Since it has some similarity to the example discussed in Section 2.2.3, the labelling of a peptide to guide radionuclides to the formyl peptide receptor and comprising a single amino acid chelator will be described.  $\alpha$ -Fmoc protected lysine was derivatized at the  $\epsilon$ -N with two quinoline moieties to obtain a tridentate neutral  $N_3$  ligand. This derivative can be conveniently integrated into the solid phase peptide synthesis of essentially any biomolecule. The corresponding rhenium complex is strongly fluorescent and its biological pathway on the cellular level can be studied with fluorescence microscopy in order to assess its functionality. At a later stage, the  $^{99m}$ Tc analogue can be used for diagnostic purposes [2.86]. After preparation of the precursor, labelling at high peptide dilution was quantitative after 30 min at  $98^\circ\text{C}$ , or at higher concentration at room temperature. The compound is stable in serum for at least 24 h. The procedure is shown in Fig. 2.9.

The advantages and disadvantages of the  $[\text{Tc}(\text{CO})_3]^+$  approach have been discussed in more detail [2.87, 2.88]. A major advantage of labelling with the  $[\text{<sup>99m</sup>Tc}(\text{CO})_3]^+$  core is the very wide variety of ligands which bind very efficiently to Tc(I). Complex stabilities are governed by kinetic stability or inertness. The complexes are all highly robust and do not, in general, decompose in serum or *in vivo*. Many different ligands have been exploited. More uncommon ones are hydrides [2.89], carboranes [2.80] and cyclopentadienyl [2.90]. Many combinations of monodentate, bidentate and tridentate ligands are possible but tridentate ones turned out to be the most versatile [2.91]. Labelling can be

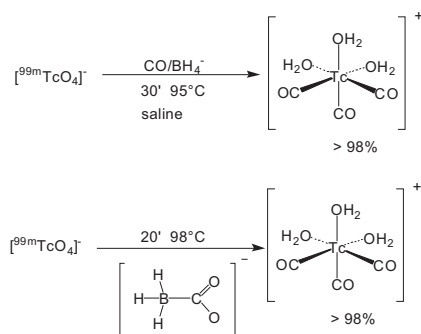


FIG. 2.8. Synthetic scheme for the preparation of the  $[\text{<sup>99m</sup>Tc}(\text{CO})_3]^+$  core.

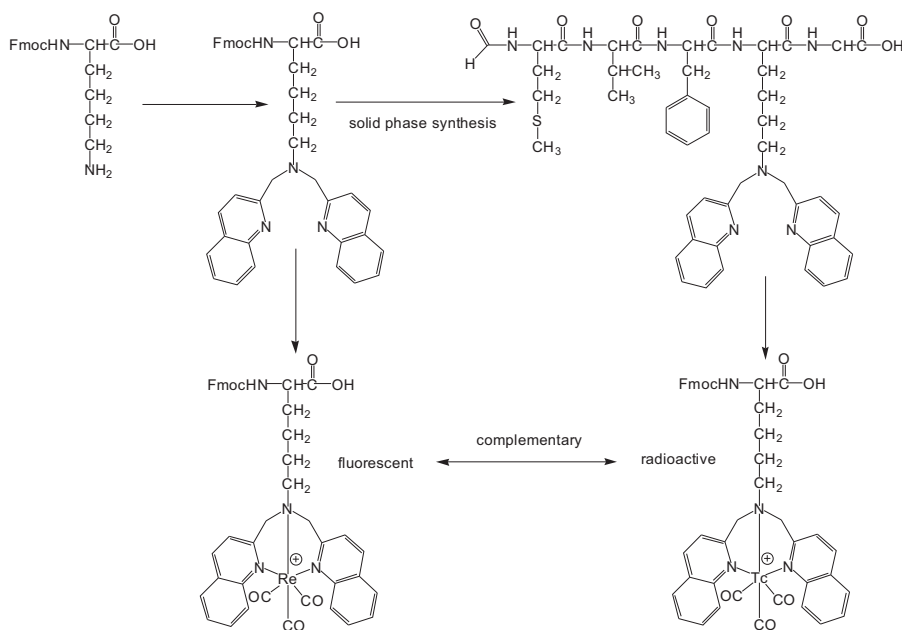


FIG. 2.9. Labelling of a peptide for fluorescent and radioactive imaging.

performed at low biomolecule concentration but heating is required in order to achieve quantitative labelling at micromolar concentrations. Here, the advantage of kinetic stability might turn into a disadvantage. The complexes tend to be lipophilic, which is a disadvantage when attempting labelling of peptides, for instance. On the other hand, newer work describes very hydrophilic complexes as well [2.84]. If the biomolecules are not sensitive towards reducing conditions, the preparation of the  $[^{99m}\text{Tc}(\text{CO})_3]^+$  core and labelling of the biomolecule can be performed in one single vial.

The approach can be adapted to  $^{188}\text{Re}$  chemistry as well. A number of studies with this analogue have been published. The conditions are slightly different, probably due to the decreased redox potential of rhenium, and an excellent procedure has recently been published [2.92].

In summary, as well as the other preceding cores,  $[^{99m}\text{Tc}(\text{CO})_3]^+$  is a very versatile building block and can be applied to a very broad variety of biomolecules. In addition to investigations towards novel radiopharmaceuticals, it has the inherent potential for relevant fundamental investigations, important not only for  $^{99m}\text{Tc}$  but also for the chemistry of other transition metals.

## 2.4. SUMMARY AND CONCLUSIONS

As discussed above, several versatile labelling procedures are available, well developed and ready to be applied for many biomolecules. As is usual in chemistry, entry into a new (labelling) method might require experience but the available labelling methods are ‘stable’ and tolerate altering conditions reasonably well. There is no preferred strategy but it should be emphasized that the selection of a particular biomolecule should be followed by the suitable labelling method and not vice versa. The labelling method should be a tool for aiming at the development of new radiopharmaceuticals, comparable to coupling methods of bifunctional chelators. The approaches introduced above, more or less, fulfil this role. Since more than one of the techniques is feasible for selected targeting biomolecules, it is of the utmost importance to compare the behaviour of the respective biomolecules conjugated to different labels. This has scarcely been done but has been at the centre of a recent coordinated research project supported by the IAEA.

Since radiopharmaceutical chemistry is basically the driving force for technetium chemistry, it is important to develop new building blocks. In the realm of technetium chemistry, there are still many possibilities for developing new cores and for exploring their respective coordination or organometallic chemistry. Clearly, research must proceed in a direction in which the new cores overcome the disadvantages of the old ones.

In conclusion, the development of versatile labelling methods is in our hands. The fact that very few new radiopharmaceuticals have emerged over the last decade is probably not a problem of chemistry or biology, but rather has its origin in the requirements imposed by the market, companies or regulatory authorities. The search has to go on, since the basic scientific conditions are very good and will ultimately lead to significant contributions to public health care.

## REFERENCES TO CHAPTER 2

- [2.1] YANG, D.J., KIM, E.E., INOUE, T., Targeted molecular imaging in oncology, *Ann. Nucl. Med.* **20** (2006) 1–11.
- [2.2] TIAN, X.B., et al., Imaging oncogene expression, *Ann. NY. Acad. Sci.* **1002** (2003) 165–188.
- [2.3] WICKSTROM, E., et al., Oncogene mRNA imaging with Tc-99m-chelator-PNA-peptides, *Russ. Chem. Bull.* **51** (2002) 1083–1099.
- [2.4] THAKUR, M.L., New radiopharmaceuticals in oncologic diagnosis and therapy, *Cancer Biother. Radiopharm.* **18** (2003) 276–276.

- [2.5] TOP, S., et al., Selective estrogen-receptor modulators (SERMs) in the cyclopentadienylrhenium tricarbonyl series: Synthesis and biological behaviour, *ChemBioChem* **5** (2004) 1104–1113.
- [2.6] TOP, S., et al., Studies on organometallic selective estrogen receptor modulators (SERMs). Dual activity in the hydroxy-ferrocifen series, *J. Organomet. Chem.* **637–639** (2001) 500–506.
- [2.7] DILWORTH, J.R., PARROTT, S.J., The biomedical chemistry of technetium and rhenium, *Chem. Soc. Rev.* **27** (1998) 43–55.
- [2.8] ALBERTO, R., ABRAM, U., (VERTES, A., NAGY, S., KLENCSAR, Z., Eds), Nuclear Chemistry, Kluwer Academic Publishers, Dordrecht (2003) 211–256.
- [2.9] MAECKE, H.R., EISENHUT, M., Technetium complexes as radiopharmaceuticals, *Bioinorg. Chem.* **2** (1995) 1079–1092.
- [2.10] MEASE, R.C., LAMBERT, C., Newer methods of labeling diagnostic agents with Tc-99m, *Semin. Nucl. Med.* **31** (2001) 278–285.
- [2.11] SCHWOCHAU, K., Technetium — Chemistry and Radiopharmaceutical Applications, Wiley-VCH, Weinheim, Germany (2000).
- [2.12] BANERJEE, S.R., et al., New directions in the coordination chemistry of Tc-99m: A reflection on technetium core structures and a strategy for new chelate design, *Nucl. Med. Biol.* **32** (2005) 1–20.
- [2.13] BLOWER, P., Towards molecular imaging and treatment of disease with radionuclides: The role of inorganic chemistry, *Dalton Trans.* (2006) 1705–1711.
- [2.14] WEINER, R.E., THAKUR, M.L., Radiolabeled peptides in oncology — Role in diagnosis and treatment, *Biodrugs* **19** (2005) 145–163.
- [2.15] MEEGALLA, S., et al., Tc-99m-labeled tropanes as dopamine transporter imaging agents, *Bioconjug. Chem.* **7** (1996) 421–429.
- [2.16] MEEGALLA, S.K., et al., Synthesis and characterization of technetium-99m-labeled tropanes as dopamine transporter-imaging agents, *J. Med. Chem.* **40** (1997) 9–17.
- [2.17] KUNG, M.P., et al., [Tc-99m]TRODAT-1: A novel technetium-99m complex as a dopamine transporter imaging agent, *Eur. J. Nucl. Med.* **24** (1997) 372–380.
- [2.18] KUNG, H.F., KUNG, M.P., CHOI, S.R., Radiopharmaceuticals for single-photon emission computed tomography brain imaging, *Semin. Nucl. Med.* **33** (2003) 2–13.
- [2.19] KUNG, H.F., Development of Tc-99m labeled tropanes: TRODAT-1, as a dopamine transporter imaging agent, *Nucl. Med. Biol.* **28** (2001) 505–508.
- [2.20] FRITZBERG, A.R., KASINA, S., ESHIMA, D., JOHNSON, D.L., Synthesis and biological evaluation of Tc-99m Mag3 as a Hippuran replacement, *J. Nucl. Med.* **27** (1986) 111–116.
- [2.21] BLOK, D., et al., New chelation strategy allows for quick and clean Tc-99m-labeling of synthetic peptides, *Nucl. Med. Biol.* **31** (2004) 815–820.
- [2.22] BORMANS, G., et al., Synthesis and biological characteristics of the 4 stereoisomers of Tc-99M-N,N'-bis-(mercaptoacetyl)-2,3-diaminopropanoate, *Nucl. Med. Biol.* **17** (1990) 499–506.
- [2.23] POLYAKOV, V., et al., Novel tat-peptide chelates for direct transduction of technetium-99m and rhenium into human cells for imaging and radiotherapy, *Bioconjug. Chem.* **11** (2000) 762–771.

- [2.24] FRIEBE, M., et al., [99mTc]oxotechnetium(V) complexes of amine-amide-dithiol chelates with dialkylaminoalkyl substituents as potential diagnostic probes for malignant melanoma, *J. Med. Chem.* **44** (2001) 3132–3140.
- [2.25] SMITH, C.J., et al., Radiochemical investigations of Tc-99m-N3S-X-BBN[7-14]NH<sub>2</sub>: An in vitro/in vivo structure-activity relationship study where X = 0-, 3-, 5-, 8-, and 11-carbon tethering moieties, *Bioconjug. Chem.* **14** (2003) 93–102.
- [2.26] NOLL, B., JOHANNSEN, B., SPIES, H., Sources of radiochemical impurities in the Tc-99M/S-unprotected Mag(3) system, *Nucl. Med. Biol.* **22** (1995) 1057–1062.
- [2.27] GUHLKE, S., et al., Re-188- and Tc-99m-MAG(3) as prosthetic groups for labeling amines and peptides: Approaches with pre- and postconjugate labeling, *Nucl. Med. Biol.* **25** (1998) 621–631.
- [2.28] ZAMORA, P.O., MAREK, M.J., KNAPP, F.F. (RUSS), Jr., Preparation of 188-Re-RC-160 somatostatin analog: A peptide for local/regional radiotherapy, *Appl. Radiat. Isotop.* **48** (1997) 305–309.
- [2.29] ZHANG, Y.-M., LIU, N., ZHU, Z.-H., RUSCKOWSKI, M., HNATOWICH, K.J., Influence of different chelators (HYNIC, MAG3 and DTPA) on tumor cell accumulation and mouse biodistribution of technetium-99m labeled to antisense DNA, *Eur. J. Nucl. Med.* **27** (2000) 1700–1707.
- [2.30] THAKUR, M.L., et al., Tc-99m-PNA-peptide: Imaging oncogene expression in breast lesions, *J. Nucl. Med.* **43** (2002) 124P–124P.
- [2.31] HNATOWICH, D.J., Pharmacokinetics of 99mTc-labeled orligonucleotides, *Q.J. Nucl. Med.* **40** (1996) 202–208.
- [2.32] HJELSTUEN, O.K., TONNESEN, H.H., BREMER, P.O., VERBRUGGEN, A.M., 3'-Tc-99m-labeling and biodistribution of a CAPL antisense oligodeoxynucleotide, *Nucl. Med. Biol.* **25** (1998) 651–657.
- [2.33] HJELSTUEN, O.K., MAELANDSMO, G.M., TONNESEN, H.H., BREMMER, P.O., VERBRUGGEN, A.M., Hybridization of Tc-99(m)-labelled oligodeoxynucleotide to CAPL RNA, *Nucl. Med. Commun.* **19** (1998) 803–812.
- [2.34] QIN, G.M., et al., Molecular imaging of atherosclerotic plaques with technetium-99m-labelled antisense oligonucleotides, *Eur. J. Nucl. Med. Mol. Imaging* **32** (2005) 6–14.
- [2.35] FRANCESCONI, L.C., et al., Preparation and characterization of [(TcO)-Tc-99] apcitide: A technetium labeled peptide, *Inorg. Chem.* **43** (2004) 2867–2875.
- [2.36] PASQUALINI, R., DUATTI, A., Synthesis and characterization of the new neutral myocardial imaging agent [(Tcn)-Tc-99m(Noet)<sub>2</sub>] (Noet = N-ethyl-N-ethoxydithiocarbamato), *J. Chem. Soc. Chem. Commun.* (1992) 1354–1355.
- [2.37] PASQUALINI, R., et al., Bis(dithiocarbamato) nitrido Tc-99m radiopharmaceuticals: A class of neutral myocardial imaging agents, *J. Nucl. Med.* **35** (1994) 334–341.
- [2.38] BOLZATI, C., et al., Synthesis, characterization, and biological evaluation of neutral nitrido technetium(V) mixed ligand complexes containing dithiolates and aminodiphosphines. A novel system for linking technetium to biomolecules, *Bioconjug. Chem.* **15** (2004) 628–637.
- [2.39] GHEZZI, C., et al., Myocardial kinetics of tcn-noet — a neutral lipophilic complex tracer of regional myocardial blood-flow, *J. Nucl. Med.* **36** (1995) 1069–1077.

- [2.40] BOLZATI, C., et al., Chemistry of the strong electrophilic metal fragment [ $\text{Tc-99(N)(PXP)}$ ](2+) (PXP = diphosphine ligand). A novel tool for the selective labeling of small molecules, *J. Am. Chem. Soc.* **124** (2002) 11468–11479.
- [2.41] BOLZATI, C., et al., Synthesis, solution-state and solid-state structural characterization of monocationic nitrido heterocomplexes [ $\text{M(N)(DTC(PNP))}(+)$ ] ( $\text{M}=\text{Tc-99, Re}$ ; DTC = dithiocarbamate; PNP = heterodiphosphane), *Eur. J. Inorg. Chem.* (2004) 1902–1913.
- [2.42] BOLZATI, C., et al., The [ $\text{Tc-99m(N)(PNP)}$ ](2+) metal fragment: A technetium-nitrido synthon for use with biologically active molecules. The N-(2-methoxyphenyl)piperazyl-cysteine analogues as examples, *Bioconjug. Chem.* **14** (2003) 1231–1242.
- [2.43] BOLZATI, C., et al., The  $\text{Tc-99m}$  fragment [ $\text{Tc-99m(N)(PXP)}$ ](2+): A novel tool for high specific-activity labeling of biomolecules, *J. Nucl. Med.* **41** (2000) 248p–248p.
- [2.44] TISATO, F., et al., The crucial role of the diphosphine heteroatom X in the stereochemistry and stabilization of the substitution-inert [ $\text{M(N)(PXP)}$ ](2+) metal fragments ( $\text{M} = \text{Tc, Re}$ ; PXP = diphosphine ligand), *Inorg. Chem.* **43** (2004) 8617–8625.
- [2.45] BOSCHI, A., et al., Asymmetrical nitrido  $\text{Tc-99m}$  heterocomplexes as potential imaging agents for benzodiazepine receptors, *Bioconjug. Chem.* **14** (2003) 1279–1288.
- [2.46] KORDE, A., et al.,  $\text{Tc-99m}$ -labeling of colchicine using [ $\text{Tc-99m(CO)(3)(H}_2\text{O)(3)}(+)$  and [ $\text{Tc-99m}$  equivalent to N](2+) core for the preparation of potential tumor-targeting agents, *Bioorgan. Med. Chem.* **14** (2006) 793–799.
- [2.47] AGOSTINI, S., et al., The ( $\text{Tc(N)(PNp)}$ )(2+) metal fragment labeled cholecystokinin-8 (CCK8) peptide for CCK-2 receptors imaging: In vitro and in vivo studies, *J. Pept. Sci.* **13** (2007) 211–219.
- [2.48] HATADA, K., et al.,  $\text{Tc-99m-N-DBODC5}$ , a new myocardial perfusion imaging agent with rapid liver clearance: Comparison with  $\text{Tc-99m}$ -sestamibi and  $\text{Tc-99m}$ -tetrofosmin in rats, *J. Nucl. Med.* **45** (2004) 2095–2101.
- [2.49] ZHANG, J.B., WANG, X.B., TIAN, C.J., Synthesis and biodistribution of ( $\text{TcN}$ )- $\text{Tc-99m(PDTC)}$ (2) as a potential brain imaging agent, *J. Radioanal. Nucl. Chem.* **262** (2004) 505–507.
- [2.50] MALLIA, M.B., et al., A novel [ $\text{Tc-99m}$  equivalent to N](2+) complex of metronidazole xanthate as a potential agent for targeting hypoxia, *Bioorg. Med. Chem. Lett.* **15** (2005) 3398–3401.
- [2.51] MAECKE, H., Radiopeptides in imaging and targeted radiotherapy: Ligands, *Eur. J. Nucl. Med. Mol. Imaging* **31** (2004) S296–S296.
- [2.52] OKARVI, S.M., Peptide-based radiopharmaceuticals: Future tools for diagnostic imaging of cancers and other diseases (Vol. 24, p. 357, 2004), *Med. Res. Rev.* **24** (2004) 685–686.
- [2.53] LIU, S., EDWARDS, D.S.,  $99\text{mTc}$ -labeled small peptides as diagnostic radiopharmaceuticals, *Chem. Rev.* **99** (1999) 2235–2268.
- [2.54] FICHNA, J., JANECKA, A., Synthesis of target-specific radiolabeled peptides for diagnostic imaging, *Bioconjug. Chem.* **14** (2003) 3–17.

- [2.55] GREENLAND, W.E.P., HOWLAND, K., HARDY, J., FOGELMAN, I., BLOWER, P.J., Solid-phase synthesis of peptide radiopharmaceuticals using Fmoc-N-epsilon-(Hynic-Boc)-lysine, a technetium-binding amino acid: Application to Tc-99m-labeled salmon calcitonin, *J. Med. Chem.* **46** (2003) 1751–1757.
- [2.56] VON GUGGENBERG, E., et al., Tc-99m-labeling and in vitro and in vivo evaluation of HYNIC- and (N alpha-His)acetic acid-modified [D-Glu(1)]-minigastrin, *Bioconjug. Chem.* **15** (2004) 864–871.
- [2.57] KIM, Y.S., HE, Z.J., HSIEH, W.Y., LIU, S., A novel ternary ligand system useful for preparation of cationic Tc-99m-diazenido complexes and Tc-99m-labeling of small biomolecules, *Bioconjug. Chem.* **17** (2006) 473–484.
- [2.58] LIU, S., EDWARDS, D.S., HARRIS, A.R., A novel ternary ligand system for Tc-99m-labeling of hydrazino nicotinamide-modified biologically active molecules using imine-N-containing heterocycles as coligands, *Bioconjug. Chem.* **9** (1998) 583–595.
- [2.59] LIU, S., EDWARDS, D.S., HARRIS, A.R., HEMINWAY, S.J., BARRETT, J.A., Technetium complexes of a hydrazinonicotinamide-conjugated cyclic peptide and 2-hydrazinopyridine: Synthesis and characterization, *Inorg. Chem.* **38** (1999) 1326–1335.
- [2.60] DECRISTOFORO, C., MELENDEZ-ALAFORT, L., SOSABOWSKI, J.K., MATHER, S.J., 99mTc-HYNIC-[Tyr3]-octreotide for imaging somatostatin-receptor-positive tumors: Preclinical evalutaion and comparison with 111In-octreotide, *J. Nucl. Med.* **41** (2000) 1114–1119.
- [2.61] BANERJEE, S.R., et al., N,N-bis(2-mercaptoethyl)methylamine: A new coligand for Tc-99m labeling of hydrazinonicotinamide peptides, *Bioconjug. Chem.* **16** (2005) 885–902.
- [2.62] ALBERTO, R., (McCLEMENTY, J.A., MEER, T.S., Eds) *Compr. Coord. Chem. II*, Vol. 5, Elsevier Science, Amsterdam (2003) 127–271.
- [2.63] SPIES, H., GLASER, M., Synthesis and reactions of trigonal-bipyramidal rhenium and technetium complexes with a tripodal, tetridentate NS<sub>3</sub> ligand, *Inorg. Chim. Acta* **240** (1995) 465–478.
- [2.64] WALThER, M., et al., Synthesis and biological evaluation of a new type of (99m)Technetium-labeled fatty acid for myocardial metabolism imaging, *Bioconjug. Chem.* **18** (2007) 216–230.
- [2.65] SEIFERT, S., et al., Novel procedures for preparing Tc-99m(III) complexes with tetridentate/monodentate coordination of varying lipophilicity and adaptation to Re-188 analogues, *Bioconjug. Chem.* **15** (2004) 856–863.
- [2.66] DREWS, A., et al., Synthesis and biological evaluation of technetium(III) mixed-ligand complexes with high affinity for the cerebral 5-HT<sub>1A</sub> receptor and the alpha<sub>1</sub>-adrenergic receptor, *Nucl. Med. Biol.* **29** (2002) 389–398.
- [2.67] PIETZSCH, H.J., et al., Synthesis, characterization, and biological evaluation of technetium(III) complexes with tridentate/bidentate S,E,S/P,S coordination (E = O, N(CH<sub>3</sub>), S): A novel approach to robust technetium chelates suitable for linking the metal to biomolecules, *Bioconjug. Chem.* **14** (2003) 136–143.

- [2.68] SEIFERT, S., PIETZSCH, H.J., The Re-188(III)-EDTA complex — a multipurpose starting material for the preparation of relevant Re-188 complexes under mild conditions, *Appl. Radiat. Isotop.* **64** (2006) 223–227.
- [2.69] SCHILLER, E., et al., Mixed-ligand rhenium-188 complexes with tetradentate/monodentate NS3/P ('4+1') coordination: Relation of structure with antioxidation stability, *Bioconjug. Chem.* **16** (2005) 634–643.
- [2.70] ALBERTO, R., ORTNER, K., WHEATLEY, N., SCHIBLI, R., SCHUBIGER, A.P., Synthesis and properties of boranocarbonate: A convenient in situ CO source for the aqueous preparation of  $[^{99m}\text{Tc}(\text{OH}_2)_3(\text{CO})_3]^+$ , *J. Am. Chem. Soc.* **123** (2001) 3135–3136.
- [2.71] ALBERTO, R., (JAOUEN, G., Ed.), *Bioorganometallics*, Wiley-VCH, Weinheim, Germany (2006) 97–124.
- [2.72] ALBERTO, R., et al., A novel organometallic aqua complex of technetium for the labeling of biomolecules: Synthesis of  $[^{99m}\text{Tc}(\text{OH}_2)_3(\text{CO})_3]^+$  from  $[^{99m}\text{TcO}_4]^-$  in aqueous solution and its reaction with a bifunctional ligand, *J. Am. Chem. Soc.* **120** (1998) 7987–7988.
- [2.73] LIU, S., The role of coordination chemistry in the development of target-specific radiopharmaceuticals, *Chem. Soc. Rev.* **33** (2004) 445–461.
- [2.74] THOMPSON, K.H., ORVIG, C., Metal complexes in medicinal chemistry: New vistas and challenges in drug design, *Dalton Trans.* (2006) 761–764.
- [2.75] LA BELLA, R., et al., In vitro and in vivo evaluation of a Tc-99m(I)-labeled bombesin analogue for imaging of gastrin releasing peptide receptor-positive tumors, *Nucl. Med. Biol.* **29** (2002) 553–560.
- [2.76] VEERENDRA, B., et al., Synthesis, radiolabeling and in vitro GRP receptor targeting studies of ( $^{99m}$ Tc-Triaza-X-BBN[7-14]NH<sub>2</sub> (X = serylserylserine, glycylglycylglycine, glycylserylglycine, or beta alanine), *Synth. React. Inorg. Me.* **36** (2006) 481–491.
- [2.77] SMITH, C.J., et al., Radiochemical investigations of gastrin-releasing peptide receptor-specific [ $\text{Tc-99m}(X)(\text{CO})(3)\text{-Dpr-Ser-Ser-Ser-Gln-Trp-Ala-Val-Gly-His-Leu-Met-(NH}_2)$ ] in PC-3, tumor-bearing, rodent models: Syntheses, radiolabeling, and in vitro/in vivo studies where Dpr=2,3-diaminopropionic acid and X=H<sub>2</sub>O or P(CH<sub>2</sub>OH)(3), *Cancer Res.* **63** (2003) 4082–4088.
- [2.78] WAIBEL, R., et al., Stable one-step technetium-99m labeling of His-tagged recombinant proteins with a novel Tc(I)-carbonyl complex, *Nat. Biotechnol.* **17** (1999) 897–901.
- [2.79] FERREIRA, C.L., et al., Glucosamine conjugates of tricarbonylcyclopentadienyl rhenium(I) and technetium(I) cores, *Inorg. Chem.* **45** (2006) 6979–6987.
- [2.80] FERREIRA, C.L., et al. Carbohydrate-appended 3-hydroxy-4-pyridinone complexes of the  $[\text{M}(\text{CO})(3)]^+$  core (M Re, Tc-99m, Re-186), *Bioconjug. Chem.* **17** (2006) 1321–1329.
- [2.81] SCHIBLI, R., et al., Synthesis and in vitro characterization of organometallic rhenium and technetium glucose complexes against glut 1 and hexokinase, *Bioconjug. Chem.* **16** (2005) 105–112.

- [2.82] BERNARD, J., ORTNER, K., SPINGLER, B., PIETZSCH, H.J., ALBERTO, R., Aqueous synthesis of derivatized cyclopentadienyl complexes of technetium and rhenium directed toward radiopharmaceutical application, *Inorg. Chem.* **42** (2003) 1014–1022.
- [2.83] TZANOPPOULOU, S., et al., Synthesis, characterization, and biological evaluation of M(I)(CO)(3)(NNO) complexes (M = Re, Tc-99m) conjugated to 2-(4-aminophenyl)benzothiazole as potential breast cancer radiopharmaceuticals, *J. Med. Chem.* **49** (2006) 5408–5410.
- [2.84] LIU, Y., et al., Amino acids labeled with [99mTc(CO)3]<sup>+</sup> and recognized by the L-type amino acid transporter LAT1, *J. Am. Chem. Soc.* **128** (2006) 15996–15997.
- [2.85] WEI, L.H., BABICH, J.W., OUELLETTE, W., ZUBIETA, J., Developing the {M(CO)3}(+) core for fluorescence applications: Rhenium tricarbonyl core complexes with benzimidazole, quinoline, and tryptophan derivatives, *Inorg. Chem.* **45** (2006) 3057–3066.
- [2.86] STEPHENSON, K.A., et al., Bridging the gap between in vitro and in vivo imaging: Isostructural Re and Tc-99m complexes for correlating fluorescence and radioimaging studies, *J. Am. Chem. Soc.* **126** (2004) 8598–8599.
- [2.87] ALBERTO, R., [Tc(CO)(3)](+) chemistry: A promising new concept for SPET? *Eur. J. Nucl. Med. Mol. Imaging* **30** (2003) 1299–1302.
- [2.88] WELCH, M., [Tc(CO)(3)](+) chemistry: A promising new concept for SPET? *Eur. J. Nucl. Med. Mol. I.* **30** (2003) 1302–1304.
- [2.89] GARCIA, R., et al., Re and Tc complexes containing B-H···M agostic interactions as building blocks for the design of radiopharmaceuticals, *J. Am. Chem. Soc.* **122** (2000) 11240–11241.
- [2.90] WALD, J., ALBERTO, R., ORTNER, K., CANDREIA, L., Aqueous one-pot synthesis of derivatized cyclopentadienyl-tricarbonyl complexes of 99mTc with an in situ CO source: Application to a serotonergic receptor ligand, *Angew. Chem. Int. Ed.* **40** (2001) 3062–3066.
- [2.91] ALBERTO, R., PAK, J.K., VAN STAVEREN, D., MUNDWILER, S., BENNY, P., Mono-, bi-, or tridentate ligands? The labeling of peptides with Tc-99m-carbonyls, *Biopolymers* **76** (2004) 324–333.
- [2.92] PARK, S.H., SEIFERT, S., PIETZSCH, H.J., Novel and efficient preparation of precursor [Re-188(OH<sub>2</sub>(3)(CO)(3)](+) for the labeling of biomolecules, *Bioconjug. Chem.* **17** (2006) 223–225.

## Chapter 3

# APPLICATION OF CLICK CHEMISTRY TO THE DESIGN OF LIGAND SYSTEMS AND FUNCTIONALIZATION OF BIOMOLECULES SUITABLE FOR RADIOLABELLING WITH THE TECHNETIUM AND RHENIUM TRICARBONYL CORE

T. L. MINDT, H. STRUTHERS, R. SCHIBLI

Centre for Radiopharmaceutical Sciences,

Paul Scherrer Institute,

Villigen, Switzerland

### Abstract

As the premier example of a click reaction, the Cu(I) catalysed cycloaddition of azides and terminal alkynes has found tremendous resonance throughout the scientific community. The reaction is characterized by mild reaction conditions, selectivity and the comparatively straightforward preparation of alkyne and azide building blocks. In addition to the numerous applications as a stable link between two chemical/biological components, triazole products are beginning to be recognized as ligands for a wide range of different metals. Combining the coordinative properties of triazole products and favourable reaction conditions, efficient triazole containing chelators for the  $M(CO)_3$  cores of technetium and rhenium can be readily synthesized and incorporated into molecules of diagnostic and therapeutic interest in a single step. In situ radiolabelling with technetium rapidly provides access to a set of radiolabelled derivatives for in vitro screening, and the viability of the approach has been demonstrated in vivo by comparing radioconjugates labelled with the tricarbonyl core via structurally analogous imidazole containing and triazole containing chelating systems.

### 3.1. INTRODUCTION

The synthesis of 1,2,3-triazoles by the 1,3-dipolar cycloaddition of azides and alkynes is known as the Huisgen cyclization [3.1]. Although the reaction was first reported decades ago, it did not find widespread application, largely due to the formation of mixtures of 1,4-substituted and 1,5-substituted isomers (Fig. 3.1, path A). In 2002, the Sharpless and Meldal groups reported the discovery of the Cu(I) catalysed version of Huisgen's cycloaddition, which selectively and efficiently provides 1,4-di-substituted 1,2,3-triazoles under mild reaction conditions (Fig. 3.1, path B) [3.2–3.6]. The copper catalysed reaction has emerged as a transformation of such practicality and broad scope, that it has

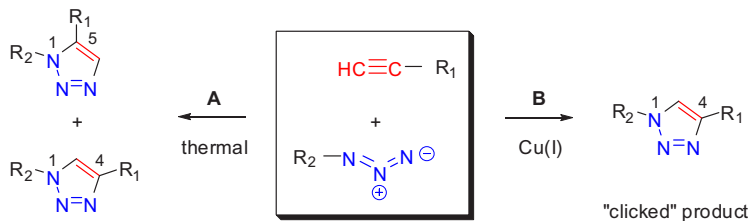


*FIG. 3.1. Huisgen cycloaddition of terminal alkynes and azides under thermal reaction conditions yields mixtures of isomers (path A) while Cu(I) catalysis results in exclusive formation of 1,4-di-substituted 1,2,3-triazoles (path B). R<sub>1</sub> and R<sub>2</sub> represent two chemical/biochemical components to be connected via a stable triazole linker.*

become the premier example of a click reaction and is synonymous with ‘click chemistry’ [3.7].

Click reactions are chemical transformations that are particularly valuable because they are efficient, selective and devoid of side reactions. In addition, they proceed under benign reaction conditions and require only simple workup and purification procedures. These characteristics enable the rapid creation of molecular diversity through the use of modular building blocks and, thus, may accelerate the process of discovery and optimization of new compounds and drugs. Not surprisingly, click chemistry has found tremendous resonance in many different fields of chemistry, biochemistry and material sciences, which is reflected by the numerous accounts of click chemistry published since the discovery of the Cu(I) catalysed Huisgen cyclization. The unique orthogonal reactivity of alkynes and azides, and the mild reaction conditions of cycloaddition are well suited for the modification of a wide variety of (bio)molecules. For click applications, alkynes and azides can be readily incorporated into such molecules by standard synthetic transformations or bioengineering [3.8–3.10]. In addition, 1,2,3-triazole forms an extraordinarily stable link between two chemical/biochemical components. The contemporary interest in click chemistry [3.11, 3.12] is likely to result in the development of a large pool of novel compounds or ‘clickable’ building blocks, some of which may have the potential to be employed in radiopharmacy. In fact, the Cu(I) catalysed cycloaddition of azides and alkynes has already found applications in molecular imaging, namely in positron emission tomography (PET) [3.13, 3.14] and fluorescence imaging [3.15, 3.16]. However, until recently [3.17], the application of click chemistry in inorganic and technetium chemistry had not been explored.

### 3.2. DESIGN OF CLICK CHELATORS FOR THE $^{99m}\text{Tc}$ TRICARBONYL CORE

Numerous bifunctional chelating systems (e.g. based on amino acid scaffolds such as cysteine, lysine and histidine) have been designed and reported [3.18] for the organometallic precursor [ $^{99m}\text{Tc}(\text{H}_2\text{O})_3(\text{CO})_3$ ]<sup>+</sup> [3.19]. However, the preparation of such chelators generally requires multistep syntheses, and their incorporation into biomolecules often lacks efficiency and is further complicated by cross-reactivity with other functional groups present. To expedite radiotracer development, the design of novel strategies that reduce the complexity of the synthesis of potent metal chelators and improve the efficiency of their incorporation into various classes of biologically relevant molecules is paramount.

1,4-di-substituted 1,2,3-triazoles share structural, electronic and, thus, coordinative features with 1,4-di-substituted imidazoles (Fig. 3.2). For example, both heterocycles are known to be extraordinarily good monodentate ligands, particularly for organometallic cores of Mo, Tc and Re [3.20–3.22]. This suggests that imidazole containing chelating systems could be modified by replacing the heterocycle with a 1,2,3-triazole via click chemistry. Surprisingly few 1,2,3-triazole chelators, obtained by click chemistry, have been reported in the literature and of those that have, the majority are used in transition metal catalysis [3.23–3.27]. Click chemistry has not yet been thoroughly explored for the design of metal chelating systems and the functionalization of biomolecules.

1,2,3-triazole containing chelating systems can be assembled and incorporated into (bio)molecules in two ways. In the first example, an azide functionalized biomolecule is reacted with an appropriate alkyne precursor to provide chelating systems which coordinate to the  $^{99m}\text{Tc}$ -tricarbonyl core via N(3)

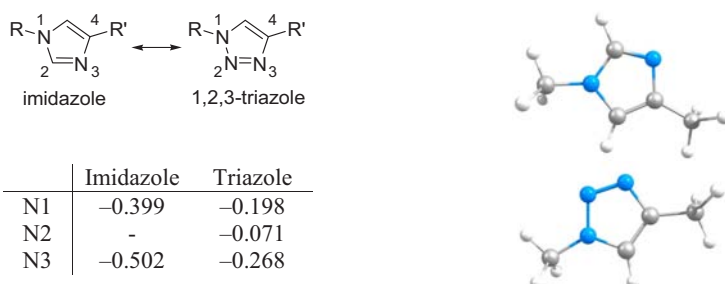


*FIG. 3.2. Structural similarity of imidazole and 1,2,3-triazole, and DFT calculated optimized geometries and natural population analyses of 1,4-dimethyl imidazole and 1,4-dimethyl 1,2,3-triazole.*

of the triazole heterocycle (Fig. 3.3(a)). Alternatively, a click reaction of an azide precursor and a biomolecule equipped with an alkyne functionality results in the formation of chelators that form complexes by coordination of N(2) (Fig. 3.3(b)). DFT calculations indicate that the electron density at N(3) of 1,4-di-substituted 1,2,3-triazoles is notably higher than at N(2) (Fig. 3.2). Coordination via N(3) is, therefore, favoured as proven in radiolabelling experiments (Fig. 3.4).

By employing appropriate click building blocks, one can readily design a large variety of novel, polydentate metal chelators tailor-made and ready for radiolabelling with the  $[^{99m}\text{Tc}(\text{H}_2\text{O})_3(\text{CO})_3]^+$  precursor and varying the ligand concentration. The most elegant feature of the ‘click-to-chelate’ strategy is the simultaneous synthesis and incorporation of the chelating system into a functionalized biomolecule. In addition, the orthogonal reactivity of azides and alkynes enables the functionalization via click chemistry, without protecting the functional groups ubiquitously present in biomolecules.

The potency of chelating systems suitable for the tricarbonyl core can be assessed by labelling with the  $[^{99m}\text{Tc}(\text{H}_2\text{O})_3(\text{CO})_3]^+$  precursor and varying the ligand concentration. This usually gives rise to step–sigmoid curves and allows the determination of EC<sub>50</sub> values (ligand concentration necessary to achieve 50% labelling yield) as a direct measurement of the chelating efficiencies of the ligand systems. In order to evaluate the structural isomers of click chelators, model chelators **1** and **2** were synthesized and their labelling efficiencies compared with structurally related N( $\tau$ )-derivatized histidine (Me-His) [3.21, 3.28, 3.29], an extraordinarily efficient chelating system for the organometallic  $^{99m}\text{Tc}$  tricarbonyl core (Fig. 3.4). Click chelator **1**, which coordinates via N(3) of the triazole, exhibits an EC<sub>50</sub> value in the sub-micromolar range. This value is comparable to that of Me-His (EC<sub>50</sub> =  $\sim 10^{-7}$  M), demonstrating the potency of the novel triazole ligand. On the other hand, the value obtained for ligand **2** is approximately two orders of magnitude higher (EC<sub>50</sub> =  $\sim 10^{-5}$  M). These findings are in agreement

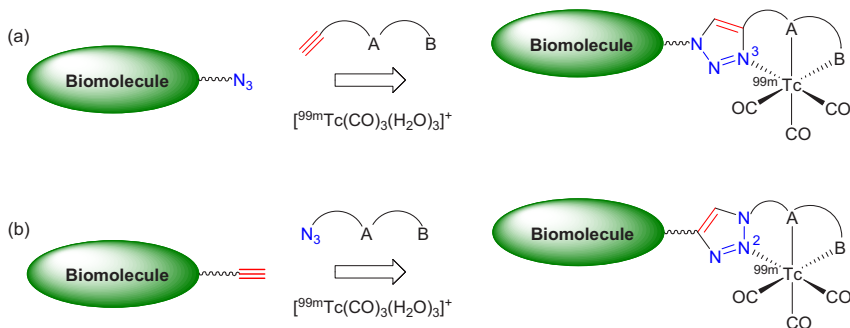


*FIG. 3.3. Schematic drawing of the synthesis, incorporation into functionalized biomolecules and radiolabelling of triazole containing chelators.*

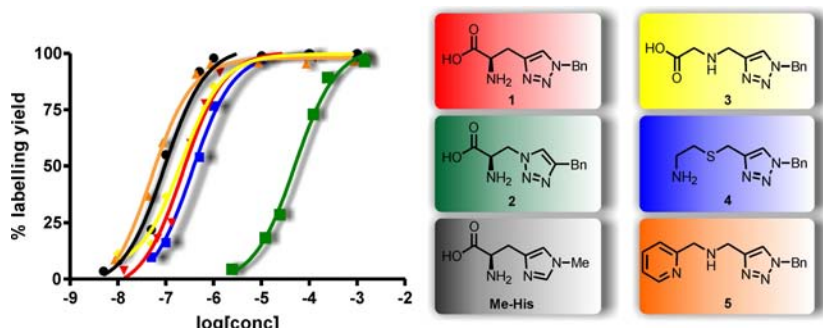


FIG. 3.4. Radiolabelling yields as a function of ligand concentration ( $10^{-3}$ – $10^{-8}$  M).

with the coordination mode proposed based on density functional theory (DFT) calculations.

### 3.3. STRUCTURAL DIVERSITY OF CLICK CHELATING SYSTEMS

In combination with small biomolecules, the physicochemical properties of metal complexes, such as size, overall charge and lipophilicity, can affect the biodistribution of the conjugates *in vivo*. Not only can these factors influence initial targeting, they may also affect the rate and route of excretion of the complex and/or its metabolites. By varying the metal chelating system, the impact of conjugation of a biomolecule to a metal can be optimized.

As described above, coordination of triazole containing chelating systems via N(3) is more favourable than via N(2). Such tridentate chelating systems can be prepared from the reaction of functionalized alkynes with any azide containing molecule. Suitable alkynes can be readily synthesized from propargyl bromide or propargyl amine, or are commercially available. Reaction with an organic azide derivative yields click chelators **1** and **3–6**, with different sizes and structures (Fig. 3.5). Reaction of the triazole ligand systems with  $M(CO)_3$  ( $M = {}^{99m}Tc$ , Re) gives rise to complexes of diverse structures and different overall charge.

Rhenium tricarbonyl complexes can be readily prepared under stoichiometric conditions. The expected tridentate coordination of the ligands and pseudo-octahedral coordination of the metal is confirmed by X ray structure determination (Fig. 3.6). The labelling efficiencies of ligands **1–6** were assessed with  $[{}^{99m}Tc(H_2O)_3(CO)_3]^+$  and were shown above (Fig. 3.4). While ligands **1–5** are all excellent chelators for the  $M(CO)_3$  core, malonate derivative **6** required a surprisingly high ligand concentration for yet unknown reasons ( $10^{-2}$  M).

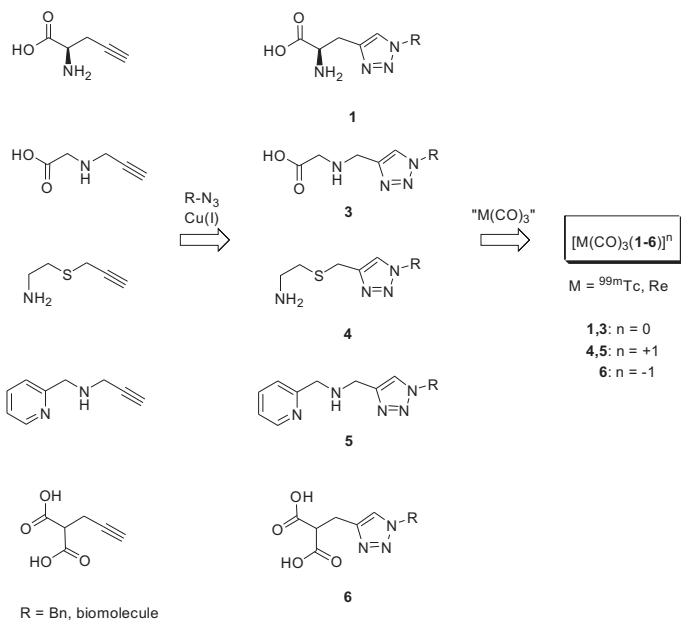


FIG. 3.5. Synthesis of diverse tridentate triazole containing ligands and complex formation with the  $M(CO)_3$  core ( $M = {}^{99m}Tc$ ,  $Re$ ).

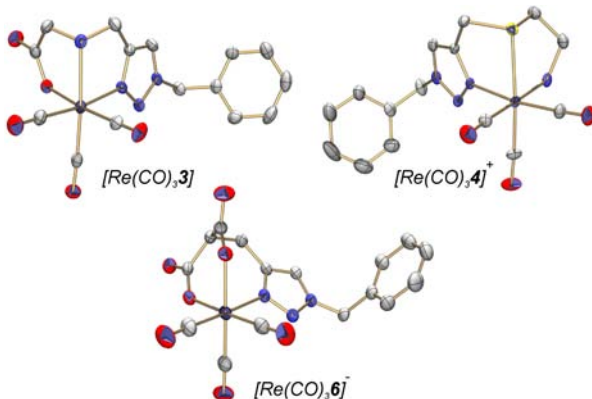


FIG. 3.6. ORTEP-3 representations of  $Re$  complexes with thermal ellipsoids shown at 50% probability.

The ‘click-to-chelate’ approach also offers the possibility of incorporating amino acid click chelators or precursors thereof into the backbone of peptides [3.30]. For example, installation of azido alanine into a peptide allows the assembly and incorporation of triazole containing ligand systems (e.g. 7) for

subsequent  $^{99m}\text{Tc}$  labelling (Fig. 3.7(a)). Alkyne containing precursors can also be incorporated into peptides and provide triazole chelators when reacted with an organic azide. Lysine derivatives functionalized at N( $\epsilon$ ) provide an opportunity for the installation of potent tridentate triazole chelating systems able to coordinate to the  $^{99m}\text{Tc}(\text{CO})_3$  core via N(3) of the triazole heterocycle (Fig. 3.7(b)).

$\text{N}(\tau)\text{-bis-triazole compound } \mathbf{8}$  (Fig. 3.7(b)) is the first example of a ‘double click’ ligand system for the  $^{99m}\text{Tc}(\text{CO})_3$  core. While chelating systems containing multiple triazole heterocycles have been reported [3.23], such an approach has not been applied to the functionalization of biomolecules. Related chelators **9** and **10**, which form stable cationic complexes with  $[\text{M}(\text{CO})_3(\text{H}_2\text{O})_3]^+$ , are readily synthesized from bis-propargyl derivatives (Fig. 3.8). The crystal structure of  $[\text{Re}(\text{CO})_3(\mathbf{10})]^+$  is shown in Fig. 3.9.

### 3.4. ONE-POT PROTOCOLS

While the clicked triazole products predominantly represent a class of extraordinarily good chelators, the individual alkyne and azide substrates do not form well defined complexes with the  $[^{99m}\text{Tc}(\text{OH}_2)_3(\text{CO})_3]^+$  precursor. These circumstances allow the deployment of a one-pot procedure in which clicked conjugates are labelled *in situ*, avoiding isolation and purification of the triazole containing ligands. A variety of azides (including azide-functionalized biomolecules) can be reacted in aqueous solutions with propargyl glycine or other

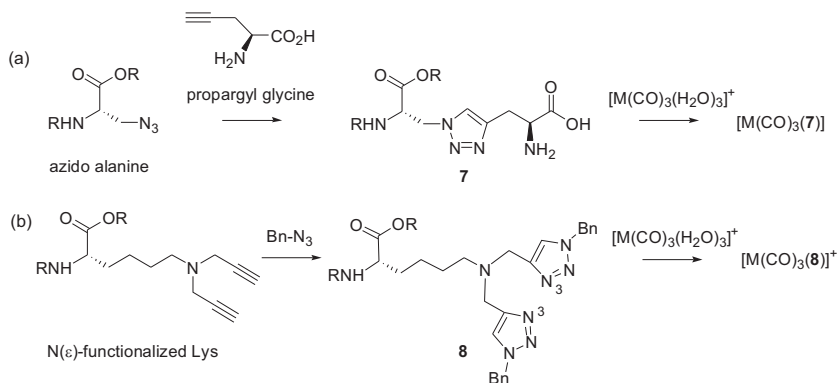


FIG. 3.7. Incorporation of click chelators into peptides.

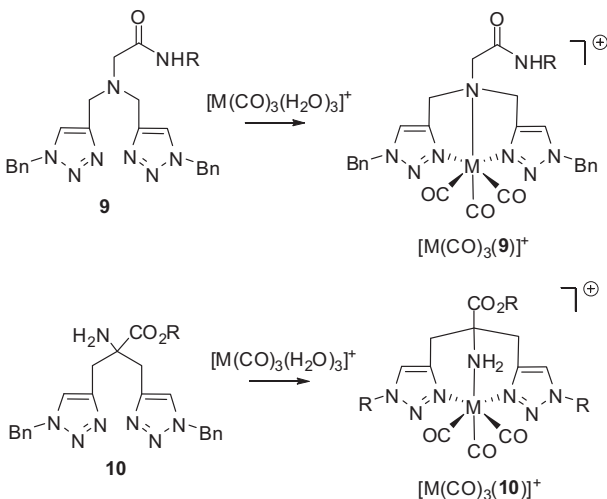


FIG. 3.8. Structure of ‘double click’ model ligands and  $M(CO)_3$  complexes thereof ( $M = {}^{99m}Tc, Re$ ).

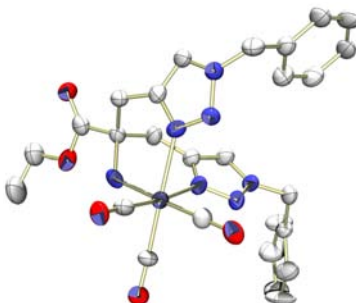


FIG. 3.9. ORTEP-3 representations of complex  $[Re(CO)_3(10)]^+$  with thermal ellipsoids shown at 20% probability.

alkynes in the presence of a Cu(I) catalyst and, subsequently, labelled in situ with the  ${}^{99m}Tc$  tricarbonyl precursor (Fig. 3.10, path A). The products formed are identical to those obtained with pre-synthesized and purified ligands (path B) as indicated by  $\gamma$ -high performance liquid chromatography ( $\gamma$ -HPLC) analysis. The one-pot procedure represents a remarkably efficient synthesis of technetium labelled conjugates for radiopharmaceutical applications.

The scope of the one-pot procedure was exemplified by technetium labelled thymidine analogues. Reaction of a suitable azido-thymidine derivative with a series of alkynes known to lead to potent triazole containing chelators, and

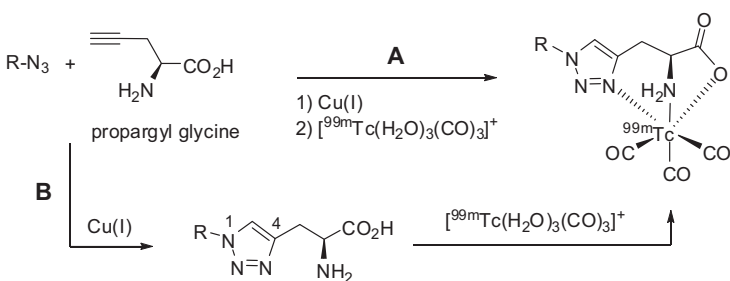


FIG. 3.10. One-pot protocol (path A) provides radiolabelled complexes identical to those obtained via isolated and purified intermediates (path B).

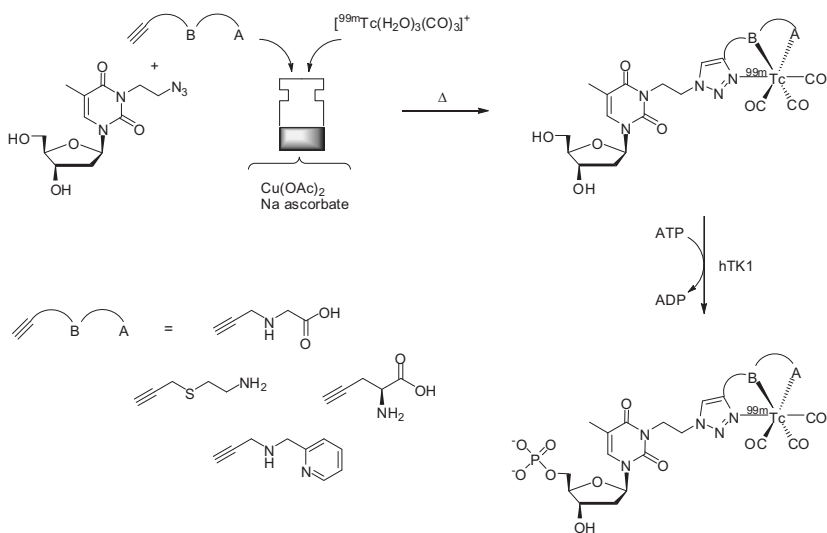


FIG. 3.11. One-pot synthesis and labelling of N3 functionalized thymidine derivatives, and their potential reaction with ATP in the presence of hTK1.

subsequent labelling with technetium provides an efficient route to a set of technetium labelled thymidine derivatives for in vitro assessment (Fig. 3.11). Thymidine was functionalized with an azide at position N3, as it is known that modification of thymidine at this position does not necessarily affect its ability to act as a substrate for human cytosolic thymidine kinase 1 (hTK1) [3.31]. However, there are no reports of Tc labelled thymidine derivatives with retained substrate activity against hTK1 [3.32]. Whether steric reasons or other properties, such as charge of the biocjugate or both, are the reason for the absence of substrate activity was unknown.

Investigation of the ability of the clicked  $^{99m}\text{Tc}$  labelled thymidine analogues to act as substrates for hTK1, and the influence of overall charge and/or structure of the complexes on phosphorylation, reveals that only the complexes with a neutral overall charge retain substrate activity. Thus, charge seemed to have a decisive influence on the acceptance as substrate of the enzyme. Using the one-pot procedure described above, the organic click syntheses radiolabelling and *in vitro* phosphorylation experiments for a set of four different thymidine derivatives could be performed in a matter of hours, which is remarkable progress compared to the classical approach.

### 3.5. IN VIVO ASSESSMENT OF CLICK CHELATORS AND COMPARISON WITH NON-CLICKED ANALOGUES

The synthetic efficiency and simplicity of the preparation of radiolabelled biomolecules functionalized via click chemistry as well as their *in vivo* properties (with respect to target affinity, pharmacokinetics and stability) were studied with a folic acid derivative. Both aspects were assessed side by side by comparison of clicked tumour targeting folate single photon emission computed tomography (SPECT) tracer **12** with the isostructural compound **11** [3.33]. First, as shown in Fig. 3.12, the five step preparation of the clicked variant **12** is considerably shorter and more efficient than the synthesis of folate tracer **11** which is equipped with a N( $\tau$ )-His-chelating system.

Second, comparison of the biodistribution of the new  $^{99m}\text{Tc}$  labelled click folate **12** with the isostructural N( $\tau$ )-His-folate **11** shows that the two tracers exhibit an almost identical pharmacological profile (Fig. 3.13(b)). Figure 3.13(a) shows a combined small animal SPECT-CT of a xenografted mouse 24 h post injection of [ $^{99m}\text{Tc}(\text{CO})_3$  (**12**)]. Specific accumulation of the radiotracer was observed only in the tumour xenografts (arrows) and in folic acid receptor-positive organs such as the kidneys and salivary glands.

### 3.6. FURTHER EXAMPLES OF THE ‘CLICK-TO-CHELATE’ APPROACH

The scope and versatility of the ‘click-to-chelate’ approach is further exemplified by its application to the functionalization and radiolabelling of azide containing compounds from different classes of biomolecules. Thus, a click reaction of propargyl glycine with appropriate azide precursors yielded triazole-chelator containing derivatives of tumour affine peptide bombesin **13**,

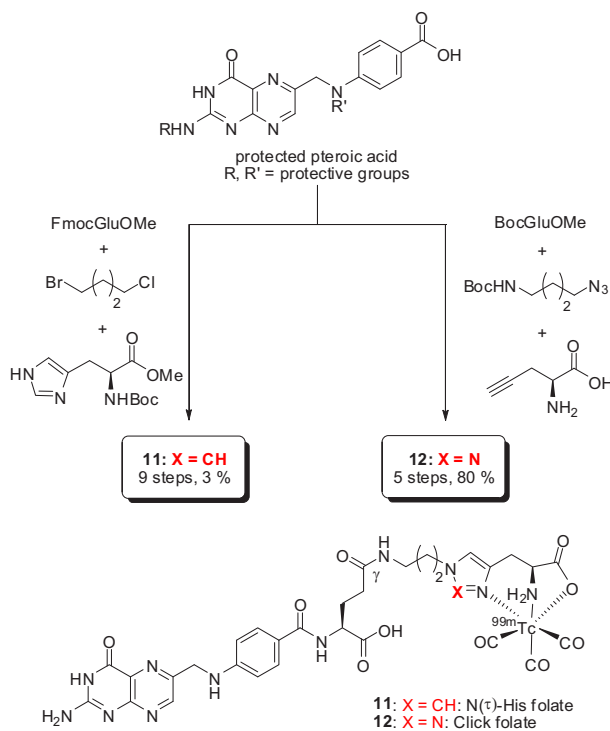


FIG. 3.12. Comparison of the synthesis of two isostructural folic acid  $^{99m}\text{Tc}$  tricarbonyl SPECT tracers.

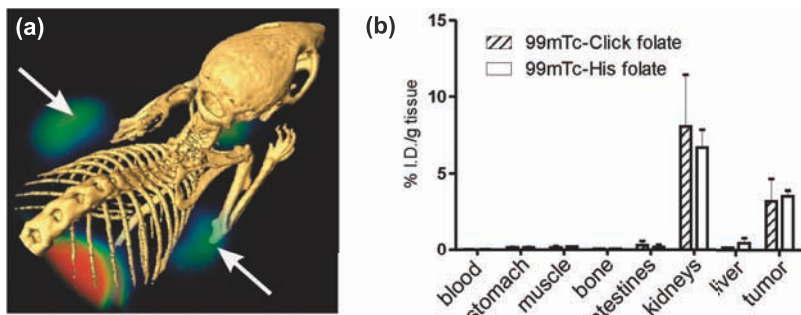
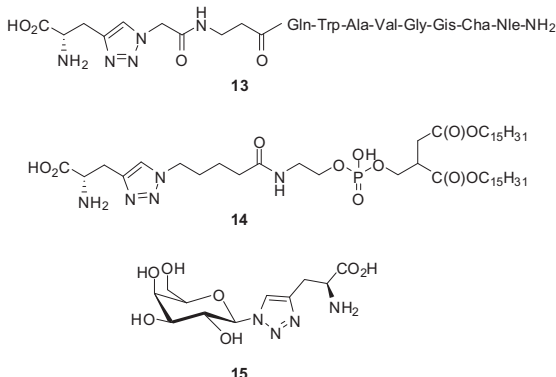


FIG. 3.13. (a) SPECT-CT of a xenografted mouse 24 h post injection of 0.4 GBq click folate 12. (b) Comparison of the biodistribution of  $^{99m}\text{Tc}$  labelled folate tracer 12 and His-folate 11 24 h post injection of 1.5 MBq.



*FIG. 3.14. Examples of biomolecules functionalized via click chemistry with a tridentate 1,2,3-triazole containing metal chelator.*

phospholipid **14** and carbohydrate **15**-deoxy- $\beta$ -D-galactopyranose **15** (Fig. 3.14). All azide precursors can be used in the unprotected form to obtain the triazole compounds as single products in quantitative yields. As expected from previous examples, the reaction of functionalized biomolecules **13–15** with  $^{99m}\text{Tc}(\text{CO})_3$  efficiently provides the corresponding radiolabelled complexes.

### 3.7. CONCLUSIONS

Click chemistry both simplifies the synthesis of efficient, structurally diverse bifunctional ligands in which 1,4-di-substituted triazoles form an integral part of the metal chelating system, and facilitates their incorporation into biologically relevant molecules. Efficient chelating systems can be incorporated into any azido functionalized biomolecule by reaction with suitable alkyne precursors. The single step click reactions are efficient and selective, and do not require protective group chemistry. Moreover, the reaction mixtures can be labelled directly with  $^{99m}\text{Tc}(\text{CO})_3$ , reducing the number of purification steps.

The preparation of potential  $^{99m}\text{Tc}$  labelled substrates for hTK1 demonstrated how the click approach facilitates preliminary *in vitro* screening without the need to synthesize large amounts of a functionalized biomolecule. The *in vitro* and *in vivo* stability of clicked bioconjugates were demonstrated with a  $^{99m}\text{Tc}(\text{CO})_3$  labelled folic acid derivative. The pharmacological profiles of the bioconjugates reveal that the triazole containing folate tracer has very similar properties to the radiolabelled derivative functionalized with an isostructural histidine chelator. Therefore, the 1,2,3-triazole chelators examined so far

represent viable alternatives to other chelators, while offering the advantages of click chemistry.

### REFERENCES TO CHAPTER 3

- [3.1] HUISGEN, R., (PADWA, A., Ed.), Wiley, New York (1984) 1–176.
- [3.2] ROSTOVTSEV, V.V., GREEN, L.G., FOKIN, V.V., SHARPLESS, K.B., A stepwise Huisgen cycloaddition process: Copper(I)-catalyzed regioselective “ligation” of azides and terminal alkynes, *Angew. Chem. Int. Ed.* **41** (2002) 2596–2599.
- [3.3] TORNOE, C.W., CHRISTENSEN, C., MELDAL, M., Peptidotriazoles on solid phase: [1,2,3]-triazoles by regiospecific copper(I)-catalyzed 1,3-dipolar cycloadditions of terminal alkynes to azides, *J. Org. Chem.* **67** (2002) 3057–3064.
- [3.4] ZHANG, L., et al., 1,5-disubstituted 1,2,3-triazoles are accessible selectively from the ruthenium-catalyzed cycloaddition of terminal alkynes and azides, *J. Am. Chem. Soc.* **127** (2005) 15998–15999.
- [3.5] YAP, A.H., WEINREB, S.M., 1,4,5-trisubstituted 1,2,3-triazoles can be obtained by either ruthenium or copper catalysis, *Tetrahedron Lett.* **47** (2006) 3035–3038.
- [3.6] DÍEZ-GONZÁLEZ, S., CORREA, A., CAVALLO, L., NOLAN, S.P., (NHC)Copper(I)-catalyzed [3+2] cycloaddition of azides and mono- or disubstituted alkynes, *Chem. Eur. J.* **12** (2006) 7558–7564.
- [3.7] KOLB, H.C., SHARPLESS, K.B., The growing impact of click chemistry on drug discovery, *Drug. Discov. Today* **8** (2003) 1128–1137.
- [3.8] PRESCHER, J.A., BERTOZZI, C.R., Chemistry in living systems, *Nature Chem. Biol.* **1** (2005) 13–21.
- [3.9] LINK, A.J., MOCK, M.L., TIRRELL, D.A., Non-canonical amino acids in protein engineering, *Curr. Opin. Biotech.* **14** (2003) 603–609.
- [3.10] WANG, L., SCHULTZ, P.G., Expanding the genetic code, *Angew. Chem. Int. Ed.* **44** (2005) 34–66.
- [3.11] MOSES, J.E., MOORHOUSE, A.D., The growing applications of click chemistry, *Chem. Soc. Rev.* **36** (2007) 1249–1262.
- [3.12] GIL, M.V., AREVALO, M.J., LOPEZ, O., Click chemistry — What’s in a name? Triazole synthesis and beyond, *Synthesis* **11** (2007) 1589–1620.
- [3.13] MARIK, J., SUTCLIFFE, J.L., Click for PET: Rapid preparation of [F-18]fluoro peptides using Cu-I catalyzed 1,3-dipolar cycloaddition, *Tetrahedron Lett.* **47** (2006) 6681–6684.
- [3.14] GLASER, M., ARSTAD, E., “Click labeling” with 2-[F-18]fluoroethylazide for positron emission tomography, *Biocjug. Chem.* **18** (2007) 989–993.
- [3.15] BASKIN, J.M., et al., Copper-free click chemistry for dynamic in vivo imaging, *Proc. Natl. Acad. Sci. USA* **104** (2007) 16793–16797.
- [3.16] ZHANG, Y.H., et al., An inexpensive fluorescent labeling protocol for bioactive natural products utilizing Cu(I)-catalyzed Huisgen reaction, *Tetrahedron* **63** (2007) 6813–6821.

- [3.17] MINDT, T.L., et al., “Click to chelate”: Synthesis and installation of metal chelates into biomolecules in a single step, *J. Am. Chem. Soc.* **128** (2006) 15096–15097.
- [3.18] ALBERTO, R., New organometallic technetium complexes for radiopharmaceutical imaging, *Top. Curr. Chem.* **252** (2005) 1–44.
- [3.19] ALBERTO, R., et al., A novel organometallic aqua complex of technetium for the labeling of biomolecules: Synthesis of  $[^{99m}\text{Tc}(\text{OH}_2)_3(\text{CO})_3]^+$  from  $[^{99m}\text{TcO}_4]^-$  in aqueous solution and its reaction with a bifunctional ligand, *J. Am. Chem. Soc.* **120** (1998) 7987–7988.
- [3.20] MOORE, D.S., ROBINSON, S.D., Catenated nitrogen ligands .2. Transition-metal derivatives of triazoles, tetrazoles, pentazoles, and hexazine, *Adv. Inorg. Chem. Radiat.* **32** (1988) 171–239.
- [3.21] VAN STAVEREN, D.R., et al., Conjugation of a novel histidine derivative to biomolecules and labelling with  $[^{99m}\text{Tc}(\text{OH}_2)_3(\text{CO})_3]^+$ , *Org. Biomol. Chem.* **2** (2004) 2593–2603.
- [3.22] RAPER, E.S., Complexes of heterocyclic thionates .1. Complexes of monodentate and chelating ligands, *Coordin. Chem. Rev.* **153** (1996) 199–255.
- [3.23] CHAN, T.R., HILGRAF, R., SHARPLESS, K.B., FOKIN, V.V., Polytriazoles as copper(I)-stabilizing ligands in catalysis, *Org. Lett.* **6** (2004) 2853–2855.
- [3.24] DAI, Q., GAO, W.Z., LIU, D., KAPES, L.M., ZHANG, X.M., Triazole-based monophosphine ligands for palladium-catalyzed cross-coupling reactions of aryl chlorides, *J. Org. Chem.* **71** (2006) 3928–3934.
- [3.25] DETZ, R.J., et al., “Clickphine”: A novel and highly versatile P,N ligand class via click chemistry, *Org. Lett.* **8** (2006) 3227–3230.
- [3.26] COLASSON, B., et al., A ditopic calix[6]arene ligand with N-methylimidazole and 1,2,3-triazole substituents: Synthesis and coordination with Zn(II) cations, *Org. Lett.* **9** (2007) 4987–4990.
- [3.27] SUIJKERUIJK, B.M.J.M., et al., “Click” 1,2,3-triazoles as tunable ligands for late transition metal complexes, *Dalton Trans.* (2007) 1273–1276.
- [3.28] VAN STAVEREN, D.R., WAIBEL, R., MUNDWILER, S., SCHUBIGER, P.A., ALBERTO, R., Conjugates of vitamin B12 with N-epsilon-functionalized histidine for labeling with  $[^{99m}\text{Tc}(\text{OH}_2)_3(\text{CO})_3]^+$ : Synthesis and biodistribution studies in tumor bearing mice, *J. Organomet. Chem.* **689** (2004) 4803–4810.
- [3.29] PAK, J.K., BENNY, P., SPINGLER, B., ORTNER, K., ALBERTO, R., N-epsilon functionalization of metal and organic protected L-histidine for a highly efficient, direct labeling of biomolecules with  $[\text{Tc}(\text{OH}_2)_3(\text{CO})_3]^+$ , *Chem. Eur. J.* **9** (2003) 2053–2061.
- [3.30] STEPHENSON, K.A., et al., Bridging the gap between in vitro and in vivo imaging: Isostructural Re and Tc-99m complexes for correlating fluorescence and radioimaging studies, *J. Am. Chem. Soc.* **126** (2004) 8598–8599.
- [3.31] AL-MADHOUN, A.S., et al., Synthesis of a small library of 3-(carboranylalkyl)thymidines and their biological evaluation as substrates for human thymidine kinases 1 and 2, *J. Med. Chem.* **45** (2002) 4018–4028.

- [3.32] CELEN, S., et al., Synthesis and evaluation of a Tc-99m-MAMA-propyl-thymidine complex as a potential probe for in vivo visualization of tumor cell proliferation with SPECT, *Nucl. Med. Biol.* **34** (2007) 283–291.
- [3.33] MÜLLER, C., FORRER, F., SCHIBLI, R., KRENNING, E.P., DE JONG, M.J., SPECT study of folate receptor-positive malignant and normal tissues in mice using a novel <sup>99m</sup>Tc-radiofolate, *Nucl. Med.* **49** (2008) 310–317.



## **Chapter 4**

# **ADVANCES IN SPECT INSTRUMENTATION (INCLUDING SMALL ANIMAL SCANNERS)**

G. DI DOMENICO, G. ZAVATTINI

Department of Physics,  
University of Ferrara,  
Ferrara, Italy

### **Abstract**

Fundamental major efforts have been devoted to the development of positron emission tomography (PET) imaging modality over the last few decades. Recently, a novel surge of interest in single photon emission computed tomography (SPECT) technology has occurred, particularly after the introduction of the hybrid SPECT-CT imaging system. This has led to a flourishing of investigations in new types of detectors and collimators, and to more accurate refinement of reconstruction algorithms. Along with SPECT-CT, new, fast gamma cameras have been developed for dedicated cardiac imaging. The existing gap between PET and SPECT in sensitivity and spatial resolution is progressively decreasing, and this trend is particularly apparent in the field of small animal imaging where the most important advances have been reported in SPECT tomographs. An outline of the basic features of SPECT technology, and of recent developments in SPECT instrumentation for both clinical applications and basic biological research on animal models is described.

### **4.1. INTRODUCTION**

In emission tomography, the source of electromagnetic radiation is a radioisotope that is distributed within the body of the patient. The objective is to provide a spatial map or image of this distribution, usually displayed as various two dimensional sections through the body. Therefore, in comparison with the CT technique, that displays absorption properties of the organs related to the anatomy information, the emission techniques reveal the distribution of radioactive tracers that often indicate various aspects of physiological functions. Thus, the interest of emission tomography is often centred around those applications in which tiny amounts of tracer follow functions which would otherwise be disturbed by the much larger amounts of contrast medium required in radiological studies.

In order to form a projection image in emission tomography, the imaging system must determine not only the photon flux density (number of X or  $\gamma$  rays for unit area) at each point in the image plane, but also the direction of the

detected photons. The flux density may be measured by using a position sensitive detector, but to define the direction of X or  $\gamma$  rays, two different methods are used, defining the two nuclear medicine specialities, namely positron emission tomography (PET) and single photon emission computed tomography (SPECT):

- The PET technique is limited to those radioisotopes that decay by emitting a positron. The positron travels a short distance (a few millimetres) before stopping and annihilating with an electron from the patient tissue. The annihilation radiation consists of two photons, each with an energy of 0.511 MeV, emitted in time coincidence and oppositely directed along the same line;
- In the SPECT techniques, the rays are isotropically emitted as single photons. Thus, to define the ray direction, the application of shadow-casting methods is required, using materials such as spatial collimators that are opaque to the photons.

Historically, the era of single photon imaging in nuclear medicine begins with the development of the first gamma camera by Hal Anger [4.1] about 50 years ago. The Anger camera was built from a 4 in scintillator plate of sodium iodide doped with thallium NaI(Tl) and seven photomultipliers. Their signals were combined and adjusted by a signal matrix circuit that allowed retrieving the position in the scintillator plate where every single  $\gamma$  ray had been absorbed. Planar images were initially obtained by pinhole collimators and later by a parallel hole collimator. Today, most clinical SPECT systems still use the Anger camera with larger NaI(Tl) crystals but new imaging systems have been built for specific clinical applications or for the emerging field of molecular imaging.

## 4.2. SPECT IMAGING SYSTEM

The ideal SPECT detector would detect every photon incident upon it, and give error free information regarding the spatial location, energy and time arrival of each event. It would also be able to handle arbitrarily fast photon-arrival rates. Real SPECT detectors fail in all of these respects to some extent. In this section, we discuss about the basic components of the SPECT camera and the physics processes involved in  $\gamma$  ray detection.

### 4.2.1. X ray and $\gamma$ ray detection

When an X ray or  $\gamma$  ray beam passes through matter, it becomes attenuated as photons are removed from it. This attenuation is due to two competitive

processes: absorption and scattering. The scattering losses refer to energy removed from the primary beam by photons that are redirected by scattering events. Absorption losses refer to the energy removed from the primary beam and transferred locally to the lattice. The dominant interactions of an X ray or  $\gamma$  ray with matter, at the energies of interest for nuclear medicine (100–600 keV), are coherent scatter, photoelectric absorption and Compton scatter. The absorbed energy is derived from the photoelectron in the photoelectric interaction and from the recoil electron in Compton events. The coherent scatter does not transfer energy to the matter. Beer's law describes the relationship between the incident photon fluence (photons per square centimetre)  $I_0$  and the photon fluence  $I_t$  after travelling a distance  $t$  in the medium as:

$$I_t = I_0 \cdot e^{-\mu t} \quad (4.1)$$

where  $\mu$  is the linear attenuation coefficient of the medium. Therefore, we can write the linear attenuation coefficient  $\mu$  as:

$$\mu = \mu_{coh} + \mu_{phe} + \mu_{Compton} \quad (4.2)$$

As an example, in Fig. 4.1 we plot the photoelectric, Compton, coherent and total mass attenuation coefficient for a NaI(Tl) scintillator, in  $\text{cm}^2/\text{g}$ , as a function of photon energy. Coherent or Rayleigh scattering is the apparent deflection of X ray beams caused by atoms being excited by the incident radiation and then re-emitting waves at the same wavelengths. This phenomenon is useful in X ray or  $\gamma$  ray diffraction studies, where the photon energies are of the order of a few keV and, thus, the wavelengths are of the same order of magnitude as atomic dimensions. It is relatively unimportant at energies used in nuclear medicine.

Experimentally,  $\mu_{coh}$  for elemental material is given by:

$$\mu_{coh} = C_R \frac{\rho}{A} N_A \frac{Z^{k+1}}{(hv_o)^l} \quad (4.3)$$

where  $N_A$  is Avogadro's number,  $C_R$  is a constant,  $\rho$  is the material density,  $A$  is the atomic weight,  $Z$  is the atomic number of the material,  $h$  is Planck's constant, and  $v_o$  is the photon frequency. The parameters  $k$  and  $l$  are experimentally determined as  $k = 2$  and  $l = 1.9$ .

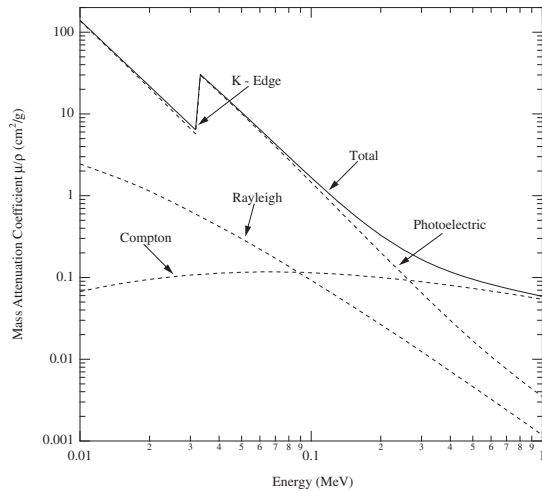


*FIG. 4.1. Gamma ray mass attenuation coefficient in NaI(Tl) as a function of energy. The density of NaI(Tl) is 3.76 g/cm<sup>2</sup>.*

At the lower energies of interest, the photoelectric effect dominates the attenuation coefficient, as seen by the plot of Fig. 4.1. The photon in this case is completely absorbed by interacting with a tightly bound electron. Its energy  $h\nu_0$  ionizes the absorbing atom and transfers kinetic energy  $E_e$  to the ejected photoelectron. The kinetic energy of the ejected electron is dissipated in the matter. The energy conservation law requires that:

$$h\nu_0 = E_e + I \quad (4.4)$$

where  $I$  is the ionization potential of the particular electron involved. All the atomic shells, with  $I \leq h\nu_0$ , contribute to the process, but the main term is due to the deepest atomic level. Experimentally,  $\mu_{phe}$  for a material composed of a single element is given by:

$$\mu_{phe} = C_p \frac{\rho}{A} N_A \frac{Z^{m+1}}{(h\nu_0)^n} \quad (4.5)$$

where  $N_A$  is Avogadro's number,  $C_p$  is a constant that depends on the shell involved,  $\rho$  is the material density,  $A$  is the atomic weight,  $Z$  is the atomic number of the material,  $h$  is Planck's constant and  $\nu_0$  is the photon frequency. The parameters  $m$  and  $n$  are functions of  $Z$  and  $\nu_0$ , but adequate values are  $m = 3.8$  and  $n = 3.2$ .

The vacancy created by knocking out an inner electron is filled in a very short period of time by an electron falling into it, usually from the next shell. This is accompanied by the emission of characteristic X ray photons, called fluorescent radiation, or by the emission of an electron, called an Auger electron, due to the direct transfer of the atomic excitation to one of the outer electrons. In high Z materials, the emission of fluorescent radiation is dominant as can be seen in Fig. 4.2. These X rays will have an energy value just below the K-edge where the linear mass attenuation is at a local minimum and will, therefore, travel relatively far compared to an X ray just above the K-edge discontinuity. In NaI(Tl), these X rays have energies of 28 and 32 keV, and their gamma mean free path in NaI(Tl) is about 0.4 mm. Thus, the effect of photoelectric interaction is the total conversion of photon energy into electron energy, which can be measured accurately.

In a Compton event, the incoming photon with energy  $h\nu_o$  is scattered by a free electron through an angle  $\theta$ . The energy conservation law requires that:

$$E_e = h\nu_o - h\nu' \quad (4.6)$$

where  $E_e$  is the kinetic energy imparted to the electron which recoils at an angle  $\phi$ ,  $h\nu_o$  is the energy of the incoming photon and  $h\nu'$  is the energy of the outgoing photon.

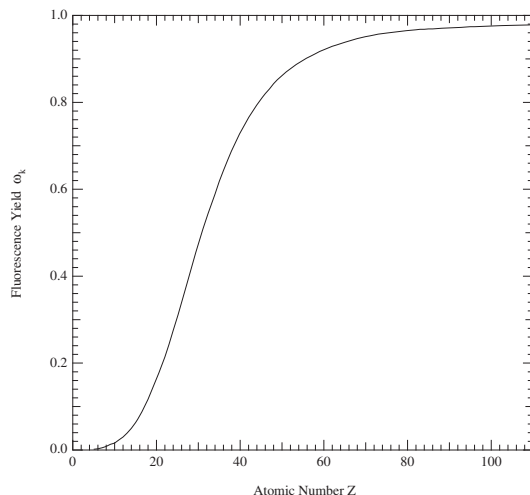


FIG. 4.2. Probability of a fluorescent photon following a K-shell vacancy due to a photoelectric interaction as a function of atomic number, Z.

The energy of the scattered photon is given by:

$$hv' = \frac{hv_o}{1 + \alpha(1 - \cos\theta)} \quad (4.7)$$

with  $\alpha = h\nu_0/m_0c^2$ . The linear absorption coefficient  $\mu_{\text{Compton}}$  is given by:

$$\mu_{\text{Compton}} = \frac{\rho}{A} N_A Z \sigma_{\text{KN}} \quad (4.8)$$

where  $N_A$  is Avogadro's number,  $\rho$  is the mass density,  $A$  is the atomic weight,  $Z$  is the atomic number of the material and  $\sigma_{KN}$  is the Klein-Nishina cross-section that only depends on the incoming photon energy  $h\nu_0$ . The ratio  $Z:A$  is near 0.5, so the important physical parameter for the Compton interaction is, therefore, the mass density.

In general, the higher the Z of the material, the higher the energy at which the Compton interaction probability crosses the photoelectric interaction probability. In Fig. 4.3, the various regions of the energy spectrum where different effects dominate are shown.

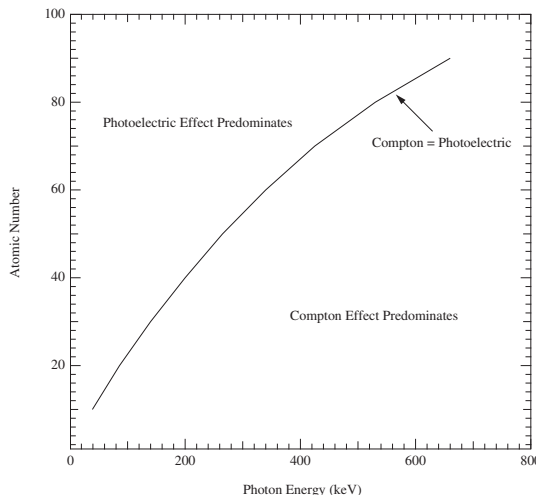


*FIG. 4.3. Relative importance of two major types of X ray interaction. The line shows the values of Z and photon energy for which the photoelectric and Compton effects are equal.*

As can be seen, higher atomic number elements will experience primarily photoelectric absorption, while those of lower atomic numbers will be dominated by Compton scattering. For composite materials, the attenuation coefficient becomes:

$$\mu = \frac{\rho}{A} N_A \left\{ \sigma_{KN} + C_R \frac{\bar{Z}_r^{k+1}}{(hv_o)^l} + C_P \frac{\bar{Z}_p^{m+1}}{(hv_o)^n} \right\} \quad (4.9)$$

where  $\bar{Z}_r$  and  $\bar{Z}_p$  are the effective atomic numbers as given by:

$$\bar{Z}_r = \left( \sum_i \alpha_i Z_i^k \right)^{1/k} \quad \bar{Z}_p = \left( \sum_i \alpha_i Z_i^m \right)^{1/m} \quad (4.10)$$

and  $\alpha_i$  is the electron fraction of the  $i$ -th element.

#### 4.2.2. Scintillation detector

The detection of ionizing radiation by the scintillation light produced by certain materials is one of the oldest techniques used by researchers. Scintillators are materials that emit visible light when they absorb energy from charged particles, X rays or  $\gamma$  rays. However, scintillators require an additional stage to convert the scintillation light into a current pulse. A photon to electron transducer (photodetector), such as a photomultiplier tube (PMT), photodiode or avalanche photodiode (APD), is generally used.

An ideal scintillator possesses the following properties [4.2]:

- It should convert the kinetic energy of a charged particle into detectable light with a high scintillation efficiency: the numbers of photons/keV should be as high as possible;
- The conversion process should be as linear as possible over the widest energy range;
- The medium should be transparent to its own emission for good light collection;
- The decay time of scintillation should be short in order to generate fast signal pulses;
- The index of refraction should be near to that of glass (1.5) for efficient coupling of the scintillator to the light sensor.

No material simultaneously meets all these criteria and the choice of a specific scintillator is a compromise among these and other factors. In nuclear medicine and molecular imaging, inorganic scintillators, such as NaI(Tl), are largely used because they offer several advantages for  $\gamma$  ray detection, including high detection efficiency, moderate cost and the possibility of being fabricated in a large variety of shapes and sizes. The physical properties of interesting inorganic scintillators for SPECT applications are listed in Table 4.1.

The first four materials shown in Table 4.1 have comparable effective atomic numbers and densities, which means that they will have similar  $\gamma$  ray detection properties: the photoelectric fraction is >70% at 140 keV, and the X ray fluorescence mean free path ranges from 180 to 340  $\mu\text{m}$ . The last scintillator, YAlO<sub>3</sub>(Ce), has a lower photoelectric fraction at 140 keV, about 50%, but a shorter X ray fluorescence mean free path, 140  $\mu\text{m}$ , so that the scintillation spot following the photoelectric interaction has a smaller size, permitting better spatial resolution. The decay time of the scintillation limits the counting rate capability of the detectors, but in SPECT, counting rate losses in the detector are rarely a problem (mainly due to the presence of a collimator). The wavelength of scintillation light determines what kind of photon transducers can be used to turn the scintillation light into an electronic pulse. The light yield of scintillation affects the energy resolution of a detector, its timing resolution and its spatial resolution.

#### *4.2.2.1. Sodium iodide activated with thallium*

NaI(Tl) is still the most used scintillator for SPECT applications. In most clinical SPECT systems, the NaI(Tl) detector is a single large rectangular crystal (50–70 cm) with a thickness of 6–10 mm. Recently, Saint-Gobain produced a StarBrite NaI(Tl) crystal that is 1 in thick to increase the efficiency for high

TABLE 4.1. PROPERTIES OF COMMONLY USED SCINTILLATORS

Scintillator	NaI(Tl)	CsI(Tl)	CsI(Na)	LaBr <sub>3</sub> (Ce)	YAlO <sub>3</sub> (Ce)
Effective atomic number	50	54	54	45	32
Density, $\rho$ (g/cm <sup>3</sup> )	3.67	4.51	4.51	5.3	5.37
Decay time, $\tau$ (ns)	230	1000	630	25	27
Wavelength, $\lambda$ (nm)	415	540	420	370	370
Refractive index	1.85	1.80	1.84	1.90	1.95
Light yield (photons/keV)	38	65	39	60	18
$\gamma$ mean free path (cm) at 140 keV	0.38	0.26	0.26	0.33	0.64

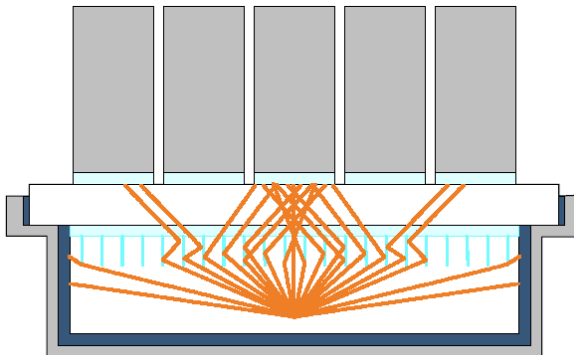


FIG. 4.4. *NaI(Tl)* scintillator plate built with StarBrite technology (courtesy of Saint Gobain).

energy  $\gamma$  emitters [4.3]. As shown in Fig. 4.4, slots (grooves) are machined into the top surface of the detector to reduce the spread of output light and to maintain intrinsic spatial resolution (4.1 mm at 140 keV).

#### 4.2.2.2. *Caesium iodide activated with thallium*

CsI(Tl) competes well with NaI(Tl) in term of efficiency and is not strongly hygroscopic. It has a longer scintillation time, leading to a larger dead time, but that is rarely a concern in SPECT. However, the scintillation light from CsI(Tl) has a longer wavelength which is not as well matched to PMTs as sodium iodide. Its performance is, therefore, inferior to that of NaI(Tl) with PMTs even though the total number of photons is higher than with NaI(Tl). However, these photons are detected with high quantum efficiency with photodiodes that can replace PMTs. DigiRad use this approach in their Cardius product.

#### 4.2.2.3. *Caesium iodide activated with sodium*

CsI(Na) is similar to CsI(Tl), but with an emission that is better matched to PMTs. It is currently used as the scintillator in the Linoview small animal SPECT system [4.4, 4.5].

#### 4.2.2.4. *Lanthanum bromide activated with cerium*

LaBr<sub>3</sub>(Ce) is a transparent scintillator material with fast emission and excellent linearity. It has a very high light output with a correspondingly improved energy resolution (<6% at 140 keV) and an intrinsic efficiency comparable to NaI(Tl) [4.6]. In addition, LaBr<sub>3</sub>(Ce) is a very fast scintillator and

is potentially very useful in the Compton gamma camera of PET imaging. Small animal SPECT systems have been recently built by using  $\text{LaBr}_3(\text{Ce})$  coupled to a position sensitive PMT [4.7, 4.8]. A disadvantage of this material is that it is highly hygroscopic.

#### 4.2.2.5. *Yttrium aluminium perovskite activated with cerium*

$\text{YAlO}_3(\text{Ce})$  is a monocrystal with the reticular structure of perovskite. It shows a high level of hardness and good chemical stability, non-hygroscopicity and no solubility in inorganic acids. The light output yield is about 55% of  $\text{NaI}(\text{Tl})$ , with a decay time of scintillation of 27 ns.

#### 4.2.3. **Photodetectors**

The detection of low levels of light is the key process in medical imaging detectors based on scintillators. For nearly three decades, PMTs have been successfully used as a photodetector for SPECT and PET applications, and are still the most commonly used light detector in this field. At the interface between the crystal detector and the photo-converter, a fraction of light is lost which can limit the energy, time and space resolution of the system. The most common camera currently used in SPECT is based on position sensitive scintillation detectors. Localizing the light flash created within the crystal is critical to good resolution and this task may be achieved by using three basic configurations as shown in Fig. 4.5.

In the configuration (1), the crystal is a single slab of inorganic scintillator coupled to a series of photodetectors with a light guide. The scintillation light diffuses and reflects throughout the crystal, and after travelling into and out of the light guide, for optimal light spread, it is converted into electrical pulses by photodetectors. The spatial coordinates of the  $\gamma$  interaction point are obtained by

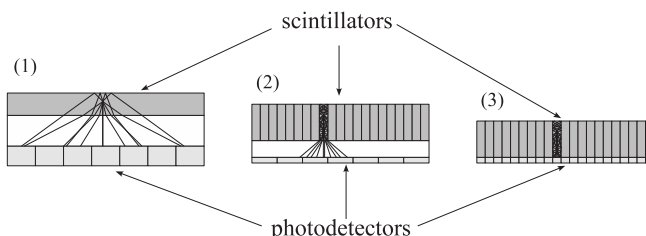


FIG. 4.5. Possible coupling schemes of crystals to photodetectors.

an appropriate weighted mean of the individual photodetector's signals, as given in Eq. (4.11):

$$x = \frac{\sum_i \omega_i V_i}{\sum_i V_i} \quad y = \frac{\sum_i v_i V_i}{\sum_i V_i} \quad (4.11)$$

where  $V_i$ ,  $\omega_i$  and  $v_i$  are the output voltage, the x-weight and y-weight of the i-th photodetector, respectively. Typically, the weights are proportional to the coordinates of the middle point of each photodetector according to an Anger type positioning scheme. One of the disadvantages of Anger logic is the loss of linearity near the edge of the scintillator that reduces the sensitive FOV of the camera. The spatial resolution  $R$  depends on the spatial spread of scintillation light  $\sigma_{\text{light}}$  and on the number of photons  $N_{\text{photons}}$  seen by the photodetectors:

$$R \approx 2.35 \frac{\sigma_{\text{light}}}{\sqrt{N_{\text{photons}}}} \quad (4.12)$$

The spatial resolution improves by reducing  $\sigma_{\text{light}}$  or increasing  $N_{\text{photons}}$ . For a smooth continuous positioning of events, it is necessary to share the light over more photodetectors, increasing  $\sigma_{\text{light}}$  intentionally. In detector design, it is, therefore, necessary to choose the right compromise between uniform positioning and spatial resolution. Despite these limitations, this scheme is still used in modern gamma cameras with a large field of view. The typical value of intrinsic spatial resolution of modern gamma cameras with Anger logic is about 3 mm full width at half maximum (FWHM). A detailed description of Anger logic has been written by Barrett and Swindell [4.9].

In configurations (2) and (3) in Fig. 4.5, the inorganic scintillation crystal is segmented into many small, optically isolated crystals to form a two dimensional array of pillar scintillators. The advantages of pixelated crystals are: (i) scintillation light is confined to a single crystal and forms a small spot on a photodetector array; (ii) the spatial resolution is determined by the crystal width; and (iii) there is no loss of linearity near the edge of the sensitive area of the detectors. Disadvantages compared to continuous crystal design are: (i) lower sensitivity due to the dead area between crystals; (ii) the output number of photons is reduced (high aspect ratio), thereby deteriorating energy resolution; (iii) inter-detector scatter causes positioning errors; and (iv) they are more expensive to manufacture. The photodetectors used with pixelated scintillators can be a position sensitive system such as position sensitive PMT (PSPMT), position sensitive APD (PSAPD) or a variety of exotic photodetectors. For

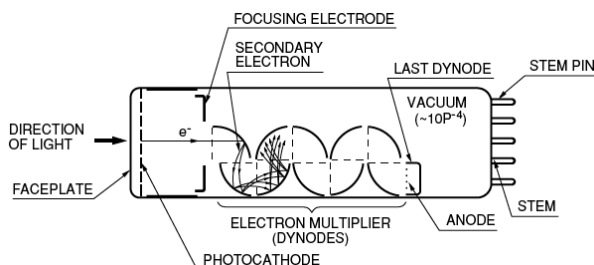
example, in the readout scheme (2), the output light from a single crystal is shared among several photodetectors, whereas with the readout scheme (3), each crystal is coupled to an individual photodetector. Widespread use of configurations (2) and (3) has been found in small field of view imagers dedicated to scintimammography, small animal imaging and intra-operative cameras [4.10–4.12].

#### 4.2.3.1. Photomultipliers

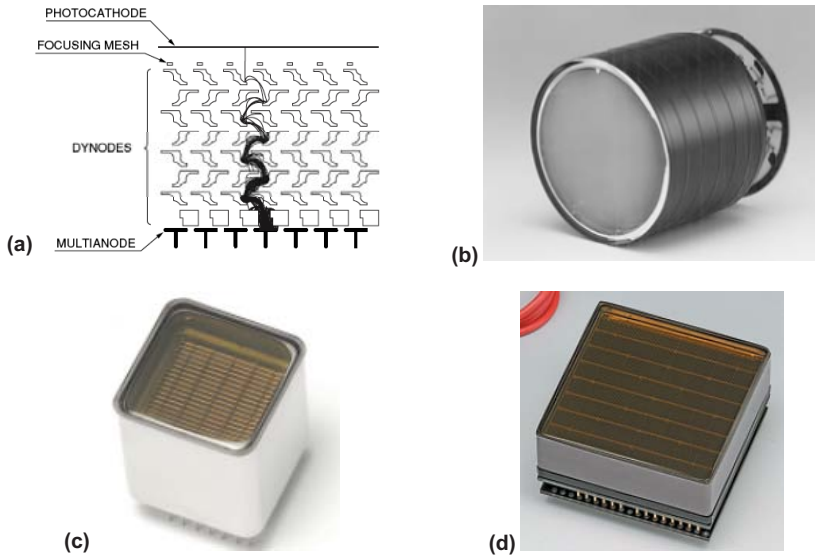
A photomultiplier tube is a vacuum tube consisting of an input window, a photocathode, focusing electrodes, an electron multiplier stage and an anode.

Figure 4.6 shows the basic structure of a photomultiplier tube. The light which enters a photomultiplier tube from the faceplate (input window) can excite the electrons in the photocathode so that photoelectrons are emitted into the vacuum. The photoelectrons are accelerated and focused by the focusing electrode onto the first dynode where they are multiplied by means of secondary electron emission. This secondary emission is repeated at each of successive dynodes. The multiplied secondary electrons, emitted from the last dynode, are finally collected by the anode. The typical PMT's gain is about  $10^6$  with relatively low noise, but their quantum conversion efficiency is low ( $\sim 20\%$ ), leading to a significant loss of signal that affects energy, spatial and timing resolution.

Nearly twenty years ago, Hamamatsu developed the first generation of the position sensitive PMTs (PSPMT): PMTs with the ability to localize events to several millimetres [4.13, 4.14]. The spatial localization of light is based on a proximity mesh dynode structure by which the charge is multiplied around the original position of the light photon striking on the photocathode (Fig. 4.7(a)). The charge distribution is sampled by crossed wire anodes and the centroid method is used for position determination. The intrinsic spatial resolution of the 3 in model is less than 0.6 mm FWHM for a light spot of 1 mm in diameter producing 1000 photoelectrons/event. These PSPMTs (Fig. 4.7(b)) have found



*FIG. 4.6. Basic structure of a photomultiplier tube (courtesy of Hamamatsu).*



*FIG. 4.7. The PSPMT schematic (a), and three PSPMT generations: R2486 (b), R8900 (c), R8500 (d). (Courtesy of Hamamatsu.)*

applications in small FOV imaging systems for SPECT and PET, but they are not useful for clinical gamma cameras due to their large peripheral dead zone (1 cm).

Following the first PSPMT generation, Hamamatsu has developed small area PSPMTs (~1 in. square) with a new dynode structure (metal channel dynode) (Fig. 4.7(c)) that produce a narrower charge distribution. The charge is collected by a multianodic system with an array of multiwire structure. The reduced peripheral dead zone (2 mm) permits arrays of tubes for large area applications to be assembled. The last generation PSPMTs are the flat panel PMTs (Fig. 4.7(d)) that combine a large active area (2 in) with the narrowest peripheral dead zone (<1 mm) and a height of only 12 mm. The flat panel imaging performances in SPECT have been investigated by Pani et al. [4.15] and the results show very good position linearity, spatial resolution and gain with pixelated scintillators. Several research groups have developed a dedicated SPECT camera by using PSPMT [4.16–4.18] for small animal imaging, breast imaging, etc. In recent years, new compact semiconductor photodetectors have become available that offer new design options and are competitive with PMTs in terms of performance and cost. Especially dedicated high resolution applications, such as small animal emission tomography, may benefit from these new detector technologies because compactness is required.

#### *4.2.3.2. Photodiode*

Photodiodes are silicon diodes that convert scintillation light into an electrical signal. They work in a reverse-bias mode with a lower voltage than PMTs. They have higher quantum efficiency (>70% at 400 nm) than PMTs but unitary gain. Thus, for SPECT applications, photodiodes must be developed with low leakage current (<0.1 nA), and a low noise pre-amplifier for readout is required. Their insensitivity to magnetic fields and their compact size make photodiodes a useful device for small animal SPECT applications in an MR environment. A modular camera has been built for breast cancer imaging at LBL [4.19] by using SiPD and CsI(Tl) scintillators.

#### *4.2.3.3. Avalanche photodiode*

APDs are high quality photodiodes with an internal gain stage [4.2]. Gain is achieved within the semiconductor material by applying a high reverse bias, so that the electric field is sufficiently high to enable the migrating electron to create secondary ionization during the collection process, so that the final electronic signal is proportional to the initial number of light photons detected. They are more rugged, very compact and largely immune to magnetic fields as compared to PMTs, and they operate at a lower voltage than PMTs, 300–400 V, with a maximum gain of about 250. In Fig. 4.8(a), a  $4 \times 8$  APD array from Hamamatsu is shown: the active area of the single photodiode is 1.6 mm  $\times$  1.6 mm with a dead zone of 0.7 mm. The typical signal rise time is 1 ns, which makes this detector suitable for small animal PET applications [4.20, 4.21]. The spatial resolution is limited to the APD array channel size, which also defines the size of the pillar crystals.

A continuous PSAPD (Fig. 4.8(b)) has been developed that uses charge sharing between additional electrodes on the back surface of the APD to improve the event localization to  $\sim 0.5$  mm. Some investigations are being performed to use PSAPD in SPECT [4.22] by cooling the photodetectors to  $-40^\circ\text{C}$  and using a matrix of CsI(Tl).

#### *4.2.3.4. Silicon photomultiplier*

The silicon photomultiplier (SiPM), which is also referred to as a multipixel photon counter, uses the technique, whereby an array of CMOS compatible photon counting (Geiger mode) photodiodes (100–1600), each with an integrated quench circuit, are connected together in parallel on a single piece of silicon. An



*FIG. 4.8. Silicon APD array (a) (courtesy of Hamamatsu); Position sensitive APD (b) (courtesy of RMD Inc.); SiPM matrix 2 × 2 pixel elements (c) (courtesy of FBK-Trento).*

incident photon on any photodiode produces a pulse of current at the sensor output. The total output is the sum of all the individual pulses of current from each photodiode detecting a photon at a moment in time. The output current is, thus, proportional to the incident photon flux. The total SiPM gain ( $10^5$ – $10^6$ ) is significantly higher than that of a normal APD, which is typically near 100. This novel device combines the main advantages of conventional silicon APDs (such as small size ( $1 \text{ mm}^2$ ), low voltage operation (<100 V) and robustness), with the main advantages of PMTs such as high gain and stability. Due to the superior time resolution ( $\ll 1 \text{ ns}$ ), these devices have been investigated in PET systems and are likely to find their way into scintillator based SPECT systems [4.23–4.25].

#### 4.2.4. Semiconductor detectors

Semiconductor detectors are solid state devices that provide direct conversion of deposited  $\gamma$  ray energy to an electronic signal [4.26–4.28]. The deposited energy from a  $\gamma$  ray interaction generates charge carriers (electrons–holes) within the depletion zone of the semiconductor (the devices work in reverse-bias). The electric field applied to the semiconductor causes the migration of the electrons and the holes, and the induced charge on the terminals generates an electronic pulse with an amplitude proportional to the deposited energy. One of the interesting features of semiconductors is their excellent energy resolution with respect to the scintillation detectors due to the larger number of information carriers produced per deposited unit of energy. For example, the measured energy resolution of a CdZnTe imager, DIGIRAD 2020TC [4.29], is 4% FWHM at 140 keV: two times better compared to a NaI based imager. This feature makes it possible to develop imaging systems which can reject Compton scattered photons more efficiently in SPECT studies, or discriminate between gamma lines close to each other in dual isotope SPECT imaging.

Among the available solid state detector materials, the most promising ones for room temperature  $\gamma$  ray imaging are CdTe and CdZnTe (CZT). However, there

are some shortcomings that prevent their broad use in imaging: poor hole collection, moderate electron collection and non-uniformity over large volumes worsen the energy resolution in thick detectors. The two main methods used to improve the energy resolution are: (i) electronic measure of lost charge using the rise time of the induced signal and its correction, and (ii) use of a segmented anode so that the collected charge depends primarily on electron movement near the anode. The intrinsic efficiency for the actual CdTe and CZT crystal is satisfactory for SPECT application, and fabrication costs limit the use in small field of view devices. Examples of applications of CZT to SPECT imaging are the PEGASE [4.30] and NUCAM3 [4.31] projects. The PEGASE project has developed a CZT gamma camera with an active area of 18 cm × 21.5 cm. Each detector module is a 4 × 4 pixel array of CZT; each pixel has dimensions of 4 mm × 4 mm × 6 mm, and the readout is based on an ASIC circuit. The PEGASE prototype currently includes 10 × 12 modules, and the measured energy resolution is 6.5% at 122 keV, with a detection efficiency of 70%.

The NUCAM3 project has been developed with the aim of replacing clinical gamma cameras in applications such as cardiology and scintimammography. The NUCAM3 camera is based on segmented pad monolithic CZT detectors covering a useful field of view of 18.5 cm × 20.1 cm. The total number of detectors used is 528. They are 5 mm thick with a planar cathode and 16 pads on the anode. The camera includes a parallel collimator with square holes registered with the pad active region to minimize the dead area. The energy resolution is 4.5% at 140 keV, the spatial resolution is 7.5 mm at 10 cm from the collimator and the sensitivity is 190 counts/min/μCi.

Recently, the CZT detectors have been proposed for MR-compatible SPECT cameras [4.32] and the first results with a prototype SPECT imaging system are very promising.

#### 4.2.5. Collimators

In modern nuclear medicine, the scene is dominated by advances in electronics and digital computing technologies. However, image quality is heavily determined by the collimator. The use of a collimator is necessary in SPECT to localize the origin of incident photons. This is accomplished by rejecting stray photons by means of absorption. The collimation process involves a great loss of information: approximately 1 photon in 10 000 is able to pass through the hole and to contribute to image formation. Collimators are basically very simple pieces of instrumentation, but there are many ways of constructing them. There are several aspects which, in principle, have to be determined while designing a collimator: hole shape (circular, triangular, rectangular, hexagonal), hole array pattern (square, rhombic, triangular), hole convergence (parallel,

convergent, divergent, fan-beam, cone-beam), hole tapering, hole diameter, collimator thickness, hole separation (septum thickness), collimator-detector distance and material. Not all of these features have the same influence on the performance of the collimator; by far the most important parameter is the ratio between the size of hole and its length.

#### 4.2.5.1. Parallel collimator

The influence of this parameter is evident if one looks at the basic formulas that give the estimates of spatial resolution and efficiency of a generic parallel hole collimator (Fig. 4.9).

The spatial resolution  $R_c$  as a function of source distance  $z$ , is usually estimated from the FWHM of a point spread function (PSF) as:

$$R_c(z) = \frac{d}{L}(L + B + z) \quad (4.13)$$

Here,  $d$  is the hole diameter,  $L$  is the thickness of the collimator and  $B$  is the distance between the collimator back face and the image plane in the crystal. Hence, spatial resolution is improved by increasing the hole length or by increasing the number of holes per unit area (provided the septum thickness is adequate), so that a large number of small diameter holes can fit into the same overall area. In addition, and importantly, the spatial resolution can be improved by minimizing the distance between the source and the collimator surface. For a multihole configuration, the geometric efficiency  $G$  is given by:

$$G = k \frac{a_{\text{hole}}}{a_{\text{cell}}} \frac{a_{\text{hole}}}{4\pi L^2} \quad (4.14)$$

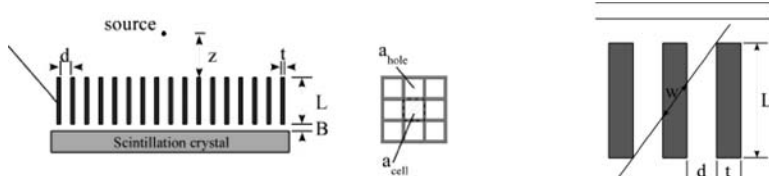


FIG. 4.9. Parallel collimator design with square holes and calculation of minimum path length.

where  $k$  is a factor depending on hole shape,  $a_{\text{hole}}$  is the area of a hole on the patient side,  $a_{\text{cell}}$  is the area of a single cell of a periodic hole array and  $L$  is the collimator thickness. The first factor in Eq. (4.14) is the ‘air-to-total’ ratio and the second factor estimates the fraction of solid angle subtended by a single hole. Note that  $G$  is independent of source–collimator distance for a point source imaged in air, since the inverse square law relationship is compensated for by the detector exposed area. An approximate relationship exists between  $R_c$  and  $G$  if  $z$  is much greater than  $L$  and if  $d$  is much greater than the septum thickness. This becomes  $G \propto R_c^2$ , thus the spatial resolution can only be improved at the expense of a reduced collimator geometric efficiency for a given septal thickness. The choice of the septum thickness is based on the necessity of reducing the penetration of the  $\gamma$  rays through the wall of the collimators. The most used criterion is to design collimators allowing a fixed fraction of photons to penetrate along the minimum path length through a single septum (Fig. 4.9).

The minimum path length  $w$  can be expressed as:

$$w = \frac{tL}{(2d + t)} \quad (4.15)$$

if the linear dimensions  $d$  of a single cell of the collimator are much smaller than the collimator thickness  $L$ . Here,  $t$  is the septum thickness. If the acceptable penetration effect is set to requiring that only 5% of the  $\gamma$  ray photons pass along the path, then  $\mu w \approx 3$  and the septum thickness  $t$  is:

$$t \approx \frac{6d}{\mu(L - 2/\mu)} \quad (4.16)$$

The performance characteristics of some commercially available parallel hole collimators are shown in Table 4.2.

TABLE 4.2. EXAMPLES OF COMMERCIALLY AVAILABLE PARALLEL HOLE COLLIMATORS AND THEIR PERFORMANCES

Type	d (mm)	L (mm)	t (mm)	$R_c$ (mm) at 10 cm	$G (\times 10^{-4})$	Septal penetration (%)
LEGP	1.4	25.4	0.31	7.89	1.6	0.8
LEHR	1.4	35.0	0.24	6.10	0.9	0.6

#### 4.2.5.2. Pinhole collimator

Currently, the most widely used collimator for small animal SPECT imaging is the pinhole. Although this collimator allows high spatial resolution, basically equal to the diameter of the pinhole, the sensitivity strongly depends on the distance from the collimators and reduces very rapidly with increasing distance. In fact, the fraction of isotropically emitted  $\gamma$  rays from the source, which pass through the pinhole, is given by the fraction of the solid angle of the pinhole, as seen from the source. If  $d$  is the diameter of the pinhole,  $b$  is the distance of the object from the pinhole and  $\theta$  is the angle shown in Fig. 4.10, the geometrical sensitivity is given by:

$$G_{\text{pinhole}} = \left( \frac{d}{4b} \right)^2 \sin^3 \theta \quad (4.17)$$

In Fig. 4.11, the sensitivity plotted as a function of the distance from the collimator hole for an on-axis point source can be seen. The field of view of a pinhole is defined by a cone projected from the pinhole onto the detector plane. It is clear that where the sensitivity is higher, the field of view is smaller. This kind of design is, therefore, suitable for very small animals such as mice. The spatial resolution of a pinhole is given by:

$$R_{\text{pinhole}} = \frac{d_e(a+b)}{a} \quad (4.18)$$

where  $a$  is the detector pinhole distance,  $b$  is the object pinhole distance and  $d_e$  is the effective pinhole diameter. The effective pinhole diameter is greater than the geometrical diameter because the incident radiation will penetrate the edge of the pinhole. An estimate of  $d_e$  can be obtained by the expression:

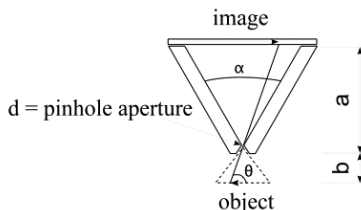


FIG. 4.10. Pinhole collimator design with square holes.

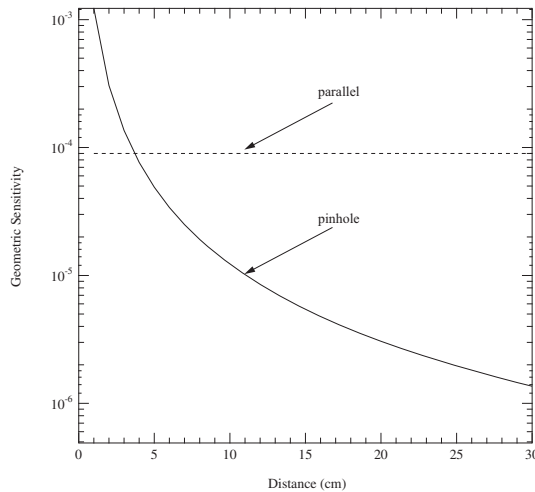


FIG. 4.11. Pinhole and parallel hole collimator sensitivity.

$$d_e = \sqrt{d \left[ d + \frac{2}{\mu} \tan\left(\frac{\alpha}{2}\right) \right]} \quad (4.19)$$

where  $d$  is the geometrical pinhole diameter,  $\mu$  is the linear attenuation coefficient of the pinhole material and  $\alpha$  is the angle of the pinhole as shown in Fig. 4.10. If the detector has a spatial resolution of  $R_d$ , the system will have a spatial resolution of:

$$R_{\text{tot}} = \sqrt{R_{\text{pinhole}}^2 + R_d^2 \left( \frac{b}{a} \right)^2} \quad (4.20)$$

where the factor  $b/a$  multiplying  $R_d$  accounts for the demagnification of the detector resolution intrinsic in pinhole systems.

It must be noted that an interesting characteristic of pinhole imaging is that, according to where the detector is placed behind the pinhole, there can be an enlargement factor of the projected image. Given a large enough detector, one can obtain a spatial resolution limited only by the pinhole even if the detector has a poor spatial resolution. Very small pinholes ( $100 \mu\text{m}$ ) have been successfully used to obtain sub-millimetre spatial resolutions. In this case,  $^{125}\text{I}$ , which emits fluorescence X rays in the range between 28 and 33 keV, is used. At these lower energies, the penetration of the X rays across the pinhole edges is small.

### 4.3. CLINICAL SYSTEMS

Most clinical SPECT systems used to perform patient studies still use a scintillation camera with NaI(Tl) coupled to an array of PMTs as the detector. These systems consist of one or more scintillation camera heads attached to a gantry that rotate around the patient to collect projection views. The most common configuration has two scintillation cameras that are fixed at 90° or 180°, or have the capability to be positioned at selected orientations. Typical imaging performances are given in Table 4.3.

One of the aims of emission tomography is the accurate measurement of activity distribution inside human or animal organs. There are several physics factors that degrade the image quality and the quantitative information as stated by Zaidi et al. [4.33]: (i) attenuation of photons travelling towards the detector, (ii) detection of scattered radiation as well as primary radiation, (iii) the finite spatial resolution of imaging systems, (iv) the limited number of counts that can be collected when imaging a patient and (v) physiological as well as patient motion. Measuring the attenuation map of the tissues inside the field of view of emission imaging system permits the attenuation and scatter corrections to be calculated [4.33]. The measurement can be performed by several techniques such as radionuclide transmission scanning, X ray transmission scanning and segmented MRI. However, the recent introduction of SPECT-CT systems has provided physicians with a new tool for handling the above problem.

#### 4.3.1. SPECT-CT

The development of SPECT-CT systems was started by Hasegawa et al. at the beginning of the 1990s [4.34, 4.35], with the goal of exploring the possibility of performing attenuation correction of the SPECT data, and to provide anatomical information for better definition of a region of interest inside a lesion

TABLE 4.3. TYPICAL PERFORMANCE VALUES FOR A CONVENTIONAL GAMMA CAMERA

No. of detectors	2
Field of view	40 cm × 55 cm
Energy resolution	10% FWHM at 140 keV
Intrinsic spatial resolution	3.8 mm FWHM
Planar count sensitivity (LEHR)	190 counts·s <sup>-1</sup> ·MBq <sup>-1</sup> (95 counts·s <sup>-1</sup> ·MBq <sup>-1</sup> per head)
SPECT spatial resolution (LEHR)	10.5 FWHM at 10 cm

for accurate radiopharmaceutical uptake. A lot of work has been done on the development of software algorithms for the co-registration of anatomical (CT) and functional (SPECT) images, and for the attenuation correction of SPECT images. Current software now gives accurate results and, hence, it is possible to visualize paired SPECT and CT images or both combined as shown in Fig. 4.12.

The first commercial SPECT-CT system, the GE Discovery Hawkeye system, was introduced in 1999 and was based on a dual-head variable geometry SPECT system. The CT system, integrated into the scanner, was composed of an X ray source operating at 140 kVp/2.5 mA and an X ray detector installed between the gamma camera heads. CT data is acquired in single slice mode over  $\pi$  radians, and CT slices are 10 mm thick with a matrix size of  $256 \times 256$ , corresponding to an in-plane resolution of approximately 1.5 mm [4.36]. During a typical imaging session, the system acquires 40 CT slices at a rate of three slices per minute. The current GE Healthcare system, the GE Infinia Hawkeye-4 system, incorporates an X ray source operating 120–140 kVp/500 mA and an X ray detector with 20 mm axial coverage (four slices, 5 mm thick). The spatial resolution is more than 3 lp/cm. The dose delivered to the patient is less than 5 mGy for a CT scan. The images acquired with this system are not of sufficient quality to be used for diagnostic purposes, but are sufficient for attenuation correction and anatomical correlation.

In 2004, the SPECT-CT systems introduced advanced CT systems, which are now being adopted in clinical practice. These systems, such as the Philips Precedence and Siemens Symbia (Fig. 4.13), join together a dual-head SPECT system with a multislice CT scanner, having similar performance to conventional diagnostic CT. The Precedence system couples a conventional 6 slice or 16 slice

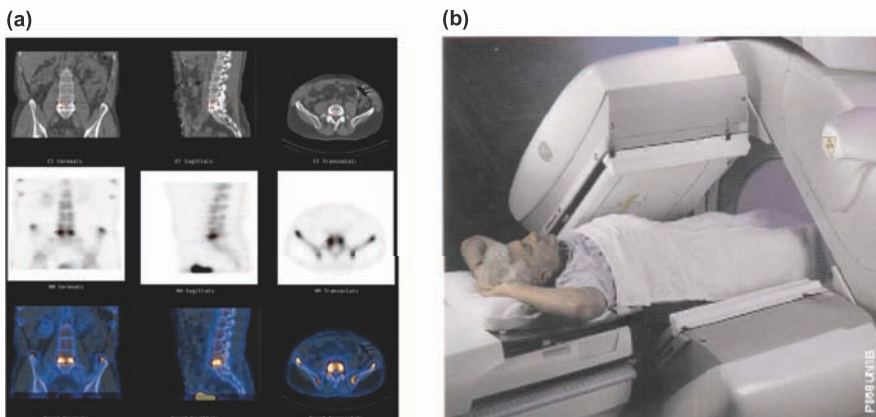


*FIG. 4.12. (a) SPECT-CT images obtained with the GE Hawkeye SPECT-CT system; (b) Picture of a GE Hawkeye. (Courtesy of GE Healthcare.)*

CT scanner, while the Symbia system incorporates a 1, 2 or 6 slice CT scanner. With both systems, CT slice thickness is variable and can be adjusted from 0.6 mm up to 10 mm. The scan speed for a 40 cm axial field is less than 30 s. These systems exhibit spatial resolutions of 13 to 15 lp/cm (line pairs), with approximately four to five times the patient dose of that from the Hawkeye system. The images acquired are of sufficient quality to be used for diagnostic purposes. However, these systems only permit the acquisition of CT studies at lower dose for attenuation correction application.

However, the SPECT-CT scanners require additional resources, including the increased cost of the system and room preparation, the quality control procedures for verifying the accuracy of registration between the two imaging modalities and the software for the correction of image artefacts due to patient motion during data acquisition.

#### 4.3.2. Cardiac SPECT systems

Many major commercial vendors offer SPECT systems optimized for myocardial perfusion imaging, the most commonly performed SPECT procedure. A major effort of customization has been performed to reduce the size of these systems, so that they can easily be placed in office size rooms. The systems offered by GE Healthcare, Siemens and Philips are dual-head systems with a fixed 90° geometry cardiac camera that rotates around the patient to acquire the projection data.

The Digirad Cardius system is available with up to three detector heads featuring pixelated CsI(Tl) crystals coupled to APD arrays. Each detector has 768 pixels with dimensions of 6 mm × 6 mm × 6 mm. During data acquisition, the gantry is kept stationary while the patient, sitting upright in a chair, is rotated. The

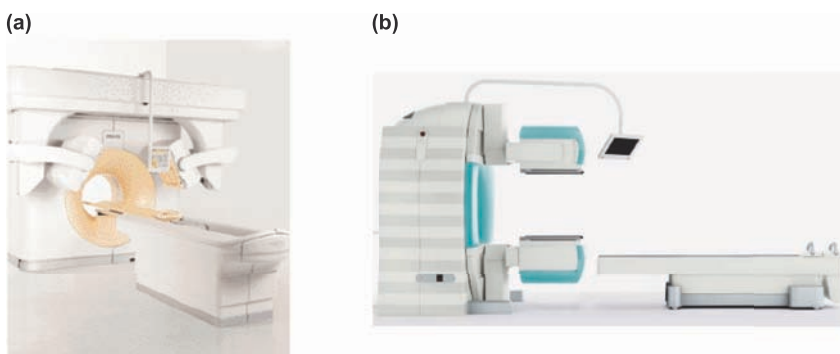


FIG. 4.13. (a) Philips Precedence system (courtesy of Philips); (b) Siemens Symbia system (courtesy of Siemens).

single detector sensitivity is 160 counts/min/ $\mu\text{Ci}$ , the energy resolution  $<10.5\%$  FWHM at 140 keV and the spatial resolution 11 mm FWHM, with an LEHR collimator and a 20 cm orbit radius [4.37]. The system is capable of performing a seven minute stress acquisition study.

Several new systems have been presented that use a different approach with respect to conventional SPECT systems, so that myocardial perfusion studies can be performed in a shorter time, thus improving throughput and patient comfort.

The CardiArc has a stationary array of detector boards (shown in green in Fig. 4.14) placed in a  $180^\circ$  arc surrounding the patient. Each detector is composed of pixelated CZT (or NaI). A thin sheet of lead (shown in grey in Fig. 4.14), called the ‘aperture arc’, is placed between the detectors and the patient. It has six vertical narrow slots that collimate incoming photons within each slot, defining a line of sight (shown in red in Fig. 4.14 (left) and 4.14 (right)) with each detector pixel. By rotating the aperture arc back and forth, each line of sight is scanned back and forth through the patient with very dense angular sampling. In a conventional system, the angular sampling is  $3^\circ$ ; in CardiArc, the angular sampling is  $0.14^\circ$ .

The vertical collimation is accomplished by stationary thin horizontal lead vanes (shown in light grey in Fig. 4.14 (right)), so that the combined effect of aperture arc and lead vanes is equivalent to an ultra long bore collimator for each detector pixel. Three different large swaths of rays are shown in Fig. 4.14 (left), corresponding to three different positions of aperture arc. The SPECT reconstructed spatial resolution is 4.3 mm FWHM at 10 cm and 6.4 mm FWHM at 20 cm. Typical scan times are 2–4 min, up to five times shorter than with a conventional scanner.

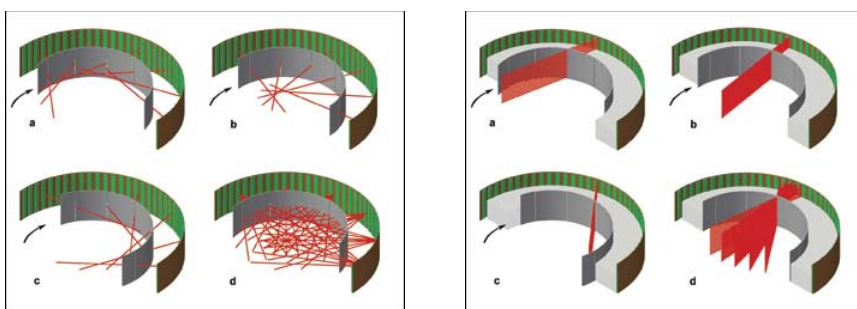


*FIG. 4.14. The CardiArc system: (left) the stationary detectors are shown in green, the aperture arc in grey, and several lines of sight are shown in red; (right) the axial collimation by lead vanes is shown in light grey. Multiple detector pixels use each aperture slot. (Courtesy of CardiArc.)*

The D-SPECT system has a different design and consists of ten individual collimated pixelated CZT modules, as shown in Fig. 4.15. Each detector is an array of  $16 \times 64$  CZT elements with dimensions of  $2.46 \text{ mm} \times 2.46 \text{ mm} \times 5 \text{ mm}$  and is equipped with a wide angle parallel hole collimator: the geometric efficiency is nearly  $7.5 \times 10^{-4}$ . The D-SPECT gantry is stationary, while each detector rotates back and forth to acquire the heart projection. Before the patient is placed on the chair, a scout scan is performed to determine the location of the heart. The average spatial resolution measured according to NEMA NU1 2001 is 5.7 mm FWHM at 15 cm and the energy resolution is 6% FWHM at 140 keV.

#### 4.4. SMALL ANIMAL SPECT

The SPECT imaging technique was originally developed for human use and was, thereafter, adapted for imaging small animals at high spatial resolution for basic and translational research. For research fields in which the development of new radiopharmaceuticals requires the evaluation of these tracers in small animals before clinical use or in which the investigation of molecular mechanisms of disease is performed by using transgenic and knockout mice, SPECT studies can be a valid alternative to ex vivo counting or autoradiography. Due to the size of the animals involved, the imaging devices need to meet specific spatial resolution and sensitivity requirements when the subjects are ten or more times smaller than humans.

In the last decade, small animal SPECT scanners have been developed following two different paths: (i) some devices are based on clinical  $\gamma$  ray detectors with a novel collimator design [4.38, 4.39] and (ii) other devices are based on dedicated small animal SPECT scanners with parallel, pinhole or

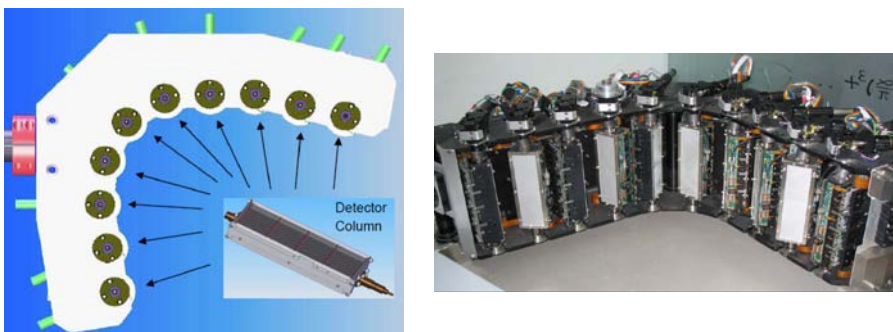


*FIG. 4.15. D-SPECT detector head consisting of ten detector columns. Each detector rotates back and forth to acquire projection data. (Courtesy of Spectrum-Dynamics.)*

slit-slat collimators [4.40–4.45, 4.4, 4.5]. Spatial resolution below 2 mm FWHM is easily achieved with investigational and commercial systems. The trend in small animal SPECT imagers is sub-millimetre spatial resolution with a high enough sensitivity. Multipinhole collimators seem to be one of the possible solutions.

#### 4.4.1. NanoSPECT

The NanoSPECT (from Bioscan) system combines patented multiplexed multipinhole (MMP) collimators [4.38] and up to a four head Mediso dedicated gamma camera with an intrinsic spatial resolution of 2.5 mm FWHM and a field of view of 23 cm × 21.5 cm. The multipinhole collimator was made in order that each pinhole views only a certain portion of the object, with all pinholes together covering the whole field of view. A certain fraction of overlap is present in the acquired projections but the iterative multipinhole algorithm makes the reconstruction of activity distribution without distortion or image artefacts possible. The detectors rotate around the animal for fast quantitative data acquisition through helical scanning.

The NanoSPECT picture is shown in Fig. 4.16(a), and has the following performance: the spatial resolution is 1.2 mm FWHM with 1.5 mm multipinholes and 0.8 mm FWHM with 1.0 mm multipinholes. The SPECT sensitivity range is from 1000 to 2500 counts/s/MBq with four detectors; the value is dependent on

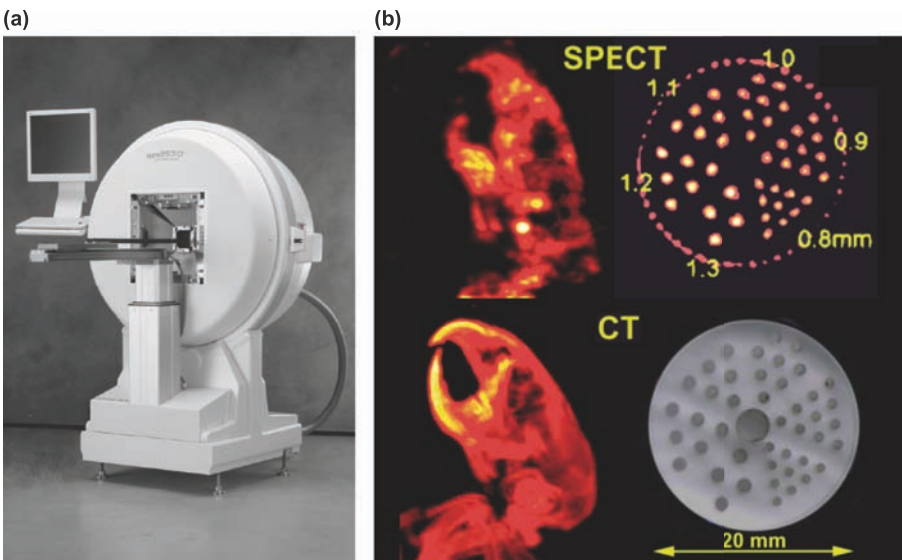


FIG. 4.16. (a) Picture of a NanoSPECT-CT scanner; (b) SPECT and CT image of a mouse brain and Jaszzczak phantom with  $^{99m}\text{Tc}$ . (Courtesy of Bioscan.)

the number of pinholes and ROR (radius of rotation). A sample image of a NanoSPECT-CT scanner is shown in Fig. 4.16(b). The commercial scanner is equipped with a cone-beam CT system: the X ray detector is a CMOS array with  $1024 \times 2048$  pixels and a  $50 \mu\text{m}$  pitch coupled to a scintillator. The CT reconstructed spatial resolution is  $<200 \mu\text{m}$ .

#### 4.4.2. U-SPECT-I

U-SPECT-I [4.39] is a stationary small animal SPECT system built by using a conventional gamma camera (PRISM3000, Picker Medial System 3 heads) and a cylindrical collimator with 75 gold micropinholes. The pinholes are placed in fivefold ring geometry (see Fig. 4.17(b)), with each ring containing an aperture of 15 pinholes. Overlap is prevented by placing a lead tube with 75 rectangular holes around the pinhole cylinder. The diameter of the pinholes is 0.6 mm. Gold was chosen as the material for the pinholes due to its higher stopping power compared to tungsten or lead, and better manufacturability and less toxicity with respect to depleted uranium. The central and longitudinal cross-section of the collimator (Fig. 4.17(c)) shows that the pinholes are tilted towards the centre of field of view so that the central portion of the field of view can be observed via 69 pinholes simultaneously: in this way, the sensitivity of the system is increased.

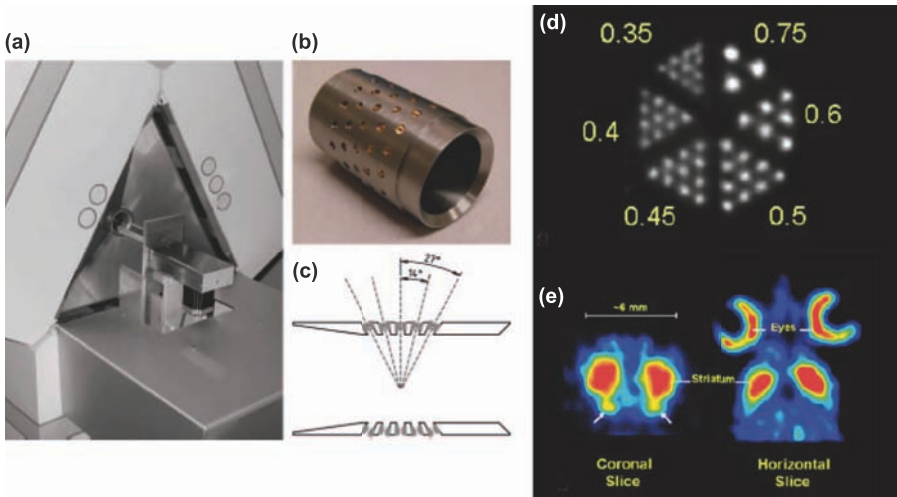


FIG. 4.17. (a) U-SPECT-I overview; (b) Cylinder with 75 gold pinholes; (c) Cross-section of cylinder. U-SPECT images: (d) Derenzo phantom image acquired with  $0.3 \text{ mm}$  pinholes; (e) Coronal and horizontal slices of an FP-CIT image of dopamine transporters in a mouse head acquired with  $0.6 \text{ mm}$  pinholes. (Courtesy of Beekman.)

The U-SPECT-I sensitivity with 0.6 mm pinholes is 0.22% at the centre (2200 counts/s/MBq) and 0.12% (1200 counts/s/MBq) within a cylindrical field of view with a diameter of 12 mm. The spatial resolution is 0.45 mm with 0.6 mm pinholes and 0.35 mm with 0.3 mm pinholes. An improved stand-alone version, U-SPECT-II, is being developed by the company MILabs. U-SPECT images are shown in Fig. 4.17(e). The next step in U-SPECT development is the use of CCD based detectors, exchanging low resolution large size  $\gamma$  ray detectors with high resolution small size ones [4.40].

#### 4.4.3. SpotImager

The SpotImager is a compact gamma camera developed at Arizona University [4.41, 4.42]. The detector is a slab of CdZnTe with dimensions of  $2.5\text{ cm} \times 2.5\text{ cm} \times 0.15\text{ cm}$ , and with a  $64 \times 64$  pixelated array of electrodes on the bottom and one continuous electrode on the top. The detector pitch is  $380\text{ }\mu\text{m}$  and the heart of the readout system is an ASIC. A high resolution parallel hole collimator, 7 mm thick, with  $64 \times 64$  holes that matches the CZT detector's pixels, is mounted in front of the gamma detector. The bore width is  $260\text{ }\mu\text{m}$  and the centre to centre spacing is  $380\text{ }\mu\text{m}$ . The collimator efficiency is  $5 \times 10^{-5}$  and the measured spatial resolution for a source 4 mm from the collimator face is  $450\text{ }\mu\text{m}$ .

#### 4.4.4. Fastspect-II

The FastSPECT-II system [4.43] is a small animal scanner that makes use of 16  $\gamma$  ray detector modules arranged as two rings. Each module is composed of a continuous NaI(Tl) scintillator 5 mm thick, a quartz light guide 1.5 cm thick and an array of  $3 \times 3$  photomultipliers with a diameter of 1.5 in. The collimator is an array of 1 mm diameter pinholes, one per module, mounted on a lead cylinder and converging towards the centre of the scanner field of view. In the basic geometry, suitable for small animal imaging, the magnification is approximately three, for a 2 in radius cylinder, and the sensitivity is 0.04%.

#### 4.4.5. A-SPECT system

The A-SPECT [4.44, 4.45] system consists of a high resolution small field of view camera head equipped with a pinhole collimator mounted on a gantry, with a rotating platform that holds the mouse or object to be imaged. The head is a compact  $15\text{ cm} \times 20\text{ cm} \times 12\text{ cm}$  scintillation camera employing a  $56 \times 56$  array of discrete  $2\text{ mm} \times 2\text{ mm} \times 6\text{ mm}$  NaI(Tl) crystals optically isolated from each other by 0.2 mm of diffuse opaque reflective material. The scintillator is coupled

to a position sensitive photomultiplier tube readout through a light guide. The detector sensitive area is approximately 12.5 cm × 12.5 cm. The pinhole collimator has a focal length of 9 cm and is equipped with several interchangeable pinhole apertures, ranging in diameter from 0.3 to 3 mm: the choice of pinhole aperture is based on the specific imaging situation. The A-SPECT tomographic spatial resolution is <1 mm, with a 0.5 mm pinhole, a radius of rotation of 3 cm and a sensitivity of ~3 counts/s/ $\mu$ Ci at 1 cm on the pinhole axis.

#### 4.4.6. Linoview

The small animal Linoview SPECT device [4.4] (Fig. 4.18 (left)) is based on four 2 in × 5 in (1 in = 2.54 cm)  $\gamma$  ray detectors. Each detector is composed of a pixelated CsI(Na) scintillator (5 mm thick, 21 × 52 pixels of 2.5 mm × 2.5 mm) coupled to ten 1 in position sensitive photomultiplier tubes (R8520-00-C12, Hamamatsu Photonics). The  $\gamma$  ray detector has an intrinsic spatial resolution of 2.5 mm, an intrinsic energy resolution of 35% at 140 keV and an intrinsic sensitivity in an energy window of 35% width centred on a photopeak of 42%.

The scanner uses linear orbit acquisition (LOrA) that generates linograms, forming a complete set of tomographic data by scanning the field of view along two orthogonal linear orbits [4.5]. The collimator has a slit aperture parallel to the longitudinal direction (Fig. 4.18 (right)). This aperture has a tuneable width,

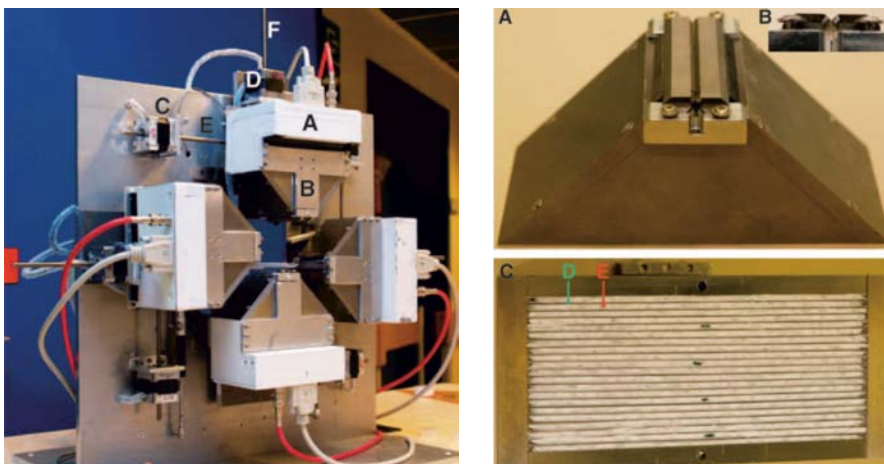


*FIG. 4.18. (left) Linoview SPECT device, consisting of four pixelated CsI(Na) detectors (A) coupled to rake collimators (B). The orbital and radial motions are obtained with a stepper motor (C and D). (right) Upper view of collimator with the slit aperture parallel to the longitudinal direction (A and B). Lateral view of the collimator showing tungsten sheets (D) sandwiched in polystyrene. (Courtesy of Linoview Systems.)*

0–5 mm, and is composed of two square iridium rods (2 mm × 2 mm × 60 mm) inserted in two linear sliding holders made of tungsten alloy. The distance between the slit aperture and the scintillator surface is 62 mm. Longitudinal collimation is achieved by 20 parallel trapezoidal tungsten sheets (55 mm high, 125 mm bottom width, 16 mm top width, 0.5 mm thick, 2 mm inter-space) sandwiched in a non-attenuating medium (extruded polystyrene). The orbit ranges of the detectors were set in such a way that the four slit apertures would draw the narrowest rectangle possible around the object to be imaged. The distance between the slit aperture and the phantom or the animal boundary was typically about 3 mm. Acquisitions were performed in a continuous motion. The acquired data were stored in list mode and including the following: detector number, ( $x, y$ ) event position, event time (ms) and event energy (256 channels).

#### 4.4.7. YAP-(S)PET

The YAP-(S)PET scanner is a small animal SPECT/PET system built by using a medium Z scintillator, the  $\text{YAlO}_3(\text{Ce})$  at Ferrara University. The commercial scanner [4.46] is made up of four detector heads, each one composed of a matrix of  $20 \times 20$  pillar crystals, 2 mm × 2 mm × 25 mm each. The matrix is directly coupled to a position sensitive photomultiplier (PS-PMT) (Hamamatsu R2486). In SPECT mode, each head is equipped with a parallel hole collimator (0.6 mm diameter, 0.15 mm septum, 20 mm thick), with an efficiency of  $2.8 \times 10^{-5}$ . The SPECT performance is: 24% energy resolution at 140 keV, 3 mm FWHM spatial resolution and 30 counts/s/MBq sensitivity. The PET performance is: 19% energy resolution at 511 keV, 2 mm FWHM spatial resolution and 18.7 counts/s/kBq sensitivity. The characteristic of this scanner is the capability to perform simultaneous PET/SPECT studies [4.47]. For this purpose, two opposing heads, equipped with a collimator and set in anticoincidence, independently acquire single events (SPECT mode); the other pair of heads detects coincidence events (PET mode). A subtraction procedure is performed to correct the SPECT images for the contribution of scattered 511 keV photons. One transverse section of a NEMA image quality phantom acquired in simultaneous modality is shown in Fig. 4.19; the phantom was filled with  $^{99\text{m}}\text{Tc}$  except for the two hollow chambers that were filled with  $^{18}\text{F}$ -FDG.

The possibility of performing simultaneous functional imaging opens the way to new and interesting protocols for the investigation of many biological phenomena.

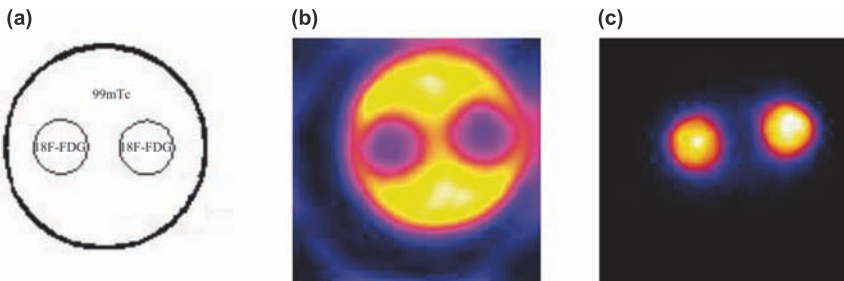


FIG. 4.19. (a) Picture of NEMA quality phantom section; (b) SPECT image; (c) PET image. (Courtesy of Del Guerra.)

#### 4.5. CONCLUSION

SPECT research in instrumentation continues to progress towards better spatial resolution and sensitivity because the limits have not yet been reached for clinical and small animal devices. At the same time, research for refinements in data reconstruction including scatter, attenuation and spatial resolution losses will permit more accurate and quantitative images, combined with anatomical information, to be acquired.

#### REFERENCES TO CHAPTER 4

- [4.1] ANGER, H.O., Scintillation camera, Rev. Sci. Instr. **29** (1958) 27.
- [4.2] KNOLL, G.F., Radiation Detection and Measurement, 3rd edn, John Wiley & Sons (2000).
- [4.3] WONG, T.Z., TURKINGTON, T.G., POLASCIK, T.J., COLEMAN, R.E., ProstaScint (capromab pentetide) imaging using hybrid gamma camera-CT technology, AJR **184** (2005) 676–680.
- [4.4] WALRAND, S., JAMAR, F., DE JONG, M., PAUWELS, S., Evaluation of novel whole-body high-resolution rodent SPECT (Linoview) based on direct acquisition of linogram projections, J. Nucl. Med. **46** (2005) 1872–1880.
- [4.5] WALRAND, S., VAN DULMEN, A., VAN ROSSEM, H., PAUWELS, S., Acquisition of linograms in SPET: implementation and benefits, Eur. J. Nucl. Med. **29** (2002) 1188–1197.
- [4.6] MOSES, W.W., SHAH, K.S., Potential for RbGd<sub>2</sub>Br<sub>7</sub>:Ce, LaBr<sub>3</sub>:Ce, LaBr<sub>3</sub>:Ce, and LuI<sub>3</sub>:Ce in nuclear medical imaging, Nucl. Instr. Meth. **A537** (2005) 317–320.

- [4.7] HAMMOND, W., et al., “Development of high performance mini gamma cameras based on LaBr<sub>3</sub> scintillator and H8500 and H9500 PSPMTs and their use in small animal studies” (Paper presented at IEEE Medical Imaging Conf. San Diego, CA, 2006).
- [4.8] KUBO, H., et al., “Development of gamma camera based on an 8×8 array of LaBr<sub>3</sub>(Ce) scintillator pixels coupled to a 64-channel multi-anode PMT” (Conf. Record IEEE Nuclear Science Symp., 2007), NM1-1, 4569–4573.
- [4.9] BARRET, H.H., SWINDELL, W., Radiological Imaging. The Theory of Image Formation, Detection, and Processing, Academic Press, New York, NY (1981).
- [4.10] PANI, R., et al., “Imaging evaluation of CsI(Tl) arrays for scintimammography” (Proc. IEEE Medical Imaging Conf. 2000), Vol. 3, 105–108.
- [4.11] SCHRAMM, N., WINWAR, A., SONNENBERG, F., HALLING, H., Compact high resolution detector for small animal SPECT, IEEE Trans. Nucl. Sci. **41** (2000) 1163–1167.
- [4.12] DEL GUERRA, A., DI DOMENICO, G., SCANDOLA, M., ZAVATTINI, G., High spatial resolution small animal YAPPET, Nucl. Instr. Meth. **A409** (1998) 537–541.
- [4.13] HAMAMATSU TECHNICAL DATA, Position Sensitive Photomultiplier Tubes With a Crossed-Wire Anode R2486 Series. August 1989 Rev., Supersedes October 1987, CR (2000).
- [4.14] KUME H., SUZUKI S., TAKEUCHI J., OBA K., Newly developed photomultiplier tubes with position sensitivity capability, IEEE Trans. Nucl. Sci. **NS-32** (1985) 448–452.
- [4.15] PANI, R., et al., Imaging detector designs based on flat panel PMT, Nucl. Instr. Meth. **A527** (2004) 54–57.
- [4.16] BELCARI, N., et al., “Tomographic approach to single-photon breast cancer imaging with a dedicated dual-head camera with VAOR (SPEMPT): Detector characterization” (Conf. Record IEEE Nuclear Science Symp., 2007), M13-61, 2901–2905.
- [4.17] SUN, X., et al., “A high resolution and high sensitivity small animal SPECT system based on H8500” (Conf. Record IEEE Nuclear Science Symp., 2007), M13-101, 2941–2943.
- [4.18] ZENIYA, T., WATANABE, H., AOI, T., et al., Use of a compact pixellated gamma camera for small animal pinhole SPECT imaging, Ann. Nucl. Med. **20** (2006) 409–416.
- [4.19] GRUBER, G.J., et al., A discrete scintillation camera module using silicon photodiode readout of CsI(Tl) crystals for breast cancer imaging, IEEE Trans. Nucl. Sci. **45** (1998) 1063–1068.
- [4.20] BERGERON, M., et al., “Performance evaluation of the LabPET™ APD-based digital PET scanner” (Conf. Record IEEE Nuclear Science Symp., 2007), 4185–4191.
- [4.21] VASKA, P., et al., RatCAP: miniaturized head-mounted PET for conscious rodent brain imaging, IEEE Trans. Nucl. Sci. **51** (2004) 2718–2722.
- [4.22] McCLISH, M., et al., Recent advances of planar silicon APD technology, Nucl. Inst. Meth. **A567** (2006) 36–40.
- [4.23] MOEHRS, S., DEL GUERRA, A., HERBERT, D.J., MANDELKERN, M.A., A detector head for small animal PET with silicon photomultipliers (SiPM), Phys. Med. Biol. **51** (2006) 1113–1127.

- [4.24] YAMAMOTO, K., et al., “Development of MultiPixel photon counter (MPPC)” (Conf. Record IEEE Nuclear Science Symp., 2007), N24-922007, 1511–1515.
- [4.25] LLOSA, G., et al., “Silicon photomultipliers and SiPM matrices as photodetectors in nuclear medicine” (Conf. Record IEEE Nuclear Science Symp., 2007), M14-4, 3220–3223.
- [4.26] DARAMBARA, D.G., TODD-POKROPEK, A., Solid state detectors in nuclear medicine, *Q. J. Nucl. Med.* **46** (2000) 3–7.
- [4.27] EISEN, Y., SHOR, A., MARDOR, I., CdTe and CdZnTe X-ray and gamma-ray detectors for imaging systems, *IEEE Trans. Nucl. Sci.* **51** (2004) 1191–1198.
- [4.28] SCHEIBER, C., GIAKOS, G.C., Medical applications of CDte and CdZnTe detectors, *Nucl. Instr. Meth.* **A458** (2001) 12–25.
- [4.29] BUTLER, J.F., et al., CdZnTe solid state gamma camera, *IEEE Trans. Nucl. Sci.* **45** (1998) 359–363.
- [4.30] MESTAIS, C., et al., A new design for a high resolution, high efficiency CZT gamma camera, *Nucl. Instr. Meth.* **A458** (2001) 62–67.
- [4.31] EISEN Y., et al., “NUCAM3 – a gamma camera based on segmented monolithic CdZnTe detectors” (Conf. Record IEEE Nuclear Science Symp., 2001), 1055–1059.
- [4.32] AZMAN, S., et al., “A nuclear detector system with integrated readout for SPECT/MR small animal imaging” (Conf. Record IEEE Nuclear Science Symp., 2007), 2311–2317.
- [4.33] ZAIDI, H., HASEGAWA, B., Determination of the attenuation map in emission tomography, *J. Nucl. Med.* **44** (2003) 291–315.
- [4.34] HASEGAWA, B.H., REILLY, S.M., GINGOLD, E.L., Design consideration for simultaneous emission-transmission CT scanner, *Radiology* **173** (1989) 414.
- [4.35] HASEGAWA, B.H., GINGOLD, E.L., REILLY, S.M., “Description of simultaneous emission-transmission CT system” (Proc. Conf. SPIE 1231, 1990), 50–60.
- [4.36] WONG, K.H., TANG, H.R., SEGALL G., HASEGAWA, B.H., “Development of quantitative imaging methods for the GE Hawkeye CT/SPECT system” (Proc. IEEE Conf., 2001), M13C-10, 2170–2173.
- [4.37] BABLA, H., BAI, C., CONWELL, R., “A triple-head solid state camera for cardiac single photon emission tomography (SPECT)” (Proc. Conf. SPIE 6319, 2006), 63190M.1–63190M.5.
- [4.38] SCHRAMM, N.U., et al., High-resolution SPECT using multiple pinhole collimation, *IEEE Trans. Nucl. Sci.* **50** (2003) 315–320.
- [4.39] BEEKMAN, F.J., et al., U-SPECT-I: a novel system for submillimeter-resolution tomography with radiolabeled molecules in mice, *J. Nucl. Med.* **46** (2005) 1194–1200.
- [4.40] BEEKMAN, F.J., VASTENHOUW, B., Design and simulation of a high-resolution stationary SPECT system for small animals, *Phys. Med. Biol.* **49** (2004) 4579–4592.
- [4.41] KASTIS, G.A., et al., Tomographic small-animal imaging using a high resolution semiconductor camera, *IEEE Trans. Nucl. Sci.* **49** (2002) 172–175.
- [4.42] KASTIS, G.A., et al., Compact CT/SPECT small-animal imaging system, *IEEE Trans. Nucl. Sci.* **51** (2004) 63–67.
- [4.43] FURENLID, L.R., et al., FastSPECT II: a second generation high-resolution dynamic SPECT imager, *IEEE Trans. Nucl. Sci.* **51** (2004) 631–635.

- [4.44] McDONALD, L.R., et al., Pinhole SPECT of mice using LumaGEM gamma camera, *IEEE Trans. Nucl. Sci.* **48** (2001) 830–836.
- [4.45] McELROY, D.P., et al., Performance evaluation of A-SPECT: a high resolution desktop pinhole SPECT system for imaging small animals, *IEEE Trans. Nucl. Sci.* **49** (2002) 2139–2147.
- [4.46] DEL GUERRA, A., et al., Performance evaluation of the fully engineered YAP-(S)PET scanner for small animal imaging, *IEEE Trans. Nucl. Sci.* **53** (2006) 1078–1083.
- [4.47] BARTOLI, A., BELCARI, N., DEL GUERRA, A., FABBRI, S., “Simultaneous PET/SPECT imaging with the small animal scanner YAP-(S)PET” (*Conf. Record IEEE Nuclear Symp.*, 2007), 3408–3413.

## **Chapter 5**

### **CATIONIC $^{99m}\text{Tc}$ COMPLEXES AS RADIOTRACERS FOR MYOCARDIAL PERFUSION IMAGING**

S. LIU

School of Health Sciences, Purdue University,  
West Lafayette, Indiana,  
United States of America

A. DUATTI

Laboratory of Nuclear Medicine, Department of Radiological Sciences,  
University of Ferrara, Ferrara,  
Italy

#### **Abstract**

Ischaemia related diseases, particularly coronary artery disease (CAD), account for the majority of deaths worldwide. Myocardial ischaemia is a serious condition and delay in reperfusion of ischaemic tissues can be life threatening. This is particularly true in the aged population. Rapid and accurate early detection of myocardial ischaemia is highly desirable, so that various therapeutic regimens can be administered before irreversible myocardial damage occurs. Myocardial perfusion imaging with radiotracers is an integral component in the evaluation of patients with known or suspected CAD. Technetium-99m-Sestamibi and  $^{99m}\text{Tc}$ -Tetrofosmin are commercial radiopharmaceuticals currently available for myocardial perfusion imaging. Despite their widespread clinical applications, neither  $^{99m}\text{Tc}$ -Sestamibi nor  $^{99m}\text{Tc}$ -Tetrofosmin meet the requirements of an ideal perfusion imaging agent, in large part, due to their high liver uptake. The intense liver uptake makes it difficult to interpret the heart activity in the inferior and left ventricular wall. Photon scattering from high liver activity remains a significant challenge for diagnosis of heart disease, despite intense efforts to reduce this interference. This review will summarize the most recent developments in ether containing and crown ether containing cationic  $^{99m}\text{Tc}$  radiotracers that have fast liver clearance with heart:liver ratios substantially better than those of  $^{99m}\text{Tc}$ -Sestamibi and  $^{99m}\text{Tc}$ -Tetrofosmin. Fast liver clearance will shorten the duration of imaging protocols (<30 min post-injection) and will allow for early acquisition of high quality heart images. Improvement of the heart:liver ratio may permit better detection of the presence and extent of CAD. Identification of such a new radiotracer that allows for the improved non-invasive delineation of myocardial perfusion would be of considerable benefit in the treatment of patients with suspected CAD.

## 5.1. INTRODUCTION

Heart diseases are the leading causes of death worldwide. Among the heart diseases, coronary artery disease (CAD) is a leading cause of premature and permanent disability. CAD arises from gradual narrowing of the coronary artery due to atherosclerotic deposits. The progressive narrowing of the coronary artery eventually predisposes the patient to myocardial ischaemia, a condition in which coronary blood flow decreases to a level below what is needed to meet the demand for oxygen and nutrients. When coronary arterial lumen diameter is reduced by 50%, perfusion abnormalities can be detected but patients are usually asymptomatic. When the diameter is reduced by 70%, clinical symptoms occur during myocardial stress because tissue oxygenation is temporarily below what is needed for adequate heart function. In advanced ischaemic CAD, blood flow and tissue oxygenation are too low to sustain cardiac function at rest. As a result, myocardial infarction occurs, and the affected muscle dies. Thus, rapid and accurate early detection of myocardial ischaemia and infarction is highly desirable so that appropriate therapeutic regimens can be administered before irreversible myocardial damage occurs.

Diagnostic radiotracers are small molecules labelled with a gamma emitter for single photon emission computed tomography (SPECT) or a positron emitter for positron emission tomography (PET). Nuclear cardiology plays a key role in CAD patient management [5.1–5.11]. Precise measurement of regional blood flow has significant clinical importance in identifying ischaemia, defining the extent and severity of disease, assessing myocardial viability, establishing the need for medical and surgical intervention, and monitoring the effects of treatment. For myocardial perfusion imaging, the radiotracer must be taken up into myocardium in proportion to blood flow in order to evaluate areas with reduced blood flow due to ischaemia. If the patient has CAD, there will be an area of reduced radiotracer uptake in myocardium, corresponding to the area of reduced blood flow. If the area of reduced uptake is worse under stress conditions than that at rest, the perfusion abnormality is most likely due to ischaemia. Information gained during perfusion imaging studies can be used not only to identify CAD but also to give insight into the patient's prognosis, such as the probability of a serious cardiac event (myocardial infarction or cardiac related death).

SPECT imaging is an integral component in current clinical practice in evaluation of patients with known or suspected CAD. The introduction of  $^{201}\text{Tl}$  in the 1970s was the turning point in the widespread clinical use of myocardial perfusion imaging and has had a profound impact on therapeutic decision making in patients with CAD over the last three decades. However, the combination of long half-life ( $t_{1/2} = 73\text{ h}$ ), attenuation artefacts due to low abundance of gamma

photons and the low count rate from dose constraints may result in suboptimal images in a significant proportion of perfusion imaging studies using  $^{201}\text{TI}$ . In addition,  $^{201}\text{TI}$  images should be taken as soon as it is injected into the patient due to its distribution and redistribution dynamics, which may not be suitable for situations where immediate imaging is not possible (e.g. patients with acute myocardial infarction). Compared to  $^{201}\text{TI}$ ,  $^{99\text{m}}\text{Tc}$  yields relatively high energy photons ( $\sim 140$  keV) and can be used at high doses due to its short half-life ( $t_{1/2} = 6.01$  h). The use of  $^{99\text{m}}\text{Tc}$  allows simultaneous assessment of myocardial perfusion and cardiac function in a single study [5.10, 5.11]. The combination of nuclear properties and diverse coordination chemistry makes  $^{99\text{m}}\text{Tc}$  the isotope of choice for the development of myocardial perfusion radiotracers. In the early 1980s, intensive efforts were focused on the development of  $^{99\text{m}}\text{Tc}$  complex radiopharmaceuticals [5.12]. As a result,  $^{99\text{m}}\text{Tc}$ -Sestamibi,  $^{99\text{m}}\text{Tc}$ -Tetrofosmin and  $^{99\text{m}}\text{Tc}$ -Teboroxime (Fig. 5.1) have been approved as commercial radiopharmaceuticals for myocardial perfusion imaging in nuclear cardiology. These cationic  $^{99\text{m}}\text{Tc}$  radiotracers are highly lipophilic with cationic or neutral charge, contain at least two ether like linkages (N-O-R or C-O-R) and are excreted through the hepatobiliary system due to their high lipophilicity.

An ideal perfusion radiotracer should have a high heart uptake with stable myocardial retention, which linearly tracks myocardial blood flow over a wide range. The uptake in the liver and lungs should be minimal, so that diagnostically

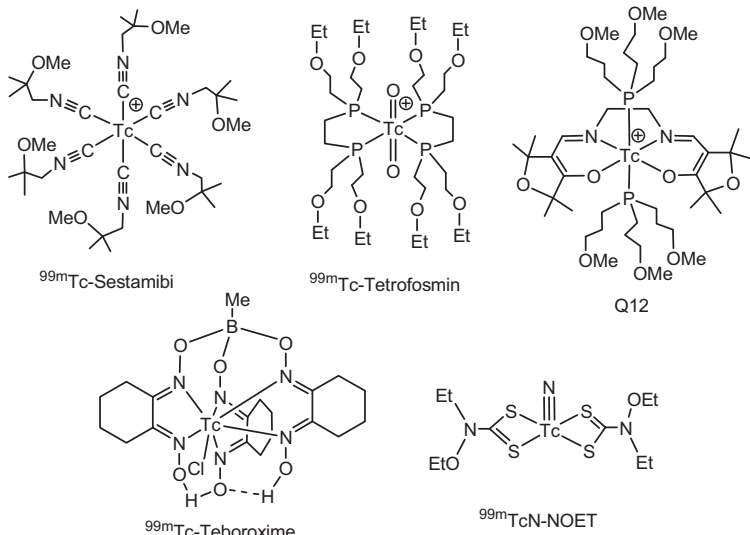


FIG. 5.1.  $^{99\text{m}}\text{Tc}$  radiotracers useful for heart imaging.  $^{99\text{m}}\text{Tc}$ -Sestamibi,  $^{99\text{m}}\text{Tc}$ -Tetrofosmin and  $^{99\text{m}}\text{Tc}$ -Teboroxime have been approved as commercial radiopharmaceuticals for myocardial perfusion imaging.

useful images can be obtained within 30 min post-injection. Despite their widespread clinical applications, both  $^{99m}\text{Tc}$ -Sestamibi and  $^{99m}\text{Tc}$ -Tetrofosmin do not meet the requirements of an ideal perfusion imaging agent due to their relatively low first-pass extraction fraction and high liver uptake [5.13]. The intense liver uptake makes it difficult to interpret the heart activity in the inferior and left ventricular wall, while a low first-pass extraction fraction often leads to inaccurate determination of blood flow characteristics. Thus, there is an unmet medical need for a new radiotracer that has a faster liver clearance and better first-pass extraction fraction than  $^{99m}\text{Tc}$ -Sestamibi and  $^{99m}\text{Tc}$ -Tetrofosmin.

This review article summarizes the most recent developments in cationic  $^{99m}\text{Tc}$  myocardial perfusion radiotracers. It focuses on the use of ether and crown ether groups to improve the liver clearance of cationic  $^{99m}\text{Tc}$  complexes. The main objective of this review is to illustrate that coordination chemistry continues to play a pivotal role in the development of new cationic  $^{99m}\text{Tc}$  radiotracers. The ultimate goal is to develop new radiotracers that will satisfy the unmet medical need and serve a large population of patients with known or suspected CAD.

## 5.2. NEW CATIONIC $^{99m}\text{Tc}$ RADIOTRACERS FOR MYOCARDIAL PERFUSION IMAGING

### 5.2.1. Improving liver clearance by ether groups

The usefulness of ether groups in reducing radiotracer liver uptake was first observed in the development of  $^{99m}\text{Tc}$ -Sestamibi [5.14–5.16]. Since then, various ether containing ligands or chelators have been used to improve T:B ratios of cationic  $^{99m}\text{Tc}$  complexes [5.17–5.21]. For example, studies on the Q-series of  $^{99m}\text{Tc}$  complexes have shown that ethers on phosphine ligands could improve heart uptake and imaging properties [5.17].  $^{99m}\text{Tc}$ -Sestamibi,  $^{99m}\text{Tc}$ -Tetrofosmin and Q12 all contain six or more ether groups, and show better liver clearance than  $^{99m}\text{Tc}$ N-Noet and  $^{99m}\text{Tc}$ -Teboroxime (Fig. 5.1).

### 5.2.2. Ether containing cationic $^{99m}\text{Tc}$ -nitrido complexes

Duatti's group recently reported a series of asymmetric cationic  $^{99m}\text{Tc}$ -nitrido complexes (Fig. 5.2), which contain a  $[^{99m}\text{Tc}\equiv\text{N}]^{2+}$  core, a bidentate dithiocarbamate (DTC) and a PNP type bisphosphine [5.22]. It has been demonstrated that the amine-N donor atom in the PNP bisphosphine is invariably in trans to the  $\text{Tc}\equiv\text{N}$  triple bond [5.22, 5.23]. The nitrogen heteroatom is important for providing stabilization for the  $[^{99m}\text{Tc}\equiv\text{N}]^{2+}$  core. It is remarkable

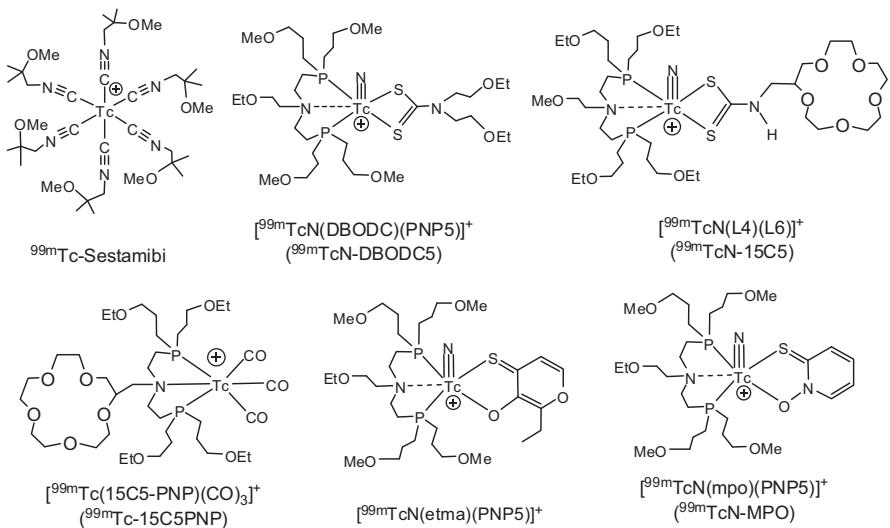
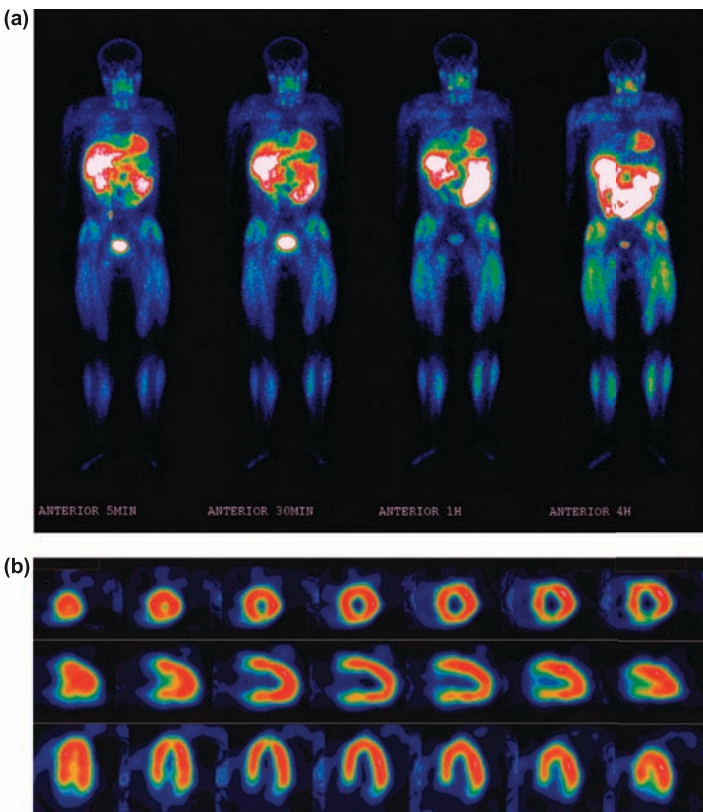


FIG. 5.2. New  $^{99m}\text{Tc}$  radiotracers useful for myocardial perfusion imaging.

that the combination of DTC and a PNP bisphosphine results in a high yield and high radiochemical purity of cationic  $^{99m}\text{Tc}$ -nitrido complexes [5.22, 5.23]. Results from animal studies show that both DTCs and bisphosphines have a significant impact on the biodistribution properties and excretion kinetics of cationic  $^{99m}\text{Tc}$ -nitrido complexes [5.24–5.27]. Among the cationic  $^{99m}\text{Tc}$ -nitrido complexes evaluated in Sprague-Dawley rats,  $^{99m}\text{TcN-DBODC5}$  (Fig. 5.2) has a high heart uptake and is retained in the rat heart for more than 2 h [5.24, 5.25]. The liver uptake is almost completely eliminated at 2 h post-injection, with the heart:liver ratio being ten times better than that of  $^{99m}\text{Tc}$ -Sestamibi [5.24, 5.25]. Results from SPECT imaging studies in Sprague-Dawley rats show that  $^{99m}\text{TcN-DBODC5}$  has a fast liver clearance, and is able to give clear images of the heart as early as 15 min post-injection [5.26]. In contrast,  $^{99m}\text{TcN-DBODC6}$  showed much lower heart uptake and T:B ratios than  $^{99m}\text{TcN-DBODC5}$  due to the higher lipophilicity of PNP6, even though they share the same DBODC ligand [5.24, 5.25]. These results clearly indicated that it is possible to develop new cationic  $^{99m}\text{Tc}$  radiotracers with much better heart:liver ratios than those of  $^{99m}\text{Tc}$ -Sestamibi by appropriate molecular design.  $^{99m}\text{TcN-DBODC5}$  was reported to have a first-pass extraction fraction between that of  $^{99m}\text{Tc}$ -Sestamibi and  $^{99m}\text{Tc}$ -Tetrofosmin [5.27].  $^{99m}\text{TcN-DBODC5}$  is currently under clinical investigation as a new SPECT myocardial perfusion radiotracer. Preliminary results from SPECT imaging studies indicate that the heart and liver (Fig. 5.3) are well separated in healthy human subjects administered with ~10 mCi of



*FIG. 5.3. Whole body planar image (a) and SPECT images of the heart (b) in a normal human subject administered with 10 mCi of  $^{99m}\text{TcN-DBODC5}$ . The heart is well separated from the liver as early as 30 min post-injection.*

$^{99m}\text{TcN-DBODC5}$ , and very clear planar and SPECT images of the heart could be obtained as early as 30 min post-injection.

Bidentate chelators (Fig. 5.4), such as 2-mercaptopypyridine oxide (Hmpo), 1,2-dimethyl-3-hydroxy-4-thiopyridinone (Hdmtp), thiomaltol (Htma) and ethylthiomaltol (Hetma) have been used to replace DTCs for the preparation of cationic complexes  $[^{99m}\text{TcN(L)(PNP)}]^+$  (L = tma, etma, dmtp and mpo; PNP = PNP5, PNP6 and L6) [5.28]. The use of these bidentate chelators offers great structural diversity and allows easy modification of the lipophilicity and biological properties of cationic  $^{99m}\text{Tc}$  radiotracers.

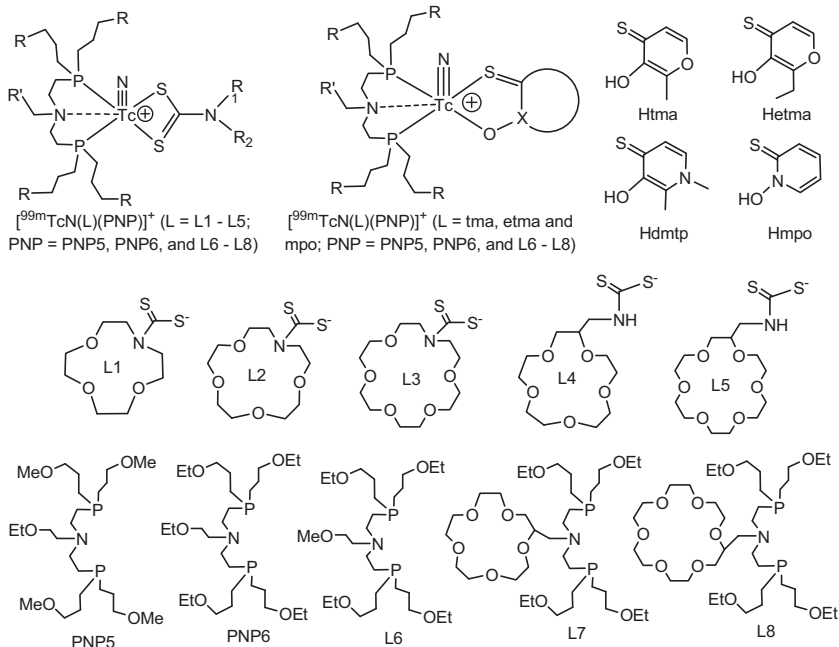


FIG. 5.4. Crown ether containing DTCs, bisphosphines and their cationic  $^{99m}\text{Tc}$ -nitrido complexes.

### 5.2.3. Crown ether containing cationic $^{99m}\text{Tc}$ -nitrido complexes

The crown ether containing DTCs and bisphosphine coligands (Fig. 5.4) are of particular interest because: (i) they form stable cationic  $^{99m}\text{Tc}$ -nitrido complexes and (ii) crown ethers are able to balance the lipophilicity of cationic  $^{99m}\text{Tc}$ -nitrido complexes without changing their overall molecular charge [5.29, 5.30]. In general, lipophilicity of the radiotracer decreases as the number of ether linkages increases. Bisphosphines also have a significant impact on the lipophilicity of their cationic  $^{99m}\text{Tc}$ -nitrido complexes. For example,  $[^{99m}\text{TcN}(\text{L})(\text{PNP6})]^+$  is much more lipophilic than  $[^{99m}\text{TcN}(\text{L})(\text{PNP5})]^+$  because of the high lipophilicity of the four ethoxy groups in PNP6 [5.30].

### 5.2.4. Crown ether containing cationic $^{99m}\text{Tc(I)}$ -tricarbonyl complexes

The rich and diverse coordination chemistry of  $[^{99m}\text{Tc}(\text{CO})_3]^+$  offers a tremendous opportunity to develop new  $^{99m}\text{Tc(I)}$ -tricarbonyl radiotracers [5.31–5.37]. The  $[^{99m}\text{Tc}(\text{CO})_3]^+$  core has also been widely used to prepare target

specific  $^{99m}\text{Tc}$  radiotracers [5.34–5.37]. In  $[^{99m}\text{Tc}(\text{H}_2\text{O})_3(\text{CO})_3]^+$ , all three water molecules are labile with respect to substitution [5.38–5.40]. Monodentate ligands, dimethyl-3-methoxypropylphosphine (DMMPP) and 2-methoxyisobutylisonitriles (MIBI), have been used to prepare complexes  $[^{99m}\text{Tc}(\text{L})_3(\text{CO})_3]^+$  ( $\text{L} = \text{DMMPP}$  and  $\text{MIBI}$ ) [5.20, 5.21]. In Sprague-Dawley rats,  $[^{99m}\text{Tc}(\text{DMMPP})_3(\text{CO})_3]^+$  and  $[^{99m}\text{Tc}(\text{MIBI})_3(\text{CO})_3]^+$  showed high heart uptake. However, their heart:liver and heart:lung ratio is not as good as that of  $^{99m}\text{Tc}$ -Sestamibi due to slow hepatobiliary excretion [5.20, 5.21]. The major challenge is to maintain the ‘true’ cationic nature of  $[^{99m}\text{Tc}(\text{L})_3(\text{CO})_3]^+$  ( $\text{L} = \text{DMMPP}$  and  $\text{MIBI}$ ) in the blood circulation.

It has been reported that monodentate and bidentate ligands form  $^{99m}\text{Tc}(\text{I})$ -tricarbonyl complexes with relatively low solution stability, which may result in high protein binding and high background activity in blood [5.34–5.37]. The chloride anions in blood may react with cationic complexes  $[^{99m}\text{Tc}(\text{L})_3(\text{CO})_3]^+$  to form neutral complexes  $[^{99m}\text{Tc}(\text{L})_2(\text{CO})_3\text{Cl}]$  that have low heart uptake and slow hepatobiliary excretion. In contrast, PNP bisphosphines are able to form highly stable cationic complexes  $[^{99m}\text{Tc}(\text{CO})_3(\text{L})]^+$  (Fig. 5.4, PNP6 and L6–L8) [5.41, 5.42]. The tridentate bisphosphines are critical for maintaining cationic nature and have a significant impact on the biodistribution characteristics of the  $^{99m}\text{Tc}(\text{I})$ -tricarbonyl complexes. The crown ether containing bisphosphines (L7 and L8) are designed in such a way that the lipophilicity and biodistribution properties of their cationic  $^{99m}\text{Tc}(\text{I})$ -tricarbonyl complexes can be modified by changing the number of oxygen heteroatoms in the macrocycle [5.29, 5.41, 5.42].

### 5.2.5. Biodistribution and excretion characteristics of cationic $^{99m}\text{Tc}$ radiotracers

Biodistribution studies were performed in Sprague-Dawley rats on cationic complexes  $[^{99m}\text{TcN}(\text{L4})(\text{L6})]^+$  ( $^{99m}\text{TcN-15C5}$ ),  $[^{99m}\text{TcN}(\text{mpo})(\text{PNP5})]^+$  ( $^{99m}\text{TcN-MPO}$ ),  $[^{99m}\text{Tc}(\text{CO})_3(\text{L7})]^+$  ( $^{99m}\text{Tc-15C5PNP}$ ),  $^{99m}\text{Tc}$ -Sestamibi and  $^{99m}\text{TcN-DBODC5}$ . Figure 5.5 shows a comparison of their heart uptake and heart:liver ratios. In general, the heart uptake of  $^{99m}\text{TcN-15C5}$ ,  $^{99m}\text{TcN-MPO}$ ,  $^{99m}\text{Tc-15C5PNP}$  and  $^{99m}\text{TcN-DBODC5}$  is comparable within the experimental error, and is slightly lower than that of  $^{99m}\text{Tc}$ -Sestamibi, particularly at >60 min post-injection. However, their heart:liver ratio is much better than that of  $^{99m}\text{Tc}$ -Sestamibi at 30–120 min post-injection [5.43]. For example, the heart:liver ratio of  $^{99m}\text{TcN-MPO}$  ( $12.75 \pm 3.34$ ) at 30 min post-injection is almost twice that of  $^{99m}\text{TcN-DBODC5}$  ( $6.01 \pm 1.45$ ) and is approximately four times better than that of  $^{99m}\text{Tc}$ -Sestamibi ( $2.90 \pm 0.22$ ). The 2 min heart uptake ( $2.55 \pm 0.36$ ,  $2.35 \pm 0.29$ ,  $2.45 \pm 0.38$ ,  $2.35 \pm 0.34$  and  $2.87 \pm 0.47$  for  $^{99m}\text{TcN-MPO}$ ,

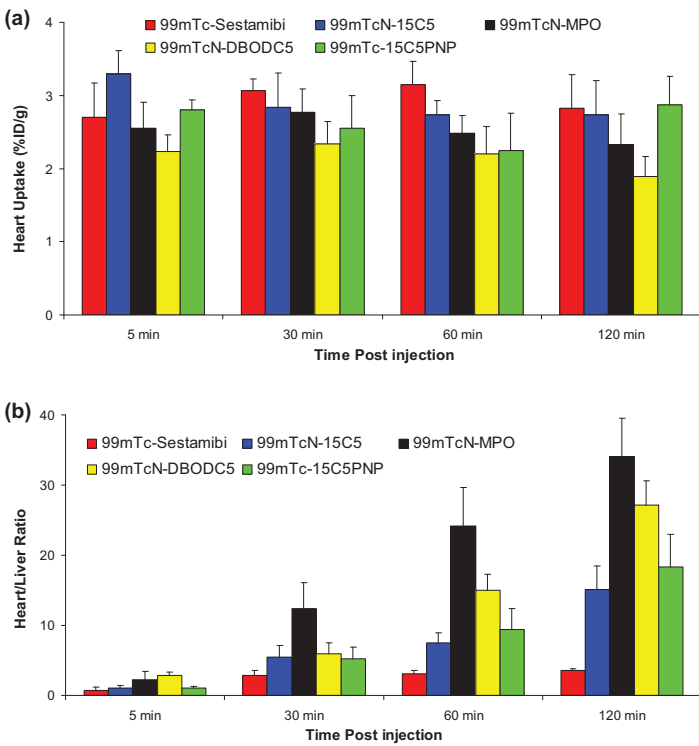


FIG. 5.5. Comparison of the heart uptake (a) and heart:liver ratios (b) between  $[^{99m}\text{TcN}(\text{L4})(\text{L6})]^+$ ,  $[^{99m}\text{TcN-15C5}]$ ,  $[^{99m}\text{TcN}(\text{mpo})(\text{PNP5})]^+$ ,  $[^{99m}\text{TcN-MPO}]$ ,  $[^{99m}\text{Tc}(\text{CO})_3(\text{L7})]^+$ ,  $[^{99m}\text{Tc-15C5PNP}]$ ,  $[^{99m}\text{Tc-Sestamibi}]$  and  $[^{99m}\text{TcN-DBODC5}]$  in Sprague-Dawley rats.

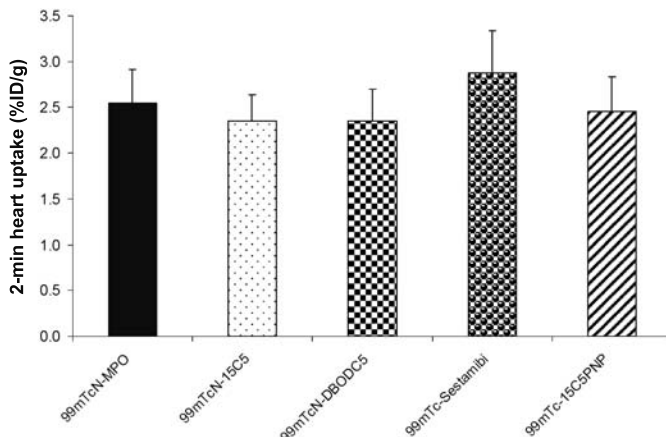


FIG. 5.6. The 2 min heart uptake (%ID/g) of  $^{99m}\text{TcN-15C5}$ ,  $^{99m}\text{TcN-MPO}$ ,  $^{99m}\text{Tc-15C5PNP}$ ,  $^{99m}\text{Tc-Sestamibi}$  and  $^{99m}\text{TcN-DBODC5}$ .

$^{99m}\text{TcN-15C5}$ ,  $^{99m}\text{Tc-15C5PNP}$ ,  $^{99m}\text{TcN-DBODC5}$  and  $^{99m}\text{Tc-Sestamibi}$ , respectively) suggests that the first-pass extraction fraction of  $^{99m}\text{TcN-MPO}$  (Fig. 5.6) is most likely between that of  $^{99m}\text{TcN-DBODC5}$  and  $^{99m}\text{Tc-Sestamibi}$  [5.43].

To further demonstrate its utility as a new radiotracer for myocardial perfusion imaging, SPECT imaging studies were performed on  $^{99m}\text{TcN-15C5}$  and  $^{99m}\text{Tc-Sestamibi}$  in canines [5.29]. In a normal dog under rest conditions,  $^{99m}\text{TcN-15C5}$  gives clear SPECT images of the heart at 30 min post-injection. In the same dog administered with  $^{99m}\text{Tc-Sestamibi}$ , however, the heart and liver are not well separated (Fig. 5.7). These promising results suggest that  $^{99m}\text{TcN-15C5}$  might be able to give clinically useful images of the heart as early as 30 min post-injection. Technetium-99m-N-15C5 has an advantage over  $^{99m}\text{Tc-Sestamibi}$  in patients with significant liver accumulation and retention. The crown ethers are

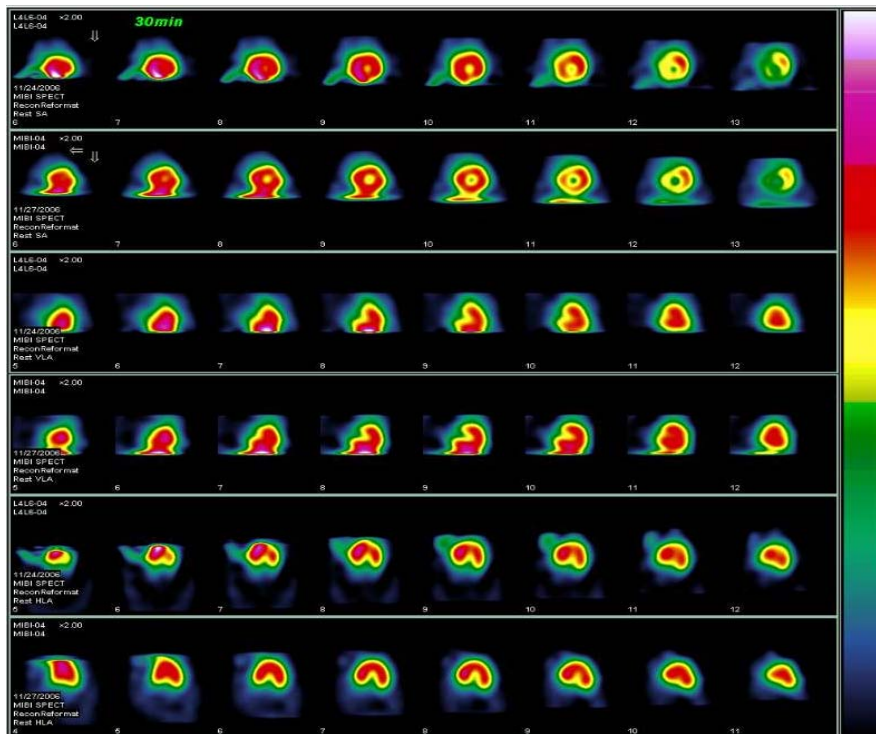


FIG. 5.7. SPECT images of the heart in a dog administered with  $^{99m}\text{TcN-15C5}$  and  $^{99m}\text{Tc-Sestamibi}$  at 30 min post-injection. Transverse (top), coronal (middle) and sagittal (bottom) views of the two tracers are given one below the other in the figure. The separation between heart and liver was clearly seen in the dog administered with  $^{99m}\text{TcN-15C5}$ , but was not well separated in the same dog administered with  $^{99m}\text{Tc-Sestamibi}$ .

very useful functional groups for the improvement of liver clearance of cationic  $^{99m}\text{Tc}$ -nitrido complexes [5.28–5.30, 5.41–5.43].

#### 5.2.6. Function of crown ethers

Crown ethers have been the subject of intense research for their potential as metal ion probes because of their ability to bind  $\text{K}^+$  and  $\text{Na}^+$  [5.44–5.46]. However, the formation of  $\text{K}^+$  and  $\text{Na}^+$  complexes with the crown ether groups in the crown ether containing cationic  $^{99m}\text{Tc}$  radiotracers is almost impossible due to the extremely low concentrations ( $<10^{-9}$  M in myocardial tissues) of the radiotracer and low stability ( $\log K = 10^3\text{--}10^5$  M) of  $\text{K}^+$  and  $\text{Na}^+$  complexes of 15-crown-5 and 18-crown-6 [5.47]. Thus, the crown ether groups in cationic  $^{99m}\text{Tc}$  radiotracers are mainly used as functional groups for modification of their lipophilicity and biological properties.

#### 5.2.7. Toxicity of crown ether containing chelators

15-crown-5 and 18-crown-6 have  $\text{LD}_{50}$  values  $>1000$  mg/kg in mice via IV injection (Sigma-Aldrich MSDS). Since the crown ether containing DTCs and bisphosphines are used at low dose ( $<1$  mg/25 mCi) during preparation of cationic  $^{99m}\text{Tc}$  radiotracers, their toxicity is expected to be minimal. In imaging studies, the amount of L4 and L7 injected into animals (rats and dogs) was as high as 0.5 mg per rat (2.0 mg/kg), which is  $>100$ -fold higher than the human dose ( $<1$  mg/25 mCi or  $\sim 15$  mg/kg for a 75 kg patient). No acute toxicity (vomiting, breathing difficulty or sudden death) has been observed during imaging studies in rats and dogs [5.30].

### 5.3. FACTORS INFLUENCING HEART UPTAKE AND LIVER CLEARANCE

#### 5.3.1. Localization mechanism

The heart localization mechanism for cationic  $^{99m}\text{Tc}$ -nitrido and  $^{99m}\text{Tc}$ (I)-tricarbonyl complexes remains unknown. Due to its similarity in molecular charge with  $^{99m}\text{Tc}$ -Sestamibi, it is reasonable to believe that they might share the same localization mechanism. It is well documented that  $^{99m}\text{Tc}$ -Sestamibi is able to penetrate plasma and mitochondrial membranes, and accumulate in mitochondria due to the negative mitochondrial potential [5.48–5.51]. Myocardium has the highest mitochondrial population, with mitochondria occupying up to 40% of the total volume of myocytes. Other mitochondrion rich organs include salivary

glands, liver and kidneys. This may explain why most lipophilic  $^{99m}\text{Tc}$  complex cations tend to have high uptake in mitochondrion rich organs, such as heart, liver and kidneys. For a  $^{99m}\text{Tc}$  radiotracer to localize in mitochondria, it must be able to cross several barriers: microvasculature, plasma membrane and mitochondrial membrane. While the contribution from mitochondrial potentials provides a driving force for the mitochondrial localization of cationic  $^{99m}\text{Tc}$  radiotracers, the lipophilicity might modulate their penetration capability across the lipophilic plasma and mitochondrial membranes.

### 5.3.2. Lipophilicity

Lipophilicity is an important factor influencing the biodistribution characteristics of cationic  $^{99m}\text{Tc}$  radiotracers [5.28–5.30, 5.41–5.43]. Studies on the localization mechanism of  $^{99m}\text{Tc}$ -Sestamibi indicate that both lipophilicity and cationic charge play a significant role in its selective localization and retention in myocardium [5.48–5.51]. In general, cationic  $^{99m}\text{Tc}$  radiotracers with a  $\log P > 1.5$  often have high protein binding and slow liver clearance, while more hydrophilic cationic radiotracers with a  $\log P < 0$  tend to show a fast washout from myocardium [5.17–5.19, 5.28–5.30, 5.41–5.43]. In both cases, the heart:liver ratio is low because of either high liver uptake or fast myocardial washout. While there is no clear-cut ‘optimal’  $\log P$  value, it is believed that cationic  $^{99m}\text{Tc}$  radiotracers should have a  $\log P$  value of 0.5–1.2 in order to achieve a high heart uptake and fast liver clearance at the same time [5.29].

### 5.3.3. Liver clearance and multidrug resistance gene expression

Many cationic  $^{99m}\text{Tc}$  radiotracers have been evaluated for their potential as radiotracers for heart imaging. However, it is not clear why certain cationic  $^{99m}\text{Tc}$  radiotracers show better liver clearance and heart:liver ratios than others even though they may have a similar lipophilicity. It is well documented that multidrug resistance (MDR) P-glycoprotein (*MDR1* Pgp), a 170 kDa plasma membrane transporter, is overexpressed in tumours [5.52–5.54], and in several organs with excretory functions, including kidneys and liver [5.55–5.57]. Many cationic  $^{99m}\text{Tc}$  radiotracers, such as  $^{99m}\text{Tc}$ -Sestamibi and  $^{99m}\text{Tc}$ -Tetrofosmin, originally developed as myocardial perfusion imaging agents, are also clinically useful for non-invasive imaging of MDR Pgp transport function in tumours [5.52–5.54, 5.58–5.60]. While several different genes have been shown to be associated with an MDR phenotype, *MDR1* Pgp represents one of the best characterized mediators of MDR, by altering the membrane permeability to cationic radiotracers and/or enhancing their efflux out of cancer cells. The *MDR1* Pgp transporter function on the biliary surface of hepatocytes would appear to explain

the difference in liver excretion kinetics of cationic  $^{99m}\text{Tc}$  radiotracers in terms of their ability to be substrates for *MDR*. Increased  $^{99m}\text{Tc}$ -Sestamibi uptake in normal liver of cancer patients after administration of G-protein inhibitors (XR9576 and SDZ PSC 833) has also been reported [5.60, 5.61].

#### 5.3.4. Metabolism

Metabolic stability is another important factor influencing the biodistribution properties of cationic  $^{99m}\text{Tc}$  radiotracers. Organic molecules can be metabolized by a number of pathways that occur mainly in the liver. The correlation between tissue metabolism and tissue residence time of metabolites relative to the parent compound might be an important factor influencing the retention of the radiotracer in the heart and other organs. Results from high performance liquid chromatography analysis of urine and faeces samples indicate that  $^{99m}\text{TcN-MPO}$ ,  $^{99m}\text{TcN-15C5}$ ,  $^{99m}\text{Tc-15C5PNP}$ ,  $^{99m}\text{TcN-DBODC5}$  and  $^{99m}\text{Tc}$ -Sestamibi all have minimal metabolism with very high metabolic stability in Sprague-Dawley rats under anaesthesia [5.30, 5.42, 5.43].

### 5.4. FUTURE DIRECTION

There are two obstacles to overcome in developing new cationic  $^{99m}\text{Tc}$  radiotracers: fast liver clearance and high first-pass extraction fraction. Through the use of ether containing and crown ether containing DTCs and bisphosphines, we are able to prepare cationic  $^{99m}\text{Tc}$ -nitrido and  $^{99m}\text{Tc}$ -tricarbonyl complexes that have much faster liver clearance with a heart:liver ratio substantially better than that of  $^{99m}\text{Tc}$ -Sestamibi. Results from a recent study suggest that the first-pass extraction fraction (~61%) of  $^{99m}\text{TcN-DBODC5}$  is between that of  $^{99m}\text{Tc}$ -Sestamibi (~65%) and  $^{99m}\text{Tc}$ -Tetrofosmin (~56%) [5.27]. Technetium- $^{99m}\text{N-DBODC5}$  does not track the blood flow as well as  $^{201}\text{Tl}$ , probably due to its relatively low first-pass extraction fraction. Thus, future research should focus on cationic  $^{99m}\text{Tc}$  radiotracers with both fast liver clearance and a better first-pass extraction fraction than  $^{99m}\text{Tc}$ -Sestamibi. In addition, other technetium cores can also be used to prepare cationic  $^{99m}\text{Tc}$  radiotracers with appropriate ether containing or crown ether containing chelators. For example, the  $^{99m}\text{Tc}$ -diazenido core has been used for preparation of cationic  $^{99m}\text{Tc(III)}$  complexes [ $^{99m}\text{Tc(NNPh)(DTC)(PNP)}]^+$  [5.62]. It was found that both DTCs and bisphosphines have a significant impact on the lipophilicity of their cationic  $^{99m}\text{Tc(III)}$  complexes. The addition of a phenyl group in the diazenido ligand imposes a significant challenge in balancing lipophilicity of cationic  $^{99m}\text{Tc}$ -diazenido complexes.

## 5.5. CONCLUSIONS

SPECT remains the modality of choice for myocardial perfusion imaging in current clinical practice. The success of SPECT in nuclear cardiology is, in large part, due to the development of new  $^{99m}\text{Tc}$  perfusion radiotracers (Fig. 5.1). Despite their wide application in nuclear medicine, neither  $^{99m}\text{Tc}$ -Sestamibi nor  $^{99m}\text{Tc}$ -Tetrofosmin meet the requirements of an ideal perfusion imaging agent due to their high liver uptake and relatively low first-pass extraction fraction. Thus, there is a continuing need for a better myocardial perfusion  $^{99m}\text{Tc}$  radiotracer that has a faster liver clearance than  $^{99m}\text{Tc}$ -Sestamibi and  $^{99m}\text{Tc}$ -Tetrofosmin.

Studies on ether containing and crown ether containing cationic  $^{99m}\text{Tc}$  complexes clearly show that it is possible to design cationic  $^{99m}\text{Tc}$  radiotracers with a heart:liver ratio substantially better than that of  $^{99m}\text{Tc}$ -Sestamibi. Fast liver clearance will shorten the duration of imaging protocols (<30 min post-injection), and allow for early acquisition of high quality images. Improvement of the heart:liver ratio will permit better detection of coronary disease with improved non-invasive delineation of myocardial perfusion. Preliminary data from animal studies on  $^{99m}\text{TcN-MPO}$ ,  $^{99m}\text{TcN-15C5}$ ,  $^{99m}\text{Tc-15C5PNP}$  and  $^{99m}\text{TcN-DBODC5}$  show that they might have a lower first-pass extraction fraction than  $^{99m}\text{Tc}$ -Sestamibi. Thus, future research should focus on cationic  $^{99m}\text{Tc}$  perfusion radiotracers with both fast liver clearance and a better first-pass extraction fraction. Identification of such a new radiotracer would be of considerable benefit in the treatment of patients with suspected CAD. It is very important to note that the overwhelming success of PET is largely due to the superiority of  $^{18}\text{FDG}$  as a proliferation specific tracer and its utility in several major areas (neurology, cardiology, oncology and infection) of nuclear medicine. Hence, radiotracer quality remains of key importance for the future of nuclear medicine.

## ACKNOWLEDGEMENTS

This work is supported, in part, by Purdue University and research grants: R01 CA115883 A2 (S.L.) from the National Cancer Institute (NCI), BCTR0503947 (S.L.) from the Susan G. Komen Breast Cancer Foundation, AHA0555659Z (S.L.) from the Greater Midwest Affiliate of American Heart Association, R21 EB003419-02 (S.L.) from the National Institute of Biomedical Imaging and Bioengineering (NIBIB) and R21 HL083961-01 from the National Heart, Lung, and Blood Institute (NHLBI).

## ABBREVIATIONS

L1 = N-(dithiocarbamato)-1-aza-12-crown-4  
L2 = N-(dithiocarbamato)-1-aza-15-crown-5  
L3 = N-(dithiocarbamato)-1-aza-18-crown-6  
L4 = N-(dithiocarbamato)-2-aminimethyl-15-crown-5  
L5 = N-(dithiocarbamato)-2-aminimethyl-18-crown-6  
L6 = N-methoxyethyl-N,N-bis[2-(bis(3-ethoxypropyl)phosphino)ethyl]amine  
L7 = N-[15-crown-5]-2-yl]-N,N-bis[2-(bis(3-ethoxypropyl)phosphino)ethyl]amine  
L8 = N-[18-crown-6]-2-yl]-N,N-bis[2-(bis(3-ethoxypropyl)phosphino)ethyl]amine  
 $[^{99m}\text{Tc}-\text{Sestamibi}] = [^{99m}\text{Tc}(\text{MIBI})_6]^+$   
MIBI = 2-methoxy-2-methylpropylisonitrile  
 $[^{99m}\text{Tc}-\text{Tetrofosmin}] = [^{99m}\text{TcO}_2(\text{Tetrofosmin})_2]^+$   
Tetrofosmin = 1,2-bis[bis(2-ethoxyethyl)phosphino]ethane  
 $[^{99m}\text{Tc}-\text{Teboroxime}] = [^{99m}\text{TcCl}(\text{CDOH})_3(\text{BCH}_3)]$   
 $\text{CDOH}_2 = \text{cyclohexanedione dioxime}$   
 $[^{99m}\text{TcN}-\text{noet}] = [^{99m}\text{TcN}(\text{Noet})_2]$   
Noet = bis(N-ethoxy-N-ethyl)dithiocarbamate  
 $[^{99m}\text{TcN}-\text{DBODC5}] = [^{99m}\text{TcN}(\text{PNP5})(\text{DBODC})]^+$   
DBODC = N,N-bis(ethoxyethyl)dithiocarbamate  
PNP5 = N-ethoxyethyl-N,N-bis[2-(bis(3-methoxypropyl)phosphino)ethyl]amine  
 $[^{99m}\text{TcN}-\text{DBODC6}] = [^{99m}\text{TcN}(\text{PNP6})(\text{DBODC})]^+$   
PNP6 = N,N-bis[2-(bis(3-ethoxypropyl)phosphino)ethyl]ethoxyethylamine

## REFERENCES TO CHAPTER 5

- [5.1] NUNN, A.D., Radiopharmaceuticals for imaging myocardial perfusion, *Semin. Nucl. Med.* **20** (1990) 111–118.
- [5.2] SAHA, G.B., GO, R.T., MACINTYRE, W.J., Radiopharmaceuticals for cardiovascular imaging, *Nucl. Med. Biol.* **19** (1992) 1–20.
- [5.3] OPIE, L.H., HESSE, B., Radionuclide tracers in the evaluation of resting myocardial ischaemia and viability, *Eur. J. Nucl. Med.* **24** (1997) 1183–1193.
- [5.4] BERMAN, D.S., GERMANO, G., SHAW, L.J., The role of nuclear cardiology in clinical decision making, *Semin. Nucl. Med.* **29** (1999) 280–297.
- [5.5] JAIN, D., Technetium-99m labeled myocardial perfusion imaging agents, *Semin. Nucl. Med.* **29** (1999) 221–236.
- [5.6] ACAMPA, W., DI BENEDETTO, C., CUOCOLO, A., An overview of radiotracers in nuclear cardiology, *J. Nucl. Cardiol.* **7** (2000) 701–707.
- [5.7] DILSIZIAN, V., The role of myocardial perfusion imaging in vascular endothelial dysfunction, *J. Nucl. Cardiol.* **7** (2000) 180–184.
- [5.8] BELLER, G.A., ZARET, B.L., Contributions of nuclear cardiology to diagnosis and prognosis of patients with coronary artery disease, *Circulation* **101** (2000) 1465–1478.

- [5.9] PARKER, J.A., Cardiac nuclear medicine in monitoring patients with coronary heart disease, *Semin. Nucl. Med.* **31** (2001) 223–237.
- [5.10] KAPUR, A., et al., A comparison of three radionuclide myocardial perfusion tracers in clinical practice: the ROBUST study, *Eur. J. Nucl. Mol. Imaging* **29** (2002) 1608–1616.
- [5.11] KAILASNATH, P., SINUSUS, A.J., Comparison of Tl-201 with Tc-99m-labeled myocardial perfusion agents: technical, physiologic, and clinic issues, *J. Nucl. Cardiol.* **8** (2001) 482–498.
- [5.12] BANERJEE, S., PILLAI, M.R.A., RAMAMOORTHY, N., Evolution of Tc-99m in diagnostic radiopharmaceuticals, *Semin. Nucl. Med.* **31** (2001) 260–277.
- [5.13] LLAURADO, J.G., The quest for the perfect myocardial perfusion indicator... still a long way to go, *J. Nucl. Med.* **42** (2001) 282–284.
- [5.14] JONES, A.G., et al., Biological studies of a new class of technetium complexes: the hexakis(alkylisonitrile)technetium(I) cations, *Int. J. Nucl. Med. Biol.* **11** (1984) 225–234.
- [5.15] WACKERS, F.J.Th., et al., Technetium-99m hexakis 2-methoxyisobutyl isonitrile: human biodistribution, dosimetry, safety, and preliminary comparison to Tl-201 for myocardial perfusion imaging, *J. Nucl. Med.* **30** (1989) 301–311.
- [5.16] ISKANDRIAN, A.S., et al., Use of technetium-99m isonitrile (RP-30A) in assessing left ventricular perfusion and function at rest and during exercise in coronary artery disease and comparison with coronary arteriography and exercise thallium-201 SPECT imaging, *Am. J. Cardiol.* **64** (1989) 270–275.
- [5.17] MARMION, M.E., et al., Preparation and characterization of technetium complexes with Schiff-base and phosphine coordination. 1. Complexes of technetium-99g and -99m with substituted acac<sub>2</sub>en and trialkyl phosphines (where acac<sub>2</sub>en = N,N'-ethylenebis[acetylacetone iminato]), *Nucl. Med. Biol.* **26** (1999) 755–770.
- [5.18] LISIC, E.C., HEEG, M.J., DEUTSH, E., <sup>99m</sup>Tc(L-L)<sub>3</sub><sup>+</sup> complexes containing ether analogs of DMPE, *Nucl. Med. Biol.* **26** (1999) 563–571.
- [5.19] TISATO, F., et al., Cationic [<sup>99m</sup>Tc<sup>III</sup>(DIARS)<sub>2</sub>(SR)<sub>2</sub>]<sup>+</sup> complexes as potential myocardial perfusion imaging agents (DIARS = o-phenylenebis(dimethylarsine); SR<sup>-</sup> = thiolate), *J. Med. Chem.* **39** (1996) 1253–1261.
- [5.20] MARMION, M.E., MACDONALD, J.R., Preparation and biodistribution of <sup>99m</sup>Tc(I)-tricarbonyl complexes containing isonitrile and phosphine ligands, *J. Nucl. Med.* **41** (2000) 124P.
- [5.21] MARESCA, K.P., et al., Novel ether containing ligand complexes of <sup>99m</sup>Tc(CO)<sub>3</sub><sup>+</sup> for cardiac imaging, *J. Nucl. Med.* **45** (2004) 215P.
- [5.22] BOLZATI, C., et al., Chemistry of the strong electrophilic metal fragment [<sup>99m</sup>Tc(N)(PXP)]<sup>2+</sup> (PXP = diphosphine ligand). A novel tool for the selective labeling of small molecules, *J. Am. Chem. Soc.* **124** (2002) 11468–11479.
- [5.23] BOLZATI, C., et al., Synthesis, solution-state and solid-state structural characterization of monocationic nitrido heterocomplexes [M(N) (DTC)(PNP)]<sup>+</sup> (M = <sup>99</sup>Tc and Re; DTC = dithiocarbamate; PNP = heterodiphosphane), *Eur. J. Inorg. Chem.* (2004) 1902–1913.

- [5.24] BOSCHI, A., et al., A class of asymmetrical nitrido  $^{99m}\text{Tc}$  heterocomplexes as heart imaging agents with improved biological properties, *Nucl. Med. Commun.* **23** (2003) 689–693.
- [5.25] BOSCHI, A., et al., Synthesis and biologic evaluation of monocationic asymmetrical  $^{99m}\text{Tc}$ -nitride heterocomplexes showing high heart uptake and improved imaging properties, *J. Nucl. Med.* **44** (2003) 806–814.
- [5.26] HATADA, K., et al.,  $^{99m}\text{Tc-N-DBODC5}$ , a new myocardial perfusion imaging agent with rapid liver clearance: comparison with  $^{99m}\text{Tc-Sestamibi}$  and  $^{99m}\text{Tc-Tetrofosmin}$  in rats, *J. Nucl. Med.* **45** (2004) 2095–2101.
- [5.27] HATADA, K., et al., Organ biodistribution and myocardial uptake, washout, and redistribution kinetics of Tc-99m N-DBODC5 when injected during vasodilator stress in canine models of coronary stenoses, *J. Nucl. Cardiol.* **13** (2006) 779–790.
- [5.28] KIM, Y.-S., et al., Impact of bidentate chelators on lipophilicity, stability and biodistribution characteristics of cationic  $^{99m}\text{Tc}$ -nitrido complexes, *Bioconjug. Chem.* **18** (2007) 929–936.
- [5.29] LIU, S., Ether and crown ether-containing cationic  $^{99m}\text{Tc}$  complexes useful as radiopharmaceuticals for heart imaging, *Dalton Trans.* (2007) 1183–1193.
- [5.30] LIU, S., HE, Z., HSIEH, W., Evaluation of novel cationic  $^{99m}\text{Tc}$ -nitrido complexes as new radiopharmaceuticals for heart imaging: improving liver clearance with crown ether groups, *Nucl. Med. Biol.* **33** (2006) 419–432.
- [5.31] ALBERTO, R., et al., A novel organometallic aqua complex of technetium for the labeling of biomolecules: synthesis of  $[^{99m}\text{Tc}(\text{H}_2\text{O})_3(\text{CO})_3]^+$  from  $[^{99m}\text{TcO}_4]^-$  in aqueous solution and its reaction with a bifunctional ligand, *J. Am. Chem. Soc.* **120** (1998) 7987–7988.
- [5.32] ALBERTO, R., et al., Synthesis and properties of boranocarbonate: a convenient in situ CO source for the aqueous preparation of  $[^{99m}\text{Tc}(\text{H}_2\text{O})_3(\text{CO})_3]^+$ , *J. Am. Chem. Soc.* **123** (2001) 3135–3136.
- [5.33] ALBERTO, R., et al., Potential of the “[M(CO)<sub>3</sub>]<sup>+</sup>” (M = Re, Tc) moiety for the labeling of biomolecules, *Radiochim. Acta* **79** (1997) 99–103.
- [5.34] ALBERTO, R., et al., Basic aqueous chemistry of  $[M(\text{H}_2\text{O})_3(\text{CO})_3]^+$  (M = Re, Tc) directed towards radiopharmaceutical application, *Coord. Chem. Rev.* **190–192** (1999) 901–919.
- [5.35] SCHIBIGER, P.A., et al., Radiopharmaceuticals: from molecular imaging to targeted radionuclide therapy, *Chimia* **58** (2004) 731–735.
- [5.36] BANERJEE, S.R., et al., New directions in the coordination chemistry of  $^{99m}\text{Tc}$ : a reflection on technetium core structures and a strategy for new chelate design, *Nucl. Med. Biol.* **32** (2005) 1–20.
- [5.37] SCHIBLI, R., SCHIBIGER, P.A., Current use and future potential of organometallic radiopharmaceuticals, *Eur. J. Nucl. Med. Mol. Imaging* **29** (2002) 1529–1542.
- [5.38] HÄFLINGER, P., et al., Structure, stability, and biodistribution of cationic  $[M(\text{CO})_3]^+$  (M = Re,  $^{99}\text{Tc}$ ,  $^{99m}\text{Tc}$ ) complexes with tridentate amine ligands, *Synth. React. Inorg. Met.-Org. Chem.* **35** (2005) 27–34.
- [5.39] RATTAT, D., et al., Comparison of tridentate ligands in competition experiments for their ability to form a  $[^{99m}\text{Tc}(\text{CO})_3]^+$  complex, *Tetrahedron Lett.* **45** (2004) 2531–2534.

- [5.40] SCHIBLI, R., et al., Influence of the denticity of ligand systems on the in vitro and in vivo behavior of  $^{99m}\text{Tc}(\text{I})$ -tricarbonyl complexes: a hint for the future functionalization of biomolecules, *Bioconjug. Chem.* **11** (2001) 345–351.
- [5.41] KIM, Y.-S., et al., Synthesis, characterization and X-ray crystal structure of  $[\text{Re}(\text{L4})(\text{CO})_3]\text{Br} \cdot 2\text{CH}_3\text{OH}$  ( $\text{L4} = \text{N,N-bis}[(2\text{-diphenylphosphino})\text{ethyl}]\text{methoxyethylamine}$ ): a model compound for novel cationic  $^{99m}\text{Tc}$  radiotracers useful for heart imaging, *Inorg. Chim. Acta* **359** (2006) 2479–2488.
- [5.42] HE, J., et al., Evaluation of novel cationic  $^{99m}\text{Tc}(\text{I})$ -tricarbonyl complexes as potential radiotracers for myocardial perfusion imaging, *Nucl. Med. Biol.* **33** (2006) 1045–1053.
- [5.43] KIM, Y.-S., et al.,  $^{99m}\text{TcN-MPO}$ : Novel cationic  $^{99m}\text{Tc}$ -nitrido radiotracer for myocardial perfusion imaging, *J. Nucl. Cardiol.* **15** (2008) 535–546.
- [5.44] VALEUR, B., LERAY, I., Design principles of fluorescent molecular sensors for cation recognition, *Coord. Chem. Rev.* **205** (2000) 3–40.
- [5.45] GUNNL AUGSSON, T., et al., Synthesis of functionalised macrocyclic compounds as  $\text{Na}^+$  and  $\text{K}^+$  receptors: a mild and high yielding nitration in water of mono and bis 2-methoxyaniline functionalised crown ethers, *J. Chem. Soc. Perkin Trans.* (2002) 1954–1962.
- [5.46] GUNNL AUGSSON, T., LEONARD, J.P., Synthesis and evaluation of colorimetric chemosensors for monitoring sodium and potassium ions in the intracellular concentration range, *J. Chem. Soc. Perkin Trans.* (2002) 1980–1985.
- [5.47] MARTELL, A.E., SMITH, R.M., MOTEKAITIS, R.J., Database 46: NIST Critical Selected Stability Constants of Metal Complexes, Version 8, Texas A&M University, TX (2004).
- [5.48] MOUSA, S.A., WILLIAMS, S.J., SANDS, H., Characterization of in vivo chemistry of cations in the heart, *J. Nucl. Med.* **28** (1987) 1351–1357.
- [5.49] CRANE, P., et al., Effect of mitochondrial viability and metabolism on technetium- $^{99m}$ -sestamibi myocardial retention, *Eur. J. Nucl. Med.* **20** (1993) 20–25.
- [5.50] CARVALHO, P.A., et al., Subcellular distribution and analysis of technetium- $^{99m}$ -MIBI in isolated perfused rat hearts, *J. Nucl. Med.* **33** (1992) 1516–1521.
- [5.51] PIWNICA-WORMS, D., et al., Uptake and retention of hexakis(2-methoxyisobutyl isonitrile) technetium(I) in cultured chick myocardial cells: Mitochondrial and plasma membrane potential dependence, *Circulation* **82** (1990) 1826–1838.
- [5.52] SHARMA, V., PIWNICA-WORMS, D., Metal complexes for therapy and diagnosis of drug resistance, *Chem. Rev.* **99** (1999) 2545–2560.
- [5.53] SHARMA, V., Radiopharmaceuticals for assessment of multidrug resistance P-glycoprotein-mediated drug transport activity, *Bioconjug. Chem.* **15** (2004) 1464–1474.
- [5.54] VAIDYANATHAN, G., ZALUTSKY, M.R., Imaging drug resistance with radiolabeled molecules, *Current Pharm. Design* **10** (2004) 2965–2979.
- [5.55] GATMAITAN, Z.C., ARIAS, I.M., Structure and function of P-glycoprotein in normal liver and small intestine, *Adv. Pharmacol.* **24** (1993) 77–97.
- [5.56] LEE, C.H., et al., Differential expression of P-glycoprotein genes in primary rat hepatocyte culture, *J. Cell Physiol.* **157** (1993) 392–402.

- [5.57] MAYER, R., et al., Expression of the MRP gene-encoded conjugate export pump in liver and its selective absence from the canalicular membrane in transport deficient mutant hepatocytes, *J. Cell Biol.* **131** (1995) 137–150.
- [5.58] DYSZLEWSKI, M., et al., Characterization of a novel  $^{99m}\text{Tc}$ -carbonyl complex as a functional probe of *MDR1* P-glycoprotein transport activity, *Mol. Imaging* **1** (2002) 24–35.
- [5.59] MUZZAMMIL, T., BALLINGER, J.R., MOORE, M.J.,  $^{99m}\text{Tc}$ -sestamibi imaging of inhibition of the multidrug resistance transporter in a mouse xenograft model of human breast cancer, *Nucl. Med. Commun.* **20** (1999) 115–122.
- [5.60] LUKER, G.D., et al., Modulation of the multidrug resistance P-glycoprotein: Detection with technetium-99m sestamibi in vivo, *J. Nucl. Med.* **38** (1997) 369–372.
- [5.61] AGRAWAL, M., et al., Increased  $^{99m}\text{Tc}$ -Sestamibi accumulation in normal liver and drug resistant-tumors after the administration of the glycoprotein inhibitor, XR9576, *Clin. Cancer Res.* **9** (2003) 650–656.
- [5.62] KIM, Y.-S., et al., A novel ternary ligand system useful for preparation of cationic  $^{99m}\text{Tc}$ -diazenido complexes and  $^{99m}\text{Tc}$ -labeling of small biomolecules, *Bioconjug. Chem.* **17** (2006) 473–484.



## Chapter 6

# TECHNETIUM-99m RADIOPHARMACEUTICALS IN NEUROLOGY

I. PIRMETTIS

Institute of Radioisotopes, Radiodiagnostic Products,  
National Centre for Scientific Research “Demokritos”,  
Athens, Greece

H.-J. PIETZSCH

Institute of Radiopharmacy, Forschungszentrum Dresden–Rossendorf,  
Dresden, Germany

### Abstract

The ideal radioisotope for single photon emission computed tomography imaging is  $^{99m}\text{Tc}$ , due to its physical decay characteristics, its availability through commercially available generator systems and its low cost per dose. Technetium-99m hydrophilic complexes are used to evaluate the integrity of the blood–brain barrier, while neutral and lipophilic complexes are used as brain perfusion imaging agents for determination of changes in regional cerebral blood flow in various neurological disorders. Radiopharmaceuticals that bind to central nervous system (CNS) receptors *in vivo* are useful for understanding the pathophysiology of a number of neurological and psychiatric disorders, their diagnosis and treatment. Nowadays, CNS receptor imaging agents are, with some exceptions, typically positron emission tomography radionuclide based radiopharmaceuticals. The reason for this is not based on principal but is rather as a result of the fact that efforts in the direction of  $^{99m}\text{Tc}$  containing agents have not been strong or consistent enough. In the chapter, the progress made in the development of  $^{99m}\text{Tc}$  complexes for imaging dopamine transporter, 5-HT<sub>1A</sub> receptor and amyloid plaques is presented.

### 6.1. INTRODUCTION

Technetium-99m radiopharmaceuticals play an important role in neurology. In the early days, pertechnetate and hydrophilic complexes such as  $^{99m}\text{Tc}$ -citrate,  $^{99m}\text{Tc}$ -DTPA and  $^{99m}\text{Tc}$ -glucoheptonate were used to evaluate the integrity of the blood–brain barrier (BBB) [6.1–6.4]. These agents cannot cross the intact BBB, but can be applied for brain imaging when the BBB is damaged, for example, by tumour or head trauma (Fig. 6.1).

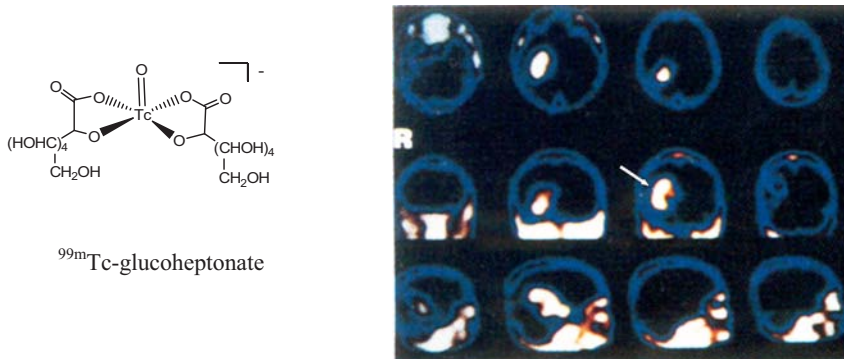


FIG. 6.1. BBB/SPECT using  $^{99m}\text{Tc}$ -glucoheptonate in a patient with malignant glioma [6.22].

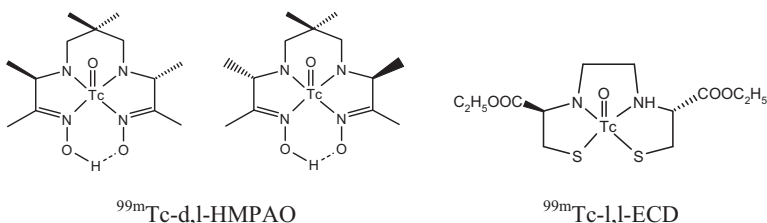
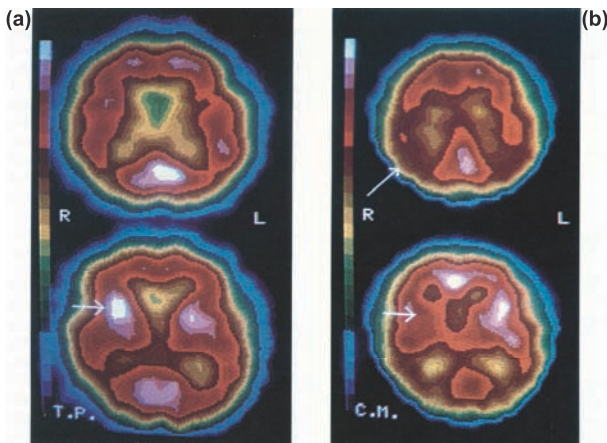


FIG. 6.2.  $[^{99m}\text{Tc}]$ -d,l-HMPAO and  $[^{99m}\text{Tc}]$ -l,l-ECD which are in clinical use.

Neutral and lipophilic complexes were synthesized and evaluated as brain perfusion imaging agents during the 1980s and 1990s, with the aim of developing  $^{99m}\text{Tc}$  agents capable of penetrating the intact BBB [6.5–6.10]. Although there is no clear cut-off, complexes with well balanced lipophilicity ( $\log P_{\text{oct/water}}$  between one and three) are considered good candidates. This effort resulted in the development of two radiopharmaceuticals,  $[^{99m}\text{Tc}]$ -d,l-HMPAO [6.11, 6.12] and  $[^{99m}\text{Tc}]$ -l,l-ECD, [6.13, 6.14] which are in clinical use (Fig. 6.2.).

After IV injection, both complexes penetrate the intact BBB and accumulate in the brain. The retention of  $[^{99m}\text{Tc}]$ -d,l-HMPAO is related to its chemical instability. Thus, after penetration of the BBB,  $^{99m}\text{Tc}$  dissociates and complexes with intracellular proteins, rendering it unable to rediffuse through the BBB and it is trapped in the brain. The redox status of the tissue and the concentration of glutathione have been identified as critical parameters for this conversion [6.11, 6.15, 6.16]. On the other hand, the retention of  $[^{99m}\text{Tc}]$ -l,l-ECD is attributed to the enzymatic hydrolysis of an ester group and the formation of a hydrophilic metabolite, which cannot diffuse back out across the BBB and, thus, is trapped in the brain, allowing for single photon emission computed tomography (SPECT) imaging [6.17, 6.18]. The distribution of



*FIG. 6.3.*  $[^{99m}\text{Tc}]\text{-d},\text{l}\text{-HMPAO/SPECT}$  images (showing cortical and basal ganglia regions) from two Parkinsonian patients with predominant left sided symptomatology. Both increased (a) and decreased (b, lower image) tracer uptake was observed in the basal ganglia contralateral to the symptomatic limbs. Additional deficits in the parietal cortex are evident in b (upper image) [6.23].

$[^{99m}\text{Tc}]\text{-d},\text{l}\text{-HMPAO}$  and  $[^{99m}\text{Tc}]\text{-l},\text{l}\text{-ECD}$  in the brain correlates well with rCBF and their use is based on monitoring the changes of rCBF in various neurological diseases such as dementia, Alzheimer's disease, epilepsy, stroke and Parkinson's disease (Fig. 6.3.) [6.19–6.23]. Epileptic seizures often cause increased blood flow in the region of discharge, which may appear as an area of increased radioactivity.

High specificity and sensitivity can be reached when the images are combined with clinical images and data from other examinations (CT, MRI). However, these agents are not specific for the diseases.

The major strength of diagnostic nuclear medicine is its unique ability to provide information on biochemical processes. This is especially true when information is required on the relationships of the densities of low capacity, high specificity receptors to disease status. High specific activity radiopharmaceuticals are ideal non-invasive probes of such receptor systems, especially for receptors in the central nervous system (CNS) [6.24–6.27]. Positron emission tomography (PET) using  $^{11}\text{C}$  and  $^{18}\text{F}$  labelled radiopharmaceuticals has led the way in studies of receptor imaging, and has provided much useful information on neurophysiology and neuropharmacology. Primarily, through the use of  $^{123}\text{I}$ , there has been a steady growth in CNS receptor imaging studies using SPECT. SPECT has slightly inferior image resolution to PET, but has the advantage that SPECT systems are readily available worldwide. Since  $^{99m}\text{Tc}$  is the ideal radioisotope for

SPECT imaging, there is considerable interest in the discovery and development of new  $^{99m}\text{Tc}$  radiopharmaceuticals for imaging CNS receptors. Like PET radiotracers for imaging CNS receptors,  $^{99m}\text{Tc}$  CNS receptor based radiopharmaceuticals will be able to provide:

- Early and accurate diagnosis, and differentiation from similar diseases;
- Guidance for the selection of the therapy and monitoring disease progression during therapy;
- Basic information about the involvement of receptors or other binding sites in various neurological diseases.

Moreover,  $^{99m}\text{Tc}$  radiopharmaceuticals are expected to aid drug development by:

- Demonstrating that drugs reach their receptor and target sites and, thus, providing proof of concept;
- Defining dose-occupancy curves for Phase I and II studies, and, thus, rationalizing dose choice in clinical trials;
- Providing biomarkers for monitoring disease progression alongside clinical rating.

Application of  $^{99m}\text{Tc}$  instead of PET radionuclides should significantly reduce the cost of performing such imaging studies, and should allow many more nuclear medicine centres access to receptor imaging radiopharmaceuticals. However, there are significant technical hurdles to overcome. While most PET radioisotopes and  $^{123}\text{I}$  can be attached to targeting molecules by a simple covalent bond, technetium, as a second row transition metal, needs to be bound to a metal binding organic molecule (a chelating agent) to be attached to a receptor-targeting molecule. The combination of technetium with a chelating agent is, generally, large in size, and will, therefore, often considerably change the physical and biochemical properties of the targeting molecule to which it is attached.

## 6.2. DESIGNING A CNS RECEPTOR BASED ON $^{99m}\text{Tc}$ RADIOPHARMACEUTICALS

The requirements for a useful  $^{99m}\text{Tc}$  labelled imaging agent for CNS receptors or binding sites are many and formidable (Table 6.1). The  $^{99m}\text{Tc}$  agent should be neutral, small in size (MW <700), with suitable lipophilicity ( $\log P$  of 1.0–3.0) and stable enough, in terms of reoxidation and trans-chelation in order to survive in the blood stream and penetrate the intact BBB. In addition, it should be

TABLE 6.1. BASIC REQUIREMENTS FOR A  $^{99m}\text{Tc}$  LABELLED CNS RECEPTOR IMAGING AGENT

	Requirements
1.	Ability to cross the BBB (neutral, MW < 700, log P 1.0–3.0)
2.	In vivo stability
3.	High and selective binding affinity for the target receptor ( $\text{IC}_{50} < 10 \text{ nM}$ )
4.	High uptake in brain
5.	Localized in target sites
6.	Formation (if any) of non-binding radiometabolites

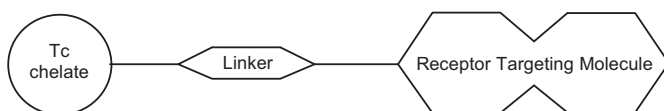


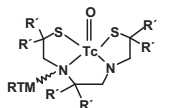
FIG. 6.4. Schematic representation of a receptor specific  $^{99m}\text{Tc}$  tracer.

capable of binding to receptors or binding sites with high affinity and selectivity. The metabolism of the  $^{99m}\text{Tc}$  agent should not result in radio-metabolites that would be able to cross the BBB and, thus, interfere with the imaging.

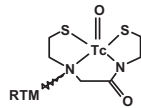
Unlike well established  $^{99m}\text{Tc}$  radiopharmaceuticals for routine nuclear medicine diagnostics, such as [ $^{99m}\text{Tc}$ ]-d,l-HMPAO and [ $^{99m}\text{Tc}$ ]-l,l-ECD, which are quite symmetrical small molecules, receptor specific agents should be asymmetrical in a specific manner, integrating building blocks for distinct functions. In general, the Tc based receptor specific molecule may be considered an entity formed by three constituents: a bifunctional chelating agent (BFCA), which on the one hand coordinates  $^{99m}\text{Tc}$  and on the other hand carries, through a linker, a receptor targeting organic moiety (Fig. 6.4).

The BFCA should, in low concentration, efficiently bind the technetium, thus providing a neutral complex that will be stable [6.28–6.32]. Coordination chemistry studies are providing a wide range of chelates, which can be used to bind technetium in various oxidation states. Among the various oxidation states of technetium explored in CNS receptor radiotracer design, Tc(V) proved to be very suitable (Fig. 6.5). One dominant structural element is the oxotechnetium core  $[\text{TcO}]^{3+}$ . The presence of the oxo ligand has a significant effect on the structure and properties of the derived complexes. Tetradentate  $\text{N}_2\text{S}_2$  diaminodithiols (DADT or BAT) were found to form neutral lipophilic complexes with three of the four ionizable protons lost upon complexation. Combining an amine-N and amide-N in an  $\text{N}_2\text{S}_2$  arrangement provides a type of

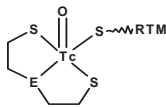
Tc(V)



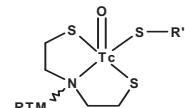
$\text{N}_2\text{S}_2$  (DADT or BAT)



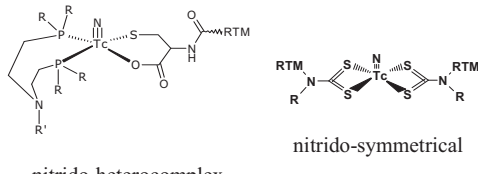
$\text{N}_2\text{S}_2$  (MAMA)



'3+1' (E = S, N-R)

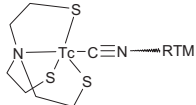


'3+1'



nitrido-heterocomplex

Tc(III)



'4+1'

Tc(I)

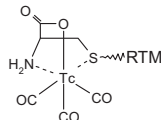
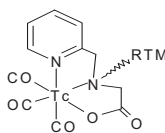
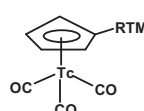
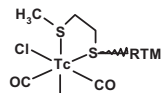
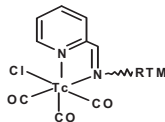


FIG. 6.5. Selected types of chelate units used in the development of CNS receptor based  $^{99m}\text{Tc}$  radiopharmaceuticals; RTM = linker bearing the receptor-targeting molecule.

tetridentate ligand called MAMA. The MAMA chelate is more polar than the diaminodithiol system. It is, therefore, particularly useful when less lipophilicity has to be imposed upon biomolecule conjugates.

Recently, a Tc-nitrido heterocomplex was proposed, an asymmetric, five coordinated  $[TcN]^{2+}$  complex containing a bidentate diphosphine ligand and a bidentate chelator associated with the receptor binding domain. Symmetrical Tc-nitrido complexes have also been prepared using two dithiocarbamate ligands [6.33, 6.34].

To reduce the synthetic expenditure necessary for tetradentate compounds, particularly for a series of complexes for structure–activity relationship studies, mixed ligand complexes were synthesized. In the technetium oxidation state +5, a combination of tridentate ( $S_3$  or  $NS_2$ ) and monodentate (S) thiol ligands was employed in ‘3+1’ complexes [6.35, 6.36]. Although stable in vitro, ligand exchange may occur in vivo [6.37–6.39].

Stable ‘4+1’ complexes in the metal oxidation state +3 no longer possess the oxo ligand as typical for Tc(V) complexes, thus avoiding the polarity of the complexes caused by the oxo group [6.40, 6.41].

The introduction of the low valency technetium(I) *fac*- $[^{99m}Tc(CO)_3(H_2O)_3]^+$  synthon produced by the gentle reduction of  $^{99m}Tc(\text{VII})$  to  $^{99m}Tc(\text{I})$  under 1 atm of CO, established the  $^{99m}Tc(\text{I})(CO)_3^+$  core as an easily accessible platform in the search for new radiopharmaceuticals [6.42]. The three aqua ligands of the *fac*- $[^{99m}Tc(CO)_3(H_2O)_3]^+$  synthon are labile and readily substituted by a variety of functional groups, including amines, thioethers, imines, thiols, carboxylates and phosphines to give stable hexacoordinated complexes [6.43]. Furthermore, the small size and kinetic inertness of the  $^{99m}Tc(\text{I})(CO)_3^+$  core make it suitable for the labelling of receptor-targeting molecules.

Between the BFCA, which coordinates the metal, and the receptor-targeting domain, which binds to the receptor, there is a linker. It is usually a simple hydrocarbon chain and is used to elongate the BFCA from the targeting moiety as well as to modify lipophilicity and the pKa of neighbouring amine nitrogens.

Several complexes were reported in which the linker had a significant effect on receptor binding and brain uptake. However, the effect on receptor binding and brain uptake cannot be predicted. For example (Fig. 6.6), extension of the methylene bridge in the  $^{99m}Tc$ -TRODAT molecule to an ethylene bridge resulted in a molecule with lower lipophilicity and negligible brain uptake [6.44].

In a series of ‘3+1’ Tc mixed ligand complexes [6.45], the replacement of a  $\text{CH}_2$  group of the linker by an ether-oxygen atom (Fig. 6.6) resulted in improvement of brain uptake. This was attributed to the lower pKa of the neighbouring nitrogen. The length of the spacer has a strong influence on the receptor binding affinity as demonstrated for Tc(III) mixed ligand complexes with high affinity for the 5-HT<sub>1A</sub> receptor [6.46].

Although these results cannot be generalized, they show that modified linkers can be used for the fine tuning of brain uptake and binding affinity.

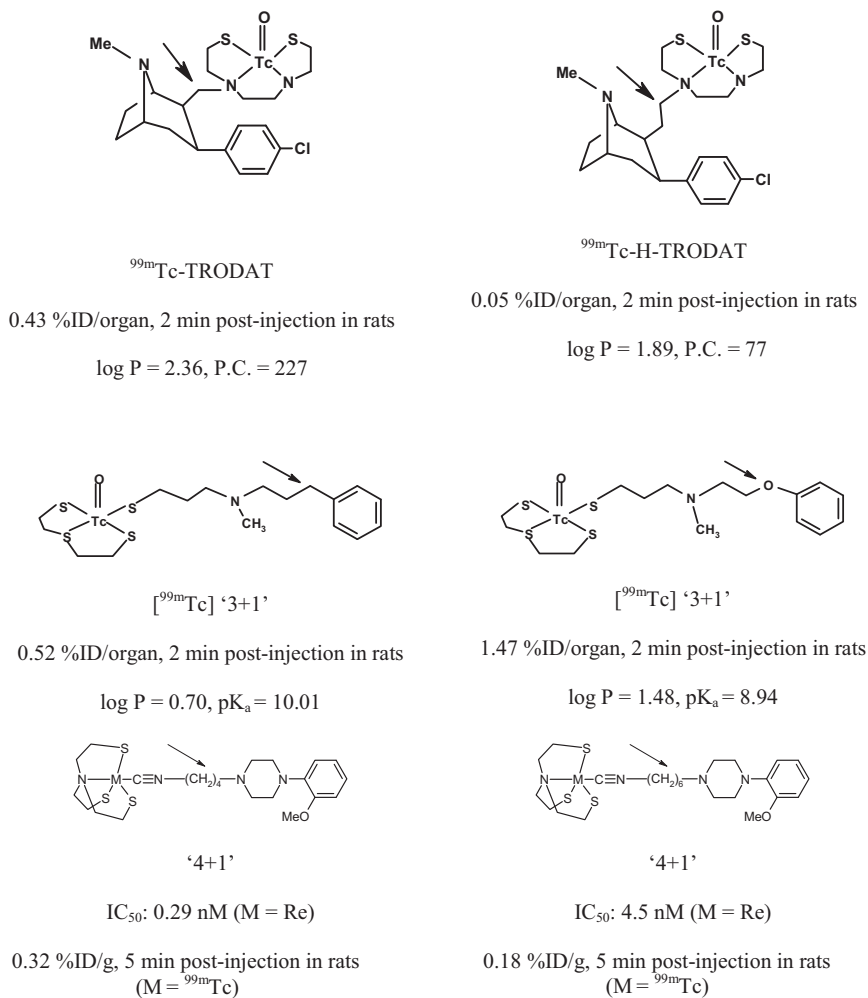


FIG. 6.6. Effect of linker modifications on brain uptake [6.44–6.46].

The targeting domain is derived from molecules with known high binding affinity to the desired receptor or binding sites ('lead structures'). The targeting domain serves as a vehicle that carries and docks the technetium to the receptor. A high concentration of the receptor in healthy brain is an important parameter, otherwise the target concentration expression level may be too low to enable sufficient levels of specific binding relative to non-target uptake for adequate imaging properties. After the selection of the receptor to be targeted, certain targeting molecules are identified, taking into consideration their availability and the degree of allowing functionalization. The topography of the various receptors

appears to accept a relatively wide array of structural types. Agonist, partial agonist and antagonist structures, known from pharmaceutical research and advances in the development of radioligands, yield an abundance of potential lead structures. Although hundreds of derivatives have been investigated for certain receptors, clear structural criteria that are responsible for their affinity and, moreover, for their selectivity are still lacking. What is rational and predictable in the design of organic receptor ligands cannot simply be extended to technetium complexes.

Over the last few years, considerable progress has been made in labelling targeting molecules with  $^{99m}\text{Tc}$  for various CNS receptors. In the following sections, the progress made in the development of  $^{99m}\text{Tc}$  complexes for imaging the dopamine transporter (DAT), the 5-HT<sub>1A</sub> receptor and amyloid plaques is discussed.

### 6.3. TECHNETIUM-99m COMPLEXES FOR THE DOPAMINE TRANSPORTER

DAT is located presynaptically on dopamine neurons and serves a critical modulatory role in dopamine neurotransmission. DAT removes the released transmitter from the synapse by transporting it back into the presynaptic terminal. Due to its crucial function, DAT is a target for drug therapy (e.g. ritaline in attention, deficit and hyperactivity disorder (ADHD)) and for drugs of abuse (e.g. cocaine). A significant reduction in the density of DAT has been reported in patients with Parkinson's disease and Alzheimer's disease, while an increased density was measured in patients with ADHD [6.47–6.51].

As the stimulant and reinforcing properties of cocaine have been ascribed to its ability to inhibit DAT, tropane became a lead structure (or receptor targeting molecule) in the development of radiolabelled PET and SPECT tracers, such as  $^{11}\text{C}$ -CFT (WIN35,428),  $^{18}\text{F}$ -FCT,  $^{123}\text{I}$ - $\beta$ -CIT (Dopascan),  $^{123}\text{I}$ -FP- $\beta$ -CIT (Datscan) and  $^{123}\text{I}$ -altropine, for imaging DAT [6.52–6.56] (Fig. 6.7). These radiopharmaceuticals are used for differentiating between Parkinson's disease

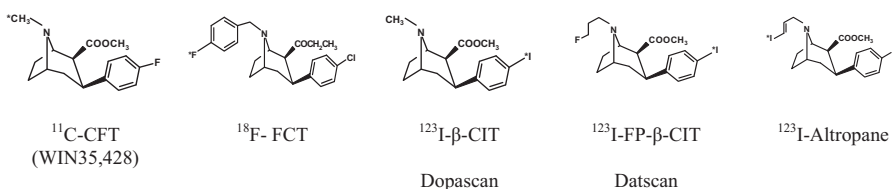
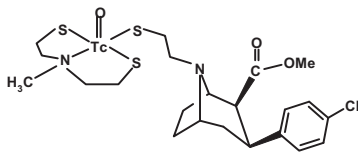
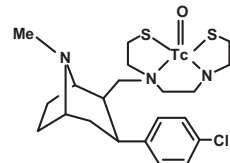


FIG. 6.7.  $^{11}\text{C}$ ,  $^{18}\text{F}$  and  $^{123}\text{I}$  labelled tropanes as DAT imaging agents.



[6.57]



$^{99m}\text{Tc}$ -TRODAT [6.59]

FIG. 6.8.  $^{99m}\text{Tc}$  labelled tropane analogues that display selective DAT binding.

and other movement disorders, drug abuse, ADHD, and evaluation of changes or involvement of DAT in psychiatric diseases, etc.

The synthesis and evaluation of the first  $^{99m}\text{Tc}$  labelled tropane analogue that displays selective dopamine transporter binding was reported more than ten years ago by Kung et al. (Fig. 6.8) [6.57, 6.58]. This was based on the [SNS + S] mixed ligand system, a system providing neutral lipophilic complexes capable of penetrating the BBB and easily modified by simply replacing the tridentate or monodentate ligand. Although this complex suffered from low brain uptake in rats (0.10 %ID/organ, 2 min post-injection), the uptake in striatum, where dopamine neurons are known to be concentrated, was higher compared to the cerebellum. Moreover, the uptake in striatum could be blocked by  $\beta$ -CIT, which competes with dopamine transporter binding, indicating that the uptake is specific. Soon after, the same group reported the development of  $^{99m}\text{Tc}$ -TRODAT, which is based on the  $\text{N}_2\text{S}_2$  system (Fig. 6.8) [6.59, 6.60].

Technetium-99m-TRODAT displayed higher initial brain uptake in rats (0.43 %ID/organ, 2 min post-injection) and a sufficient striatal:cerebellum ratio (2.66 at 60 min post-injection). The results were confirmed in baboons, and in an initial human study showed excellent localization of radioactivity in striatum. After a long march,  $^{99m}\text{Tc}$ -TRODAT has succeeded in entering evaluation in the European Union (Fig. 6.9) [6.61, 6.62].

Several research groups have also reported potential  $^{99m}\text{Tc}$  labelled DAT imaging agents [6.63–6.72]. All are based on the tropane moiety. From Fig. 6.10, it can be seen that there is obviously a large degree of bulk tolerance in the bridgehead nitrogen region for in vitro binding to DAT. Likewise, the good binding affinity of  $^{99m}\text{Tc}$ -TRODAT towards DAT in the brain indicates that  $2\beta$  substitution is well tolerated.

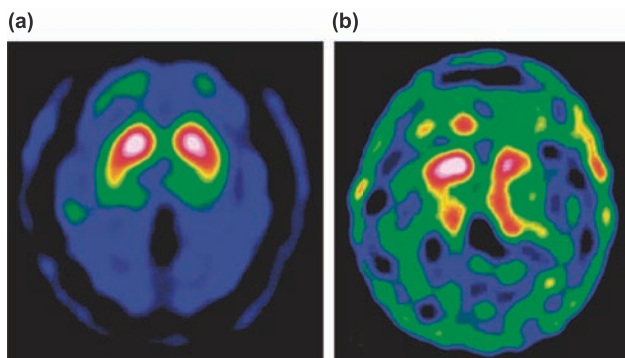


FIG. 6.9.  $^{99m}\text{Tc}$ -TRODAT/SPECT images of a control (a) and a patient with Parkinson's disease (b). The uptake decreased on both sides of the striatal region in the patient with Parkinson's disease [6.61].

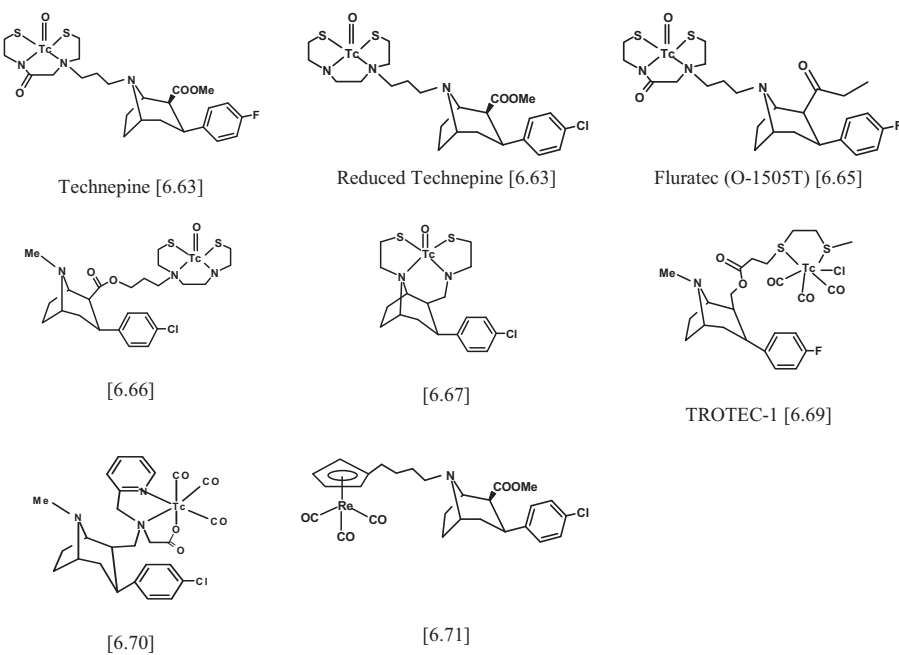


FIG. 6.10.  $^{99m}\text{Tc}$  labelled tropane derivatives studied as potential DAT imaging agents.

#### 6.4. TECHNETIUM-99m COMPLEXES FOR THE 5-HT<sub>1A</sub> RECEPTOR

The development of radiopharmaceuticals for imaging serotonergic (5-HT) receptors is of particular interest since alterations in the concentration or function of these receptors are implicated in neurological and psychological disorders such as anxiety, depression, schizophrenia and Alzheimer's disease [6.73–6.76]. Soon after its discovery, WAY 100635 (N-(2-[4-(2-methoxyphenyl)-1-piperazinyl]ethyl)-N-2-pyridinylcyclohexanecarboxamide), which is a potent and selective 5-HT<sub>1A</sub> antagonist [6.77, 6.78], became the lead structure for the development of radioligands for in vivo imaging of 5-HT<sub>1A</sub> receptors [6.79–6.81]. Carbon-11 and <sup>18</sup>F derivatives of WAY 100635 have been synthesized and evaluated for use in PET [6.82–6.86], while its iodinated analogues have been reported for use in SPECT imaging of 5-HT<sub>1A</sub> receptors [6.87, 6.88] (Fig. 6.11).

Since <sup>99m</sup>Tc is the radionuclide of choice in diagnostic nuclear medicine, many efforts have been focused on developing <sup>99m</sup>Tc based radioligands for 5-HT<sub>1A</sub> receptors. In order to imitate this prototypic organic compound, several neutral and lipophilic oxotechnetium complexes have been synthesized and evaluated as potential imaging agents for 5-HT<sub>1A</sub> receptors. Derivatives and fragments of WAY 100635 were combined with different technetium tetradeятate N<sub>2</sub>S<sub>2</sub> chelates, such as amine–amide dithiols or diamine dithiols [6.89–6.92] with different linkers

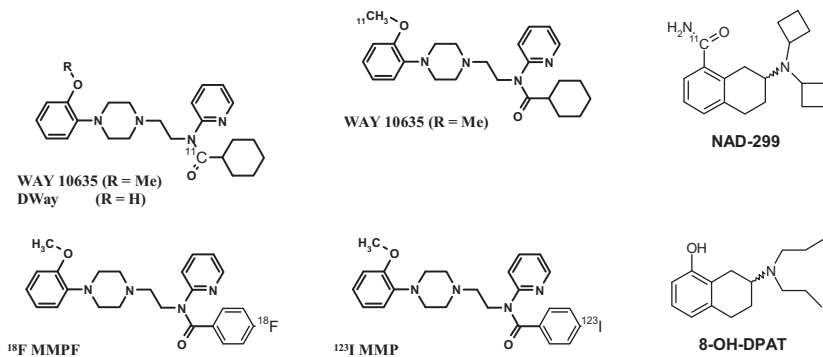
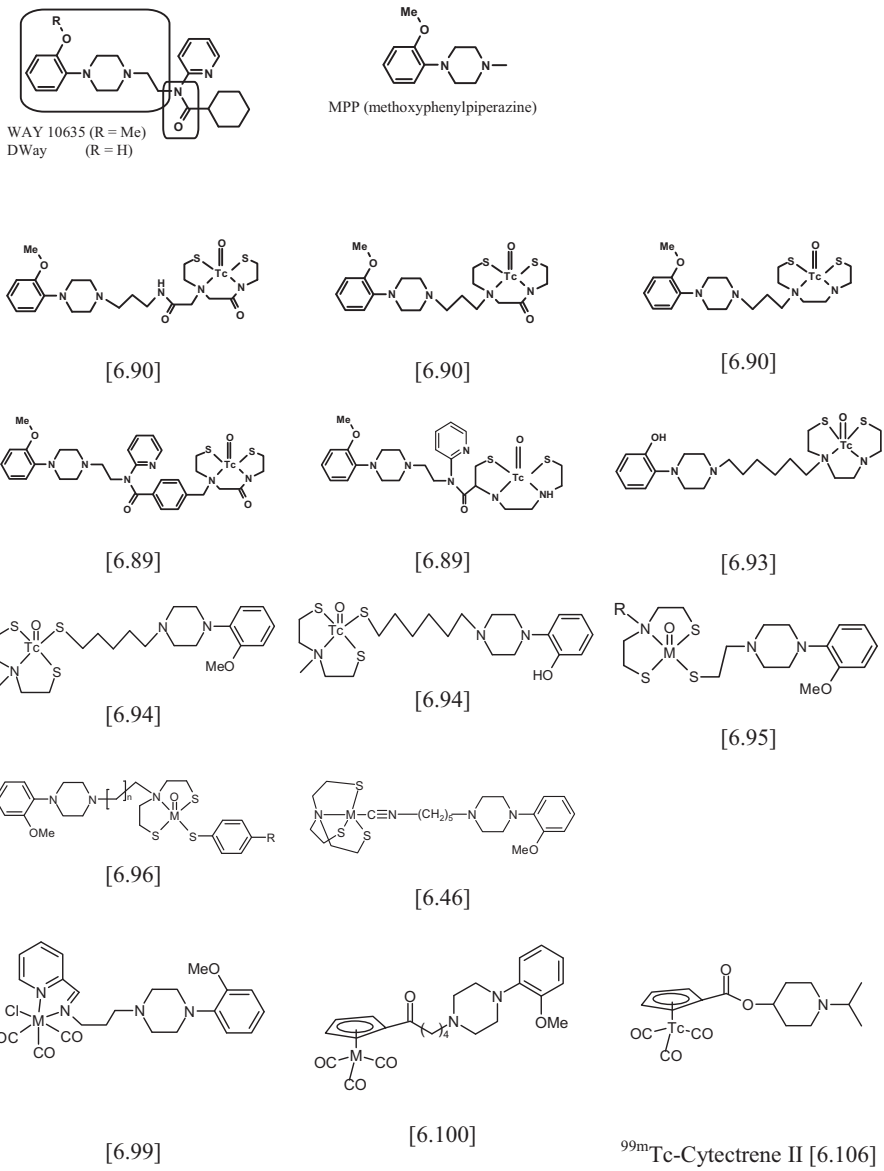


FIG. 6.11. <sup>11</sup>C, <sup>18</sup>F and <sup>123</sup>I labelled agents for imaging the 5-HT<sub>1A</sub> receptor.



*FIG. 6.12. Design features of technetium based 5-HT<sub>1A</sub> ligands employing structural elements of the selective antagonist WAY 100635.*

between the receptor binding moiety, 1-(2-methoxyphenyl)piperazine and the metal chelate (Fig. 6.12). The major disadvantage of these compounds is their poor brain uptake in experimental animals, which precludes their usefulness as brain receptor imaging agents. This has been attributed mainly to their large molecular size. However, a  $^{99m}\text{TcON}_2\text{S}_2$  complex with promising characteristics, carrying the 2-(1-piperazino)phenol via a 6-carbon alkyl chain, has been reported recently [6.93]. Furthermore, '3+1' oxotechnetium mixed ligand complexes of the general type  $^{99m}\text{TcO}[\text{SN}(\text{R})\text{S}][\text{S}]$  have been synthesized as 5-HT<sub>1A</sub> radioligands by introducing the receptor binding 1-(2-methoxyphenyl)piperazine moiety on the monodentate ligand [S] [6.94, 6.95]. The complexes showed in vitro affinity for 5-HT<sub>1A</sub> in the nanomolar range and moderate brain uptake in mice and rats. In a study [6.96] with a series of  $^{99m}\text{TcO}[\text{SN}(\text{R})\text{S}][\text{S}]$  complexes carrying the 1-(2-methoxyphenyl)piperazine moiety on the tridentate ligand [SN(R)S], it was observed that all oxorhenium analogues have affinity for the 5-HT<sub>1A</sub> receptor binding sites with IC<sub>50</sub> values in the nanomolar range (IC<sub>50</sub> = 5.8–103 nM). All of the  $^{99m}\text{TcO}[\text{SN}(\text{R})\text{S}][\text{S}]$  complexes showed significant brain uptake in rats at 2 min post-injection (0.24–1.31 %ID/organ). However, a clear correlation between distribution of radioactivity in the brain and distribution of 5-HT<sub>1A</sub> receptors could not be established.

Technetium and rhenium complexes carrying the 1-(2-methoxyphenyl)piperazine moiety have been synthesized using the '4+1' mixed ligand approach. In vitro binding studies demonstrated the high affinity, for 5-HT<sub>1A</sub> receptors, of the technetium and rhenium complexes [6.46]. The IC<sub>50</sub> values are in the sub-nanomolar range. Technetium-99m complexes showed moderate brain uptake in rats. Although regional distribution is inhomogeneous, only low ratios between areas rich and poor in 5-HT<sub>1A</sub> receptors were observed.

Recently, many efforts have been made to find an improved system or alternative methods for labelling various CNS receptor binding agents based on the *fac*-[Tc(CO)<sub>3</sub>]<sup>+</sup> synthon. This was promoted by the development of a single vial freeze-dried kit for the preparation of [ $^{99m}\text{Tc}(\text{OH}_2)_3(\text{CO})_3$ ]<sup>+</sup> without the requirement of using free CO [6.97].

Several new chelating systems were tested and 1-(2-methoxyphenyl)piperazine (o-MPP) was attached to various chelating agents [6.98–6.105]. The attachment of o-MPP to a hynic chelating unit resulted in a  $^{99m}\text{Tc}$  tricarbonyl complex with low brain uptake and a low concentration in the hippocampus [6.98]. For imino-pyridine derivatives of o-MPP, a strong dependence on IC<sub>50</sub> values of the chain length spacer was observed [6.99]. This was also true for o-MPP bearing cyclopentadienyl derivatives [6.100].

Technetium tricarbonyl complexes with derivatized cyclopentadienyl ligands were prepared starting from pertechnetate and an appropriate ferrocene ligand. The complexes (Tc(CO)<sub>3</sub>cp-COOCH<sub>2</sub>NH<sub>2</sub>R, R = Me, isopropyl) could also

be obtained starting from the precursor complexes  $[^{99m}\text{Tc}(\text{CO})_3(\text{H}_2\text{O})_3]^+$ . The biodistribution of the  $^{99m}\text{Tc}$  complexes (cytectrene I and cytectrene II) was studied in Wistar rats. Both compounds show high uptake in the brain and fast blood clearance. The pattern of regional distribution in the brain demonstrated in autoradiographic studies indicates binding to the 5-HT<sub>1A</sub> and  $\alpha_1$  adrenergic receptors [6.106].

## 6.5. TECHNETIUM-99m COMPLEXES FOR AMYLOID PLAQUES

Alzheimer's disease, which is the most common form of dementia, is one of the most prevalent neurodegenerative disorders among the elderly and will cause an enormous economic and emotional cost on society. The clinical impairments in Alzheimer's disease include cognitive dysfunction and behavioural abnormality with increasing mortality. Neuronal cell death is the central abnormality occurring in brains suffering from Alzheimer's disease. Clinical diagnosis of Alzheimer's disease is based on definitions by the NINDS\_ADRDA Working group and the DSM-IV. A definite diagnosis of Alzheimer's disease can be made by biopsy or by autopsy [6.107–6.109]. The main histopathological features of Alzheimer's disease is the formation of amyloid plaques in the extracellular space of the brain and the amyloid deposits on the wall of the brain blood vessels, which can be seen after staining with histological dyes (Congo Red, Chrysamine G, Thioflavine S and Thioflavine T). The amyloid plaque is a composite formation, the main component of which is the  $\beta$ -amyloid peptide.

Amyloid- $\beta$  (A $\beta$ ) is 39–42 amino acids in length and is secreted from neurons into brain interstitial fluid, where it is eliminated by proteolytic degradation, passive back flow and active transport across the BBB. The low-density lipoprotein receptor-related protein (LRP-1) and P-glycoprotein (Pgp; ABCB1) have been described as the major efflux transporters. Dysfunction of the efflux transporters results in an increasing concentration of A $\beta$ , which induces a change in the conformation of A $\beta$  to  $\beta$ -sheet and progressively aggregates, forming the insoluble amyloid fibrils, which eventually form the amyloid plaque [6.110–6.113]. The amyloid plaques have, therefore, been recognized as a target for the development of specific radiopharmaceuticals. These radiopharmaceuticals, when administered to the patient, are expected to cross the BBB and to be retained in the brain by binding specifically to amyloid plaques. Subsequent SPECT or PET imaging of the brain will provide information about the location of the plaques and will allow quantitative evaluation of the progress of the disease [6.114–6.116].

The design of these radiopharmaceuticals is mainly based on the structures of the dyes Congo Red, Chrysamine G and Thioflavin T (Fig. 6.13), which

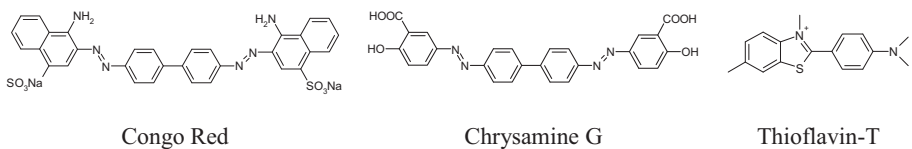


FIG. 6.13. Organic dyes serving as lead structures for amyloid plaque avid  $^{99m}\text{Tc}$  tracers.

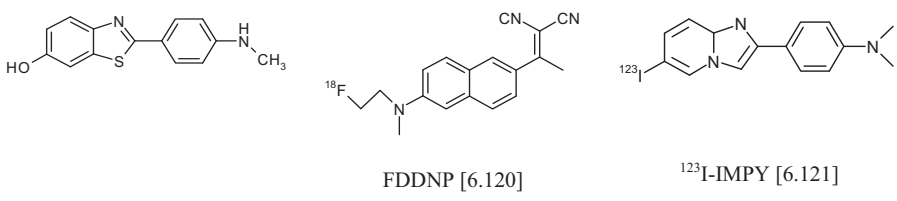


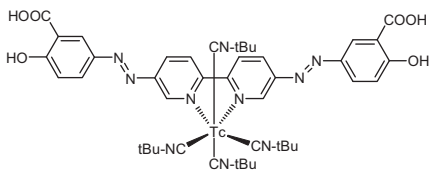
FIG. 6.14.  $^{11}\text{C}$ ,  $^{18}\text{F}$  and  $^{123}\text{I}$  labelled amyloid plaque imaging agents.

display great selectivity for amyloid plaques and are extensively used in medical practice for in vitro staining of brain tissue of Alzheimer's patients. The basic structure of these dyes can, therefore, be considered as the target specific compound that will bind to amyloid plaques. The use of other derivatives such as biphenyl and stilbene has also been reported.

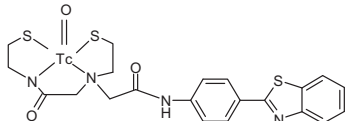
Although the majority of efforts in developing cerebral amyloid probes have been focused on PET radionuclides and  $^{123}\text{I}$  (Fig. 6.14) [6.117–6.123], some progress has also been made on the development of  $^{99m}\text{Tc}$  agents (Fig. 6.15). The  $^{99m}\text{Tc}$  complexes studied so far showed good binding affinity for the amyloid in vitro, but their brain uptake was too low [6.124–6.130]. As is obvious from these few experiments, more systematic studies are required to improve brain uptake.

## 6.6. PERSPECTIVES AND CONCLUSIONS

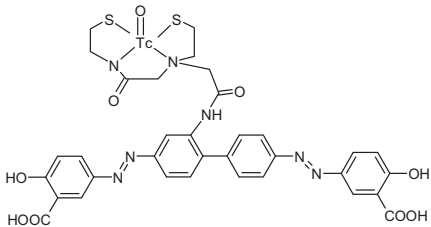
Nowadays, CNS receptor imaging agents are, with some exceptions, typically PET radionuclide based radiopharmaceuticals. The reason for this is not based on principal but is rather as a result of the fact that efforts in the direction of  $^{99m}\text{Tc}$  containing agents have not been strong or consistent enough. Early detection of a neurodegenerative disease and assessment of success or failure of therapy are equally important roles for radiopharmaceuticals. It requires highly specific radiopharmaceuticals, which pass the BBB to a good extent and lead to clear images with a high target:non-target ratio. This is not yet ideally established,



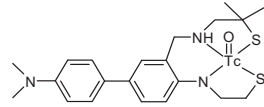
[6.124]



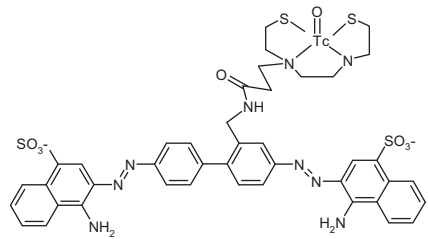
[6.127]



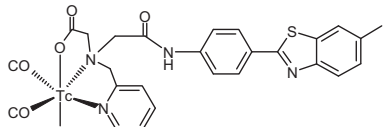
[6.125]



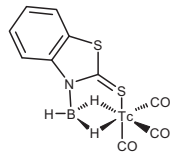
[6.129]



[6.126]



[6.128]



[6.130]

FIG. 6.15. Potential  $^{99m}\text{Tc}$  labelled amyloid imaging agents derived from organic dyes.

either for  $^{99\text{m}}\text{Tc}$  based radiopharmaceuticals or for PET radiopharmaceuticals. However,  $^{99\text{m}}\text{Tc}$ -TRODAT has provided proof of principle although its relatively low uptake through the BBB is a weak point that has to be improved. Technetium-99m-TRODAT (and similar compounds) is the only  $^{99\text{m}}\text{Tc}$  based CNS receptor targeting agent studied in depth so far. In addition, the type of receptors to be targeted is still narrow and should be extended substantially according to the practical needs of clinicians and company marketing studies. The selection of the targeted receptors (and, hence, the targeting molecules) has

to be performed very carefully and various aspects, such as availability, not only radiopharmacy, have to be considered since it will impact on synthetic strategies, cores and new chemistry to be investigated. After selecting the receptor to be targeted, a decision has to be made about which labelling method should be chosen. Since lipophilicity, charge and molecular weight are crucial factors, the TcN, TcO, Tc(CO)<sub>3</sub> and Tc(III) cores can be exploited. It is recommended that differently labelled compounds of the same receptor ligand are compared. Since most of the previously available compounds suffer from low to very low brain uptake (and not from receptor affinity), a major focus should be put on the coordination chemistry in order to improve the percentage of compound, which passes the BBB. This task will, to a large extent, be based on new chemistry, either with the available cores or with new ones. Ligand development, coupling strategies and labelling techniques play a major role for improving the critical issue of brain uptake.

The development of new <sup>99m</sup>Tc based radiopharmaceuticals for brain receptor imaging will contribute to health care for a significant part of the population and will add to the knowledge of biological and biochemical processes taking place in the brain.

## REFERENCES TO CHAPTER 6

- [6.1] RAMSEY, R.G., QUINN, R.G., Comparison of accuracy between initial and delayed <sup>99m</sup>Tc-pertechnetate brain scans, *J. Nucl. Med.* **13** (1972) 131–134.
- [6.2] CASTAGNOLI, A., et al., Brain scintigraphy with <sup>99m</sup>Tc-citrate and <sup>99m</sup>Tc-DTPA: A clinical comparison of the results, *Eur. J. Nucl. Med.* **7** (1982) 184–186.
- [6.3] REYRSON, T.W., SPIES, S.M., SINGH, N.B., ZEMAN, R.K., A quantitative clinical comparison of three <sup>99m</sup>Technetium labeled brain imaging radiopharmaceuticals, *Radiology* **127** (1978) 429–432.
- [6.4] NIR, I., LEVANON, D., IOSILEVSKY, G., Permeability of blood vessels in experimental gliomas: uptake of <sup>99m</sup>Tc-glucoheptonate and alteration in blood-brain barrier as determined by cytochemistry and electron microscopy, *Neurosurgery* **25** (1989) 523–531.
- [6.5] KUNG, H.F., New Technetium <sup>99m</sup>-labeled brain perfusion imaging agents, *Semin. Nucl. Med.* **20** (1990) 150–158.
- [6.6] NOWOTNIK, D.P., “Technetium-based brain perfusion agents”, *Radiopharmaceuticals: Chemistry and Pharmacology* (NUNN, A., Ed.), Marcel Dekker, New York, NY (1992) 37–95.
- [6.7] KUNG, H.F., MOLNAR, M., BILLINGS, J., WICKS, R., BLAU, M., Synthesis and biodistribution of neutral lipid soluble Tc-<sup>99m</sup> complexes that cross the blood brain barrier, *J. Nucl. Med.* **25** (1984) 326–332.

- [6.8] LEVER, S.Z., et al., Design preparation and biodistribution of a technetium-99m triaminedithiol complex to assess regional cerebral blood flow, *J. Nucl. Med.* **28** (1985) 1287–1294.
- [6.9] TROUTNER, D.E., VOLKERT, W.A., HOFFMAN, T.J., A neutral lipophilic complex of  $^{99m}\text{Tc}$  with a multidentate amine oxime, *Int. J. Appl. Radiat. Isotop.* **35** (1984) 467–470.
- [6.10] NOWOTNIK, D.P., et al., Development of  $^{99m}\text{Tc}$ -labelled radiopharmaceutical for SPECT imaging, *Nucl. Med. Commun.* **6** (1985) 499–506.
- [6.11] NEIRINCKX, R.D., et al., Technetium-99m d,1-HM-PAO: a new radiopharmaceutical for SPECT imaging of regional cerebral blood perfusion, *J. Nucl. Med.* **28** (1987) 191–202.
- [6.12] JURISSON, S., et al., Synthesis and characterization and X-ray structural determinations of technetium (V)-oxo-tetradeятate amine oxime complexes, *Inorg. Chem.* **25** (1986) 543–549.
- [6.13] WALOVITCH, R.C., et al., Characterization of Technetium-99m-L-L-ECD for brain perfusion imaging, Part 1: Pharmacology of Technetium-99m ECD in nonhuman primates, *J. Nucl. Med.* **30** (1989) 1892–1901.
- [6.14] LEVEILLE, J., et al., Characterization of Technetium-99m-L-L-ECD for brain perfusion imaging, Part 2: Biodistribution and brain imaging in humans, *J. Nucl. Med.* **30** (1989) 1902–1910.
- [6.15] ROTH, C.A., HOFFMAN, T.J., CORLIJA, M., VOLKERT, W.A., HOLMES, R.A., The effect of ligand structure on glutathione-mediated decomposition of propylene amine oxime derivatives, *Nucl. Med. Biol.* **19** (1992) 783–790.
- [6.16] JACQUIER-SARLIN, M.R., POLLA, B.S., SLOSMAN, D.O., Oxido-reductive state: The major determinant for cellular retention of Technetium-99m-HMPAO, *J. Nucl. Med.* **37** (1996) 1413–1416.
- [6.17] EDWARDS, D.S., et al., “Synthesis and characterization of technetium and rhenium complexes of N,N'-1,2-ethylenediylbis-L-cysteine. Neurolite and its metabolites”, *Technetium and Rhenium in Chemistry and Nuclear Medicine 3* (NICOLINI, M., BANDOLI, G., MAZZI, U., Eds), Raven Press, New York, NY (1990) 433–444.
- [6.18] WALOVITCH, R.C., et al., Metabolism of  $^{99m}\text{Tc}$ -L-L-ethyl cysteinate dimer in healthy volunteers, *Neuropharmacology* **30** (1991) 283–292.
- [6.19] HOLMAN, B.L., DEVOUS, M.D., Functional brain SPECT: The emergence of a powerful clinical method, *J. Nucl. Med.* **33** (1992) 1888–1904.
- [6.20] MORETTI, J.L., CAGLAR, M., WEINMANN, P., Cerebral perfusion imaging tracers for SPECT: Which one to choose? *J. Nucl. Med.* **36** (1995) 359–363.
- [6.21] DEVOUS, M.D., Functional brain imaging in the dementias: role in early detection, differential diagnosis, and longitudinal studies, *Eur. J. Nucl. Med.* **29** (2002) 1685–1687.
- [6.22] “Ceretec” brochure PJ.Ell (Institute of Nuclear Medicine, Middlesex Hospital, University College London Hospitals Trusts, London, UK).
- [6.23] PIZZOLATO, G., et al., [ $^{99m}\text{Tc}$ ]-HM-PAO SPECT in Parkinson’s disease, *J. Cereb. Blood Flow Metab.* **8**(Suppl. 1) (1988) S101–S108.

- [6.24] HAMMOUD, D.A., HOFFMAN, J.M., POMPER, M.G., Molecular neuroimaging: From conventional to emerging techniques, *Radiology* **245** (2007) 21–42.
- [6.25] TASCH, K., ELL, P.J., PET and SPECT in common neuropsychiatric disease, *Clin. Med.* **6** (2006) 259–262.
- [6.26] VERHOEFF, N.P.L.G., Radiotracer imaging of dopaminergic transmission in neuropsychiatric disorders, *Psychopharmacology* **147** (1999) 217–249.
- [6.27] ECKELMAN, W.C., Accelerating drug discovery and development through in vivo imaging, *Nucl. Med. Biol.* **29** (2002) 777–782.
- [6.28] ECKELMAN, W.C., Radiolabeling with technetium-99m to study high-capacity and low-capacity biochemical systems, *Eur. J. Nucl. Med.* **22** (1995) 249–263.
- [6.29] LIU, S., EDWARDS, S., <sup>99m</sup>Tc-labeled small peptides as diagnostic radiopharmaceuticals, *Chem. Rev.* **99** (1999) 2235–2268.
- [6.30] JURISSON, S.S., LYDON, J.D., Potential technetium small molecule radiopharmaceuticals, *Chem. Rev.* **99** (1999) 2205–2218.
- [6.31] DILWORTH, J.R., PARROTT, J., The biomedical chemistry of technetium and rhenium, *Chem. Soc. Rev.* **27** (1998) 43–55.
- [6.32] JOHANNSEN, B., SPIES, H., Technetium(V) chemistry as relevant to nuclear medicine, *Top. Curr. Chem.* **176** (1996) 77–121.
- [6.33] BOLZATI, C., et al., Synthesis and biodistribution in rats of a nitrido-technetium-99m radiopharmaceutical incorporating a benzodiazepine-receptor-specific ligand, *J. Labelled Comp. Radiopharm.* **42** (1999) S579–S580.
- [6.34] BOLZATI, C., et al., Geometrically controlled selective formation of nitridotechnetium(V) asymmetrical heterocomplexes with bidentate ligands, *J. Am. Chem. Soc.* **122** (2000) 4510–4511.
- [6.35] PIETZSCH, H.-J., SPIES, H., HOFFMANN, S., STACH, J., Lipophilic technetium complexes-V. Synthesis and characterization of (3-thiapentane-1,5-dithiolato)(thiophenolato) oxotechnetium (V), *Inorg. Chem. Acta* **161** (1989) 15–16.
- [6.36] MASTROSTAMATIS, S.G., et al., Tridentate ligands containing the SNS donor atom set as a novel backbone for the development of technetium brain-imaging agents, *J. Med. Chem.* **37** (1994) 3212–3218.
- [6.37] GUPTA, A., et al., Reactivity of <sup>99m</sup>Tc(V) “3+1” mixed-ligand complexes towards glutathione, *Radiochim. Acta* **89** (2001) 43–49.
- [6.38] NOCK, B.A., et al., Glutathione-mediated metabolism of technetium-99m SNS/S mixed ligand complexes: a proposed mechanism of brain retention, *J. Med. Chem.* **42** (1999) 1066–1075.
- [6.39] SEIFERT, S., GUPTA, A., SYHRE, R., SPIES, H., JOHANNSEN, B., Ligand exchange reaction of labile “3+1” Tc(V) complexes with SH group-containing proteins, *Int. J. Appl. Radiat. Isotop.* **54** (2001) 637–644.
- [6.40] PIETZSCH, H.-J., GUPTA, A., SYHRE, R., LEIBNITZ, P., SPIES, H., Mixed-ligand technetium(III) complexes with tetradendate/monodendate NS3/isocyanide coordination: A new nonpolar technetium chelate system for the design of neutral and lipophilic complexes stable in vivo, *Bioconjug. Chem.* **12** (2001) 538–544.

- [6.41] SEIFERT, S., et al., Novel procedures for preparing  $^{99m}\text{Tc}(\text{III})$  complexes with tetradeinate/monodentate coordination of varying lipophilicity and adaptation to  $^{188}\text{Re}$  analogues, *Bioconjug. Chem.* **15** (2004) 856–863.
- [6.42] ALBERTO, R., SCHIBLI, R., EGLI, A., SCHUBIGER, A.P., Novel organometallic aqua complex of technetium for the labeling of biomolecules: Synthesis of  $[^{99m}\text{Tc}(\text{OH}_2)_3(\text{CO})_3]^+$  from  $[^{99m}\text{TcO}_4]^-$  in aqueous solution and its reaction with a bifunctional ligand, *J. Am. Chem. Soc.* **120** (1998) 7987–7988.
- [6.43] ALBERTO, R., New organometallic technetium complexes for radiopharmaceutical imaging, *Top. Curr. Chem.* **252** (2005) 1–44.
- [6.44] ZHUANG, Z.P., MU, M., KUNG, M.P., PLÖSSL, K., KUNG, H.F., Homologue of  $^{99m}\text{Tc}$ -TRODAT as dopamine transporter imaging agent, *J. Labelled Comp. Radiopharm.* **42** (1999) S351–S353.
- [6.45] JOHANNSEN, B., et al., Structural modification of receptor-binding technetium- $99m$  complexes in order to improve brain uptake, *Eur. J. Nucl. Med.* **24** (1997) 316–319.
- [6.46] DREWS, A., et al., Synthesis and biological evaluation of Tc(III) mixed-ligand complexes with high affinity for the cerebral 5-HT1A receptor and the alpha1-adrenergic receptor, *Nucl. Med. Biol.* **29** (2002) 389–398.
- [6.47] MADRAS, B.K., MILLER, G.M., FISHMAN, A.J., The dopamine transporter and attention-deficit/hyperactivity disorder, *Biol. Psychiatry* **57** (2005) 1397–1409.
- [6.48] SPENCER, T.J., et al., In vivo neuroreceptor imaging in attention-deficit/hyperactivity disorder: A focus on the dopamine transporter, *Biol. Psychiatry* **57** (2005) 1293–1300.
- [6.49] BROOKS, D.J., Imaging studies in drug development: Parkinson's disease, *Drug Disc. Today* **2** (2005) 317–321.
- [6.50] RAVINA, B., et al., The role of radiotracer imaging in Parkinson's disease, *Neurology* **64**(2) (2005) 208–215.
- [6.51] INNIS, R.B., Single photon emission tomography imaging of dopamine terminal innervation: a potential clinical tool in Parkinson's disease, *Eur. J. Nucl. Med.* **21** (1994) 1–5.
- [6.52] SHAYA, E.K., et al., In vivo imaging of dopamine reuptake sites in the primate brain using single photon emission computed tomography (SPECT) and iodine-123 labeled RTI-55, *Synapse* **10** (1992) 169–172.
- [6.53] FROST, J.J., et al., Positron emission tomographic imaging of the dopamine transporter with  $[^{11}\text{C}]\text{-WIN } 35,428$  reveals marked declines in mild Parkinson's disease, *Ann. Neurol.* **34** (1993) 423–431.
- [6.54] KUNG, M.-P., et al., IPT: a novel iodinated ligand for the CNS dopamine transporter, *Synapse* **20** (1995) 316–324.
- [6.55] NEUMEYER, J.L., et al., N- $\omega$ -fluoroalkyl analogs of (1R)- $2\beta$ -carbomethoxy- $3\beta$ -(4-iodophenyl)-tropane ( $\beta$ -CIT): radiotracers for positron emission tomography and single photon emission computed tomography imaging of dopamine transporters, *J. Med. Chem.* **37** (1994) 1558–1561.
- [6.56] WILSON, A.A., DASILVA, J.N., HOULE, S., In vivo evaluation of  $[^{11}\text{C}]$ - and  $[^{18}\text{F}]$ -labelled cocaine analogues as potential dopamine transporter ligands for positron emission tomography, *Nucl. Med. Biol.* **23** (1996) 141–146.

- [6.57] MEEGALLA, S., et al., First example of a  $^{99m}\text{Tc}$  complex as a dopamine transporter imaging agent, *J. Am. Chem. Soc.* **117** (1995) 11037–11038.
- [6.58] MEEGALLA, S., et al., Tc-99m-labeled tropanes as dopamine transporter imaging agents, *Bioconjug. Chem.* **7** (1996) 421–429.
- [6.59] MEEGALLA, S., et al., Synthesis and characterization of Tc-99m labelled tropanes as dopamine transporter imaging agents, *J. Med. Chem.* **40** (1997) 9–17.
- [6.60] KUNG, H.F., et al., Imaging of dopamine transporters in humans with technetium-99m TRODAT-1, *Eur. J. Nucl. Med.* **23** (1996) 1527–1530.
- [6.61] KUNG, H.F., KUNG, M.-P., WEY, S.-P., LIN, K.-J., YEN, T.-C., Clinical acceptance of a molecular imaging agent: a long march with [ $^{99m}\text{Tc}$ ]TRODAT, *Nucl. Med. Biol.* **34** (2007) 787–789.
- [6.62] KOCH, W., et al., Extented studies of the striatal uptake of  $^{99m}\text{Tc}$ -NC100697 in healthy volunteers, *J. Nucl. Med.* **48** (2007) 27–34.
- [6.63] MADRAS, B.K., et al., Technepine: a high affinity  $^{99m}\text{Tc}$ Technetium probe to label the dopamine transporter in brain by SPECT imaging, *Synapse* **22** (1996) 239–246.
- [6.64] MELTZER, P.C., et al., A technetium-99m SPECT imaging agent which targets the dopamine transporter in primate brain, *J. Med. Chem.* **40** (1997) 1835–1844.
- [6.65] MELTZER, P.C., et al., A second-generation  $^{99m}\text{Tc}$ Technetium single photon emission computed tomography agent that provides *in vivo* images of the dopamine transporter in primate brain, *J. Med. Chem.* **46** (2003) 3483–3496.
- [6.66] VALBILLOEN, H.P., et al., Development and biological evaluation of  $^{99m}\text{Tc}$ -BAT-tropane esters, *Nucl. Med. Biol.* **32** (2005) 607–612.
- [6.67] CLEYNHENS, B.J., et al., Technetium-99m labelled integrated tropane-BAT as potential dopamine transporter trace, *Bioorg. Med. Chem.* **13** (2005) 1053–1058.
- [6.68] KIEFFER, D.M., et al., Biological evaluation of a technetium-99m labelled integrated tropane-BAT and its piperidine congener as potential dopamine transporter imaging agent, *Nucl. Med. Biol.* **33** (2006) 125–133.
- [6.69] HOEPPING, A., et al., TROTEC-1: a new high-affinity ligand for labeling of the dopamine transporter, *J. Med. Chem.* **41** (1998) 4429–4432.
- [6.70] KIEFFER, D.M., et al., Synthesis and biological evaluation of a technetium-99m(I) tricarbonyl labelled phenyltropane derivative, *Bioorg. Med. Chem. Lett.* **16** (2006) 382–386.
- [6.71] CESATI, R.R., III, et al., Synthesis of cyclopentadienyltricarbonyl rhenium phenyltropanes by double ligand transfer: Organometallic ligands for the dopamine transporter, *Bioconjug. Chem.* **13** (2002) 29–39.
- [6.72] VANBILLOEN, H.P., KIEFFER, D.M., CLEYNHENS, B.J., BORMANS, G.M., VERBRUGGEN, A.M., Evaluation of  $^{99m}\text{Tc}$ -labeled tropanes with alkyl substituents on the  $3\beta$ -phenyl ring as potential dopamine transporter tracers, *Nucl. Med. Biol.* **33** (2006) 413–418.
- [6.73] PASSCHIER, J., VAN WAARDE, A., Visualisation of serotonin-1A (5-HT1A) receptors in the central nervous system, *Eur. J. Nucl. Med.* **28** (2001) 113–129.
- [6.74] LANFUMEY, L., HAMON, M., Central 5-HT1A receptors: Regional distribution and functional characteristics, *Nucl. Med. Biol.* **27** (2000) 429–435.

- [6.75] KEPE, V., et al., Serotonin 1A receptors in the living brain of Alzheimer's disease patients, *Proc. Natl. Acad. Sci. USA* **103** (2006) 702–707.
- [6.76] MERENS, W., WILLEM VAN DER DOES, A.J., SPINHOVEN, P., The effects of serotonin manipulations on emotional information processing and mood, *J. Aff. Disorders* **103** (2007) 43–62.
- [6.77] FORSTER, E.A., et al., A pharmacological profile of the selective silent 5-HT<sub>1A</sub> receptor antagonist, WAY-100635, *Eur. J. Pharmacol.* **281** (1995) 81–88.
- [6.78] LAPORTE, A.-M., LIMA, L., GOZLAN, H., HAMON, M., Selective in vivo labeling of brain 5-HT<sub>1A</sub> receptors by [<sup>3</sup>H]WAY 100635 in the mouse, *Eur. J. Pharmacol.* **271** (1994) 505–514.
- [6.79] CLIFFE, I.A., A retrospect on the discovery of WAY-100635 and the prospect for improved 5-HT<sub>1A</sub> receptor PET radioligands, *Nucl. Med. Biol.* **27** (2000) 441–447.
- [6.80] JOHANNSEN, B., PIETZSCH, H.J., Development of technetium-99m-based CNS receptor ligands: have there been any advances? *Eur. J. Nucl. Med.* **29** (2002) 263–275.
- [6.81] PIKE, V.W., HALLDIN, C., WILKSTRÖM, H.V., “Radioligands for the study of brain 5-HT<sub>1A</sub> receptors in vivo”, *Progress in Medicinal Chemistry* (KING, F.D., OXFORD, A.W., Eds), Elsevier Science B.V. (2001) 189–247.
- [6.82] LANG, L., et al., Fluoro analogues of WAY-100635 with varying pharmacokinetic properties, *Nucl. Med. Biol.* **27** (2000) 457–462.
- [6.83] PIKE, V.W., et al., Radioligands for the study of brain 5-HT<sub>1A</sub> receptors in vivo—development of some new analogues of WAY, *Nucl. Med. Biol.* **27** (2000) 449–455.
- [6.84] PIKE, V.W., et al., [Carbonyl-<sup>11</sup>C] Desmethyl-WAY 100635 (DWAY) is a potent and selective radioligand for the central 5-HT<sub>1A</sub> receptors in vitro and in vivo, *Eur. J. Nucl. Med.* **25** (1998) 338–346.
- [6.85] WILSON, A.A., et al., Derivatives of WAY 100635 as potential imaging agents for 5-HT<sub>1A</sub> receptors: syntheses, radiosyntheses, and in vitro and in vivo evaluation, *Nucl. Med. Biol.* **25** (1998) 769–776.
- [6.86] PIKE, V.W., et al., Exquisite delineation of 5-HT<sub>1A</sub> receptors in human brain with PET and [carbonyl-<sup>11</sup>C] WAY 100635, *Eur. J. Pharmacol.* **301** (1996) R5–R7.
- [6.87] VANDECAPELLE, M., et al., In vivo evaluation of 4-[<sup>123</sup>I]iodo-N-{2-[4-(6-trifluoromethyl-2-pyridinyl)-1-piperazinyl]ethyl}benzamide, a potential SPECT radioligand for the 5-HT<sub>1A</sub> receptor, *Nucl. Med. Biol.* **28** (2001) 639–643.
- [6.88] ZHUANG, Z-P., KUNG, M-P., KUNG, H.F., Synthesis and evaluation of 4-(2'-methoxyphenyl)-1-[2'-(N-(2"-pyridinyl)-p-iodobenzamido)ethyl]piperazine (p-MPPI): A new iodinated 5-HT<sub>1A</sub> ligand, *J. Med. Chem.* **37** (1994) 1406–1407.
- [6.89] KUNG, H., et al., “New TcO(III) and ReO(III)N<sub>2</sub>S<sub>2</sub> complexes as potential CNS 5-HT<sub>1A</sub> receptor imaging agents”, *Technetium and Rhenium in Chemistry and Nuclear Medicine* (NICOLINI, M., BANDOLI, G., MAZZI, U., Eds), SGE, Padova (1995) 293–298.
- [6.90] MAHMOOD, A., et al., “Technetium(V) and rhenium (V) analogues of WAY 100635 5HT<sub>1A</sub> receptor-binding complexes”, *Technetium, Rhenium and other Metals in Chemistry and Nuclear Medicine* (NICOLINI, M., MAZZI, U., Eds), SGE, Padova (1999) 393–399.

- [6.91] PLÖSSL, K., et al., Tc-99m[MPP] complexes: potential 5-HT<sub>1A</sub> receptor imaging agents, *J. Labelled Comp. Radiopharm.* **37** (1995) 306–308.
- [6.92] VANBILLOEN, H., CLEYNHENS, B., CROMBEZ, D., VERBRUGGEN, A., “Synthesis and biological evaluation of a conjugate of <sup>99m</sup>Tc-ECC with 1-(2-methoxyphenyl)-4-(2-pyridylamino)ethylpiperazine (Way-100634)”, *Technetium, Rhenium and other Metals in Chemistry and Nuclear Medicine* (NICOLINI, M., MAZZI, U., Eds), SGE, Padova (1999) 479–484.
- [6.93] HEIMBOLD, I., et al., A novel Tc-99m radioligand for the 5-HT<sub>1A</sub> receptor derived from Desmethyl-WAY-100635 (DWAY), *Eur. J. Nucl. Med.* **29** (2002) 82–87.
- [6.94] DREWS, A., et al., Autoradiographical evaluation of novel high-affinity Tc-99m ligands for the serotonin-HT<sub>1A</sub> receptor, *J. Labelled Comp. Radiopharm.* **44** (2001) S544–S546.
- [6.95] LEÓN, A., et al., Novel mixed ligand technetium complexes as 5-HT<sub>1A</sub> receptor imaging agents, *Nucl. Med. Biol.* **29** (2002) 217–226.
- [6.96] PAPAGIANNOPOLOU, D., et al., Oxotechnetium <sup>99m</sup>TcO[SN(R)S][S] complexes as potential 5-HT<sub>1A</sub> receptor imaging agents, *Nucl. Med. Biol.* **29** (2002) 825–832.
- [6.97] DYSZLEWSKI, M.E., et al., Kit formulation and preliminary toxicity of [<sup>99m</sup>Tc(CO)<sub>3</sub>]<sup>+</sup> intermediate: A novel technetium radiopharmaceutical platform, *J. Labelled Comp. Radiopharm.* **44** (2001) S483–S485.
- [6.98] PIRMETTIS, I., et al., Synthesis, labelling with <sup>99m</sup>Tc and biological study of a novel 5-HT<sub>1A</sub> receptor ligand, *J. Labelled Comp. Radiopharm.* **44** (2001) S550–S552.
- [6.99] ALBERTO, R., et al., First application of fac-[<sup>99m</sup>Tc(OH<sub>2</sub>)<sub>3</sub>(CO)<sub>3</sub>]<sup>+</sup> in bioorganometallic chemistry: Design, structure, and in vitro affinity of a 5-HT<sub>1A</sub> receptor ligand labeled with <sup>99m</sup>Tc, *J. Am. Chem. Soc.* **121** (1999) 6076–6077.
- [6.100] BERNARD, J., ORTNER, K., SPINGLER, B., PIETZSCH, H.-J., ALBERTO, R., Aqueous synthesis of derivatized cyclopentadienyl complexes of technetium and rhenium directed toward radiopharmaceutical application, *Inorg. Chem.* **42** (2003) 1014–1022.
- [6.101] WEI, L., BANERJEE, S.A., LEVEDALA, M.K., BABICH, J., ZUBIETA, J., Complexes of the fac- $\{\text{Re}(\text{CO})_3^+\}$  core with tridentate ligands derived from arylpiperazines, *Inorg. Chim. Acta* **57** (2004) 1499–1516.
- [6.102] BOLZATI, C., et al., The [<sup>99m</sup>Tc(N)(PNP)]<sup>2+</sup> metal fragment: A technetium-nitrido synthon for use with biologically active molecules, The N-(2-methoxyphenyl)piperazyl-cysteine analogues as example, *Bioconjug. Chem.* **14** (2003) 1231–1242.
- [6.103] PALMA, E., et al., Rhenium tricarbonyl complexes anchored by 5-HT<sub>1A</sub> receptor-binding ligands containing P,O/N donor atom sets, *J. Organomet. Chem.* **689** (2004) 4811–4819.
- [6.104] FERNANDES, C., et al., Dramatic effect of the tridentate ligand on the stability of <sup>99m</sup>Tc “3+1” oxo complexes bearing arylpiperazine derivatives, *Bioconjug. Chem.* **16** (2005) 660–688.
- [6.105] INTERNATIONAL ATOMIC ENERGY AGENCY, Development of <sup>99m</sup>Tc Agents for Imaging Central Neural System Receptors, Technical Reports Series No. 426, IAEA, Vienna (2004).

- [6.106] SAIDI, M., SEIFERT, S., KRETZSCHMAR, M., BERGMANN, R., PIETZSCH, H.-J., Cyclopentadienyl tricarbonyl complexes of  $^{99m}\text{Tc}$  for the *in vivo* imaging of the serotonin 5-HT<sub>1A</sub> receptor in the brain, *J. Organomet. Chem.* **689** (2004) 4739–4744.
- [6.107] MCKHAN, G., et al., Clinical diagnosis of Alzheimer's disease: report of the NINCDS-ADRDA Work Group under the auspices of Department of Health and Human Services Task Force on Alzheimer's Disease, *Neurology* **34** (1984) 939–944.
- [6.108] AMERICAN PSYCHOLOGICAL ASSOCIATION, Diagnostic and Statistical Manual of Mental Disorders, 4th edn, American Psychological Association, Washington, DC (1994).
- [6.109] MULLER, S.G., et al., Ways toward an early diagnosis in Alzheimer's disease: The Alzheimer's disease neuroimaging initiative (ADNI), *Alzheimer's & Dementia* **1** (2005) 55–66.
- [6.110] ZLOKOVIC, B.V., Neurovascular mechanisms of Alzheimer's neurodegeneration, *Trends Neurosci.* **28** (2005) 202–208.
- [6.111] FARRIS, W., et al., Insulin-degrading enzyme regulates the levels of insulin, amyloid beta-protein, and the beta-amyloid precursor protein intracellular domain *in vivo*, *Proc. Natl. Acad. Sci. USA* **100** (2003) 4162–4167.
- [6.112] DEMATTOS, R.B., BALES, K.R., CUMMINS, D.J., PAUL, S.M., HOLTZMAN, D.M., Brain to plasma amyloid-beta efflux: a measure of brain amyloid burden in a mouse model of Alzheimer's disease, *Science* **295** (2002) 2264–2267.
- [6.113] CIRRITO, J.R., et al., P-glycoprotein deficiency at the blood-brain barrier increases amyloid- $\beta$  deposition in an Alzheimer disease mouse model, *J. Clin. Invest.* **115** (2005) 3285–3290.
- [6.114] WU, C., PIKE, V.W., WANG, Y., Amyloid imaging: From benchtop to bedside, *Curr. Top. Develop. Biol.* **70** (2005) 171–213.
- [6.115] SAIR, D., DORAISWAMY, P.M., PETRELLA, J.R., In vivo imaging in Alzheimer's disease, *Neuroradiology* **46** (2004) 93–104.
- [6.116] MATHIS, C.A., KLUNK, W.E., PRICE, J.C., DEKOSKY, S.T., Imaging technology for neurodegenerative diseases, *Arch. Neurol.* **62** (2005) 196–200.
- [6.117] ENGLER, H., NORDBERG, A., BLOMQVIST, G., et al., First human study with a benzothiazole amyloid-imaging agent in Alzheimer's disease and control subjects, *Neurobiol. Aging* **23**(Suppl. 1) (2002) S429.
- [6.118] MATHIS, C.A., et al., Synthesis and evaluation of  $^{11}\text{C}$ -labeled 6-substituted 2-arylbenzothiazoles as amyloid imaging agents, *J. Med. Chem.* **46** (2003) 2740–2754.
- [6.119] KUDO, Y., et al., 2-(2-[2-dimethylaminothiazol-5-yl]ethenyl)-6-(2-[fluoro]ethoxy)benzoxazole: A novel PET agent for *in vivo* detection of dense amyloid plaques in Alzheimer's disease patients, *J. Nucl. Med.* **48** (2007) 553–561.
- [6.120] AGDEPA, E.D., et al., Binding characteristics of radiofluorinated 6-dialkylamino-2-naphthylethylidene derivatives as positron emission tomography imaging probes for beta-amyloid plaques in Alzheimer's disease, *J. Neurosci.* **21** (2001) RC189.
- [6.121] KUNG, H.F., et al., Iodinated tracers for imaging amyloid plaques in the brain, *Mol. Imag. Biol.* **5** (2003) 418–426.

- [6.122] NEWBERG, A.B., et al., Safety, biodistribution and dosimetry of  $^{123}\text{I}$ -IMPY: A novel amyloid plaque-imaging agent for the diagnosis of Alzheimer's disease, *J. Nucl. Med.* **47** (2006) 748–754.
- [6.123] WU, C., WEI, J., GAO, K., WANG, Y., Dibenzothiazoles as novel amyloid-imaging agents, *Bioorg. Med. Chem.* **15** (2007) 2789–2796.
- [6.124] HAN, H., CHO C.-G., LANSBURY, P.T., Technetium complexes for quantification of brain amyloid, *J. Am. Chem. Soc.* **118** (1996) 4506–4507.
- [6.125] DEZUTTER, N.A., DOM, R.J., DE GROOT, T.J., BORMANS, G.M., VERBRUGGEN, A.M.,  $^{99\text{m}}\text{Tc}$ -MAMA-chrysamine G a probe for beta amyloid protein of Alzheimer's disease, *Eur. J. Nucl. Med.* **26** (1999) 1392–1399.
- [6.126] ZHEN, W., et al., Synthesis and amyloid binding properties of rhenium complexes: Preliminary progress toward a reagent for SPECT imaging of Alzheimer's disease, *Brain. J. Med. Chem.* **42** (1999) 2805–2815.
- [6.127] SERDONS, K., et al., Synthesis and evaluation of a  $^{99\text{m}}\text{Tc}$ -BAT-phenylbenzothiazole conjugate as a potential in vivo tracer for visualization of amyloid  $\beta$ , *Bioorg. Med. Chem. Lett.* **17** (2007) 6086–6090.
- [6.128] TZANOPOLOU, S., et al., "Synthesis and characterization of M(I)(CO)<sub>3</sub>(NNO) complexes (M = Re,  $^{99\text{m}}\text{Tc}$ ) conjugated to 6-methyl-2-(4'-aminophenyl)benzothiazole towards the development of Alzheimer's disease radiodiagnostics", *Technetium, Rhenium and Other Metals in Chemistry and Nuclear Medicine*, 7 (MAZZI, U., Ed.), SGE Ditorialli, Padova (2006) 103–104.
- [6.129] ZHUANG, Z.-P., KUNG, M.-P., HOU, C., PLOESSL, K., KUNG, H.F., Biphenyls with technetium 99m for imaging  $\beta$ -amyloid plaques in the brain, *Nucl. Med. Biol.* **32** (2005) 171–184.
- [6.130] MARIA, L., et al., Very small and soft scorpionates: Water stable technetium tricarbonyl complexes combining a bis-agostic (K<sub>3</sub>-H, H, S) binding motif with pendant and integrated bioactive molecules, *J. Am. Chem. Soc.* **128** (2006) 14590–14598.

## **Chapter 7**

### **TECHNETIUM-99m LABELLED INFECTION IMAGING AGENTS**

M. WELLING

Department of Radiology, Division of Nuclear Medicine,  
Leiden University Medical Center,  
Leiden, Netherlands

G. FERRO-FLORES

Instituto Nacional de Investigaciones Nucleares,  
Departamento de Materiales Radiactivos,  
Carretera México-Toluca S/N, La Marquesa, Ocoyoacac,  
Estado de México, Mexico

I. PIRMETTIS

Institute of Radioisotopes, Radiodiagnostic Products,  
National Centre for Scientific Research “Demokritos”,  
Athens, Greece

#### **Abstract**

Infection specific radiopharmaceuticals can be used for diagnosis as well as for decision making in therapy and treatment follow-up. Most of the currently used tracers are not able to discriminate between infection and inflammation. Research has been going on to develop infection specific markers, and radiolabelled anti-infective agents look promising towards developing infection specific agents. Technetium-99m labelled antibiotics might also have the potential to differentiate sterile inflammation from infection. There are numerous ongoing studies reporting the use of other radiolabelled antibacterial and antifungal agents for detecting infection. Other promising agents are antimicrobial peptides as they preferentially bind to membranes of bacteria over mammalian cells and, therefore, will discriminate between infection and sterile inflammation. Clinical studies are now being undertaken with these agents and further evaluation with different types of pathogens such as viruses, fungi, parasites and intracellular pathogens in humans will provide new infection specific diagnostic agents.

#### **7.1. INTRODUCTION**

An important aspect in medicine is the emergence of infections with multidrug resistant microorganisms. Multidrug resistant microorganisms, such as

methicillin resistant *Staphylococcus aureus* (MRSA) are the first priority target on the list of the Infectious Diseases Society of America (March 2006) of bad bugs that need drugs, the reason being that: “*MRSA* infections constitute the majority of health care-associated infections, increasing lengths of hospital stay, severity of illness, deaths, and costs”. While these infections used to be limited primarily to hospitals and especially to immunocompromised patients, the increase in number of *MRSA* carriers in communities is striking, especially where groups of people are in close quarters, including military facilities, sports teams and prisons ([www.idsociety.org](http://www.idsociety.org)).

## 7.2. PATHOPHYSIOLOGY OF INFECTION

After invasion of a foreign particle, such as a microorganism, an inflammatory response takes place, aiming at the elimination of the pathogenic insult. In addition, the inflammatory process tries to remove the injured tissue and stimulates the regeneration of the normal tissue architecture. Next, the immune system generates memory on behalf of dealing with re-infections with the same microorganism more effectively [7.1]. Once this objective has been reached, specific compounds inhibit the chemical mediators which act in a pro-inflammatory way. Inflammation is usually characterized as either acute or chronic in nature. In acute inflammation, various local events occur and these are summarized below:

- Vascular changes featuring vasodilation and increased vascular permeability;
- Formation of exudate, an extracellular fluid with high protein content and much cellular debris;
- Cellular events such as diapedesis (the emigration of leukocytes from the smaller blood vessels and accumulation at the site of tissue injury), chemotaxis and phagocytosis involving polymorphonuclear leukocytes (PMNs) and macrophages ingesting foreign particles. Cellular migrations and triggering is mediated by chemokines and cytokines as well as by killed pathogens;
- Generation of antimicrobial peptides produced by phagocytes, epithelial cells, endothelial cells and many other cell types. They can be expressed constitutively or induced during inflammation or microbial challenge.

Infection by pathogenic microorganisms is usually followed by an acute inflammatory response. Tissue macrophages represent the first line of defence. As a second line of defence, within a few hours, the infection site is invaded with

large numbers of PMNs. These cells primarily attack by phagocytosis and the engulfed microorganism is exposed to corrosive enzymes, thereby destroying the pathogen.

Chronic inflammation may be the result of acute inflammation. Under this condition, the number of PMNs is reduced and there is marked proliferation of fibroblasts and infiltration by macrophages, lymphocytes and plasma cells. This third line of defence is active only days or weeks after the initial event. During this delayed period, immature monocytes present in blood and bone marrow are transformed into potent phagocytic macrophages and the result is the production of PMNs and monocytes. In addition, lymphocytes and plasma cells are recruited, extending the fighting capability.

The effectors of the innate immune response have traditionally been thought to include phagocytic cells, such as neutrophils and macrophages, other leukocyte-like cells (e.g. mast cells) and serum proteins such as complement. Over the past two decades, living organisms of all types have been found to produce a large repertoire of antimicrobial peptides that play an important role in innate immunity to microbial invasion.

### 7.3. DIAGNOSIS OF INFECTION

To optimize treatment of the postulated infection, febrile patients are exposed to a large array of diagnostic studies. These include laboratory tests, which often reveal non-specific parameters, due to the host's immune response, such as the erythrocyte sedimentation rate, white blood cell counts and cytokine reactions. For obvious reasons, these tests are not specific enough to differentiate between bacterial infections, sterile inflammation and tumours. This differentiation is of crucial importance for further clinical analysis and/or treatment. Imaging studies such as X ray, CT and MRI show abnormalities caused by morphological changes and are insufficient to provide a reliable diagnosis [7.2]. Moreover, such abnormalities can only be detected at advanced stages of disease and it is, therefore, obvious that morphological imaging does not really contribute to an early diagnosis in which phase therapy might be more successful. On the other hand, nuclear medicine imaging is based on changes in function, rather than on morphology. Once the proposed compounds are radiolabelled, their biodistribution and pharmacokinetics can be visualized and quantitated at the site of pathology revealed by scintigraphy. Selection of multidrug resistant MRSA as a target for the development of infection seeking tracers is driven by the significant health risks that are associated with these bacteria.

## 7.4. RADIOPHARMACEUTICALS FOR THE IMAGING OF INFECTION

The primary medicinal use of radiopharmaceuticals is in the diagnosis and therapy of cancer. Early identification and localization of the site of infection is crucial in the appropriate treatment of patients and, in this respect, over the past few decades scintigraphy has contributed significantly. In clinical practice, however, it is of the utmost importance to distinguish aseptic inflammation from infection [7.3]. The treatment of, for example, aseptic loosening of a hip implant (caused by an immune response initiated by the phagocytic reaction of the host in an effort to clean the area around the implant from particulate debris produced by component destruction) is very different from an infected prosthesis, whereas the clinical signs are often similar. Aseptic loosening usually requires a relatively simple revision arthroplasty as opposed to the complex treatment of infection, which involves excision arthroplasty and several weeks of intensive antibiotic therapy, followed by a new joint replacement. Inflammatory diseases vary greatly in etiology, pathology, severity and the extent of complications. Infection specific radiopharmaceuticals can be used not only for diagnosis, but also for decision making in therapy and treatment follow-up.

A wide variety of radiopharmaceutical markers has been developed for infection and inflammation: (i) radiolabelled IgG monoclonal anti-granulocyte antibody fragments and chimeric monoclonal antibodies against the tumour necrosis factor (TNF- $\alpha$ ) developed during the last century [7.4–7.7]; (ii) radiolabelled peptides that bind to specific receptors expressed on granulocytes [7.8]; and (iii) radiolabelled cytokines that bind to a receptor expressed on granulocytes [7.9]. However, the radiopharmaceuticals described above cannot discriminate between infection and inflammation because they are not specific for bacteria, thus ongoing research is still necessary to develop infection specific markers. An ideal radiopharmaceutical for infection imaging should satisfy the following criteria: high and specific uptake at the site of infection, rapid detection of infection, rapid background clearance, minimal accumulation in non-target tissues, low toxicity and zero immune response, and, in particular, an ability to differentiate infection from sterile inflammation [7.10].

In order to be clinically useful, an imaging test should, therefore, be able to differentiate between both entities. Moreover, it should be both sensitive and specific. Specificity is especially important as an unspecific test can easily lead to unnecessary and costly operations and hospitalization, apart from the morbidity and unavoidable mortality associated with surgical interventions. In this context, it is clear that the clinical need for infection specific radiopharmaceuticals cannot be overemphasized [7.11].

TABLE 7.1. RADIOPHARMACEUTICALS FOR INFLAMMATION/INFECTION IMAGING

Mechanism	Tracers
Migration of white blood cells to infection site	Indium-111 labelled leukocytes Technetium-99m labelled leukocytes
Increased vascular permeability	Indium-111 and technetium-99m human polyclonal IgG Gallium-67 citrate Technetium-99m nanocolloid
Binding to lactoferrin and transferrin at the infection site	Gallium-67 citrate
Increased glycolysis of inflammatory cells	Fluoro-18 fluorodeoxyglucose
Binding to bacteria	Gallium-67 citrate

From Table 7.1, it can be concluded that the majority of scintigraphic tests does not allow the distinction between inflammation and infection. Gallium-67 does bind to bacteria, but also to proteins, accumulating at both sites of sterile inflammation and bacterial infection. Other agents interact with receptors or domains on circulating and infiltrating leukocytes, such as <sup>99m</sup>Tc labelled anti-granulocyte monoclonal antibodies (or fragments thereof), and <sup>99m</sup>Tc labelled chemotactic peptides and interleukins. Since antimicrobial compounds often display preferential binding to microorganisms, radiopharmaceuticals for discriminating infections from inflammations may be recruited from the array of antibiotics.

## 7.5. ANTIBIOTICS

Labelled antibiotics might have the potential to differentiate sterile inflammation from infection. Ciprofloxacin is a fluoroquinoline-type antibiotic which binds to the DNA gyrase and DNA present in dividing bacteria. Infecton, the first <sup>99m</sup>Tc labelled ciprofloxacin, has been substantially studied in clinical trials. The largest trial, that included about 900 patients, was conducted in the framework of an IAEA coordinated research project. In this study, the overall sensitivity was 87.6%, while the specificity was 81.7% [7.12]. These encouraging results promoted studies with other fluoroquinolones, such as norfloxacin, sparfloxacin, enrofloxacin, levofloxacin and ofloxacin, as well as with other antibiotics [7.13]. While improved methods for the preparation and quality

control of these radiopharmaceuticals have been developed [7.14], parallel studies determined no specific binding of  $^{99m}\text{Tc}$ -ciprofloxacin, with controversial results regarding its uptake in aseptic inflammation [7.15–7.19]. Moreover, recently published data from a Phase II clinical study carried out in the United States of America and sponsored by the manufacturers of Infecton® [7.20], showed poor specificity and accuracy in patients with osteomyelitis both in 2 and 24 h images. The tracer disappeared from sites of infection as well as from inflammation with equal rapidity. This raises the issue of whether the uptake is nothing more than a blood pool effect [7.21].

Given that the structure of the investigational agent Infecton is still unknown, controversial results could be attributed mainly to variations in the labelling procedure followed and insufficient quality control. It is known that small variations during the preparation of  $^{99m}\text{Tc}$  radiopharmaceuticals can lead to the formation of different complexes with a different biodistribution. These problems were overcome by the development of freeze-dried kit formulations for each radiopharmaceutical as well as by the availability of analytical methods (high performance liquid chromatography (HPLC) and TLC) that give robust information about the radiochemical purity of these radiopharmaceuticals. Taking into consideration that, until recently, precise methods of preparation and quality control were not widely available, it is most likely that different  $^{99m}\text{Tc}$ -ciprofloxacin complexes or mixtures were prepared and evaluated in various laboratories. In most cases, including the patient studies with Infecton, the presence of  $^{99m}\text{Tc}$ -colloid, a potential by-product that is trapped in sites of inflammation, was not investigated. The presence of  $^{99m}\text{Tc}$ -colloid could lead to a high number of true positives and a low number of false positives (in cases where the infection was not confirmed by other methods). The opposite (low true positives and high false positives) will be seen in cases where the infection was confirmed by other methods. Thus, the development of a freeze-dried kit, preferably single vial, as well as the development of analytical methods capable of distinguishing the potential radiochemical impurities is required to avoid these discrepancies. Additionally, solid testing in laboratory animals is warranted in order to obtain insight into the specificity of the radilabelled compounds.

Another important parameter that contributes to the discrepancies in the reported specificity is the ‘way of reading’ the scans. The evaluation of scans was more or less ‘qualitative’ and there was no clear-cut boundary between positive and negative. This could easily lead to over and under estimates. More recently, claims about the specificity of Infecton in detecting bacterial infections in humans (depending on the discrepancy between early and late imaging) were refuted by Palestro et al. as his group conducted a Phase II trial sponsored by Draximage, the manufacturer of Infecton, and they experienced that this tracer disappeared from sites of infection as well as from inflammation with equal

rapidity [7.21]. As Infecton detects bacterial infections with poor specificity and accuracy, this group seriously considered that it is unlikely that this radiolabelled antibiotic will ever be a viable method for imaging infection. Moreover, a recent press release from Draximage clearly states that formulation development of Infecton targeting orthopaedic indications has to date not been successful and Draximage will allocate the resources devoted to this product to other projects ([http://www.draxishealth.com/pdf/Draxis\\_Q3\\_PR\\_US\\_GAAP.pdf](http://www.draxishealth.com/pdf/Draxis_Q3_PR_US_GAAP.pdf)).

Together with the recent finding that synthesized <sup>18</sup>F-ciprofloxacin shows no specific uptake in bacterial infected lesions [7.22, 7.23], suggests that ciprofloxacin is not suited as a bacteria specific imaging agent. Current studies are focused on developing other well defined <sup>99m</sup>Tc labelled antibiotics [7.24]. Preliminary studies with ciprofloxacin or norfloxacin derivatives have shown significant in vitro uptake in bacteria as well as low accumulation in sterile inflammatory sites [7.25]. Critical evaluation (e.g. interaction with host cells and adequate control experiments) with these investigational compounds is warranted to prove their value for specific imaging of infections [7.26]. Recently, the antifungal drug fluconazole, which binds to fungal cytochrome P450, has been successfully labelled with <sup>99m</sup>Tc. In mice infected with *Candida albicans* or *Aspergillus fumigatus*, <sup>99m</sup>Tc labelled fluconazole detects these infections but not tissues infected with bacteria or sites injected with LPS [7.27], indicating that this tracer is a specific fungal infection marker. Another issue is the role of these tracers in infections with drug resistant microorganisms as these pathogens develop various routes of neutralizing antibiotics by producing large quantities of free LPS or they upregulate their efflux pumps to remove intracellular antibiotics [7.28].

## 7.6. ANTIMICROBIAL PEPTIDES

Another promising class of specific infection imaging agents is <sup>99m</sup>Tc labelled antimicrobial peptides as they preferentially bind to membranes of bacteria over mammalian cells. Due to the discovery of antibiotics, the bactericidal effect of cationic antimicrobial peptides was ignored but interest was restored after the emergence of microorganisms resistant to the most widely used antibiotic agents. These agents have gained renewed attention as therapeutic drugs after the discovery that these antimicrobial peptides are widely distributed throughout the animal and plant world. Hundreds of antimicrobial peptides have been isolated so far and irrespective of their origin, spectrum of activity and structure, most of these peptides share several common properties. They are generally composed of less than 60 amino acid residues (mostly common

L-amino acids), their net charge is positive, they are amphipathic and, in most cases, they are membrane active [7.29].

Cationic antimicrobial peptides can be broadly categorized into four classes on the basis of their secondary structure: (i) amphipathic  $\alpha$ -helices, such as cecropin, magainins, mellitin and ubiquicidin; (ii) peptides with two or more disulphide bridges, such as  $\alpha$ -and  $\beta$ -defensins, cathelicidins and protegrins; (iii) peptides with one intermolecular disulphide bond that have a loop/hairpin-like structure; and (iv) linear peptides lacking cysteine and with a high content of certain residues such as tryptophan-rich indolicidin or proline-arginine-rich PR39.

In higher organisms, antimicrobial peptides are mainly produced on epithelial surfaces and in phagocytic cells that play a crucial role in the innate as well as the adaptive defence systems [7.30–7.33]. Antimicrobial peptides exhibit rapid killing, often within minutes *in vitro*, and a broad spectrum of activity against various targets, including Gram-positive and Gram-negative bacteria, fungi, parasites, enveloped viruses and tumour cells [7.30]. In addition, their antimicrobial activity can be enhanced by the synergy between individual cationic peptides within a host, and between the peptides and other host factors, such as lysozyme [7.32].

Their mode of action against invading pathogens, rather than against mammalian cells, is based upon the architectural and biochemical composition of the cellular membrane [7.34]. These differences translate into varying degrees of antimicrobial toxicity by perforation, membrane destabilization, metabolic inhibitors and triggering of bacteriolysis, and, as such, they are an important component of innate immunity against pathogenic infections [7.35, 7.36]. Antimicrobial peptides display activity against bacteria, viruses and fungi *in vitro* [7.37–7.39], and against experimental infections in laboratory animals [7.40–7.42]. Besides direct microbial killing properties, antimicrobial peptides neutralize bacterial toxins and upregulate host defence as chemo-attractants or by other immunostimulatory effects [7.29, 7.30]. Additionally, antimicrobial peptides may play an important role in anti-tumour activity [7.34], bone repair [7.43] and neoangiogenesis [7.44].

These peptides have a net positive charge due to an excess of basic residues, such as lysine and arginine, and are predominantly produced by phagocytes, and epithelial and endothelial cells. The induction occurs, in principle, upon contact with microorganisms or microbial products such as lipopolysaccharides or pro-inflammatory cytokines. The basis of the antimicrobial activity is the interaction of the cationic (positively charged) domains of the peptide with the (negatively charged) surface of microorganisms. The membranes of the latter expose negatively charged lipoteichoic acid and phospholipids, while in normal mammalian cells, negatively charged lipids face the cytoplasm. This difference

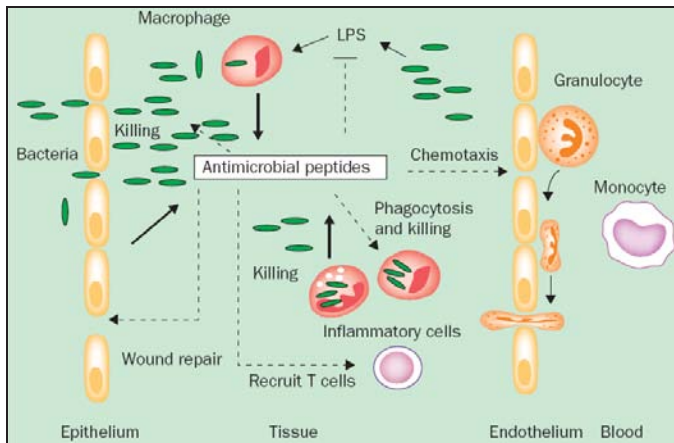


*FIG. 7.1. The role of antimicrobial peptides in innate immunity.*

explains the poor binding of cationic peptides to mammalian cells [7.32]. The interactions of these peptides with the bacterial cytoplasmic membrane results in destabilization and pore formation in the membrane, allowing leakage of cellular constituents such as potassium ions, thus destroying the proton gradient across the membrane resulting in bacterial death. In addition, intercellular activity leading to disturbed metabolic processes has been observed [7.34]. Figure 7.1 outlines the role of antimicrobial peptides in the network of innate immunity in a schematic way. It is generally thought that the development of resistance against antimicrobial peptides is very limited in nature. This is conceivable as, during evolution, multiple antimicrobial activities of the host remained active and effective in withstanding invasions by microorganisms. Nevertheless, a mechanism of developing resistance could be the modification of the lipid membrane composition, thereby reducing attractive electrostatic interactions, triggering pathogen virulence, or by releasing proteases that can degrade the antimicrobial peptides [7.45–7.47].

The killing mechanism of antimicrobial peptides is so different to that of conventional antibiotics that antimicrobial peptides are considered as an attractive substitute and/or as additional drugs. In view of the emergence of pathogens with increased resistance to conventional anti-infective drugs, the use of antimicrobial peptides alone or in combination with current antifungal drugs could lead to the development of new therapies to combat otherwise resistant infections [7.48].

Large quantities of purified antimicrobial peptides are required to investigate their possible applications. Difficulties arising in purifying natural antimicrobial peptides from various sources have prompted the recombinant

production of antimicrobial peptides by genetically engineered bacteria, transgenic animals or by peptide synthesis [7.49–7.51]. Such methods may yield sufficient amounts of antimicrobial peptides produced under good manufacturing practice conditions (GMP), which is essential for future approval to use the peptides in clinical trials. Peptide synthesis also allows the production of chemical variants, such as D-enantiomers, which are less easily degraded by enzymatic decomposition, peptides that have amino acid substitutions at various positions and incorporation of various linkers at desired places in order to change the pharmacology or to incorporate markers [7.52, 7.23]. The study of different domains of native molecules may result in the identification of biologically active regions, for example, those ones in antimicrobial cationic peptides which are responsible for binding and killing the target. Eventually, this knowledge and techniques can be used to select peptide fragments that preferentially bind to specific species of pathogens and show favourable pharmacological behaviour for scintigraphic imaging.

Human defensins, lactoferrin, ubiquicidin and histatins have been proposed as they serve as the first line of defence against microbial infiltration [7.53, 7.54]. As the natural peptides rapidly accumulate in infected tissues, they show strong microbicidal activity. For this reason, bacterial binding domains from these human antimicrobial peptides were selected and synthesized. After labelling with  $^{99m}\text{Tc}$ , the synthetic peptides accumulated rapidly in tissues from mice, rats and rabbits infected with bacteria or fungi, and do not accumulate in sterile inflammatory lesions [7.55]. The nearest to this goal are analogues of a natural mammalian antimicrobial agent, a 59 amino acid peptide, ubiquicidin (UBI 1–59) [7.56]. Its shorter analogues, UBI 18–35, UBI 22–35, UBI 29–41 and UBI 31–38, significantly and specifically bind to bacteria [7.55]. The most studied analogue,  $^{99m}\text{Tc}$ -UBI 29–41 [7.55, 7.27, 7.57, 7.58], rendered promising results in animal models, demonstrating fast infection imaging with high *in vivo* infection specificity that led to its recent entry into successful clinical use in bacteria specific imaging [7.59, 7.60] and therapy monitoring [7.40, 7.61]. For future developments, it should be considered that antimicrobial peptides may function as carrier molecules to bring drugs, either microbicidal compounds or  $\beta$ -emitters, to sites of pathology which are hard to reach (e.g. the blood–brain barrier (BBB)) because of the nature or pharmacology of these drugs [7.62].

## 7.7. TECHNETIUM LABELLING TECHNIQUES

In general, antibiotics and peptides show rapid pharmacokinetics. They exhibit fast clearance from the circulation, rapid excretion and, most importantly, rapid penetration of extravascular tissues, leading to fast accumulation in the

target. With the aid of a gamma camera, the pathway of the radiolabelled compounds can be followed over time by scintigraphy *in vivo*. This tool is not only for pharmacological studies, but also serves an important purpose in clinical patient care in diagnosis and therapy.

The most suitable radionuclide for diagnostic patient studies is  $^{99m}\text{Tc}$ , which is readily available, at low cost, from a molybdenum generator as  $^{99m}\text{Tc}$ -pertechnetate. Moreover, its relatively short half-life of 6 h results in a low radiation burden for the patient and no measurable contamination of the environment. The energy of the photons emitted by this radionuclide is 140 keV, which is ideal for scintigraphic detection with a gamma camera, thus permitting high quality imaging. Another advantage is that the chemistry of  $^{99m}\text{Tc}$  is similar to that of the  $\beta$ -emitters  $^{186}\text{Re}$  (half-life = 90 h, 137 keV) and  $^{188}\text{Re}$  (half-life = 17 h, 155 keV), which are applied for targeted therapeutic purposes. The labelled  $^{99m}\text{Tc}$  should be firmly attached to the carrier and the  $^{99m}\text{Tc}$  complex should be sufficiently robust to withstand metabolism itself, as radiolytic degradation and reactive labelling conditions affect biological properties of both proteins and peptides [7.63, 7.64, 7.14]. Technetium-99m complexes, in which this element is in oxidation states -1 to +7 are known, although  $^{99m}\text{Tc}$  in the +5 oxidation state is the most suited oxidation state for incorporation into other molecules. Donor atoms may be sulphur and nitrogen. Except for radiopharmaceuticals in which the small radioactive metal is bound to a large biologically active molecule, prediction of a given biological property remains a difficult task for such types of compounds. A better understanding of the biological properties of  $^{99m}\text{Tc}$  labelled radiopharmaceuticals would be expected if metal chelates with well defined chemical structure and with a known stability were used in biological experiments [7.65]. On the other hand, it is difficult to orchestrate the chelators to a well defined position and attachment to the bioactive core, and this may lead to reduced biological activity.

To circumvent this issue, the chelating group for the  $^{99m}\text{Tc}$  radionuclide has to be incorporated during synthesis. This makes it possible to attach this chelating group at a site, which is remote from the biologically active binding site. In this way, the metal complex is supposed not to disturb the biochemical actions of the compound. Most of these tetradeinate ligands contain one of two thiol groups and the remainder are N-donor atoms such as amine or amide groups. They are usually indicated as  $\text{N}_3\text{S}$  or  $\text{N}_2\text{S}_2$  chelators. Especially  $\text{N}_2\text{S}_2$  (bisamine bisthiol) based chelators have the supposed chemical structure of this  $^{99m}\text{Tc}$  complex [7.66]. Another approach is the use of the hydrazinonicotinamide (hynic) system developed by Babich et al. [7.67]. This conjugation uses a single tether to bind  $^{99m}\text{Tc}$  to the peptide, thereby offering the possibility of modifying the pharmacokinetics of the radiolabelled peptide [7.68].

Besides the above mentioned labelling methods,  $^{99m}\text{Tc}$  labelling is also possible using reducing conditions under which the +7 oxidation state in pertechnetate is reduced to the +5 oxidation state. This is problematic for peptides containing intramolecular disulphide bonds, which are usually reduced, resulting in an altered chemical structure, and an altered biodistribution and biological activity. Stannous ions, the most commonly used agents to reduce  $^{99m}\text{Tc}$ , may reduce such disulphide bonds and are, therefore, often unsuitable for  $^{99m}\text{Tc}$  binding to peptides, although a recently developed method employs a unique mild reaction process that leads to end products that still have intact biological characteristics [7.64, 7.69]. This method is very valuable, especially for compounds that do not contain disulphide bridges. This direct labelling method is a simple, rapid and cheap procedure, without the need for a chelating agent, and has been used to label an array of peptides successfully, even those with disulphide bridges, leaving their biological features intact [7.37, 7.70]. This method has been extensively tested for UBI 29-41 in a CRP (2000–2003) by the IAEA [7.71]. This multicentre study, involving 12 laboratories, concluded that the labelling method is highly reproducible, leading to a potential clinical utility. The CRP made a major contribution by providing the first validated specific  $^{99m}\text{Tc}$  labelled infection imaging agent.

The mechanism underlying this direct labelling method involves the reduction of  $^{99m}\text{Tc}$ -pertechnetate by low concentrations of stannous ions, in the presence of another reducing agent,  $\text{KBH}_4$ , the production of a stabilized  $\text{TcO}$  intermediate followed by a substitution reaction [7.72]. According to a recent finding by the group of Ferro Flores et al., the labelling of a fragment of the synthetic cationic antimicrobial peptide ubiquicidin 29–41 results in a dimeric peptide complex with Arg7 and Lys being the most suitable binding sites for  $^{99m}\text{Tc}$ , indicating that residual amines are involved [7.73, 7.74].

The direct labelling method was used to label numerous cationic antimicrobial peptides with  $^{99m}\text{Tc}$ . Under alkaline conditions (final pH9) and with a relatively short reaction time of 10–20 min, a high labelling yield of more than 95% has been achieved as determined by techniques including HPLC, instant layer chromatography and Sep-Pak analysis. Furthermore, it appeared that the stability of this complex in human serum albumin was excellent (less than 5% release of free  $^{99m}\text{Tc}$  at 24 h) as well as in laboratory animals, and that the labelling preparation had retained its biological activity, which was demonstrated by in vitro competitor bacteria binding assays, and comparing its in vitro and in vivo bacterial killing capability with the unlabelled peptide [7.69, 7.57].

Direct and chelator labelling techniques have been applied to select tracers with the most preferential biodistribution, fastest targeting properties and the ability to discriminate between infection and inflammation. In this respect, UBI 29–41 derived from human ubiquicidin and directly labelled with  $^{99m}\text{Tc}$  is the

most promising and well tolerated compound to specifically detect infections and monitor antimicrobial therapy. Labelling of antimicrobial peptides with  $^{99m}\text{Tc}$  also offers the perspective of selecting and modifying the preferential amino acid sequence in order to design a microorganism specific seeking tracer at reasonable cost. Additionally, this methodology may also make alterations in biodistribution, possible, if desired. It is challenging to select for such infection specific markers from the array of other antimicrobial peptides. Another issue is the specific coordination of the radioisotope to the peptide, and a complete chemical and biochemical characterization. For this reason, the well established peptide synthesis technique offers the possibility of introducing new chelators to the peptide backbone.

## 7.8. PHARMACOKINETICS

The classical method for studying the pharmacokinetics of drugs in animals is to measure their levels in different organs at various intervals after injection using biochemical or immunological assays. A major disadvantage of this approach is that it does not allow whole body, early real time monitoring of the biodistribution of the drugs *in vivo*. To circumvent this drawback, these compounds need to be labelled to assess the biodistribution of the labelled peptides in animals [7.75]. In the case of small peptides, it is not feasible to analyse their pharmacokinetics by preparing a fusion protein of the peptide under study with, for example, green fluorescent protein or luciferase, both of which can be monitored in animals in real time. Alternatively, peptides can be tagged with  $\gamma$  emitting radioisotopes, such as  $^{99m}\text{Tc}$ ,  $^{111}\text{In}$  and  $^{125}\text{I}$ , and scintigraphic techniques can be used to quantify the amount of radiolabelled peptides in different organs at various intervals [7.76–7.78]. Recently, the solid phase synthesis of  $^{18}\text{F}$  labelled linear peptides and antibiotics enabled positron emission tomography (PET) [7.79, 7.23]. Due to its favourable radiation characteristics, easy radiopharmacy, costs and ready availability,  $^{99m}\text{Tc}$  is the preferred label to determine the pharmacokinetics of cationic antimicrobial peptides [7.69].

Progress can also be made with improvements in instrumentation. In clinical settings, it is of importance to correlate functional scintigraphic studies with anatomical imaging. Single photon emission computed tomography (SPECT) as well as PET provide images for direct correlation to anatomical modalities such as CT and MRI. These fusion methods include side by side software and hardware fusion [7.80]. It is believed that fusion imaging would increase the specificity of the physiological modality and the sensitivity of the anatomical modality.

Recent innovations in small animal SPECT have led to advantages in resolution and sensitivity, which could easily withstand the competition from small animal PET cameras. This is of importance considering the radiation issues raised with PET, high costs, and logistics in tracer preparation and development [7.81, 7.82].

## 7.9. CONCLUSIONS

The development of infection imaging agents will help clinicians to monitor the success of antimicrobial therapy for infection with multidrug resistant pathogens. The specific and fast accumulation of  $^{99m}\text{Tc}$  labelled antibiotics and antimicrobial peptides makes them the infection seeking agents of choice. They have now been successfully applied in clinical settings and further evaluation with different types of infections in humans will determine the future of these promising compounds. Infection imaging with radiopharmaceuticals is unique, considering that neither CT nor MRI is able to detect microorganisms, as such, and monitor the effect of antimicrobial therapy on the basis of the number of bacteria.

## 7.10. FUNDAMENTAL QUESTIONS

- (1) Will radiopharmaceuticals continue to play a useful role in the new field of infection imaging? Infection specific radiopharmaceuticals can be used for diagnosis, decision making in therapy and treatment follow-up. It is necessary to continue with the research on developing agents to address the infections caused by microorganisms such as viruses, fungi, parasites and intracellular pathogens. The diseases caused by the above mentioned microorganisms are widespread and if effective radiopharmaceuticals are developed for such applications, nuclear medicine will have the potential to enter into areas of wider impact, especially in the developing world.
- (2) Is  $^{99m}\text{Tc}$  still the most ideal radionuclide for nuclear imaging? Labelling methods with  $^{99m}\text{Tc}$  have attained an extremely high degree of efficiency and sophistication. High specific activities needed for targeting low concentration targets are easily achievable through advanced chemical procedures employing the novel  $^{99m}\text{Tc}$ -carbonyl,  $^{99m}\text{Tc}$ -nitrido and  $^{99m}\text{Tc}(\text{III})$  cores.

- (3) Will  $^{99m}\text{Tc}$  continue to be employed in a specific clinical field or will it be replaced by other radionuclides (PET) or imaging modalities? It has been recognized that the overwhelming success of PET is because of the superiority of  $^{18}\text{FDG}$  as a proliferation specific tracer and due to its utility in several areas including neurology, cardiology, oncology, infection, etc. Hence, the quality of the radiopharmaceutical is the key issue, the superiority of the instrumentation technique playing a secondary role. Recently,  $^{18}\text{F}$ -UBI 29–41 was synthesized and, in contrast to  $^{18}\text{F}$ -ciprofloxacin, showed specific binding to bacteria *in vitro*. Animal studies need to be performed to show its effectiveness in imaging infections. A review of current advances in detector technologies and reconstruction algorithms clearly showed that spatial resolution in SPECT is rapidly approaching that of PET, without a decrease in sensitivity. The recent introduction of SPECT-CT has pursued this imaging modality a step further towards approaching detection characteristics of PET. Hence, the development of successful Tc based radiopharmaceuticals is the challenge to radiopharmaceuticals chemists.
- (4) Which type of novel  $^{99m}\text{Tc}$  radiopharmaceuticals are required for the new molecular medicine? The development of new  $^{99m}\text{Tc}$  based radiopharmaceuticals for targeting intracellular pathogens and compounds that could pass the BBB to allow brain infection imaging (and therapy) should be given high priority. Achievements will contribute to health care for a significant part of the population and will add to the knowledge of biological and biochemical processes taking place in the brain.
- (5) Will  $^{99m}\text{Tc}$  only have relevance in connection with the development of  $^{188}\text{Re}$  therapeutic radiopharmaceuticals? Labelling of antimicrobial peptides with  $^{188}\text{Re}$  may be the answer for antimicrobial therapy of infections with multidrug resistant microorganisms as it specifically targets bacteria and fungi. Moreover, its fast clearance via the kidneys and urinary bladder indicate a low radiation burden. Viral infections, especially AIDS, when HIV-1 viruses are displayed on the surface of infected cells, will become interesting targets for radiotherapy.

## REFERENCES TO CHAPTER 7

- [7.1] WEINER, R.E., THAKUR, M.L., Imaging infection/inflammations: Pathophysiologic basis and radiopharmaceuticals, *Q. J. Nucl. Med.* **43** (1999) 2–8.
- [7.2] BOERMAN, O.C., DAMS, E.T.M., OYEN, W.J.G., CORSTENS, F.H.M., STORM, G., Radiopharmaceuticals for scintigraphic imaging of infection and inflammation, *Inflammation Res.* **50** (2001) 55–64.
- [7.3] BECKER, W., The contribution of nuclear medicine to the patient with infection, *Eur. J. Nucl. Med.* **22** (1995) 1195–1211.
- [7.4] BUSCOMBE, J., Radiolabelled human immunoglobulins, *Nucl. Med. Commun.* **16** (1995) 990–1001.
- [7.5] HAZRA, D.K., et al., Immunotechnological trends in radioimmunotargeting: from magic bullet to smart bomb, *Nucl. Med. Commun.* **16** (1995) 66–75.
- [7.6] BECKER, W., et al., Detection of soft-tissue infections and osteomyelitis using a Technetium-99m-labeled anti-granulocyte monoclonal antibody fragment, *J. Nucl. Med.* **35** (1994) 1436–1443.
- [7.7] BECKER, W., et al., Rapid imaging of infections with a monoclonal antibody fragment (LeukoScan), *Clin. Orthop. Relat. Res.* **329** (1996) 263–272.
- [7.8] RAO, P.S., PALLELA, V.R., VASSILEVA-BELNIKOLOVSKA, D., JUNGKIND, D., THAKUR, M.L., A receptor-specific peptide for imaging infection and inflammation, *Nucl. Med. Commun.* **21** (2000) 1063–1070.
- [7.9] SIGNORE, A., CHIANELLI, M., BEI, R., OYEN, W., MODESTI, A., Targeting cytokine/chemokine receptors: a challenge for molecular nuclear medicine, *Eur. J. Nucl. Med. Mol. Imaging* **30** (2003) 801–802.
- [7.10] NIBBERING, P.H., et al., Radiolabelled antimicrobial peptides for imaging of infections: A review, *Nucl. Med. Commun.* **19** (1998) 1117–1121.
- [7.11] BECKER, W., MELLER, J., The role of nuclear medicine in infection and inflammation, *Lancet Infect. Dis.* **1** (2001) 326–333.
- [7.12] DAS, S.S., HALL, A.V., WAREHAM, D.W., BRITTON, K.E., Infection imaging with radiopharmaceuticals in the 21<sup>st</sup> century, *Braz. Arch. Biol. Techn.* **45** (2002) 25–37.
- [7.13] MULLER, M., PENA, A.D., DERENDORF, H., Issues in pharmacokinetics and pharmacodynamics of anti-infective agents: Distribution in tissue, *Antimicrob. Agents Ch.* **48** (2004) 1441–1453.
- [7.14] RODRIGUEZ-PUIG, D., et al., A new method of [Tc-99m]-ciprofloxacin preparation and quality control, *J. Labelled Comp. Radiopharm.* **49** (2006) 1171–1176.
- [7.15] WELLING, M.M., et al., Imaging of bacterial infections with Tc-99m-labeled human neutrophil peptide-1, *J. Nucl. Med.* **41** (2000) 2100–2102.
- [7.16] SARDA, L., et al., Evaluation of Tc-99m-ciprofloxacin scintigraphy in a rabbit model of *Staphylococcus aureus* prosthetic joint infection, *J. Nucl. Med.* **43** (2002) 239–245.
- [7.17] DUMAREY, N., BLOCKLET, D., APPELBOOM, T., TANT, L., SCHOUTENS, A., Infecton is not specific for bacterial osteo-articular infective pathology, *Eur. J. Nucl. Med. Mol. Imaging* **29** (2002) 530–535.
- [7.18] SARDA, L., et al., Inability of Tc-99m-ciprofloxacin scintigraphy to discriminate between septic and sterile osteoarticular diseases, *J. Nucl. Med.* **45** (2003) 920–926.

- [7.19] SIAENS, R.H., RENNEN, H.J., BOERMAN, O.C., DIERCKX, R., SLETERS, G., Synthesis and comparison of Tc-99m-enrofloxacin and Tc-99m-ciprofloxacin, *J. Nucl. Med.* **45** (2004) 2088–2094.
- [7.20] PALESTRO, C.J., et al., Phase II study of <sup>99m</sup>Tc-ciprofloxacin uptake in patients with high suspicion of osteomyelitis, *J. Nucl. Med.* **47**(Suppl. 1) (2007) P152.
- [7.21] PALESTRO, C.J., LOVE, C., MILLER, T.T., Diagnostic imaging tests and microbial infections, *Cell. Microbiol.* **9** (2007) 2323–2333.
- [7.22] LANGER, O., et al., In vitro and in vivo evaluation of [F-18]ciprofloxacin for the imaging of bacterial infections with PET, *Eur. J. Nucl. Med. Mol. Imaging* **32** (2005) 143–150.
- [7.23] ZIJLSTRA, S., GUNAWAN, J., FREYTAG, C., BURCHERT, W., Synthesis and evaluation of fluorine-18 labelled compounds for imaging of bacterial infections with pet, *Appl. Radiat. Isotop.* **64** (2006) 802–807.
- [7.24] BENITEZ, A., ROCA, M., MARTIN-COMIN, J., Labeling of antibiotics for infection diagnosis, *Q. J. Nucl. Med. Mol. Imaging* **50** (2006) 147–152.
- [7.25] PIRMETTIS, I., LIMOURIS, G.S., PAPADOPOULOS, M., CHIOTELLIS, E., Potential infection imaging agents: preparation and biodistribution of Tc-99m-norfloxacin and Tc99m-ciprofloxacin, *Eur. J. Nucl. Med.* **26** (1999) 1108.
- [7.26] GEMMEL, F., DUMAREY, N., PALESTRO, C.J., Radionuclide imaging of spinal infections, *Eur. J. Nucl. Med. Mol. Imaging* **33** (2006) 1226–1237.
- [7.27] LUPETTI, A., WELLING, M.M., MAZZI, U., NIBBERING, P.H., PAUWELS, E.K.J., Technetium-99m labelled fluconazole and antimicrobial peptides for imaging of *Candida albicans* and *Aspergillus fumigatus* infections, *Eur. J. Nucl. Med. Mol. Imaging* **29** (2002) 674–679.
- [7.28] MAHAMOUD, A., CHEVALIER, J., ALIBERT-FRANCO, S., KEM, W.V., PAGES, J.M., Antibiotic efflux pumps in gram-negative bacteria: the inhibitor response strategy, *J. Antimicrob. Chemother.* **59** (2007) 1223–1229.
- [7.29] HANCOCK, R.E.W., Peptide antibiotics, *Lancet* **349** (1997) 418–422.
- [7.30] MCPHEE, J.B., HANCOCK, R.E.W., Function and therapeutic potential of host defence peptides, *J. Pept. Sci.* **11** (2005) 677–687.
- [7.31] MARTIN, E., GANZ, T., LEHRER, R.I., Defensins and other endogenous peptide antibiotics of vertebrates, *J. Leukocyte Biol.* **58** (1995) 128–136.
- [7.32] HANCOCK, R.E.W., SCOTT, M.G., The role of antimicrobial peptides in animal defenses, *Proc. Natl. Acad. Sci. USA* **97** (2000) 8856–8861.
- [7.33] YANG, D., CHERTOV, O., OPPENHEIM, J.J., The role of mammalian antimicrobial peptides and proteins in awakening of innate host defenses and adaptive immunity, *Cell. Mol. Life Sci.* **58** (2001) 978–989.
- [7.34] OTVOS, L., Antibacterial peptides and proteins with multiple cellular targets, *J. Pept. Sci.* **11** (2005) 697–706.
- [7.35] GINSBURG, I., The role of bacteriolysis in the pathophysiology of inflammation, infection and post-infectious sequelae, *Apmis* **110** (2002) 753–770.
- [7.36] BROGDEN, K.A., Antimicrobial peptides: pore formers or metabolic inhibitors in bacteria? *Nat. Rev. Microbiol.* **3** (2005) 238–250.

- [7.37] WELLING, M.M., et al., Antibacterial activity of human neutrophil defensins in experimental infections in mice is accompanied by increased leukocyte accumulation, *J. Clin. Invest.* **108** (1998) 1583–1590.
- [7.38] COLE, A.M., et al., Retrocyclin: a primate peptide that protects cells from infection by T- and M-tropic strains of HIV-1, *Proc. Natl. Acad. Sci. USA* **99** (2002) 1813–1818.
- [7.39] LUPETTI, A., et al., Candidacidal activities of human lactoferrin peptides derived from the N terminus, *Antimicrob. Agents Ch.* **44** (2000) 3257–3263.
- [7.40] NIBBERING, P.H., et al., Tc-99m-labeled UBI 29-41 peptide for monitoring the efficacy of antibacterial agents in mice infected with *Staphylococcus aureus*, *J. Nucl. Med.* **45** (2004) 321–326.
- [7.41] SHAMA, S., VERMA, I., KHULLER, G.K., Therapeutic potential of human neutrophil peptide 1 against experimental tuberculosis, *Antimicrob. Agents Ch.* **45** (2001) 639–640.
- [7.42] BROUWER, C.P.J.M., BOGAARDS, S.J.P., WULFERINK, M., VELDERS, M.P., WELLING, M.M., Synthetic peptides derived from human antimicrobial peptide ubiquicidin accumulate at sites of infections and eradicate (multi-drug resistant) *Staphylococcus aureus* in mice, *Peptides* **27** (2006) 2585–2591.
- [7.43] COMISH, J., et al., Lactoferrin is a potent regulator of bone cell activity and increases bone formation in vivo, *Endocrinology* **145** (2004) 4366–4374.
- [7.44] STEINSTRAESSER, L., et al., The human host defense peptide LL37/hCAP accelerates angiogenesis in PEGT/PBT biopolymers, *Ann. Plas. Surg.* **56** (2006) 93–98.
- [7.45] PESCHEL, A., How do bacteria resist human antimicrobial peptides? *Trends Microbiol.* **10** (2002) 179–186.
- [7.46] BISHOP, J.L., FINLAY, B.B., Friend or foe? Antimicrobial peptides trigger pathogen virulence, *Trends Mol. Med.* **12** (2006) 3–6.
- [7.47] JIN, T., et al., *Staphylococcus aureus* resists human defensins by production of staphylokinase, a novel bacterial evasion mechanism, *J. Immunol.* **172** (2004) 1169–1176.
- [7.48] LUPETTI, A., et al., Synergistic activity of the N-terminal peptide of human lactoferrin and fluconazole against *Candida* species, *Antimicrob. Agents Ch.* **47** (2003) 262–267.
- [7.49] HWANG, S.W., et al., A simple method for the purification of an antimicrobial peptide in recombinant *Escherichia coli*, *Mol. Biotechnol.* **18** (2001) 193–198.
- [7.50] DAWSON, N.F., et al., Chemical synthesis, characterization and activity of RK-1, a novel alpha-defensin-related peptide, *J. Pept. Sci.* **6** (2000) 19–25.
- [7.51] VAN BERKEL, P.H.C., et al., Large scale production of recombinant human lactoferrin in the milk of transgenic cows, *Nature Biotechnol.* **20** (2002) 484–487.
- [7.52] DE KOSTER, H.S., et al., The use of dedicated peptide libraries permits the discovery of high-affinity binding peptides, *J. Immunol. Methods* **187** (1995) 179–188.
- [7.53] LUPETTI, A., WELLING, M.M., PAUWELS, E.K.J., NIBBERING, P.H., Radiolabelled antimicrobial peptides for infection detection, *Lancet Infect. Dis.* **3** (2003) 223–229.
- [7.54] LUPETTI, A., NIBBERING, P.H., WELLING, M.M., PAUWELS, E.K.J., Radiopharmaceuticals: new antimicrobial agents, *Trends Biotechnol.* **21** (2003) 70–73.

- [7.55] WELLING, M.M., PAULUSMA-ANNEMA, A., BALTER, H.S., PAUWELS, E.K.J., NIBBERING, P.H., Technetium-99m labelled antimicrobial peptides discriminate between bacterial infections and sterile inflammations, *Eur. J. Nucl. Med.* **27** (2000) 292–301.
- [7.56] HIEMSTRA, P.S., VAN DEN BARSELAAR, M.T., ROEST, M., NIBBERING, P.H., VAN FURTH, R., Ubiquicidin, a novel murine microbicidal protein present in the cytosolic fraction of macrophages, *J. Leukocyte Biol.* **66** (1999) 423–428.
- [7.57] FERRO-FLORES, G., et al., In vitro and in vivo assessment of Tc-99m-UBI specificity for bacteria, *Nucl. Med. Biol.* **30** (2003) 597–603.
- [7.58] SARDA-MANTEL, L., et al., Evaluation of  $^{99\text{m}}\text{Tc}$ -UBI 29-41 scintigraphy for specific detection of experimental *Staphylococcus aureus* prosthetic joint infections, *Eur. J. Nucl. Med. Mol. Imaging* **34** (2007) 1302–1309.
- [7.59] MELENDEZ-ALAFORT, L., et al., Biokinetics of Tc-99m-UBI 29-41 in humans, *Nucl. Med. Biol.* **31** (2004) 373–379.
- [7.60] AKHTAR, M.S., et al., Antimicrobial peptide Tc-99m-ubiquicidin 29-41 as human infection-imaging agent: clinical trial, *J. Nucl. Med.* **46** (2005) 567–573.
- [7.61] AKHTAR, M.S., et al., An imaging analysis of  $^{99\text{m}}\text{Tc}$ -UBI (29–41) uptake in *S. aureus* infected thighs of rabbits on ciprofloxacin treatment, *Eur. J. Nucl. Med. Mol. Imaging* **35** (2008) 1056–1064.
- [7.62] PETERS, A.M., JAMAR, F., The importance of endothelium and interstitial fluid in nuclear medicine, *Eur. J. Nucl. Med.* **25** (1998) 801–815.
- [7.63] FRITZBERG, A.R., BEAUMIER, P.L., Targeted proteins for diagnostic imaging: Does chemistry make a difference? *J. Nucl. Med.* **33** (1992) 394–397.
- [7.64] PAUWELS, E.K.J., WELLING, M.M., FEITSMA, R.I.J., ATSMA, D.E., NIEUWENHUIZEN, W., The labeling of proteins and LDL with Tc-99m: A new direct method employing  $\text{KBH}_4$  and stannous chloride, *Nucl. Med. Biol.* **20** (1993) 825–833.
- [7.65] DECRISTOFORO, C., MATHER, S.J., The influence of chelator on the pharmacokinetics of Tc-99m-labelled peptides, *Q. J. Nucl. Med.* **46** (2002) 195–205.
- [7.66] GARIEPY, J., et al., A simple two-step approach for introducing a protected diaminedithiol chelator during solid-phase assembly of peptides, *Bioconjug. Chem.* **13** (2002) 679–684.
- [7.67] BABICH, J.W., et al., Tc-99m-labeled hydrazino-nicotinamide derivatized chemotactic peptide analogs for imaging focal sites of bacterial-infection, *J. Nucl. Med.* **34** (1993) 1964–1974.
- [7.68] WELLING, M.M., et al., Infection detection in mice using Tc-99m-labeled HYNIC and  $\text{N}_2\text{S}_2$  chelate conjugated to the antimicrobial peptide UBI 29-41, *Nucl. Med. Biol.* **31** (2004) 503–509.
- [7.69] WELLING, M.M., et al., Radiochemical and biological characteristics of Tc-99m-UBI 29-41 for imaging of bacterial infections, *Nucl. Med. Biol.* **29** (2002) 413–422.
- [7.70] WELLING, M.M., et al., Imaging of bacterial infections with Tc-99m-labeled human neutrophil peptide-1, *J. Nucl. Med.* **40** (1999) 2073–2080.
- [7.71] INTERNATIONAL ATOMIC ENERGY AGENCY, Development of Kits for  $^{99\text{m}}\text{Tc}$  Radiopharmaceuticals for Infection Imaging, IAEA-TECDOC-1414, IAEA, Vienna (2004).

- [7.72] ROSSIN, R., et al., Tc-99m-labeling experiments on CCK4 by a direct method, *Nucl. Med. Biol.* **28** (2001) 865–873.
- [7.73] MELENDEZ-ALAFORT, L., et al., Lys and Arg in UBI: A specific site for a stable Tc-99m complex? *Nucl. Med. Biol.* **30** (2003) 605–615.
- [7.74] FERRO-FLORES, G., RAMIREZ, F.D., MELENDEZ-ALAFORT, L., DE MURPHY, C.A., PEDRASA-LOPEZ, M., Molecular recognition and stability of Tc-99m-UBI 29-41 based on experimental and semiempirical results, *Appl. Radiat. Isotop.* **61** (2004) 1261–1268.
- [7.75] HONIGMAN, A., et al., Imaging transgene expression in live animals, *Mol. Ther.* **4** (2001) 239–249.
- [7.76] JURISSON, S.S., LYDON, J.D., Potential technetium small molecule radiopharmaceuticals, *Chem. Rev.* **99** (1999) 2205–2218.
- [7.77] ANDERSON, C.J., WELCH, M.J., Radiometal labeled agents (non-technetium) for diagnostic imaging, *Chem. Rev.* **99** (1999) 2219–2234.
- [7.78] LIU, S., EDWARDS, D.S., Tc-99m-labeled small peptides as diagnostic radiopharmaceuticals, *Chem. Rev.* **99** (1999) 2235–2268.
- [7.79] SUTCLIFFE-GOULDEN, J.L., et al., Rapid solid phase synthesis and biodistribution of F-18-labelled linear peptides, *Eur. J. Nucl. Med. Mol. Imaging* **29** (2002) 754–759.
- [7.80] BUNYAVIROCH, T., AGGARWAL, A., OATES, M.E., Optimized scintigraphic evaluation of infection and inflammation: role of single-photon emission computed tomography/computed tomography fusion imaging, *Semin. Nucl. Med.* **36** (2006) 295–311.
- [7.81] MARKS, C.L., CONTI, P.S., Session 4: instrumentation and animal models, *J. Nucl. Med.* **47** (2007) 48N–50N.
- [7.82] ECKELMAN, W.C., MATHIS, C.A., Molecular targets, *Nucl. Med. Biol.* **33** (2006) 1.

## **Chapter 8**

### **GENE AND MOLECULAR IMAGING USING $^{99m}\text{Tc}$ LABELLED RADIOPHARMACEUTICALS**

L. I. WIEBE

Cross Cancer Institute, University of Alberta,  
Edmonton, Canada

#### **Abstract**

Classical  $^{99m}\text{Tc}$  labelled radiopharmaceuticals are either particulate or highly lipophilic. Consequently, they have generally been characterized as receptor averse, with relatively low and often non-specific binding affinities, and as poor candidates as false substrates for enzymes. These properties, together with the challenges of attaining high radioactive specific activity  $^{99m}\text{Tc}$  from generators, has led to the view that such radiopharmaceuticals are ineffective and uninteresting for use as radiotracers of molecular processes in the body. New  $^{99m}\text{Tc}$  chelation moieties have changed this paradigm, providing compact, relatively hydrophilic and even charged products that are specific substrates or markers of functional macromolecules. Molecular imaging of gene encoded processes can focus on pathologically skewed expression or can, in the case of gene therapy, react with products of transgene expression. Thus, several classes of  $^{99m}\text{Tc}$  labelled compounds have been designed to interact with enzymes, transport proteins, nucleic acids and other vital macromolecules. The chapter provides a view of current  $^{99m}\text{Tc}$  radiotracers that have already been applied in molecular imaging, including labelled peptides, proteins, oligonucleotides, as well as  $^{99m}\text{Tc}$ -pertechnetate itself for sodium iodide symporter imaging.

#### **8.1. INTRODUCTION**

Nuclear imaging has evolved from an imaging modality that depicts anatomy and physiology, to a method of visualizing and quantifying biochemical events in animals and man. These events primarily occur within individual cells or on their surfaces, but their images are based on combined effects occurring in millions of cells during the data collection (imaging) period. The molecular/functional imaging paradigms in vogue today are built on overlapping contributions from biology, chemistry and imaging physics, with biochemical targets characteristic of numerous pathologies in cardiology, neurology/psychiatry/psychology, oncology and metabolism/internal medicine. Recent advances in the biomolecular sciences, particularly those using imaging technologies, can be attributed to the broad selection of overlapping but not redundant ‘molecular’ imaging technologies including the nuclear techniques

positron emission tomography (PET) and single photon emission computed tomography (SPECT), MRI and optical imaging. X ray CT is less important in terms of functional imaging, but is invaluable when co-registered for interpretation of images with low resolution. Refinements and advances in ultrasound are of growing importance for selected applications.

## 8.2. DEFINITIONS

Brief definitions of modern imaging related terminology are necessary to ensure clarity of meaning and intent when referring to molecular biology, molecular imaging, gene transfer, gene therapy and gene (therapy/transfer) imaging.

Gene therapy is a relatively recent biological concept, a modern subset of molecular biology that can be defined as the use of genetic material to modify a patient's cells for the treatment of an inherited or acquired disease [8.1]; in other words, gene transfer for therapeutic benefit. The first human gene therapy protocol, for correction of adenosine deaminase (ADA) deficiency, was begun in September 1990 [8.2] and the first use of a retroviral vector in human cancer gene therapy followed in 1993 [8.3]. The objectives of gene therapy are to correct cellular function through expression of a deficient or poorly expressed endogenous gene, to add a new function by transferring an exogenous gene or to counteract a normal gene [8.4].

Gene transfer is defined simply as the transfer of genomic DNA from one cell to another. The gene involved may be referred to as the transgene.

The term molecular biology was coined by W. Weaver in 1938 [8.5] in reference to the then growing knowledge of biological molecules derived through new analytical techniques. It was only later that Avery, a Canadian who obtained his medical degree from Columbia University, demonstrated that DNA, not proteins, stored the genetic code [8.6], thereby confirming the centrality of nucleic acids to molecular biology. This pivotal discovery, together with philosophical [8.7] and additional experimental [8.8] endeavours form the basis of today's definition: the processes involved in DNA replication, DNA transcription to RNA and RNA translation to protein.

Molecular imaging, on the other hand, has a much broader definition. Today's meaning is perhaps best taken from the Society of Nuclear Medicine [8.9]: the visualization, characterization and measurement of biological processes at the molecular and cellular levels in humans and other living systems.

Suicide gene therapy is a therapeutic paradigm in which the transgene (step one) activates a cell cytotoxin (step two) to destroy the transgene expressing cells.

Transgene imaging (gene therapy/transfer imaging) describes the application of one or more imaging technologies for spatial and temporal characterization of the result(s) of a therapeutic gene transfer. The imaging process may be directed to assessment of expression of the therapeutic gene (e.g. the receptor, enzyme, etc. encoded by the gene), or a physiological response generated through expression of the gene (e.g. regional perfusion).

### 8.3. GENE TRANSFER AND GENE THERAPY IMAGING: A BRIEF HISTORY

Gene transfer, originally termed genetic engineering, was coined at the Sixth International Congress of Genetics in 1932. This field advanced rapidly once the ‘transforming principle’ had been identified [8.6]. Although the ‘non-molecular’ principles of inheritance were already known, new structural information and the knowledge that DNA ‘transferred’ the genetic code quickly led to experiments involving the transfer of genes within species (inheritance). Horizontal (also called lateral) gene transfer involves the transfer of genetic material (i.e. transgenic DNA) from one cell to another cell that is not its offspring, whereas vertical transfer occurs when an organism receives genetic material from its ancestor. Horizontal transfer may involve transformation, the uptake and incorporation of ‘naked’ DNA (DNA not in a chromosome) into the genome of competent target cells [8.10], or transfection, in which gene transfer is mediated by genetic parasites such as plasmids, viruses or bacteriophages.

Regardless of the method by which a transgene is introduced, the transgenic DNA must be optimized to cross species barriers and enter genomes. Transgenic constructs contain new combinations of genes that have never existed, and they may be designed to amplify gene products that are new to the host. Gene transfer may involve germinal cells or somatic cells (including progenitor cells). The development of recombinant DNA technology [8.11] and retroviral vectors [8.12] made gene transfer into mammalian cells possible. The promises, risks and ethics of human gene transfer for therapy were hot long before the technical breakthroughs were realized [8.13], but once the tools were functional, human gene transfer found its opening [8.2].

The objectives of gene therapy fall into three broad categories: (i) to replace/augment or inactivate a dysfunctional gene, (ii) to replace or add a functional gene, or (iii) to insert a gene that will induce an immune or cytotoxic response. The latter has been of particular interest in cancer gene therapy, using an approach termed suicide gene therapy. Suicide gene therapy, also referred to as virus directed enzyme prodrug therapy (VDEPT) or gene directed enzyme prodrug therapy (GDEPT), is a gene based two step treatment in which the gene

for the exogenous enzyme is targeted to the tumour by the use of a selective (viral) vector, followed by administration of a prodrug that is activated to a cytotoxic product by the enzyme.

### 8.3.1. Transgene imaging

The acyclovir-ganciclovir/herpes simplex virus type 1 thymidine kinase (HSV-TK) system was among the earliest suicide gene therapy paradigms utilized in medicine. This ganciclovir/HSV-TK system was based on the pioneering development of selective antiviral nucleoside drugs which were not activated (phosphorylated) by mammalian thymidine kinase 1 (TK-1) but were activated to toxic nucleotides by HSV-TK [8.14]. The natural transfection model (i.e. herpes infection from a wild-type virus) built on the successful transfection of mammalian cells using the HSV-*tk* gene [8.15] and the demonstration that the antiviral nucleoside drugs activated by HSV-TK inhibited DNA synthesis in HSV-*tk* transfected cells [8.16]. The natural infection model was used to develop radiotracers to detect brain cells ‘naturally’ transfected by the herpes virus (i.e. herpes encephalitis). The early techniques were based on tissue autoradiography with  $^{14}\text{C}$  labelled 2'-deoxy-2'-fluoro-5-methyl-1-β-D-arabinofuranosyluracil ( $^{14}\text{C}$ -FMAU) [8.17, 8.18], 5-iodovinyldeoxyuridine ( $^{131}\text{I}$ VdU) in cell culture [8.19] and in vivo [8.20], and other antiviral nucleosides including 2'-fluoroarabino-5-ioduridine ( $^{131}\text{I}$ -FIAU) [8.21, 8.22]. It was also at this time that a  $^{99\text{m}}\text{Tc}$  labelled radiopharmaceutical ( $^{99\text{m}}\text{Tc}$ -HMPAO) was used (unsuccessfully) to image the effects of herpes encephalitis [8.23].

In the early 1990s, the advent of clinical gene therapy trials based on the ganciclovir/HSV-TK paradigm drew the attention of radiopharmaceutical designers: Balzarini et al. [8.24] published evaluations of nucleosides suitable for imaging the ganciclovir/HSV-TK suicide gene therapy paradigm, the first gene therapy imaging patent application was filed [8.25] and the first in vivo imaging report using  $^{131}\text{I}$ -FIAU was published [8.26]. The latter study confirmed the potential usefulness of radiolabelled FIAU for imaging HSV-TK in mammalian systems naturally infected by the herpes simplex virus [8.21]. Today, numerous similar studies continue, using FIAU [8.27, 8.28] and other antiviral pyrimidine [8.29, 8.30] and purine [8.31, 8.32] nucleosides.

Over the past 15 years, numerous gene therapy protocols have been developed. Those models that are of particular interest to the nuclear medicine community have been reviewed from numerous perspectives. The reviews by Haberkorn et al. [8.33, 8.34] provide a comprehensive overview of gene expression imaging in oncology, as well as an excellent introduction to DNA/RNA products that are of interest because of their ability to interact with nucleic acids (e.g. antisense nucleotides) and expression products (e.g. aptamers). An

equally excellent review of imaging in cardiac gene therapy [8.35] also covers gene therapy imaging in a more general sense. Table 8.1, adapted from Inubushi and Tamaki's review [8.36], lists examples of gene therapy systems in current use. Many other reviews of gene and molecular imaging are found in the

TABLE 8.1. TRANSFECTION IMAGING SYSTEMS IN EXPERIMENTAL AND CLINICAL INVESTIGATION (ADAPTED FROM INUBUSHI AND TAMAKI, 2007 [8.36])

Type of reporter	Reporter gene	Radiolabelled reporter probe
Enzyme	Herpes simplex virus type-1 thymidine kinase (HSV1-tk)	[ <sup>14</sup> C/ <sup>123</sup> I/ <sup>124</sup> I/ <sup>125</sup> I/ <sup>131</sup> I]FIAU, [ <sup>11</sup> C/ <sup>14</sup> C/ <sup>18</sup> F]FMAU, [ <sup>18</sup> F/ <sup>76</sup> Br]FBAU, [ <sup>18</sup> F]FCAU, [ <sup>3</sup> H]FEAU, [ <sup>3</sup> H/ <sup>18</sup> F]FFAU, [ <sup>18</sup> F]FFEAU, [ <sup>18</sup> F]FPAU, [ <sup>18</sup> F]FBrVAU, [ <sup>18</sup> F]FTMAU, [ <sup>123</sup> I/ <sup>125</sup> I]FIRU, [ <sup>123</sup> I/ <sup>125</sup> I/ <sup>131</sup> I]IVFRU, [ <sup>125</sup> I]IVDU, [ <sup>3</sup> H]IUDR, [ <sup>18</sup> F]FUDR, [ <sup>3</sup> H]TdR, [ <sup>3</sup> H]ACV, [ <sup>3</sup> H/ <sup>14</sup> C]GCV, [ <sup>18</sup> F]FGCV, [ <sup>3</sup> H]PCV, [ <sup>18</sup> F]FPCV, [ <sup>18</sup> F]FHPG, [ <sup>18</sup> F]FHGB, [ <sup>11</sup> C]ABE
	HSV1-sr39tk (mutant HSV1-tk)	[ <sup>14</sup> C]FIAU, [ <sup>3</sup> H]PCV, [ <sup>18</sup> F]FPCV, [ <sup>18</sup> F]FHGB
Enzyme	Cytosine deaminase (CD)	[ <sup>18</sup> F]fluorocytosine
Enzyme	LacZ	[ <sup>125</sup> I]PETG
Receptor type	Dopamine type-2 receptor (D2R)	[ <sup>18</sup> F]FESP, [ <sup>3</sup> H]spiperone, [ <sup>123</sup> I]iodobenzamine, [ <sup>11</sup> C]isorexopipride (FLB457)
Receptor type	Somatostatin receptor subtype-2 (SSTr2)	[ <sup>18</sup> F/ <sup>64</sup> Cu/ <sup>67</sup> Ga/ <sup>68</sup> Ga/ <sup>86</sup> Y/ <sup>111</sup> In/ <sup>123</sup> I-octreotide, <sup>99m</sup> Tc-depreotide (P829), <sup>99m</sup> Tc-vapreotide (RC160), <sup>99m</sup> Tc-P2045, <sup>99m</sup> Tc-sandostatin, <sup>94m</sup> Tc-demotate 1, <sup>111</sup> In-pentetretide]
Receptor type	Oestrogen receptor ligand (ERL)	[ <sup>18</sup> F]FES
Transporter type	Sodium iodide symporter (NIS)	[ <sup>123</sup> I/ <sup>124</sup> I/ <sup>125</sup> I/ <sup>131</sup> I-iodide, <sup>99m</sup> TcO <sub>4</sub> <sup>-</sup> , <sup>76</sup> Br <sup>-</sup> bromide]
Transporter type	Norepinephrine transporter (NET)	[ <sup>131</sup> I]MIBG, [ <sup>11</sup> C]mHED
Transporter type	Dopamine transporter (DAT)	[ <sup>99m</sup> Tc-TRODAT-1]

literature, with a focus on topics such as hepatocellular cancer [8.35], brain function [8.37], Alzheimer's disease [8.38] and lymphatics [8.39]. Figure 8.1 provides a diagrammatic representation of cellular structure and function, which represent potential targets for selective interaction and trapping of radiopharmaceuticals to generate image contrast.

An interesting but clearly under utilized imaging technology lies in the use of radiolabelling technologies to track gene vector biodistributions *in vivo*. In one such report, recombinant adenovirus serotype 5 knob (Ad5K) was radiolabelled with  $^{99m}\text{Tc}$ . The product,  $^{99m}\text{Tc}$ -Ad5K, was highly active after radiolabelling, showed specific high affinity binding to U293 cells ( $K_d = 1.4 \pm 0.5 \text{ nM}$ ), and *in vivo* dynamic imaging with an Anger gamma camera revealed that hepatic binding increased exponentially to 100% extraction efficiency, equivalent to approximately 17 000 Ad5K molecules per liver cell. These data demonstrated that *in vivo* imaging is a sensitive tool for measuring changes to liver tropism and that imaging techniques can be applied to adenovirus vectors to measure specific targeting for gene therapy [8.40].

The advantages and shortcomings of  $^{99m}\text{Tc}$  and  $^{99m}\text{Tc}$  labelled radiopharmaceuticals have been discussed at length in other forums. In biomolecular imaging, the  $^{99m}\text{Tc}$  labelled tracer/reporter radiopharmaceutical is frequently disadvantaged or even ineffective because of its lipophilicity, charge, size and general lack of appropriate bio-isosteric properties. In each case, it is

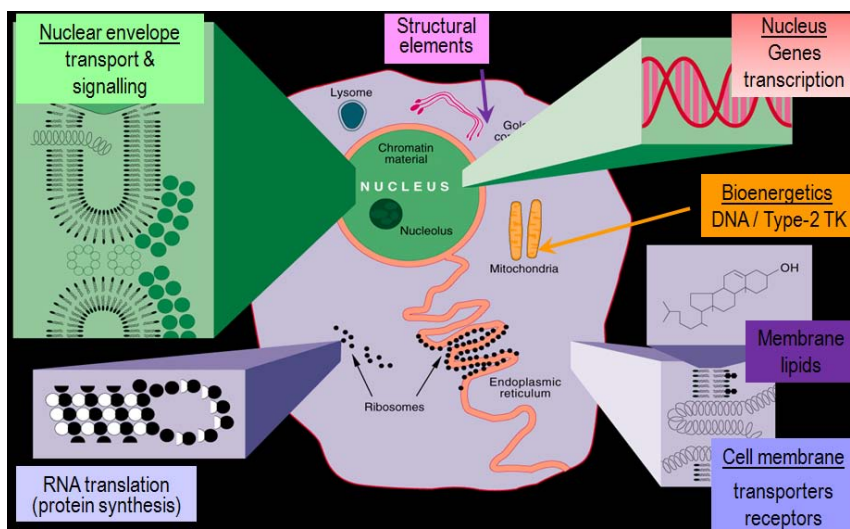


FIG. 8.1. Diagrammatic representation of a mammalian cell. Functional targets suitable for gene therapy imaging, including enzyme, receptor and transporter proteins, structural elements and intermediary metabolites are identified.

crucial for the investigator to ensure that the ‘novel’  $^{99m}\text{Tc}$  labelled tracer actually meets the specific requirements of the target, be it as an enzyme substrate or as a binding/transport ligand. The ‘down-side’ properties are most frequently encountered when the reporter molecule is small, but these are usually not an issue for large molecules such as monoclonal antibodies and oligonucleotides. A recent review of  $^{99m}\text{Tc}$  ligands and their application in medicine [8.41] is highly recommended to interested readers.

#### *8.3.1.1. Technetium-99m substrates for imaging HSV-TK expression*

The enzymes responsible for the activation (i.e. phosphorylation) have exacting demands for the chemical structures of their substrates. Thus, the narrow range of structures accepted by thymidine kinase severely constrains the application of technetium labelled and, for that matter, all coordination labelled radiopharmaceuticals in imaging this important gene therapy paradigm. A review of the literature reveals only two reports of  $^{99m}\text{Tc}$  labelled nucleosides for HSV-TK gene expression imaging. Yang et al. [8.42] prepared  $^{99m}\text{Tc}$ -ethylenedicycysteine-guanine (EC-Guan) ( $^{99m}\text{Tc}$ -ethylenedicycysteine-9-[4-amino-3-(hydroxy-methyl)butyl] guanine), but found that despite incorporation into cellular DNA in vitro, there was no difference in uptake between prostate tumour cell lines and overexpressing counterparts. Although the authors suggest that this agent may have a role in cell proliferation imaging, phosphorylation by nucleoside kinase was not established. More recently, a second guanine derivative, 3-((1,3-dihydroxypropan-2-yloxy)-methyl)-6-(4-(3-((2-mercaptopethyl)(2-(2-mercaptopethyl-amino)-ethyl)amino)-propoxy)phenyl)-3H-imidazopurin-9(5H)-one-oxo-Tc(V), was synthesized as an HSV-TK substrate, but no biological properties have been reported [8.43]. Rigorous validation of the method of action of these agents will be required before they can be considered as substrates for indigenous and/or transferred nucleoside phosphorylases.

#### *8.3.1.2. Technetium-99m-pertechnetate for imaging the sodium iodide symporter*

The sodium iodide symporter (NIS) is a basolateral plasma membrane glycoprotein that actively transports iodide into thyroid follicular cells and into several non-thyroid tissues, including the salivary glands, gastric mucosa and lactating mammary gland. NIS specific complementary DNA (cDNA) based studies have found the human NIS (hNIS) gene to have highest expression in the thyroid gland, with lesser degrees of expression in the salivary gland, parotid gland, submandibular gland, pituitary gland, pancreas, testis, mammary gland, gastric mucosa, prostate and ovary, adrenal gland, heart, thymus and lung [8.44].

Expression is regulated through complex interactions of numerous hormones, of which thyroid stimulating hormone (thyrotropin) is the most potent. The NIS co- transports two sodium ions ( $\text{Na}^+$ ), which serve as the driving force, for the uptake of one iodide ion ( $\text{I}^-$ ) [8.45]. This transporter is also capable of transporting a wide variety of anions, including  $\text{ClO}_3^-$ ,  $\text{SCN}^-$ ,  $\text{SeCN}^-$ ,  $\text{NO}_3^-$ ,  $\text{Br}^-$ ,  $\text{BF}_4^-$ ,  $\text{IO}_4^-$ ,  $\text{BrO}_3^-$  [8.46] and, importantly from a nuclear medicine perspective,  $\text{ReO}_4^-$ ,  $\text{TcO}_4^-$  [8.47] and  $^{211}\text{At}^-$  [8.48]. The importance of the NIS in clinical and nuclear medicine has been the subject of detailed reviews [8.45, 8.49, 8.50].

In the decade since the NIS was first cloned [8.51, 8.52], the NIS has been seen as both a near ideal reporter gene and as a genetic portal for radionuclide based radiotherapy [8.53, 8.54]. Since the transport of pertechnetate ( $\text{TcO}_4^-$ ), like that of iodide, is NIS mediated,  $^{99\text{m}}\text{TcO}_4^-$  could have a role in the assessment of tumours derived from organs expressing NIS and their metastases (Fig. 8.2.). Although the diagnostic and therapeutic applications of NIS would appear to be applicable primarily to pathologies of the thyroid, NIS expression in non-thyroid tissues, including salivary glands, stomach, thymus and breast may make these and other tissues ‘natural’ sites for exploitation of NIS. Indeed, nuclear imaging based visualization of some abnormal non-thyroid tissue has been attributed to NIS expression. NIS is known to be expressed in up to 80% of breast tumours [8.55] and NIS expression in pre-neoplastic stages of liver carcinogenesis and in human cholangiocarcinoma has been reported [8.56].

The first link between an NIS defect (mutation) and photopenic  $^{99\text{m}}\text{TcO}_4^-$  thyroid images [8.57] were followed by reports of the use of  $^{99\text{m}}\text{TcO}_4^-$  in NIS gene therapy models in cell culture [8.58] and in vivo in an adenoviral mediated NIS gene transfer model in mice [8.59]. Research into NIS gene cassette design [8.60], NIS gene delivery vectors [8.61] and murine NIS-expressing genetic models [8.62] continues to advance the field. No clinical trials based on NIS have been reported (NIH database search, July 2007), but design considerations for using NIS reporter gene imaging in prostate cancer gene therapy trials have been published [8.63].

### 8.3.1.3. Imaging VEGF transgene expression

Technetium-99m-Sestamibi has been used to measure reduction in myocardial infarct size following transfection in a porcine model of chronic myocardial ischaemia [8.64]. Although this is in itself not a direct measure of the expressed protein (VEGF), it does indicate the utility of a functional tracer to validate a gene therapy intervention.

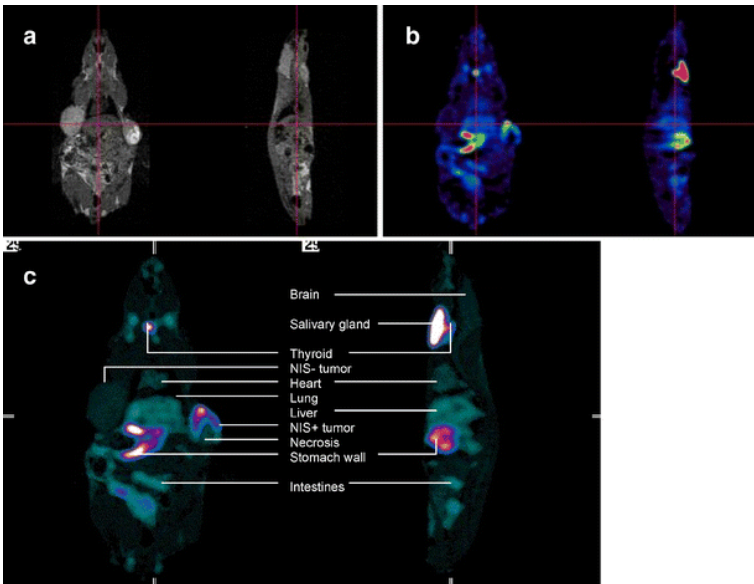


**FIG. 8.2.** SPECT and MRI images of a nude mouse with NIS expressing and control neuroendocrine tumour xenografts. (a) MRI coronal and sagittal slices; (b) Corresponding single pinhole SPECT images 60 min after IV injection of 15 mCi of  $^{99m}\text{TcO}_4^-$ ; (c) Corresponding slices of co-registered data sets. Red lines (a,b) indicate the localization of corresponding planes. (The figure and text are adapted from Schipper et al. 2007 [8.73].)

#### 8.3.1.4. Imaging transgene expression of the somatostatin receptor

The potential of the somatostatin receptor (SSTR) as a transgenic reporter/therapeutic molecule has been reviewed [8.65], and there are several reports of the utility of Tc labelled somatostatin/octreotide analogues as reporter probes for somatostatin transgene research. For example, the somatostatin receptor subtype 2 (SSTR2) has been used as a reporter probe for experimental transgene imaging. The somatostatin analogue  $^{94m}\text{Tc}$ -Demotate 1 ( $^{94m}\text{Tc}$  chelated to Tyr(3)-octreotide via 1,4,8,11-tetraazaundecane) was targeted to SSTR2. The biodistribution and microPET in mice, bearing A-427 tumour xenografts, showed that the  $^{94m}\text{Tc}$ -Demotate 1-microPET system could detect expression of the SSTR2 transgene [8.66]. This group also demonstrated the feasibility of imaging with a  $^{99m}\text{Tc}$  anti-HA antibody to detect expression of the fused haemagglutinin (HA)-HSSTR2 gene (e.g. the epitope tagged HSSTR2 human reporter receptor) [8.67].

In other work,  $^{99m}\text{Tc}$ -Demotate 2 was successfully used to monitor virus induced SSTR2 expression in a murine model [8.68], and the somatostatin

analogue,  $^{99m}\text{Tc}$ -P2045, was used for *in vivo* imaging of adenoviral vectors encoding SSTR [8.69]. Using a bicistronic adenoviral construct to express both HSSTR2 and HSV-TK,  $^{99m}\text{Tc}$ -P2045 imaging consistently depicted HSSTR2 gene transfer in tumours at all adenovirus doses, and tumour uptake of  $^{99m}\text{Tc}$ -P2045 positively correlated with viral vector dose, whereas  $^{131}\text{I}$ -FIAU tumour uptake did not correlate with vector dose [8.70], following earlier work using  $^{99m}\text{Tc}$ -P829 for visualization of transgene HSSTR2 expressing tumours [8.71].

#### *8.3.1.5. Imaging artificial receptors expressed by transgenes*

A novel approach to transgene imaging is to engineer a transgene that expresses an artificial target. In a demonstration case, Simonova et al. [8.72] engineered reporter gene constructs for expression of membrane proteins with a  $^{99m}\text{Tc}$ -oxotechnetate binding domain and a membrane anchoring domain, one consisting of osteonectin (Type II: secretable protein, acidic, rich in cysteine), the other a metallothionein (Types I and II: cysteine rich, metal binding) protein. Translation in cell culture (DNA to RNA) was confirmed using the reverse transcription polymerase chain reaction (RT-PCR) and expression on cell membranes by immunofluorescence, cell fractionation and immunoblotting. The oxotechnetate cation was readily prepared by reduction of  $^{99m}\text{Tc}$ -pertechnetate in a glucoheptanate kit formulation. High uptake, especially by the Type I membrane proteins, and high contrast (experiment to control ratios) support further development of this approach.

#### **8.3.2. Imaging pathology upregulated gene expression**

Abnormal expression of a large number of genes is known to occur during the progression of disease. Some of these genes have a profound ‘downstream’ impact not only through the function of their expression products (e.g. enzymes, receptors, transporters), but also through the ‘activation’ of other genes. Regardless of the breadth of impact, it may be of great importance to measure specific gene expression end product function. Of these systems (see Table 8.1), imaging research and the clinical impact of only three will be discussed: multidrug resistance (MDR), anti-apoptosis and apoptosis. Imaging of hypoxia using approaches based on up-regulation of a cascade of events beginning with hypoxia inducible factors (e.g. HIF-1 $\alpha$ ) is not discussed in this chapter.

### *8.3.2.1. Multidrug resistance: P-glycoprotein expression*

A 1970s report about drug resistance due to active daunomycin efflux in a daunomycin resistant cell line is generally recognized as the beginning of research into what is referred to today as MDR [8.74], and the molecular basis for MDR was attributed to a surface glycoprotein shortly thereafter [8.75]. The genetics and molecular mechanisms responsible for the resistance of cells to a broad range of drugs (i.e. MDR) have been studied for almost two decades [8.76–8.78], and today include additional efflux transporters such as multidrug resistance associated protein-1 (MRP1) or ABCC1 [8.79] and others [8.80].

In summary, one MDR process is based on the expression of the mammalian multidrug resistance gene MDR1 to produce P-glycoprotein (Pgp). Pgp, an ATPase, is only one of a family of molecules responsible for MDR. It is an ATP-binding cassette (ABC) type energy dependent transmembrane drug efflux pump [8.75]. Its structure comprises 1280 amino acids expressed as a single chain glycoprotein containing two homologous portions of six transmembrane domains and two ATP binding regions [8.81, 8.82]. Several models of its mechanism of action have been proposed [8.83]. Reviews of the phylogenetic relationship of the 48 human ABC transporters and the diseases caused by mutations in the genes encoding ABC transporters [8.84], as well as current knowledge/status [8.85] have been published.

The literature of MDR imaging is large and will not be reviewed in detail in this chapter. Instead, clinical work using  $^{99m}$ Tc-Sestamibi,  $^{99m}$ Tc-Tetrofosmin and  $^{99m}$ Tc-antisense DNA will be summarized. Comparisons between  $^{99m}$ Tc labelled radiopharmaceuticals and other MDR tracers (e.g.  $^{18}$ F PET;  $^{111}$ In and  $^{123}$ I SPECT) will not be reviewed; interested readers are referred to recent literature [8.86, 8.87].

#### Multidrug resistance imaging:

$^{99m}$ Tc-Sestamibi ( $^{99m}$ Tc-hexakis(2-methoxy)-isobutyl isonitrile;  $^{99m}$ Tc-MIBI) (Fig. 8.3.)

Nuclear imaging of multidrug resistance P-glycoprotein (MDR-Pgp), the molecular product of MDR1 overexpression, was first reported in 1993 [8.88] using cells genetically engineered to overexpress MDR1. These investigators presented a detailed study of the interactions of hexakis(2-methoxyisobutylisonitrile)technetium(I) ( $^{99m}$ Tc-Sestamibi), a lipophilic cationic radiopharmaceutical, *in vitro* (Chinese hamster V79 lung fibroblasts; 77A and LZ derivative cell lines) and *in vivo* in human multidrug resistant cell lines (drug resistant KB-8-5 cells) [8.89] injected into the flanks of athymic BALB/c/nu/nu mice. This work was expanded to determine structural features essential for

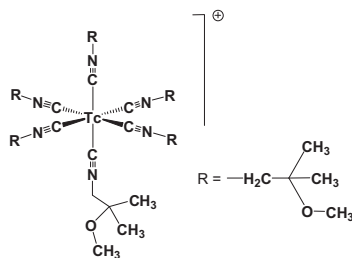


*FIG. 8.3. Chemical structure of Tc-Sestamibi (Courtesy of Roger Alberto, 2007).*

transport of hexakis(areneisonitrile) technetium(1) complexes [8.90], and to the use of microPET with  $^{94m}\text{Tc}$ -Sestamibi to assess MDR [8.91] (Fig. 8.4.).

$^{99m}\text{Tc}$ -Sestamibi was initially developed as a lipophilic cationic Tc complex for myocardial perfusion imaging [8.92, 8.93]. Its biodistribution features high uptake by well perfused myocardial tissue and little redistribution from myocardium after uptake. Substantial hepatic uptake and biliary elimination [8.94], which is sufficient to support scintigraphic determination of gall bladder ejection fraction [8.95], also occurs. Pharmacokinetic studies in patients have shown that hepatic scanning of  $^{99m}\text{Tc}$ -Sestamibi is a potential in vivo probe of hepatic ABCB1 activity that is significantly associated with the presence of common single nucleotide polymorphisms (SNPs) in ABCB1.  $^{99m}\text{Tc}$ -MIBI hepatic scanning may provide a useful pretreatment indicator of MDR mediated drug clearance in cancer patients [8.96]. Importantly for model studies, the pharmacokinetic models of in vitro and in vivo hepatobiliary clearance of  $^{99m}\text{Tc}$ -Sestamibi have been validated [8.97].  $^{99m}\text{Tc}$ -Sestamibi is also taken up by the thyroid, possibly through hydrolysis to pertechnetate [8.93], and by the parathyroid. It can be used for parathyroid imaging due to slower washout than from the thyroid [8.98, 8.99]. The slower washout is possibly as a result of low or lower expression of Pgp in parathyroid [8.100], but a decade later, clear evidence of the role of Pgp in hyperparathyroid disease remains to be confirmed [8.101]. Regardless of the mechanism, delayed clearance forms the basis of its use as the radiodiagnostic for radioguided parathyroidectomy [8.102].

Technetium-99m-Sestamibi is taken up by lactating breast, but is not excreted in human milk [8.103]. Uptake by human brown adipose tissue has been reported recently [8.104]. In summary, various tissues accumulate  $^{99m}\text{Tc}$ -Sestamibi as part of their normal physiological function, making it necessary to establish correlations between uptake and expression of MDR elements before it can be used as a diagnostic for MDR overexpression and as a monitoring tool for MDR inhibition therapies. Liu (2007) has provided a review

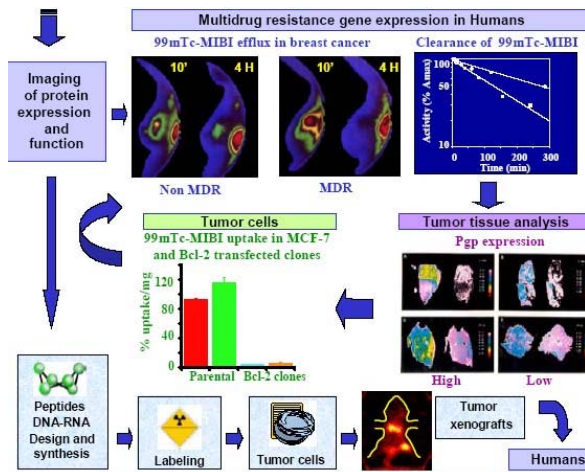


*FIG. 8.4. Graphic presentation of  $^{99m}\text{Tc}$ -Sestamibi in MDR (taken from the European Molecular Imaging Laboratories (EMIL) Centers of Excellence web site [8.130]).*

of the applications of the broad class of cationic Tc complexes in cardiology [8.105].

MDR remains a major obstacle to successful chemotherapeutic treatment of cancer, and overexpression of Pgp, the MDR1 gene product, is thought to be a major player in MDR. The value of a rapid, readily available, non-invasive and economical method to detect MDR in target tissues is obvious, and  $^{99m}\text{Tc}$ -Sestamibi is probably the current agent of choice.

There are numerous reports of inverse correlations between  $^{99m}\text{Tc}$ -Sestamibi uptake and Pgp levels in a variety of cancers. For example, increased levels of MDR1 mRNA and MRP1 mRNA have been shown to correlate with a low accumulation of  $^{99m}\text{Tc}$ -Sestamibi in bone marrow areas in patients with acute leukaemia [8.106]. Similarly, low uptake of  $^{99m}\text{Tc}$ -Sestamibi has been correlated to high levels of expressed Pgp in malignant lymphomas [8.107]. However, although  $^{99m}\text{Tc}$ -Sestamibi scans can be used to demonstrate lymphoma and other tumours of the brain, nasopharynx, thyroid, parathyroid, lung, breast and kidney in Kaposi's sarcoma (KS). Post-therapy scans can provide additional information on the extent of lymph node involvement and more precise staging and therapeutic planning [8.108], but direct or casual relationships have not been validated with respect to MDR and Pgp (over)expression. Fonti et al. [8.109] have concluded, following Pgp-washout relationships, that washout of  $^{99m}\text{Tc}$ -Sestamibi may be used for *in vivo* whole body imaging of Pgp expression and function in multiple myeloma patients.

Importantly, and perhaps surprisingly, in view of expression of MRD proteins by normal hepatocytes, a measurable inverse relationship between  $^{99m}\text{Tc}$ -Sestamibi and Pgp in hepatocellular cancers has been reported [8.110]. Wong et al. [8.96] confirmed this relationship for Pgp as well as for  $^{99m}\text{Tc}$ -Sestamibi and MRP, but found no relationship between  $^{99m}\text{Tc}$ -Sestamibi uptake and lung resistance protein (LRP) expression in patients with hepatocellular carcinoma. In a 21 patient imaging study of intracranial meningiomas, Kunishio et al. [8.111] concluded that it may not be useful for determining proliferative potential and histological malignancy, but that it could predict anticancer drug resistance related to the expression of MDR-1 mRNA and its gene product Pgp in patients with intracranial meningiomas. Similar inverse correlations between  $^{99m}\text{Tc}$ -Sestamibi accumulation and Pgp expression have been reported for pituitary adenomas [8.112].

Technetium-99m-Sestamibi is currently in use as a breast tumour imaging agent [8.113], based, in part, on earlier studies in a smaller patient cohort in which it was concluded that despite moderate sensitivity and specificity, visual and quantitative indices of DSMM could be used to determine and predict Pgp and MRP expression in untreated breast cancer [8.114]. In a less supportive case, deep breast cancer with satellite tumours in multifocal disease failed to find correlations between the tumour/blood indices and Pgp overexpression on baseline  $^{99m}\text{Tc}$ -Sestamibi scans. Objective clinical results after neoadjuvant chemotherapy corresponded to scintigraphic results in 75% of the patients with minimal response [8.115].

There is a substantial literature reporting the relationship between  $^{99m}\text{Tc}$ -Sestamibi uptake and MDR/Pgp expression in cell culture models and in vivo cancer xenografts. For example, Gomes et al. [8.116] report the relationship and its applicability to drug resistance chemotherapy in an orthotopic model of osteosarcoma in nude mice, and Liu et al. [8.117] detected MDR in human breast cancer xenografts using an imaging technique. The downregulation of Pgp expression by short hairpin RNA interference (shRNAi), using a number of in vitro and in vivo molecular techniques, including  $^{99m}\text{Tc}$ -Sestamibi and luciferase optical imaging, has been used to rationalize the feasibility of a knockdown approach to reversing MDR in vivo [8.118]. Other studies have also reported that  $^{99m}\text{Tc}$ -Sestamibi is a sensitive probe for monitoring Pgp inhibition using mdrl antisense oligodeoxynucleotides in vitro and in vivo tumour xenografts [8.119], and that it can be used to monitor antisense oligodeoxynucleotide treatment in an MDR induced human breast cell line [8.120].

It is reported that lipophilic Pgp ligands modify the biphasic accumulation kinetics of  $^{99m}\text{Tc}$ -Sestamibi in MDR negative and positive tumour cells in different and complex ways, and could, therefore, mask the Pgp pump dependent changes in tracer accumulation [8.121].

### Multidrug resistance imaging:

$^{99m}\text{Tc}$ -Tetrofosmin ( $^{99m}\text{Tc}$ -1,2-bis[bis(2-ethoxyethyl phosphino]-ethane)

MDR studies have also been based on another commonly used  $^{99m}\text{Tc}$  radiopharmaceutical,  $^{99m}\text{Tc}$ -Tetrofosmin ( $^{99m}\text{Tc}$ -1,2-bis[bis(2-ethoxyethyl phosphino]-ethane). Clinical studies revealed a sensitivity value of 87.5% with a specificity of 100% when correlating washout rate with Pgp overexpression [8.122], and its function as an indicator of MDR expression has been validated in animal models [8.117]. It has been suggested that  $^{99m}\text{Tc}$ -Tetrofosmin scintigraphy may overestimate the reversal effects of modulators on chemoresistance caused by MRP1 when the modulators simultaneously affect ion transporters [8.123]. Although both  $^{99m}\text{Tc}$ -Sestamibi and  $^{99m}\text{Tc}$ -Tetrofosmin have been acknowledged as being appropriate for MDR imaging, interchangeable use is not recommended [8.124]. The value of  $^{99m}\text{Tc}$ -Tetrofosmin in predicting tumour response has been reviewed [8.125]. Chemical derivatives of this class have been studied [8.126].

### Multidrug resistance imaging: $^{99m}\text{Tc}$ -antisense DNA

A novel approach to determine the involvement of MDR1 in MDR is to use antisense oligonucleotides complimentary to MDR1 mRNA. In a cell culture study using a 20-mer uniform phosphorothioate DNA oligonucleotide  $^{99m}\text{Tc}$  labelled via mercaptoacetyltriglycine (MAG3), uptake of the DNA oligomers was greater than for the corresponding  $^{99m}\text{Tc}$  sense oligonucleotides, and only the antisense oligonucleotide affected  $^{99m}\text{Tc}$ -Sestamibi in cell lines transfected to overexpress MDR1 mRNA to Pgp. These findings support the utilization of radiolabelled antisense for imaging MDR [8.127, 8.128].

### Multidrug resistance gene therapy

Combating MDR through gene therapy has been raised but, to date, no reports have been published [8.129]. Imaging applications in this field could be expected to be substantial, both with labelled MDR substrates and with other reporters associated with the technique.

#### 8.3.2.2. *Imaging gene expression in apoptosis*

Cell death is usually described in terms of necrosis (traumatic cell death) and apoptosis (programmed or orderly cell death); both are complex and not fully understood, but apoptosis has become a major area of research in understanding cell mechanisms important to the development of cytotoxic drugs (i.e. for cancer therapy) and for cell recovery (i.e. in cardiology). Numerous reviews of the

mechanisms and roles of apoptosis in cell biology and medicine are available [8.131–8.133].

#### Bcl-2 (anti-apoptotic gene):

Imaging with  $^{99m}\text{Tc}$ -Sestamibi or  $^{99m}\text{Tc}$ -Tetrofosmin

B-cell lymphoma 2 (Bcl-2) is one of a family of genes that regulates mitochondrial outer membrane permeation and affects apoptotic processes in cells. Of the 25 genes in this family, some are pro-apoptotic (e.g. Bax, BAD) and others are anti-apoptotic — Bcl-2 falls into the latter category [8.134]. Their mechanisms of action have not been fully revealed, but cooperation with other cell proteins such as c-myc are known to be important to their final action. In the case of Bcl-2, cooperation with *c-myc* (oncogene) immortalizes cells [8.135].

A possible link between MDR and the apoptotic pathway was alluded to in a breast cancer study that reported correlations among the apoptotic index, MDR expression and  $^{99m}\text{Tc}$ -Sestamibi efflux rate [8.136]. At about the same time that the role of  $^{99m}\text{Tc}$ -Sestamibi was reviewed in a positive light [8.137], the same group reported a strong link between reduced uptake and Bcl-2 expression in a 42 patient breast cancer study [8.138], introducing concern that reduced  $^{99m}\text{Tc}$ -Sestamibi uptake solely reflects MDR. The Bcl-2 relationship to low  $^{99m}\text{Tc}$ -Sestamibi was validated in breast cell studies *in vitro* [8.139]. A case of a malignant pheochromocytoma refractory to  $^{131}\text{I}$ -MIBG, which showed early intense uptake and rapid washout of  $^{99m}\text{Tc}$ -Tetrofosmin, was similarly interpreted in terms of (anti-apoptotic) Bcl-2 overexpression [8.140].

Other investigators have concluded that  $^{99m}\text{Tc}$ -Sestamibi is unable to differentiate tumours with ongoing apoptosis from those developing drug resistance [8.141].

#### $^{99m}\text{Tc}$ -annexins for apoptosis imaging

The annexins comprise a superfamily of  $\text{Ca}^{2+}$  and phospholipid binding proteins expressed by a multigene (12 genes in humans) family. Some annexins occur ubiquitously, whereas others are limited to only certain tissues/cells. Their function broadly relates to calcium traffic across cell membranes, but their actual functions, exerted through binding to cell surface proteins, range from intracellular signalling by enzyme modulation to ion flux and growth control [8.142, 8.143].

Recognition of apoptotic cell death and subsequent clearance of dying cells are essential to tissue homeostasis. Alterations on the surfaces of dying cells create characteristic membrane signatures for unequivocal distinction from viable cells, and the exposure of phosphatidylserine on the apoptotic cell surface

represents one of the key signals [8.144]. Annexin-A5 (formerly named annexin V) is a highly specific binding partner of phosphatidylserine, a property used as a basis for using labelled annexin-A5 for the identification of apoptotic cells [8.145]. Interested readers are referred to the review by Gaipl et al. [8.146] and references therein.

The first radiolabel based imaging of apoptosis using annexin-A5 was reported in 1998 using succinimidyl 6-hydrazinonicotinamide (hynic) to prepare  $^{99m}$ Tc hynic-annexin V; the decayed  $^{99m}$ Tc-hynic-annexin V inhibited 50% of the binding of a fluorescently tagged annexin V product [8.147]. This preparation ( $^{99m}$ Tc-hynic-annexin prepared optimally via hydrazino nicotinate [8.148] has been applied in numerous animal imaging studies supporting its use in humans as a non-invasive means to assess tumour response [8.149–8.151], and using pre-and post-conditioning in cardiological applications [8.152]. Approaches to achieve improved imaging through altered biodistribution, excretion and binding have been reported. Radiolabelling recombinant annexin V (rh-annexin V) via MAG3 instead of hynic showed a significant decrease in kidney and liver uptake for  $^{99m}$ Tc-MAG3-rh-annexin compared to the  $^{99m}$ Tc-hynic-rh-annexin with lower retention of radioactivity in the whole body, but with small intestine accumulation over fivefold higher [8.153]. The introduction of an endogenous Tc chelation site (Ala-Gly-Gly-Cys-Gly-His) at the N-terminus of annexin V creates ‘annexin V-128’. The annexin V-128 was mutated in calcium binding sites to reduce  $\text{Ca}^{2+}$  binding, and other mutations were made in other residues to alter molecular charge without altering membrane binding affinity. These studies showed that  $^{99m}$ Tc-annexin V-128 detects cell death as well as  $^{99m}$ Tc-hynic-annexin V, but with 88% less renal retention of radioactivity [8.154]. A preliminary study of annexin-13 fragments derivatized to contain cysteine, cysteine-cysteine and histidine in their sequence at the N terminal and labelled with  $^{99m}$ Tc-nitrido and  $^{99m}$ Tc-carbonyl precursors was reported in Ref. [8.155]. In vitro cell uptake and in vivo biodistribution studies showed sufficient specific uptake in apoptotic tumour cells to warrant further study [8.155].

Although clinical validation of the annexin imaging approach is sparse, pre and post cis-platinum therapy uptake studies detected a significant prognostic value of  $^{99m}$ Tc-hynic-rh-annexin V for treatment response in therapy naive patients [8.156].

#### Cyclooxygenases and apoptosis imaging: $^{99m}$ Tc-celebrex

Cyclooxygenases (COX-1 and COX-2) play important roles in tissue function. COX-1 is a housekeeping gene, constitutively expressed in most tissues, and is responsible for the production of homeostatic prostaglandins. COX-2, the product of an immediate early, rapidly inducible and tightly regulated

gene, expression is highly restricted, but dramatically upregulated during inflammation. Increased COX-2 expression occurs upon stimulation with cytokines such as interleukin 1 (IL-1) and tumour necrosis factor-alpha (TNF- $\alpha$ ). COX-2 is increased in some types of human cancers, particularly colon cancer. Mechanisms underlying the association between COX-2 overexpression and tumourigenic potential may include resistance to apoptosis [8.157]. Interaction of cyclooxygenases and apoptotic principles [8.158], and the apoptotic effects of COX-2 inhibitors [8.159] are well known. COX-2 is recognized as a target for both therapy and diagnostic imaging [8.160].

Celebrex (N-4-(5-p-tolyl-3-trifluoromethyl-pyrazol-1-yl) benzene-sulphonylamine) has been labelled with  $^{99m}$ Tc via L,L-ethylenedicycysteine (EC) (e.g. the EC-ethylamino celebrex conjugate) for in vitro and in vivo studies of COX-2 expression; these studies showed some promise as imaging agents, but target validation in vivo, including apoptosis marker correlations, were not included in this study [8.161].

#### *8.3.2.3. Somatostatin receptor imaging*

Early imaging of overexpressed somatostatin receptors was based on radioiodinated peptides such as  $^{123}$ I-tyr-3-octreotide, and although coordination labelled peptides were reported soon thereafter (e.g. [ $^{111}$ In-DTPA-D-Phe1]-octreotide [8.162]), the first  $^{99m}$ Tc labelled peptides followed much later [8.163, 8.164]. The radiolabelling methodology and peptide sequence of Tc labelled somatostatin imaging agents has been reviewed [8.165]. Newer peptides include  $^{99m}$ Tc-tricine-hynic-D-Phe1-Tyr3-octreotide [8.166] and  $^{99m}$ Tc-hydrazinonicotinyl-Tyr3-octreotide (hynic-TOC) [8.167], which compared favourably with [ $^{111}$ In-DTPA-D-Phe1]-octreotide. Recent reports address the use of  $^{99m}$ Tc-depreotide, first labelled in 1994 [8.168] and studied in vivo several years later [8.169]. Reported uses include measurement of oestrogen mediated somatostatin receptor expression in cell culture [8.170]; a comparison to FDG in pulmonary lesion evaluation has been published [8.171]. Technetium-99m-EDDA/hynic-TOC was reported to be clinically useful for scintigraphic follow-up of patients with medullary thyroid cancer, as well as for pre-operative evaluation and for localization of local recurrence or distant metastases [8.172].

#### *8.3.2.4. Angiogenesis: RGD based alpha<sub>1</sub>beta<sub>3</sub> integrin imaging with $^{99m}$ Tc-RGD peptides*

Imaging angiogenesis is a major objective in oncology, cardiology and other diseases. A review of the current status of this field has been published [8.173]. Of the range of potential molecular targets, overexpression of angiogenic

genes encoding the alpha integrins presents one of the most alluring targets. Alpha v integrins, absent or virtually absent in normal tissue blood vessels, are among a number of proteins expressed in endothelial cells of the angiogenic vasculature in solid tumours [8.174, 8.175]. The arginine-glycine-aspartic acid (RGD) peptide sequence is highly selective for binding to alpha<sub>v</sub>beta<sub>3</sub> ( $\alpha_v\beta_3$ ) integrin and related alpha<sub>v</sub>-integrins [8.176], and is the functional targeting moiety in a variety of RGD containing peptides and drug conjugates which display preferential binding to alpha<sub>v</sub>beta<sub>3</sub>, including therapeutic and diagnostic molecules. Several reviews provide excellent orientations to these medically important molecular targets and their targeted drugs [8.177–8.182].

The current status of integrin based angiogenesis imaging has been reviewed [8.183]. Several classes of peptides have been studied to optimize RGD based binding. These include monomer peptides [8.184–8.186], cyclic peptides [8.187–8.189], dimeric peptides [8.190], tetrameric peptides [8.191], RGD-polymer conjugates [8.192] and glucosamino-peptide [8.193]. Methods used to introduce the Tc label vary widely, with  $^{99m}\text{Tc}$ -hynic [8.194] and  $^{99m}\text{Tc}(\text{CO})_3$  [8.195] being the most common.

Direct comparisons among the various RGD based integrin ligands are limited, but investigators report that cyclic RGD peptides labelled via  $[^{99m}\text{Tc}(\text{H}_2\text{O})_3(\text{CO})_3]^+$  may exhibit better tumour uptake than linear counterparts [8.196]. In a study with [2-[[[5-[carbonyl]-2-pyridinyl]hydrazono]methyl]benzenesulphonic acid]-Glu(cyclo{Lys-Arg-Gly-Asp-d-Phe})-cyclo{Lys-Arg-Gly-Asp-d-Phe} in a murine U87MG human glioma xenografts model, the Tc-tricine-TPPTS (trisodium triphenylphosphine-3,3',3'-trisulphonate) labelled complex performed better than either the Tc-EDDA (ethylenediamine-N,N'-diacetic acid) complex or the Tc-tricine-PDA (2,5-pyridinedicarboxylic acid) complex. Dechristoforo et al. [8.197] compared Tc-c(RGDyK), a cyclic pentapeptide labelled via either hynic- $[^{99m}\text{Tc}]$ EDDA, Cys- $[^{99m}\text{Tc}]$ nitridophosphine] (PNP), L2- $[^{99m}\text{Tc}]$ isonitrile-NS(3)-coligand] or Pz-1(pyrazole)  $[^{99m}\text{Tc}(\text{CO})_3]$ . Although these investigators reported highest uptakes of  $[^{99m}\text{Tc}]$ EDDA/hynic-c(RGDyK),  $[^{99m}\text{Tc}]$ nitrido-PNP-Cys-c(RGDyK) and  $[^{99m}\text{Tc}(\text{CO})_3]$ -Pz1-c(RGDyK) in a tumour model, they caution that, in each case, other properties affecting overall pharmacokinetics, such as renal and hepatobiliary uptake and clearance must be taken into account, together with in vitro assays of binding, in order to make a final selection [8.197].

## **8.4. TECHNETIUM-99m LABELLED DNA/RNA PRODUCTS FOR IMAGING COMPLEMENTARY mRNA**

Oligonucleotides play central roles in living organisms; as large molecules, they hold the genetic code (DNA and genes) and mediate between DNA and protein (RNA). As shorter chains, they have equally vital roles in a myriad of homeostatic processes. Imaging biological processes using radiolabelled oligonucleotides has been reviewed [8.33, 8.34, 8.198–8.200].

### **8.4.1. Chemistry: $^{99\text{m}}\text{Tc}$ labelling of oligonucleotides and polynucleotides**

Early reports of DNA labelling with  $^{99\text{m}}\text{Tc}$  used the hydrazinonicotinamide (SHNH) moiety. Single strand oligonucleotides with a primary amine attached to either the 3' or 5' end, and with a biotin moiety on the opposite end, were conjugated with SHNH by an N-hydroxysuccinimide derivative with DTPA via the cyclic anhydride, and the purified SHNH-DNA was radiolabelled with  $^{99\text{m}}\text{Tc}$  by trans-chelation from glucoheptonate at labelling efficiencies of up to 60% [8.201]. MAG3 based chelation via a two step synthesis of the N-hydroxysuccinimide ester of MAG3 in which the sulphur was protected with an acetyl group (i.e. S-acetyl NHS-MAG3), coupling S-acetyl NHS-MAG3 to single strand amine-derivatized DNA and finally radiolabelling at room temperature and neutral pH by trans-chelation from  $^{99\text{m}}\text{Tc}$ -tartrate has become the most commonly used Tc labelling technique for this class of compounds [8.202]. It has been used for locked peptide nucleic acids [8.203], nucleic acids [8.204] and phosphorodiamidate morpholino nucleic acids [8.204–8.209]. One report has compared three labelling methods with the in vitro properties and murine biodistributions of an antisense phosphorothioate labelled by NHS ester conjugation with hynic(tricene), MAG3 and the cyclic anhydride of DTPA. Surface plasmon resonance measurements of the association rate constants for hybridization were identical for all three chelators and the native DNA. The order of accumulation of  $^{99\text{m}}\text{Tc}$  in the RIalpha mRNA-positive cancer cell line was DTPA > hynic > MAG3, and the rate of  $^{99\text{m}}\text{Tc}$  egress from cells was MAG3 > hynic > DTPA. The biodistribution in normal mice was heavily influenced by the labelling method. The authors concluded that the success of antisense imaging may depend on the method of radiolabelling [8.210].

### **8.4.2. Targeting and delivery of $^{99\text{m}}\text{Tc}$ labelled DNA/RNA products**

Most drugs, and many diagnostics, must find passage across cell membranes before they can exert their biochemical/molecular effect(s). This applies equally to radiotracers for molecular imaging [8.211]. Atherosclerotic

lesions induced in rabbits were successfully imaged with [ $^{99m}\text{Tc}$ ]c-myc antisense oligonucleotides but not the corresponding sense oligonucleotides with no atherosclerotic lesions found in the vessel wall and no positive imaging in animals of the control group [8.212]. This study represents a case in which transmembrane passage of the oligonucleotide is not required in order to find and bind the complementary target. In most cases, passage of the highly charged oligonucleotide is blocked, and even in cases with limited charge, passage of large molecules into cells is constrained.

#### *8.4.2.1. Drug formulation approaches*

Carriers have been used as a means of introducing both radiolabelled and non-labelled oligonucleotides into cells. Pharmaceutical carriers such as cyclodextrins [8.213, 8.214], liposomes [8.215, 8.216] and electrostatic complexation using transfecting carriers [8.128], and peptides [8.216] are under investigation.

#### *8.4.2.2. Medicinal chemistry approaches*

Perhaps the most substantial developments in targeting and delivery of oligonucleotides (antisense, aptamers, siRNA, DNAzymes, etc.) have come through chemical modifications of the basic oligonucleotide. In the first instance, this involved the development of nuclease resistant molecules, achieved through changes in the phosphodiester backbone, replacing phosphate with phosphorodiamidate, phosphorothioate, amino acid or morpholino moieties, making ‘locked’ nucleic acids and changing the stereochemistry (spiegelmers). Readers are referred to Haberkorn et al. [8.33] for a succinct review of ‘oligo’ backbone and sugar modification design.

#### Phosphorothioate nucleic acids

A comparison between a synthetic 22-base single stranded phosphodiester DNA and its phosphorothioate analogue, both  $^{99m}\text{Tc}$  labelled via hynic, found that the phosphodiester label was almost quantitatively converted to lower molecular weight catabolites after only 15 min, whereas the phosphorothioate label was primarily on proteins. They concluded, however, that phosphodiester DNA may be preferred in certain circumstances to avoid the high and persistent liver uptake observed with the phosphorothioate DNA [8.217]. The influence of base composition on non-specific accumulation in MCF-7 breast cancer cells was investigated using ten uniform phosphorothioate and five uniform phosphodiester oligonucleotides. Three of the phosphorothioates were antisense against different

sites within survivin mRNA, two were the corresponding sense and scrambled controls, and the remaining five were polynucleotides of adenosine, cytidine, deoxythymidine and guanine-guanine-guanine-adenine. Guanine content was identified as an important determinant of non-specific cellular accumulations under the conditions of this investigation [8.218].

#### Peptide nucleic acids

Studies of a  $^{99m}\text{Tc}$ -MAG3 radiolabelled, amine-derivatized 15 base peptide nucleic acid (PNA) oligomer showed rapid whole body clearance in mice, and whole body images showed only bladder, kidneys and the left thigh, which contained implanted beads conjugated with complimentary DNA, supporting the conclusion that  $^{99m}\text{Tc}$ -PNA may provide the stability and pharmacokinetic properties suitable for use as radiopharmaceuticals [8.203].

#### Locked nucleic acids

In a study comparing various RIalpha mRNA antisense molecules, a 15-mer locked nucleic acid (LNA) was compared with sense LNAs, uniform 18-mer phosphorothioate DNA and uniform 18-mer phosphodiamidate morpholinos, all labelled with  $^{99m}\text{Tc}$  via MAG3. The antisense LNA showed a favourable dissociation constant for the 15-mer LNA-DNA duplex compared to the 18-mer DNA duplex and 18-mer morpholino nucleic acids (MORFs)-duplex. Cellular accumulation of antisense LNA was higher than that of sense, both when added naked and with a liposome carrier. As much as 2.9% of the antisense LNA (with carrier) was in the cytoplasmic or nuclear fractions, demonstrating that the LNA was internalized [8.216].

#### Morpholino nucleic acids

For investigations of 15-mer and 18-mer MORFs with a nuclease resistant non-ionic and water-soluble phosphorodiamidate backbone, a primary amine was added via a  $\beta$ -alanine linker to the 3' equivalent end, and this amino group was used to conjugate NHS-MAG3 for  $^{99m}\text{Tc}$  radiolabelling. Hybridization of this  $^{99m}\text{Tc}$ -MORF in vitro to free cMORF (complimentary MORF), to a cMORF polymer and to cMORF beads was nearly quantitative, and it was stable in vitro with minimal protein binding. In normal mice, it was rapidly cleared, and uptake by implanted cMORF labelled beads confirmed in vivo hybridization [8.208]. Technetium-99m-NHS-MAG3 was still largely intact after 48 h in saline or serum, and was rapidly cleared after IV injection into normal mice [8.219].

#### *8.4.2.3. Targeting techniques for improved delivery based on molecular derivatization*

##### Structurally altered probes

Several approaches to targeting and delivery using complex molecular probes have been published. Chain length and base sequence, particularly the presence of cytosines, appear to be determinants of uptake and/or hybridization of DNA/RNA complementary binding probes [8.220, 8.221]. The use of duplex oligonucleotide probes may also provide improved imaging. Chain length, homoduplexes and heteroduplexes have been investigated [8.222]. Duplex formation appears to improve performance over single strand antisense oligomers. This involves duplex formation between the antisense phosphorothioate DNA against the *mdr1* mRNA and the uniform phosphorothioate or uniform phosphodiester sense DNAs [8.223].

##### Oligomer chimeras

A second approach targets mRNA via  $^{99m}\text{Tc}$  labelled peptide-PNA chimeras. Previous attempts to image *c-myc* mRNA were based on  $^{111}\text{In}$  labelled antisense phosphodiester and phosphorothioate oligonucleotides [8.224]. In the current approach, a dodecamer antisense PNA, specific for the c-MYC oncogene overexpressed in human breast cancer cells, is coupled to a chelating moiety that facilitates quantitative radiolabelling with  $^{99m}\text{Tc}$ . Inhibition of reverse transcription by the c-MYC specific chimera as compared to that of the mismatch control *in vitro*, and tissue distribution studies of antisense and mismatch chimeras showed modest accumulation of the antisense chimera in liver, and appreciable levels in tumours [8.225]. A second ‘chimera’ has been reported for imaging the cyclin D gene [8.226]. This gene, called the CCND1 gene, encodes the cell cycle regulatory protein cyclin D1; cyclin D1 mRNA and ER mRNA are positively correlated in primary breast cancer [8.227]. Tian and co-workers exploited breast cancer overexpression of CCND1 mRNA together with the known overexpression of insulin like growth factor 1 receptor (IGF1R mRNA), creating a  $^{99m}\text{Tc}$  labelled PNA peptide chimera (CCND1 PNA-IGF1 peptide) to image breast cancer. Successful imaging of cancer xenograft models was reported [8.226]. A similar approach for preparation of a chelator-peptide-PNA-peptide chimera specific for *KRAS*, coupling a C terminal insulin like growth factor 1 (IGF1) ligand and an N terminal bis(s-benzoyl thioglycoloyl) diaminopropanoate chelator for radionuclide labelling has been reported [8.228]. This approach was recently reviewed [8.229].

## Oligomer pretargeting

The concept that pretargeting antisense using polymers of PNA for amplification can improve localization was introduced by Wang et al. [8.230]. An 80 kilodalton poly(methyl vinyl ether-alt-maleic acid) (PA) polymer was conjugated with multiple copies of PNA and with multiple copies of poly(ethylene glycol) (PEG) by reacting the NHS derivative of PA with the amine derivatives of PNA and PEG, followed by  $^{99m}\text{Tc}$ -MAG3 labelling. About 80 PNAs could be conjugated to PA, requiring conjugation of about 200 PEGs to improve aqueous solubility. The authors concluded that the application of pretargeting using pegylated PA polymers of PNA for amplification improved localization. In another case, an amine derivatized 25-mer MORF, MAG3-radiolabelled  $^{99m}\text{Tc}$ , was conjugated to three polymers of succinylated polylysine (PL) (average molecular weight: 30, 100 and 200 kilodaltons), and one PA (molecular weight: 45 kilodaltons). The 30 kilodalton PL showed the most favourable pharmacokinetic profile [8.222].

The effective use of antibody pretargeting for MORFs was demonstrated with an 18-mer MORF and its 18-mer cMORF linked via a 3-member alkyl amine linker on the 3' end to an anti-carcinoembryonic antigen IgG antibody (MN14) and  $^{99m}\text{Tc}$  labelled via MAG3. High uptake in tumours and low uptake in normal tissues of the study mice confirmed the effectiveness of this pretargeting approach [8.231]. A semi-empirical description of the biodistribution of labelled cMORF was capable of predicting the biodistribution of the radiolabelled effector in the pretargeted tumour bearing mouse model, demonstrating that the underlying pretargeting concepts are correct [8.232].

### 8.4.3. Aptamers

Aptamers are short DNA or RNA oligonucleotides, or peptides that assume specific, stable conformations *in vivo*. They can bind specifically and tightly to small rigid molecules (drugs), peptides, proteins and other oligonucleotides. As opposed to antisense oligonucleotides, their targets are frequently extracellular rather than intracellular, thus avoiding the necessity of crossing cell membranes. Aptamers were discovered in the early 1990s. Their importance has given rise to innumerable investigations, and many reviews of their properties and applications appear in the recent literature [8.233–8.235].

Somewhat surprisingly, with the exception of Dougan's pioneering work with radioiodinated aptamers for thrombosis imaging using an aptamer avid for crosslinked fibrin [8.236–8.238] (Fig. 8.5), aptamers have not yet received the attention one might have anticipated.

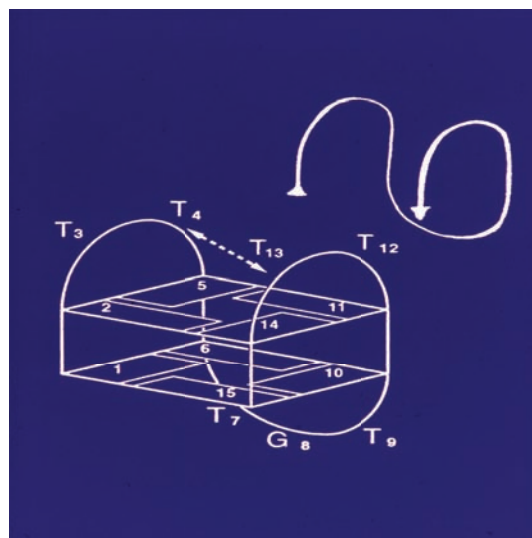


*FIG. 8.5. A diagrammatic representation of the 15-mer thrombin binding DNA aptamer d(GGTTGGTGTGGTTGG), a guanine quartet DNA aptamer that binds to exosite 1, the fibrinogen binding site on thrombin (courtesy of Hayes Dougan).*

Very recently, an aptamer to the extracellular matrix protein tenascin-C was prepared in fluorescent and radiolabelled forms, and <sup>99m</sup>Tc labelled aptamer images of glioblastoma and breast tumours were obtained by planar scintigraphy. Aptamer uptake in several different human tumour xenografts required the presence of the target protein (human tenascin-C). Interestingly, selection of the radiometal chelator [mercapto-acetyl diglycine (MAG2); diethylenetriaminepentaacetic acid; MAG2-3,400-molecular-weight PEG (PEG3,400)] dramatically altered the uptake and clearance patterns [8.239].

## REFERENCES TO CHAPTER 8

- [8.1] American Society of Gene Therapy (2007), <http://www.asgt.org>
- [8.2] ANDERSON, W.F., BLAESE, R.M., CULVER, K., The ADA human gene therapy clinical protocol: Points to consider response with clinical protocol, *Hum. Gene. Ther.* **1** (1990) 331–362.
- [8.3] ROSENBERG, S.A., et al., The development of gene-therapy for the treatment of cancer, *Ann. Surg.* **218** (1993) 455–464.
- [8.4] IMAI, E., AKAGI, Y., ISAKA, Y., Towards gene therapy for renal diseases, *Nephrologie* **19** (1998) 397–402.

- [8.5] GLASS, H.B., The Rockefeller Foundation: Warren Weaver and the launching of molecular biology, *Quart. Rev. Biol.* **66** 3 (1991) 303.
- [8.6] AVERY, T., MACLEOD, C.M., MCCARTY, M., Studies on the chemical nature of the substance inducing transformation of pneumococcal types, *J. Exp. Med.* (1944) 137–158.
- [8.7] SCHRODINGER, E., *What is Life? The Physical Aspect of the Living Cell, and Mind and Matter*, Cambridge University Press (1947).
- [8.8] HERSEY, A.D., CHASE, M., Independent functions of viral protein and nucleic acid in growth of bacteriophage, *J. Gen. Physiol.* **36** (1952) 39–56.
- [8.9] SOCIETY OF NUCLEAR MEDICINE (2007), <http://interactive.snm.org/>
- [8.10] WOLFF, J.A., LEDERBERG, J., An early history of gene-transfer and therapy, *Hum. Gene. Ther.* **5** (1994) 469–480.
- [8.11] GRAHAM, F.L., VANDEREB, A.J., Transformation of rat cells by DNA of human adenovirus-5, *Virology* **54** (1973) 536–539.
- [8.12] DUBENSKY, T.W., CAMPBELL, B.A., VILLARREAL, L.P., Direct transfection of viral and plasmid DNA into the liver or spleen of mice, *Proc. Natl. Acad. Sci. USA* **81** (1984) 7529–7533.
- [8.13] APOSHIAN, H.V., Use of DNA for gene therapy - Need, experimental approach, and implications, *Perspect. Biol. Med.* **14** (1970) 98–108.
- [8.14] ELION, G.B., et al., Selectivity of action of an anti-herpetic agent, 9-(2-hydroxyethoxymethyl)guanine, *Proc. Natl. Acad. Sci. USA* **74** (1977) 5716–5720.
- [8.15] WIGLER, M., et al., Transfer of purified herpes-virus thymidine kinase gene to cultured mouse cells, *Cell* **11** (1977) 223–232.
- [8.16] FURMAN, P.A., MCGUIRT, P.V., KELLER, P.M., FYFE, J.A., ELION, G.B., Inhibition by acyclovir of cell-growth and DNA-synthesis of cells biochemically transformed with Herpesvirus genetic information, *Virology* **102** (1980) 420–430.
- [8.17] SAITO, Y., et al., Quantitative autoradiographic mapping of Herpes-Simplex Virus encephalitis with a radiolabeled antiviral drug, *Science* **217** (1982) 1151–1153.
- [8.18] SAITO, Y., RUBENSTEIN, R., PRICE, R.W., FOX, J.J., WATANABE, K.A., Diagnostic-imaging of Herpes-Simplex Virus encephalitis using a radiolabeled antiviral drug - Autoradiographic assessment in an animal-model, *Ann. Neurol.* **15** (1984) 548–558.
- [8.19] GILL, M.J., SAMUEL, J., WIEBE, L.I., KNAUS, E.E., TYRRELL, D.L., Quantitative uptake studies of I-131-labeled (E)-5-(2-iodovinyl)-2'-deoxyuridine in herpes simplex virus-infected cells in vitro, *Antimicrob. Agents Chemother.* **25** (1984) 476–478.
- [8.20] SAMUEL, J., et al., Pharmacokinetics and metabolism of E-5-(2-[I-131]-iodovinyl)-2'-deoxyuridine in dogs, *Antimicrob. Agents Chemother.* **29** (1986) 320–324.
- [8.21] TOVELL, D.R., et al., Effect of acyclovir on the uptake of I-131-labeled 1-(2'-fluoro-2'-deoxy-beta-D-arabinofuranosyl)-5-iodouracil in Herpes infected-cells, *J. Med. Virol.* **22** (1987) 183–188.

- [8.22] TOVELL, D., et al., The in vitro evaluation of nucleoside analogues as probes for use in the non-invasive diagnosis of herpes simplex encephalitis, *Drug Des. Deliv.* (1988) 213–221.
- [8.23] CLEATOR, G.M., LEWIS, A.G., KLAPPER, P.E., SHARMA, H.L., SMITH, A.M., Hm-Pao-imaging and herpes encephalitis, *Arch. Virol.* **109** (1989) 263–268.
- [8.24] BALZARINI, J., MORIN, K.W., KNAUS, E.E., WIEBE, L.I., DECLERCQ, E., Novel (E)-5-(2-iodovinyl)-2'-deoxyuridine derivatives as potential cytostatic agents against Herpes-Simplex Virus thymidine kinase gene transfected tumors, *Gene Ther.* **2** (1995) 317–322.
- [8.25] KNAUS, E.E., WIEBE, L.I., MORIN, K.W., Combined Use of Nucleoside Analogues and Gene Transfection for Tissue Imaging and Therapy, Canadian Patent 2,202,891 (1994) 21.
- [8.26] TJUVAJEV, J.G., et al., Imaging the expression of transfected genes in vivo, *Cancer Res.* **55** (1995) 6126–6132.
- [8.27] ALAUDDIN, M.M., et al., In vivo evaluation of 2'-deoxy-2'-[F-18]fluoro-5-iodo-1-beta-D-arabinofuranosyluracil ([F-18]FIAU) and 2'-deoxy-2'-[F-18]fluoro-5-ethyl-1-beta-D-arabinofuranosyluracil ([F-18]FEAU) as markers for suicide gene expression, *Eur. J. Nucl. Med. Mol. Imaging* **34** (2007) 822–829.
- [8.28] DEMPSEY, M.F., et al., Assessment of I-123-FIAU imaging of herpes simplex viral gene expression in the treatment of glioma, *Nucl. Med. Commun.* **27** (2006) 611–617.
- [8.29] CRISTOFOLI, W.A., et al., 5-alkynyl analogs of arabinouridine and 2'-deoxyuridine: Cytostatic activity against herpes simplex virus and varicella-zoster thymidine kinase gene-transfected cells, *J. Med. Chem.* **50** (2007) 2851–2857.
- [8.30] NIMMAGADDA, S., MANGNER, T.J., DOUGLAS, K.A., MUZIK, O., SHIELDS, A.F., Biodistribution, PET, and radiation dosimetry estimates of HSV-tk gene expression imaging agent 1-(2'-deoxy-2'-F-18-fluoro-beta-D-arabinofuranosyl)-5-iodouracil in normal dogs, *J. Nucl. Med.* **48** (2007) 655–660.
- [8.31] ALAUDDIN, M.M., et al., Biodistribution and PET imaging of [F-18]-fluoroadenosine derivatives, *Nuc.l Med. Biol.* **34** (2007) 267–272.
- [8.32] KUMMER, C., et al., Multitracer positron emission tomographic imaging of exogenous gene expression mediated by a universal herpes simplex virus I amplicon vector, *Mol. Imaging* **6** (2007) 181–192.
- [8.33] HABERKORN, U., MIER, W., EISENHUT, M., Scintigraphic imaging of gene expression and gene transfer, *Curr. Med. Chem.* **12** (2005) 779–794.
- [8.34] BOY, R.G., KNAPP, E.M., EISENHUT, M., HABERKORN, U., MIER, W., Enzymes/transporters, *Handb. Exp. Pharmacol.* (2008) 131–143.
- [8.35] GHARIB, A.M., THOMASSON, D., LI, K.C.P., Molecular imaging of hepatocellular carcinoma, *Gastroenterology* **127** (2004) S153–S158.
- [8.36] INUBUSHI, M., TAMAKI, N., Radionuclide reporter gene imaging for cardiac gene therapy, *Eur. J. Nucl. Med. Mol. Imaging* **34** (2007) S27–S33.
- [8.37] HARGREAVES, R., New migraine and pain research, *Headache* **47** (2007) S26–S43.
- [8.38] REIMAN, E.M., Linking brain imaging and genomics in the study of Alzheimer's disease and aging, *Ann. NY. Acad. Sci.* **1097** (2007) 94–113.

- [8.39] BARRETT, T., CHOYKE, P.L., KOBAYASHI, H., Imaging of the lymphatic system: new horizons, *Contrast Media Mol. Imaging* **1** (2006) 230–245.
- [8.40] ZINN, K.R., et al., Imaging and tissue biodistribution of Tc-99m-labeled adenovirus knob (serotype 5), *Gene Ther.* **5** (1998) 798–808.
- [8.41] ABRAM, U., ALBERTO, R., Technetium and rhenium – Coordination chemistry and nuclear medical applications, *J. Brazil Chem. Soc.* **17** (2006) 1486–1500.
- [8.42] YANG, D.J.J., et al., Tc-99m-EC-guanine: Synthesis, biodistribution, and tumor imaging in animals, *Pharm. Res.* **22** (2005) 1471–1479.
- [8.43] ZHANG, Y., LIN, J., PAN, D.F., Synthesis of a technetium-99m labeled tricyclic ganciclovir analog for non-invasive reporter gene expression imaging, *Bioorg. Me. Chem. Lett.* **17** (2007) 741–744.
- [8.44] SPITZWEG, C., JOBA, W., EISENMENGER, W., HEUFELDER, A.E., Analysis of human sodium iodide symporter gene expression in extrathyroidal tissues and cloning of its complementary deoxyribonucleic acids from salivary gland, mammary gland, and gastric mucosa, *J. Clin. Endocr. Metab.* **83** (1998) 1746–1751.
- [8.45] DOHAN, O., et al., The sodium/iodide symporter (NIS): Characterization, regulation, and medical significance, *Endocr. Rev.* **24** (2003) 48–77.
- [8.46] ESKANDARI, S., et al., Thyroid Na<sup>+</sup>/I<sup>-</sup> symporter - Mechanism, stoichiometry, and specificity, *J. Biol. Chem.* **272** (1997) 27230–27238.
- [8.47] VAN SANDE, J., et al., Anion selectivity by the sodium iodide symporter, *Endocrinology* **144** (2003) 247–252.
- [8.48] PETRICH, T., HELMEKE, H.J., MEYER, G.J., KNAPP, W.H., POTTER, E., Establishment of radioactive astatine and iodine uptake in cancer cell lines expressing the human sodium/iodide symporter, *Eur. J. Nucl. Med. Mol. Imaging* **29** (2002) 842–854.
- [8.49] RIESCO-EIZAGUIRRE, G., SANTISTEBAN, P., A perspective view of sodium iodide symporter research and its clinical implications, *Eur. J. Endocrinol.* **155** (2006) 495–512.
- [8.50] CHUNG, J.K., Sodium iodide symporter: Its role in nuclear medicine, *J. Nucl. Med.* **43** (2002) 1188–1200.
- [8.51] DAI, G., LEVY, O., CARRASCO, N., Cloning and characterization of the thyroid iodide transporter, *Nature* **379** (1996) 458–460.
- [8.52] SMANIK, P.A., et al., Cloning of the human sodium iodide symporter, *Biochem. Biophys. Res. Co.* **226** (1996) 339–345.
- [8.53] DADACHOVA, E., CARRASCO, N., The Na<sup>+</sup>/I<sup>-</sup> symporter (NIS): Imaging and therapeutic applications, *Semin. Nucl. Med.* **34** (2004) 23–31.
- [8.54] CHEN, L.B., et al., Tc-99m-pertechnetate uptake in hepatoma cells due to tissue-specific human sodium iodide symporter gene expression, *Nucl. Med. Biol.* **33** (2006) 575–580.
- [8.55] TAZEBAY, U.H., et al., The mammary gland iodide transporter is expressed during lactation and in breast cancer, *Nature Med.* **6** (2000) 871–878.
- [8.56] LIU, B.K., et al., Sodium iodide symporter is expressed at the preneoplastic stages of liver carcinogenesis and in human cholangiocarcinoma, *Gastroenterology* **132** (2007) 1495–1503.

- [8.57] FUJIWARA, H., et al., Recurrent T354P mutation of the Na<sup>+</sup>/I<sup>-</sup> symporter in patients with iodide transport defects, *J. Clin. Endocr. Metab.* **83** (1998) 2940–2943.
- [8.58] SHIN, J.H., et al., Feasibility of sodium/iodide symporter gene as a new imaging reporter gene: comparison with HSV1-tk, *Eur. J. Nucl. Med. Mol. Imaging* **31** (2004) 425–432.
- [8.59] LEE, W.W., et al., Imaging of adenovirus-mediated expression of human sodium iodide symporter gene by (99)mTcO(4)<sup>-</sup> scintigraphy in mice, *Nucl. Med. Biol.* **31** (2004) 31–40.
- [8.60] HWANG, D.W., et al., Development of a dual membrane protein reporter system using sodium iodide symporter and mutant dopamine D-2 receptor transgenes, *J. Nucl. Med.* **48** (2007) 588–595.
- [8.61] LIM, S.J., et al., Enhanced expression of adenovirus-mediated sodium iodide symporter gene in MCF-7 breast cancer cells with retinoic acid treatment, *J. Nucl. Med.* **48** (2007) 398–404.
- [8.62] KANG, J.H., et al., Development of a sodium/iodide symporter (NIS)-transgenic mouse for imaging of cardiomyocyte-specific reporter gene expression, *J. Nucl. Med.* **46** (2005) 479–483.
- [8.63] SIDDIQUI, F., et al., Design considerations for incorporating sodium iodide symporter reporter gene imaging into prostate cancer gene therapy trials, *Hum. Gene. Ther.* **18** (2007) 312–322.
- [8.64] CROTTOGINI, A., et al., Arteriogenesis induced by intramyocardial vascular endothelial growth factor 165 gene transfer in chronically ischemic pigs, *Hum. Gene. Ther.* **14** (2003) 1307–1318.
- [8.65] ZINN, K.R., CHAUDHURI, T.R., The type 2 human somatostatin receptor as a platform for reporter gene imaging, *Eur. J. Nucl. Med. Mol. Imaging* **29** (2002) 388–399.
- [8.66] ROGERS, B.E., et al., MicroPET imaging of gene transfer with a somatostatin receptor-based reporter gene and Tc-94m-demotate 1, *J. Nucl. Med.* **46** (2005) 1889–1897.
- [8.67] ROGERS, B.E., CHAUDHURI, T.R., REYNOLDS, P.N., DELLA MANNA, D., ZINN, K.R., Non-invasive gamma camera imaging of gene transfer using an adenoviral vector encoding an epitope-tagged receptor as a reporter, *Gene Ther.* **10** (2003) 105–114.
- [8.68] TER HORST, M., et al., Locoregional delivery of adenoviral vectors, *J. Nucl. Med.* **47** (2006) 1483–1489.
- [8.69] HEMMINKI, A., et al., In vivo molecular chemotherapy and noninvasive imaging with an infectivity-enhanced adenovirus, *J. Natl. Cancer Inst.* **94** (2002) 741–749.
- [8.70] ZINN, K.R., et al., Gamma camera dual imaging with a somatostatin receptor and thymidine kinase after gene transfer with a bicistronic adenovirus in mice, *Radiology* **223** (2002) 417–425.
- [8.71] ZINN, K.R., et al., Noninvasive monitoring of gene transfer using a reporter receptor imaged with a high-affinity peptide radiolabeled with Tc-99m or Re-188, *J. Nucl. Med.* **41** (2000) 887–895.

- [8.72] SIMONOVA, M., SHTANKO, O., SERGEYEV, N., WEISSLEDER, R., BOGDANOV, A., Engineering of technetium-99m-binding artificial receptors for imaging gene expression, *J. Gene. Med.* **5** (2003) 1056–1066.
- [8.73] SCHIPPER, M.L., et al., Efficacy of Tc-99m pertechnetate and I-131 radioisotope therapy in sodium/iodide symporter (NIS)-expressing neuroendocrine tumors *in vivo*, *Eur. J. Nucl. Med. Mol. Imaging* **34** (2007) 638–650.
- [8.74] DANO, K., Active outward transport of daunomycin in resistant Ehrlich ascites tumor cells, *Biochim. Biophys. Acta* **323** (1973) 466–483.
- [8.75] JULIANO, R.L., LING, V., Surface glycoprotein modulating drug permeability in chinese-hamster ovary cell mutants, *Biochim. Biophys. Acta* **455** (1976) 152–162.
- [8.76] CROOP, J.M., GROS, P., HOUSMAN, D.E., Genetics of multidrug resistance, *J. Clin. Invest.* **81** (1988) 1303–1309.
- [8.77] GOTTESMAN, M.M., PASTAN, I., The multidrug transporter, a double-edged sword, *J. Biol. Chem.* **263** (1988) 12163–12166.
- [8.78] ENDICOTT, J.A., LING, V., The biochemistry of P-glycoprotein-mediated multidrug resistance, *Annu. Rev. Biochem.* **58** (1989) 137–171.
- [8.79] COLE, S.P.C., et al., Overexpression of a transporter gene in a multidrug-resistant human lung-cancer cell line, *Science* **258** (1992) 1650–1654.
- [8.80] TSURUO, T., Molecular cancer therapeutics: Recent progress and targets in drug resistance, *Internal Med.* **42** (2003) 237–243.
- [8.81] SCHINKEL, A.H., KEMP, S., DOLLE, M., RUDENKO, G., WAGENAAR, E., N-glycosylation and deletion mutants of the human Mdr1 P-glycoprotein, *J. Biol. Chem.* **268** (1993) 7474–7481.
- [8.82] AMBUDKAR, S.V., et al., Biochemical, cellular, and pharmacological aspects of the multidrug transporter, *Annu. Rev. Pharmacol.* **39** (1999) 361–398.
- [8.83] VARMA, M.V.S., ASHOKRAJ, Y., DEY, C.S., PANCHAGNULA, R., P-glycoprotein inhibitors and their screening: a perspective from bioavailability enhancement, *Pharmacol. Res.* **48** (2003) 347–359.
- [8.84] SHERVINGTON, A., LU, C., Expression of multidrug resistance genes in normal and cancer stem cells, *Cancer Invest.* **26** (2008) 535–542.
- [8.85] SZAKACS, G., PATERSON, J.K., LUDWIG, J.A., BOOTH-GENTHE, C., GOTTESMAN, M.M., Targeting multidrug resistance in cancer, *Nat. Rev. Drug Discov.* **5** (2006) 219–234.
- [8.86] DE GEUS-OEI, L.F., et al., Tracers to monitor the response to chemotherapy: In vitro screening of four radiopharmaceuticals, *Cancer Biother. Radiopharm.* **19** (2004) 457–465.
- [8.87] VAN EERD, J.E.M., DE GEUS-OEI, L.F., OYEN, W.J.G., CORSTENS, F.H.M., BOERMAN, O.C., Scintigraphic imaging of P-glycoprotein expression with a radiolabelled antibody, *Eur. J. Nucl. Med. Mol. Imaging* **33** (2006) 1266–1272.
- [8.88] PIWNICA-WORMS, D., et al., Functional imaging of multidrug-resistant P-glycoprotein with an organotechnetium complex, *Cancer Res.* **53** (1993) 977–984.
- [8.89] SHEN, D.W., et al., Human multidrug-resistant cell-lines: increased Mdr1 expression can precede gene amplification, *Science* **232** (1986) 643–645.

- [8.90] HERMAN, L.W., et al., Novel hexakis(areneisonitrile)technetium(I) complexes as radioligands targeted to the multidrug-resistance P-glycoprotein, *J. Med. Chem.* **38** (1995) 2955–2963.
- [8.91] BIGOTT, H.M., PRIOR, J.L., PIWNICA-WORMS, D.R., WELCH, M.J., Imaging multidrug resistance P-glycoprotein transport function using microPET with technetium-94m-sestamibi, *Mol. Imaging* **4** (2005) 30–39.
- [8.92] TAMAKI, N., Myocardial perfusion imaging with Tc-99m isonitriles, *Rinsho Hoshasen* (1987) 471–477.
- [8.93] SAVI, A., et al., Biodistribution of Tc-99m methoxy-isobutyl-isonitrile (Mibi) in humans, *Eur. J. Nucl. Med.* **15** (1989) 597–600.
- [8.94] TAILLEFER, R., et al., Myocardial perfusion imaging with Tc-99m-methoxy-isobutyl-isonitrile (Mibi) - Comparison of short and long-time intervals between rest and stress injections — Preliminary-results, *Eur. J. Nucl. Med.* **13** (1988) 515–522.
- [8.95] KAKHKI, V.R., ZAKAVI, S.R., DAVOUDI, Y., Normal values of gallbladder ejection fraction using 99mTc-sestamibi scintigraphy after a fatty meal formula, *J. Gastrointestin. Liver Dis.* (2007) 157–161.
- [8.96] WONG, M., et al., Hepatic technetium Tc 99m-labeled sestamibi elimination rate and ABCB1 (MDR1) genotype as indicators of ABCB1 (P-glycoprotein) activity in patients with cancer, *Clin. Pharmacol. Ther.* **77** (2005) 33–42.
- [8.97] GHIBELLINI, G., et al., In vitro-in vivo correlation of hepatobiliary drug clearance in humans, *Clin. Pharmacol. Ther.* **81** (2007) 406–413.
- [8.98] ISHIBASHI, M., et al., Comparison of technetium-99m-MIBI, technetium-99m-tetrofosmin, ultrasound and MRI for localization of abnormal parathyroid glands, *J. Nucl. Med.* **39** (1998) 320–324.
- [8.99] LAVELY, W.C., et al., Comparison of SPECT/CT, SPECT, and planar imaging with single- and dual-phase Tc-99m-Sestamibi parathyroid scintigraphy, *J. Nucl. Med.* **48** (2007) 1084–1089.
- [8.100] MITCHELL, B.K., et al., Mechanism of technetium 99m sestamibi parathyroid imaging and the possible role of p-glycoprotein, *Surgery* **120** (1996) 1039–1045.
- [8.101] CHUDZINSKI, W., et al., P-glycoprotein expression influences the result of Tc-99m-MIBI scintigraphy in tertiary hyperparathyroidism, *Int. J. Mol. Med.* **16** (2005) 215–219.
- [8.102] RUBELLA, D., MARIANI, G., PELIZZO, M.R., GISCRIS, A., Minimally invasive radio-guided parathyroidectomy on a group of 452 primary hyperparathyroid patients — Refinement of preoperative imaging and intraoperative procedure, *Nuklearmedizin* **46** (2007) 85–92.
- [8.103] RUBOW, S.M., ELLMANN, A., LEROUX, J., KLOPPER, J., Excretion of Tc-99m hexakismethoxyisobutylisonitrile in milk, *Eur. J. Nucl. Med.* **18** (1991) 363–365.
- [8.104] BELHOCINE, T., SHAstry, A., DRIEDGER, A., URBAIN, J.L., Detection of Tc-99m-sestamibi uptake in brown adipose tissue with SPECT-CT, *Eur. J. Nucl. Med. Mol. Imaging* **34** (2007) 149–149.
- [8.105] LIU, S., Ether and crown ether-containing cationic Tc-99m complexes useful as radiopharmaceuticals for heart imaging, *Dalton Trans.* (2007) 1183–1193.

- [8.106] AK, Y., DEMIREL, G., GULBAS, Z., MDR1, MRP1 and LRP expression in patients with untreated acute leukaemia: Correlation with Tc-99m-MIBI bone marrow scintigraphy, *Nucl. Med. Commun.* **28** (2007) 541–546.
- [8.107] LAZAROWSKI, A., et al., 99mTechnetium-SESTAMIBI uptake in malignant lymphomas. Correlation with chemotherapy response, *Lymphat. Res. Biol.* (2006) 23–28.
- [8.108] PEER, F.I., PUI, M.H., MOSAM, A., RAE, W.I.D., Tc-99m-MIBI imaging of cutaneous AIDS-associated Kaposi's sarcoma, *Int. J. Dermatol.* **46** (2007) 166–171.
- [8.109] FONTI, R., et al., Functional imaging of multidrug resistant phenotype by Tc-99m-MIBI scan in patients with multiple myeloma, *Cancer Biother. Radiopharm.* **19** (2004) 165–170.
- [8.110] CHANG, C.S., YANG, S.S., YEH, H.Z., KAO, C.H., CHEN, G.H., Tc-99m MIBI liver imaging for hepatocellular carcinoma: Correlation with P-glycoprotein-multidrug-resistance gene expression, *Hepato-Gastroenterol.* **51** (2004) 211–214.
- [8.111] KUNISHIO, K., MORISAKI, K., MATSUMOTO, Y., NAGAO, S., NISHIYAMA, Y., Technetium-99m sestamibi single photon emission computed tomography findings correlated with P-glycoprotein expression, encoded by the multidrug resistance gene-1 messenger ribonucleic acid, in intracranial meningiomas, *Neurol. Med-Chir.* **43** (2003) 573–580.
- [8.112] KUNISHIO, K., OKADA, M., MATSUMOTO, Y., NAGAO, S., NISHIYAMA, Y., Technetium-99m sestamibi single photon emission computed tomography findings correlated with P-glycoprotein expression in pituitary adenoma, *J. Med. Invest.* (2006) 285–291.
- [8.113] KIM, S.J., BAE, Y.T., LEE, J.S., KIM, I.J., KIM, Y.K., Diagnostic performances of double-phase Tc-99m MIBI scintimammography in patients with indeterminate ultrasound findings: visual and quantitative analyses, *Ann. Nucl. Med.* **21** (2007) 145–150.
- [8.114] KIM, I.J., et al., Determination and prediction of P-glycoprotein and multidrug-resistance-related protein expression in breast cancer with double-phase technetium-99m sestamibi scintimammography - Visual and quantitative analyses, *Oncology* **70** (2006) 403–410.
- [8.115] SERGIEVA, S., TIMCHEVA, K.V., HADJILOV, N.D., 99mTc-MIBI scintigraphy as a functional method for the evaluation of multidrug resistance in breast cancer patients, *J. Buon.* (2006) 61–68.
- [8.116] GOMES, C.M., et al., Functional imaging of multidrug resistance in an orthotopic model of osteosarcoma using 99mTc-sestamibi, *Eur. J. Nucl. Med. Mol. Imaging* **34** (2007) 1793–1803.
- [8.117] LIU, Z.L., et al., Imaging recognition of inhibition of multidrug resistance in human breast cancer xenografts using Tc-99m-labeled sestamibi and tetrofosmin, *Nucl. Med. Biol.* **32** (2005) 573–583.
- [8.118] PICHLER, A., ZELCER, N., PRIOR, J.L., KUIL, A.J., PIWNICA-WORMS, D., In vivo RNA interference - Mediated ablation of MDR1 P-glycoprotein, *Clin. Cancer Res.* **11** (2005) 4487–4494.

- [8.119] JEKERLE, V., et al.,  $^{99m}\text{Tc}$ -Sestamibi, a sensitive probe for in vivo imaging of p-glycoprotein inhibition by modulators and mdr1 antisense oligodeoxynucleotides, *Mol. Imaging Biol.* **8** (2006) 333–339.
- [8.120] KINUYA, S., et al., Tc-99m-sestamibi to monitor treatment with antisense oligodeoxynucleotide complementary to MRP mRNA in human breast cancer cells, *Ann. Nucl. Med.* **20** (2006) 29–34.
- [8.121] MARIAN, T., et al., Biphasic accumulation kinetics of [ $\text{Tc-99m}$ ]-hexakis-2-methoxyisobutyl isonitrile in tumour cells and its modulation by lipophilic P-glycoprotein ligands, *Eur. J. Pharm. Sci.* **25** (2005) 201–209.
- [8.122] YAPAR, Z., et al., The value of  $\text{Tc-99m}$ -tetrofosmin scintigraphy in the assessment of P-glycoprotein in patients with malignant bone and soft-tissue tumors, *Ann. Nucl. Med.* **17** (2003) 443–449.
- [8.123] KINUYA, S., et al., Limitations of  $\text{Tc-99m}$  tetrofosmin in assessing reversal effects of verapamil on the function of multi-drug resistance associated protein 1, *Nucl. Med. Commun.* **25** (2004) 585–589.
- [8.124] BALLINGER, J.R.,  $\text{Tc-99m}$ -tetrofosmin for functional imaging of P-glycoprotein modulation in vivo, *J. Clin. Pharmacol.* (2001) 39s–47s.
- [8.125] FUSTER, D., et al., Tetrofosmin as predictor of tumour response, *Q. J. Nucl. Med.* **47** (2003) 58–62.
- [8.126] LE JEUNE, N., PEREK, N., DENOYER, D., DUBOIS, F., Study of monoglutathionyl conjugates TC-99M-sestamibi and TC-99M-tetrofosmin transport mediated by the multidrug resistance-associated protein isoform 1 in glioma cells, *Cancer Biother. Radiopharm.* **20** (2005) 249–259.
- [8.127] NAKAMURA, K., KUBO, A., HNATOWICH, D.J., Antisense targeting of P-glycoprotein expression in tissue culture, *J. Nucl. Med.* **46** (2005) 509–513.
- [8.128] NAKAMURA, K., WANG, Y., LIU, X.R., KUBO, A., HNATOWICH, D.J., Influence of two transfectors on delivery of  $\text{Tc-99m}$  antisense DNA in tumor-bearing mice, *Mol. Imaging Biol.* **8** (2006) 188–192.
- [8.129] LABIALLE, S., et al., Gene therapy of the typical multidrug resistance phenotype of cancers: A new hope? *Semin. Oncol.* **32** (2005) 583–590.
- [8.130] EUROPEAN MOLECULAR IMAGING LABORATORIES, Centers of Excellence, <http://www.emilnet.org/scripts/home/publigen/content/templates/show.asp?P=203&L=EN&SYNC=Y>
- [8.131] DOMINGOS, P.M., STELLER, H., Pathways regulating apoptosis during patterning and development, *Curr. Opin. Genet. Dev.* **17** (2007) 294–299.
- [8.132] KARUNAGARAN, D., JOSEPH, J., KUMAR, T.R.S., Cell growth regulation, *Adv. Exp. Med. Biol.* **595** (2007) 245–268.
- [8.133] ELMORE, S., Apoptosis: A review of programmed cell death, *Toxicol. Pathol.* **35** (2007) 495–516.
- [8.134] CHAO, D.T., KORSMEYER, S.J., BCL-2 FAMILY: Regulators of cell death, *Annu. Rev. Immunol.* **16** (1998) 395–419.
- [8.135] VAUX, D.L., CORY, S., ADAMS, J.M., Bcl-2 gene promotes hematopoietic-cell survival and cooperates with C-Myc to immortalize pre-B-cells, *Nature* **335** (1988) 440–442.

- [8.136] DEL VECCHIO, S., et al., Dynamic coupling of Tc-99m-MIBI efflux and apoptotic pathway activation in untreated breast cancer patients, *Eur. J. Nucl. Mol. Imaging* **29** (2002) 809–814.
- [8.137] DEL VECCHIO, S., ZANNETTI, A., ALOJ, L., SALVATORE, M., MIBI as prognostic factor in breast cancer, *Q. J. Nucl. Med.* **47** (2003) 46–50.
- [8.138] DEL VECCHIO, S., et al., Inhibition of early Tc-99m-MIBI uptake by Bcl-2 anti-apoptotic protein overexpression in untreated breast carcinoma, *Eur. J. Nucl. Mol. Imaging* **30** (2003) 879–887.
- [8.139] ALOJ, L., ZANNETTI, A., CARACO, C., DEL VECCHIO, S., SALVATORE, M., Bcl-2 overexpression prevents Tc-99m-MIBI uptake in breast cancer cell lines, *Eur. J. Nucl. Mol. Imaging* **31** (2004) 521–527.
- [8.140] WAKASUGI, S., et al., A case of malignant pheochromocytoma with early intense uptake and immediate rapid washout of Tc-99m-tetrofosmin characterizing the overexpression of anti-apoptotic Bcl-2, *Ann. Nucl. Med.* **20** (2006) 325–328.
- [8.141] MORETTI, J.L., HAUET, N., CAGLAR, M., REBILLARD, O., BURAK, Z., To use MIBI or not to use MIBI? That is the question when assessing tumour cells, *Eur. J. Nucl. Mol. Imaging* **32** (2005) 836–842.
- [8.142] MOSS, S.E., MORGAN, R.O., The annexins, *Genome Biol.* **5** (2004) 219.
- [8.143] GERKE, V., MOSS, S.E., Annexins: From structure to function, *Physiol. Rev.* **82** (2002) 331–371.
- [8.144] HIRT, U.A., LEIST, M., Rapid, noninflammatory and PS-dependent phagocytic clearance of necrotic cells, *Cell Death Differ.* **10** (2003) 1156–1164.
- [8.145] VERMES, I., HAANEN, C., STEFFENSNAKKEN, H., REUTELINGSPERGER, C., A novel assay for apoptosis - Flow cytometric detection of phosphatidylserine expression on early apoptotic cells using fluorescein-labeled annexin-V, *J. Immunol. Methods* **184** (1995) 39–51.
- [8.146] GAIPL, U.S., et al., Modulation of the immune system by dying cells and the phosphatidylserine-ligand annexin A5, *Autoimmunity* **40** (2007) 254–259.
- [8.147] BLANKENBERG, F.G., et al., In vivo detection and imaging of phosphatidylserine expression during programmed cell death, *Proc. Natl. Acad. Sci. USA* **95** (1998) 6349–6354.
- [8.148] BLANKENBERG, F.G., VANDERHEYDEN, J.L., STRAUSS, H.W., TAIT, J.F., Radiolabeling of HYNIC-annexin V with technetium-99m for in vivo imaging of apoptosis, *Nature Protoc.* **1** (2006) 108–110.
- [8.149] OHTSUKI, K., et al., Technetium-99m HYNIC-annexin V: a potential radiopharmaceutical for the in-vivo detection of apoptosis, *Eur. J. Nucl. Med.* **26** (1999) 1251–1258.
- [8.150] MOCHIZUKI, T., et al., Detection of apoptotic tumor response in vivo after a single dose of chemotherapy with Tc-99m-annexin V, *J. Nucl. Med.* **44** (2003) 92–97.
- [8.151] KUGE, Y., et al., Feasibility of Tc-99m-annexin V for repetitive detection of apoptotic tumor response to chemotherapy: An experimental study using a rat tumor model, *J. Nucl. Med.* **45** (2004) 309–312.

- [8.152] TAKI, J., et al., Effect of postconditioning on myocardial Tc-99m-annexin-V uptake: Comparison with ischemic preconditioning and caspase inhibitor treatment, *J. Nucl. Med.* **48** (2007) 1301–1307.
- [8.153] VANDERHEYDEN, J.L., et al., Evaluation of Tc-99m-MAG(3)-annexin V: influence of the chelate on in vitro and in vivo properties in mice, *Nucl. Med. Biol.* **33** (2006) 135–144.
- [8.154] TAIT, J.F., SMITH, C., BLANKENBERG, F.G., Structural requirements for in vivo detection of cell death with Tc-99m-annexin V, *J. Nucl. Med.* **46** (2005) 807–815.
- [8.155] MUKHERJEE, A., et al., Tc-99m-labeled annexin V fragments: a potential SPECT radiopharmaceutical for imaging cell death, *Nucl. Med. Biol.* **33** (2006) 635–643.
- [8.156] KARTACHOVA, M., et al., Prognostic significance of Tc-99m Hynic-rh-annexin V scintigraphy during platinum-based chemotherapy in advanced lung cancer, *J. Clin. Oncol.* **25** (2007) 2534–2539.
- [8.157] CROFFORD, L.J., COX-1 and COX-2 tissue expression: Implications and predictions, *J. Rheumatol.* **24** (1997) 15–19.
- [8.158] BALLIF, B.A., MINCEK, N.V., BARRATT, J.T., WILSON, M.L., SIMMONS, D.L., Interaction of cyclooxygenases with an apoptosis- and autoimmunity-associated protein, *Proc. Natl. Acad. Sci. USA* **93** (1996) 5544–5549.
- [8.159] HARA, A., YOSHIMI, N., NIWA, M., INO, N., MORI, H., Apoptosis induced by NS-398, a selective cyclooxygenase-2 inhibitor, in human colorectal cancer cell lines, *Jpn. J. Cancer Res.* **88** (1997) 600–604.
- [8.160] HERSCHEMAN, H.R., TALLEY, J.J., DUBOIS, R., Cyclooxygenase 2 (COX-2) as a target for therapy and noninvasive imaging, *Mol. Imaging Biol.* (2003) 286–303.
- [8.161] YANG, D.J., et al., Assessment of cyclooxygenase-2 expression with Tc-99m-labeled celebrex, *Anticancer Drugs* **15** (2004) 255–263.
- [8.162] BAKKER, W.H., et al., [In-111-Dtpa-D-Phe1]-octreotide, a potential radiopharmaceutical for imaging of somatostatin receptor-positive tumors – synthesis, radiolabeling and in vitro validation, *Life Sci.* **49** (1991) 1583–1591.
- [8.163] PEARSON, D.A., et al., Somatostatin receptor-binding peptides labeled with technetium-99m: Chemistry and initial biological studies, *J. Med. Chem.* **39** (1996) 1361–1371.
- [8.164] VALLABHAJOSULA, S., et al., Preclinical evaluation of technetium-99m-labeled somatostatin receptor-binding peptides, *J. Nucl. Med.* **37** (1996) 1016–1022.
- [8.165] DECRISTOFORO, C., MATHER, S.J., Technetium-99m somatostatin analogues: effect of labelling methods and peptide sequence, *Eur. J. Nucl. Med.* **26** (1999) 869–876.
- [8.166] BANGARD, M., et al., Detection of somatostatin receptor-positive tumours using the new Tc-99m-tricine-HYNIC-D-Phe(1)-Tyr(3)-octreotide: first results in patients and comparison with In-111-DTPA-D-Phe(1)-octreotide, *Eur. J. Nucl. Med.* **27** (2000) 628–637.
- [8.167] DECRISTOFORO, C., MELENDEZ-ALAFORT, L., SOSABOWSKI, J.K., MATHER, S.J., Tc-99m-HYNIC-[Tyr(3)]-octreotide for imaging somatostatin-receptor-positive tumors: Preclinical evaluation and comparison with In-111-octreotide, *J. Nucl. Med.* **41** (2000) 1114–1119.

- [8.168] LISTER-JAMES, J., MOYER, B.R., DEAN T., Small peptides radiolabeled with  $^{99m}\text{Tc}$ , *Q. J. Nucl. Med.* (1996) 221–233.
- [8.169] VIRGOLINI, I., et al., Somatostatin receptor subtype specificity and in vivo binding of a novel tumor tracer,  $\text{Tc-99m-P829}$ , *Cancer Res.* **58** (1998) 1850–1859.
- [8.170] VAN DEN BOOSCHE, B., et al., Oestrogen-mediated regulation of somatostatin receptor expression in human breast cancer cell lines assessed with  $\text{Tc-99m}$ -depreotide, *Eur. J. Nucl. Med. Mol. Imaging* **31** (2004) 1022–1030.
- [8.171] FERRAN, N., et al., Characterization of radiologically indeterminate lung lesions:  $\text{Tc-99m}$ -depreotide SPECT versus F-18-FDG PET, *Nucl. Med. Commun.* **27** (2006) 507–514.
- [8.172] CZEPCZYNSKI, R., et al., Somatostatin receptor scintigraphy using  $\text{Tc-99m-EDDA/HYNIC-TOC}$  in patients with medullary thyroid carcinoma, *Eur. J. Nucl. Med. Mol. Imaging* **34** (2007) 1635–1645.
- [8.173] CHO, Y.S., LEE, K.H., Targeted in vivo imaging of angiogenesis: Present status and perspectives, *Curr. Pharm. Design* **13** (2007) 17–31.
- [8.174] BROOKS, P.C., CLARK, R.A.F., CHERESH, D.A., Requirement of vascular integrin alpha(V)beta(3) for angiogenesis, *Science* **264** (1994) 569–571.
- [8.175] FOLKMAN, J., Angiogenesis in cancer, vascular, rheumatoid and other disease, *Nature Med.* **1** (1995) 27–31.
- [8.176] KOIVUNEN, E., WANG, B.C., RUOSLAHTI, E., Phage libraries displaying cyclic-peptides with different ring sizes - Ligand specificities of the Rgd-directed integrins, *Biotechnology (NY)* **13** (1995) 265–270.
- [8.177] OCAK, I., BALUK, P., BARRETT, T., MCDONALD, D.M., CHOYKE, P., The biologic basis of in vivo angiogenesis imaging, *Front Biosci.* **12** (2007) 3601–3616.
- [8.178] MEYER, A., AUEMHEIMER, J., MODLINGER, A., KESSLER, H., Targeting RGD recognizing integrins: Drug development, biomaterial research, tumor imaging and targeting, *Curr. Pharm. Design* **12** (2006) 2723–2747.
- [8.179] LIM, E.H., DANTHI, N., BEDNARSKI, M., LI, K.C., A review: Integrin alphavbeta3-targeted molecular imaging and therapy in angiogenesis, *Nanomedicine* (2005) 110–114.
- [8.180] TEMMING, K., SCHIFFELERS, R.M., MOLEMA, G., KOK, R.J., RGD-based strategies for selective delivery of therapeutics and imaging agents to the tumour vasculature, *Drug Resist. Update* **8** (2005) 381–402.
- [8.181] ARAP, W., PASQUALINI, R., RUOSLAHTI, E., Cancer treatment by targeted drug delivery to tumor vasculature in a mouse model, *Science* **279** (1998) 377–380.
- [8.182] HAUBNER, R., WESTER, H.J., WEBER, W.A., SCHWAIGER, M., Radiotracer-based strategies to image angiogenesis, *Q. J. Nucl. Med.* **47** (2003) 189–199.
- [8.183] HAUBNER, R., Alpha(v)beta(3)-integrin imaging: a new approach to characterise angiogenesis? *Eur. J. Nucl. Med. Mol. Imaging* **33** (2006) S54–S63.
- [8.184] JANSSEN, M.L., et al., Tumor targeting with radiolabeled alpha(v)beta(3) integrin binding peptides in a nude mouse model, *Cancer Res.* **62** (2002) 6146–6151.
- [8.185] LEE, K.H., et al., Radiolabeled RGD uptake and alpha(v) integrin expression is enhanced in ischemic murine hindlimbs, *J. Nucl. Med.* **46** (2005) 472–478.

- [8.186] HUA, J., et al., Noninvasive imaging of angiogenesis with a Tc-99m-labeled peptide targeted at alpha(v)beta(3) integrin after murine hindlimb ischemia, *Circulation* **111** (2005) 3255–3260.
- [8.187] HAUBNER, R., et al., Synthesis and biological evaluation of a Tc-99m-labelled cyclic RGD peptide for imaging the alpha v beta 3 expression, *Nuklearmedizin* **43** (2004) 26–32.
- [8.188] JIA, B., et al., Tc-99m-labeled cyclic RGDFK dimer: Initial evaluation for SPECT imaging of glioma integrin alpha(v)beta(3) expression, *Bioconjug. Chem.* **17** (2006) 1069–1076.
- [8.189] ALVES, S., et al., In vitro and in vivo evaluation of a novel Tc-99m(CO)(3)-pyrazolyl conjugate of cyclo-(Arg-Gly-Asp-D-Tyr-Lys), *Bioconjug. Chem.* **18** (2007) 530–537.
- [8.190] JANSSEN, M., et al., Comparison of a monomeric and dimeric radiolabeled RGD-peptide for tumor targeting, *Cancer Biother. Radiopharm.* **17** (2002) 641–646.
- [8.191] LIU, S., et al., Evaluation of a Tc-99m-labeled cyclic RGD tetramer for noninvasive imaging integrin alpha(v)beta(3)-positive breast cancer, *Bioconjug. Chem.* **18** (2007) 438–446.
- [8.192] MITRA, A., et al., Targeting tumor angiogenic vasculature using polymer-RGD conjugates, *J. Control. Release* **102** (2005) 191–201.
- [8.193] JUNG, K.H., et al., Favorable biokinetic and tumor-targeting properties of Tc-99m-labeled glucosamino RGD and effect of paclitaxel therapy, *J. Nucl. Med.* **47** (2006) 2000–2007.
- [8.194] DECRISTOFORO, C., et al., [99mTc]HYNIC-RGD for imaging integrin alpha(v)beta(3) expression, *Nucl. Med. Biol.* **33** (2006) 945–952.
- [8.195] ZHANG, X.Z., CHEN, X.Y., Preparation and characterization of Tc-99m(CO)(3)-BPy-RGD complex as alpha(v)beta(3) integrin receptor-targeted imaging agent, *Appl. Radiat. Isotop.* **65** (2007) 70–78.
- [8.196] FANI, M., et al., Comparative evaluation of linear and cyclic Tc-99m-RGD peptides for targeting of integrins in tumor angiogenesis, *Anticancer Res.* **26** (2006) 431–434.
- [8.197] DECRISTOFORO, C., et al., Comparison of in vitro and in vivo properties of [Tc-99m]cRGD peptides labeled using different novel Tc-cores, *Q. J. Nucl. Med. Mol. Imaging* **51** (2007) 33–41.
- [8.198] DEWANJEE, M.K., HAIDER, N., NARULA, J., Imaging with radiolabeled antisense oligonucleotides for the detection of intracellular messenger RNA and cardiovascular disease, *J. Nucl. Cardiol.* **6** (1999) 345–356.
- [8.199] DUATTI, A., In vivo imaging of oligonucleotides with nuclear tomography, *Curr. Drug Targets* **5** (2004) 753–760.
- [8.200] HNATOWICH, D.J., NAKAMURA, K., Antisense targeting in cell culture with radiolabeled DNAs - a brief review of recent progress, *Ann. Nucl. Med.* **18** (2004) 363–368.
- [8.201] HNATOWICH, D.J., et al., Tc-99m labeling of DNA oligonucleotides, *J. Nucl. Med.* **36** (1995) 2306–2314.
- [8.202] WINNARD, P., CHANG, F., RUSCKOWSKI, M., MARDIROSSIAN, G., HNATOWICH, D.J., Preparation and use of NHS-MAG(3) for technetium-99m labeling of DNA, *Nucl. Med. Biol.* **24** (1997) 425–432.

- [8.203] MARDIROSSIAN, G., et al., In vivo hybridization of technetium-99m-labeled peptide nucleic acid (PNA), *J. Nucl. Med.* **37** (1996) 924–924.
- [8.204] ZHANG, Y.M., et al., Initial observations of Tc-99m labelled locked nuclear acids for antisense targeting, *Nucl. Med. Commun.* **25** (2004) 1113–1118.
- [8.205] LIU, G.Z., et al., Pretargeting in tumored mice with radiolabeled morpholino oligomer showing low kidney uptake, *Eur. J. Nucl. Med. Mol. Imaging* **31** (2004) 417–424.
- [8.206] HE, J., LIU, G.Z., ZHANG, S.R., RUSCKOWSKI, M., HNATOWICH, D.J., Pharmacokinetics in mice of four oligomer-conjugated polymers for amplification targeting, *Cancer Biother. Radiopharm.* **18** (2003) 941–947.
- [8.207] LIU, C.B., et al., Radiolabeling morpholinos with Y-90, In-111, Re-188 and Tc-99m, *Nucl. Med. Biol.* **30** (2003) 207–214.
- [8.208] MANG'ERA, K.O., et al., Initial investigations of Tc-99m-labeled morpholinos for radiopharmaceutical applications, *Eur. J. Nucl. Med.* **28** (2001) 1682–1689.
- [8.209] ZHANG, Y.M., RUSCKOWSKI, M., LIU, N., LIU, C.B., HNATOWICH, D.J., Cationic liposomes enhance cellular/nuclear localization of Tc-99m-antisense oligonucleotides in target tumor cells, *Cancer Biother. Radiopharm.* **16** (2001) 411–419.
- [8.210] ZHANG, Y.M., LIU, N., ZHU, Z.H., RUSCKOWSKI, M., HNATOWICH, D.J., Influence of different chelators (HYNIC, MAG(3) and DTPA) on tumor cell accumulation and mouse biodistribution of technetium-99m labeled to antisense DNA, *Eur. J. Nucl. Med.* **27** (2000) 1700–1707.
- [8.211] BRITZ-CUNNINGHAM, S.H., ADELSTEIN, S.J., Molecular targeting with radionuclides: State of the science, *J. Nucl. Med.* **44** (2003) 1945–1961.
- [8.212] QIN, G.M., et al., Molecular imaging of atherosclerotic plaques with technetium-99m-labelled antisense oligonucleotides, *Eur. J. Nucl. Med. Mol. Imaging* **32** (2005) 6–14.
- [8.213] PUN, S.H., et al., Targeted delivery of RNA-cleaving DNA enzyme (DNAzyme) to tumor tissue by transferrin-modified, cyclodextrin-based particles, *Cancer Biol. Ther.* **3** (2004) 641–650.
- [8.214] GUTHRIE, J.W., RYU, J.H., LE, X.C., WIEBE, L.I., Characterization of a cyclodextrin-oligonucleotide complex by capillary electrophoresis using laser-induced fluorescence, *J. Pharm. Pharmaceut. Sci.* **10** (2007) 246–255.
- [8.215] ZHENG, J.G., TAN, T.Z., Antisense imaging of colon cancer-bearing nude mice with liposome-entrapped 99m-technetium-labeled antisense oligonucleotides of c-myc mRNA, *World J. Gastroenterol.* (2004) 2563–2566.
- [8.216] ZHANG, Y.M., et al., Electrostatic binding with tat and other cationic peptides increases cell accumulation of 99mTc-antisense DNAs without entrapment, *Mol. Imaging Biol.* (2003) 240–247.
- [8.217] HNATOWICH, D.J., et al., Comparative properties of a Technetium-99m-labeled single-stranded natural DNA and a phosphorothioate derivative in vitro and in mice, *J. Pharmacol Exp. Ther.* **276** (1996) 326–334.
- [8.218] WANG, Y., et al., Nonspecific cellular accumulation of Tc-99m-labeled oligonucleotides in culture is influenced by their guanine content, *Nucl. Med. Biol.* **34** (2007) 47–54.

- [8.219] LIU, G., et al., Investigations of Tc-99m morpholino pretargeting in mice, *Nucl. Med. Commun.* **24** (2003) 697–705.
- [8.220] LIU, G., et al., The influence of chain length and base sequence on the pharmacokinetic behavior of Tc-99m-morpholinos in mice, *Q. J. Nucl. Med.* **46** (2002) 233–243.
- [8.221] LIU, G.Z., et al., Tumor pretargeting in mice using Tc-99m-labeled morpholino, a DNA analog, *J. Nucl. Med.* **43** (2002) 384–391.
- [8.222] HE, J., et al., A comparison of in vitro and in vivo stability in mice of two morpholino duplexes differing in chain length, *Bioconjug. Chem.* **14** (2003) 1018–1023.
- [8.223] LIU, X.R., et al., Improved delivery in cell culture of radiolabeled antisense DNAs by duplex formation, *Mol. Imaging Biol.* **8** (2006) 278–283.
- [8.224] DEWANJEE, M.K., et al., Noninvasive imaging of c-myc oncogene messenger-RNA with indium-111-antisense probes in a mammary tumor-bearing mouse model, *J. Nucl. Med.* **35** (1994) 1054–1063.
- [8.225] RAO, P.S., et al., 99(m)Tc-peptide-peptide nucleic acid probes for imaging oncogene mRNAs in tumours, *Nucl. Med. Commun.* **24** (2003) 857–863.
- [8.226] TIAN, X.B., et al., External imaging of CCND1 cancer gene activity in experimental human breast cancer xenografts with Tc-99m-peptide-peptide nucleic acid-peptide chimeras, *J. Nucl. Med.* **45** (2004) 2070–2082.
- [8.227] HUI, R., et al., Cyclin D1 and estrogen receptor messenger RNA levels are positively correlated in primary breast cancer, *Clin. Cancer Res.* **2** (1996) 923–928.
- [8.228] CHAKRABARTI, A., ARUVA, M.R., SAJANKILA, S.P., THAKUR, M.L., WICKSTROM, E., Synthesis of novel peptide nucleic acid-peptide chimera for non-invasive imaging of cancer, *Nucleos. Nucleot. Nucl.* **24** (2005) 409–414.
- [8.229] WICKSTROM, E., THAKUR, M.L., Imaging cancer gene activity in patients from outside the body, *Biotech. Healthcare* (2006) 45–48.
- [8.230] WANG, Y., et al., Pretargeting with amplification using polymeric peptide nucleic acid, *Bioconjug. Chem.* **12** (2001) 807–816.
- [8.231] HE, J., et al., An improved method for covalently conjugating morpholino oligomers to antitumor antibodies, *Bioconjug. Chem.* **18** (2007) 983–988.
- [8.232] LIU, G.Z., et al., Predicting the biodistribution of radiolabeled cMORF effector in MORF-pretargeted mice, *Eur. J. Nucl. Med. Mol. Imaging* **34** (2007) 237–246.
- [8.233] IRESON, C.R., KELLAND, L.R., Discovery and development of anticancer aptamers, *Mol. Cancer Ther.* **5** (2006) 2957–2962.
- [8.234] PROSKE, D., BLANK, M., BUHMANN, R., RESCH, A., Aptamers - basic research, drug development, and clinical applications, *Appl. Microbiol. Biotechnol.* **69** (2005) 367–374.
- [8.235] NIMJEE, S.M., RUSCONI, C.P., SULLENGER, B.A., Aptamers: An emerging class of therapeutics, *Annu. Rev. Med.* **56** (2005) 555–583.
- [8.236] DOUGAN, H., HOBBS, J.B., WEITZ, J.I., LYSTER, D.M., Synthesis and radioiodination of a stannyloligodeoxyribonucleotide, *Nucleic Acids Res.* **25** (1997) 2897–2901.
- [8.237] DOUGAN, H., et al., Extending the lifetime of anticoagulant oligo-deoxynucleotide aptamers in blood, *Nucl. Med. Biol.* **27** (2000) 289–297.

- [8.238] DOUGAN, H., et al., Evaluation of DNA aptamers directed to thrombin as potential thrombus imaging agents, *Nucl. Med. Biol.* **30** (2003) 61–72.
- [8.239] HICKE, B.J., et al., Tumor targeting by an aptamer, *J. Nucl. Med.* **47** (2006) 668–678.

## BIBLIOGRAPHY

- CHANG, X.B., A molecular understanding of ATP-dependent solute transport by multidrug resistance-associated protein MRP1, *Cancer Metastasis Rev.* **26** (2007) 15–37.
- DRONAMRAJU, K.R., Erwin Schrödinger and the origins of molecular biology, *Genetics* **153** (1999) 1071–1076.
- FRIEDMANN, T., A brief history of gene therapy, *Nature Genet.* **2** (1992) 93–98.
- GLUNDE, K., PATHAK, A.P., BHUJWALLA, Z.M., Molecular-functional imaging of cancer: to image and imagine, *Trends Mol. Med.* **13** (2007) 287–297.
- QUE-GEWIRTH, N.S., SULLENGER, B.A., Gene therapy progress and prospects: RNA aptamers, *Gene Ther.* **14** (2007) 283–291.
- ROME, C., COUILAUD, F., MOONEN, C.T., Gene expression and gene therapy imaging, *Eur. Radiol.* **17** (2007) 305–319.
- SCHELLINGERHOUT, D., Molecular imaging of novel cell- and viral-based therapies, *Neuroimaging Clin. N. Am.* **16** (2006) 55–679.
- SPRINGER, C.J., Suicide Gene Therapy, Methods in Molecular Medicine Series, Methods and Reviews, Humana Press, New Jersey (2004).
- WOLFF, J.A., LEDERBERG, J., An early history of gene transfer and therapy, *Human Gene Ther.* **5** (1994) 469–480.

## Chapter 9

# TECHNETIUM-99m LABELLED RGD PEPTIDES AS INTEGRIN $\alpha_v\beta_3$ -TARGETED RADIOTRACERS FOR TUMOUR IMAGING

S. LIU

School of Health Sciences, Purdue University,  
West Lafayette, Indiana  
United States of America

### Abstract

Integrin  $\alpha_v\beta_3$  plays a significant role in tumour angiogenesis, and is a receptor for the extracellular matrix proteins with the exposed arginine-glycine-aspartic acid (RGD) tripeptide sequence. Integrin  $\alpha_v\beta_3$  is normally expressed at low levels on epithelial cells and mature endothelial cells; but it is overexpressed on the activated endothelial cells of tumour neovasculature and some tumour cells. The highly restricted expression of integrin  $\alpha_v\beta_3$  presents an interesting molecular target for early detection and treatment of rapidly growing tumours. Over the last decade, significant progress has been made on the use of radiolabelled RGD peptides for imaging tumours by single photon emission computed tomography (SPECT) or positron emission tomography (PET). Fluorine-18-galacto-RGD is under clinical investigation as an  $\alpha_v\beta_3$ -targeted radiotracer for non-invasive visualization of integrin  $\alpha_v\beta_3$  in cancer patients. The chapter focuses on  $^{99m}\text{Tc}$  labelled RGD peptides as SPECT radiotracers to image tumour integrin  $\alpha_v\beta_3$  expression. Technetium-99m is of particular importance due to its optimal nuclear properties and its ready availability at low cost. Despite wide availability of PET isotopes (such as  $^{18}\text{F}$ ,  $^{62/64}\text{Cu}$  and  $^{68}\text{Ga}$ ) in Western countries,  $^{99m}\text{Tc}$  remains the radionuclide of choice for diagnostic radiotracers in most developing countries.

### 9.1. INTRODUCTION

Tumours produce many angiogenic factors, which are able to activate endothelial cells in the established blood vessels and induce endothelial proliferation, migration and new vessel formation (angiogenesis). Angiogenesis is a requirement for tumour growth and metastasis [9.1–9.5]. Without the formation of neovasculature to provide oxygen and nutrients, tumours cannot grow beyond 1–2 mm in size. The angiogenic process is regulated by cell adhesion receptors. Integrins are such a family of proteins that facilitate cellular adhesion to and migration on the extracellular matrix proteins found in intercellular spaces and basement membranes, and regulate cellular entry and exit from the cell cycle [9.5–9.8]. Integrin  $\alpha_v\beta_3$  serves as a receptor for extracellular

matrix proteins, including vitronectin, fibronectin, fibrinogen, lamin, collagen, Von Willibrand's factor, osteoponin and adenovirus particles, with the exposed arginine-glycine-aspartic acid (RGD) tripeptide sequence [9.6–9.11]. Integrin  $\alpha_v\beta_3$  is expressed at low levels on epithelial cells and mature endothelial cells; but is highly expressed on activated endothelial cells in the neovasculature of tumours, including osteosarcomas, neuroblastomas, glioblastomas, melanomas, lung carcinomas and breast cancer [9.12–9.18]. A recent study shows that the integrin  $\alpha_v\beta_3$  is overexpressed on both endothelial cells and tumour cells in human breast cancer xenografts [9.18]. Integrin  $\alpha_v\beta_3$  expression correlates well with tumour progression and invasiveness of melanoma, glioma, ovarian and breast cancers [9.8–9.18]. The highly restricted expression of integrin  $\alpha_v\beta_3$  during tumour growth, invasion and metastasis presents an interesting molecular target for early diagnosis of rapidly growing and metastatic tumours [9.19–9.26].

Over the last several years, a number of radiolabelled RGD peptides have been evaluated as integrin  $\alpha_v\beta_3$ -targeted radiotracers by single photon emission computed tomography (SPECT) or positron emission tomography (PET) in preclinical animal models and human clinical trials. Several review articles appeared recently, covering different aspects of integrin  $\alpha_v\beta_3$ -targeted radiotracers [9.19–9.26]. This chapter is not intended as an exhaustive review of current literature on radiolabelled RGD peptides. Instead, it focuses on  $^{99m}\text{Tc}$  labelled RGD peptides as SPECT radiotracers for imaging integrin  $\alpha_v\beta_3$  expression in tumours of different origin. Despite the wide availability of PET isotopes (such as  $^{18}\text{F}$ ,  $^{62/64}\text{Cu}$  and  $^{68}\text{Ga}$ ) in Western countries,  $^{99m}\text{Tc}$  remains the radionuclide of choice for development of diagnostic radiotracers in most developing countries.

## 9.2. RADIOPHARMACEUTICAL DESIGN

### 9.2.1. Radiotracer composition

In general, the integrin  $\alpha_v\beta_3$ -targeted radiopharmaceutical can be divided into four parts (Fig. 9.1): the RGD peptide as the targeting biomolecule, a PKM (pharmacokinetic modifying) linker, a bifunctional chelator (BFC) and the radionuclide. Technetium-99m is of particular importance due to its optimal nuclear properties (half-life = 6.02 h with 140 keV gamma photons) and its ready availability at low cost [9.27, 9.28]. The RGD peptide serves as a vehicle to carry  $^{99m}\text{Tc}$  to integrin  $\alpha_v\beta_3$  overexpressed on tumour cells and activated endothelial cells of tumour neovasculature. For successful  $^{99m}\text{Tc}$  labelling, a BFC is needed. An ideal BFC is able to form a stable  $^{99m}\text{Tc}$  complex in high yield at very low concentration of BFC–RGD conjugate. The PKM linkers are used for modifying

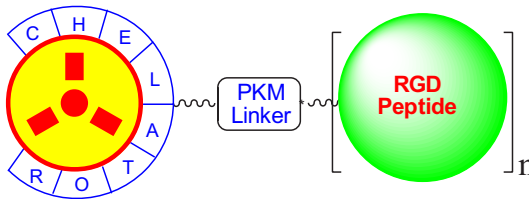


*FIG. 9.1. Schematic diagram of the integrin  $\alpha_v\beta_3$ -targeted  $^{99m}\text{Tc}$  radiopharmaceutical.*

the pharmacokinetics of the  $^{99m}\text{Tc}$  radiotracer. The choice of both BFC and PKM linker is critical for the successful development of a clinically useful integrin  $\alpha_v\beta_3$ -targeted  $^{99m}\text{Tc}$  radiotracer.

### 9.2.2. Clinical requirements

A successful integrin  $\alpha_v\beta_3$ -targeted  $^{99m}\text{Tc}$  radiotracer must show clinical indications for high incidence tumours (e.g. breast, colorectal and lung). The radiotracer should have high tumour uptake with a diagnostically useful target:background (T:B) ratio in a short period of time. To achieve this goal, the  $^{99m}\text{Tc}$  radiotracer should have fast clearance kinetics to minimize non-target radioactivity accumulation. The integrin  $\alpha_v\beta_3$  binding rate should be fast and its dissociation rate slow. In this way, radiotracer tumour uptake can be optimized. Since most high incidence tumours (namely lung, colorectal and breast cancers) occur in the torso, renal excretion is highly recommended to avoid accumulation of radioactivity in the liver and gastrointestinal tract, which may interfere with interpretation of tumour activity in chest and abdominal regions. The integrin  $\alpha_v\beta_3$ -targeted radiotracer should also be able to: (i) distinguish between benign and malignant tumours; (ii) follow the course of a particular tumour type and its response to anti-angiogenic therapy; and (iii) predict the success or failure of a specific therapeutic regimen for a given type of tumour in a particular cancer patient.

### 9.2.3. Advantages over other radiotracers

Most modalities currently available for tumour imaging rely on features of tumour cells (enhanced uptake of  $^{99m}\text{Tc}$ -Sestamibi due to the increased mitochondrial potential), their metabolic rate (basis for  $^{18}\text{FDG}$  PET imaging) or tumour cell specific receptors, such as the somatostatin receptor ( $^{111}\text{In}$ -DTPA-octreotide and  $^{99m}\text{Tc}$ -depreotide). Radiotracers targeting integrin  $\alpha_v\beta_3$  would be used not only for early tumour detection but also for staging the extent of the disease (local, regional or widespread) and monitoring the therapeutic response of a specific treatment regimen. These applications would take advantage of the

unique ability of nuclear medicine procedures to do simultaneous whole body imaging. Radiotracers targeting integrin  $\alpha_v\beta_3$  have direct contact with intravascular space, so that it is also possible for the radiotracer to avoid barriers associated with extravasation and penetration into tumour cells. The radiotracers targeting integrin  $\alpha_v\beta_3$  would be more specific for rapidly growing and metastatic tumours than those targeting tumour cell associated receptors.

#### 9.2.4. Selection of targeting biomolecules

The selection of a targeting biomolecule depends on its integrin  $\alpha_v\beta_3$  affinity and selectivity. In general, the targeting biomolecule should be an antagonist since the use of an agonist may cause unwanted side effects, even at low dose. It should have high affinity and selectivity for integrin  $\alpha_v\beta_3$  over glycoprotein IIb/IIIa. Many RGD peptide antagonists induce endothelial apoptosis [9.29] and inhibit angiogenesis of tumours [9.30–9.32]. Figure 9.2 shows examples of cyclic RGD peptides, such as EMD 121974, that have high affinity and selectivity for integrin  $\alpha_v\beta_3$ , with an  $IC_{50}$  in the nanomolar range [9.33–9.35]. These cyclic RGD peptides are early ‘lead’ compounds and have been successfully used as targeting biomolecules for the development of an integrin  $\alpha_v\beta_3$ -targeted  $^{99m}\text{Tc}$  radiotracer.

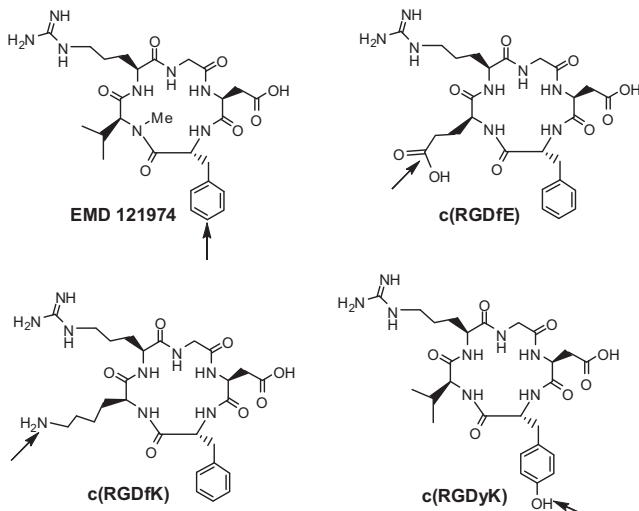


*FIG. 9.2. Cyclic RGD peptides useful as targeting biomolecules for integrin  $\alpha_v\beta_3$ -targeted radiotracers. Arrows indicate possible sites for attachment of the  $^{99m}\text{Tc}$  chelate.*

#### *9.2.4.1. Why small peptides?*

There are several advantages to using small RGD peptides. The RGD tripeptide sequences are natural binding units that are responsible for interactions between integrin  $\alpha_v\beta_3$  and extracellular matrix proteins, such as vitronectin and fibronectin. Small RGD peptides can tolerate harsh conditions for radiolabelling and chemical modification [9.22, 9.23, 9.26]. Unlike antibodies, they are less likely to be immunogenic. Due to their small size, the radiolabelled cyclic RGD peptides have rapid blood clearance. The faster blood clearance results in adequate T:B ratios earlier, so that it is practical to use  $^{99m}\text{Tc}$  for SPECT imaging.

#### *9.2.4.2. Why cyclic RGD peptides?*

A major challenge in designing integrin  $\alpha_v\beta_3$  antagonists is to improve integrin  $\alpha_v\beta_3$  binding affinity. In theory, targeting biomolecules can be linear or cyclic if they contain one or more RGD tripeptide sequences. The disadvantage of using linear RGD peptides is that they are often degraded rapidly in serum by proteases. The combination of low binding affinity ( $\text{IC}_{50} > 100 \text{ nM}$ ), lack of specificity (integrin  $\alpha_v\beta_3$  versus GPIIb/IIIa) and rapid degradation, makes them non-optimal for tumour imaging [9.22, 9.23, 9.26]. Cyclization of RGD peptides via linkers, such as S–S disulphide, thioether and rigid aromatic rings or heterocycles, often leads to increased integrin  $\alpha_v\beta_3$  binding affinity and selectivity [9.36, 9.37]. Although there is little evidence to show that any particular mode of cyclization will result in high affinity integrin  $\alpha_v\beta_3$  binding, it is clear that cyclic RGD peptides with a conformation at the receptor binding motif similar to that of the natural ligand are likely to have a higher integrin  $\alpha_v\beta_3$  binding affinity and better selectivity [9.33, 9.36, 9.37]. After extensive structure–activity relationship studies, it was found that incorporation of RGD into a cyclic pentapeptide framework (Fig. 9.2) significantly increases the binding affinity and selectivity for integrin  $\alpha_v\beta_3$  [9.36, 9.37]. The amino acid at position five has no significant impact on integrin  $\alpha_v\beta_3$  binding. For example, the valine residue in c(RGDFV) (Fig. 9.2) can be replaced by lysine (K) or glutamic acid (E) to afford c(RGDfK) and c(RGDfE), respectively, without changing their integrin  $\alpha_v\beta_3$  binding affinity.

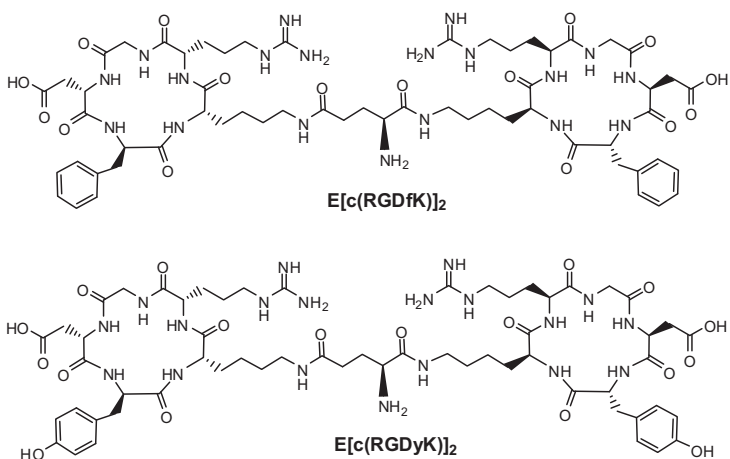


FIG. 9.3. Cyclic RGD peptide dimers:  $E[c(RGDfK)]_2$  and  $E[c(RGDyK)]_2$ .

#### 9.2.4.3. Multivalency concept

Since the natural mode of interactions between integrin  $\alpha_v\beta_3$  and RGD containing proteins may involve multiple binding sites, the idea to improve integrin  $\alpha_v\beta_3$  affinity with multivalent cyclic RGD peptides may provide more effective antagonists with better targeting capability and higher cellular uptake through the integrin dependent endocytosis pathway [9.38]. Multivalent interactions are used so that weak ligand–receptor interactions may become biologically relevant [9.39]. The multivalent concept was first used by Rajopadhye et al. to prepare cyclic RGD dimers, such as  $E[c(RGDfK)]_2$  (Fig. 9.3), for the development of diagnostic ( $^{99m}Tc$  and  $^{111}In$ ) and therapeutic ( $^{90}Y$  and  $^{177}Lu$ ) radiotracers [9.40–9.46]. Chen et al. [9.47, 9.48] reported the use of  $E[c(RGDyK)]_2$  (Fig. 9.3) for preparation of  $^{64}Cu$  and  $^{18}F$  based PET radiotracers. Poethko et al. [9.49–9.52] reported the  $^{18}F$  labelled RGDFE dimer (Fig. 9.4;  $[c(RGDfE)HEG]_2$ -K-Dpr-[ $^{18}F$ ]FBOA) and found that  $[c(RGDfE)HEG]_2$ -K-Dpr-[ $^{18}F$ ]FBOA had much higher integrin  $\alpha_v\beta_3$  binding affinity to the immobilized integrin  $\alpha_v\beta_3$  than its monomeric analogue,  $c(RGDfE)HEG$ -Dpr-[ $^{18}F$ ]FBOA.

The multivalent concept has been used to prepare cyclic RGD tetramers. For example, Boturyn et al. reported a series of cyclic RGDFK tetramers [9.38], and found that the increase of peptide multiplicity significantly enhances integrin  $\alpha_v\beta_3$  binding affinity and internalization in CHO3a (Chinese hamster ovary) in vitro assays. Kessler et al. [9.49–9.52] reported a cyclic RGDFE peptide tetramer (Fig. 9.4) that had better integrin  $\alpha_v\beta_3$  binding affinity than its monomeric and dimeric analogues. The minimum linker length was reported to

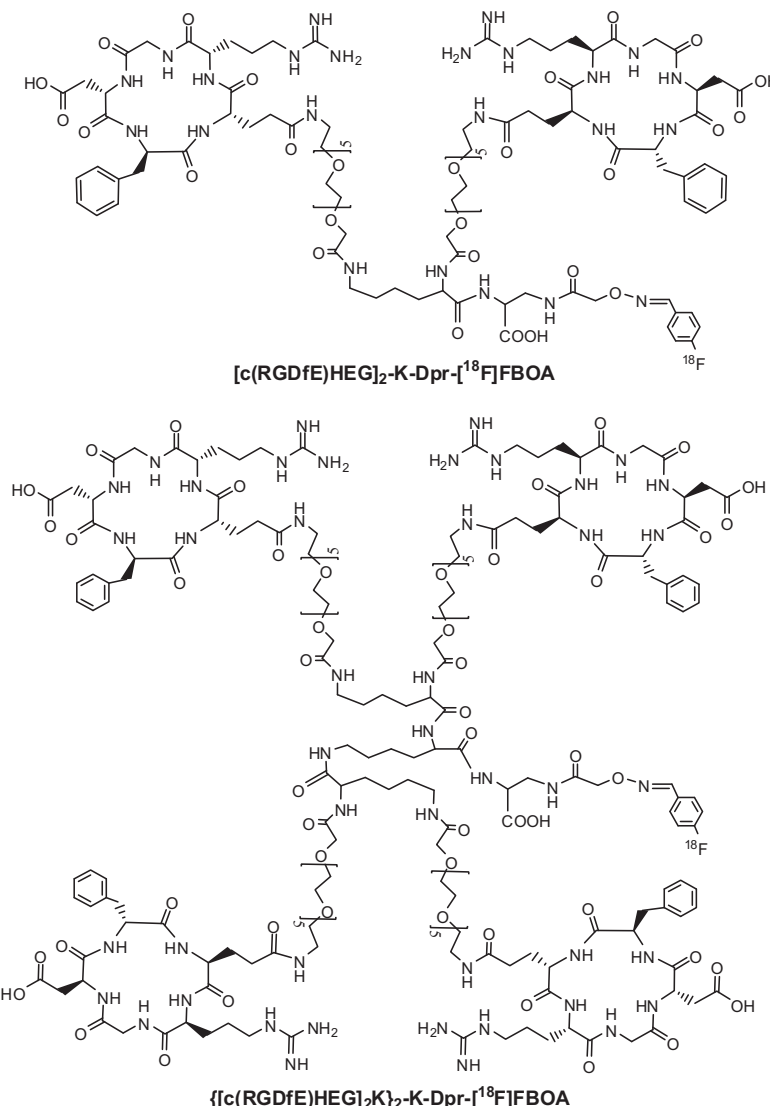


FIG. 9.4. Cyclic RGDfE peptide dimer ( $[c(RGDfE)HEG]_2\text{-K-Dpr-[}^{18}\text{F]FBOA}$ ) and tetramer ( $\{[c(RGDfE)HEG]_2\text{K}\}_2\text{-Dpr-[}^{18}\text{F]FBOA}$ ).

be ~25 bond distances for simultaneous binding of two c(RGDfE) motifs [9.49]. Liu et al. [9.53–9.55] used an RGDFK tetramer, E{E[c(RGDFK)]<sub>2</sub>}<sub>2</sub> (Fig. 9.5), to develop integrin  $\alpha_v\beta_3$ -targeted radiotracers for SPECT and PET imaging. It was found that the RGDFK tetramer E{E[c(RGDFK)]<sub>2</sub>}<sub>2</sub> has higher integrin  $\alpha_v\beta_3$  affinity ( $IC_{50} = 15.1 \pm 1.1$  nM) than the dimer analogue,

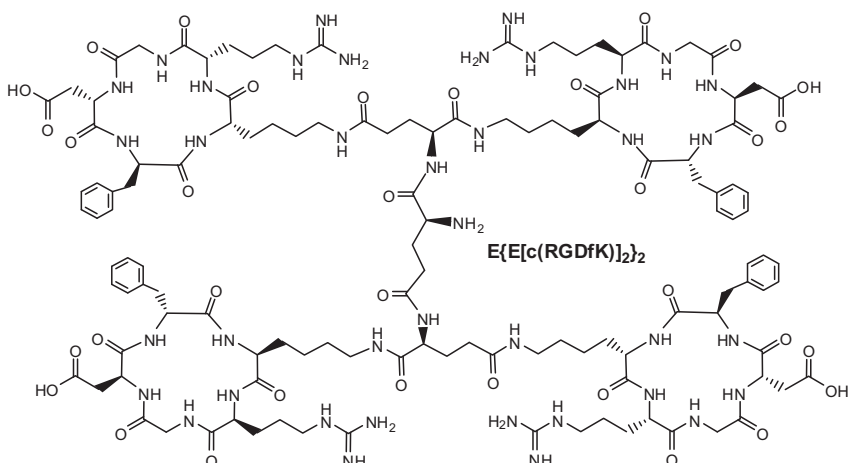


FIG. 9.5. Cyclic RGDfK tetramer  $E\{E[c(RGDfK)]_2\}_2$ .

$E[c(RGDfK)]_2$  ( $IC_{50} = 32.2 \pm 2.1$  nM), against the binding of  $^{125}\text{I}$ -echistatin to integrin  $\alpha_v\beta_3$ -positive U87MG human glioma cells [9.54]. The longest distance between two RGD motifs is  $\sim 30$  bond lengths, which is long enough for them to bind to adjacent integrin  $\alpha_v\beta_3$  receptors simultaneously. Results from biodistribution and imaging studies also showed that the use of  $E\{E[c(RGDfK)]_2\}_2$  enhances the tumour targeting capability of radiotracers ( $^{99\text{m}}\text{Tc}$ ,  $^{111}\text{In}$  and  $^{64}\text{Cu}$ ) [9.53–9.55].

The success of  $E[c(RGDfK)]_2$  and  $E[c(RGDyK)]_2$  (Fig. 9.3) as targeting biomolecules is intriguing. Given the short distance ( $\sim 20$  bond lengths) between two cyclic RGD peptides, it is unlikely that they would bind to adjacent integrin  $\alpha_v\beta_3$  simultaneously. However, binding of one RGD motif to integrin  $\alpha_v\beta_3$  will significantly increase the ‘local concentration’ of the second RGD motif in the vicinity of another integrin  $\alpha_v\beta_3$ , and lead to the enhanced integrin  $\alpha_v\beta_3$  binding rate or reduced dissociation rate of the cyclic RGD peptide from the integrin  $\alpha_v\beta_3$ . The high ‘local RGD peptide concentration’ may explain the higher tumour uptake and longer tumour retention times of the radiolabelled cyclic RGD dimers over their monomeric analogues [9.40–9.52].

### 9.2.5. Selection of bifunctional chelators

In general, the technetium core determines the design of BFCs and the choice of donor atoms. Different BFCs useful for  $^{99\text{m}}\text{Tc}$  labelling of biomolecules have been reviewed extensively [9.26–9.28, 9.56, 9.57]. Figure 9.6 shows examples of  $^{99\text{m}}\text{Tc}$  cores and BFCs that have successfully been used for

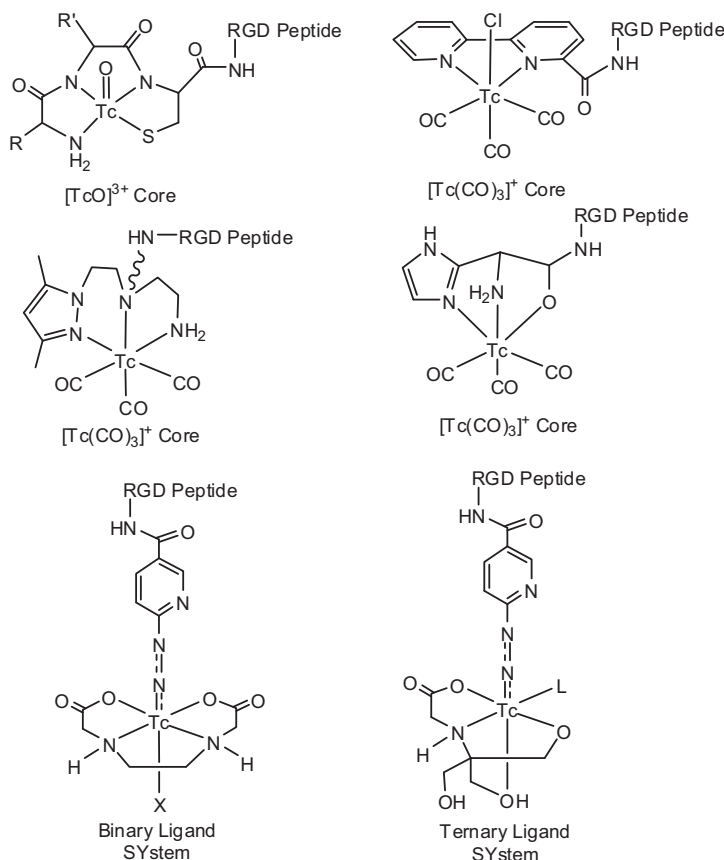


FIG. 9.6.  $^{99m}\text{Tc}$  cores and bifunctional chelating systems for  $^{99m}\text{Tc}$  labelling of RGD peptides.

$^{99m}\text{Tc}$  labelling of RGD peptides. The  $[\text{Tc}=\text{O}]^{3+}$  core is the most frequently used technetium core for  $^{99m}\text{Tc}$  labelling of biomolecules, and forms square pyramidal oxotechnetium complexes with tetradentate chelators, such as  $\text{N}_3\text{S}$  monoamindiamidethiols (Fig. 9.6). The  $^{99m}\text{Tc}(\text{CO})_3^+$  core has also been successfully used for  $^{99m}\text{Tc}$  labelling of RGD peptides [9.58–9.60]. Hynic (6-hydrazinonicotinamide) is of particular interest due to its high  $^{99m}\text{Tc}$  labelling efficiency (rapid and high yield radiolabelling), the high solution stability of its  $^{99m}\text{Tc}$  complexes and the easy use of coligands for modification of the biodistribution characteristics of  $^{99m}\text{Tc}$  labelled small biomolecules [9.61].

### **9.2.6. Selection of pharmacokinetic modifying linkers**

An important aspect for the successful development of integrin  $\alpha_v\beta_3$ -targeted radiotracers is to improve T:B ratios by modifying the excretion kinetics of radiolabelled cyclic RGD peptides with various PKM linkers, depending on the pharmacokinetic requirements. Many PKM linkers have been used to improve the excretion kinetics of radiolabelled cyclic RGD peptides. For example, a sugar moiety was used to increase tumour:liver ratios of  $^{125}\text{I}$  labelled and  $^{18}\text{F}$  labelled cyclic RGD peptides [9.62–9.65]. The di(cysteic acid) linker has been used to improve blood clearance and to minimize liver accumulation of radiolabelled integrin  $\alpha_v\beta_3$  non-peptide antagonists [9.66–9.69]. It has been reported that the introduction of the polyethylene glycol (PEG) linker can improve not only tumour uptake but also excretion kinetics of the  $^{125}\text{I}$  labelled and  $^{18}\text{F}$  labelled cyclic RGD monomer, c(RGDyK), and the  $^{64}\text{Cu}$  labelled cyclic RGD dimer, E[c(RGDyK)]<sub>2</sub> [9.70, 9.71]. PEG<sub>4</sub> and amino acid linkers, such as E and K, have also been used to improve excretion kinetics of  $^{111}\text{In}$  and  $^{99\text{m}}\text{Tc}$  labelled E[c(RGDfK)]<sub>2</sub> [9.72, 9.73]. The ultimate goal of using PKM linkers is to modify the radiotracer excretion kinetics so that its T:B ratios can be optimized by minimizing its uptake in non-tumour organs, while maintaining its high tumour uptake. Different PKM linkers and their applications to improve excretion kinetics of radiolabelled small biomolecules have been reviewed recently [9.23, 9.26–9.28, 9.56, 9.74].

## **9.3. TECHNETIUM-99m LABELLED RGD PEPTIDES AS RADIOTRACERS FOR IMAGING TUMOUR ANGIOGENESIS**

### **9.3.1. Linear RGD peptides**

A synthetic linear decapeptide  $\alpha\text{P2}$  (RGDSCRGDSY) has been radiolabelled with  $^{99\text{m}}\text{Tc}$  by ligand exchange with [ $^{99\text{m}}\text{Tc}$ ]glucoheptonate [75]. The linear peptide contains two RGD sequences for integrin  $\alpha_v\beta_3$  receptor binding. It was believed that the cysteine residue inserted in the primary structure is responsible for the  $^{99\text{m}}\text{Tc}$  binding. However, there is no structural information reported for the corresponding  $^{99\text{m}}\text{Tc}$  complex. In humans, six out of eight lymph node metastases (75%) and all other neoplastic sites (11 sites) were successfully imaged using the  $^{99\text{m}}\text{Tc}$  labelled peptide  $\alpha\text{P2}$ . The  $^{99\text{m}}\text{Tc}$  labelled  $\alpha\text{P2}$  also shows a rapid clearance from circulation via the renal system [9.75].

### 9.3.2. Cyclic RGD peptide monomers

Su et al. [9.76] recently reported the in vitro and in vivo evaluation of a  $^{99m}\text{Tc}$  labelled cyclic RGD peptide, RGD-4C, which contains four cysteine residues for cyclization. Hynic was used as the BFC and tricine as the coligand for the  $^{99m}\text{Tc}$  labelling. The tumour uptake of  $^{99m}\text{Tc}$  labelled RGD-4C in nude mice bearing xenotransplanted ACHN (human renal adenocarcinoma) tumours was very disappointing, which has been attributed to the limited numbers of integrin  $\alpha_v\beta_3$  per tumour cell and the relatively low binding affinity of the  $^{99m}\text{Tc}$  complex [9.76]. The solution instability and high protein binding of the radiotracer may also contribute to the poor performance of the  $^{99m}\text{Tc}$  labelled RGD-4C, [ $^{99m}\text{Tc}(\text{hynic-RGD-4C})(\text{tricine})_2$ ].

Decristoforo et al. [9.77] recently published a report on the  $^{99m}\text{Tc}$  labelled cyclic RGD peptide monomer, hynic-c(RGDyK). It was found that hynic-RGD could be labelled with  $^{99m}\text{Tc}$  with very high specific activity ( $\sim 100 \text{ GBq}/\mu\text{mol}$ ) using tricine, EDDA, tricine/TPPTS and tricine/nicotinic acid (NA) as coligands. [ $^{99m}\text{Tc}(\text{hynic-RGD})(\text{EDDA})$ ] and [ $^{99m}\text{Tc}(\text{hynic-RGD})(\text{tricine})(\text{L})$ ] (Fig. 9.7; L = TPPTS and NA) had lower protein binding than [ $^{99m}\text{Tc}(\text{hynic-RGD})(\text{tricine})_2$ ] and [ $^{99m}\text{Tc}(\text{CO})_3(\text{hynic-RGD})$ ]. [ $^{99m}\text{Tc}(\text{hynic-RGD})(\text{EDDA})$ ] showed a high tumour uptake ( $\sim 2.7 \% \text{ID/g}$  at 1 h post-injection), along with the rapid renal excretion, low blood retention, and low uptake in liver and muscle. The tumour uptake studies also showed specific targeting of integrin  $\alpha_v\beta_3$  in mice bearing small cell lung tumours. All tumours could be readily visualized using gamma scintigraphy. It was claimed that [ $^{99m}\text{Tc}(\text{hynic-RGD})(\text{EDDA})$ ] had tumour:organ ratios comparable to those of [ $^{18}\text{F}$ ]galacto-RGD [9.77].

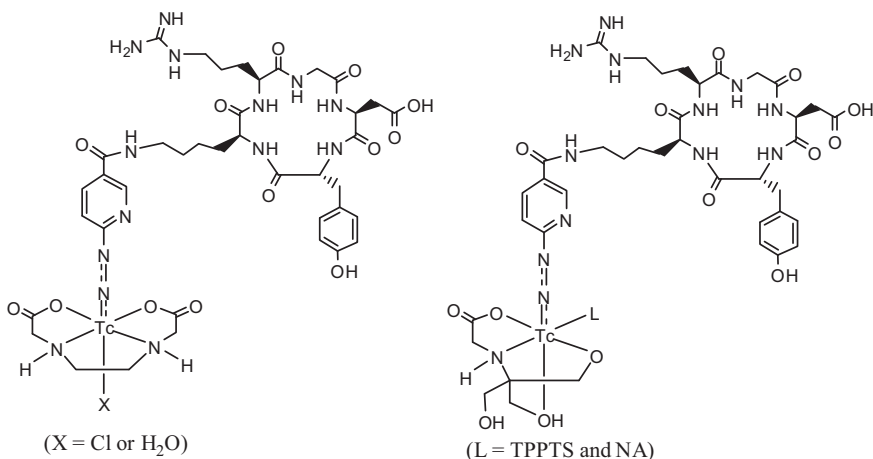


FIG. 9.7.  $^{99m}\text{Tc}$  complexes of a hynic-conjugated cyclic RGD peptide c(RGDyK).

Histidine (His) is considered to be a very effective tridentate BFC for the  $[^{99m}\text{Tc}(\text{CO})_3]^+$  core since it provides one imine-N, one amine-N and, potentially, one carbonyl-O for  $^{99m}\text{Tc}$  chelation. Fani et al. [9.58] recently evaluated  $^{99m}\text{Tc}$  labelled linear and cyclic RGD peptides (Fig. 9.8; RGDFK-His and His-c(RGDyK)). The results from the biodistribution studies in athymic nude mice bearing MDA-MB-435 breast tumour xenografts showed that the tumour uptake of  $[^{99m}\text{Tc}(\text{CO})_3(\text{His}-\text{c}(\text{RGDFK}))]$  ( $3.74 \pm 1.51$  %ID/g at 30 min post-injection) was fourfold higher than that of  $[^{99m}\text{Tc}(\text{CO})_3(\text{RGDFK}-\text{His})]$  ( $0.91 \pm 0.08$  %ID/g at 30 min post-injection) due to the higher integrin  $\alpha_v\beta_3$  binding affinity of His-c(RGDFK) than that of RGDFK-His, even though both radiotracers have similar lipophilicity, solution stability and blood clearance [9.58].

Zhang and Chen [9.59] also reported in vitro and in vivo evaluation of the  $^{99m}\text{Tc}$  labelled cyclic RGD peptide monomer c(RGDyK). Bipyridine-5-carboxylic acid (BPy) was used as the BFC in bonding to the  $[^{99m}\text{Tc}(\text{CO})_3]^+$  core (Fig. 9.8). The BPy-c(RGDyK) conjugate (BPy-RGD) has an  $\text{IC}_{50}$  value of  $92.5 \pm 22.69$  nM against  $^{125}\text{I}$ -echistatin in binding to integrin  $\alpha_v\beta_3$ . As a result, the complex  $[^{99m}\text{Tc}(\text{CO})_3(\text{BPy}-\text{c}(\text{RGDyK}))]$  (Fig. 9.8) had a relatively low tumour uptake ( $1.45 \pm 0.25$  nM at 1.5 h post-injection) in athymic nude mice bearing the MDA-MB-425 breast tumour xenografts. The radiotracer specificity for integrin

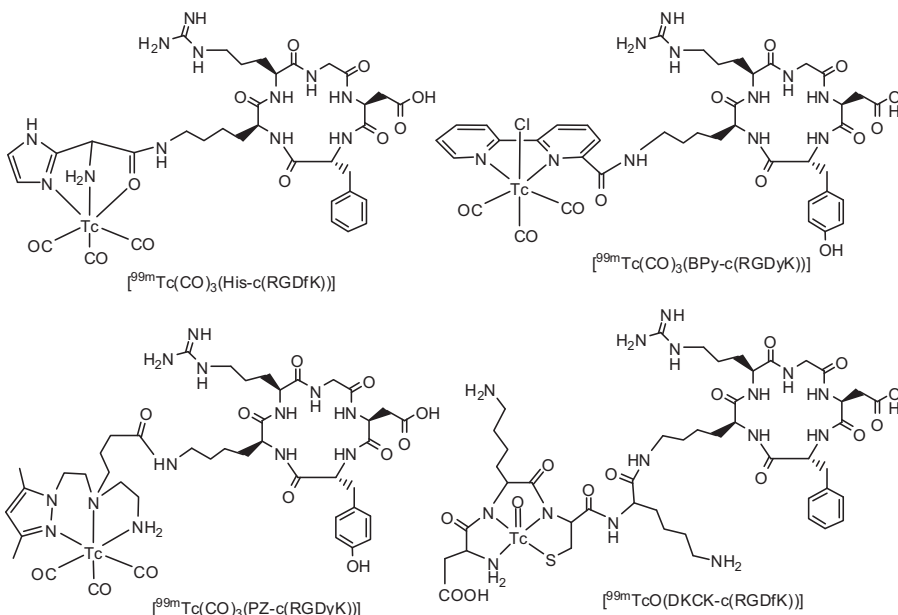


FIG. 9.8. Examples of  $^{99m}\text{Tc}$  labelled cyclic RGD peptide monomers c(RGDyK) and c(RGDyK).

$\alpha_v\beta_3$  was demonstrated by co-injection of excess c(RGDyK), a known integrin  $\alpha_v\beta_3$  antagonist. The low tumour uptake was attributed to the low integrin  $\alpha_v\beta_3$  binding affinity of the BPy-RGD conjugate. Compared to that of [ $^{99m}$ Tc(CO)<sub>3</sub>(His-c(RGDfK))], the high liver uptake of [ $^{99m}$ Tc(CO)<sub>3</sub>(BPy-c(RGDyK))] is most likely caused by the higher lipophilicity of the BPy moiety and its  $^{99m}$ Tc(I)-tricarbonyl chelate as compared to the histidine residue.

The [ $^{99m}$ Tc(CO)<sub>3</sub>]<sup>+</sup> core has also been used for  $^{99m}$ Tc labelling of c(RGDyK) with 3,5-Me<sub>2</sub>-PZ-(CH<sub>2</sub>CH<sub>2</sub>)N(CH<sub>2</sub>CH<sub>2</sub>CH<sub>2</sub>COOH)(CH<sub>2</sub>CH<sub>2</sub>NH<sub>2</sub>) (PZ) as the BFC [9.60]. It was found that [ $^{99m}$ Tc(CO)<sub>3</sub>(PZ-c(RGDyK))] (Fig. 9.8) had a tumour uptake ( $2.50 \pm 0.29$  %ID/g at 1 h post-injection) very similar to that of [ $^{99m}$ Tc(hynic-RGD)(EDDA)] ( $\sim 2.7$  %ID/g at 1 h post-injection) in the same animal model [9.77]. The liver uptake of [ $^{99m}$ Tc(CO)<sub>3</sub>(PZ-c(RGDyK))] ( $8.89 \pm 0.71$  %ID/g) was significantly higher than that of [ $^{99m}$ Tc(hynic-RGD)(EDDA)] ( $2.63 \pm 0.14$  %ID/g) at 1 h post-injection. This suggests that the  $^{99m}$ Tc(hynic) core has an advantage over the [ $^{99m}$ Tc(CO)<sub>3</sub>]<sup>+</sup> core with respect to hydrophilicity of the  $^{99m}$ Tc chelate and to radiotracer clearance kinetics from the liver.

The [Tc=O]<sup>3+</sup> core has also been successfully used for  $^{99m}$ Tc labelling of cyclic RGD peptide c(RGDfK) [9.78]. The BFC is a very hydrophilic DKC-tripeptide sequence (Fig. 9.8). Results of biodistribution studies in Balb/c nude mice bearing M21-L human melanoma xenografts showed that the tumour uptake of the complex [ $^{99m}$ TcO(DKCK-c(RGDfK))] was 1.1 %ID/g at 4 h post-injection. Planar gamma images of the tumour bearing mice clearly showed a good contrast between the tumour and non-tumour tissues. Metabolite analysis indicated that ~60% of [ $^{99m}$ TcO(DKCK-c(RGDfK))] remained intact in the kidneys and 80% in the tumour at 4 h post-injection, while only 24% of [ $^{99m}$ TcO(DKCK-c(RGDfK))] was intact in the blood at 30 min post-injection.

### 9.3.3. Cyclic RGD dimers

Liu et al. has been using cyclic RGD peptides, such as c(RGDfK) and E[c(RGDfK)]<sub>2</sub>, to develop  $^{99m}$ Tc radiotracers for imaging integrin  $\alpha_v\beta_3$  expression in tumours [9.22, 9.41, 9.46]. More than 20  $^{99m}$ Tc labelled cyclic RGD monomers and dimers were screened in the c-neu Oncomouse® model [9.22]. The results of biodistribution studies showed that [ $^{99m}$ Tc(hynic-E[c(RGDfK)]<sub>2</sub>)(tricine)(TPPTS)] (RP593) has the best biodistribution characteristics in terms of tumour uptake, and tumour:liver and tumour:lung ratios. RP593 showed much higher tumour uptake and longer retention than [ $^{99m}$ Tc(hynic-c(RGDfK))(tricine)(TPPTS)] (RP582). The tumour uptake of RP593 can be blocked by co-injection of excess c(RGDfV), suggesting that its tumour localization is indeed due to integrin  $\alpha_v\beta_3$  binding. RP593 and RP582

were also evaluated in the female Balb/c mice with subcutaneously growing OVCAR-3 ovarian carcinoma xenografts [9.43, 9.44]. The tumour uptake of RP593 was significantly higher than that of RP582 at 1, 2 and 4 h post-injection. These results strongly suggest that the cyclic RGD dimer E[c(RGDfK)]<sub>2</sub> has a significant advantage over its monomer counterpart with respect to tumour uptake and retention times of their <sup>99m</sup>Tc radiotracers. A similar conclusion was also made for <sup>18</sup>F labelled and <sup>64</sup>Cu labelled cyclic RGD <sup>64</sup>Cu-DOTA-E[c(RGDfK)]<sub>2</sub> and <sup>64</sup>Cu-DOTA-E[c(RGDyK)]<sub>2</sub>.

PKM linkers also have a significant impact on the biological properties of the <sup>99m</sup>Tc labelled cyclic RGDfK dimer hynic-PKM-E[c(RGDfK)]<sub>2</sub> (Fig. 9.9; PKM = E, K and PEG<sub>4</sub>) [9.72]. Even though they have a minimal impact on the integrin  $\alpha_v\beta_3$  binding capability of E[c(RGDfK)]<sub>2</sub>, all three PKM linkers are able to reduce the radiotracer uptake in blood, kidneys, liver and lungs. It was concluded that E and K linkers have advantages over PEG<sub>4</sub> due to the low liver uptake and high tumour:liver ratios of the <sup>99m</sup>Tc labelled E[c(RGDfK)]<sub>2</sub> [9.72].

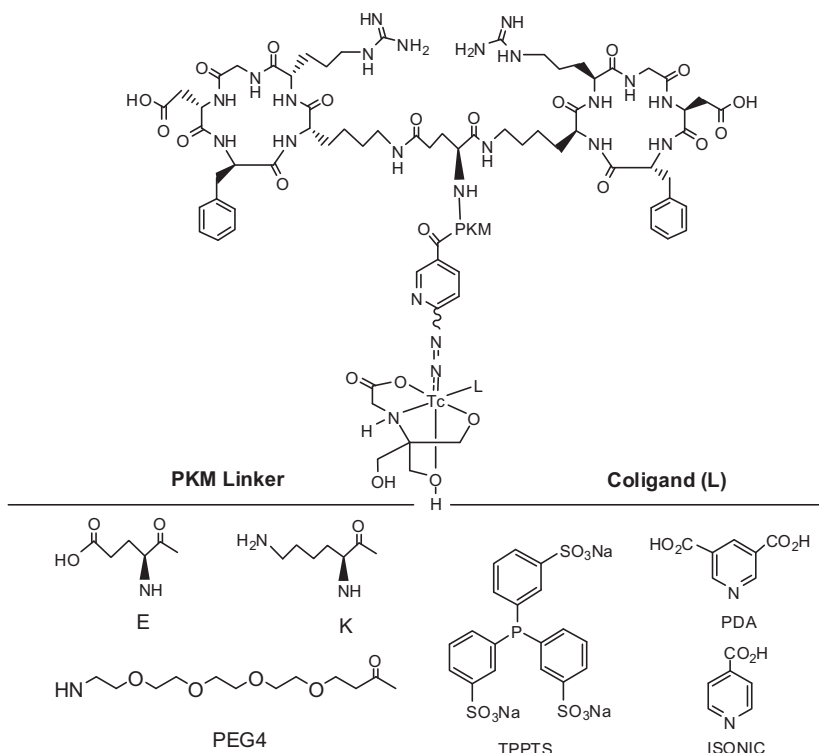
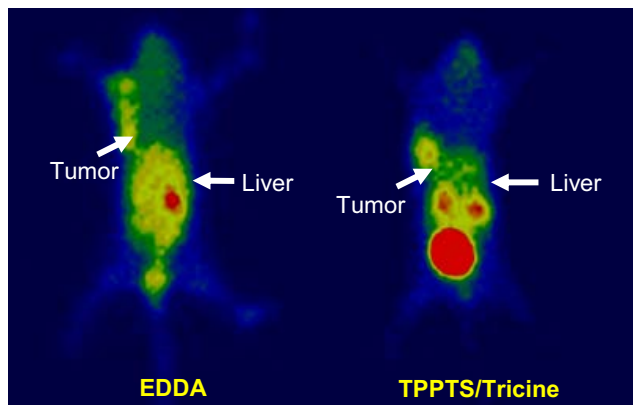


FIG. 9.9. Structures of ternary ligand <sup>99m</sup>Tc complexes: [<sup>99m</sup>Tc(hynic-dimer)(tricine)(L)] (dimer = E[c(RGDfK)]<sub>2</sub>; PKM = E, K and PEG<sub>4</sub>; L = TPPTS, ISONIC and PDA).



*FIG. 9.10. Planar gamma images of Balb/c mice administered with ~400  $\mu$ Ci of RP593 (right) and [ $^{99m}$ Tc(SQ168)(EDDA)] (left) at 4 h post-injection.*

Similar linker effects were also observed for the  $^{111}$ In labelled DOTA-PKM-E[c(RGDfK)]<sub>2</sub> (PKM = E, K and PEG<sub>4</sub>) [9.73].

Coligands have a significant impact on the tumour uptake, metabolic stability and excretion kinetics of [ $^{99m}$ Tc(hynic-E[c(RGDfK)]<sub>2</sub>)(tricine)(L)] (L = TPPTS, ISONIC and PDA). For example, [ $^{99m}$ Tc(hynic-E[c(RGDfK)]<sub>2</sub>)(tricine)(PDA)] had a tumour uptake comparable to that of RP593 in athymic nude mice bearing MDA-MB-435 human breast cancer xenografts; but its liver uptake was significantly lower than that of RP593 [9.46]. The tumour uptake of RP593 in athymic nude mice bearing U87MG glioma xenografts was  $3.10 \pm 0.35$  %ID/g, which was significantly ( $p < 0.01$ ) higher than that of [ $^{99m}$ Tc(hynic-E[c(RGDfK)]<sub>2</sub>)(EDDA)] ( $1.99 \pm 0.44$  %ID/g) at 4 h post-injection. The liver uptake of RP593 was significantly lower than that of [ $^{99m}$ Tc(hynic-E[c(RGDfK)]<sub>2</sub>)(EDDA)] during the same period [9.79]. Figure 9.10 illustrates planar images of tumour bearing BALB/c mice (U87MG glioma xenografts) administered with RP593 (right) and [ $^{99m}$ Tc(hynic-E[c(RGDfK)]<sub>2</sub>)(EDDA)] (left) at 4 h post-injection. It was found that RP593 has much better tumour:liver contrast than [ $^{99m}$ Tc(hynic-E[c(RGDfK)]<sub>2</sub>)(EDDA)] [9.79]. RP593 is a promising radiotracer for SPECT imaging of tumour integrin  $\alpha_v\beta_3$  expression in tumours.

#### 9.3.4. Monitoring tumour metastasis

RP593 was also evaluated for its capability to stage the extent of tumour metastasis in canines with mammary adenocarcinomas confirmed by biopsy. Figure 9.11 illustrates planar images of the same dog administered with RP593 on three different dates [9.22]. Both primary and the rapidly growing metastatic

cancer (on the left side of each image) are clearly seen. When the first imaging study was performed, the image showed no indication of the metastatic tumour. Two months later, the metastatic tumour is clearly seen 60 min after injection of RP593 [9.22, 9.23]. As the size increases, images show increased localization of radioactivity in the tumour, suggesting that the integrin  $\alpha_v\beta_3$ -targeted radiotracers, such as RP593, have the capability to monitor metastasis and tumour growth.

### 9.3.5. Dimer versus tetramer

Liu et al. published a report on hynic-E{E[c(RGDfK)]<sub>2</sub>}<sub>2</sub> and its ternary ligand <sup>99m</sup>Tc complex [<sup>99m</sup>Tc(hynic-E{E[c(RGDfK)]<sub>2</sub>}<sub>2</sub>)(tricine)(TPPTS)] [9.53]. Biodistribution studies of RP593 and [<sup>99m</sup>Tc(hynic-E{E[c(RGDfK)]<sub>2</sub>}<sub>2</sub>)(tricine)(TPPTS)]) were performed in athymic nude mice bearing MDA-MB-435 human breast cancer xenografts. It was found that the tumour uptake of [<sup>99m</sup>Tc(hynic-E{E[c(RGDfK)]<sub>2</sub>}<sub>2</sub>)(tricine)(TPPTS)] was significantly higher than that of RP593 at 120 min post-injection (Fig. 9.12), due to the much higher integrin  $\alpha_v\beta_3$  binding affinity of E{E[c(RGDfK)]<sub>2</sub>}<sub>2</sub>. It is interesting to note that there was a steady increase in tumour uptake for [<sup>99m</sup>Tc(hynic-E{E[c(RGDfK)]<sub>2</sub>}<sub>2</sub>)(tricine)(TPPTS)], while the tumour uptake of RP593 remained relatively unchanged over the 2 h study period. Due to the increased tumour uptake, the T:B ratios of this compound were also significantly increased. The advantage of the cyclic RGDFK tetramer over the corresponding dimer was also demonstrated in different tumour bearing animal models for <sup>111</sup>In-DOTA-E{E[c(RGDfK)]<sub>2</sub>}<sub>2</sub> [9.55] and <sup>64</sup>Cu-DOTA-E{E[c(RGDfK)]<sub>2</sub>}<sub>2</sub> [9.53].

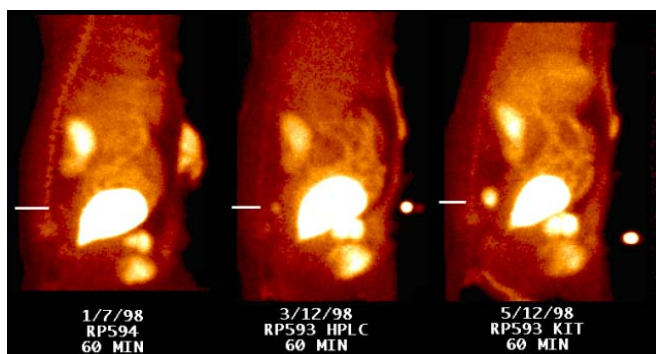


*FIG. 9.11. Representative images of the dog with RP593 at 60 min post-injection. This dog had metastatic mammary adenocarcinoma confirmed by biopsy. Arrows indicate the presence of tumours.*

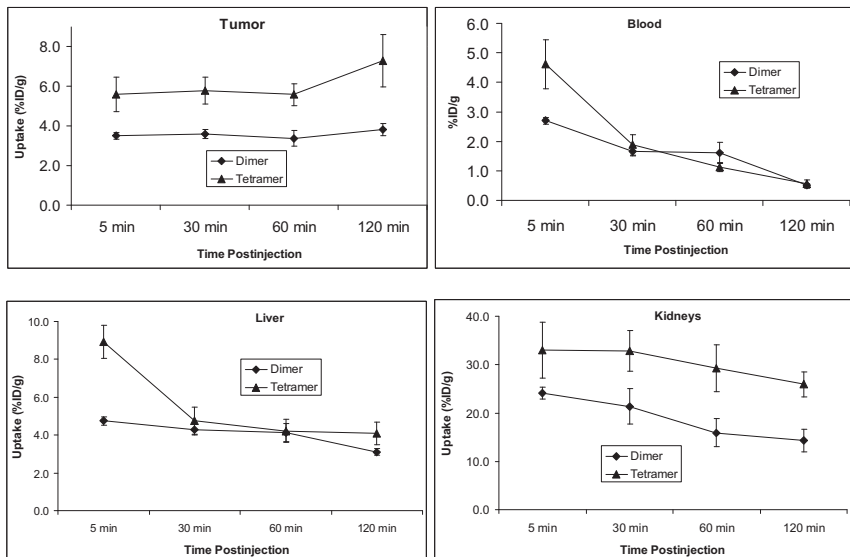


FIG. 9.12. Direct comparison of the biodistribution characteristics of RP593 (dimer: left) and  $[^{99m}\text{Tc}(\text{hynic-}E\{\text{E}[c(\text{RGDfK})_2]_2\}\text{tricine})(\text{TPPTS})]$  (tetramer: right) in athymic nude mice bearing MDA-MB-435 human breast cancer xenografts.

#### 9.4. CONCLUSIONS

Radiolabelled RGD peptides represent a new class of radiotracers with the potential for early tumour detection, and for monitoring tumour metastasis and therapeutic response of various treatment regimens. For the last several years, significant progress has been made on the use of radiolabelled RGD peptides to visualize tumours by SPECT or PET in various tumour bearing animal models. Fluorine-18-galacto-RGD has been under clinical investigations as the first integrin  $\alpha_v\beta_3$ -targeted radiotracer for non-invasive visualization of activated integrin  $\alpha_v\beta_3$  in cancer patients. Based on the experience gained from imaging studies with  $^{99m}\text{Tc}$  labelled peptide  $\alpha\text{P2}$  and  $[^{18}\text{F}]$ galacto-RGD in cancer patients with metastatic melanoma, it is clear that there is sufficient integrin  $\alpha_v\beta_3$  expression for SPECT and PET imaging. Since most rapidly growing and metastatic cancers involve extensive angiogenesis, radiotracers targeting integrin  $\alpha_v\beta_3$  would be useful for a large population of cancer patients with integrin  $\alpha_v\beta_3$  positive tumours.

Peptide multiplicity has been successfully used to enhance integrin  $\alpha_v\beta_3$  binding affinity of cyclic RGD peptides, and to improve radiotracer tumour targeting capability. Among several cyclic RGDFK peptides (monomer, dimer and tetramer), E{E[c(RGDFK)]<sub>2</sub>}<sub>2</sub> is the best targeting biomolecule with respect to its integrin  $\alpha_v\beta_3$  binding affinity and the tumour targeting capability of its radiotracers (<sup>99m</sup>Tc, <sup>111</sup>In, <sup>18</sup>F and <sup>64</sup>Cu). From this point of view, a further increase of RGD peptide multiplicity may result in the formation of oligomeric or polymeric cyclic RGD peptides with improved integrin  $\alpha_v\beta_3$  binding affinity and tumour targeting capability. However, the radiotracer uptake in non-tumour organs, such as kidneys, is also significantly increased as the peptide multiplicity increases. In this situation, the modification of the *in vivo* pharmacokinetics of the radiolabelled oligomeric or multimeric cyclic RGD peptides will become a challenge.

## ACKNOWLEDGEMENTS

The author would like to thank Prof. Xiaoyuan Chen, Stanford Medical School and Prof. Otto C. Boerman, University Nijmegen Medical Centre for their collaboration on the radiolabelled cyclic RGDFK peptides as new radiotracers for imaging rapidly growing and metastatic tumours by SPECT and PET. This work is supported, in part, by research grants: R01 CA115883 A2 (S.L.) from the National Cancer Institute (NCI), BCTR0503947 (S.L.) from the Susan G. Komen Breast Cancer Foundation, AHA0555659Z (S.L.) from the Greater Midwest Affiliate of American Heart Association, R21 EB003419-02 (S.L.) from the National Institute of Biomedical Imaging and Bioengineering (NIBIB), and R21 HL083961-01 (S.L.) from the National Heart, Lung, and Blood Institute (NHLBI).

## REFERENCES TO CHAPTER 9

- [9.1] MOUSA, S.A., Integrins as novel drug discovery targets: potential therapeutic and diagnostic implications, *Expert Opini. Ther. Targets* **4** (2000) 143–153.
- [9.2] CARMELIET, P., Mechanisms of angiogenesis and atherogenesis, *Nature Med.* **6** (2000) 389–395.
- [9.3] BÖGLER, O., MIKKELSEN, T., Angiogenesis in glioma: molecular mechanisms and roadblocks to translation, *Cancer J.* **9** (2003) 205–213.
- [9.4] FOLKMAN, J., Role of angiogenesis in tumor growth and metastasis, *Semin. Oncol.* **29** (2002) 15–18.

- [9.5] HWANG, R., VARNER, J., The role of integrins in tumor angiogenesis, *Hematol. Oncol. Clin. N. Am.* **18** (2004) 991–1006.
- [9.6] JIN, H., VARNER, J., Integrins: roles in cancer development and as treatment targets, *Br. J. Cancer* **90** (2004) 561–565.
- [9.7] KUMMAR, C.C., Integrin  $\alpha_v\beta_3$  as a therapeutic target for blocking tumor-induced angiogenesis, *Curr. Drug Targets* **4** (2003) 123–131.
- [9.8] BROOKS, P.C., CLARK, R.A., CHERESH, D.A., Requirement of vascular integrin  $\alpha_v\beta_3$  for angiogenesis, *Science* **264** (1994) 569–571.
- [9.9] FREDLANDER, M., et al., Definition of two angiogenic pathways by distinct  $\alpha_v$  integrins, *Science* **270** (1995) 1500–1502.
- [9.10] HORTON, M.A., The  $\alpha_v\beta_3$  integrin “vitronectin receptor”, *Int. J. Biochem. Cell Biol.* **29** (1997) 721–725.
- [9.11] BELLO, L., et al., Alpha(v)beta3 and alpha(v)beta5 integrin expression in glioma periphery, *Neurosurgery* **49** (2001) 380–389.
- [9.12] MEITAR, D., et al., Tumor angiogenesis correlates with metastatic disease, *N-myc*-amplification, and poor outcome in human neuroblastoma, *J. Clin. Oncol.* **14** (1996) 405–414.
- [9.13] GASPARINI, G., et al., Vascular integrin  $\alpha_v\beta_3$ : a new prognostic indicator in breast cancer, *Clin. Cancer Res.* **4** (1998) 2625–2634.
- [9.14] ALBELDA, S.M., et al., Integrin distribution in malignant melanoma: association of the beta3 subunit with tumor progression, *Cancer Res.* **50** (1990) 6757–6764.
- [9.15] FALCIONI, R., et al., Expression of beta 1, beta 3, beta 4, and beta 5 integrins by human lung carcinoma cells of different histotypes, *Exp. Cell Res.* **210** (1994) 113–122.
- [9.16] SENGUPTA, S., et al., Role of  $\alpha_v\beta_3$  integrin receptors in breast tumor, *J. Exp. Clin. Cancer Res.* **20** (2001) 585–590.
- [9.17] FELDING-HABERMANN, B., et al., Involvement of integrin alpha V gene expression in human melanoma tumorigenicity, *J. Clin. Invest.* **89** (1992) 2018–2022.
- [9.18] ZITZMANN, S., EHEMANN, V., SCHAB, M., Arginine-Glycine-Aspartic acid (RGD)-peptide binds to both tumor and tumor endothelial cells in vivo, *Cancer Res.* **62** (2002) 5139–5143.
- [9.19] WEBER, W.A., et al., Tumor angiogenesis targeting using imaging agents, *Q. J. Nucl. Med.* **45** (2001) 179–182.
- [9.20] COSTOUROS, N.G., DIEHN, F.E., LIBUTTI, S.K., Molecular imaging of tumor angiogenesis, *J. Cell Biochem. Suppl.* **39** (2002) 72–78.
- [9.21] VAN DE WIELE, C., et al., Tumor angiogenesis pathways: related clinical issues and implications for nuclear medicine imaging, *Eur. J. Nucl. Med. Mol. Imaging* **29** (2002) 699–709.
- [9.22] LIU, S., ROBINSON, S.P., EDWARDS, D.S., Integrin  $\alpha_v\beta_3$  directed radiopharmaceuticals for tumor imaging, *Drugs Future* **28** (2003) 551–564.
- [9.23] LIU, S., ROBINSON, S.P., EDWARDS, D.S., Radiolabeled integrin  $\alpha_v\beta_3$  antagonists as radiopharmaceuticals for tumor radiotherapy, *Top. Curr. Chem.* **252** (2005) 193–216.

- [9.24] HAUBNER, R., WESTER, H.J., Radiolabeled tracers for imaging of tumor angiogenesis and evaluation of anti-angiogenic therapies, *Curr. Pharm. Des.* **10** (2004) 1439–1455.
- [9.25] CHEN, X., Multimodality imaging of tumor integrin  $\alpha_v\beta_3$  expression, *Mini Rev. Med. Chem.* **6** (2006) 227–234.
- [9.26] LIU, S., Radiolabeled multimeric cyclic RGD peptides as integrin  $\alpha_v\beta_3$ -targeted radiotracers for tumor imaging, *Mol. Pharm.* **3** (2006) 472–487.
- [9.27] LIU, S., EDWARDS, D.S.,  $^{99m}\text{Tc}$ -labeled small peptides as diagnostic radiopharmaceuticals, *Chem. Rev.* **99** (1999) 2235–2268.
- [9.28] LIU, S., EDWARDS, D.S., Fundamentals of receptor-based diagnostic metalloradiopharmaceuticals, *Top. Curr. Chem.* **222** (2002) 259–278.
- [9.29] BROOKS, P.C., et al., Integrin  $\alpha_v\beta_3$  antagonists promote tumor regression by inducing apoptosis of angiogenic blood vessels, *Cell* **79** (1994) 1157–1164.
- [9.30] GIANNIS, A., RÜBSAM, F., Integrin antagonists and other low molecular weight compounds as inhibitors of angiogenesis: new drugs in cancer therapy, *Angew. Chem. Int. Ed.* **36** (1997) 588–590.
- [9.31] MILLER, W.H., et al., Identification and in vivo efficacy of small-molecule antagonists of integrin  $\alpha_v\beta_3$  (the vitronectin receptor), *DDT* **5** (2000) 397–408.
- [9.32] BURKE, P.A., DEDARDO, S.J., Antiangiogenic agents and their promising potential in combined therapy, *Critical Rev. Oncol. Hematol.* **39** (2001) 155–171.
- [9.33] HAUBNER, R., et al., Structural and functional aspect of RGD-containing cyclic pentapeptides as highly potent and selective integrin  $\alpha_v\beta_3$  antagonists, *J. Am. Chem. Soc.* **118** (1996) 7461–7472.
- [9.34] DRAKE, C.J., CHARESH, D.A., LITTLE, C.D., An antagonist of integrin  $\alpha_v\beta_3$  prevents maturation of blood vessels during embryonic neovascularization, *J. Cell Sci.* **108** (1995) 2655–2661.
- [9.35] AUMAILLEY, M., et al., Arg-Gly-Asp constrained within cyclic pentapeptides strong and selective inhibitors of cell adhesion to vitronectin and laminin fragment P1, *FEBS Lett.* **291** (1991) 50–54.
- [9.36] HAUBNER, R., FINSINGER, D., KESSLER, H., Stereoisomeric peptide libraries and peptidomimetics for designing selective inhibitors of the  $\alpha_v\beta_3$  integrin for a new cancer therapy, *Angew. Chem. Int. Ed.* **36** (1997) 1374–1389.
- [9.37] GOTTSCHALK, K.E., KESSLER, H., The structures of integrins and integrin-ligand complexes: Implications for drug design and signal transduction, *Angew. Chem. Int. Ed.* **41** (2002) 3767–3774.
- [9.38] BOTURYN, D., et al., Template assembled cyclopeptides as multimeric system for integrin targeting and endocytosis, *J. Am. Chem. Soc.* **126** (2004) 5730–5739.
- [9.39] MAMMEN, M., et al., Polyvalent interactions in biological systems: Implications for design and use of multivalent ligands and inhibitors, *Angew. Chem. Int. Ed.* **37** (1998) 2755–2794.
- [9.40] RAJOPADHYE, M., et al., RP593, a  $^{99m}\text{Tc}$ -labeled  $\alpha_v\beta_3/\alpha_v\beta_5$  antagonist, rapidly detects spontaneous tumors in mice and dogs, *J. Nucl. Med.* **41** (2000) 34P.
- [9.41] LIU, S.,  $^{99m}\text{Tc}$ -labeling of a hydrazinonicotinamide-conjugated vitronectin receptor antagonist useful for imaging tumors, *Bioconjug. Chem.* **12** (2001) 624–629.

- [9.42] LIU, S.,  $^{90}\text{Y}$ - and  $^{177}\text{Lu}$ -labeling of a DOTA-conjugated vitronectin receptor antagonist useful for tumor therapy, *Bioconjug. Chem.* **12** (2001) 559–568.
- [9.43] JANSSEN, M., et al., Tumor targeting with radiolabeled  $\alpha,\beta_3$  integrin binding peptides in a nude mouse model, *Cancer Res.* **62** (2002) 6146–6151.
- [9.44] JANSSEN, M., et al., Comparison of a monomeric and dimeric radiolabeled RGD-peptide for tumor targeting, *Cancer Biother. Radiopharm.* **17** (2002) 641–646.
- [9.45] JANSSEN, M., et al., Improved tumor targeting of radiolabeled RGD-peptides using rapid dose fractionation, *Cancer Biother. Radiopharm.* **19** (2004) 399–404.
- [9.46] LIU, S., et al., Effect of coligands on biodistribution characteristics of ternary ligand  $^{99\text{m}}\text{Tc}$  complexes of a HYNIC-conjugated cyclic RGDFK dimer, *Bioconjug. Chem.* **16** (2005) 1580–1588.
- [9.47] CHEN, X.Y., et al., MicroPET imaging of breast cancer  $\alpha_v$ -integrin expression with  $^{64}\text{Cu}$ -labeled dimeric RGD peptides, *Mol. Imaging Biol.* **6** (2004) 350–359.
- [9.48] CHEN, X.Y., et al., MicroPET imaging of breast cancer  $\alpha_v$ -integrin expression with  $^{18}\text{F}$ -labeled dimeric RGD peptide, *Mol. Imaging* **3** (2004) 96–104.
- [9.49] POETHKO, T., et al., Improved tumor uptake, tumor retention and tumor/background ratios of pegylated RGD multimers, *J. Nucl. Med.* **44** (2003) 46P.
- [9.50] POETHKO, T., et al., Chemoselective pre-conjugate radiohalogenation of unprotected mono- and multimeric peptides via oxime formation, *Radiochim. Acta* **92** (2004) 317–328.
- [9.51] THUMSHIRN, G., et al., Multimeric cyclic RGD peptides as potential tools for tumor targeting: solid-phase peptide synthesis and chemoselective oxime ligation, *Chem. Eur. J.* **9** (2003) 2717–2725.
- [9.52] POETHKO, T., et al., Two-step methodology for high yield routine radiohalogenation of peptides:  $^{18}\text{F}$ -labeled RGD and octreotide analogs, *J. Nucl. Med.* **45** (2004) 892–902.
- [9.53] LIU, S., et al., Evaluation of a  $^{99\text{m}}\text{Tc}$ -labeled cyclic RGD tetramer for non-invasive imaging integrin  $\alpha,\beta_3$ -positive breast cancer, *Bioconjug. Chem.* **18** (2007) 438–446.
- [9.54] WU, Y., et al., MicroPET imaging of glioma integrin  $\alpha,\beta_3$  expression using  $^{64}\text{Cu}$ -labeled tetrameric RGD peptide, *J. Nucl. Med.* **46** (2005) 1707–1718.
- [9.55] DIJKRAAF, I., et al., Improved targeting of the  $\alpha,\beta_3$  integrin by multimerization of RGD peptides, *Eur. J. Nucl. Med. Mol. Imaging* **34** (2007) 267–273.
- [9.56] LIU, S., The role of coordination chemistry in development of target-specific radiopharmaceuticals, *Chem. Soc. Rev.* **33** (2004) 445–461.
- [9.57] JURISSON, S.S., LYDON, J.D., Potential technetium small molecule radiopharmaceuticals, *Chem. Rev.* **99** (1999) 2205–2218.
- [9.58] FANI, M., et al., Comparative evaluation of linear and cyclic  $^{99\text{m}}\text{Tc}$ -RGD peptides for targeting of integrins in tumor angiogenesis, *Anticancer Res.* **26** (2006) 431–434.
- [9.59] ZHANG, X., CHEN, X., Preparation and characterization of  $^{99\text{m}}\text{Tc}(\text{CO})_3\text{-BPy-RGD}$  complex as  $\alpha,\beta_3$  integrin receptor-targeted imaging agent, *Appl. Radiat. Isotop.* **65** (2007) 70–78.
- [9.60] ALVES, S., et al., In vitro and in vivo evaluation of a novel  $^{99\text{m}}\text{Tc}(\text{CO})_3$ -pyrazolyl conjugate of *cyclo*-(Arg-Gly-Asp-D-Tyr-Lys), *Bioconjug. Chem.* **18** (2007) 530–537.
- [9.61] LIU, S., 6-Hydrazinonicotinamide derivatives as bifunctional coupling agents for  $^{99\text{m}}\text{Tc}$ -labeling of small biomolecules, *Top. Curr. Chem.* **252** (2005) 117–153.

- [9.62] HAUBNER, R., et al., RGD-peptides for tumor targeting: biological evaluation of radioiodinated analogs and introduction of a novel glycosylated peptide with improved biokinetics, *J. Labelled Comp. Radiopharm.* **40** (1997) 383–385.
- [9.63] HAUBNER, R., et al., Radiolabeled  $\alpha_v\beta_3$  integrin antagonists: a new class of tracers for tumor imaging, *J. Nucl. Med.* **40** (1999) 1061–1071.
- [9.64] HAUBNER, R., et al., Glycolated RGD-containing peptides: tracer for tumor targeting and angiogenesis imaging with improved biokinetics, *J. Nucl. Med.* **42** (2001) 326–336.
- [9.65] HAUBNER, R., et al., Noninvasive imaging of  $\alpha_v\beta_3$  integrin expression using  $^{18}\text{F}$ -labeled RGD-containing glycopeptide and positron emission tomography, *Cancer Res.* **61** (2001) 1781–1785.
- [9.66] HARRIS, T.D., et al., Design, synthesis and evaluation of radiolabeled integrin  $\alpha_v\beta_3$  receptor antagonists for tumor imaging and radiotherapy, *Cancer Biother. Radiopharm.* **18** (2003) 627–641.
- [9.67] ONTHANK, D.C., et al.,  $^{90}\text{Y}$  and  $^{111}\text{In}$  complexes of A DOTA-conjugated integrin  $\alpha_v\beta_3$  receptor antagonist: different but biologically equivalent, *Bioconjug. Chem.* **15** (2004) 235–241.
- [9.68] HARRIS, T.D., et al., Structure-activity relationships of  $^{111}\text{In}$ - and  $^{99\text{m}}\text{Tc}$ -labeled quinolin-4-one peptidomimetics as ligands for the vitronectin receptor: potential tumor imaging agents, *Bioconjug. Chem.* **17** (2006) 1294–1313.
- [9.69] HARRIS, T.D., et al., Radiolabeled divalent peptidomimetic vitronectin receptor antagonists as potential tumor radiotherapeutic and imaging agents, *Bioconjug. Chem.* **18** (2007) 1266–1279.
- [9.70] CHEN, X., et al., Pharmacokinetics and tumor retention of  $^{125}\text{I}$ -labeled RGD peptide are improved by PEGylation, *Nucl. Med. Biol.* **31** (2004) 11–19.
- [9.71] CHEN, X., et al., Integrin  $\alpha_v\beta_3$ -targeted imaging of lung cancer, *Neoplasia* **7** (2005) 271–279.
- [9.72] LIU, S., et al., Impact of PKM linkers on biodistribution characteristics of the  $^{99\text{m}}\text{Tc}$ -labeled cyclic RGDFK dimer, *Bioconjug. Chem.* **17** (2006) 1499–1507.
- [9.73] DIJKGRAAF, I., et al., Effect of linker variation on the in vitro and in vivo characteristics of an  $^{111}\text{In}$ -labeled RGD Peptide, *Nucl. Med. Biol.* **34** (2007) 29–35.
- [9.74] LIU, S., EDWARDS, D.S., Bifunctional chelators for therapeutic lanthanide radiopharmaceuticals, *Bioconjug. Chem.* **12** (2001) 7–34.
- [9.75] SIVOLAPENKO, G.B., et al., Imaging of metastatic melanoma utilizing a technetium- $99\text{m}$  labeled RGD-containing synthetic peptide, *Eur. J. Nucl. Med.* **25** (1998) 1383–1389.
- [9.76] SU, Z.F., et al., In vitro and in vivo evaluation of a technetium- $99\text{m}$ -labeled cyclic RGD peptide as specific marker of  $\alpha_v\beta_3$  integrin for tumor imaging, *Bioconjug. Chem.* **13** (2002) 561–570.
- [9.77] DECRISTOFORO, C., et al., [ $^{99\text{m}}\text{Tc}$ ]HYNIC-RGD for imaging integrin  $\alpha_v\beta_3$  expression, *Nucl. Med. Biol.* **33** (2006) 945–952.

- [9.78] HAUBNER, R., et al., Synthesis and biological evaluation of  $^{99m}\text{Tc}$ -labeled cyclic RGD peptide for imaging integrin  $\alpha_v\beta_3$  expression, Nuklearmedizin **43** (2004) 26–32.
- [9.79] JIA, B., et al.,  $^{99m}\text{Tc}$ -labeled cyclic RGDFK dimer: initial evaluation for SPECT imaging of glioma integrin  $\alpha_v\beta_3$  expression, Bioconjug. Chem. **17** (2006) 1069–1076.



## **Chapter 10**

# **TECHNETIUM-99m LABELLED REGULATORY PEPTIDE FOR TUMOUR IMAGING**

**C. DECRISTOFORO**

Clinical Department of Nuclear Medicine,  
Medical University Innsbruck,  
Innsbruck, Austria

### **Abstract**

The chapter deals with  $^{99m}\text{Tc}$  labelled peptides for tumour targeting. Receptors of regulatory peptides are overexpressed in a variety of tumours and can be targeted using different radiolabelled peptides, such as analogues of somatostatin, gastrin, bombesin or substance P. The pharmacokinetics of  $^{99m}\text{Tc}$  labelled peptides are dependent on the stability of the peptide, lipophilicity and charge, the radionuclide and the choice of chelator. The ideal characteristics of radiolabelled peptides for tumour diagnosis are predominant renal excretion, rapid elimination from circulation and low tissue retention. It has been shown that the chelator has a great influence on the pharmacokinetic properties and that the use of pharmacokinetic modifiers may overcome potential limitations. Technetium-99m labelled somatostatin analogues are described in detail, as these have had the greatest impact on patient management so far. These were labelled with  $^{99m}\text{Tc}$  using  $\text{N}_3\text{S}$ , hynic,  $\text{Tc}(\text{CO})_3$  and other strategies. Other  $^{99m}\text{Tc}$  labelled peptide analogues described in the chapter include neuropeptides Y and alpha-MSH, cholecystokinin, bombesin, vasoactive intestinal peptide, neuropeptide Y and alpha-MSH analogues.

### **10.1. INTRODUCTION: REGULATORY PEPTIDES AND HUMAN CANCER**

The most important group of peptides for targeting tumour cells are physiologically occurring regulatory peptides. Their regulatory functions are mediated through specific membrane bound receptors that influence a number of intracellular effector systems. The great majority of these peptides belong to the family of G protein-coupled receptors. Receptor subtypes with their own ligand specificity and second messenger systems, are known for almost every regulatory peptide. This results in an increased diversity in their mode of action. While these peptide receptors are physiologically found in a variety of tissues including the brain, they can be highly overexpressed in primary human cancers. Table 10.1 shows the expression of the most important regulatory peptide receptors in human tumours. A detailed review on regulatory peptide receptors as molecular targets for cancer diagnosis and therapy was recently published by Reubi et al. [10.1].

TABLE 10.1. RECEPTORS OF REGULATORY PEPTIDES  
OVEREXPRESSED IN HUMAN TUMOURS

Peptide receptor	Known subtypes	Tumour type
Somatostatin	SSTR 1–5	Neuroendocrine tumours, non-Hodgkin's lymphoma, melanoma, breast cancer
Gastrin/CCK	CCK1,2	MTC, SCLC, pancreatic, astrocytoma, stromal ovarian cancer
Bombesin/GRP	BB1–4 (BB2=GRP)	SCLC, colon, breast, glioblastoma, prostate
Neurotensin	NT1–3	Exocrine pancreatic tumours, small cell lung cancer, neuroblastoma, colon cancer
$\alpha$ -MSH	$\alpha$ -MSH	Melanoma
VIP/PACAP	VPAC1,2	SCLC, colon, gastric, pancreatic
NPY	Y1–6	Breast cancer, neuroblastoma
Substance P	NK1	Glioblastoma, astrocytoma, MTC, breast cancer, intra-tumoural and peritumoural blood vessels
LNRH	LNRH	Breast, prostate, ovarian cancer
GLP	GLP-1	Insulinoma
ANP	ANP A–C	Neuroblastoma
Oxytocin	Oxytocin	Glial tumours, neuroblastoma, breast and endometrial cancers
Calcitonin	Calcitonin	Bone, MTC
Endothelin	ET A,B	Breast, ovary, lung cancer

Note: MTC = medullary thyroid carcinoma; SCLC = small cell lung cancer.

## 10.2. PHARMACOKINETICS AND PHARMACODYNAMICS

For the application of radiolabelled peptides as diagnostic tools to target cancer cells, an optimal pattern of biodistribution, such as rapid transport, binding and retention in the target, is needed. Any radioactivity not bound to the tumour should rapidly be cleared from the blood and efficiently excreted without significant retention in normal organs. Since hepatobiliary clearance is necessarily accompanied by a relatively slow gastrointestinal transit before the radioactivity leaves the body, an entirely renal route of excretion is preferred.

Several factors determine this biodistribution pattern (i.e. the pharmacokinetics) as well as the interaction with the target receptor. In recent years, research has focused on the optimization of parameters that affect the pharmacokinetics of radiolabelled peptides and many improvements have been made which have had a considerable impact on clinical applications. The major parameters are addressed below.

### 10.2.1. Stability of the peptide

Naturally occurring peptides that bind to regulatory receptors have an intrinsic instability in biological systems. The peptides transmit a signal to other cells by binding to their receptors and are rapidly degraded by enzymes to limit their action to the vicinity of their release and not throughout the body. Radiolabelled naturally occurring peptide sequences have rarely proven to be suitable as radiopharmaceuticals, except for locoregional applications [10.2]. For example, the natural form of vasoactive intestinal peptide (VIP) has been radioiodinated and used for imaging studies [10.3]. However, its very low in vivo stability has hampered its further development towards, for example,  $^{99m}\text{Tc}$  labelled compounds [10.4]. For systemic application, stabilization of the peptide is, therefore, usually required to achieve a high target:non-target ratio. If the stability of the radiolabelled peptide appears to be too low, a higher uptake of radioactivity in non-target tissues such as liver as well as a lower tumour uptake can be expected. Stabilization may be achieved by identifying the binding sequence of the peptide to its receptor and subsequent optimization by replacing single amino acids. An introduction of D amino acids, formation of non-peptide bonds, replacement of a carboxylic group by amide or alcohol are typical strategies for enhancing the stability of peptides for imaging purposes. However, it must be ensured that the binding affinity to the target is not impaired. Neurotensin (NT) analogues provide an example of where stabilization of the peptide sequence is important for improving the targeting properties. Subsequent modification of cleavage bonds in the peptide resulted in highly stable analogues for labelling with  $^{99m}\text{Tc}$  with a high tumour uptake (Table 10.2).

### 10.2.2. Lipophilicity and peptide charge

Other important factors decisive for the pharmacokinetic properties of peptides as radiopharmaceuticals are lipophilicity and charge. The lipophilicity of a peptide will determine its elimination pathways and tissue retention. For somatostatin analogues, it is known that higher lipophilic derivatives such as lanreotide or  $1\text{-Na}^3\text{-octreotide}$  (NOC) show higher blood activities and slower renal elimination rates as compared to their octreotide counterparts. The charge of

TABLE 10.2. OPTIMIZATION OF THE PEPTIDE SEQUENCE NT ANALOGUES FOR  $^{99m}\text{Tc}$  LABELLING STARTING FROM THE NATIVE SEQUENCE NT(8–13) AND SUBSEQUENT REPLACEMENT OF AMINO ACIDS FOR IMPROVED PLASMA STABILITY. COMPARISON OF BINDING AFFINITIES OF THE  $^{99m}\text{Tc}$  LABELLED NT ANALOGUES TO HT29 CELLS, STABILITY IN HUMAN PLASMA (1 mg/mL), AND TUMOUR UPTAKE 5 h POST-INJECTION IN AN HT29 NUDE MOUSE TUMOUR MODEL (from Refs [10.16, 10.48])

Peptide	Sequence	Kd (nM)	$T_{1/2}$	Tumour uptake
NT(8–13)	Arg-Arg-Pro-Tyr-Ile-Leu	1.6	10–20 min	n.d.
NT-I	HisArg-Arg-Pro-Tyr-Ile-Leu	0.6	10–20 min	1.8%
NT-II	(N $\alpha$ -His)Ac-Arg-Arg-Pro-Tyr-Ile-Leu	0.3	3.5–4 h	0.4%
NT-IV	His-Lys-C(CH <sub>2</sub> NH)Arg-Pro-Tyr-Ile-Leu	0.3	1–3 h	n.d.
NT-VI	(N $\alpha$ -His)Ac-Lys-C(CH <sub>2</sub> NH)Arg-Pro-Tyr-Ile-Leu	0.5	3 h	0.8%
NT-XI	(N $\alpha$ -His)Ac-Lys-C(CH <sub>2</sub> NH)-Arg-Pro-Tyr-Tle-Leu	0.5	>24 h	n.d.
NT-XII	(N $\alpha$ -His)Ac-Arg-(N-CH <sub>3</sub> )-Arg-Pro-Tyr-Tle-Leu	2.0	>24 h	4.6%
NT-XIII	(N $\alpha$ -His)A-h3Arg-Arg-Pro-Tyr-Tle-Leu	6.5	>24 h	0.98%
NT-XVIII	(N $\alpha$ -His)Ac-Lys(shikimic)-Arg-(N-CH3)-Arg-Pro-Tyr-Tle-Leu	4.5	>24 h	0.76%
NT-XIX 2	(N $\alpha$ -His)Ac-Arg-NMeArg-Pro-Dmt-Tle-Leu	15.0	>24 h	5.2%

the peptide is, specifically, important for the renal accumulation of a peptide. The majority of glomerularly-filtered radiolabelled peptides are reabsorbed by the renal tubule, resulting in prolonged renal retention of radioactivity. This renal uptake is thought to be mediated by the megalin receptor [10.5] and may be more pronounced for peptides that are mainly positively charged than for neutral or negatively charged peptides.

### 10.2.3. Affinity and receptor interaction of the peptide

The affinity of radiolabelled peptides for their target receptors should, generally, be very high, i.e. dissociation constants (Kd values) should be in the low nanomolar range. However, the subsequent fate of the radiolabelled peptide at the target site has also been a focus of research in recent years. Upon binding to

the receptor, regulatory peptides act as agonists and show receptor mediated internalization of the receptor/peptide complex [10.6]. Once inside the cell, the peptide may be further metabolized and stored in lysosomes, actively recycled onto the cell surface or radiolabelled metabolites may passively diffuse out of the cell. The rate of internalization is highly correlated with tumour uptake [10.7]. Research has, therefore, focused on peptide receptor agonists. These, however, have the disadvantage of being very pharmacologically active. Recently, using somatostatin receptor antagonists, it has been shown that even higher tumour uptake values can be achieved [10.8]. This issue will certainly remain a matter of interest in the future.

#### **10.2.4. Radionuclide**

Concerning the radionuclide used for radiolabelling peptides, radiometals in general have proven to be advantageous for a variety of reasons. In contrast to radiohalogenated peptides, they show a tendency towards higher stability in biological systems and are not as readily released from target cells once taken up. Additionally, chelators may also serve as pharmacokinetic modifiers, which will be discussed in detail later. Another advantage lies in a straightforward labelling approach using the bifunctional chelator approach, where the chemically modified peptide readily reacts with a radiometal in high yields, rendering post-labelling purification steps for patient studies unnecessary. While  $^{111}\text{In}$ ,  $^{90}\text{Y}$ ,  $^{177}\text{Lu}$  and  $^{68}\text{Ga}$  are frequently used for SPECT, radiotherapy and PET applications,  $^{99\text{m}}\text{Tc}$  is advantageous in terms of its availability and cost, as well as its high specific activity.

#### **10.2.5. The choice of chelator**

A very high specific activity is generally required for labelling regulatory peptides due to their high pharmacological activity, especially when they act in an agonistic manner. For potential clinical application, a  $^{99\text{m}}\text{Tc}$  labelled peptide cannot be separated from an unbound ligand. Thus, the total amount of peptide used in the labelling reaction would not result in any pharmacological actions. The chelator must be designed to allow labelling at sufficiently high specific activities.

Different chelating systems have been employed in an attempt to develop  $^{99\text{m}}\text{Tc}$  labelled probes for targeting regulatory peptide receptors with highly specific activities. These include systems based on  $\text{N}_3\text{S}$  and  $\text{N}_2\text{S}_2$  systems with Tc-oxo core, tetramines with Tc-dioxo core, Tc-tricarbonyl core, Tc-hynic, etc. An excellent review on labelling strategies for small peptides was published by Edwards and Liu [10.9]. It is well recognized that the introduction of a radiolabel

alone or after attachment of a chelating moiety will considerably influence the specific interaction between the peptide sequence and the receptor, depending on the individual targeting sequence. Information about the site of chelator attachment without impairing receptor binding ability can be derived from basic research on the peptides themselves and their respective receptors. However, it remains very difficult to predict the influence of the radiolabelling approach on the resulting pharmacokinetics of the peptide [10.10].

#### **10.2.6. Lipophilicity, charge of the chelator and stability of the complex**

Although it is well recognized that the influence of the chelator on the imaging characteristics of  $^{99m}\text{Tc}$  labelled peptides is decisive, clear structure-activity relationships in this respect are rare. The charge of a metal complex is certainly an important factor, similar to the charge of the peptide itself. A comparison of the biodistribution of two similar radiopharmaceuticals, P587 and P829, has been published [10.11]. It is shown that a chelator with an additional +2 charge resulted in faster blood clearance, lower hepatobiliary excretion, but also higher kidney retention. There also seems to be a clear correlation between lipophilicity and pharmacokinetic behaviour. High lipophilicity introduced using a labelling approach results in a higher degree of hepatobiliary excretion. For example, a replacement of glycine for serine in an  $\text{N}_3\text{S}$  chelator for  $^{99m}\text{Tc}$  labelling resulted in a considerable shift towards renal excretion in monkeys [10.12]. For RC160, a somatostatin analogue, rather lipophilic chelators such as MAG3 based ligands resulted in predominant and rapid hepatobiliary excretion both in rats and in mouse tumour models, whereas hynic derivatized peptides with a hydrophilic coligand such as EDDA resulted in almost exclusive renal elimination and low retention in liver and muscle [10.13]. For these peptides, tumour uptake was also considerably reduced for lipophilic derivatives as compared to their hydrophilic counterparts based on hynic or  $\text{N}_4$  labelling approaches. Comparative gamma camera images of the  $^{99m}\text{Tc}$  labelled somatostatin analogue RC160 are shown in Fig. 10.1.

On the other hand, it has been demonstrated that the coligand used for radiolabelling plays a crucial role in the stability of hynic-conjugated peptides. If the complex is not sufficiently stable (e.g. use of tricine as coligand), then at least partial trans-chelation can occur between the hynic-coligand-technetium complex and plasma proteins [10.14]. This also results in increased GI clearance as well as higher levels of retention in the blood and normal tissues. Another example of the importance of complex stability can be seen from the application of the  $\text{Tc}(\text{CO})_3$  core for labelling peptides. While complexes with tridentate coordinated ligand systems generally exhibited a fast and complete clearance

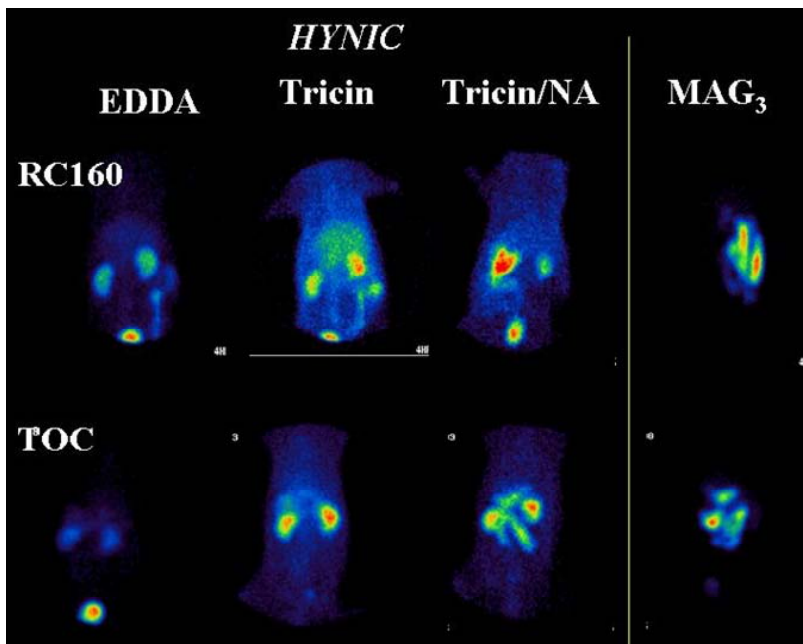


*FIG. 10.1. Influence of the chelator and peptide on pharmacokinetics: gamma camera images of rats at 1 h post-injection of  $^{99m}\text{Tc}$  labelled somatostatin analogues. Top row: RC160 derivatives (vapreotide), bottom row TOC ( $\text{Tyr}^3$ -octreotide) derivatives. This influence of the more lipophilic peptide sequence of vapreotide as well as the influence of the chelator lipophilicity ( $\text{MAG}_3$  = hepatobiliary elimination,  $\text{hynic}$  = predominantly renal excretion) is clearly shown. In the case of  $\text{hynic}$ , higher stable complexes (EDDA or tricine/nicotinic acid (NA) as coligand) resulted in lower blood levels and liver uptake as compared to tricine as a coligand, resulting in unstable  $^{99m}\text{Tc}$  complexes.*

from all organs and tissues, complexes with only bidentate coordinated ligands showed a significantly higher retention of radioactivity in the liver, the kidneys and the blood pool [10.15]. The likely explanation for this behaviour is that the coordination site of Tc, which is unfilled by bidentate ligands, becomes filled by a donor atom from circulating plasma proteins, resulting in a high degree of protein binding and a radically altered pattern of biodistribution. In the case of Tc labelled NT derivatives, Garcia-Garayoa et al. demonstrated that a replacement of the N terminal His with an acetyl  $\text{N}\alpha$ -His analogue can provide tridentate coordination of the Tc-carbonyl, which resulted in a more rapid blood clearance, lower retention by normal tissues and a much lower proportion of hepatobiliary clearance of the labelled peptide [10.16]. In the case of bombesin (BBN) derivatized with diaminepropionic acid as a bidentate chelator for the  $\text{Tc}(\text{CO})_3$  core [10.17], tris(hydroxymethyl)-phosphine, a strong  $\pi$ -acid donor, was

used as a third ligand to eliminate potential dissociation or coordination with endogenous proteins. Moreover, by choosing appropriate water soluble phosphines, this monodentate ligand could be used to modulate and, possibly, to tune the pharmacokinetic properties.

#### 10.2.7. Pharmacokinetic modifiers

Some labelling moieties themselves modify pharmacokinetic properties. This is especially true for the hynic system. Here, the distribution profile and rate of excretion can be widely altered by using different coligands. Tetramine ( $N_4$ ) based chelators also positively influence pharmacokinetics, leading to hydrophilic complexes with predominant renal excretion and low tissue retention. Besides hydrophilicity and charge, however, further factors need to be considered for achieving optimized pharmacokinetics. One of the serious challenges for radiolabelled peptides is, in many cases, the high retention of radioactivity in the kidney due to a tubular reabsorption mechanism. Béhé et al. have shown that the initial high renal uptake of a radiolabelled minigastrin analogue could be blocked by a specific penta-glutamic acid sequence, and suggested that a modification of the peptide sequence would lead to much lower levels of kidney uptake and retention [10.18]. Another way of reducing renal retention of radiolabelled peptides may be the introduction of a cleavable linker between the peptide and the chelating moiety [10.19]. Introducing a linker may also help to optimize receptor targeting and target retention. Introducing additional amino acids or a sugar between a somatostatin analogue and a radiometal chelate may help to increase receptor affinity and internalization rates [10.20]. Chemical modification of linker moieties was also performed to accelerate the elimination rate from the kidney. This may be achieved, for example, by introducing carbohydrate chains [10.21] or PEG residues.

### 10.3. TECHNETIUM-99m LABELLED SOMATOSTATIN ANALOGUES

Due to the success of  $^{111}\text{In}$ -DTPA-octreotide as a receptor imaging agent, somatostatin analogues have been the peptides most widely studied for scintigraphic purposes, including  $^{99\text{m}}\text{Tc}$  labelling. Somatostatin receptors (SSTs) are integral membrane glycoproteins that are distributed in a variety of tissues throughout the body [10.22]. SSTs are found throughout the endocrine system. They have multiple physiological functions, including inhibition of secretion of a growth hormone, glucagon, insulin, gastrin and other human peptide hormones. In addition, somatostatin plays an inhibitory role in the immune system and acts as a neuromodulatory peptide in the central nervous system (CNS). Alterations of

SST expression during disease, such as overexpression in many types of neoplasia, can be exploited by imaging techniques.

Receptor-positive tumours, such as pituitary adenomas, gastroenteropancreatic tumours, and pancreatic islet cell tumours, can originate in the neuroendocrine system, but other tumours, such as lymphomas and breast cancer, may possess these receptors as well. Of the six SST subtypes, SST1, SST2A, SST2B, SST3, SST4 and SST5, SST2A is the most important one because of its high overexpression in malignant tumours and its high affinity for the clinically available somatostatin analogues. Somatostatin naturally occurs in two forms, somatostatin-14 and somatostatin-28. However, these compounds are very unstable in biological systems and metabolically stabilized analogues, such as octreotide, lanreotide, vaptoreotide (RC-160) and segreotide, have, therefore, been developed and have been exploited for scintigraphic applications. All of them show a high affinity for SST2, but variable affinity for other receptor subtypes. The most widely used analogue is octreotide and derivatives thereof. Replacing Phe<sup>3</sup> with Tyr (Tyr<sup>3</sup>-octreotide (TOC)) resulted in higher affinity and more rapid internalization as compared to octreotide. Replacing Thr(ol)<sup>8</sup> with Thr (Tyr<sup>3</sup>-octreotide, (TATE)) was reported to have even higher internalization rates, which resulted in higher tumour uptake [10.23]. Recently, somatostatin analogues were reported with a broader receptor profile based on octreotide, such as Nal<sup>3</sup> and BzThi<sup>3</sup> substituted octreotide and octreotide derivatives [10.24]. Thus, today a broad range of somatostatin analogues is available for potential radiolabelling with <sup>99m</sup>Tc.

One of the first strategies for <sup>99m</sup>Tc labelling of these analogues was the direct labelling approach. Analogous to the labelling of antibodies, the disulphide bridge of octreotide and vaptoreotide was cleaved by reduction, creating high affinity binding sites for <sup>99m</sup>Tc and <sup>186/188</sup>Re [10.25, 10.26]. For the resulting agents, no receptor binding data were reported and biodistribution was unfavourable; the main excretion pathway was via the hepatobiliary system. Moreover, tumour uptake was low.

Early attempts for radiolabelling octreotide using bifunctional chelators were based on propylenediamine-dioxime (PnAO) or MAG3. The <sup>99m</sup>Tc labelled (PnAO) octreotide derivative bound specifically and possessed high affinity to SRIF receptors in vitro ( $K_d = 9.8 \text{ nM}$ ) [10.27]. Biodistribution studies of <sup>99m</sup>Tc-PnAO-octreotide showed rapid blood clearance but relatively low tumour and high liver uptake, and excreted predominantly via the hepatobiliary system. Similar properties were found for <sup>99m</sup>Tc-MAG3 derivatized RC160, which had low tumour uptake and a high degree of hepatobiliary excretion [10.28].

The first successful candidate used in patient studies was P829 (depreotide, NeoSPECT) [10.29]. It is based on the segreotide backbone with an N<sub>3</sub>S monothiol-bisamide-monoamine ligand derivative with an additional lysine

residue. In patients, it has proven successful in imaging solitary pulmonary nodes [10.30], but failed in gastrointestinal tumours. Further improvement of the peptide ( $^{99m}\text{Tc}$ -P2045) resulted in a dramatic increase in tumour uptake, with an improved biodistribution pattern suitable for  $^{188/186}\text{Re}$  labelling for therapeutic applications [10.31].

A potential problem with the use of octreotide is the disulphide bridge that might be opened when using reducing agents. However, it could be shown that it remains intact during labelling processes [10.32]. Hynic-conjugated octreotide analogues have been proven to be particularly suitable for  $^{99m}\text{Tc}$  labelling [10.33]. Among them, [hynic-DPhe<sup>1</sup>,Tyr<sup>3</sup>]-octreotide was proven to be superior in patients compared to  $^{111}\text{In}$ -DTPA octreotide [10.34]. The resulting  $^{99m}\text{Tc}$  labelled peptide becomes highly stable and hydrophilic, especially when EDDA was used as the coligand. So far,  $^{99m}\text{Tc}$ -EDDA/hynic-TOC can be considered to be the most widely used  $^{99m}\text{Tc}$  labelled octreotide derivative [10.35]. A TATE derivative has also shown excellent diagnostic properties [10.36], allowing tumour visualization at an early post-injection interval.

A tetramine (N<sub>4</sub>) constitutes another promising chelator for preparing  $^{99m}\text{Tc}$  labelled peptides [10.37]. The tetramine chelator can be labelled at high specific activities under relatively mild conditions and is hydrophilic, due to the formation of a positively charged Tc-dioxo unit. The TATE derivative Demotate binds with high affinity to a SST receptor, and revealed high and specific uptake in a tumour model [10.38]. In a small number of patients,  $^{99m}\text{Tc}$ -Demotate showed excellent visualization of tumours as early as 1 h post-injection [10.39]. Figure 10.2 shows

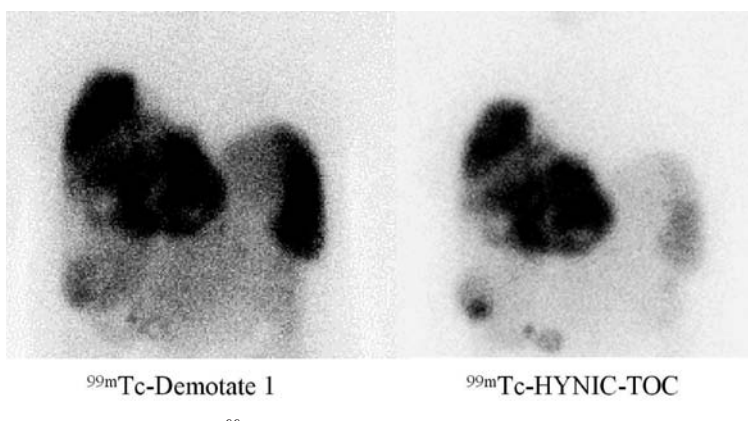


FIG. 10.2. Comparison of two  $^{99m}\text{Tc}$  labelled somatostatin analogues in the same patient. Left:  $^{99m}\text{Tc}$ -EDDA/hynic-TOC; right:  $^{99m}\text{Tc}$ -N<sup>4</sup>-Tyr<sup>3</sup>-octreotate (Demotate 1). Both images are planar images 4 h post-injection with an anterior view. Both peptides show a comparable biodistribution with clear delineation of massive tumour masses in the liver and visualization of metastases in the intestinal tract.

a comparison of two  $^{99m}\text{Tc}$  labelled somatostatin analogues based on hynic and N<sub>4</sub> chelators in the same patient. Cyclopentadienyltricarbonyltechnetium has also been used to prepare somatostatin analogues [10.40]. Due to its apolar character, cyclopentadienyl derivatization is not the method of choice for labelling highly hydrophilic small peptides.

## 10.4. OTHER $^{99m}\text{TC}$ LABELLED PEPTIDES TARGETING REGULATORY RECEPTORS

### 10.4.1. Neurotensin analogues

NT, a tridecapeptide with the sequence pGlu-Leu-Tyr-Glu-Asn-Lys-Pro-Arg-Arg-Pro-Tyr-Ile-Leu-OH, was originally isolated from bovine hypothalamus [10.41]. In mammals, NT is localized in the CNS as well as in peripheral tissues, where it is mainly found in the gastrointestinal tract. NT exerts a spectrum of physiological functions both in the CNS and in the periphery. Three NT receptor subtypes have been cloned so far [10.42], two of which (NTS1-R and NTS2-R) belong to the superfamily of G-protein-coupled receptors having the typical seven transmembrane domain configuration. A variety of tumours has been found to overexpress NT receptors. These include pancreatic adenocarcinoma, Ewing's sarcoma, astrocytoma and meningiomas, whereas expression in colorectal cancer is still controversial [10.43].

Technetium-99m labelled NT analogues are almost exclusively prepared by modifying the C terminal hexapeptide, H-Arg-Arg-Pro-Tyr-Ile-Leu-OH (NT(8–13)), which is the minimal fragment for biological activity [10.44]. One of the initial attempts to label NT analogues with  $^{99m}\text{Tc}$  was conducted using an N<sub>3</sub>S chelator (dimethylglycine-L-serine-L-cysteine-acetamidomethylglycine) [10.45]. Although these compounds showed high in vitro binding affinity, in vivo stability was very low. Accordingly, NT analogues stabilized at the most rapidly biodegradable sites in the NT(8–13) sequence, namely the Arg<sup>8</sup>–Arg<sup>9</sup> and the Tyr<sup>11</sup>–Ile<sup>12</sup> bonds, have been applied to  $^{99m}\text{Tc}$  labelling. A series of NT analogues derivatized with (N $\alpha$ -His)Ac for the  $^{99m}\text{Tc}(\text{CO})_3$  core or tetramines (N<sub>4</sub>) for the  $^{99m}\text{Tc}$ -dioxo core was developed based on increasing knowledge of sequence stabilization.

Technetium-99m(CO)<sub>3</sub> labelled (N $\alpha$ -His)Ac-Lys<sup>8</sup>- $\psi$ (CH<sub>2</sub>NH)-Arg<sup>9</sup>-Pro-Tyr-Tle-Leu-OH is the first compound that satisfies both high stability and highly specific tumour uptake in an animal model [10.46]. This  $^{99m}\text{Tc}$  labelled peptide was used for an initial clinical study [10.47]. Four patients with ductal pancreatic adenocarcinoma were followed by scintigraphy up to 4 h post-injection. Although immunohistochemistry revealed NT receptor expression in two of the

four patients, only one patient with higher receptor expression showed tracer accumulation in the tumour. In a continuation of their work, Garcia-Garoya developed analogues with improved stability, which resulted in higher tumour uptake [10.48].

Another group developed  $^{99m}\text{Tc}$  labelled NT analogues using  $\text{N}_4$  chelators. A first series of compounds showed considerably improved stability compared to  $^{99m}\text{Tc}$  labelled analogues of native sequence, while high and specific tumour uptake in a mouse model was shown [10.49]. In a continuation of their work, the group introduced further improvements in the synthetic strategy, developing analogues based on a Dab9 substitution and stabilizing Pos 11–12 [10.50]. One analogue (Demotensin 6) showed high stability, high tumour uptake and can be conveniently synthesized on a solid phase support. This analogue seems to be the most promising candidate for this chelator at this stage.

All together, a number of  $^{99m}\text{Tc}$  labelled NT analogues are available. However, their clinical impact still has to be proven in clinical trials.

#### 10.4.2. Bombesin analogues targeting the gastrin-releasing peptide receptor

BBN is a neuropeptide consisting of 14 amino acids, which was originally isolated from the skin of the frog *Bombina bombina*. It shows high affinity for the gastrin-releasing peptide (GRP) receptor. BBN and its mammalian counterpart, GRP, which consists of 27 amino acids, share the amidated seven amino acid C terminal sequence, Trp-Ala-Val-Gly-His-Leu-Met-NH<sub>2</sub>. Four BBN receptor subtypes have been characterized [10.51]. The subtypes are classified as the neuromedin B subtype (BB1), the GRP subtype (BB2), the orphan receptor subtype (BB3) and the BBN receptor subtype (BB4). It has been shown that BB2 is especially overexpressed in prostate, breast, pancreas and small cell lung cancer (SCLC). A special focus of application has been dedicated to target prostate cancer with radiolabelled BBN analogues, as the expression of BB2 receptors in non-neoplastic prostatic tissue and in benign prostatic hyperplasia incidence was low or lacking [10.52]. In addition, endogenous expression of the receptor is limited to neuroendocrine cells in the pulmonary and gastrointestinal tracts. Consequently, a number of radiolabelled analogues have been developed, utilizing the C terminal seven amino acid sequence. Besides radiolabelling with trivalent metals,  $^{99m}\text{Tc}$  labelling has been a major focus of development [10.53]. Most  $^{99m}\text{Tc}$  labelled BBN derivatives developed so far are based on BBN(7–14)NH<sub>2</sub>.

A variety of chelating systems have been applied, including P<sub>2</sub>S<sub>2</sub>, N<sub>2</sub>S<sub>2</sub>, N<sub>3</sub>S and N<sub>4</sub> chelator systems, as well as chelators for the  $^{99m}\text{Tc}(\text{CO})_3$  core. [ $^{99m}\text{Tc}] \text{P}_2\text{S}_2\text{-5-Ava-BBN}(7\text{--}14)\text{NH}_2$  was synthesized [10.54] with high affinity and stability using a prelabelling procedure. A subsequent study using

6,8-bis-[3-(bis(hydroxymethyl)phosphanyl)-propylsulphanyl]octanoic acid as a bifunctional chelator system [10.55] indicated that the P<sub>2</sub>S<sub>2</sub> systems can be conveniently used for labelling peptides with diagnostic (<sup>99m</sup>Tc) and therapeutic (<sup>188</sup>Re) radionuclides via a post-conjugation approach in high yields. Derivatives based on the P<sub>2</sub>S<sub>2</sub> system showed both a renal and hepatobiliary excretion pattern.

A number of approaches have been conducted using N<sub>3</sub>S systems. A limited series of <sup>99m</sup>Tc labelled N<sub>3</sub>S-X-BBN(7–14)NH<sub>2</sub> derivatives were synthesized by covalent coupling of the N<sub>3</sub>S chelator system, (dimethyl)Gly-Ser-Cys-Gly, via a spacer group X (X = 0, β-Ala, 5-Ava, 8-Aoc, or 11-Aun) with the peptide [10.56]. The biodistribution in non-tumour bearing CF-1 mice, along with cell binding studies, suggested that conjugates with X = β-Ala, 5-Ava or 8-Aoc were promising candidates for further evaluation. Further investigations were carried out with a 5-aminovaleric acid (5-Ava) spacer containing analogue, [<sup>99m</sup>Tc]N<sub>3</sub>S-5-Ava-BBN(7–14)NH<sub>2</sub> (<sup>99m</sup>Tc-RP527). An initial study in patients showed selective uptake in four of six breast carcinomas and in one of four prostate carcinomas, irrespectively of lesion size at 5 to 6 h post-injection [10.57]. GPR receptor mediated uptake was supported by visualization of the pancreas, a GPR receptor expressing organ, in those patients where the pancreas was in the field of view.

Another group used hynic derivatized Lys-BBN [10.58] and labelled with <sup>99m</sup>Tc using EDDA as a coligand. The resulting complex showed rapid internalization in PC3 cells and high tumour (PC3 cells) uptake in a mouse model.

N<sub>4</sub> chelator systems [10.59] were applied to prepare <sup>99m</sup>Tc labelled BBN analogues based on the Tc-dioxo core. The resulting conjugates showed high affinity and good tumour:background ratios, allowing visualization of the tumour in murine models using a gamma camera. It is especially interesting to note that the receptor antagonist [<sup>99m</sup>Tc]Demobesin 1, showed very promising imaging characteristics, with a high tumour uptake value despite lacking internalization.

A number of attempts to radiolabel BBN derivatives have also been performed using the Tc(I)-tricarbonyl core with a combination of a variety of chelators. Whereas 2-picolyamine-N,N-diacetic acid (PADA) showed selectivity problems [10.60], BBN(7–14)N derivatized with Na-histidinyl acetate achieved high specific activity [10.61]. The <sup>99m</sup>Tc labelled compound showed high affinity and receptor mediated uptake in the pancreas. However, low tumour uptake in a PC3 model was also observed. Smith et al. [10.62] used a bidentate chelating system combined with a four amino acid spacer (Dpr-Ser-Ser-Ser) for labelling BBN(7–14)NH<sub>2</sub>. The addition of a monodentate ligand reduced the organ and blood retention of the <sup>99m</sup>Tc labelled compound, whereas receptor mediated uptake in the tumour and pancreas was higher in a mouse PC3 model.

Overall, a number of  $^{99m}\text{Tc}$  labelled BBN derivatives has been developed. The high proportion of hepatobiliary excretion for most derivatives, which hinders abdominal imaging, still constitutes a major challenge. Clinical data are limited to date and further studies are warranted.

#### **10.4.3. Gastrin/cholecystokinin analogues**

Gastrin and cholecystokinin (CCK) are regulatory peptides with multiple functions in the gastrointestinal tract and the brain. These functions are mediated by two specific receptors, CCK-1 and CCK-2/gastrin receptors. CCK-2 (formerly CCK-B/gastrin) receptors have recently become increasingly interesting as targets for nuclear medicine applications. A high incidence of CCK-2 receptors has been found on human samples of medullary thyroid cancer (MTC), SCLC and stromal ovarian cancers [10.63]. The expression of CCK-2 receptors in gastrointestinal neuroendocrine tumours is of high importance in patients with negative somatostatin receptor scintigraphy [10.64]. Indium-111 labelled analogues of both CCK [10.65] and gastrin [10.66] have been developed and have shown that detection of CCK-2 receptor positive tissue in patients is feasible.

In a comparison to  $^{99m}\text{Tc}$  labelled analogues of minigastrin, von Guggenberg reported a very high receptor affinity for  $^{99m}\text{Tc}-(\text{CO})_3(\text{Na}-\text{His})\text{Ac}$  minigastrin. The same peptide derivatized with hydrazide and labelled with  $^{99m}\text{Tc}$  using EDDA as a coligand resulted in rapid uptake and high retention in CCK-2 receptor positive tumours, with very low retention in tissues except for an extraordinarily high kidney uptake [10.67]. Shortening of the peptide sequence resulted in an improvement of targeting properties but also lower in vitro stability [10.68]. Similar results were observed by others using a HIS-modified sequence [10.69]. Using an N<sub>4</sub> chelator, Nock et al. prepared  $^{99m}\text{Tc}$  labelled minigastrin analogues with high receptor affinity. These  $^{99m}\text{Tc}$  labelled peptides also exhibited lower kidney uptake than their hydrazide counterparts [10.70]. Clear visualization of the tumour was observed in a patient with medullary thyroid carcinoma. Laverman et al. used cholecystokinin (CCK8) peptides derivatized with hydrazide for labelling with  $^{99m}\text{Tc}$ . Using tricine/nicotinic acid as coligands, high specific activity and high stability were achieved. Using the sulphated analogue, high affinity for the CCK-1 receptor was also reached and specific uptake in a mouse tumour model was shown [10.71].

#### **10.4.4. Other peptides**

Melanocortin-1 (MC1) receptors are overexpressed in melanomas, and a number of radiolabelled  $\alpha$ -melanocyte stimulating hormone derivatives have been

developed [10.72]. Interestingly, a directly  $^{99m}\text{Tc}$  labelled derivative resulted in a cyclization of the peptide via technetium, leading to an increase in stability and, finally, to a very high tumour uptake in an animal model [10.73]. Clinical studies have not been reported so far and the clinical impact remains a matter of discussion.

VIP is another interesting candidate for receptor scintigraphy. However, it exemplifies the challenges that have to be tackled when dealing with regulatory peptides. VIP regulates its functions via VPAC1 and VPAC2 receptors. VPAC1, especially, is overexpressed in adenocarcinomas and  $^{123}\text{I}$  labelled VIP has been successfully used for targeting these receptors [10.74]. The challenges are, on the one hand, receptor expression as VPAC1 receptors also show a high physiological expression, especially in liver and lung tissues, making imaging of tumours in these tissues difficult. Secondly, VIP is intrinsically very unstable and limited knowledge is available to stabilize the peptide. Additionally, derivatization with chelators is difficult, since both carboxyl and amino terminals seem to be required for receptor interaction [10.75]. Thakur et al. attempted to label VIP using an H-Gly-DAla-Gly-Gly sequence attached to an amino butyric acid linker at the C terminal of VIP<sub>28</sub> [10.76]. Eleven patients were studied and breast tumours could be delineated as early as 20 min post-injection of [ $^{99m}\text{Tc}$ ]TP3654. However, limited results have been reported about the stability of this peptide and the characterization of the complex.

The possible use of neuropeptide Y (NPY) as a novel radiopeptide was investigated by Langer et al. [10.77]. NPY is a 36 amino acid peptide, and exerts its action via six different receptor subtypes (Y1–6). Its receptors are overexpressed in neuroblastoma and breast cancer. The Tc-tricarbonyl technology using PADA as a bifunctional chelating agent was applied. The resulting peptide, Ac-[Ahx5-24,K4( $^{99m}\text{Tc}(\text{CO})_3\text{-PADA}$ )]-NPY, showed high affinity to the Y2 receptor and promising in vivo properties. Further studies on this receptor have not so far been reported.

## 10.5. SUMMARY AND CONCLUSION

Technetium-99m remains a very good choice for labelling highly selective regulatory peptides. The last decade has seen a vast increase in labelling technologies and in knowledge about receptor targeting, including pharmacokinetic tailoring leading to development of a number of  $^{99m}\text{Tc}$  labelled peptides for tumour targeting. For targeting the somatostatin receptor, several peptide conjugates have been proven to be of significant clinical impact and value. For other receptors, several candidates are in the pipeline, especially targeting gastrin/CCK-2, BBN/GRP and NT receptors. Clinical evaluation will show which of these compounds will be of diagnostic significance in the future.

## REFERENCES TO CHAPTER 10

- [10.1] REUBI, J.C., Peptide receptors as molecular targets for cancer diagnosis and therapy, *Endocr. Rev.* **24** (2003) 389–427.
- [10.2] KNEIFEL, S., et al., Local targeting of malignant gliomas by the diffusible peptidic vector 1,4,7,10-tetraazacyclododecane-1-glutaric acid-4,7,10-triacetic acid-substance p, *Clin. Cancer Res.* **12** (2006) 3843–3850.
- [10.3] VIRGOLINI, I., et al., Vasoactive intestinal peptide-receptor imaging for the localization of intestinal adenocarcinomas and endocrine tumors, *N. Engl. J. Med.* **331** (1994) 1116–1121.
- [10.4] HESSENIUS, C., et al., Vasoactive intestinal peptide receptor scintigraphy in patients with pancreatic adenocarcinomas or neuroendocrine tumours, *Eur. J. Nucl. Med. Mol. Imaging* **27** (2000) 1684–1693.
- [10.5] MELIS, M., et al., Localisation and mechanism of renal retention of radiolabelled somatostatin analogues, *Eur. J. Nucl. Med. Mol. Imaging* **32** (2005) 1136–1143.
- [10.6] DE JONG, M., et al., Internalization of radiolabelled [DTPA<sup>0</sup>]octreotide and [DOTA<sup>0</sup>,Tyr<sup>3</sup>]octreotide: peptides for somatostatin receptor-targeted scintigraphy and radionuclide therapy, *Nucl. Med. Commun.* **19** (1998) 283–288.
- [10.7] STORCH, D., et al., Evaluation of [<sup>99m</sup>Tc/EDDA/HYNIC0]octreotide derivatives compared with [<sup>111</sup>In-DOTA<sup>0</sup>,Tyr<sup>3</sup>, Thr<sup>8</sup>]octreotide and [<sup>111</sup>In-DTPA<sup>0</sup>]octreotide: Does tumor or pancreas uptake correlate with the rate of internalization? *J. Nucl. Med.* **46** (2005) 1561–1569.
- [10.8] GINJ, M., et al., Radiolabeled somatostatin receptor antagonists are preferable to agonists for in vivo peptide receptor targeting of tumors, *Proc. Natl. Acad. Sci. USA* **103** (2006) 16436–16441.
- [10.9] LIU, S., EDWARDS, D.S., <sup>99m</sup>Tc-labeled small peptides as diagnostic radiopharmaceuticals, *Chem. Rev.* **99** (1999) 2235–2268.
- [10.10] DECristoforo, C., MATHER, S.J., The influence of chelator on the pharmacokinetics of <sup>99m</sup>Tc-labeled peptides, *Q. J. Nucl. Med.* **46** (2002) 195–205.
- [10.11] LISTER-JAMES, J., MOYER, B.R., DEAN, R.T., Small peptides radiolabeled with <sup>99m</sup>Tc, *Q. J. Nucl. Med.* **40** (1996) 221–233.
- [10.12] RUSCKOWSKI, M., et al., A comparison in monkeys of <sup>99m</sup>Tc labelled to a peptide by 4 methods, *J. Nucl. Med.* **42** (2001) 1870–1877.
- [10.13] DECristoforo, C., MATHER, S.J., <sup>99m</sup>Tc-somatostatin analogues — effect of labelling methods and peptide sequence, *Eur. J. Nucl. Med.* **26** (1999) 869–876.
- [10.14] ONO, M., et al., Plasma protein binding of <sup>99m</sup>Tc-labeled hydrazino nicotinamide derivatized polypeptides and peptides, *Nucl. Med. Biol.* **28** (2001) 155–164.
- [10.15] SCHIBLI, R., et al., Influence of the denticity of ligand systems on the in vitro and in vivo behavior of <sup>99m</sup>Tc(I)-tricarbonyl complexes: a hint for the future functionalization of biomolecules, *Bioconjug. Chem.* **11** (2000) 345–351.
- [10.16] GARCIA-GARAYOA, E., et al., In vitro and in vivo evaluation of new radiolabeled neurotensin(8-13) analogues with high affinity for NT1 receptors, *Nucl. Med. Biol.* **28** (2001) 75–84.

- [10.17] SMITH, C.J., et al., Radiochemical investigations of gastrin-releasing peptide receptor-specific [ $^{99m}\text{Tc}(\text{X})(\text{CO})_3$ -Dpr-Ser-Ser-Ser-Gln-Trp-Ala-Val-Gly-His-Leu-Met-(NH<sub>2</sub>)] in PC-3, tumor-bearing, rodent models: syntheses, radiolabeling, and in vitro/in vivo studies where Dpr = 2,3-diaminopropionic acid and X = H<sub>2</sub>O or P(CH<sub>2</sub>OH)<sub>3</sub>, *Cancer Res.* **63** (2003) 4082–4088.
- [10.18] BÉHÉ, M., et al., Use of polyglutamic acids to reduce uptake of radiometal-labeled minigastrin in the kidneys, *J. Nucl. Med.* **46** (2005) 1012–1015.
- [10.19] UEHARA, T., et al., Design, synthesis, and evaluation of [ $^{188}\text{Re}$ ]organorhenium-labeled antibody fragments with renal enzyme-cleavable linkage for low renal radioactivity levels, *Bioconjug. Chem.* **18** (2007) 190–198.
- [10.20] ANTUNES, P., et al., Influence of different spacers on the biological profile of a DOTA-somatostatin analogue, *Bioconjug. Chem.* **18** (2007) 84–92.
- [10.21] WESTER, H.J., et al., Comparison of radioiodinated TOC, TOCA and Mtr-TOCA: the effect of carbohydration on the pharmacokinetics, *Eur. J. Nucl. Med. Mol. Imaging* **29** (2002) 28–38.
- [10.22] PATEL, Y.C., et al., The somatostatin receptor family, *Life Sci.* **57** (1995) 1249–1265.
- [10.23] DE JONG, M., et al., Comparison of  $^{111}\text{In}$ -labeled somatostatin analogues for tumor scintigraphy and radionuclide therapy, *Cancer Res.* **58** (1998) 437–441.
- [10.24] GINJ, M., et al., Preclinical evaluation of new and highly potent analogues of octreotide for predictive imaging and targeted radiotherapy, *Clin. Cancer Res.* **11** (2005) 1136–1145.
- [10.25] KOLAN, H., LI, J., THAKUR, M.L., Sandostatin labeled with  $^{99m}\text{Tc}$ : in vitro stability, in vivo validity and comparison with  $^{111}\text{In}$ -DTPA-octreotide, *Peptide Res.* **9** (1996) 144–150.
- [10.26] ZAMORA, P.O., et al., Experimental radiotherapy of receptor-positive human prostate adenocarcinoma with  $^{188}\text{Re}$ -RC-160, a directly-radiolabeled somatostatin analogue, *Int. J. Cancer* **66** (1996) 214–220.
- [10.27] MAINA, T., et al., Synthesis, radiochemistry and biological evaluation of a new somatostatin analogue (SDZ 219-387) labelled with technetium-99m, *Eur. J. Nucl. Med.* **21** (1994) 437–444.
- [10.28] GUHLKE, S., et al.,  $^{188}\text{Re}$ -and  $^{99m}\text{Tc}$ -MAG3 as prosthetic groups for labeling amines and peptides: approaches with pre-and postconjugate labelling, *Nucl. Med. Biol.* **25** (1998) 621–631.
- [10.29] PEARSON, D.A., et al., Somatostatin receptor-binding peptides labeled with technetium-99m: chemistry and initial biological studies, *J. Med. Chem.* **36** (1996) 1361–1371.
- [10.30] BLUM, J.E., HANDMAKER, H., RINNE, N.A., The utility of a somatostatin-type receptor binding peptide radiopharmaceutical (P829) in the evaluation of solitary pulmonary nodules, *Chest* **115** (1999) 224–232.
- [10.31] CYR, J.E., et al., Somatostatin receptor-binding peptides suitable for tumor radiotherapy with Re-188 or Re-186. Chemistry and initial biological studies, *J. Med. Chem.* **50** (2007) 1354–1364.
- [10.32] UEHARA, T., et al., The integrity of the disulfide bond in a cyclic somatostatin analog during  $^{99m}\text{Tc}$  complexation reactions, *Nucl. Med. Biol.* **26** (1999) 883–890.

- [10.33] DECRISTOFORO, C., et al.,  $^{99m}\text{Tc}$ -HYNIC-[Tyr<sup>3</sup>]-octreotide for imaging somatostatin-receptor-positive tumors: preclinical evaluation and comparison with  $^{111}\text{In}$ -octreotide, *J. Nucl. Med.* **41** (2000) 1114–1119.
- [10.34] DECRISTOFORO, C., et al.,  $^{99m}\text{Tc}$ -EDDA/HYNIC-TOC: a new  $^{99m}\text{Tc}$ -labelled radiopharmaceutical for imaging somatostatin receptor-positive tumours: first clinical results and intra-patient comparison with  $^{111}\text{In}$ -labelled octreotide derivatives, *Eur. J. Nucl. Med.* **27** (2000) 1318–1325.
- [10.35] GABRIEL, M., et al., An intrapatient comparison of  $^{99m}\text{Tc}$ -EDDA/HYNIC-TOC with  $^{111}\text{In}$ -DTPA-octreotide for diagnosis of somatostatin receptor-expressing tumors, *J. Nucl. Med.* **44** (2003) 708–716.
- [10.36] HUBALEWSKA-DYDEJCZYK, A., et al.,  $^{99m}\text{Tc}$ -EDDA/HYNIC-octreotate scintigraphy, an efficient method for the detection and staging of carcinoid tumours: results of 3 years' experience, *Eur. J. Nucl. Med. Mol. Imaging* **33** (2006) 1123–1133.
- [10.37] MAINA, T., et al., “Synthesis, radiochemistry and biological evaluation of  $^{99m}\text{Tc}[\text{N}4-(\text{D})\text{-PHE}^1]$ -octreotide, a new octreotide derivative with high affinity for somatostatin receptors”, *Technetium and Rhenium in Chemistry and Nuclear Medicine* (NICOLINI, M., BANOLI, M., MAZZI, U., Eds), Vol. 4, SG Editoriali, Padova (1995) 395–400.
- [10.38] MAINA, T., et al., [ $^{99m}\text{Tc}$ ]Demotate, a new  $^{99m}\text{Tc}$ -based [Tyr<sup>3</sup>]octreotate analogue for the detection of somatostatin receptor-positive tumours: synthesis and preclinical results, *Eur. J. Nucl. Med. Mol. Imaging* **29** (2002) 742–753.
- [10.39] DECRISTOFORO, C., et al.,  $^{99m}\text{Tc}$ -Demotate 1: first data in tumour patients-results of a pilot/phase I study, *Eur. J. Nucl. Med. Mol. Imaging* **30** (2003) 1211–1219.
- [10.40] SPRADAU, T.W., et al., Synthesis and biological evaluation of Tc-99m-cyclopentadienyltricarbonyltechnetium-labeled octreotide, *Nucl. Med. Biol.* **26** (1999) 1–7.
- [10.41] CARRAWAY, R., LEEMAN, S.E., The isolation of a new hypotensive peptide, neurotensin, from bovine hypothalami, *J. Biol. Chem.* **248** (1973) 6854–6861.
- [10.42] VINCENT, J.P., MAZELLA, J., KITABGI, P., Neurotensin and neurotensin receptors, *Trends Pharmacol. Sci.* **20** (1999) 302–309.
- [10.43] REUBI, J.C., et al., Neurotensin receptors in human neoplasms: high incidence in Ewing's sarcomas, *Int. J. Cancer* **82** (1999) 213–218.
- [10.44] GRANIER, C., et al., Synthesis and characterization of neurotensin analogues for structure/activity relationship studies. Acetyl-neurotensin-(8–13) is the shortest analogue with full binding and pharmacological activities, *Eur. J. Biochem.* **124** (1982) 117–124.
- [10.45] CHAVATTE, K., et al., “Rhenium and technetium-99m oxocomplexes of neurotensin (8–13)”, *Technetium, Rhenium and Other Metals in Chemistry and Nuclear Medicine* (NICOLINI, M., MAZZI, U., Eds), Vol. 5, SEG Editoriali, Padova (1999) 513–525.
- [10.46] BRUEHLMEIER, M., et al., Stabilization of neurotensin analogues: effect on peptide catabolism, biodistribution and tumor binding, *Nucl. Med. Biol.* **29** (2002) 321–327.
- [10.47] BUCHEGGER, F., et al., Radiolabeled neurotensin analog,  $^{99m}\text{Tc}$ -NT-XI, evaluated in ductal pancreatic adenocarcinoma patients, *J. Nucl. Med.* **44** (2003) 1649–1454.

- [10.48] GARCIA-GARAYOA, E., et al., Double-stabilized neuropeptides as potential radiopharmaceuticals for NTR-positive tumors, *Nucl. Med. Biol.* **33** (2006) 495–503.
- [10.49] NOCK, B.A., et al., Toward stable N4-modified neuropeptides for NTS1-receptor-targeted tumor imaging with  $^{99m}\text{Tc}$ , *J. Med. Chem.* **49** (2006) 4767–4776.
- [10.50] MAINA, T., et al., [ $^{99m}\text{Tc}$ ]Demobesin 5 and 6 in the NTS1-R-targeted imaging of tumors: synthesis and preclinical results, *Eur. J. Nucl. Med. Mol. Imaging* **34** (2007) 1804–1814.
- [10.51] OHKI-HAMAZAKI, H., IWABUCHI, M., MAEKAWA, F., Development and function of bombesin-like peptides and their receptors, *Int. J. Dev. Biol.* **49** (2005) 293–300.
- [10.52] MARKWALDER, R., REUBI, J.C., Gastrin-releasing peptide receptors in the human prostate: relation to neoplastic transformation, *Cancer Res.* **59** (1999) 1152–1159.
- [10.53] MAINA, T., NOCK, B., MATHER, S., Targeting prostate cancer with radiolabelled bombesins, *Cancer Imaging* **6** (2006) 153–157.
- [10.54] KARRA, S.R., et al.,  $^{99m}\text{Tc}$ -labeling and in vivo studies of a bombesin analogue with a novel water-soluble dithiadiphosphine-based bifunctional chelating agent, *Bioconjug. Chem.* **10** (1999) 254–260.
- [10.55] GALI, H., et al., Synthesis, characterization, and labeling with  $^{99m}\text{Tc}/^{188}\text{Re}$  of peptide conjugates containing a dithia-bisphosphine chelating agent, *Bioconjug. Chem.* **12** (2001) 354–363.
- [10.56] SMITH, C.J., et al., Radiochemical investigations of  $^{99m}\text{Tc}-\text{N}_3\text{S-X-BBN}[7\text{-}14]\text{NH}_2$ : an in vitro/in vivo structure-activity relationship study where X = 0-, 3-, 5-, 8-, and 11-carbon tethering moieties, *Bioconjug. Chem.* **14** (2003) 93–102.
- [10.57] VAN DE WIELE, C., et al., Technetium-99m RP527, a GRP analogue for visualisation of GRP receptor-expressing malignancies: a feasibility study, *Eur. J. Nucl. Med.* **27** (2000) 1694–1699.
- [10.58] FERRO-FLORES, G., et al., Preparation and evaluation of  $^{99m}\text{Tc}$ -EDDA/HYNIC-[Lys<sup>3</sup>]-bombesin for imaging gastrin-releasing peptide receptor-positive tumors, *Nucl. Med. Commun.* **27** (2006) 371–376.
- [10.59] NOCK, B.A., et al., [ $^{99m}\text{Tc}$ ]Demobesin 1, a novel potent bombesin analogue for GRP receptor-targeted tumour imaging, *Eur. J. Nucl. Med. Mol. Imaging* **30** (2003) 247–258.
- [10.60] LA BELLA, R., et al., In vitro and in vivo evaluation of a  $^{99m}\text{Tc(I)}$ -labeled bombesin analogue for imaging of gastrin releasing peptide receptor-positive tumors, *Nucl. Med. Biol.* **29** (2002) 553–560.
- [10.61] LA BELLA, R., et al., A  $^{99m}\text{Tc(I)}$ -postlabeled high affinity bombesin analogue as a potential tumor imaging agent, *Bioconjug. Chem.* **13** (2002) 599–604.
- [10.62] SMITH, C.J., et al., Radiochemical investigations of gastrin-releasing peptide receptor-specific [ $^{99m}\text{Tc(X)(CO)3-Dpr-Ser-Ser-Gln-Trp-Ala-Val-Gly-His-Leu-Met-(NH}_2\text{)}$ ] in PC-3, tumor-bearing, rodent models: syntheses, radiolabeling, and in vitro/in vivo studies where Dpr = 2,3-diaminopropionic acid and X =  $\text{H}_2\text{O}$  or  $\text{P}(\text{CH}_2\text{OH})_3$ , *Cancer Res.* **63** (2003) 4082–4088.
- [10.63] REUBI, J.C., SCHÄFER, J.C., WASER, B., Cholecystokinin (CCK)-A and CCK-B/gastrin receptors in human tumors, *Cancer Res.* **57** (1997) 1377–1386.

- [10.64] GOTTHART, M., et al., Scintigraphy with In-111-DTPA-D-Glu<sup>1</sup>-Minigastrin and In-111-DTPA-D-Phe<sup>1</sup>-Octreotide in patients with gastrointestinal neuroendocrine tumors: results of the first 60 patients, *Eur. J. Nucl. Med. Mol. Imaging* **30** (2003) S181–S189.
- [10.65] DE JONG, M., et al., Preclinical and initial clinical evaluation of <sup>111</sup>In-labeled nonsulfated CCK<sub>8</sub> analog: a peptide for CCK-B receptor-targeted scintigraphy and radionuclide therapy, *J. Nucl. Med.* **40** (1999) 2081–2087.
- [10.66] BÉHÉ, M.P., et al., Improved kinetic stability of DTPA-D-Glu as compared with conventional monofunctional DTPA in chelating indium and yttrium: preclinical and initial clinical evaluation of radiometal labelled minigastrin derivatives, *Eur. J. Nucl. Med. Mol. Imaging* **30** (2003) 1140–1146.
- [10.67] VON GUGGENBERG, E., et al., <sup>99m</sup>Tc-labeling, in vitro and in vivo evaluation of HYNIC and (N<sub>α</sub>-His)-acetic acid modified [D-Glu<sup>1</sup>]-Minigastrin, *Bioconjug. Chem.* **15** (2004) 864–871.
- [10.68] VON GUGGENBERG, E., et al., <sup>99m</sup>Tc-labelled HYNIC-minigastrin with reduced kidney uptake for targeting of CCK-2 receptor-positive tumours, *Eur. J. Nucl. Med. Mol. Imaging* **34** (2007) 1209–1218.
- [10.69] MATHER, S.J., et al., Selection of radiolabeled gastrin analogs for peptide receptor-targeted radionuclide therapy, *J. Nucl. Med.* **48** (2007) 615–622.
- [10.70] NOCK, B.A., et al., CCK-2/gastrin receptor-targeted tumor imaging with <sup>99m</sup>Tc-labeled minigastrin analogs, *J. Nucl. Med.* **46** (2005) 1727–1736.
- [10.71] LAVERMAN, P., et al., Two technetium-99m-labeled cholecystokinin-8 (CCK8) peptides for scintigraphic imaging of CCK receptors, *Bioconjug. Chem.* **15** (2004) 561–568.
- [10.72] MIAO, Y., QUINN, T.P., Alpha-melanocyte stimulating hormone peptide-targeted melanoma imaging, *Front. Biosci.* **12** (2007) 4514–4524.
- [10.73] CHEN, J., et al., Melanoma-targeting properties of (99m)technetium-labeled cyclic alpha-melanocyte-stimulating hormone peptide analogues, *Cancer Res.* **60** (2000) 5649–5658.
- [10.74] VIROGOLINI, I., et al., Vasoactive intestinal peptide-receptor imaging for the localization of intestinal adenocarcinomas and endocrine tumors, *N. Engl. J. Med.* **331** (1994) 1116–1121.
- [10.75] CHAKDER, S., RATTAN, S., The entire vasoactive intestinal polypeptide molecule is required for the activation of the vasoactive intestinal polypeptide receptor: functional and binding studies on opossum internal anal sphincter smooth muscle, *J. Pharmacol. Exp. Ther.* **266** (1993) 392–399.
- [10.76] THAKUR, M.L., et al., <sup>99m</sup>Tc-labeled vasoactive intestinal peptide analog for rapid localization of tumors in humans, *J. Nucl. Med.* **41** (2000) 107–110.
- [10.77] LANGER, M., et al., <sup>99m</sup>Tc-labeled neuropeptide Y analogues as potential tumor imaging agents, *Bioconjug. Chem.* **12** (2001) 1028–1034.

## Chapter 11

### TECHNETIUM-99m ANNEXIN-A5 FOR APOPTOSIS IMAGING

Y. KUGE

Department of Pathofunctional Bioanalysis,  
Graduate School of Pharmaceutical Sciences,  
Kyoto University, Kyoto, Japan

#### Abstract

The chapter highlights  $^{99m}\text{Tc}$  labelled annexin-A5 (annexin V) for single photon emission computed tomography imaging of apoptosis. Annexin-A5 specifically binds to membrane bound phosphatidylserine that is exposed on the outer surface of the cell membrane during apoptosis. Accordingly, apoptotic cells can be detected using annexin-A5 labelled with radioactive agents, such as  $^{99m}\text{Tc}$ . To date, several  $^{99m}\text{Tc}$ -annexin-A5 radioligands have been developed using different types of bifunctional chelating agents. Each  $^{99m}\text{Tc}$ -annexin-A5 radioligand has different pharmaceutical properties and biological behaviours. Among these  $^{99m}\text{Tc}$ -annexin-A5 radioligands,  $^{99m}\text{Tc}$ -hynic-annexin-A5-(tricine)<sub>2</sub> has been the most widely applied radiopharmaceutical for basic and clinical studies. So far,  $^{99m}\text{Tc}$ -hynic-annexin-A5(tricine)<sub>2</sub> is the best candidate for apoptosis imaging; however, the biodistribution profiles of these compounds are not optimal. Improvement of the biodistribution profile of radiolabelled annexin-A5 is a key issue in the development of apoptosis imaging agents. The main features, limitations and future perspectives of apoptosis imaging with a variety of  $^{99m}\text{Tc}$  labelled annexin-A5 derivatives are discussed.

#### 11.1. INTRODUCTION

Apoptosis plays a crucial role in normal physiology and many disease processes [11.1]. Apoptosis is also deeply involved in tumour pathology, as pronounced loss in normal apoptosis leads to excessive cell proliferation and subsequent tumour development [11.2]. In addition, it is known that several chemotherapeutic drugs and irradiation induce apoptosis in both normal tissues and tumours [11.3]. Induction of apoptosis is directly connected with tumour response to chemotherapy or radiotherapy. Thus, non-invasive assessment of apoptosis appears to provide clinicians with useful information on tumour pathology and therapeutic efficacy. In these regards, apoptosis detecting radiopharmaceuticals have been extensively studied. This review highlights  $^{99m}\text{Tc}$

labelled annexin-A5 (annexin V) for single photon emission computed tomography (SPECT) imaging of apoptosis and discusses the main features, limitations and future perspectives of apoptosis imaging with  $^{99m}\text{Tc}$  labelled annexin-A5.

## 11.2. PRINCIPLE OF APOPTOSIS IMAGING WITH ANNEXIN-A5

One of the earliest events in apoptosis is the externalization of phosphatidylserine (PS), a membrane phospholipid normally restricted to the inner leaflet of the lipid bilayer [11.4, 11.5]. Annexin-A5, a 36 kilodalton human protein, specifically binds to membrane bound PS with nanomolar affinity in the presence of calcium [11.6–11.9]. Accordingly, apoptotic cells can be detected using annexin-A5 labelled with fluorescent markers or radioactive agents, such as  $^{99m}\text{Tc}$  (Fig. 11.1). The annexin-A5 apoptosis assay was first reported by Koopman et al. to detect apoptosis in vitro using fluorescent labelled annexin-A5 [11.10, 11.11], and it was further developed by labelling annexin-A5 with a radionuclide for in vivo imaging of apoptosis [11.12, 11.13].

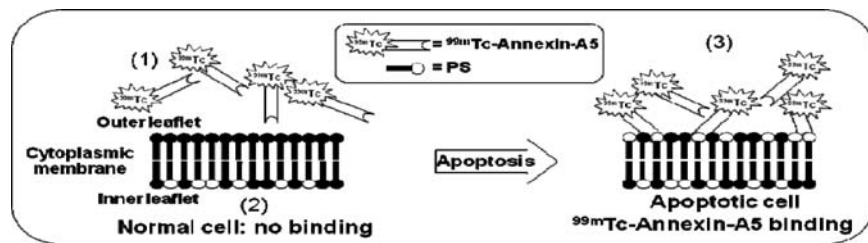


FIG. 11.1. Principle of apoptosis imaging with  $^{99m}\text{Tc}$ -annexin-A5. (1) Annexin-A5, a human protein with a high affinity for phosphatidylserine (PS), can be labelled with radionuclides such as  $^{99m}\text{Tc}$  ( $^{99m}\text{Tc}$ -annexin-A5). (2) In viable (normal) cells,  $^{99m}\text{Tc}$ -annexin-A5 cannot bind to PS since viable cells retain PS predominantly in the inner leaflet of the lipid bilayer. (3) During apoptosis, PS is exposed on the cell surface (outer leaflet) and apoptotic cells can be imaged with  $^{99m}\text{Tc}$ -annexin-A5.

### 11.3. TECHNETIUM-99m LABELLED ANNEXIN-A5 BY USE OF BIFUNCTIONAL CHELATING AGENTS

To date, several  $^{99\text{m}}\text{Tc}$ -annexin-A5 radioligands have been developed by different groups using different types of bifunctional chelating agents. Each  $^{99\text{m}}\text{Tc}$ -annexin-A5 radioligand has different pharmaceutical properties and biological behaviours (Table 11.1).

TABLE 11.1. PHARMACEUTICAL PROPERTIES AND BIOLOGICAL BEHAVIOUR OF VARIOUS  $^{99\text{m}}\text{Tc}$ -ANNEXIN-A5 CONJUGATED COMPLEXES [11.12, 11.13]

Radiopharmaceutical	Pharmaceutical properties and biological behaviours	Refs
$^{99\text{m}}\text{Tc}$ -BTAP-annexin-A5	<ul style="list-style-type: none"> <li>• <math>^{99\text{m}}\text{Tc}</math>-(4,5-bis(thioacetamido)pentanoyl)-annexin-A5</li> <li>• First <math>^{99\text{m}}\text{Tc}</math> labelled annexin-A5</li> <li>• <math>^{99\text{m}}\text{Tc}</math>-N2S2 complex by way of <math>^{99\text{m}}\text{Tc}</math>-gluconate and <math>^{99\text{m}}\text{Tc}</math>-N2S2-tetrafluorophenyl (TFP) ester</li> <li>• Complex labelling procedures (multistep reaction, including purification step)</li> <li>• Low radiochemical yield (RCY) (25–30%)</li> <li>• High uptake in the liver, kidneys and gut, with a relatively short biological half-life</li> <li>• Imaging apoptosis in the abdominal region is precluded</li> </ul>	[11.43–11.45]
$^{99\text{m}}\text{Tc}$ -hynic-annexin-A5-(tricine) <sub>2</sub>	<ul style="list-style-type: none"> <li>• <math>^{99\text{m}}\text{Tc}</math>-hydrazinonicotinamide-annexin-A5-(tricine)<sub>2</sub></li> <li>• Most widely used <math>^{99\text{m}}\text{Tc}</math> labelled annexin-A5; Broad applicability for apoptosis imaging</li> <li>• <math>^{99\text{m}}\text{Tc}</math>-hynic complex with tricine as a coligand</li> <li>• High RCY (<math>\approx 90\%</math>); No purification required</li> <li>• One step reaction with 30 min incubation</li> <li>• High uptake in the liver and kidneys, with a relatively long biological half-life</li> <li>• Relatively low abdominal uptake; Favourable imaging conditions in the abdominal region</li> <li>• Imaging apoptosis around the liver and kidneys is precluded</li> </ul>	[11.14, 11.17, 11.20]

TABLE 11.1. PHARMACEUTICAL PROPERTIES AND BIOLOGICAL BEHAVIOUR OF VARIOUS  $^{99m}\text{Tc}$ -ANNEXIN-A5 CONJUGATED COMPLEXES [11.12, 11.13] (cont.)

Radiopharmaceutical	Pharmaceutical properties and biological behaviours	Refs
$^{99m}\text{Tc}$ -imino-annexin-A5	<ul style="list-style-type: none"> <li>• <math>^{99m}\text{Tc}</math>-(N-1-imino-4-mercaptopbutyl)-annexin-A5</li> <li>• First nuclear probe used to image apoptosis in humans</li> <li>• Low RCY (<math>\approx 80\%</math>) with a 2 h incubation period</li> <li>• High uptake in the liver, kidneys, and gut with a long biological half-life</li> <li>• Imaging apoptosis in the abdominal region is precluded</li> </ul>	[11.44, 11.46]
$^{99m}\text{Tc}$ -EC-annexin-A5	<ul style="list-style-type: none"> <li>• <math>^{99m}\text{Tc}</math>-ethylenedicystein-annexin-A5</li> <li>• N2S2 complex: ethylenedicysteine is conjugated to annexin-A5 using sulphonyl-N-hydroxy-succinimide and 1-ethyl-3-(3-dimethylaminopropyl) carbodiimide-HCl as coupling agents</li> <li>• Easy labelling procedure; Low RCY (<math>\approx 70\%</math>)</li> <li>• High uptake in the liver and kidneys</li> </ul>	[11.47]
$^{99m}\text{Tc}$ -hynic-EDDA-annexin-A5 ( $^{99m}\text{Tc}$ -EDDA-hynexin)	<ul style="list-style-type: none"> <li>• <math>^{99m}\text{Tc}</math>-hydrazinonicotinamide-annexin-A5 (N,N-ethylenediamine diacetic acid)</li> <li>• Low RCY (<math>\approx 30\%</math>)</li> <li>• Significantly higher uptake in the kidneys, but lower uptake in the liver, compared with <math>^{99m}\text{Tc}</math>-hynic-annexin-A5(tricine)<sub>2</sub></li> </ul>	[11.21, 11.22]
$^{99m}\text{Tc}$ -MAG3-annexin-A5	<ul style="list-style-type: none"> <li>• <math>^{99m}\text{Tc}</math>-mercaptoacetyltriglycine-annexin-A5</li> <li>• Annexin-A5 is conjugated with an N-hydroxysuccinimide ester of MAG3</li> <li>• High RCY (<math>\approx 90\%</math>); No purification required (1 h incubation at pH8.6)</li> <li>• Significantly lower uptake in the kidneys and liver, but higher uptake in the small intestine, compared with <math>^{99m}\text{Tc}</math>-hynic-annexin-A5-(tricine)<sub>2</sub></li> </ul>	[11.23]

TABLE 11.1. PHARMACEUTICAL PROPERTIES AND BIOLOGICAL BEHAVIOUR OF VARIOUS  $^{99m}\text{Tc}$ -ANNEXIN-A5 CONJUGATED COMPLEXES [11.12, 11.13] (cont.)

Radiopharmaceutical	Pharmaceutical properties and biological behaviours	Refs
$[^{99m}\text{Tc}(\text{CO})_3\text{PADA}]\text{-annexin-A5}$	<ul style="list-style-type: none"> <li>Tc(I)-tricarbonyl complex with pycolylamine-N,N-diacetic acid (PADA)</li> <li>Lower uptake in the kidneys, compared with <math>^{99m}\text{Tc}</math>-hynic-annexin-A5-(tricine)<sub>2</sub></li> </ul>	[11.24]
$[^{99m}\text{Tc}(\text{CO})_3\text{hynic}]\text{-annexin-A5}$	<ul style="list-style-type: none"> <li>Tc(I)-tricarbonyl complex with hynic</li> <li>Major uptake and retention in the liver and kidneys</li> </ul>	[11.25]
$^{99m}\text{Tc-C}_3(\text{BHam})_2\text{-annexin-A5}$	<ul style="list-style-type: none"> <li><math>^{99m}\text{Tc}</math>-N,N'-trimethylenedibenzohydroxamamide-annexin-A5</li> <li>High RCY (&gt;95%); No purification required</li> <li>Remarkably lower uptake in the kidneys, but slower blood clearance, compared with <math>^{99m}\text{Tc}</math>-hynic-annexin-A5-(tricine)<sub>2</sub></li> </ul>	[11.26]
$^{99m}\text{Tc}$ -annexin-A5-117	<ul style="list-style-type: none"> <li><math>^{99m}\text{Tc}</math>-(NH<sub>2</sub>Ala-Gly-Gly-Cys-Gly-His-Met)-annexin-A5</li> <li>Annexin-A5 mutant with endogenous chelation sites for <math>^{99m}\text{Tc}</math></li> <li>Rapid labelling reaction; RCY ≈ 90% after 40 min at room temperature</li> <li>Remarkably lower uptakes in the kidneys and liver, but slightly higher uptake in the gut, compared with <math>^{99m}\text{Tc}</math>-hynic-annexin-A5-(tricine)<sub>2</sub></li> </ul>	[11.30, 11.31]
$^{99m}\text{Tc}$ -annexin-A5-123	<ul style="list-style-type: none"> <li><math>^{99m}\text{Tc}</math>-(NH<sub>2</sub>Ala-His-His-His-His-His-Ala-Gln-Val)-Annexin-A5</li> <li>Annexin-A5 mutant with endogenous chelation sites for <math>^{99m}\text{Tc}</math></li> <li>Tc(I)-tricarbonyl complex; RCY ≈ 80% after 60 min at 37°C</li> </ul>	[11.33]

TABLE 11.1. PHARMACEUTICAL PROPERTIES AND BIOLOGICAL BEHAVIOUR OF VARIOUS  $^{99m}\text{Tc}$ -ANNEXIN-A5 CONJUGATED COMPLEXES [11.12, 11.13] (cont.)

Radiopharmaceutical	Pharmaceutical properties and biological behaviours	Refs
$^{99m}\text{Tc}$ -annexin-A5-128	<ul style="list-style-type: none"> <li><math>^{99m}\text{Tc}</math>-(NH<sub>2</sub>Ala-Gly-Gly-Cys-His)-annexin-A5</li> <li>Annexin-A5 mutant with endogenous chelation sites for <math>^{99m}\text{Tc}</math></li> <li>Rapid labelling reaction; RCY ≈ 90% after 60 min at 37°C</li> <li>Remarkably lower uptake in the kidneys and liver, but slightly higher uptake in the gut, compared with <math>^{99m}\text{Tc}</math>-hynic-annexin-A5(tricine)<sub>2</sub></li> </ul>	[11.32]
$^{99m}\text{Tc}$ -CC-annexin-13	<ul style="list-style-type: none"> <li><math>^{99m}\text{Tc}</math>-(Cys-Cys-Ala-Glu-Val-Leu-Arg-Gly-Thr-Val-Thr-Asp-Phe-Pro-Gly-OH)</li> <li>Labelled via <math>^{99m}\text{Tc}</math> nitrido intermediate; RCY ≈ 90%</li> <li>Remarkably lower accumulation in soft tissues, including the liver and kidneys, in comparison to <math>^{99m}\text{Tc}</math>-hynic-annexin-A5(tricine)<sub>2</sub></li> </ul>	[11.35]

Among these  $^{99m}\text{Tc}$ -annexin-A5 radioligands,  $^{99m}\text{Tc}$ -hynic-annexin-A5-(tricine)<sub>2</sub> has been the most widely applied radiopharmaceutical for basic [11.14–11.16] and clinical studies [11.17–11.19] (Fig. 11.2). Hynic annexin-A5 can be labelled rapidly and efficiently with  $^{99m}\text{Tc}$  by using tricine as a coligand in the presence of stannous ions. This conjugation method provides a stable  $^{99m}\text{Tc}$ -annexin-A5 complex with a radiochemical purity of >90%, without requiring additional purification [11.14, 11.20]. Initially, Blankenberg et al. successfully demonstrated the potential of  $^{99m}\text{Tc}$ -hynic-annexin-A5-(tricine)<sub>2</sub> in three animal models: hepatic apoptosis induced by an anti-Fas antibody, acute cardiac allograft rejection and cyclophosphamide treatment of B cell lymphoma [11.14]. Numerous studies have demonstrated the broad applicability of  $^{99m}\text{Tc}$ -hynic-annexin-A5-(tricine)<sub>2</sub> as a radiopharmaceutical for imaging apoptosis. In addition, clinical studies showed a relatively low accumulation of  $^{99m}\text{Tc}$ -hynic-annexin-A5-(tricine)<sub>2</sub> in the gut [11.17], compared with  $^{99m}\text{Tc}$ -BTAP-annexin-A5 and  $^{99m}\text{Tc}$ -imino-annexin-A5 (Table 11.1). The results indicate that  $^{99m}\text{Tc}$ -hynic-annexin-A5-(tricine)<sub>2</sub> provides favourable imaging conditions, particularly in the abdominal region. However, the high accumulation of  $^{99m}\text{Tc}$ -hynic-annexin-A5-(tricine)<sub>2</sub> in the kidneys and liver is still a major

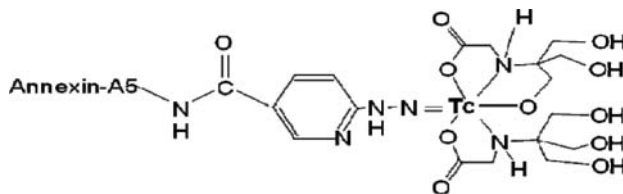


FIG. 11.2. Chemical structure of  $^{99m}\text{Tc}$ -hynic-annexin-A5-(tricine)<sub>2</sub>.

obstacle for imaging apoptosis around these organs. The development of conjugates with a better biodistribution profile, namely reduced accumulation in the kidneys and liver, is essential.

In an effort to decrease the high kidney and liver accumulation of  $^{99m}\text{Tc}$ -hynic-annexin-A5-(tricine)<sub>2</sub>, several bifunctional chelating agents have been examined [11.21–11.26] (Table 11.1). Vanderheyden et al. utilized MAG3 (mercaptoacetyltriglycine) as a chelator with  $^{99m}\text{Tc}$  [11.23], based on previous evidence that this method of radiolabelling can encourage rapid renal clearance of labelled biomolecules [11.27, 11.28]. They conjugated MAG3 to annexin-A5 using an N-hydroxysuccinimide ester of MAG3. High radiochemical purity (RCP  $\approx$  90%) was achieved without further purification by incubating MAG3 conjugated annexin-A5 with  $^{99m}\text{Tc}$ -pertechnetate under mildly basic pH conditions. Biodistribution data in normal mice clearly showed a significant decrease in kidney and liver accumulation of  $^{99m}\text{Tc}$ -MAG3-annexin-A5 at 1 h post-injection, compared with  $^{99m}\text{Tc}$ -hynic-annexin-A5-(tricine)<sub>2</sub> (from 45% injected dose (ID) to 15 %ID for the kidneys and 24 %ID to 4 %ID for the liver). Technetium-99m-MAG3-annexin-A5 also showed lower retention in the whole body, but higher accumulation in the small intestine than  $^{99m}\text{Tc}$ -hynic-annexin-A5-(tricine)<sub>2</sub>. These results indicate that the MAG3 radioligand provides better imaging conditions in the kidneys and liver, but worse conditions in the lower abdomen. Two different  $^{99m}\text{Tc}$ -tricarbonyl labelling methods [11.29] have also been applied to label annexin-A5 and were reported in abstracts [11.24, 11.25]. Han et al. reported a  $^{99m}\text{Tc}(\text{CO})_3(\text{H}_2\text{O})_3]^+$  was complexed with pycolylamine-N,N-diacetic acid (PADA) [11.24]. The remaining carboxylic group of PADA was then converted to an activated trifluorophenyl (TFP) ester and conjugated to annexin-A5. Preliminary biodistribution studies suggested that the kidney accumulation of this compound was improved, compared with that of  $^{99m}\text{Tc}$ -hynic-annexin-A5-(tricine)<sub>2</sub>. On the other hand, Chang et al. utilized hynic-annexin-A5 to obtain a  $\text{Tc(I)}$ -tricarbonyl complex [11.25]. Further investigation of the biodistribution profiles of these radiolabelled annexin-A5 derivatives and for targeting apoptosis is warranted. However, improvement of the biodistribution profile of

radiolabelled annexin-A5 is still a key issue in the development of apoptosis imaging agents.

#### 11.4. TECHNETIUM-99m LABELLED ANNEXIN-A5 MUTANTS WITH ENDOGENOUS CHELATION SITES

To simplify the preparation and radiolabelling of annexin-A5, Tait et al. investigated the addition of peptide sequences that directly form endogenous chelation sites for  $^{99m}\text{Tc}$  [11.30] (Table 11.1). Three annexin-A5 mutants called annexin-A5-116, annexin-A5-117 and annexin-A5-118 were constructed with N terminal extensions of seven amino acids containing either one or two cysteine residues and were expressed cytoplasmically in *Escherichia coli*. These annexin-A5 mutants could be labelled with  $^{99m}\text{Tc}$ , using  $\text{SnCl}_2$  as a reducing agent and glucoheptonate as an exchange agent. The labelling reaction was rapid, reaching a maximum ( $\text{RCY} \approx 90\%$ ) after 40 min at room temperature. The proteins retained binding activity for erythrocyte membranes with exposed PS after radiolabelling. In addition, cyclophosphamide induced apoptosis could be detected with  $^{99m}\text{Tc}$ -annexin-A5-117 [11.30, 11.31]. Biodistribution data in normal mice showed a marked decrease in the kidney and liver accumulation of  $^{99m}\text{Tc}$ -annexin-A5 mutants, particularly  $^{99m}\text{Tc}$ -annexin-A5-117 (6 %ID for the kidneys and 6 %ID for the liver), at 1 h post-injection, compared with  $^{99m}\text{Tc}$ -hynic-annexin-A5-(tricine)<sub>2</sub> (39 %ID for the kidneys and 16 %ID for the liver) [11.30]. On the other hand,  $^{99m}\text{Tc}$ -annexin-A5-117 showed slightly higher accumulation in the gut than  $^{99m}\text{Tc}$ -hynic-annexin-A5-(tricine)<sub>2</sub>. Results similar to  $^{99m}\text{Tc}$ -annexin-A5-117 were also obtained with  $^{99m}\text{Tc}$ -annexin-A5-128 [11.32]. Tait et al. also constructed two other annexin-A5 mutants (annexin-A5-122 and annexin-A5-123) with N terminal extensions containing either three or six histidine residues, in order to investigate whether the  $^{99m}\text{Tc}$ -carbonyl labelling method [11.29] would be suitable for annexin-A5 [11.33]. Using the Tc-carbonyl reagent, both mutant proteins could be labelled with  $^{99m}\text{Tc}$  with full retention of bioactivity. Unfortunately, the biodistribution profiles of  $^{99m}\text{Tc}$ -annexin-A5-122 and  $^{99m}\text{Tc}$ -annexin-A5-123 have not been reported.

#### 11.5. OTHER APPROACHES TO IMPROVE BIODISTRIBUTION PROFILES OF LABELLED COMPOUNDS

To improve the biodistribution profiles of  $^{99m}\text{Tc}$  labelled annexin-A5, small fragments of annexin-A5 were considered [11.34, 11.35] (Table 11.1). Mukherjee et al. investigated  $^{99m}\text{Tc}$  labelled 13 amino acid fragments of annexin-A5

(annexin-13), based on evidence that the PS specific sequence is attributable to the 13 amino acid sequence at the N terminal [11.35]. The annexin fragment was derivatized to contain cysteine, cysteine–cysteine or histidine in the amino acid sequence at the N terminus and was labelled with  $^{99m}\text{Tc}$  via nitrido and carbonyl precursors. The  $^{99m}\text{Tc}$  nitrido complex of cysteine-cysteine-annexin-13 ( $^{99m}\text{Tc}$ -CC-annexin-13) and the  $^{99m}\text{Tc}$  carbonyl complex of histidine-annexin-13 were obtained with high radiochemical yields. In vitro cell uptake studies with  $^{99m}\text{Tc}$ -CC-annexin-13 showed specific uptake in apoptotic HL-60 cells. Biodistribution studies of  $^{99m}\text{Tc}$ -CC-annexin-13 in fibrosarcoma tumour bearing mice revealed optimum tumour uptake with a remarkably lower accumulation in soft tissues, including the liver and kidneys, in comparison to  $^{99m}\text{Tc}$ -hynic-annexin-A5-(tricine)<sub>2</sub>. Thus,  $^{99m}\text{Tc}$ -CC-annexin-13 may deserve further evaluation, although Tait et al. indicated that all four domains of annexin-A5 are needed for maximum uptake in apoptotic organs *in vivo* [11.32].

Recently, Cauchon et al. attempted to visualize tumour apoptosis by PET using  $^{64}\text{Cu}$  labelled streptavidin (SAv), following pretargeting of apoptotic cells with biotinylated annexin-A5 [11.36]. In this study, apoptotic cells were first pretargeted with commercially available biotinylated annexin-A5. This was followed by an avidin chase to eliminate free biotinylated products. Subsequent administration of  $^{64}\text{Cu}$  labelled SAv allowed apoptotic tissues to be imaged by positron emission tomography. In this method, biodistribution of radioactivity follows that of  $^{64}\text{Cu}$  labelled SAv. The procedure can be applied to  $^{99m}\text{Tc}$  labelled SAv. In addition, other pretargeting methods that use hapten-antibody or complimentary DNA analogues have been reported to date [11.37]. Accordingly, the procedure may offer flexibility for controlling the biodistribution of radioactivity for imaging apoptosis with annexin-A5.

On the other hand, to improve the biodistribution profiles of  $^{99m}\text{Tc}$  labelled annexin-A5, it is essential to understand the reasons for the different biodistribution profiles among the radiolabelled annexin-A5. Although the mechanisms behind the different biodistribution profiles remain unclear, several studies have indicated the involvement of *in vivo* stability and protein binding of the labelled conjugates, in addition to the molecular sizes and lipophilicity of the chelating agents [11.38, 11.39]. Systematic investigation of these factors should help understand the mechanisms and improve the biodistribution profiles of  $^{99m}\text{Tc}$  labelled annexin-A5.

## 11.6. ANNEXIN-A5 LABELLED WITH OTHER RADIONUCLIDES

Although this review focused on  $^{99m}\text{Tc}$  labelled annexin-A5, there have been many reports on annexin-A5 labelled with other radionuclides, including

halogen radioisotopes ( $^{18}\text{F}$ ,  $^{123}\text{I}$ ,  $^{124}\text{I}$ ,  $^{125}\text{I}$ ) [11.12, 11.13]. Annexin-A5 was, in fact, first radiolabelled with  $^{125}\text{I}$  using the Iodo-Gen method by Tail et al. [11.40]. In humans, acquired images with  $^{123}\text{I}$  labelled annexin-A5 showed low lung uptake, resulting in good imaging conditions for the thoracic region. On the other hand, delayed imaging of the abdominal region was impeded due to extensive bowel activity [11.41]. Recently, Wen et al. developed a PEGylated annexin-A5 to increase the biological half-life of the protein [11.42]. The PEGylated annexin-A5 was labelled with  $^{111}\text{In}$ , taking advantage of the longer physical half-life of  $^{111}\text{In}$ . Approaches making good use of various radionuclides appear to be indispensable for the development of suitable radiolabelled annexin-A5 and in responding to wide ranging clinical demands, which may also provide useful information for improving  $^{99\text{m}}\text{Tc}$  labelled annexin-A5.

## 11.7. CONCLUSION

A variety of  $^{99\text{m}}\text{Tc}$  labelled annexin-A5 derivatives have been extensively studied as radiopharmaceuticals for detecting apoptosis. So far,  $^{99\text{m}}\text{Tc}$ -hynic-annexin-A5(tricine)<sub>2</sub> is the best candidate for apoptosis imaging. However, the biodistribution profiles of these compounds are not optimal. Improvement of the biodistribution profile of radiolabelled annexin-A5 is a key issue in the development of apoptosis imaging agents.

## REFERENCES TO CHAPTER 11

- [11.1] THOMPSON, C.B., Apoptosis in the pathogenesis and treatment of disease, *Science* **267** (1995) 1456–1462.
- [11.2] EVAN, G.I., VOUSDEN, K.H., Proliferation, cell cycle and apoptosis in cancer, *Nature* **411** (2001) 342–348.
- [11.3] KERR, J.F., WINTERFORD, C.M., HARMON, B.V., Apoptosis. Its significance in cancer and cancer therapy, *Cancer* **73** (1994) 2013–2026.
- [11.4] FADOK, V.A., et al., Exposure of phosphatidylserine on the surface of apoptotic lymphocytes triggers specific recognition and removal by macrophages, *J. Immunol.* **148** (1992) 2207–2216.
- [11.5] ZWAAL, R.F., SCHROIT, A.J., Pathophysiologic implications of membrane phospholipid asymmetry in blood cells, *Blood* **89** (1997) 1121–1132.
- [11.6] TAIT, J.F., GIBSON, D., FUJIKAWA, K., Phospholipid binding properties of human placental anticoagulant protein-I, a member of the lipocortin family, *J. Biol. Chem.* **264** (1989) 7944–7949.
- [11.7] ANDREE, H.A., et al., Binding of vascular anticoagulant alpha (VAC alpha) to planar phospholipid bilayers, *J. Biol. Chem.* **265** (1990) 4923–4928.

- [11.8] VAN HEERDE, W.L., DE GROOT, P.G., REUTELINGSPERGER, C.P., The complexity of the phospholipid binding protein Annexin V, *Thromb. Haemost.* **73** (1995) 172–179.
- [11.9] GERKE, V., MOSS, S.E., Annexins: from structure to function, *Physiol. Rev.* **82** (2002) 331–371.
- [11.10] KOOPMAN, G., et al., Annexin V for flow cytometric detection of phosphatidylserine expression on B cells undergoing apoptosis, *Blood* **84** (1994) 1415–1420.
- [11.11] VAN ENGELAND, M., NIELAND, L.J., RAMAEKERS, F.C., SCHUTTE, B., REUTELINGSPERGER, C.P., Annexin V-affinity assay: a review on an apoptosis detection system based on phosphatidylserine exposure, *Cytometry* **3** (1998) 1–9.
- [11.12] LAHORTE, C.M., et al., Apoptosis-detecting radioligands: current state of the art and future perspectives, *Eur. J. Nucl. Med. Mol. Imaging* **31** (2004) 887–919.
- [11.13] BOERSMA, H.H., et al., Past, present, and future of annexin A5: from protein discovery to clinical applications, *J. Nucl. Med.* **46** (2005) 2035–2050.
- [11.14] BLANKENBERG, F.G., et al., In vivo detection and imaging of phosphatidylserine expression during programmed cell death, *Proc. Natl Acad. Sci. USA* **95** (1998) 6349–6354.
- [11.15] BLANKENBERG, F.G., NAUMOVSKI, L., TAIT, J.F., POST, A.M., STRAUSS, H.W., Imaging cyclophosphamide-induced intramedullary apoptosis in rats using  $^{99m}\text{Tc}$ -radiolabeled annexin V, *J. Nucl. Med.* **42** (2001) 309–316.
- [11.16] MOCHIZUKI, T., et al., Detection of apoptotic tumor response in vivo after a single dose of chemotherapy with  $^{99m}\text{Tc}$ -annexin V, *J. Nucl. Med.* **44** (2003) 92–97.
- [11.17] KEMERINK, G.J., et al., Safety, biodistribution, and dosimetry of  $^{99m}\text{Tc}$ -HYNIC-annexin V, a novel human recombinant annexin V for human application, *J. Nucl. Med.* **44** (2003) 947–952.
- [11.18] VAN DE WIELE, C., et al., Quantitative tumor apoptosis imaging using technetium- $^{99m}\text{HYNIC}$  annexin V single photon emission computed tomography, *J. Clin. Oncol.* **21** (2003) 3483–3487.
- [11.19] ROTTEY, S., SLEGERS, G., VAN BELLE, S., GOETHALS, I., VAN DE WIELE, C., Sequential  $^{99m}\text{Tc}$ -hydrazinonicotinamide-annexin V imaging for predicting response to chemotherapy, *J. Nucl. Med.* **47** (2006) 1813–1818.
- [11.20] BLANKENBERG, F.G., VANDERHEYDEN, J.L., STRAUSS, H.W., TAIT, J.F., Radiolabeling of HYNIC-annexin V with technetium-99m for in vivo imaging of apoptosis, *Nature Protoc.* **1** (2006) 108–110.
- [11.21] VERBEKE, K., et al., Optimization of the preparation of  $^{99m}\text{Tc}$ -labeled Hynic-derivatized Annexin V for human use, *Nucl. Med. Biol.* **30** (2003) 771–778.
- [11.22] VERBEKE, K., et al., Influence of the co-ligand on the labeling and biodistribution of Tc-99m labeled Hynic-Annexin V, *Eur. J. Nucl. Med. Mol. Imaging* **29**(Suppl. 1) (2002) S369.
- [11.23] VANDERHEYDEN, J.L., et al., Evaluation of  $^{99m}\text{Tc}$ -MAG3-annexin V: influence of the chelate on in vitro and in vivo properties in mice, *Nucl. Med. Biol.* **33** (2006) 135–144.
- [11.24] HAN, E.S., et al., Labeling annexin V with  $^{99m}\text{Tc}$ -tricarbonyl PADA improved its organ clearance property, *J. Nucl. Med.* **43**(Suppl.) (2002) 374P.

- [11.25] CHANG, S.M., LAI, P.H., CHENG, H.W., LO, J.M.,  $^{99m}$ Tc(I) tricarbonyl labeled HYNIC-annexin V as a potential apoptosis imaging agent, *J. Nucl. Med.* **44**(Suppl.) (2003) 316P.
- [11.26] OGAWA, K., et al., A novel  $^{99m}$ Tc-labeled annexin V using bis(hydroxamamide)-based bifunctional chelating agent, *J. Nucl. Med.* **46**(Suppl.) (2005) 365P.
- [11.27] ZHANG, Y.M., LIU, N., ZHU, Z.H., RUSCKOWSKI, M., HNATOWICH, D.J., Influence of different chelators (HYNIC, MAG3 and DTPA) on tumor cell accumulation and mouse biodistribution of technetium-99m labeled to antisense DNA, *Eur. J. Nucl. Med.* **27** (2000) 1700–1707.
- [11.28] RUSCKOWSKI, M., et al., Inflammation and infection imaging with a  $^{99m}$ Tc-neutrophil elastase inhibitor in monkeys, *J. Nucl. Med.* **41** (2000) 363–374.
- [11.29] ALBERTO, R., SCHIBLI, R., EGLI, A., SCHUBIGER, A.P., A novel organometallic aqua complex of technetium for labeling of biomolecules: synthesis of  $[^{99m}\text{Tc}(\text{OH}_2)_3(\text{CO})_3]^+$  from  $[^{99m}\text{TcO}_4]^-$  in aqueous solution and its reaction with a bifunctional ligand, *J. Am. Chem. Soc.* **120** (1998) 7987–7988.
- [11.30] TAIT, J.F., BROWN, D.S., GIBSON, D.F., BLANKENBERG, F.G., STRAUSS, H.W., Development and characterization of annexin V mutants with endogenous chelation sites for  $^{99m}$ Tc, *Bioconjug. Chem.* **11** (2000) 918–925.
- [11.31] KUGE, Y., et al., Feasibility of  $^{99m}$ Tc-annexin V for repetitive detection of apoptotic tumor response to chemotherapy: an experimental study using a rat tumor model, *J. Nucl. Med.* **45** (2004) 309–312.
- [11.32] TAIT, J.F., SMITH, C., BLANKENBERG, F.G., Structural requirements for in vivo detection of cell death with  $^{99m}$ Tc-annexin V, *J. Nucl. Med.* **46** (2005) 807–815.
- [11.33] TAIT, J.F., SMITH, C., GIBSON, D.F., Development of annexin V mutants suitable for labeling with Tc(i)-carbonyl complex, *Bioconjug. Chem.* **13** (2002) 1119–1123.
- [11.34] BOISGARD, R., et al., A new SPECT tracer for improved apoptosis imaging in tumor bearing mice, *J. Nucl. Med.* **44**(Suppl.) (2003) 98P.
- [11.35] MUKHERJEE, A., et al.,  $^{99m}$ Tc-labeled annexin V fragments: a potential SPECT radiopharmaceutical for imaging cell death, *Nucl. Med. Biol.* **33** (2006) 635–643.
- [11.36] CAUCHON, N., et al., PET imaging of apoptosis with  $^{64}\text{Cu}$ -labeled streptavidin following pretargeting of phosphatidylserine with biotinylated annexin-V, *Eur. J. Nucl. Med. Mol. Imaging* **34** (2007) 247–258.
- [11.37] SHARKEY, R.M., GOLDENBERG, D.M., Advances in radioimmunotherapy in the age of molecular engineering and pretargeting, *Cancer Invest.* **24** (2006) 82–97.
- [11.38] ONO, M., et al., Control of radioactivity pharmacokinetics of  $99\text{mTc}$ -HYNIC-labeled polypeptides derivatized with ternary ligand complexes, *Bioconjug. Chem.* **13** (2002) 491–501.
- [11.39] ONO, M., et al., Plasma protein binding of ( $99\text{m}$ Tc)-labeled hydrazino nicotinamide derivatized polypeptides and peptides, *Nucl. Med. Biol.* **28** (2001) 155–164.
- [11.40] THIAGARAJAN, P., TAIT, J.F., Binding of annexin V/placental anticoagulant protein I to platelets. Evidence for phosphatidylserine exposure in the procoagulant response of activated platelets, *J. Biol. Chem.* **265** (1990) 17420–17423.
- [11.41] LAHORTE, C.M., et al., Biodistribution and dosimetry study of  $^{123}\text{I}$ -rh-annexin V in mice and humans, *Nucl. Med. Commun.* **24** (2003) 871–880.

- [11.42] WEN, X., et al., Improved radiolabeling of PEGylated protein: PEGylated annexin V for noninvasive imaging of tumor apoptosis, *Cancer Biother. Radiopharm.* **18** (2003) 819–827.
- [11.43] STRATTON, J.R., et al., Selective uptake of radiolabeled annexin V on acute porcine left atrial thrombi, *Circulation* **92** (1995) 3113–3121.
- [11.44] BOERSMA, H.H., et al., Comparison between human pharmacokinetics and imaging properties of two conjugation methods for  $^{99m}\text{Tc}$ -annexin A5, *Br. J. Radiol.* **76** (2003) 553–560.
- [11.45] KEMERINK, G.J., et al., Biodistribution and dosimetry of  $^{99m}\text{Tc}$ -BTAP-annexin-V in humans, *Eur. J. Nucl. Med. Mol. Imaging* **28** (2001) 1373–1378.
- [11.46] HOFSTRA, L., et al., Visualisation of cell death in vivo in patients with acute myocardial infarction, *Lancet* **356** (2000) 209–212.
- [11.47] YANG, D.J., et al., In vivo and in vitro measurement of apoptosis in breast cancer cells using  $^{99m}\text{Tc}$ -EC-annexin V, *Cancer Biother. Radiopharm.* **16** (2001) 73–83.



## Chapter 12

# TECHNETIUM-99m RADIOPHARMACEUTICALS FOR MONITORING DRUG RESISTANCE

H. AKIZAWA, T. UEHARA, Y. ARANO

Graduate School of Pharmaceutical Sciences, Chiba University,  
Chuo-ku, Chiba, Japan

### Abstract

Resistance to chemotherapy constitutes a major obstacle to cancer cures. Cellular mechanisms of resistance involve efflux pumps, P-glycoprotein (Pgp), the product of the MDR1 gene and the related membrane glycoprotein, multidrug resistance associated protein 1 (MRP1). Multidrug resistant cell lines overexpressing Pgp are resistant to a structurally and functionally diverse group of chemotherapeutic agents. Many of these drugs tend to be lipophilic and positively charged at neutral pH. This suggested the application of the two lipophilic cationic  $^{99m}$ Tc radiopharmaceuticals currently used for myocardial perfusion,  $^{99m}$ Tc-MIBI and  $^{99m}$ Tc-Tetrofosmin. Efforts were also made to develop specific  $^{99m}$ Tc labelled substrates for Pgp based on lipophilic cationic  $^{99m}$ Tc complexes. A large number of studies indicated that  $^{99m}$ Tc-MIBI,  $^{99m}$ Tc-Tetrofosmin and some related  $^{99m}$ Tc compounds are substrates for Pgp. However, it remains uncertain whether these  $^{99m}$ Tc labelled compounds are substrates for MRP1. Thus, both  $^{99m}$ Tc-MIBI and  $^{99m}$ Tc-Tetrofosmin would be general probes of transporter mediated multidrug resistance in tumour cells.

### 12.1. INTRODUCTION

Resistance to chemotherapy constitutes a major obstacle to cancer cures. Some tumours are intrinsically resistant to chemotherapy, whereas others initially respond to treatment but then acquire resistance during the treatment. Acquired resistance to a single drug may result in resistance to a diverse group of drugs that are structurally and functionally unrelated. Cellular mechanisms of resistance involve efflux pumps, P-glycoprotein (Pgp), the product of the MDR1 gene, and the related membrane glycoprotein, multidrug resistance associated protein 1 (MRP1). Both Pgp and MRP1 are members of the ATP-binding cassette (ABC) family of membrane transport proteins. Riordan et al. cloned a cDNA encoding p170, a glycoprotein that is increased in membranes from multidrug resistant cells [12.1] and Ueda et al. confirmed that the MDR1 gene codes for Pgp [12.2]. McGrath et al. found MRP1, a 190 kilodalton protein [12.3], and demonstrated that a cell line which exhibited a multidrug resistance (MDR) phenotype overexpressed MRP1 rather than Pgp [12.4]. Thus, a non-invasive method to

monitor the *in vivo* status of drug resistance constitutes an important diagnostic procedure for management and prognostic stratification of cancer patients. In this chapter,  $^{99m}\text{Tc}$  radiopharmaceuticals developed for monitoring MDR are described.

## 12.2. TECHNETIUM-99m-MIBI

Hexakis(2-methoxyisobutyl-isonitrile)technetium(I) ( $^{99m}\text{Tc}$ -MIBI) is a lipophilic complex cation that has been widely used for myocardial perfusion imaging (Fig. 12.1(a)). The fundamental myocardium uptake mechanism of  $^{99m}\text{Tc}$ -MIBI involves passive distribution across plasma and mitochondrial membranes, and at equilibrium,  $^{99m}\text{Tc}$ -MIBI is sequestered within mitochondria by the large negative transmembrane potentials [12.5]. Malignant tumours show increased transmembrane potentials due to increased metabolic requirements which induce increased accumulation of  $^{99m}\text{Tc}$ -MIBI [12.6].

Multidrug resistant cell lines overexpressing Pgp are resistant to a structurally and functionally diverse group of chemotherapeutic agents. Many of these drugs tend to be lipophilic and positively charged at neutral pH [12.7]. These features and the broad ligand binding properties of Pgp raised the

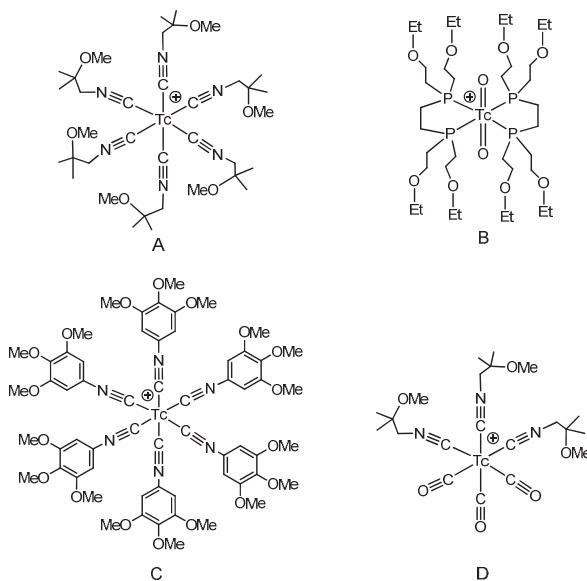


FIG. 12.1. Chemical structures of  $^{99m}\text{Tc}$ -MIBI (a),  $^{99m}\text{Tc}$ -Tetrofosmin (b),  $^{99m}\text{Tc}$ -TMPI (c) and  $^{99m}\text{Tc}$ -CO-MIBI (d).

possibility that a cationic lipophilic organotechnetium complex,  $^{99m}\text{Tc}$ -MIBI, would also be a transport substrate for Pgp. Piwnica-Worms and co-workers examined the cellular pharmacological profile of  $^{99m}\text{Tc}$ -MIBI transport in cell lines which express modestly low, intermediate and very high levels of Pgp, respectively. Steady state contents of  $^{99m}\text{Tc}$ -MIBI were consistent with enhanced extrusion of the agent by Pgp enriched cells. In vivo evaluation using  $^{201}\text{Tl}$  chloride as a perfusion tracer demonstrated that functional expression of Pgp was successfully visualized with  $^{99m}\text{Tc}$ -MIBI [12.8].

Ballinger et al. performed a similar study using a rat breast adenocarcinoma cell line and its drug resistant variant [12.9]. In vitro experiments showed that wild type cell lines exhibited higher accumulation of  $^{99m}\text{Tc}$ -MIBI than the drug resistant variant. The drug resistant variant showed enhanced accumulation of  $^{99m}\text{Tc}$ -MIBI in the presence of a Pgp modulator. When injected into rats bearing wild type and drug resistant tumours,  $^{99m}\text{Tc}$ -MIBI was excreted from the resistant tumours at three times the rate as from wild type tumours. The correlation between  $^{99m}\text{Tc}$ -MIBI accumulation and Pgp expression was also established by in vitro experiments [12.10, 12.11]. The level of Pgp expression determined by Western blotting was compared to  $^{99m}\text{Tc}$ -MIBI accumulation. Rao et al. confirmed that  $^{99m}\text{Tc}$ -MIBI accumulation declined as membrane Pgp expression increased in insect cells that were infected with a recombinant baculovirus carrying the human MDR1 cDNA [12.11]. Cordobes et al. showed that  $^{99m}\text{Tc}$ -MIBI uptake by cells expressing non-immunodetectable levels of Pgp was significantly higher than in cells expressing high Pgp levels using nine human breast tumour cell lines. Technetium- $^{99m}$ -MIBI uptake increased by a factor of two in the cells expressing no detectable Pgp and by a factor of 12 in the cells with high Pgp levels in the presence of verapamil, a known reverser of Pgp functions.

Clinical studies in patients with leukaemia, neural crest tumour, hepatocellular carcinoma or breast carcinoma demonstrated that  $^{99m}\text{Tc}$ -MIBI accumulation was inversely related to Pgp levels, as determined by flow cytometry, reverse transcription-polymerase chain reaction (RT-PCR) or immunohistochemical study [12.12–12.16].

The relationship between  $^{99m}\text{Tc}$ -MIBI accumulation in the tumour and the response to chemotherapy was determined in patients with small cell lung cancer and breast cancer [12.12, 12.17–12.20]. Kao et al. reported that 13 of 15 patients (ages 54–64 years) showed that the response to chemotherapy was correctly predicted by  $^{99m}\text{Tc}$ -MIBI chest single photon emission computed tomography (SPECT) images and that the correlation between tumour uptake ratios obtained by planar images and survival was both positive and good (correlation coefficient = 0.83). Del Vecchio et al. correlated  $^{99m}\text{Tc}$ -MIBI efflux rate to Pgp level in untreated breast carcinoma [12.21]. The efflux rates of  $^{99m}\text{Tc}$ -MIBI, calculated

from time–activity curves, were directly correlated with Pgp levels measured in the same tumours using an  $^{125}\text{I}$  labelled monoclonal antibody and in vitro quantitative autoradiography ( $r = 0.62$ ,  $p < 0.001$ ). Taki et al. also performed a similar study in patients with bone and soft tissue tumours [12.22]. The washout rates determined by comparing the images at 15 min and 3 h post-injection were higher in patients with high Pgp expression levels than in those with lower Pgp expression levels. These results demonstrated that  $^{99\text{m}}\text{Tc}$ -MIBI scintigraphy with washout analysis may be useful for the in vivo evaluation of Pgp status.

Since MRP1 is also involved in MDR, Hendrikse et al. conducted in vitro experiments to elucidate whether  $^{99\text{m}}\text{Tc}$ -MIBI is a substrate for MRP1 [12.23]. Technetium-99m-MIBI concentration decreased in the MRP1-overexpressing, but not in the Pgp-overexpressing GLC4/ADR sublines, and was lower in the MRP1-transfected subline S1-MRP than in the non-infected S1 cell line. Glutathione depletion elevated  $^{99\text{m}}\text{Tc}$ -MIBI concentration in GLC4/ADR. These results suggest that  $^{99\text{m}}\text{Tc}$ -MIBI efflux is influenced by MDR1 and MRP expression, and that this fact should be taken into consideration when  $^{99\text{m}}\text{Tc}$ -MIBI is tested for tumour efflux measurement.

Kao et al. also estimated the relationship between the degree of  $^{99\text{m}}\text{Tc}$ -MIBI accumulation and Pgp or MRP1 expression in patients with breast cancers [12.24]. The tumour:background ratios of  $^{99\text{m}}\text{Tc}$ -MIBI were lowest in the group with positive Pgp and MRP1 expression, and highest in the group with both negative Pgp and MRP1 expression. These results also showed that  $^{99\text{m}}\text{Tc}$ -MIBI scintigraphy is useful for determining Pgp and MRP1 expression in patients with breast cancers. Similar studies were performed by Burak et al. to evaluate the relationship between  $^{99\text{m}}\text{Tc}$ -MIBI washout rates and Pgp or MRP1 expression levels in patients with osteosarcoma. The level of MRP1 expression was significantly correlated with the washout rate of  $^{99\text{m}}\text{Tc}$ -MIBI. There was no significant difference between the  $^{99\text{m}}\text{Tc}$ -MIBI washout rate in tumours which co-expressed both proteins and tumours with high expression of either Pgp or MRP1. From these findings, they concluded that while  $^{99\text{m}}\text{Tc}$ -MIBI can be used as a general probe for functional imaging of both Pgp and MRP1, it is not capable of differentiating the functional status of either MRP-related glycoprotein [12.25].

Zhou et al. searched for correlations between both tumour uptake and washout of  $^{99\text{m}}\text{Tc}$ -MIBI with an MDR phenotype (Pgp, MRP and lung resistant protein) on protein and mRNA levels. A close correlation was found to exist between  $^{99\text{m}}\text{Tc}$ -MIBI late imaging, washout rates and Pgp expression. Contrary to the findings of other studies, they did not observe a correlation between tumour accumulation or efflux of  $^{99\text{m}}\text{Tc}$ -MIBI and the expression of MRP1 on protein or mRNA levels in lung cancer [12.26]. It has been documented that cardiac muscle shows low washout of  $^{99\text{m}}\text{Tc}$ -MIBI and a low level of Pgp expression, but a high

level of MRP expression [12.27, 12.28]. Depleted glutathione levels have been reported with reduced MRP mediated  $^{99m}$ Tc-MIBI transport [12.29]. Increased glutathione levels have been observed with resistance to alkylating agents and cisplatin [12.30]. A significant correlation was also found between resistance to doxorubicin and the expression of glutathione-S-transferase (GST), an enzyme that catalyses the glutathione conjugation reaction [12.31]. From these studies, they suggested that  $^{99m}$ Tc-MIBI imaging may be related to the levels of glutathione and GST, which reflects the functionality of MRP mediated transport.

Thus, there has been a lot of evidence that  $^{99m}$ Tc-MIBI is a substrate for Pgp and that the radiopharmaceutical is useful for monitoring Pgp expression levels in tumour cells by *in vivo* imaging. However, further studies on the relationship between MRP1, glutathione and GST expression levels, and  $^{99m}$ Tc-MIBI efflux rates should be undertaken to elucidate MRP1 mediated washout of  $^{99m}$ Tc-MIBI.

### 12.3. TECHNETIUM-99m-TETROFOSMIN

A  $^{99m}$ Tc(V) complex of 1,2-bis[bis(2-ethoxyethyl)phosphino]ethane called  $^{99m}$ Tc-Tetrofosmin (Fig. 12.1(b)) is another radiopharmaceutical currently being used as a myocardial perfusion imaging agent; it is also a lipophilic cationic compound. Ballinger et al. studied  $^{99m}$ Tc-Tetrofosmin in sensitive and multidrug resistant rodent and human breast tumour cell lines *in vitro* to determine whether  $^{99m}$ Tc-Tetrofosmin, as  $^{99m}$ Tc-MIBI, is a substrate for Pgp [12.32]. Technetium-99m-Tetrofosmin and  $^{99m}$ Tc-MIBI accumulated extensively in both sensitive cell lines. In contrast, multidrug resistant cell lines accumulated very little of either tracer, but the accumulation was increased by addition of a modulator in a dose dependent manner. From these results, the researchers concluded that  $^{99m}$ Tc-Tetrofosmin shares with  $^{99m}$ Tc-MIBI the property of being a substrate for Pgp and is, thus, potentially useful for functional imaging of tumour Pgp status.

Technetium-99m-Tetrofosmin offers possible formulation advantages over  $^{99m}$ Tc-MIBI, such as room temperature reconstitution from a lyophilized kit and faster clearance from the liver. Thus, Chen et al. undertook a full characterization of  $^{99m}$ Tc-Tetrofosmin as a transport substrate of Pgp and related ABC transporters, and evaluated the radiopharmaceutical as a reporter of the relative potency of newer MDR modulators that are in clinical trials [12.33]. Their studies supported the hypothesis that  $^{99m}$ Tc-Tetrofosmin is outwardly transported to the extracellular space by Pgp. They also found that while  $^{99m}$ Tc-Tetrofosmin may be transported by human MRP1, the differences in  $^{99m}$ Tc-Tetrofosmin net uptake produced by MRP1 expression were significantly less than the differences produced by Pgp expression. Utsunomiya et al. compared the accumulation and efflux kinetics of  $^{99m}$ Tc-MIBI and  $^{99m}$ Tc-Tetrofosmin in an MRP expressing

tumour cell line [12.34]. They observed that both  $^{99m}\text{Tc}$ -Tetrofosmin and  $^{99m}\text{Tc}$ -MIBI exhibited similar transport characteristics. In particular,  $^{99m}\text{Tc}$ -MIBI and  $^{99m}\text{Tc}$ -Tetrofosmin displayed similar accumulation and efflux rates and comparable inhibition profiles. The only difference worth noting was that  $^{99m}\text{Tc}$ -MIBI accumulated in the cells to a two times greater degree than did  $^{99m}\text{Tc}$ -Tetrofosmin.

In clinical studies, Pgp or MRP1 expression limits the sensitivity of  $^{99m}\text{Tc}$ -Tetrofosmin parathyroid imaging for localizing parathyroid adenomas [12.35, 12.36]. The same research group also showed that  $^{99m}\text{Tc}$ -Tetrofosmin scintigraphy correlated well with Pgp or MRP1 expression and concluded that the reagent is useful for predicting the response to chemotherapy in patients with small cell lung cancer, non-small cell lung cancer and lymphoma [12.37–12.40]. The other group also demonstrated a correlation between  $^{99m}\text{Tc}$ -Tetrofosmin retention and therapeutic resistance in patients with lung and breast cancer although Pgp and MRP1 expression were not determined [12.41, 12.42].

Thus, a number of studies show that  $^{99m}\text{Tc}$ -Tetrofosmin is useful for predicting the response to chemotherapy in a manner similar to  $^{99m}\text{Tc}$ -MIBI. However, Le Jeune et al. reported that the two radiopharmaceuticals may not be used interchangeably. They compared the behaviour of  $^{99m}\text{Tc}$ -Tetrofosmin and  $^{99m}\text{Tc}$ -MIBI in MRP1 positive and negative human glioma cell lines and demonstrated that  $^{99m}\text{Tc}$ -MIBI levels were inversely proportional to the cell MDR phenotype, while  $^{99m}\text{Tc}$ -Tetrofosmin levels were not [12.43]. This result indicated that, in contrast with  $^{99m}\text{Tc}$ -MIBI,  $^{99m}\text{Tc}$ -Tetrofosmin was not an MRP1 probe in glioma cells. Their later study suggested that the difference between the two agents was attributable to a relatively slower catalytic efficiency of formation of monoglutathionyl-conjugates of  $^{99m}\text{Tc}$ -Tetrofosmin compared to  $^{99m}\text{Tc}$ -MIBI [12.44]. Further studies of the reaction of the two  $^{99m}\text{Tc}$  complexes with glutathione may provide further insight into understanding the role played by the two radiopharmaceuticals for clinical applications of MDR monitoring.

## 12.4. OTHER COMPOUNDS

The successful application of  $^{99m}\text{Tc}$ -MIBI for Pgp functional imaging stimulated the development of more specific substrates for Pgp based on lipophilic cationic  $^{99m}\text{Tc}$  labelled compounds. A combination of potent functionalities of known MDR transport substrates and reversal agents (such as methoxyaryl moieties of colchicines, verapamil or reserpine analogues) with the lipophilic cationic character of the hexakis metal(I)-isonitrile complexes was used to design new agents for functional detection and in vivo modulation of MDR Pgp. A series of substituted aromatic isonitriles of  $^{99m}\text{Tc}$  and Re complexes

was synthesized and evaluated [12.16]. In vitro tracer accumulation studies in cells overexpressing Pgp suggested that methoxy functionalities confer Pgp recognition. Together with the results of biodistribution and imaging studies, they concluded that 8 of 21 complexes showed biological promise. Based on the results, the same research group evaluated a 3,4,5-trimethoxyphenylisonitrile analogue,  $^{99}\text{Tc}$ -TMPI (Fig. 12.1(c)), to assess its potential as a Pgp modulator [12.45].  $^{99\text{m}}\text{Tc}$ -TMPI showed net cellular accumulation in inverse proportion to its Pgp level, and accumulation was enhanced by the addition of classic MDR modulators. The carrier-added  $^{99}\text{Tc}$ -TMPI complex at pharmacological concentrations showed potent inhibition of Pgp-mediated  $^{99\text{m}}\text{Tc}$ -MIBI transport. These results suggest that this compound may serve as a convenient template for development of non-radioactive Re(I) analogues as novel MDR modulators.

The advent of  $[\text{Tc}(\text{CO})_3(\text{OH}_2)_3]^+$  chemistry also stimulated the application of the novel Tc(I) precursor for the development of functional imaging agents of MDR. Dyszlewski et al. prepared a  $^{99\text{m}}\text{Tc}$ (I)-tricarbonyl complex,  $[^{99\text{m}}\text{Tc}(\text{CO})_3(\text{MIBI})_3]^+$  (Tc-CO-MIBI, Fig. 12.1(d)) [12.46]. Technetium-99m-CO-MIBI showed sixtyfold higher accumulation in drug sensitive cells compared to colchicine selected drug resistant cells. However, the transport of  $^{99\text{m}}\text{Tc}$ -CO-MIBI by MRP1 was modest. From these results, they suggested that  $^{99\text{m}}\text{Tc}$ -CO-MIBI would be specifically excluded by overexpression of Pgp and that the agent would constitute a functional probe of Pgp transport activity *in vivo*.

$\text{N}_2\text{O}_2\text{P}_2$ -technetium(III) complexes (the so called Q series, Fig. 12.2(a)) are a general class of non-reducible mixed ligand  $^{99\text{m}}\text{Tc}$  coordination molecules also developed for myocardial perfusion imaging agents [12.47]. These compounds are stable monocovalent cations where two lipophilic phosphine substituents and a planar Schiff base ligand fill the coordination sphere of the technetium(III) core. Since the phosphine compounds and the Schiff base ligand can be modified to prepare appropriate lipophilic  $^{99\text{m}}\text{Tc}$  cationic complexes, efforts were also made to prepare  $^{99\text{m}}\text{Tc}$  labelled compounds for MDR imaging.

Piwnica-Worms and co-workers evaluated the potential of a series of  $^{99\text{m}}\text{Tc}$ -Q compounds as agents for functional imaging of MDR [12.48, 12.49]. Thirty-seven  $^{99\text{m}}\text{Tc}$ -Q compounds were synthesized, screened by tracer assay with human drug sensitive epidermal carcinoma and drug resistant cells that expressed non-immunodetectable and modest levels of Pgp. Only three of the compounds showed transport distinctions between drug sensitive and drug resistant cell lines that were equal to or greater than  $^{99\text{m}}\text{Tc}$ -MIBI and  $^{99\text{m}}\text{Tc}$ -Tetrofosmin. A biodistribution study showed that two of the three compounds, trans-(2,2'-(1,2-ethanediyldiimino)bis(1,5-methoxy-5-methyl-4-

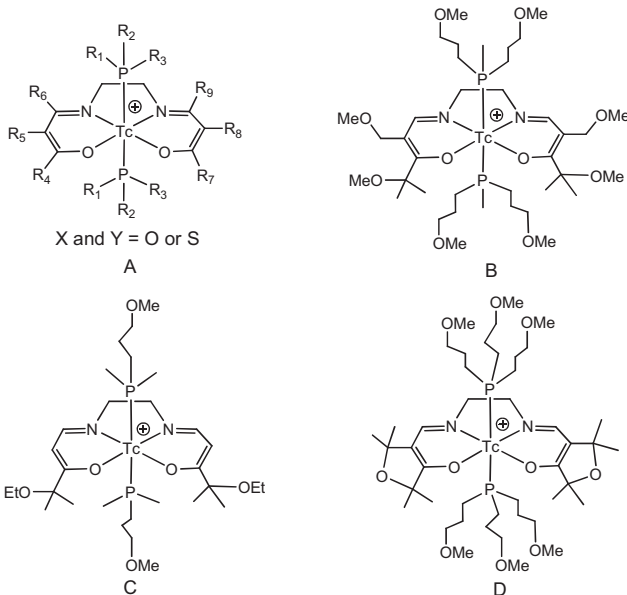


*FIG. 12.2. Chemical structures of  $^{99m}\text{Tc}$ -Q compounds (a),  $^{99m}\text{Tc}$ -Q58 (b),  $^{99m}\text{Tc}$ -Q63 (c) and  $^{99m}\text{Tc}$ -Q12 (d).*

oxo-hexenyl))bis[methylbis(3-methoxy-1-propyl)phosphine]Tc(III) ( $^{99m}\text{Tc}$ -Q58, Fig. 12.2(b)) and trans-[5,5'-(1,2-ethanediylidimino)bis(2-ethoxy-2-methyl-3-oxo-4-pentenyl)]bis[dimethyl(3-methoxy-1-propyl)phosphine]]Tc(III) ( $^{99m}\text{Tc}$ -Q63, Fig. 12.2(c)), would satisfy the requirement of a radiopharmaceutical for imaging the functional status of Pgp at the blood-brain barrier *in vivo*. Ballinger et al. also evaluated another Q compound, Q12, trans-(1,2-bis(dihydro-2,2,5,5-tetramethyl-3(2H)furanone-4-methyleneimino)ethane)bis(tris(3-methoxy-1-propyl) phosphine) technetium(III)-99m ( $^{99m}\text{Tc}$ -furifosmin, Fig. 12.2(d)) [12.50], which was originally developed as a myocardial perfusion agent [12.51]. The *in vitro* behaviour of  $^{99m}\text{Tc}$ -furifosmin was similar to that of  $^{99m}\text{Tc}$ -MIBI and  $^{99m}\text{Tc}$ -TFos, in that drug sensitive cells accumulated much more radioactivity than drug resistant cells, and the addition of a Pgp modulator increased the accumulation in the resistant cells but not in the sensitive cells. Technetium-99m-furifosmin accumulated rapidly in drug sensitive cells and washed out with a mean half-life of 78 min, which was significantly slower than from drug resistant cells (46 min). From these results, the researchers concluded that  $^{99m}\text{Tc}$ -furifosmin was suitable for functional imaging of MDR. Despite promising results, further studies of  $^{99m}\text{Tc}$ -Q compounds have not been reported so far.

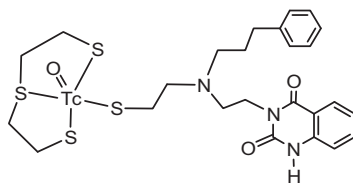


*FIG. 12.3. Chemical structure of a Pgp substrate  $^{99\text{m}}\text{Tc}$  compound based on the '3+1' concept.*

The '3+1' mixed ligand Tc complex constitutes another chemical design of  $^{99\text{m}}\text{Tc}$  radiopharmaceuticals [12.52, 12.53]. Based on their previous studies of this series of  $^{99\text{m}}\text{Tc}$  complexes, Johannsen and co-workers investigated the applicability of this kind of compounds for functional imaging of MDR [12.54]. Five complexes were prepared using 2-mercaptoproethyl sulphide as a tridentate ligand and five different monothiol compounds as a monodentate ligand. Among them, (3-thiapentane-1,5-dithiolato)[[N-(3-phenylpropyl)-N-2(3-quinazoline-2,4-dionyl)-ethyl]amino-ethylthiolato] oxotechnetium(V) ( $^{99/99\text{m}}\text{Tc}1$ , Fig. 12.3) showed the most effective inhibition of efflux of  $^{99\text{m}}\text{Tc}$ -MIBI from rat brain endothelial cells expressing Pgp. Two-dimensional scatter plots of  $^{99\text{m}}\text{Tc}$ -MIBI/[<sup>18</sup>F]FDG uptake showed typical changes of known Pgp inhibitors. The effect of  $^{99}\text{Tc}1$  on in vivo distribution of  $^{99\text{m}}\text{Tc}$ -MIBI and [<sup>18</sup>F]FDG in rats was also comparable with the effects of verapamil. From these studies, the researchers concluded that  $^{99/99\text{m}}\text{Tc}1$  is a transporter substrate and a potential inhibitor of Pgp.

## 12.5. CONCLUSIONS

Technetium-99m radiopharmaceuticals for monitoring drug resistance have been briefly reviewed. Although efforts have been made to develop new  $^{99\text{m}}\text{Tc}$  labelled compounds that improve diagnostic information,  $^{99\text{m}}\text{Tc}$ -MIBI and  $^{99\text{m}}\text{Tc}$ -Tetrofosmin are the current radiopharmaceuticals of choice in clinical studies to monitor MDR of tumour cells. However, it should be kept in mind that a deficit of  $^{99\text{m}}\text{Tc}$ -MIBI activity within tumour cells can be related to several contradictory biological phenomena: poor accessibility of  $^{99\text{m}}\text{Tc}$ -MIBI to the tumour, decreased viability and electrical gradients in 'over-aged' and hypoxic cells, loss of influx in cells at an early stage of apoptosis owing to a decrease in their electrical gradient, lack of retention in resistant cells mediated by multidrug resistant proteins and/or overexpression of the anti-apoptotic protein Bcl-2, preventing mitochondrial accumulation [12.55]. Thus,  $^{99\text{m}}\text{Tc}$ -MIBI and probably other related  $^{99\text{m}}\text{Tc}$  radiopharmaceuticals are unable to differentiate tumours with ongoing apoptosis from the developing drug resistance. MRP1 mediated

transport is a double edged sword when monitoring MDR of tumour cells. On the one hand, the apparent specificity of the tracers for functional imaging of Pgp in tumours is reduced; but on the other hand, this property may favourably enable  $^{99m}$ Tc-MIBI and some related  $^{99m}$ Tc radiopharmaceuticals to be general probes of transporter mediated MDR in tumour cells [12.33]. Further development of  $^{99m}$ Tc radiopharmaceuticals is required to differentiate the above mentioned status of tumour cells.

## REFERENCES TO CHAPTER 12

- [12.1] RIORDAN, J.R., et al., Amplification of P-glycoprotein genes in multidrug-resistant mammalian cell lines, *Nature* **316** (1985) 817–819.
- [12.2] UEDA, K., et al., The mdr1 gene, responsible for multidrug-resistance, codes for P-glycoprotein, *Biochem. Biophys. Res. Commun.* **141** (1986) 956–962.
- [12.3] MCGRATH, T., CENTER, M.S., Adriamycin resistance in HL60 cells in the absence of detectable P-glycoprotein, *Biochem. Biophys. Res. Commun.* **145** (1987) 1171–1176.
- [12.4] MCGRATH, T., et al., Mechanisms of multidrug resistance in HL60 cells. Analysis of resistance associated membrane proteins and levels of mdr gene expression, *Biochem. Pharmacol.* **38** (1989) 3611–3619.
- [12.5] PIWNICA-WORMS, D., KRONAUGE, J.F., CHIU, M.L., Uptake and retention of hexakis (2-methoxyisobutyl isonitrile) technetium(I) in cultured chick myocardial cells. Mitochondrial and plasma membrane potential dependence, *Circulation* **82** (1990) 1826–1838.
- [12.6] KABASAKAL, L., et al., Technetium-99m sestamibi uptake in human breast carcinoma cell lines displaying glutathione-associated drug-resistance, *Eur. J. Nucl. Med.* **23** (1996) 568–570.
- [12.7] FORD, J.M., HAIT, W.N., Pharmacology of drugs that alter multidrug resistance in cancer, *Pharmacol. Rev.* **42** (1990) 155–199.
- [12.8] PIWNICA-WORMS, D., et al., Functional imaging of multidrug-resistant P-glycoprotein with an organotechnetium complex, *Cancer Res.* **53** (1993) 977–984.
- [12.9] BALLINGER, J.R., et al.,  $^{99}\text{Tc}^{\text{m}}$ -sestamibi as an agent for imaging P-glycoprotein-mediated multi-drug resistance: In vitro and in vitro studies in a rat breast tumour cell line and its doxorubicin-resistant variant, *Nucl. Med. Commun.* **16** (1995) 253–257.
- [12.10] CORDOBES, M.D., et al., Technetium-99m-sestamibi uptake by human benign and malignant breast tumor cells: Correlation with mdr gene expression, *J. Nucl. Med.* **37** (1996) 286–289.
- [12.11] RAO, V.V., et al., Expression of recombinant human multidrug resistance P-glycoprotein in insect cells confers decreased accumulation of technetium-99m-sestamibi, *J. Nucl. Med.* **35** (1994) 510–515.
- [12.12] TAKAMURA, Y., et al., Prediction of chemotherapeutic response by Technetium 99m-MIBI scintigraphy in breast carcinoma patients, *Cancer* **92** (2001) 232–239.

- [12.13] DE MOERLOOSE, B., et al., Technetium-99m sestamibi imaging in pediatric neuroblastoma and ganglioneuroma and its relation to P-glycoprotein, *Eur. J. Nucl. Med.* **26** (1999) 396–403.
- [12.14] KIM, Y.S., et al., Tc-99m MIBI SPECT is useful for noninvasively predicting the presence of MDR1 gene-encoded P-glycoprotein in patients with hepatocellular carcinoma, *Clin. Nucl. Med.* **24** (1999) 874–879.
- [12.15] KOSTAKOGLU, L., et al., P-glycoprotein expression by technetium-99m-MIBI scintigraphy in hematologic malignancy, *J. Nucl. Med.* **39** (1998) 1191–1197.
- [12.16] HERMAN, L.W., et al., Novel hexakis(areneisonitrile)technetium(I) complexes as radioligands targeted to the multidrug resistance P-glycoprotein, *J. Med. Chem.* **38** (1995) 2955–2963.
- [12.17] CIARMIELLO, A., et al., Tumor clearance of technetium 99m-sestamibi as a predictor of response to neoadjuvant chemotherapy for locally advanced breast cancer, *J. Clin. Oncol.* **16** (1998) 1677–1683.
- [12.18] KAO, A., et al., Technetium-99m methoxyisobutylisonitrile chest imaging of small cell lung carcinoma: Relation to patient prognosis and chemotherapy response — A preliminary report, *Cancer* **83** (1998) 64–68.
- [12.19] YAMAMOTO, Y., et al., Comparative study of technetium-99m-sestamibi and thallium-201 SPECT in predicting chemotherapeutic response in small cell lung cancer, *J. Nucl. Med.* **39** (1998) 1626–1629.
- [12.20] MORETTI, J.L., et al., Sequential functional imaging with technetium-99m hexakis-2-methoxyisobutylisonitrile and indium-111 octreotide: Can we predict the response to chemotherapy in small cell lung cancer? *Eur. J. Nucl. Med.* **22** (1995) 177–180.
- [12.21] DEL VECCIO, S., et al., In vivo detection of multidrug-resistant (MDR1) phenotype by technetium-99m sestamibi scan in untreated breast cancer patients, *Eur. J. Nucl. Med.* **24** (1997) 150–159.
- [12.22] TAKI, J., et al., Assessment of P-glycoprotein in patients with malignant bone and soft-tissue tumors using technetium-99m-MIBI scintigraphy, *J. Nucl. Med.* **39** (1998) 1179–1184.
- [12.23] HENDRIKES, N.H., et al., <sup>99m</sup>Tc-sestamibi is a substrate for P-glycoprotein and the multidrug resistance-associated protein, *Br. J. Cancer* **77** (1998) 353–358.
- [12.24] KAO, A., et al., P-glycoprotein and multidrug resistance-related protein expressions in relation to technetium-99m methoxyisobutylisonitrile scintimammography findings, *Cancer Res.* **61** (2001) 1412–1414.
- [12.25] BURAK, Z., et al., <sup>99m</sup>Tc-MIBI imaging as a predictor of therapy response in osteosarcoma compared with multidrug resistance-associated protein and P-glycoprotein expression, *J. Nucl. Med.* **44** (2003) 1394–1401.
- [12.26] ZHOU, J., et al., Expression of multidrug resistance protein and messenger RNA correlate with <sup>99m</sup>Tc-MIBI imaging in patients with lung cancer, *J. Nucl. Med.* **42** (2001) 1476–1483.
- [12.27] FLENS, M.J., et al., Tissue distribution of the multidrug resistance protein, *Am. J. Pathol.* **148** (1996) 1237–1247.
- [12.28] FOJO, A.T., et al., Expression of a multidrug-resistance gene in human tumors and tissues, *Proc. Natl. Acad. Sci. USA* **84** (1987) 265–269.

- [12.29] MORETTI, J.L., et al., Involvement of glutathione in loss of technetium-99m-MIBI accumulation related to membrane MDR protein expression in tumor cells, *J. Nucl. Med.* **39** (1998) 1214–1218.
- [12.30] LEWIS, A.D., et al., Amplification and increased expression of alpha class glutathione S-transferase-encoding genes associated with resistance to nitrogen mustards, *Proc. Natl. Acad. Sci. USA* **85** (1988) 8511–8515.
- [12.31] VOLM, M., RITTGEN, W., Cellular predictive factors for the drug response of lung cancer, *Anticancer Res.* **20** (2000) 3449–3458.
- [12.32] BALLINGER, J.R., et al., Technetium-99m-tetrofosmin as a substrate for P-glycoprotein: In vitro studies in multidrug-resistant breast tumor cells, *J. Nucl. Med.* **37** (1996) 1578–1582.
- [12.33] CHENA, W.S., et al., Effects of MDR1 and MDR3 P-glycoproteins, MRP1, and BCRP/MXR/ABCP on the transport of  $^{99m}\text{Tc}$ -Tetrofosmin, *Biochem. Pharmacol.* **60** (2000) 413–426.
- [12.34] UTSUNOMIYA, K., et al., Comparison of the accumulation and efflux kinetics of technetium-99m sestamibi and technetium-99m tetrofosmin in an MRP-expressing tumour cell line, *Eur. J. Nucl. Med.* **27** (2000) 1786–1792.
- [12.35] SHIAU, Y., et al., Detecting parathyroid adenoma using technetium-99m tetrofosmin: Comparison with P-glycoprotein and multidrug resistance related protein expression — A preliminary report, *Nucl. Med. Biol.* **29** (2002) 339–344.
- [12.36] WU, H.-S., et al., Using technetium 99m tetrofosmin parathyroid imaging to detect parathyroid adenoma and its relation to P-glycoprotein expression, *Surgery* **132** (2002) 456–460.
- [12.37] LIANG, J.A., et al., Using technetium-99m-tetrofosmin scan to predict chemotherapy response of malignant lymphomas, compared with P-glycoprotein and multidrug resistance related protein expression, *Oncol. Rep.* **9** (2002) 307–312.
- [12.38] SHIAU, Y., et al., Technetium-99m tetrofosmin chest imaging related to P-glycoprotein expression for predicting the response with paclitaxel-based chemotherapy for non-small cell lung cancer, *Lung* **179** (2002) 197–207.
- [12.39] SHIAU, Y., et al., Predicting chemotherapy response and comparing with P-glycoprotein expression using technetium-99m tetrofosmin scan in untreated malignant lymphomas, *Cancer Lett.* **170** (2001) 139–146.
- [12.40] SHIAU, Y., et al., To predict chemotherapy response using technetium-99m tetrofosmin and compare with p-glycoprotein and multidrug resistance related protein-1 expression in patients with untreated small cell lung cancer, *Cancer Letters* **169** (2001) 181–188.
- [12.41] TATSUMI, M., TSURUO, T., NISHIMURA, T., Evaluation of MS-209, a novel multidrug-resistance-reversing agent, in tumour-bearing mice by technetium-99m-MIBI imaging, *Eur. J. Nucl. Med.* **29** (2002) 288–294.
- [12.42] FUKUMOTO, M., et al., Scintigraphic prediction of resistance to radiation and chemotherapy in patients with lung carcinoma: technetium 99m-tetrofosmin and thallium-201 dual single photon emission computed tomography study, *Cancer* **86** (1999) 1470–1479.

- [12.43] LE LEUNE, N., et al., Influence of glutathione depletion on plasma membrane cholesterol esterification and on Tc-99m-sestamibi and Tc-99m-tetrofosmin uptakes: A comparative study in sensitive U-87-MG and multidrug-resistant MRP1 human glioma cells, *Cancer Biother. Radiopharm.* **19** (2004) 411–421.
- [12.44] LE LEUNE, N., et al., Study of monoglutathionyl conjugates Tc-99m-sestamibi and Tc-99m-tetrofosmin transport mediated by the multidrug resistance-associated protein isoform 1 in glioma cells, *Cancer Biother. Radiopharm.* **20** (2005) 249–259.
- [12.45] RAO, W., et al., A novel areneisonitrile Tc complex inhibits the transport activity of MDR P-glycoprotein, *Nucl. Med. Biol.* **25** (1998) 225–232.
- [12.46] DYSLEWSKI, M., et al., Characterization of a novel  $^{99\text{m}}\text{Tc}$ -carbonyl complex as a functional probe of MDR1 P-glycoprotein transport activity, *Mol. Imaging* **1** (2002) 24–35.
- [12.47] DEUTSCH, E., et al., Development of nonreducible technetium-99m(III) cations as myocardial perfusion imaging agents: initial experience in humans, *J. Nucl. Med.* **28** (1987) 1870–1880.
- [12.48] CRANKSHAW, C.L., et al., Novel technetium (III)-Q complexes for functional imaging of multidrug resistance (MDR1) P-glycoprotein, *J. Nucl. Med.* **39** (1998) 77–86.
- [12.49] LUKER, G.D., et al., Characterization of phosphine complexes of technetium(III) as transport substrates of the multidrug resistance P-glycoprotein and functional markers of P-glycoprotein at the blood-brain barrier, *Biochemistry* **36** (1997) 14218–14227.
- [12.50] BALLINGER, J.R., MUZZMMIL, T., MOORE, M.J., Technetium-99m-furifosmin as an agent for functional imaging of multidrug resistance in tumors, *J. Nucl. Med.* **38** (1997) 1915–1919.
- [12.51] ROSSETTI, C., et al., Human biodistribution, dosimetry and clinical use of technetium(III)-99m-Q12, *J. Nucl. Med.* **35** (1994) 1571–1580.
- [12.52] SYHRE, R., et al., Stability versus reactivity of “3+1” mixed-ligand technetium-99m complexes in vitro and in vivo, *Eur. J. Nucl. Med.* **25** (1998) 793–796.
- [12.53] PIRMETTIS, I.C., PAPADOPOULOS, M.S., CHIOTELLIS, E., Novel  $^{99\text{m}}\text{Tc}$  aminobisthiolato/monothiolato “3 + 1” mixed ligand complexes: structure-activity relationships and preliminary in vivo validation as brain blood flow imaging agents, *J. Med. Chem.* **40** (1997) 2539–2546.
- [12.54] BERGMANN, R., et al., Assessment of the in vitro and in vivo properties of a  $^{99\text{m}}\text{Tc}$ -labeled inhibitor of the multidrug resistant gene product P-glycoprotein, *Nucl. Med. Biol.* **27** (2000) 135–141.
- [12.55] MORETTI, J.L., et al., To use MIBI or not to use MIBI? That is the question when assessing tumour cells, *Eur. J. Nucl. Med. Mol. Imaging* **32** (2005) 836–842.



## Chapter 13

# TECHNETIUM-99m RADIOPHARMACEUTICALS FOR LYMPHOSCINTIGRAPHY

T. UEHARA, H. AKIZAWA, Y. ARANO

Graduate School of Pharmaceutical Sciences, Chiba University,  
Chuo-ku, Chiba, Japan

### Abstract

Lymphoscintigraphy is a safe, well tolerated and reproducible technique for imaging regional lymph node drainage systems. Recent validation of the sentinel lymph node (SLN) concept in clinical care has attracted interest in lymphoscintigraphy. Technetium-99m labelled colloidal particles, such as  $^{99m}\text{Tc}$ -sulphur colloid,  $^{99m}\text{Tc}$ -antimony trisulphide colloid,  $^{99m}\text{Tc}$ -colloidal albumin,  $^{99m}\text{Tc}$ -tin colloid and  $^{99m}\text{Tc}$ -phytate, have been used for both purposes. Technetium-99m labelled colloids slow elimination rates from the injection site and the uptake of radioactivity by lymph nodes is dependent on both particle size and the functional state of the reticuloendothelial system. Thus, non-colloidal particles have been developed as alternatives. These include  $^{99m}\text{Tc}$  labelled human serum albumin,  $^{99m}\text{Tc}$ -dextran,  $^{99m}\text{Tc}$ -Haemaccel and  $^{99m}\text{Tc}$ -hydroxyethyl starch. Although these  $^{99m}\text{Tc}$  labelled compounds showed good visualization of lymphatic channels, these polymer molecules will be only partially retained by the SLN and will continue to diffuse towards distant lymph nodes, which makes identification of the SLN difficult. Recently, another approach for SLN identification has been developed based on the specific binding of  $^{99m}\text{Tc}$  labelled compounds to mannose receptors on macrophages in the SLN. The  $^{99m}\text{Tc}$  radiopharmaceuticals used in lymphoscintigraphy and/or SLN detection are described.

### 13.1. INTRODUCTION

Lymphoscintigraphy is a safe, well tolerated and reproducible technique, utilizing radionuclides for imaging regional lymph node drainage systems, for providing functional and morphological information [13.1, 13.2]. This technique was first reported by Sherman et al. [13.3] in 1953 in lymph node accumulation of interstitially injected radioactive colloidal gold ( $^{198}\text{Au}$ ). Lymph nodes are common sites of metastatic deposits of melanoma and carcinomas of lung, colon, breast and testis [13.1, 13.4, 13.5]. Lymph node status is, therefore, important in staging many malignancies. Additionally, it is useful to determine the etiology of oedema of the extremities [13.6, 13.7]. Meanwhile, multidisciplinary interest in lymphoscintigraphy emerged because of the recent validation of the sentinel node concept in clinical care

[13.4, 13.8–13.10]. The sentinel node concept states that if there is any lymphatic spread of the tumour, the tumour cells should be present in the first lymph node to receive lymphatic drainage from a tumour site and the sentinel node is the best tissue to sample for histopathological examination. This concept was originally proposed in 1977 by Cabanas in the management of patients with penile carcinoma [13.11]. As morbidities such as lymphoedema and sensory disturbances are much reduced compared with lymph node dissection, sentinel lymph node (SLN) biopsy is rapidly entering common practice of tumours [13.4, 13.9, 13.12]. Current applications of lymphoscintigraphy and SLN detection are listed in Table 13.1.

The radiopharmaceuticals for lymphoscintigraphy should rapidly migrate from the injection sites to lymphatic channels and travel through the lymph node chain. On the other hand, the radiopharmaceuticals for SLN detection should migrate rapidly from the injection sites to the draining SLN but have prolonged retention in the SLN, as shown in Fig. 13.1. Thus, the properties of lymphoscintigraphic agents should be different from those of SLN detecting agents. However, in many cases, the same radiopharmaceuticals have been used for both lymphoscintigraphy and SLN detection. The  $^{99m}\text{Tc}$  radiopharmaceuticals used in lymphoscintigraphy and/or SLN detection are described.

TABLE 13.1. PATHOLOGIES IN WHICH LYMPHOSCINTIGRAPHY AND SENTINEL NODE DETECTION ARE USED

Sentinel node detection	Lymphoscintigraphy
Penile cancer	Tumour staging
Melanoma	Define radiotherapy fields
Breast cancer	Evaluate lymphoedema versus venous oedema
Colorectal cancer	Evaluate drainage patterns (leaks)
Head and neck cancer	Lymphangiectasia
Other	Chyle stasis

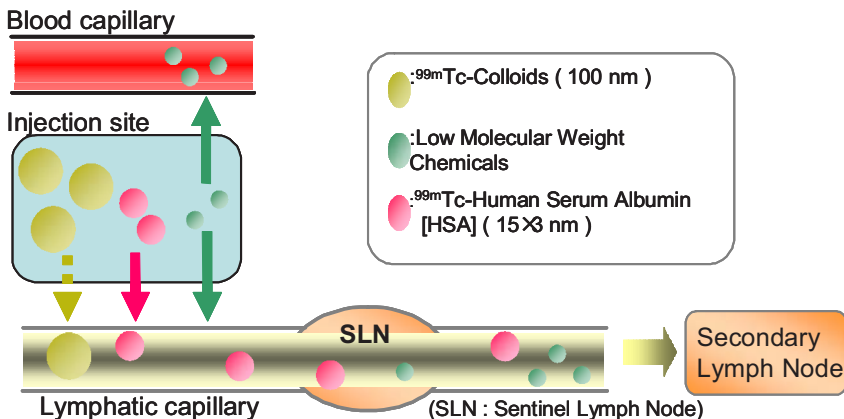


*FIG. 13.1. Entry of particulates into the lymphatic system, depicting the relationship between particle size and uptake by the sentinel node.*

## 13.2. TECHNETIUM-99m LABELLED COLLOIDAL PARTICLES

There is no consensus regarding optimal methods for lymphoscintigraphy. The intra-lymphatic kinetics of lymphoscintigraphic radiopharmaceuticals are not well understood. Radioactive colloidal gold ( $^{198}\text{Au}$ ) was initially introduced for lymphoscintigraphy but suffers from the disadvantage of  $\beta^-$  emission, which results in local damage at the injection sites. Subsequently,  $^{99\text{m}}\text{Tc}$  colloidal tracers were introduced to circumvent this problem. These include  $^{99\text{m}}\text{Tc}$ -sulphur colloid [13.13–13.16],  $^{99\text{m}}\text{Tc}$ -antimony trisulphide colloid [13.4, 13.17, 13.18],  $^{99\text{m}}\text{Tc}$ -colloidal albumin [13.19, 13.20],  $^{99\text{m}}\text{Tc}$ -tin colloid [13.21, 13.22] and  $^{99\text{m}}\text{Tc}$ -phytate [13.23–13.26]. The particle size and surface characteristics of colloidal particles can influence the rate of drainage from the injection site to the dermal lymphatic capillaries and phagocytotic uptake by lymph node macrophages [13.14, 13.17, 13.22, 13.27–13.29]. Particles of up to 100 nm in diameter are necessary for the colloid to translocate from the interstitial injection site to lymphatic channels and nodes. Larger particles (500–2000 nm) remain trapped at the injection site [13.30], whereas particles smaller than 4–5 nm penetrate the capillary membranes and, consequently, would not migrate through the lymphatic channel [13.31].

There are two methods of preparing  $^{99\text{m}}\text{Tc}$ -sulphur colloid.  $^{99\text{m}}\text{Tc}$ -sulphur colloid produced by passing hydrogen sulphide gas through an acidic pertechnetate solution, produces particle sizes of less than 100 nm, and the product provides satisfactory lymph node scans [13.30, 13.32]. On the other

hand,  $^{99m}\text{Tc}$ -sulphur colloid produced by the reaction of thiosulphate with acid is unsatisfactory for lymphoscintigraphy because of the relatively large particle size and range (100–1000 nm), because the migration rate of the particles from the injection site is slow [13.30]. Thus,  $^{99m}\text{Tc}$ -sulphur colloid produced by the latter method is filtered through a 0.1–0.2  $\mu\text{m}$  filter to obtain particles of smaller and even sizes [13.14]. The filtered  $^{99m}\text{Tc}$ -sulphur colloid is commonly used in clinical studies.

Technetium-99m-antimony trisulphide colloid prepared by slowly adding a solution of potassium antimonyl tartrate to a hot saturated aqueous hydrogen sulphide solution has a particle size of 3–30 nm [13.4, 13.17]. Polyvinylpyrrolidone is added to stabilize the colloid. This polymer builds a protective layer around the antimony trisulphide particle [13.8]. For clinical application, the addition of a buffered solution is required to bring the pH of the colloid to physiological pH. Although  $^{99m}\text{Tc}$ -antimony trisulphide colloid provides satisfactory lymph node scans [13.4, 13.17, 13.18], several adverse reactions requiring medical treatment have been reported [13.33].

The biodistribution of colloidal albumin depends on particle size. More than 95% of the particles of nanocolloidal albumin are smaller than 80 nm and less than 4% of the particles are 80–100 nm. Only 1% is larger than 100 nm [13.8]. Nanocolloidal albumin is licensed in Europe for lymphoscintigraphy and bone marrow scintigraphy. On the other hand, microcolloidal albumin is licensed for scintigraphy of liver and spleen. Microcolloidal particles have a size distribution of 200–3000 nm, which is not ideal for lymphoscintigraphy, although good results have been reported by Paganelli et al. [13.34].

The particle size of  $^{99m}\text{Tc}$ -tin colloid depends on the ratio between the  $^{99m}\text{Tc}$  solution and the tin solution [13.26]. As the ratio of tin solution decreases, the size of colloidal particles increases. Technetium-99m-tin colloid has a particle size of 50–1500 nm. Uenosono et al. recommended 100 nm as a suitable colloidal size for detecting SLN in gastric cancer [13.35].

Technetium-99m-phytate possesses a wide size distribution (100–1000 nm), since the particle size depends on the concentration of extracellular calcium [13.26, 13.36]. Although direct measurement of the particle size *in vivo* is difficult, some groups used  $^{99m}\text{Tc}$ -phytate for SLN mapping, and good results have been reported [13.37–13.39]. Among these agents, only  $^{99m}\text{Tc}$ -colloidal albumin and  $^{99m}\text{Tc}$ -sulphur colloid are licensed for use in lymphoscintigraphy. In the United States of America,  $^{99m}\text{Tc}$ -sulphur colloid is the only tracer approved for lymphoscintigraphy. Particle size data are summarized in Table 13.2.

TABLE 13.2. PARTICLE SIZES OF SELECTED RADIOPHARMACEUTICALS USED FOR SENTINEL NODE SCINTIGRAPHY

Product	Particle size (nm)
<sup>198</sup> Au-colloid	3–5
<sup>99m</sup> Tc-antimony-sulphide colloid	45
<sup>99m</sup> Tc-sulphur colloid (modified)	200–600
<sup>99m</sup> Tc-micro-aggregated albumin	200–1000
<sup>99m</sup> Tc-HSA-colloid	80

### 13.3. TECHNETIUM-99m LABELLED NON-COLLOIDAL PARTICLES

Although <sup>99m</sup>Tc labelled colloids are used for lymphoscintigraphy, they have two major problems [13.24, 13.40]: (i) slow elimination rates from the injection site, which requires several hours to visualize lymph nodes after administration, and (ii) the uptake of radioactivity by lymph nodes is dependent on both particle size and functional state of the reticuloendothelial system. To circumvent these problems, non-colloidal particles have been developed as alternatives. These include <sup>99m</sup>Tc labelled human serum albumin (<sup>99m</sup>Tc-HSA) [13.7, 13.41, 13.42], <sup>99m</sup>Tc-dextran [13.31], <sup>99m</sup>Tc-Haemaccel [13.43] and <sup>99m</sup>Tc-hydroxyethyl starch [13.44]. HSA is a physiological substance with a particle size of 3.8 nm × 15 nm [13.41]; it can be labelled with <sup>99m</sup>Tc directly or indirectly via DTPA as a bifunctional chelating agent. Technetium-99m-HSA clears rapidly from injection sites and travels through the lymph node chain to the systemic circulation [13.45–13.47]. Although this radiopharmaceutical is useful for assessment of the lymphatic system [13.7], the use of substances of human origin may result in a potential biohazard.

It has been reported that polymer molecules of high molecular weight (>35 kilodaltons) do not penetrate blood capillary membranes after intradermal administration [13.44]. Technetium-99m labelled dextran (average molecular weight = 110 kilodaltons) [13.31, 13.44], Technetium-99m labelled hydroxyethyl starch (average molecular weight = 450 kilodaltons) [13.44, 13.48] and <sup>99m</sup>Tc labelled haemaccel (average molecular weight = 35 kilodaltons) [13.44] have been evaluated in animals and patients as lymphoscintigraphic agents. These <sup>99m</sup>Tc labelled compounds showed fast migration from the injection site and good visualization of lymphatic channels [13.31, 13.43, 13.44, 13.48]. Since

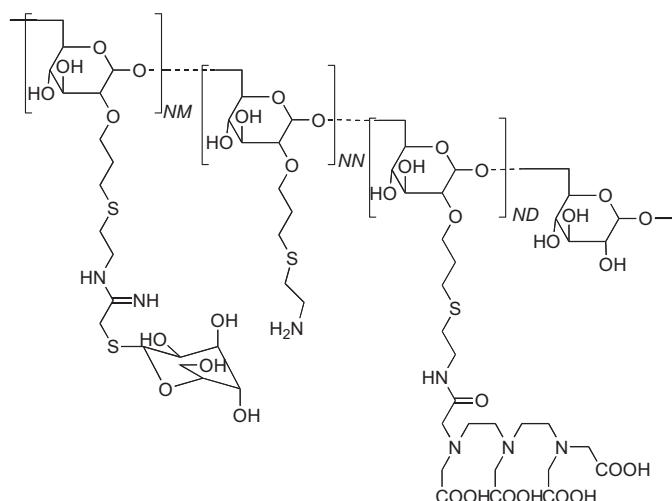
these  $^{99m}$ Tc labelled compounds travel through the lymph node chain, these compounds are also utilized as agents for SLN detection [13.8]. However, while  $^{99m}$ Tc labelled colloidal particles are taken up by the macrophages in the SLN via active and saturable phagocytosis, these polymer molecules will only be partially retained by the SLN and will continue to diffuse towards distant lymph nodes (similar to colloidal particles of smaller sizes), which makes identification of the SLN difficult.

Thus,  $^{99m}$ Tc labelled compounds developed to date are not designed for SLN detection and do not exhibit properties of both rapid injection site clearance and high SLN extraction [13.49].

To circumvent these problems, Vera et al. proposed new radiopharmaceuticals based on the receptor binding technology, as shown in Fig. 13.2(a) [13.49–13.51]. It has been recognized that the mannose binding protein (receptor) binds mannose-terminated glycoproteins and is present in high densities in macrophages [13.52–13.55]. Based on these findings, the researchers attached a large number of mannose units to dextran-DTPA to produce DTPA-mannosyl-dextran [13.49]. The unlabelled product, DTPA-mannosyl-dextran, has a molecular weight of 35.8 kilodaltons and a molecular diameter of 7.1 nm. Preclinical studies showed that  $^{99m}$ Tc-DTPA-mannosyl-dextran would constitute a useful radiopharmaceutical for SLN detection. This compound is now under clinical investigation [13.56–13.59]. Although this approach demonstrated the possibility of yielding a  $^{99m}$ Tc radiopharmaceutical for SLN detection, selection of the DTPA moiety as the  $^{99m}$ Tc chelating group may suffer from some limitations. Further improvement of  $^{99m}$ Tc chemistry would be warranted to provide  $^{99m}$ Tc labelled compounds in high radiochemical yields in a reproducible manner. In addition, it remains uncertain whether the size distribution of the dextran molecules will be within acceptance levels, since it is well known that molecular size significantly affects the migration rates and pathway (through lymph drainage or through the capillary wall) of the resulting compounds.

Since the specific binding of mannosyl-neoglycoalbumin (NMA) to mannose receptors on macrophages is well documented [13.52–13.55], and human serum albumin (HSA) rapidly clears from injection sites [13.46], we evaluated  $^{99m}$ Tc-hynic-NMA (Fig. 13.2(b)) as an SLN detection reagent [13.60]. A monodisperse molecular weight of HSA would be advantageous to reduce variation in the biodistribution associated with the heterogeneous molecular weight of backbone molecules. Such products are available today through synthetic macromolecule methodology. After subcutaneous injection of  $[^{99m}\text{Tc}](\text{hynic-NMA})(\text{tricine})_2$  into the murine foot pad,  $[^{99m}\text{Tc}](\text{hynic-NMA})(\text{tricine})_2$  demonstrated significantly higher radioactivity levels in the popliteal lymph node, the SLN in this model, than did  $[^{99m}\text{Tc}](\text{hynic-HSA})(\text{tricine})_2$  and  $[^{99m}\text{Tc}]\text{rhenium-colloid}$  at 0.5, 1 and 6 h post-injection.

(a)



(b)

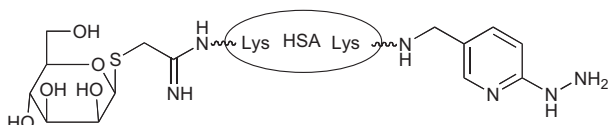


*FIG. 13.2. Chemical structures of  $^{99m}\text{Tc}$  labelled compounds designed for SLN identification.  
(a)  $^{99m}\text{Tc}$  labelled mannose-dextran and (b)  $^{99m}\text{Tc}$ -labelled mannocyl-neoglycoalbumin.*

Radioactivity levels of both  $[^{99m}\text{Tc}](\text{hynic-NMA})(\text{tricine})_2$  and  $[^{99m}\text{Tc}](\text{hynic-HSA})(\text{tricine})_2$  were similar to each other at the injection sites. These findings indicate that the addition of a macrophage binding function to  $^{99m}\text{Tc}$  labelled HSA provides high and selective accumulation of the radioactivity in the SLN without affecting the elimination rate from the injection site. This study also shows that  $^{99m}\text{Tc}$  radiopharmaceuticals of high specific activities are required to achieve high and selective accumulation of radioactivity in the SLN. These findings provide a good basis for the future design of  $^{99m}\text{Tc}$  radiopharmaceuticals for SLN identification using high molecular weight synthetic polymers of narrow size distribution that are safe and cost effective.

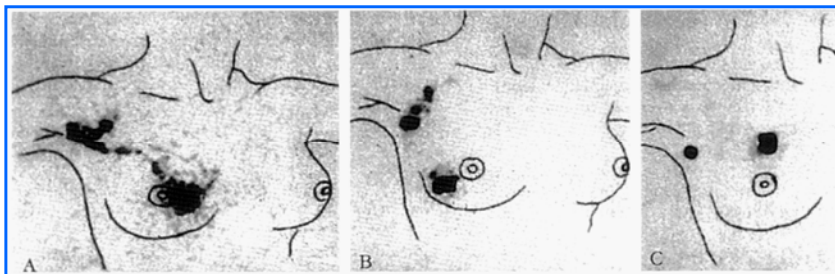


*FIG. 13.3. A depiction of lymph node scintigraphy in a breast cancer study (from Ref. [13.61]).*

#### 13.4. CONCLUSIONS

Although numerous radiopharmaceuticals have been used for lymphoscintigraphy and SLN detection, there is no consensus regarding the optimal tracers for them. Recently, multidisciplinary interest in lymphoscintigraphy emerged because of validation of the SLN concept in clinical care. However, SLN detection is currently being performed by injecting small radiolabelled particles that do not exhibit the ideal properties of both rapid injection site clearance and high SLN extraction. In general, the relationship between colloid particle size and number of nodes imaged is a function of particle size, with the smaller the particles, the greater the number of nodes imaged.

Typical images using colloidal particles are shown in Fig. 13.3.

Recent studies of  $^{99m}\text{Tc}$  labelled compounds targeting mannose receptors on macrophages provide a good basis for the future development of  $^{99m}\text{Tc}$  radiopharmaceuticals that satisfy the following criteria: (i) higher specificity for the target in the lymph node, (ii) smaller size for rapid and efficient migration from the injection site, (iii) high specific activities, (iv) use of safe starting material (e.g. not originating from humans to avoid viruses), (v) high reproducibility and (vi) high cost effectiveness. Technetium-99m chemistry to prepare radiolabelled compounds of high *in vivo* stability with high radiochemical yields and high specific activities has been well developed. The chemical strategy of targeting SLNs has been well developed. Thus, the selection of a backbone molecule of appropriate molecular size and narrow size distribution would constitute a key step to developing a  $^{99m}\text{Tc}$  radiopharmaceutical for both lymphoscintigraphy and SLN identification.

## REFERENCES TO CHAPTER 13

- [13.1] MOGHIMI, S.M., BONNEMAIN, B., Subcutaneous and intravenous delivery of diagnostic agents to the lymphatic system: Applications in lymphoscintigraphy and indirect lymphography, *Adv. Drug Delivery Rev.* **37** (1999) 295–312.
- [13.2] PETRONIS, J.D., LAFRANCE, N.D., KAELIN, W., Lymphoscintigraphy, *Eur. J. Nucl. Med.* **10** (1985) 560–562.
- [13.3] SHERMAN, A.I., TER-POGOSSIAN, M., Lymph-node concentration of radioactive colloidal gold following interstitial injection, *Cancer* **6** (1953) 1238–1240.
- [13.4] ALAZRAKI, N.P., et al., Lymphoscintigraphy, the sentinel node concept, and the intraoperative gamma probe in melanoma, breast cancer, and other potential cancers, *Semin. Nucl. Med.* **27** (1997) 55–67.
- [13.5] HADWAY, P., LYNCH, M., HEENAN, S., WATKIN, N.A., Current status of dynamic lymphoscintigraphy and sentinel lymph-node biopsy in urological malignancies, *BJU Int.* **96** (2005) 1235–1239.
- [13.6] PERRYMORE, W.D., HAROLDS, J.A., Technetium-99m-albumin colloid lymphoscintigraphy in postoperative lymphocele, *J. Nucl. Med.* **37** (1996) 1517–1518.
- [13.7] MCNEILL, G.C., et al., Whole-body lymphangioscintigraphy: preferred method for initial assessment of the peripheral lymphatic system, *Radiology* **172** (1989) 495–502.
- [13.8] WILHELM, A.J., MIJNHOUT, G.S., FRANSSEN, E.J., Radiopharmaceuticals in sentinel lymph-node detection - an overview, *Eur. J. Nucl. Med.* **26** (1999) S36–42.
- [13.9] NEWMAN, L.A., Lymphatic mapping and sentinel lymph node biopsy in breast cancer patients: a comprehensive review of variations in performance and technique, *J. Am. Coll. Surg.* **199** (2004) 804–816.
- [13.10] PEREZ, N., et al., A practical approach to intraoperative evaluation of sentinel lymph node biopsy in breast carcinoma and review of the current methods, *Ann. Surg. Oncol.* **12** (2005) 313–321.
- [13.11] CABANAS, R.M., An approach for the treatment of penile carcinoma, *Cancer* **39** (1977) 456–466.
- [13.12] SCHNEEBAUM, S., et al., Clinical applications of gamma-detection probes — radioguided surgery, *Eur. J. Nucl. Med.* **26** (1999) S26–35.
- [13.13] MEYER, C.M., et al., Technetium-99m sulfur-colloid cutaneous lymphoscintigraphy in the management of truncal melanoma, *Radiology* **131** (1979) 205–209.
- [13.14] HUNG, J.C., et al., Filtered technetium-99m-sulfur colloid evaluated for lymphoscintigraphy, *J. Nucl. Med.* **36** (1995) 1895–1901.
- [13.15] ESHIMA, D., et al., Technetium-99m-sulfur colloid for lymphoscintigraphy: effects of preparation parameters, *J. Nucl. Med.* **37** (1996) 1575–1578.
- [13.16] KERN, K.A., ROSENBERG, R.J., Preoperative lymphoscintigraphy during lymphatic mapping for breast cancer: improved sentinel node imaging using subareolar injection of technetium 99m sulfur colloid, *J. Am. Coll. Surg.* **191** (2000) 479–489.
- [13.17] STRAND, S.E., PERSSON, B.R., Quantitative lymphoscintigraphy I: Basic concepts for optimal uptake of radiocolloids in the parasternal lymph nodes of rabbits, *J. Nucl. Med.* **20** (1979) 1038–1046.

- [13.18] O'BRIEN, C.J., et al., Prediction of potential metastatic sites in cutaneous head and neck melanoma using lymphoscintigraphy, *Am. J. Surg.* **170** (1995) 461–466.
- [13.19] PIJPERS, R., et al., Impact of lymphoscintigraphy on sentinel node identification with technetium-99m-colloidal albumin in breast cancer, *J. Nucl. Med.* **38** (1997) 366–368.
- [13.20] FOWLER, J.C., et al., Dual-isotope lymphoscintigraphy using albumin nanocolloid differentially labeled with  $^{111}\text{In}$  and  $^{99\text{m}}\text{Tc}$ , *Acta Oncol.* **46** (2007) 105–110.
- [13.21] KIM, R., OSAKI, A., KOJIMA, J., TOGE, T., Significance of lymphoscintigraphic mapping with Tc-99m human serum albumin and tin colloid in sentinel lymph node biopsy in breast cancer, *Int. J. Oncol.* **19** (2001) 991–996.
- [13.22] JINNO, H., et al., Sentinel lymph node biopsy in breast cancer using technetium-99m tin colloids of different sizes, *Biomed. Pharmacother.* **56**(Suppl. 1) (2002) 213s–216s.
- [13.23] ALAVI, A., STAUM, M.M., SHESOL, B.F., BLOCH, P.H., Technetium-99m stannous phytate as an imaging agent for lymph nodes, *J. Nucl. Med.* **19** (1978) 422–426.
- [13.24] KAPLAN, W.D., DAVIS, M.A., ROSE, C.M., A comparison of two technetium-99m-labeled radiopharmaceuticals for lymphoscintigraphy: concise communication, *J. Nucl. Med.* **20** (1979) 933–937.
- [13.25] SUTTON, R., et al., Sentinel node biopsy and lymphoscintigraphy with a technetium 99m labeled blue dye in a rabbit model, *Surgery* **131** (2002) 44–49.
- [13.26] HIGASHI, H., et al., Particle size of tin and phytate colloid in sentinel node identification, *J. Surg. Res.* **121** (2004) 1–4.
- [13.27] GULEC, S.A., et al., Sentinel lymph node localization in early breast cancer, *J. Nucl. Med.* **39** (1998) 1388–1393.
- [13.28] SATO, K., et al., Sentinel lymph node identification for patients with breast cancer using large-size radiotracer particles: technetium-99m-labeled tin colloids produced excellent results, *Breast J.* **7** (2001) 388–391.
- [13.29] IKOMI, F., HANNA, G.K., SCHMID-SCHONBEIN, G.W., Mechanism of colloidal particle uptake into the lymphatic system: basic study with percutaneous lymphography, *Radiology* **196** (1995) 107–113.
- [13.30] EGE, G.N., Internal mammary lymphoscintigraphy. The rationale, technique, interpretation and clinical application: a review based on 848 cases, *Radiology* **118** (1976) 101–107.
- [13.31] HENZE, E., et al., Lymphoscintigraphy with Tc-99m-labeled dextran, *J. Nucl. Med.* **23** (1982) 923–929.
- [13.32] RICHARDS, T.B., MCBILES, M., COLLINS, P.S., An easy method for diagnosis of lymphedema, *Ann. Vasc. Surg.* **4** (1990) 255–259.
- [13.33] PONTO, J.A., Adverse reactions to technetium-99m colloids, *J. Nucl. Med.* **28** (1987) 1781–1782.
- [13.34] PAGANELLI, G., et al., Optimized sentinel node scintigraphy in breast cancer, *Q. J. Nucl. Med.* **42** (1998) 49–53.
- [13.35] UENOSONO, Y., et al., Evaluation of colloid size for sentinel nodes detection using radioisotope in early gastric cancer, *Cancer Lett.* **200** (2003) 19–24.
- [13.36] CAMPBELL, J., BELLEN, J.C., BAKER, R.J., COOK, D.J., Technetium-99m calcium phytate-optimization of calcium content for liver and spleen scintigraphy: concise communication, *J. Nucl. Med.* **22** (1981) 157–160.

- [13.37] TAKEI, H. et al.,  $^{99m}\text{Tc}$ -phytate is better than  $^{99m}\text{Tc}$ -human serum albumin as a radioactive tracer for sentinel lymph node biopsy in breast cancer, *Surg. Today* **36** (2006) 219–224.
- [13.38] SILVA, L.B., et al., Sentinel node detection in cervical cancer with  $^{99m}\text{Tc}$ -phytate, *Gynecol. Oncol.* **97** (2005) 588–595.
- [13.39] TAVARES, M.G., et al., The use of  $^{99m}\text{Tc}$ -phytate for sentinel node mapping in melanoma, breast cancer and vulvar cancer: a study of 100 cases, *Eur. J. Nucl. Med.* **28** (2001) 1597–1604.
- [13.40] EGE, G.N., Radiocolloid lymphoscintigraphy in neoplastic disease, *Cancer Res.* **40** (1980) 3065–3071.
- [13.41] KATAOKA, M., et al., Quantitative lymphoscintigraphy using  $^{99}\text{Tc}^m$  human serum albumin in patients with previously treated uterine cancer, *Br. J. Radiol.* **64** (1991) 1119–1121.
- [13.42] NISHIYAMA, Y., et al., Usefulness of Technetium-99m human serum albumin lymphoscintigraphy in chyluria, *Clin. Nucl. Med.* **23** (1998) 429–431.
- [13.43] SADEK, S., OWUNWANNE, A., YACOUB, T., ABDEL-DAYEM, H.M., Technetium-99m haemaccel: a new lymphoscintigraphic agent, *Am. J. Physiol. Imaging* **4** (1989) 464–469.
- [13.44] SADEK, S., DAYEM, H.A., OWUNWANNE, A., YACOUB, T.,  $^{99}\text{Tc}^m$  hydroxyethyl starch: a potential radiopharmaceutical for lymphoscintigraphy, *Nucl. Med. Commun.* **8** (1987) 395–405.
- [13.45] BEDROSIAN, I., et al.,  $^{99m}\text{Tc}$ -human serum albumin: an effective radiotracer for identifying sentinel lymph nodes in melanoma, *J. Nucl. Med.* **40** (1999) 1143–1148.
- [13.46] NATHANSON, S.D., et al., Sentinel lymph node uptake of two different technetium-labeled radiocolloids, *Ann. Surg. Oncol.* **4** (1997) 104–110.
- [13.47] NATHANSON, S.D., et al., Sentinel lymph node metastasis in experimental melanoma: relationships among primary tumor size, lymphatic vessel diameter and  $^{99m}\text{Tc}$ -labeled human serum albumin clearance, *Ann. Surg. Oncol.* **4** (1997) 161–168.
- [13.48] SADEK, S., OWUNWANNE, A., ABDEL-DAYEM, H.M., YACOUB, T., Preparation and evaluation of Tc-99m hydroxyethyl starch as a potential radiopharmaceutical for lymphoscintigraphy: comparison with Tc-99m human serum albumin, Tc-99m dextran, and Tc-99m sulfur microcolloid, *Lymphology* **22** (1989) 157–166.
- [13.49] VERA, D.R., WALLACE, A.M., HOH, C.K., MATTREY, R.F., A synthetic macromolecule for sentinel node detection:  $^{99m}\text{Tc}$ -DTPA-mannosyl-dextran, *J. Nucl. Med.* **42** (2001) 951–959.
- [13.50] VERA, D.R., WISNER, E.R., STADALNIK, R.C., Sentinel node imaging via a nonparticulate receptor-binding radiotracer, *J. Nucl. Med.* **38** (1997) 530–535.
- [13.51] VERA, D.R., WALLACE, A.M., HOH, C.K.,  $[^{99m}\text{Tc}]MAG_3$ -mannosyl-dextran: A receptor-binding radiopharmaceutical for sentinel node detection, *Nucl. Med. Biol.* **28** (2001) 493–498.
- [13.52] ARANO, Y., et al., A biological method to evaluate bifunctional chelating agents to label antibodies with metallic radionuclides, *J. Nucl. Med.* **35** (1994) 890–898.

- [13.53] ASHWELL, G., HARFORD, J., Carbohydrate-specific receptors of the liver, *Annu. Rev. Biochem.* **51** (1982) 531–554.
- [13.54] ROBBINS, J.C., et al., Synthetic glycopeptide substrates for receptor-mediated endocytosis by macrophages, *Proc. Natl. Acad. Sci. USA* **78** (1981) 7294–7298.
- [13.55] HUBBARD, A.L., WILSON, G., ASHWELL, G., STUKENBROK, H., An electron microscope autoradiographic study of the carbohydrate recognition systems in rat liver. I. Distribution of  $^{125}\text{I}$ -ligands among the liver cell types, *J. Cell. Biol.* **83** (1979) 47–64.
- [13.56] WALLACE, A.M., et al., Lymphoseek: a molecular imaging agent for melanoma sentinel lymph node mapping, *Ann. Surg. Oncol.* **14** (2007) 913–921.
- [13.57] WALLACE, A.M., et al., Minimally invasive sentinel lymph node mapping of the pig colon with Lymphoseek, *Surgery* **139** (2006) 217–223.
- [13.58] ELLNER, S.J., et al., Sentinel lymph node mapping of the colon and stomach using lymphoseek in a pig model, *Ann. Surg. Oncol.* **11** (2004) 674–681.
- [13.59] WALLACE, A.M., et al., Lymphoseek: a molecular radiopharmaceutical for sentinel node detection, *Ann. Surg. Oncol.* **10** (2003) 531–538.
- [13.60] TAKAGI, K., et al.,  $^{99\text{m}}\text{Tc}$ -labeled mannosyl-neoglycoalbumin for sentinel lymph node identification, *Nucl. Med. Biol.* **31** (2004) 893–900.
- [13.61] KESHTGAR, M.R.S., The Sentinel Node in Surgical Oncology.

# **Chapter 14**

## **RADIOPHARMACEUTICALS FOR BONE METASTASIS IMAGING**

**K. OGAWA**

Division of Tracer Kinetics, Advanced Science Research Center,  
Kanazawa University, Kanazawa, Japan

### **Abstract**

Although there has been a significant advancement in imaging technologies, such as CT and MR, nuclear medicine bone scanning has been the optimum test for the detection of bone metastases. Technetium-99m-bisphosphonate complexes, which are complexes of bisphosphonate compounds with reduced  $^{99m}\text{Tc}$ , have been widely used as radiopharmaceuticals for detecting bone metastases. They cannot be obtained as well defined single chemical species, but as mixtures of short chain and long chain oligomers, which may reduce the efficacy of the radiopharmaceutical. Recently,  $^{99m}\text{Tc}$ -complex conjugated bisphosphonates and  $^{99m}\text{Tc}$ -complex conjugated oligopeptides were developed as chemically well characterized and highly stable new  $^{99m}\text{Tc}$  labelled bone seekers. Some of them showed superior results in preclinical studies. Moreover, the strategy could be applied to  $^{186/188}\text{Re}$  labelled bone seeking radiopharmaceuticals for palliation therapy. Meanwhile, pentavalent  $^{99m}\text{Tc}$ -dimercaptosuccinic acid ( $^{99m}\text{Tc(V)}$ -DMSA), which accumulated not only in tumours but also in lesions of bone metastases, could be used in the functional diagnosis of bone diseases, particularly osteoclastic type metastases, which is not possible with  $^{99m}\text{Tc}$  labelled bisphosphonates.

### **14.1. INTRODUCTION**

The skeleton is the most common organ to be affected by metastatic cancer. Bone metastases from carcinomas of the breast, lung, prostate, kidney and thyroid are frequent [14.1]. In these bone metastases, the prevalence of skeletal disease is greatest in breast and prostate carcinoma.

Although there have been significant advances in imaging technologies, such as CT and MR, over the last decade, nuclear medicine bone scanning has been the optimum test for the detection of bone metastases, because of its high sensitivity, namely that bone seeking radiopharmaceuticals usually localize in skeletal lesions before the appearance of symptoms and radiograph changes, and the easy evaluation of the entire skeleton [14.2]. This report reviews the history of currently available  $^{99m}\text{Tc}$  radiopharmaceuticals, and recent efforts towards the

development of new radiopharmaceuticals that circumvent the problems associated with the currently available  $^{99m}\text{Tc}$  radiopharmaceuticals are followed.

## 14.2. TECHNETIUM-99m-BISPHOSPHINE COMPLEXES (POLYNUCLEAR)

Although some radionuclides, such as lanthanide and rare earth radiometal cations, localize in bone, little bone uptake occurs when  $^{99m}\text{Tc}$  sodium pertechnetate ( $\text{NaTcO}_4$ ) is administered intravenously [14.3]. The first bone seeking  $^{99m}\text{Tc}$  compound, a complex of reduced  $^{99m}\text{Tc}$  and sodium tripolyphosphate, was reported in 1971 [14.4], followed by longer chain linear polyphosphate [14.5]. Soon,  $^{99m}\text{Tc}$ -pyrophosphate was developed. Pyrophosphate (Fig. 14.1) is composed of only two phosphate moieties and is the simplest polyphosphate. Technetium-99m-pyrophosphate is now seldom used for skeletal imaging because of its high soft tissue background activity but is still employed to determine myocardial infarct. Unfortunately,  $^{99m}\text{Tc}$ -pyrophosphate and  $^{99m}\text{Tc}$ -polyphosphate are subject to in vivo enzymatic degradation, resulting in the release of free technetium from the complexes. Subsequently, three groups almost simultaneously reported a  $^{99m}\text{Tc}$  complex of 1-hydroxyethyliden-1,1-diphosphonate (HEDP) as a new bone imaging agent (Fig. 14.1) [14.6–14.8]. HEDP is a bisphosphonate (diphosphonate) compound and is known as an inhibitor of bone resorption. Bisphosphonate has a P-C-P central structure that affords greater resistance to in vivo phosphatase hydrolysis rather than the P-O-P configuration of pyrophosphate. As a result,  $^{99m}\text{Tc}$ -HEDP exhibited more rapid blood clearance and higher skeletal uptake. In clinical studies,  $^{99m}\text{Tc}$ -HEDP showed significantly higher lesion:normal bone ratios when compared with either  $^{99m}\text{Tc}$ -pyrophosphate or  $^{99m}\text{Tc}$ -polyphosphate [14.9].

Following the introduction of  $^{99m}\text{Tc}$ -methylene diphosphonate (MDP) (Fig. 14.1(c)) by Subramanian et al. [14.10] in 1973 and  $^{99m}\text{Tc}$ -hydroxymethylene diphosphonate (HMDP) (Fig. 14.1(d)) by Bevan et al. [14.11] in 1980,  $^{99m}\text{Tc}$ -MDP and  $^{99m}\text{Tc}$ -HMDP have been widely used as radiopharmaceuticals for bone scintigraphy [14.12–14.14]. Subramanian et al. suggested that  $^{99m}\text{Tc}$ -MDP was superior to  $^{99m}\text{Tc}$ -HEDP as a bone imaging agent due to higher bone accumulation of the tracer in rats, higher whole body retention in dogs and faster plasma clearance in human volunteers [14.10]. On the other hand, other groups claimed that  $^{99m}\text{Tc}$ -HMDP showed faster blood clearance and higher bone retention than  $^{99m}\text{Tc}$ -MDP [14.11, 14.15–14.17].

Technetium-99m-MDP is postulated to form a bidentate–bidentate bridge with hydroxyapatite, while the presence of a hydroxyl group in  $^{99m}\text{Tc}$ -HMDP

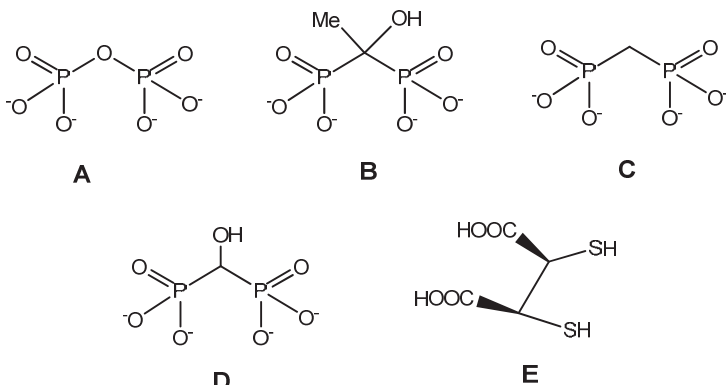


*FIG. 14.1. Structures of pyrophosphate (A), 1-hydroxyethylidene-1,1-diphosphonate (HEDP) (B), methylene diphosphonate (MDP) (C), hydroxymethylene diphosphonate (HMDP) (D) and dimercaptosuccinic acid (DMSA) (E) useful for the preparation of bone targeted  $^{99m}\text{Tc}$  radiopharmaceuticals.*

would convert the ligand to form a bidentate–tridentate bridge and is expected to enhance the hydroxyapatite affinity of the  $^{99m}\text{Tc}$  complex [14.15, 14.18]. However, the lower bone accumulation of  $^{99m}\text{Tc}$ -HEDP, which also has a hydroxyl group at the central carbon, compared to  $^{99m}\text{Tc}$ -HMDP is not well understood, although both compounds may form bidentate–tridentate binding. Increasing steric hindrance associated with the methyl group at the central carbon atom of HEDP, difference in solubility and differences in molecular size, as well as in the bisphosphonate polymeric complexes themselves have all been suggested [14.15, 14.16]. Meanwhile, Fogelman [14.19] described that it is not clear that higher bone uptake will be equally valuable in the identification of disease. Visualization of a focal lesion depends upon the contrast between the lesion and the surrounding bone, that is to say the ratio of radioactivity counts in the lesion to those in background bone. Subramanian et al. [14.20] reported that  $^{99m}\text{Tc}$ -HMDP had higher normal bone concentration than  $^{99m}\text{Tc}$ -MDP without improving the contrast in experiments using rabbits, because high accumulation in normal bone does not result in an improved contrast between bone lesion and normal bone.

The uptake mechanisms of  $^{99m}\text{Tc}$ -bisphosphonate complexes have not been completely elucidated. One of the factors contributing to increased radiopharmaceutical uptake should be caused by the increased vascularity and regional distribution of blood flow that result from disease. However, it has been shown that regional bone blood flow alone does not account for the increased uptake of these radiopharmaceuticals [14.21]. Other factors are involved in their binding and interaction with the bone. It is generally assumed that

$^{99m}$ Tc-bisphosphonate complexes accumulate at sites of active bone metabolism, that is to say areas of new bone formation or calcification [14.22, 14.23]. It was also reported that the accumulation mechanisms might be both the adsorption onto the surface of hydroxyapatite in the bone and incorporation into the crystalline structure of hydroxyapatite [14.24]. The newly formed bone has a much larger surface area than the stable bone, namely the crystalline structure of hydroxyapatite in the newly formed bone is amorphous and has a greater surface area than in normal bone [14.25]. An in vitro study demonstrated that bisphosphonate compounds have a significantly higher adsorption on amorphous calcium phosphate than on a crystalline one [14.16]. There are conflicting views about the mechanism of bone uptake in the literature as to whether  $^{99m}$ Tc-bisphosphonate complexes are hydrolysed during transport to the bone or whether  $^{99m}$ Tc-bisphosphonate complexes are transported to the bone intact. There is another hypothesis that the bisphosphonate moieties in  $^{99m}$ Tc-bisphosphonate complexes act as carriers for the reduced  $^{99m}$ Tc. After reaching the bone surface intact,  $^{99m}$ Tc-bisphosphonate complexes dissociate because (i)  $^{99m}$ Tc-bone adsorption is stronger than  $^{99m}$ Tc-bisphosphonate coordination or (ii) bisphosphonate–bone binding is stronger than  $^{99m}$ Tc-bisphosphonate coordination. In this hypothesis, the dissociation would then allow reduced  $^{99m}$ Tc to deposit as the hydrolysed oxide. Schwartz et al. reported that the dissociation of  $^{99m}$ Tc-bisphosphonate resulted in the absorption of  $^{99m}$ Tc onto the organic phase of bone and MDP onto the inorganic phase, as determined by  $^{99m}$ Tc labelled [ $^{32}$ P]MDP in an animal model [14.26].

Another explanation argues that  $^{99m}$ Tc-bisphosphonate complexes also reach the bone surface intact, and the bisphosphonate moiety of  $^{99m}$ Tc-bisphosphonate provides another coordination with calcium of hydroxyapatite in the bone. A follow-up study using  $^{99m}$ Tc-HEDP supported this hypothesis. The researchers prepared  $^{99m}$ Tc-HEDP from  $^{99m}$ TcO<sub>4</sub><sup>-</sup>,  $^{113}$ Sn and 1-[ $^{14}$ C]HEDP, and found that  $^{99m}$ Tc-HEDP travels as a unit and is deposited as a unit in bone because the radioactivity rates of all radioisotopes in bone were roughly equal percentages of dose [14.8, 14.27]. Jurisson et al. [14.18] reported that since the mechanism of action of  $^{99m}$ Tc-bisphosphonate complexes presumably involves binding of the  $^{99m}$ Tc-bisphosphonate complexes to calcium (either in the hydroxyapatite of bone or the amorphous calcium phosphate), it is not unreasonable that the affinity for the coordination between the bisphosphonate ligand and calcium should strongly influence biodistribution.

Bisphosphonate compounds form multiple complexes with reduced  $^{99m}$ Tc. Using high performance liquid chromatography (HPLC), the relative composition of  $^{99m}$ Tc-bisphosphonate complexes in a reaction mixture has been found to vary with pH and with technetium and oxygen concentrations [14.28]. It has been postulated that  $^{99m}$ Tc-bisphosphonate complexes would be a mixture of

monomers, oxobridged dimers and oligomeric clusters with varying technetium-oxo core configurations, oxidation states and ligand coordination numbers [14.29]. These radiolabelled species have different biodistribution properties. It was reported that the smallest low charged mononuclear  $^{99m}$ Tc-bisphosphonate complexes have the greatest uptake in bone lesions, and the highest lesion:muscle and lesion:normal bone ratios in experiments using each isolated complex by HPLC [14.30]. Thus, despite extensive studies over the past two decades, the exact structures and mechanisms of action of  $^{99m}$ Tc labelled bisphosphonate remain uncertain.

#### 14.3. MONONUCLEAR $^{99m}$ TC LABELLED BISPHOSHPONATE COMPOUNDS ( $^{99m}$ TC COMPLEX CONJUGATED BISPHOSPHONATE COMPOUNDS)

As mentioned above,  $^{99m}$ Tc-bisphosphonate complexes cannot be obtained as well defined single chemical species, but as mixtures of short chain and long chain oligomers, which may reduce the efficacy of the radiopharmaceutical. The biological behaviour of this type of tracer is also affected by the different degrees of ionization and by the variation of the relative amount of the oligomers after preparation [14.28].

In clinical studies, an interval of 2 to 6 h is required between an injection of  $^{99m}$ Tc labelled bisphosphonates and bone images [14.14]. Shortening this interval would lessen the burden to patients in terms of the total length of the examination and the dose of radiation absorbed. To enable imaging at an earlier time after injection, a radiopharmaceutical with higher affinity for the bone may be advantageous. This led to the development of  $^{99m}$ Tc-mononuclear complex conjugated bisphosphonate compounds [14.31–14.33]. Although the accumulation of bisphosphonate compounds in the bone is achieved by binding the phosphonate groups with  $\text{Ca}^{2+}$  of hydroxyapatite crystals [14.34], the phosphonate groups in  $^{99m}$ Tc-MDP and  $^{99m}$ Tc-HMDP serve as both coordinating ligands and  $\text{Ca}^{2+}$  binding functional groups [14.35], which might decrease the inherent accumulation of MDP and HMDP in the bone. It was hypothesized that the bone affinity of  $^{99m}$ Tc labelled bisphosphonate would be enhanced by conjugating a stable mononuclear  $^{99m}$ Tc chelating group with a bisphosphonate moiety so that the conjugation does not impair the inherent chemical and biological properties of bisphosphonate compounds. Technetium-99m-L,L-ethylene dicysteine (EC),  $^{99m}$ Tc-mercaptoacetylglycylglycylglycine (MAG3),  $^{99m}$ Tc-6-hydrazinonicotinic acid (hynic) and  $^{99m}$ Tc-tricarbonyl anchored by a pyrazolyl containing ligand were selected as  $^{99m}$ Tc chelating molecules, and were conjugated with bisphosphonate compounds, as shown in Fig. 14.2

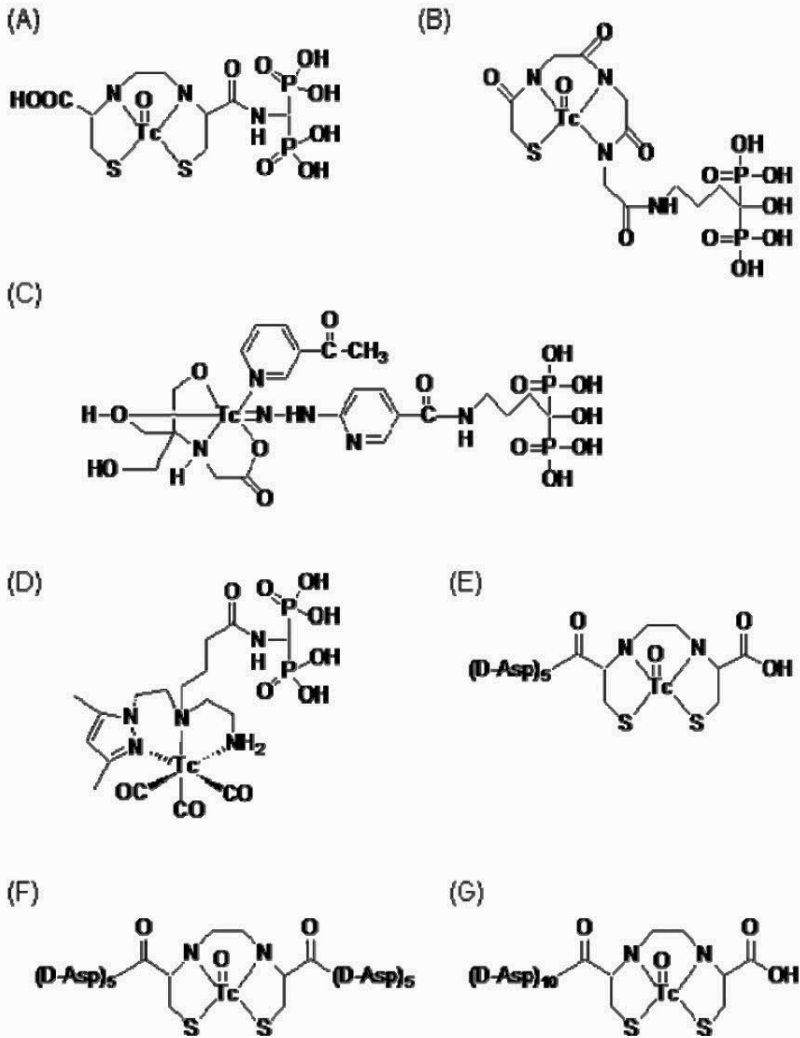


FIG. 14.2.  $^{99m}\text{Tc}$  complex conjugated bisphosphonate or oligopeptide compounds.  $^{99m}\text{Tc}$ -EC-AMDP (A),  $^{99m}\text{Tc}$ -MAG3-HBP (B),  $^{99m}\text{Tc}$ -hynic-HBP (C),  $[^{99m}\text{Tc}(\text{CO})_3(\kappa^3\text{-pz-BPOH})]^+$  (D),  $^{99m}\text{Tc}$ -EC-(D-Asp)<sub>5</sub> (E),  $^{99m}\text{Tc}$ -EC-[{(D-Asp)<sub>5</sub>}<sub>2</sub>] (F) and  $^{99m}\text{Tc}$ -EC-(D-Asp)<sub>10</sub> (G).

( $^{99m}\text{Tc}$ -EC-AMDP,  $^{99m}\text{Tc}$ -MAG3-HBP,  $^{99m}\text{Tc}$ -hynic-HBP,  $[^{99m}\text{Tc}(\text{CO})_3(\kappa^3\text{-pz-BPOH})]^+$ , respectively). Among these compounds,  $^{99m}\text{Tc}$ -EC-AMDP and  $^{99m}\text{Tc}$ -hynic-HBP showed superior results in preclinical studies;  $^{99m}\text{Tc}$ -EC-AMDP and  $^{99m}\text{Tc}$ -hynic-HBP showed significantly higher bone:blood ratios of radioactivity than  $^{99m}\text{Tc}$ -MDP [14.31] and  $^{99m}\text{Tc}$ -HMDP [14.32], respectively.

Meanwhile, because of similar chemical properties between rhenium and technetium,  $^{186/188}\text{Re}$  labelled 1-hydroxyethylidene-1,1-diphosphonate ( $^{186/188}\text{Re}$ -HEDP) has also been proposed for the palliation of metastatic bone pain [14.36–14.38]. However, since rhenium is easier to oxidize than technetium [14.39, 14.40], in vivo decomposition of  $^{186}\text{Re}$ -HEDP to  $^{186}\text{ReO}_4^-$  was observed. This resulted in a delayed blood clearance and higher gastric uptake of radioactivity [14.41, 14.42]. The molecular design of chelate-conjugated bisphosphonate has also been applied to stabilize  $^{186/188}\text{Re}$  in vivo [14.43–14.47]. A recent study showed that while an HPLC-purified chelate-conjugated bisphosphonate exhibited higher hydroxyapatite binding and bone accumulation than  $^{186}\text{Re}$ -HEDP, bone accumulation of the chelate-conjugated bisphosphonate decreased to levels similar to those of  $^{186}\text{Re}$ -HEDP when co-injected with HEDP equivalent to that in  $^{186}\text{Re}$ -HEDP. These results suggested that the specific activity of  $^{186}\text{Re}$  labelled bisphosphonates would play a crucial role in bone accumulation and blood clearance. These findings also suggested that the molecular design of chelate-conjugated bisphosphonate would be useful for the development of bone seeking radiopharmaceuticals with a variety of radionuclides by selecting chelating molecules that provide high specific activities [14.47].

#### 14.4. TECHNETIUM-99m-COMPLEX CONJUGATED OLIGOPEPTIDES

Several bone non-collagenous proteins have a repeating sequence of acidic amino acids (Asp or Glu) in their structures as a possible hydroxyapatite binding site. For example, osteopontin and bone sialoprotein, two major non-collagenous proteins in the bone, have Asp and Glu repeating sequences, respectively [14.48–14.50]. It has been reported that polyglutamic acid or polyaspartic acid is effective as a bone targeting moiety to deliver drugs to bone [14.51–14.53]. In addition, a prior study suggested that the presence of free bisphosphonate would impair blood clearance of radiolabelled bisphosphonate by competing for glomerular filtration [14.54]. On these bases, a  $^{99\text{m}}\text{Tc}$ -EC complex conjugated with one or two  $(\text{D-Asp})_5$  peptides ( $^{99\text{m}}\text{Tc}$ -EC-(D-Asp)<sub>5</sub> and  $^{99\text{m}}\text{Tc}$ -EC-[ $(\text{D-Asp})_5$ ]<sub>2</sub>) and  $^{99\text{m}}\text{Tc}$ -EC conjugated with a  $(\text{D-Asp})_{10}$  peptide ( $^{99\text{m}}\text{Tc}$ -EC-(D-Asp)<sub>10</sub>) (Fig. 14.2) have been evaluated as a new class of bone seeking radiopharmaceuticals [14.54]. Technetium-99m-EC-[ $(\text{D-Asp})_5$ ]<sub>2</sub> provided the most preferable pharmacokinetics for bone imaging of the three, and  $^{99\text{m}}\text{Tc}$ -EC-[ $(\text{D-Asp})_5$ ]<sub>2</sub> may constitute a lead compound for bone seeking radiopharmaceuticals without bisphosphonate moieties.

## 14.5. TECHNETIUM-99m-DMSA

Pentavalent  $^{99\text{m}}\text{Tc}$ -dimercaptosuccinic acid ( $^{99\text{m}}\text{Tc(V)}$ -DMSA) (Fig. 14.1) is a tumour seeking radiopharmaceutical that is chemically distinct from the well established trivalent renal imaging radiopharmaceutical. Technetium-99m(V)-DMSA has been used to evaluate medullary carcinoma of the thyroid [14.55, 14.56] and various soft tissue tumours [14.57–14.59]. Furthermore, recent studies have shown that  $^{99\text{m}}\text{Tc(V)}$ -DMSA could constitute a reliable marker of proliferation [14.60–14.62], which may render  $^{99\text{m}}\text{Tc(V)}$ -DMSA useful for improving prognosis estimation and therapy optimization.

Technetium-99m(V)-DMSA was originally designed to generate a  $^{99\text{m}}\text{TcO}_4^{3-}$  ion following dissociation of the complex at sites of tumours. The resulting  $^{99\text{m}}\text{Tc}$  anion would be incorporated into tumour cells due to structural similarity to the phosphate anion [14.57, 14.63, 14.64]. Recent studies showed that  $^{99\text{m}}\text{Tc(V)}$ -DMSA is pH sensitive, and tumour uptake is enhanced by an acidic pH environment and inhibited by an alkaline pH [14.65, 14.66]. Such chemical properties may partially explain the mechanism of tumour accumulation of this tracer, as it is now well established that malignant tumours are more acidic than normal tissues. More recently, it has been demonstrated that  $^{99\text{m}}\text{Tc(V)}$ -DMSA is specifically mediated by a type III  $\text{Na}^+$ -dependent inorganic phosphate (NaPi) co-transporter in cancer cells [14.67]. (The transporters constitute three different protein families denoted NaPi Type I, Type II and Type III [14.68]). These findings support the concept of the molecular design. In addition, the uptakes of both  $^{99\text{m}}\text{Tc(V)}$ -DMSA and phosphate were stimulated by acidic pH and inhibited by alkaline pH in cell line experiments. It has been reported that tumour cells overexpress the type III NaPi co-transporter, and the type III NaPi co-transporter is inhibited by alkaline pH [14.69]. In contrast, the activity of the type II NaPi co-transporter is increased by raising pH, and the type I NaPi co-transporter is not modified by pH changes [14.70].

Technetium-99m(V)-DMSA has also been reported to accumulate in lesions of bone metastases [14.71–14.74]. However, Lam et al. [14.71] reported that the role of  $^{99\text{m}}\text{Tc(V)}$ -DMSA as a routine imaging agent for bone metastases is limited because it showed inferior and variable uptake in diseased bone compared with  $^{99\text{m}}\text{Tc-HMDP}$ . On the other hand, Sahin et al. [14.74] reported that  $^{99\text{m}}\text{Tc(V)}$ -DMSA imaging of bone metastases had a similar diagnostic value to a  $^{99\text{m}}\text{Tc-MDP}$  scan. The mechanism of  $^{99\text{m}}\text{Tc(V)}$ -DMSA accumulation to the lesion of bone metastases has not yet been well elucidated. Lam et al. [14.75] suggested that  $^{99\text{m}}\text{Tc(V)}$ -DMSA binds to calcium phosphates in a chemically unaltered form and that bone affinity might be dependent on the mineral phase of bone. They also reported that the mineral binding of  $^{99\text{m}}\text{Tc(V)}$ -DMSA was stronger than that of  $^{99\text{m}}\text{Tc-HMDP}$  under a narrower range of conditions, and that  $^{99\text{m}}\text{Tc(V)}$ -DMSA

might be more selective among different types of calcified deposits than  $^{99m}\text{Tc}$ -HMDP. On the other hand, using isolated bone cells, Horiuchi et al. [14.76] reported the preferential accumulation of  $^{99m}\text{Tc(V)}$ -DMSA by osteoclasts, and this accumulation responded to the acidification of the pH environment. They suggested that along with the cellular response to differential pH, physicochemical properties of  $^{99m}\text{Tc(V)}$ -DMSA should also be mentioned; the occurrence of some active  $^{99m}\text{Tc}$  species derived from the pH sensitive  $^{99m}\text{Tc(V)}$ -DMSA might trigger cellular accumulation. This also suggests that a  $^{99m}\text{Tc(V)}$ -DMSA scan could be used in the functional diagnosis of bone diseases, particularly osteoclastic type metastases that is not possible with  $^{99m}\text{Tc}$  labelled bisphosphonates. Indeed,  $^{99m}\text{Tc(V)}$ -DMSA accumulates in some types of bone metastases. However, normal skeleton is not visualized above the soft tissue background on  $^{99m}\text{Tc(V)}$ -DMSA patient scintigrams [14.75]. In some lung cancer metastases showing no  $^{99m}\text{Tc-MDP}$  uptake,  $^{99m}\text{Tc(V)}$ -DMSA uptake was observed [14.74].

The accumulation of  $^{99m}\text{Tc(V)}$ -DMSA in tumour and bone metastases lesions suggested that molecular design may pave the way to developing radiopharmaceuticals for targeted radiotherapy when considering the similar chemical properties of rhenium and technetium. Indeed, similar pharmacokinetics were observed between  $^{188}\text{Re(V)}$ -DMSA and  $^{99m}\text{Tc(V)}$ -DMSA in mice and humans [14.77, 14.78]. Rhenium-186/188(V)-DMSA has two advantages over  $^{186/188}\text{Re}$  labelled bisphosphonate compounds. First,  $^{186/188}\text{Re(V)}$ -DMSA could be applied not only to bone metastases but also to soft tissue tumours. Secondly, the lower normal bone accumulation of  $^{186/188}\text{Re-DMSA}$  is advantageous for reducing bone marrow toxicity, which constitutes the dose limiting factor of therapeutic bone seeking radiopharmaceuticals. Thus,  $^{99m}\text{Tc(V)}$ -DMSA is predictive of  $^{186/188}\text{Re(V)}$ -DMSA biodistribution and could be used to estimate the tumour and non-target tissue dosimetry, and to assess suitability of patients for  $^{186/188}\text{Re(V)}$ -DMSA.

#### 14.6. CONCLUSION

Over the past two decades,  $^{99m}\text{Tc-MDP}$  and  $^{99m}\text{Tc-HMDP}$  have been used for detecting bone metastases, although their mechanisms of accumulation remain uncertain. Recent efforts of chelate-conjugated bisphosphonates and their derivatives have provided chemically well characterized and highly stable new  $^{99m}\text{Tc}$  labelled bone seekers. Although some studies suggested involvement in hydroxyapatite binding, further studies are required to elucidate the ‘molecule’ responsible for the accumulation of these new  $^{99m}\text{Tc}$  labelled compounds. These studies would provide reliable information about the changes in the

‘specific-molecule’ of the bone in normal and diseased states. At the same time, further studies on the mechanism of localization of  $^{99m}\text{Tc(V)}$ -DMSA may open a new window in the differential diagnosis of bone pathology.

## REFERENCES TO CHAPTER 14

- [14.1] COLEMAN, R.E., Skeletal complications of malignancy, *Cancer* **80** (1997) 1588–1594.
- [14.2] KRASNOW, A.Z., et al., Diagnostic bone scanning in oncology, *Semin. Nucl. Med.* **27** (1997) 107–141.
- [14.3] FRANCIS, M.D., SLOUGH, C.L., TOFE, A.J., Factors affecting uptake and retention of technetium-99m-diphosphonate and 99m-pertechnetate in osseous, connective and soft tissues, *Calcif. Tissue Res.* **20** (1976) 303–311.
- [14.4] SUBRAMANIAN, G., MCAFEE, J.G., A new complex of  $^{99m}\text{Tc}$  for skeletal imaging, *Radiology* **99** (1971) 192–196.
- [14.5] SUBRAMANIAN, G., et al.,  $^{99m}\text{Tc}$ -labeled polyphosphate as a skeletal imaging agent, *Radiology* **102** (1972) 701–704.
- [14.6] SUBRAMANIAN, G., et al.,  $^{99m}\text{Tc}$ -EHDP: a potential radiopharmaceutical for skeletal imaging, *J. Nucl. Med.* **13** (1972) 947–950.
- [14.7] CASTRONOVO, F.P., Jr., CALLAHAN, R.J., New bone scanning agent:  $^{99m}\text{Tc}$ -labeled 1-hydroxy-ethylidene-1,1-disodium phosphonate, *J. Nucl. Med.* **13** (1972) 823–827.
- [14.8] YANO, Y., MCRAE, J., VAN DYKE, D.C., ANGER, H.O., Technetium-99m-labeled stannous ethane-1-hydroxy-1,1-diphosphonate: a new bone scanning agent, *J. Nucl. Med.* **14** (1973) 73–78.
- [14.9] CITRIN, D.L., et al., A comparison of phosphate bone-scanning agents in normal subjects and patients with malignant disease, *Br. J. Radiol.* **48** (1975) 118–121.
- [14.10] SUBRAMANIAN, G., et al., Technetium-99m-methylene diphosphonate—a superior agent for skeletal imaging: comparison with other technetium complexes, *J. Nucl. Med.* **16** (1975) 744–755.
- [14.11] BEVAN, J.A., et al., Tc-99m HMDP (hydroxymethylene diphosphonate): a radiopharmaceutical for skeletal and acute myocardial infarct imaging. II. Comparison of Tc-99m hydroxymethylene diphosphonate (HMDP) with other technetium-labeled bone-imaging agents in a canine model, *J. Nucl. Med.* **21** (1980) 967–970.
- [14.12] DOMSTAD, P.A., et al.,  $^{99m}\text{Tc}$ -hydroxymethane diphosphonate: a new bone imaging agent with a low tin content, *Radiology* **136** (1980) 209–211.
- [14.13] MARI, C., CATAFAU, A., CARRIO, I., Bone scintigraphy and metabolic disorders, *Q. J. Nucl. Med.* **43** (1999) 259–267.
- [14.14] LOVE, C., et al., Radionuclide bone imaging: an illustrative review, *Radiographics* **23** (2003) 341–358.
- [14.15] BEVAN, J.A., et al., Tc-99m HMDP (hydroxymethylene diphosphonate): a radiopharmaceutical for skeletal and acute myocardial infarct imaging. I. Synthesis and distribution in animals, *J. Nucl. Med.* **21** (1980) 961–966.

- [14.16] FRANCIS, M.D., et al., Comparative evaluation of three diphosphonates: in vitro adsorption (C-14 labeled) and in vivo osteogenic uptake (Tc-99m complexed), *J. Nucl. Med.* **21** (1980) 1185–1189.
- [14.17] FOGELMAN, I., et al., A comparison of skeletal uptakes of three diphosphonates by whole-body retention: concise communication, *J. Nucl. Med.* **22** (1981) 880–883.
- [14.18] JURRISSON, S.S., et al., Calcium affinity of coordinated diphosphonate ligand. Single-crystal structure of  $[(en)_2Co(O_2P(OH)CH_2P(OH)O_2)]ClO_4 \cdot H_2O$ . Implication for the chemistry of technetium-99m-diphosphonate skeletal imaging agents, *Inorg. Chem.* **22** (1983) 1332–1338.
- [14.19] FOGELMAN, I., Diphosphonate bone scanning agents — Current concepts, *Eur. J. Nucl. Med.* **7** (1982) 506–509.
- [14.20] SUBRAMANIAN, G., et al., New diphosphonate compounds for skeletal imaging: comparison with methylene diphosphonate, *Radiology* **149** (1983) 823–828.
- [14.21] LAVENDER, J.P., KHAN, R.A., HUGHES, S.P., Blood flow and tracer uptake in normal and abnormal canine bone: comparisons with Sr-85 microspheres, Kr-81m, and Tc-99m MDP, *J. Nucl. Med.* **20** (1979) 413–418.
- [14.22] BUDD, R.S., HODGSON, G.S., HARE, W.S., The relation of radionuclide uptake by bone to the rate of calcium mineralization. I: Experimental studies using  $^{45}Ca$ ,  $^{32}P$  and  $^{99}Tc^m$ -MDP, *Br. J. Radiol.* **62** (1989) 314–317.
- [14.23] BUDD, R.S., HODGSON, G.S., HARE, W.S., The relation of radionuclide uptake by bone to the rate of calcium mineralization. II: Patient studies using  $^{99}Tc^m$ -MDP, *Br. J. Radiol.* **62** (1989) 318–320.
- [14.24] KANISHI, D.,  $^{99m}Tc$ -MDP accumulation mechanisms in bone, *Oral Surg. Oral Med. Oral Pathol.* **75** (1993) 239–246.
- [14.25] GALASKO, C.S., Mechanism of uptake of bone imaging isotopes by skeletal metastases, *Clin. Nucl. Med.* **5** (1980) 565–568.
- [14.26] SCHWARTZ, Z., et al., Uptake and biodistribution of technetium-99m-MD $^{32}P$  during rat tibial bone repair, *J. Nucl. Med.* **34** (1993) 104–108.
- [14.27] TOFE, A.J., FRANCIS, M.D., Optimization of the ratio of stannous tin: ethane-1-hydroxy-1,1-diphosphonate for bone scanning with  $^{99m}Tc$ -pertechnetate, *J. Nucl. Med.* **15** (1974) 69–74.
- [14.28] TANABE, S., et al., Effect of pH on the formation of Tc(NaBH<sub>4</sub>)-MDP radiopharmaceutical analogues, *Int. J. Appl. Radiat. Isotop.* **34** (1983) 1577–1584.
- [14.29] WILSON, G.M., PINKERTON, T.C., Determination of charge and size of technetium diphosphonate complexes by anion-exchange liquid chromatography, *Anal. Chem.* **57** (1985) 246–253.
- [14.30] PINKERTON, T.C., et al., Influence of complex charge and size on the uptake of  $^{99m}Tc$ -diphosphonates in osteogenic tissue, *Int. J. Radiat. Appl. Instrum. B* **13** (1986) 49–56.
- [14.31] VERBEKE, K., et al., Development of a conjugate of  $^{99m}Tc$ -EC with aminomethylenediphosphonate in the search for a bone tracer with fast clearance from soft tissue, *Bioconjug. Chem.* **13** (2002) 16–22.

- [14.32] OGAWA, K., et al., Development of a novel  $^{99m}\text{Tc}$ -chelate-conjugated bisphosphonate with high affinity for bone as a bone scintigraphic agent, *J. Nucl. Med.* **47** (2006) 2042–2047.
- [14.33] PALMA, E., et al. A new bisphosphonate-containing  $^{99m}\text{Tc}(\text{I})$  tricarbonyl complex potentially useful as bone-seeking agent: synthesis and biological evaluation, *J. Biol. Inorg. Chem.* **12** (2007) 667–679.
- [14.34] MEYER, J.L., NANCOLLAS, G.H., The influence of multidentate organic phosphonates on the crystal growth of hydroxyapatite. *Calcif. Tissue Int.* **13** (1973) 295–303.
- [14.35] LIBSON, K., DEUTSCH, E., BARNETT, B.L., Structural characterization of a technetium-99-diphosphonate complex. Implications for the chemistry of technetium-99m skeletal imaging agents, *J. Am. Chem. Soc.* **102** (1980) 2476–2478.
- [14.36] LAM, M.G., DE KLERK, J.M., VAN RIJK, P.P.,  $^{186}\text{Re}$ -HEDP for metastatic bone pain in breast cancer patients, *Eur. J. Nucl. Med. Mol. Imaging* **31**(Suppl. 1) (2004) S162–S170.
- [14.37] LI, S., et al., Rhenium-188 HEDP to treat painful bone metastases, *Clin. Nucl. Med.* **26** (2001) 919–922.
- [14.38] ELDER, R.C., et al., Studies of the structure and composition of rhenium-1,1-hydroxyethylidenediphosphonate (HEDP) analogues of the radiotherapeutic agent  $^{186}\text{Re}$ HEDP, *Inorg. Chem.* **36** (1997) 3055–3063.
- [14.39] DEUTSCH, E., et al., The chemistry of rhenium and technetium as related to the use of isotopes of these elements in therapeutic and diagnostic nuclear medicine, *Nucl. Med. Biol.* **13** (1986) 465–477.
- [14.40] ARANO, Y., et al. Synthesis and biodistribution studies of  $^{186}\text{Re}$  complex of 1-hydroxyethylidene-1,1-diphosphonate for treatment of painful osseous metastases, *Radioisotopes* **44** (1995) 514–522.
- [14.41] DE KLERK, J.M., et al., Pharmacokinetics of rhenium-186 after administration of rhenium-186-HEDP to patients with bone metastases, *J. Nucl. Med.* **33** (1992) 646–651.
- [14.42] DE WINTER, F., et al., Visualization of the stomach on rhenium-186 HEDP imaging after therapy for metastasized prostate carcinoma, *Clin. Nucl. Med.* **24** (1999) 898–899.
- [14.43] OGAWA, K., et al., Therapeutic effects of a  $^{186}\text{Re}$ -complex-conjugated bisphosphonate for the palliation of metastatic bone pain in an animal model, *J. Nucl. Med.* **48** (2007) 122–127.
- [14.44] OGAWA, K., et al., Rhenium-186-monoaminemonoamidedithiol-conjugated bisphosphonate derivatives for bone pain palliation, *Nucl. Med. Biol.* **33** (2006) 513–520.
- [14.45] OGAWA, K., et al., Development of a rhenium-186-labeled MAG3-conjugated bisphosphonate for the palliation of metastatic bone pain based on the concept of bifunctional radiopharmaceuticals, *Bioconjug. Chem.* **16** (2005) 751–757.
- [14.46] OGAWA, K., et al., Design of a radiopharmaceutical for the palliation of painful bone metastases: rhenium-186-labeled bisphosphonate derivative, *J. Labelled Comp. Radiopharm.* **47** (2004) 753–761.

- [14.47] UEHARA, T., et al., Assessment of  $^{186}\text{Re}$  chelate-conjugated bisphosphonate for the development of new radiopharmaceuticals for bones, *Nucl. Med. Biol.* **34** (2007) 79–87.
- [14.48] BUTLER, W.T., The nature and significance of osteopontin, *Connect. Tissue Res.* **23** (1989) 123–136.
- [14.49] OLDBERG, A., FRANZEN, A., HEINEGARD, D., The primary structure of a cell-binding bone sialoprotein, *J. Biol. Chem.* **263** (1988) 19430–19432.
- [14.50] OLDBERG, A., FRANZEN, A., HEINEGARD, D., Cloning and sequence analysis of rat bone sialoprotein (osteopontin) cDNA reveals an Arg-Gly-Asp cell-binding sequence, *Proc. Natl. Acad. Sci. USA* **83** (1986) 8819–8823.
- [14.51] KASUGAI, S., et al., Selective drug delivery system to bone: small peptide (Asp)<sub>6</sub> conjugation, *J. Bone Miner. Res.* **15** (2000) 936–943.
- [14.52] YOKOGAWA, K., et al., Selective delivery of estradiol to bone by aspartic acid oligopeptide and its effects on ovariectomized mice, *Endocrinology* **142** (2001) 1228–1233.
- [14.53] WANG, D., et al., Synthesis and evaluation of water-soluble polymeric bone-targeted drug delivery systems, *Bioconjug. Chem.* **14** (2003) 853–859.
- [14.54] UEHARA, T., et al., Mononuclear Tc-99m-chelate-conjugated oligo-aspartic acid as a new bone imaging agent, *J. Nucl. Med.* **47** (2006) 520P.
- [14.55] OHTA, H., et al., A new imaging agent for medullary carcinoma of the thyroid, *J. Nucl. Med.* **25** (1984) 323–325.
- [14.56] MIYAUCHI, A., et al.,  $^{99\text{m}}\text{Tc}(\text{V})$ -dimercaptosuccinic acid scintigraphy for medullary thyroid carcinoma, *World J. Surg.* **10** (1986) 640–645.
- [14.57] OHTA, H., et al., Imaging of head and neck tumors with technetium(V)-99m DMSA. A new tumor-seeking agent, *Clin. Nucl. Med.* **10** (1985) 855–860.
- [14.58] KOBAYASHI, H., et al., Soft-tissue tumors: diagnosis with Tc-99m (V) dimercaptosuccinic acid scintigraphy, *Radiology* **190** (1994) 277–280.
- [14.59] HIRANO, T., et al., Differentiating histologic malignancy of primary brain tumors: pentavalent technetium-99m-DMSA, *J. Nucl. Med.* **38** (1997) 20–26.
- [14.60] PAPANTONIOU, V.J., et al., Relationship of cell proliferation (Ki-67) to  $^{99\text{m}}\text{Tc}(\text{V})$ DMSA uptake in breast cancer, *Breast Cancer Res.* **6** (2004) R56–R62.
- [14.61] LE LEUNE, N., PEREK, N., DUBOIS, F., Influence of Pi3-K and PKC activity on  $^{99\text{m}}\text{Tc}-(\text{V})$ -DMSA uptake: correlation with tumour aggressiveness in an in vitro malignant glioblastoma cell line model, *Eur. J. Nucl. Med. Mol. Imaging* **33** (2006) 1206–1213.
- [14.62] TSIOURIS, S., et al., Pentavalent technetium-99m dimercaptosuccinic acid [ $^{99\text{m}}\text{Tc}-(\text{V})$ DMSA] brain scintitomography — a plausible non-invasive depicter of glioblastoma proliferation and therapy response, *J. Neurooncol.* **85** (2007) 291–295.
- [14.63] BLOWER, P.J., SINGH, J., CLARKE, S.E., The chemical identity of pentavalent technetium-99m-dimercaptosuccinic acid, *J. Nucl. Med.* **32** (1991) 845–849.
- [14.64] YOKOYAMA, A., et al., The design of a pentavalent  $^{99\text{m}}\text{Tc}$ -dimercaptosuccinate complex as a tumor imaging agent, *Int. J. Nucl. Med. Biol.* **12** (1985) 273–279.

- [14.65] HORIUCHI, K., SAJI, H., YOKOYAMA, A., Tc(V)-DMS tumor localization mechanism: a pH-sensitive Tc(V)-DMS-enhanced target/nontarget ratio by glucose-mediated acidosis, *Nucl. Med. Biol.* **25** (1998) 549–555.
- [14.66] HORIUCHI, K., SAJI, H., YOKOYAMA, A., pH sensitive properties of Tc(V)-DMS: analytical and in vitro cellular studies, *Nucl. Med. Biol.* **25** (1998) 689–695.
- [14.67] DENOYER, D., et al., Evidence that  $^{99m}\text{Tc}$ -(V)-DMSA uptake is mediated by NaPi cotransporter type III in tumour cell lines, *Eur. J. Nucl. Med. Mol. Imaging* **31** (2004) 77–84.
- [14.68] WERNER, A., DEHMELT, L., NALBANT, P.,  $\text{Na}^+$ -dependent phosphate cotransporters: the NaPi protein families, *J. Exp. Biol.* **201** (1998) 3135–3142.
- [14.69] FERNANDES, I., et al.,  $\text{NaPO}_4$  cotransport type III (PiT1) expression in human embryonic kidney cells and regulation by PTH, *Am. J. Physiol.* **277** (1999) F543–F551.
- [14.70] BIBER, J., et al., Renal Na/Pi-cotransporters, *Kidney Int.* **49** (1996) 981–985.
- [14.71] LAM, A.S., et al., Pentavalent  $^{99}\text{Tc}^{\text{m}}$ -DMSA imaging in patients with bone metastases, *Nucl. Med. Commun.* **18** (1997) 907–914.
- [14.72] KASHYAP, R., et al., Tc-99m(V) DMSA imaging. A new approach to studying metastases from breast carcinoma, *Clin. Nucl. Med.* **17** (1992) 119–122.
- [14.73] HIRANO, T., et al., Primary lung cancer SPECT imaging with pentavalent technetium-99m-DMSA, *J. Nucl. Med.* **36** (1995) 202–207.
- [14.74] SAHIN, T., et al., Evaluation of metastatic bone disease with pentavalent  $^{99}\text{Tc}^{\text{m}}$ -dimercaptosuccinic acid: a comparison with whole-body scanning and 4/24 hour quantitation of vertebral lesions, *Nucl. Med. Commun.* **21** (2000) 251–258.
- [14.75] LAM, A.S., PUNCHER, M.R., BLOWER, P.J., In vitro and in vivo studies with pentavalent technetium-99m dimercaptosuccinic acid, *Eur. J. Nucl. Med.* **23** (1996) 1575–1582.
- [14.76] HORUCHI-SUZUKI, K., et al., Skeletal affinity of Tc(V)-DMS is bone cell mediated and pH dependent, *Eur. J. Nucl. Med. Mol. Imaging* **31** (2004) 388–398.
- [14.77] GARCIA-SALINAS, L., et al., Uptake of the  $^{188}\text{Re}$ (V)-DMSA complex by cervical carcinoma cells in nude mice: pharmacokinetics and dosimetry, *Appl. Radiat. Isotop.* **54** (2001) 413–418.
- [14.78] BLOWER, P.J., et al., Pentavalent rhenium-188 dimercaptosuccinic acid for targeted radiotherapy: synthesis and preliminary animal and human studies, *Eur. J. Nucl. Med.* **25** (1998) 613–621.

## Chapter 15

# TECHNETIUM-99m LABELLED MOLECULES FOR HYPOXIA IMAGING

M. B. MALLIA, S. BANERJEE, M. VENKATESH

Radiopharmaceuticals Division, Bhabha Atomic Research Centre,  
Mumbai, India

### Abstract

In the field of diagnostic imaging, the concept of imaging hypoxia constitutes an important development and  $^{99\text{m}}\text{Tc}$  labelled vectors have taken a long stride in this direction. Delineation of hypoxic cells amidst oxygenated cells has a strong bearing on treatment strategies and regimes, since hypoxic cells are normally resistant to therapy, thus having a direct influence on the extent of tumour propagation and malignant progression. Inherent drawbacks in the invasive methods currently available for measuring hypoxia led to the development of non-invasive modalities such as use of radiolabelled molecules for imaging hypoxia. In the chapter, an attempt is made to provide a comprehensive overview of  $^{99\text{m}}\text{Tc}$  based radiopharmaceutical agents as well as a brief discussion of other radiolabelled agents that show considerable promise in diagnostic imaging of tumour hypoxia. The review also discusses the phenomenon of hypoxia, other non-invasive methods of detecting hypoxia currently available and the evolution of radiopharmaceuticals to image hypoxia.

### 15.1. INTRODUCTION

Tumour hypoxia is an important factor that influences treatment prognosis in cancer patients, both for radiation therapy as well as for most chemotherapy regimens. This fact has been recognized for more than five decades, which has led to efforts to detect the extent of hypoxia in tumours and to develop drugs that could selectively act on hypoxic tissues to enhance the efficacy of treatment. However, owing to the difficulties in invasive sampling of tumour mass for hypoxia measurement and due to the heterogeneity of hypoxic regions in tumours, these efforts have not been fully successful. Imaging hypoxia would be an invaluable non-invasive tool for this purpose and several investigators have addressed this issue over the past few decades. Several good reviews have appeared on this topic [15.1–15.4]. Identification of hypoxic regions in ischaemic brain and heart has significant implications for treatment planning and a hypoxia imaging agent would be very useful in such instances.

In order to image hypoxia, it is desirable to have increased accumulation of the tracer with decreasing oxygenation in the cell. This inverse relation is possible if the biochemical reaction of the radiolabelled molecule inside the cell is oxygen dependent, wherein the molecule is trapped under hypoxic conditions inside the cell. A variety of molecules that are selectively trapped in hypoxic cells, while remaining untrapped in normoxic cells, have been reported for their utility in radiosensitization. One category, known as oxygen mimetics, fit this requirement well. Among these, nitroimidazoles, such as misonidazole, have been explored extensively and have also shown promise for development into radiopharmaceuticals. Halogenated misonidazoles were the first set in the series of radiolabelled molecules reported for hypoxia imaging. Another approach is the use of metallic complexes in which the redox potential of the metal in a complex is adequately low to allow reduction followed by irreversible trapping inside oxygen starved hypoxic cells. Following this approach, extensive work has been reported with Cu(II)-diacetyl-bis(N<sup>4</sup>-methylthiosemicarbazone) (Cu-ATSM).

All of these compounds suffer from some kind of shortcoming, leading to further work in this area. Although <sup>18</sup>F based nitroimidazoles are now being used in clinical settings in many places, and many other molecules are actively being pursued through clinical trials, <sup>99m</sup>Tc based agents are still of interest due to their possible wider utility. Efforts in this direction, thus far, have led to several <sup>99m</sup>Tc labelled nitroimidazole molecules, labelled via a variety of functional moieties such as BAT0, PnAO, etc. However, the search for an ideal <sup>99m</sup>Tc based hypoxia imaging agent is still on, and in the recent past, with the new <sup>99m</sup>Tc synthons such as <sup>99m</sup>Tc-tricarbonyl and <sup>99m</sup>Tc-nitrido moieties, a few more potential hypoxia imaging <sup>99m</sup>Tc agents have been reported. An overview of the biochemical mechanism behind hypoxia and the <sup>99m</sup>Tc based agents for hypoxia imaging is given below.

## 15.2. HYPOXIA

The normal functioning of a cell requires an adequate supply of oxygen. However, in diseases where there is a reduction in the supply of oxygen to a tissue, cell or in a region of the body, the metabolic demands of the affected part can exceed the amount of energy supplied by the lower oxygen concentrations present in the cell. In such a physiological condition, where the supply of oxygen to the cell is exceeded by the metabolic requirement of the cell, the cell is said to be ‘hypoxic’. That a fundamental role is played by hypoxia in solid tumours is evidenced from experimental and clinical studies.

While addressing the condition related to oxygen deficiency, the term ‘hypoxia’ has been used by researchers in a variety of ways without a clear

definition of experimental conditions. Thus, while a biochemist may define hypoxia as oxygen limited electron transport, physiologists and clinicians define it as decreased oxygen partial pressure that restricts or even abolishes the function of organs, tissues and cells. Anoxia describes the state where no O<sub>2</sub> is detected in the tissue (oxygen partial pressure = 0 mmHg). Since malignant tumours no longer produce adequate amounts of adenosine triphosphate for homeostasis, the definitions of the term ‘hypoxia’ based on physiology are not necessarily valid for malignant tumours. Instead, alternative definitions based on oxygen partial pressures below a critical level are applied. Critical values of oxygen tension, below which certain events take place at the cellular level are outlined in Table 15.1 [15.1].

Since the clinical importance of tumour hypoxia is increasing, there must be a unanimous and unambiguous understanding between biologists, physiologists and clinicians with respect to ascertaining what is actually meant by the state of hypoxia.

### 15.2.1. Causes of hypoxia

The causes leading to hypoxia are manifold. These include low oxygen partial pressure in arterial blood due to pulmonary diseases or high altitude, the reduced ability of blood to carry oxygen as a result of anaemia, methemoglobin formation or poisoning with carbon monoxide or similar agents, reduced tissue perfusion or diffusion abnormalities, and inability of cells to use oxygen due to intoxication, as in cyanide poisoning [15.1]. Hypoxia may be present due to one

TABLE 15.1. CRITICAL VALUES OF OXYGEN TENSION,  
BELOW WHICH CERTAIN EVENTS TAKE PLACE AT THE  
CELLULAR LEVEL

Critical O <sub>2</sub> tension (mmHg)	Function or parameter observed
30–35	Effectiveness of certain immunotherapies
15–35	Cell death with photodynamic therapy
25–30	Cell death on exposure to X and $\gamma$ radiation
10–20	Binding of hypoxia markers
1–15	Proteome changes
0.2–1	Genome changes

or more of the above reasons in several pathological conditions. Thus, hypoxia can be associated with oncology, cardiovascular disease, cerebrovascular disease, diabetes, infection, during wound healing, joint hypoxia, etc. [15.2].

Generally, biological systems have feedback mechanisms which can meet the varying oxygen demands of the tissue. Thus, an increased demand for oxygen in a tissue is met by increasing the blood supply to that tissue. However, under certain conditions, such as in myocardial ischaemia, cerebrovascular ischaemia, tumour hypoxia, etc., this biological mechanism does not work and the tissue becomes hypoxic. The terms ‘ischaemia’ and ‘hypoxia’ imply the identical physiological state related to reduced oxygen partial pressure, but are used in different contexts, depending on the cause which led to the condition. In myocardium or in brain, a block in the artery may lead to reduced tissue perfusion, thus reducing the oxygen partial pressure in the concerned tissue, which may or may not lead to a state of hypoxia of pathophysiological importance. Such ‘ischaemic’ conditions refer to perfusion related abnormalities. In tumours, the fast growing cells require more oxygen. As a response to this condition, the tumour vasculature starts developing, a process called angiogenesis. However, tumour growth almost always outpaces the development of new supply lines within the tissue, resulting in very poor diffusion geometry, severe abnormalities of tumour microvessels and disturbed microcirculation inside tumour tissue, which fail to cater for the needs of all the cells [15.3]. Thus, in solid tumours, a heterogeneous situation prevails with regard to oxygenation, since, while the tumour cells situated near the blood capillary may be well oxygenated, those further away will be hypoxic.

### **15.2.2. Importance of hypoxia in clinical management**

As already mentioned, one of the major problems associated with hypoxic tissue is its resistance to radiation therapy and chemotherapy. It has been observed that a dose of up to three times as high is required to cause the same biological effect in a tissue in the absence of oxygen compared to in the presence of oxygen. This was attributed to a phenomenon called the ‘oxygen enhancement effect’ [15.4–15.7]. During the treatment of a hypoxic tumour, while the well oxygenated cells are killed, the hypoxic cells survive and become re-oxygenated, which results in regeneration and contributes to the recurrence of tumour growth [15.7]. The second factor is that hypoxia is not static and can be chronic (diffusion limited) or acute, which arises due to temporary occlusion of the blood vessels [15.8]. The period of hypoxia is generally short and, hence, cell proliferation will not be inhibited. The existence of such proliferating hypoxic cells has been observed in preclinical tumours [15.9]. Such ‘transiently hypoxic’ cells, just like other hypoxic cells, are resistant to therapy and once they become

re-oxygenated, they are again in a position to contribute to tumour re-population. The third problem associated with hypoxic cells is that tumour cells which survive hypoxic stress become increasingly tolerant of hypoxia. The next generation of cells originating from such tumour cells are more malignant and difficult to treat than the initial ones. This has been clearly proven by Graeber et al. [15.10]. Fourth, it has been observed in several preclinical studies that a hypoxic environment induces gene amplification, chromosomal rearrangements, DNA over-replication and DNA strand breaks, indicating that hypoxic stress offers a conducive environment for genetic modifications [15.11–15.13]. One of the marked consequences of these events is the acquisition of drug resistance [15.14]. Such genetic instabilities can also be a consequence of new pathways of DNA repair after hypoxic exposure [15.15, 15.16]. Genetic instability can lead to a more aggressive phenotype, which may be even more difficult to treat than the primary tumour cells. Finally, the cells exposed to hypoxic conditions can adapt to survive under low partial pressures of oxygen. The transcription factor, hypoxia-inducible factor-1 (HIF-1), is responsible for this survival mechanism [15.17]. HIF-1, a heterodimer which consists of  $\alpha$  and  $\beta$  subunits, is also expressed in normal cells. However, in normal cells, HIF-1 $\alpha$  is degraded by the enzyme prolyl hydroxylase. In hypoxic cells, low levels of oxygen inhibit prolyl hydroxylase, resulting in the buildup of HIF-1 $\alpha$ . HIF-1 $\alpha$ , when stabilized by hypoxic conditions, upregulates several genes to promote survival in low oxygen conditions. These include glycolytic enzymes, which allow ATP synthesis in an oxygen independent manner, and vascular endothelial growth factor (VEGF), which promotes angiogenesis [15.17, 15.18]. These factors make hypoxia a formidable challenge and it is, hence, very important to identify hypoxic tumours and to sensitize them to achieve complete therapy.

#### *15.2.2.1. What is the critical level of hypoxia to look for?*

It has already been mentioned that hypoxia is associated with several pathological conditions. However, the prime concerns of clinicians are related to tumour hypoxia. This is because hypoxia plays a negative role in cancer treatment, either by radiation therapy or chemotherapy [15.5–15.7]. Any tissue or cell that has an oxygen partial pressure below that of normal oxygen partial pressure can be called hypoxic. Thus, cells which are anoxic (have no oxygen), extremely hypoxic, moderately hypoxic, less hypoxic, etc., can exist within the same tumour, and there is no clear boundary between these different groups of hypoxic cells. However, there is a certain upper threshold level of oxygen partial pressures below which certain cellular functions progressively become restricted with a decreased oxygen partial pressure. This could, thus, be the basis on which the critical hypoxic level can be set. Hence, in the case of tumour hypoxia, the

interest will be in quantifying the cells with hypoxic levels below which they are resistant to radiation therapy and chemotherapy (radiobiological hypoxia fraction (RHF)).

### 15.3. METHODS FOR DETECTING TUMOUR HYPOXIA

While there are several methods for detecting tumour hypoxia, many factors need to be considered for deciding the most appropriate one for a particular experimental or clinical situation. The feasibility of the method, approaches available in terms of invasiveness, the degree of resolution required and the cost are the prime factors in this context. In the past, the oxygenation status of solid tumours was evaluated to assess the degree of hypoxia. Despite various limitations in the techniques used, several key findings resulted, such as: (i) most tumours have lower median oxygen partial pressures than their tissue of origin; (ii) many solid tumours contain areas of low oxygen partial pressure that cannot be predicted by clinical size, stage, grade histology and site; (iii) tumour to tumour variability in oxygenation is usually greater than intratumour variability in oxygenation; and (iv) recurring tumours have a poorer oxygenation status than the corresponding primary tumours. Intratumour polarographic measurement of oxygen partial pressures using microsensor techniques is, at present, the ‘gold standard’ and makes use of the systematic random sampling principle [15.18]. However, no single method will probably be suitable for all situations. The use of more than one technique is, therefore, recommended and careful interpretation of the data obtained in all cases is of prime importance, keeping in mind the limitations of the specific methods used.

Assessment of tumour oxygenation status by invasive and non-invasive procedures has been reviewed [15.1, 15.19–15.22], and can be categorized as follows:

#### *Invasive techniques*

- Polarographic O<sub>2</sub> sensors; luminescence based optical sensors;
- Electron paramagnetic resonance oximetry;
- Cryospectrophotometry [HbO<sub>2</sub> saturation]; Near-infrared spectroscopy [HbO<sub>2</sub> saturation]; phosphorescence imaging;
- Immunohistochemical hypoxia marker techniques using misonidazole [<sup>3</sup>H labelled pimonidazole, etanidazole, nitroimidazole-theophylline].

### *Non-invasive techniques*

- NMR spectroscopy and imaging techniques (blood oxygen level dependent BOLD MRI,  $^1\text{H}$  MRI,  $^{19}\text{F}$  magnetic resonance oximetry);
- Nuclear medicine imaging following *in vivo* administration of radiolabelled molecules which become trapped in hypoxic cells forming adducts [ $^{18}\text{F}$ ]fluoromisonidazole (PET), [ $^{123}\text{I}$ ]iodoazomycin-arabinoside (SPECT),  $^{60/62/64}\text{Cu}$ -ATSM (PET).

Invasive techniques suffer from serious drawbacks, namely the need to place a needle directly into the tumour, the high cost of the equipment, tumour inaccessibility, high inter-observer variability, failure to distinguish necrosis from hypoxia and lack of spatial information. Invasive techniques are, therefore, not popular.

Another method for assessing tumour hypoxia is through the administration of an injectable hypoxia marker such as pimonidazole (1-(2-nitro-1-imidazolyl)-3-N-piperidino-2-propanol) and EF5 [2-(2-nitro-1H-imidazol-1-yl)-N-(2,2,3,3,3-pentafluoropropyl) acetamide]. As all 2-nitroimidazoles, these compounds form stable adducts with intracellular macromolecules and this binding is proportionally inhibited as a function of increasing oxygen concentration. Detection of these adducts with antibodies can provide information on the relative oxygenation of the tissue at a cellular resolution. This approach is limited by the requirement for exogenous drug administration and additional biopsies for staining.

The inherent drawbacks in the invasive methods available today for measuring hypoxia have provided the impetus for development of non-invasive modalities for the purpose. The detection of tumour hypoxia by radionuclide imaging techniques was proposed by Chapman in 1979 [15.23] using radiolabelled 2-nitroimidazoles which are reduced enzymatically and trapped in regions of low oxygen concentration. Since then,  $^{18}\text{F}$ -fluoromisonidazole (FMISO) has been developed and evaluated for detecting hypoxia in tumours [15.24] and myocardium [15.25] with PET. A series of  $^{123}\text{I}$  labelled 2-nitroimidazole derivatives for imaging have been investigated with the more widely available single photon emission computed tomography (SPECT), culminating in  $^{123}\text{I}$ -iodoazomycin arabinoside (IAZA), which is in clinical trials [15.26–15.28]. The majority of nitroaromatics studied for targeting hypoxia are based on nitroimidazoles. The mechanism of reduction of nitroimidazoles has been well documented by Nunn et al. [15.29]. In essence, the agent enters cells by passive diffusion owing to its lipophilicity, which is the major determinant governing its entry. Inside the cell, the nitroimidazole undergoes a series of one electron reductions, mediated by various nitro-reductase enzymes. However,

because the initial single electron reduction step, which results in the formation of a radical anion  $\text{RNO}_2^-$ , is reversible in the presence of oxygen, further reduction of nitroimidazole is prevented in normoxic cells and the unchanged nitroimidazole is eventually cleared. On the other hand, in hypoxic cells, the reduction proceeds further, resulting in the formation of hydroxylamine derivative ( $\text{RNHOH}$ ), amine derivative ( $\text{RNH}_2$ ), followed by ring fragmentation and subsequent binding of the fragments to cellular components.

Apart from the nitroimidazole based agents, there has been a keen interest in using radiolabelled Cu(II) complexes of substituted dithiosemicarbazones. Such complexes are non-selectively taken up in cells, but selectively undergo bioreduction in hypoxic cells, followed by dissociation of the complex and binding of copper to cellular components [15.30]. In the presence of  $\text{O}_2$ , the Cu(I)-ATSM is rapidly reoxidized to Cu(II)-ATSM, which can freely diffuse out of cells. Among these, Cu(II)diacetyl-bis(N4-methylthio semi carbazone) (ATSM) [15.31–15.34] is being tested in clinical situations, since the redox potential of Cu(II) to be reduced to Cu(I) in this complex is amenable for its entrapment in oxygen deficient cells. Although very promising results have been reported from some groups, the utility of  $^{62}\text{Cu}$ (II)-ATSM to delineate hypoxic regions in all types of solid tumours has not been unequivocally proven.

Owing to the limited availability and high cost of cyclotron produced  $^{18}\text{F}$ ,  $^{123}\text{I}$  and  $^{62}\text{Cu}$ ,  $^{99\text{m}}\text{Tc}$  based agents could serve as more desirable alternatives.

### **15.3.1. Technetium-99m labelled radiopharmaceuticals for targeting tumour hypoxia: An overview**

The development of  $^{99\text{m}}\text{Tc}$  labelled radiopharmaceuticals for targeting hypoxia has been pursued for the past few decades. One common factor in these studies is the use of nitroimidazole derivatives as the basic hypoxia targeting moiety. In the beginning,  $[^{99\text{m}}\text{Tc}=\text{O}]^{3+}$  (the mono-oxo core) was used for labelling the molecules, while in the recent past, novel cores such as the  $[^{99\text{m}}\text{Tc}=\text{N}]^{2+}$  and  $[^{99\text{m}}\text{Tc}(\text{CO})_3(\text{H}_2\text{O})_3]^+$  cores have been employed. In this article, the  $^{99\text{m}}\text{Tc}$  labelled radiopharmaceuticals for targeting hypoxia are grouped based on the  $^{99\text{m}}\text{Tc}$  core used for labelling the molecule, with one category detailing molecules labelled with the  $[^{99\text{m}}\text{Tc}=\text{O}]^{3+}$  core and the second category the molecules labelled with other  $^{99\text{m}}\text{Tc}$  cores, such as the  $[^{99\text{m}}\text{Tc}=\text{N}]^{2+}$  and  $[^{99\text{m}}\text{Tc}(\text{CO})_3(\text{H}_2\text{O})_3]^+$  cores. A few selected molecules which showed some promise for targeting tumour hypoxia are discussed in detail, while the others have been grouped together, in order to provide a brief overview of the developments that have taken place so far in this area of research.

### *15.3.1.1. Molecules based on $[^{99m}\text{Tc}=\text{O}]^{3+}$ or $[\text{O}=\text{^{99m}Tc}=\text{O}]^+$ cores*

- (a) BMS181321(oxo[[3,3,9,9-tetramethyl-1-(2-nitro-1H-imidazol-1-yl)-4,8-diazaundecane-2,10-dione dioximato](3-)N,N',N'',N''']-technetium)

This molecule is 2-nitroimidazole linked via a methylene group to a PnAO (propylene amine oxime). The  $^{99m}\text{TcO}$  complex could be prepared by mixing the ligand and sodium pertechnetate at room temperature using stannous tartrate as the reducing agent. The four nitrogen atoms of the PnAO ring coordinate with the  $[^{99m}\text{Tc}=\text{O}]^{3+}$  core to form a neutral complex (Fig. 15.1). This complex was initially explored for its potential as a myocardial and cerebral hypoxia targeting agent by Rumsey et al. [15.35]. The in vitro studies carried out in a perfused heart model showed preferential uptake of the complex in the myocardium under hypoxic conditions compared to normoxic conditions. Ballinger et al. investigated the same complex for its potential to target tumour hypoxia [15.36]. In vitro studies carried out in Chinese hamster ovary (CHO) cells maintained at different partial pressures of oxygen, extremely hypoxic (<10 ppm of oxygen) to normoxic, demonstrated selective accumulation and retention of this complex in hypoxic cells compared to normoxic cells. The study also revealed a dependency of accumulation and retention of this complex on oxygen, with decreasing trends observed in the accumulation and retention with increases in partial pressure of oxygen. In vivo biodistribution and imaging studies were carried out in C3H/HeJ male mice bearing KHT (fibrosarcoma), SCC-VII (squamous cell carcinoma) and RIF-1 (radiation induced fibrosarcoma) tumours. Dynamic gamma camera imaging showed rapid distribution of the agent, upon intravenous injection, throughout the body with major clearance through the hepatobiliary route. This was attributed to the very high lipophilicity of the complex ( $\log P_{\text{o/w}} = 40$ ). In all of the tumour models, steady retention of activity was observed until 8 h post-injection. The tumour:muscle ratio obtained was high, but the tumour:blood ratio remained suboptimal (below one). The tumour could be visualized at 2 h post-injection in the gamma camera image of mice bearing an SCC-VII tumour, but only after masking the abdominal activity. This was a major drawback that prevented imaging of tumours situated in and around the abdominal region. Other limitations of this agent, apart from its very high lipophilicity, included chemical decomposition in saline and cell culture medium with a half-life of 16–20 h.

- (b) BRU59-21(oxo[[3,3,9,9-tetramethyl-5-oxa-6-(2-nitro-1H-imidazol-1-yl)-4,8-diazaundecane-2,10-dione dioximato](3-N,N',N'',N'')]technetium)

BRU59-21, previously known as BMS194796, was reported by Melo et al. [15.37]. This molecule was the successor to BMS181321 and had improved characteristics as far as lipophilicity and stability are concerned. The structural features of BRU59-21 (Fig. 15.1) were also different from its predecessor; for example, the substitution of one of the methylene groups in the propylene bridge with oxygen, and changing the point of attachment of the 2-nitroimidazole moiety, which, the authors claim, is the reason for the improved stability of the complex and its lower lipophilicity ( $\log P_{o/w} = 12$ ). These modifications effectively improved the pharmacokinetics of the complex compared to BMS181321 (faster clearance, hence lower background activity), which resulted in a higher target:background ratio, and at the same time retaining the favourable in vitro properties exhibited by BMS181321. The complex could be prepared by mixing the ligand and sodium pertechnetate at room temperature using stannous chloride as the reducing agent. As mentioned earlier, BRU59-21 showed similar in vitro properties, but in terms of absolute uptake, BRU59-21 showed lower uptake compared to BMS181321, probably due to the lower lipophilicity of the former compound. However, the hypoxic–aerobic differential (ratio of the uptake of radioactivity under extremely hypoxic conditions to the uptake of radioactivity under aerobic conditions) was similar. The biodistribution and imaging study of BRU59-21 in mice bearing a KHT-C tumour showed rapid distribution of activity in various organs/tissue, albeit to a lower extent as compared to BMS181321. This was again attributed to the lower lipophilicity of BRU59-21 as compared to BMS181321. The maximum tumour:muscle ratios obtained with both the agents are similar. However, BRU59-21 showed a slightly higher tumour:blood ratio. Despite the lower lipophilicity of BRU59-21, the major clearance of activity was through the hepatobiliary route. Hence, the problem of high abdominal activity associated with BMS181321 persisted with BRU59-21, making it difficult to image tumours in the vicinity of the abdominal region.

- (c) HL-91

The  $^{99m}\text{Tc}$ -HL-91 (BnAO (butylene amine oxime), PROGNOX) (Fig. 15.1) is a non-nitroimidazole based complex, which shows hypoxia specific accumulation [15.38]. The utility of this compound was discovered accidentally, while it was being used as a non-targeted control in the evaluation of a series of mono- and bis-2-nitroimidazoles coupled to amine oxime chelators. The in vivo properties of this complex were also found to be good, with extensive renal

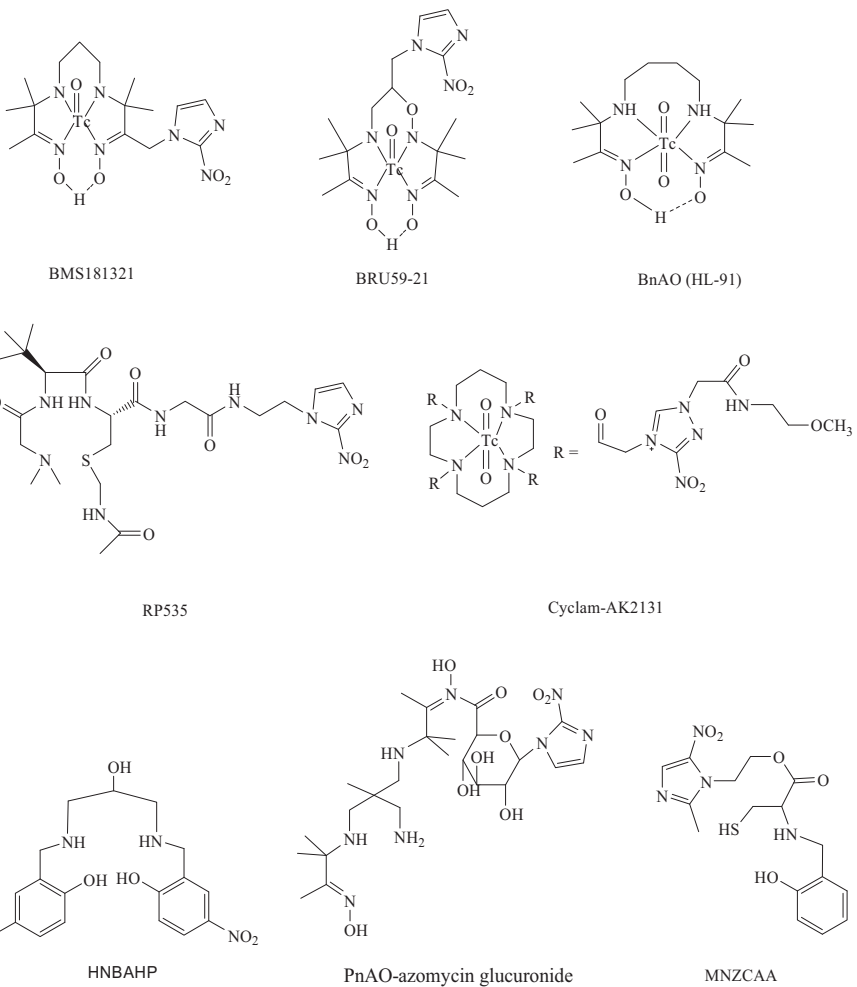


FIG. 15.1.  $^{99m}\text{Tc}$  based molecules studied for their hypoxia imaging properties.

clearance, thus considerably reducing the background activity. The  $\log P_{\text{o/w}}$  was found to be 0.1, which was considerably less than that of BMS181321 and BRU59-21 complexes. The accumulation of the  $^{99m}\text{Tc}$ -BnAO complex in hypoxic cells was found to be much lower than that of either BMS181321 or BRU59-21 complexes, but a ninefold hypoxic:aerobic ratio was observed [15.38]. Reports on preclinical evaluations of this agent in murine and xenograft systems *in vivo* clearly demonstrate the utility of this complex to target tumour hypoxia. An excellent correlation was observed between  $^{99m}\text{Tc}$ -HL91 retention and hypoxia measured with an Eppendorf oxygen electrode [15.39]. The structure of

$^{99m}$ Tc-HL91 has not been conclusively determined. However, studies carried out by Brauers et al. suggested the possibility that  $^{99m}$ Tc-HL91 could adopt both the mono-oxo form as well as the dioxo form in solution [15.40]. The study also indicated that this could be important in the uptake of this complex in hypoxic cells, as the mono-oxo form is lipophilic, while the dioxo form is hydrophilic. The authors also demonstrated that the bioreducibility of  $^{99m}$ Tc-HL91 is technetium essential, as in the Cu-ATSM compounds mentioned earlier.

#### (d) Other molecules

Linder et al. studied a series of nitroimidazole-BATO (BATO (boronic acid adduct of technetium dioximes)) complexes of technetium containing either 2-nitroimidazole or 4-nitroimidazole [15.41]. They were found to form neutral complexes with technetium. In vitro enzyme assays of these complexes showed that these complexes are recognized and reduced by nitroreductase and xanthine oxidase under anaerobic conditions. However, the results indicated that the rate of reduction of the complexes is much slower than that of the unchelated form, thus limiting the utility of this complex *in vivo*.

Ramalingam et al. synthesized and compared a new class of bis(amine-phenol) based 2-nitroimidazole complexes [15.42] of technetium with BMS181321. However, the in vitro studies of this complex carried out to evaluate the permeability and uptake of this compound in normoxic and anoxic myocytes, revealed that the complex is neither permeable through cultured bovine brain endothelial cells, nor showed any preferential uptake in anoxic myocytes.

Zhang et al. synthesized a  $^{99m}$ Tc labelled complex of an amine nitrophenol ligand (HNBAHP) [15.43]. This was a non-nitroimidazole containing complex where the radiosensitizer property of an aromatic nitro-compound is utilized to target hypoxic cells. The complex could be prepared with a radiochemical yield of more than 97%, and was found to be stable for up to 24 h. Paper electrophoresis studies showed that the complex is neutral. Whole body imaging studies with this complex, performed in balb/c mice bearing an EMT-6 tumour, revealed that the tumour could only be visualized after 20 h, which the authors ascribed to slow blood clearance and slow uptake into the tumour.

The same group of workers reported two more  $^{99m}$ Tc complexes of peptides containing a 2-nitroimidazole moiety, namely 1-[(diphenylphosphino)acetylglycylglycyl-2-aminoethyl]-2-nitroimidazole (HL-501) and 1-[N-(benzoylthioglycolyl)glycylglycyl-2-aminoethyl]-2-nitroimidazole (HL-601) [15.44]. The respective complexes,  $^{99m}$ Tc-HL501 and  $^{99m}$ Tc-HL601, could be prepared in high radiochemical yields and are found to be neutral. However, the biodistribution studies and imaging studies performed in balb/c mice bearing an EMT-6 tumour showed negligible tumour uptake.

Su et al. reported two peptidic agents containing a 2-nitroimidazole moiety, namely dimethylglycyl-L-seryl-L-cysteinyl-lysyl{N<sub>c</sub>-[1-(2-nitro-1H-imidazolyl)acetamido]} glycine (RP453) and dimethylglycyl-tert-butylglycyl-L-cysteinyl-glycine-[2-(2-nitro-1H-imidazolyl) ethyl] amide (RP535, Fig. 15.1) [15.45]. Both of the molecules contained an NS<sub>3</sub> class chelator, which coordinated with the [<sup>99m</sup>Tc=O]<sup>3+</sup> core forming the complex. While <sup>99m</sup>TcO-RP453 was formed as a mixture of syn-isomer and anti-isomer, <sup>99m</sup>TcO-RP535 could be prepared as a single species. In vitro studies carried out in CHO cells, following the procedure used for BMS181321 and BRU59-21, showed selective accumulation of both the complexes in cells under hypoxic conditions. However, <sup>99m</sup>TcO-RP535 performed better than <sup>99m</sup>TcO-RP453 and the authors proposed RP535 as a lead compound for further investigation. The same group reported another series of <sup>99m</sup>TcO complexes of 2-nitroimidazole and 4-nitroimidazole linked to amine-dioxime, a bidentate chelator [15.46]. Two such molecules can, therefore, form '2+2' types of complexes with the [<sup>99m</sup>Tc=O]<sup>3+</sup> core. In studies carried out in an in vitro model of hypoxia, while the 2-nitroimidazole complexes showed selective accumulation in hypoxic conditions, the 4-nitroimidazole counterpart showed variable selectivity.

Murugesan et al. reported a cyclam based nitrotriazole complex of <sup>99m</sup>Tc (Fig. 15.1) [15.47]. It has four nitrotriazole (AK2123) molecules linked to the four nitrogens of cyclam. The resultant <sup>99m</sup>Tc complex was positively charged with a log P<sub>o/w</sub> value of 0.1. The complex showed extensive renal clearance and exhibited a high tumour:muscle ratio in studies carried out in rats bearing carcinogen induced mammary tumours, and in immune deficient mice bearing EMT-6 tumours.

Kumar et al. synthesized a PnAO derivative of azomycin glucuronate and labelled it with <sup>99m</sup>Tc [15.48]. The structural features of the prepared ligand led to multiple possibilities of coordination with <sup>99m</sup>Tc. Eventually, two different formulations were prepared at different pH, pH7.6 and pH8.6, and were then tested both in vitro and in vivo. While the in vitro evaluation of the two labelled complexes indicated selective binding to hypoxic EMT-6 cells, the in vivo studies indicated different results. The complex prepared at pH7.6 did not show much promise, whereas with the complex prepared at pH8.6, the tumour could be visualized after 3 h post-injection.

Das et al. reported a metronidazole derivative with a cysteine based chelator, MNZCAA (Fig. 15.1), to label with the [<sup>99m</sup>Tc=O]<sup>3+</sup> core [15.49]. As generally observed while labelling the [<sup>99m</sup>Tc=O]<sup>3+</sup> core, excess ligand concentration was required for obtaining a satisfactory complexation yield in this case as well. Although the complex was not tested in an in vitro hypoxia model, biodistribution in Swiss mice bearing a fibrosarcoma tumour showed accumulation of activity in the tumour that cleared with time. While the complex

exhibited a high tumour:muscle ratio, fast clearance of activity from the tumour limited its applicability. Chu et al. reported a 4-nitroimidazole derivative with a hydroxyiminoamide chelator [15.50]. Although the complex was not well characterized, the biodistribution studies in the S180 tumour demonstrated uptake and slow clearance from the tumour.

#### *15.3.1.2. Molecules based on $[^{99m}\text{Tc}\equiv\text{N}]^{2+}$ and $[^{99m}\text{Tc}(\text{CO})_3]^{+}$ cores*

The classical method of  $^{99m}\text{Tc}$  labelling, either directly with  $^{99m}\text{Tc}$  metal, via the oxo  $[\text{O}=\text{O}]^{3+}$  core or dioxo  $[\text{O}=\text{O}=\text{O}]^{+}$  core, is often associated with the drawback of the requirement of a high ligand concentration for obtaining satisfactory labelling yields. This is because the labelling procedure involves in situ generation of the  $^{99m}\text{Tc}$  core, using a suitable reducing agent; the absence of sufficient ligand to stabilize the  $^{99m}\text{Tc}$  core may lead to further reduction of  $^{99m}\text{Tc}$ , thus affecting the complexation yields. Another problem associated with technetium oxo cores is their stability. They are prone to atmospheric oxidation resulting in decomposition of the complex.

Introduction of novel technetium cores, namely the  $[\text{C}\equiv\text{N}]^{2+}$  core [15.51, 15.52] by A. Duatti et al. and the  $[\text{O}=\text{O}=\text{O}]^{+}$  core [15.53] by R. Alberto et al. opened up a new avenue in  $^{99m}\text{Tc}$  labelling chemistry of small molecules and biomolecules. The significant advantage of these cores is that they can be prepared in the form of a precursor and that they are very stable with respect to the re-oxidation of the metal, thus overcoming the stability issues encountered with  $^{99m}\text{TcO}$  complexes, such as BMS181321. It is not yet clear whether these novel cores of technetium are bioreducible, as in the case of  $^{99m}\text{Tc}$ -HL91. Hence, for the time being, they just offer another efficient labelling route with an added benefit of achieving high complexation yields with a very low ligand concentration.

##### (a) Molecules labelled with the $[\text{C}\equiv\text{N}]^{2+}$ core

The soft metal centre in the  $[\text{C}\equiv\text{N}]^{2+}$  core prefers coordination with a chelator having soft donor atoms such as sulphur and phosphorus [15.54]. Hence, target specific molecules could be modified to incorporate chelators with soft donor atoms as in dithiocarbamate, cysteine, xanthate, etc., which could then be complexed with the  $[\text{C}\equiv\text{N}]^{2+}$  core. The  $[\text{C}\equiv\text{N}]^{2+}$  core forms a  $^{99m}\text{TcNL}_2$  ( $\text{L}$ , a bidentate ligand) type square pyramidal complex. Probably the first attempt to utilize the  $[\text{C}\equiv\text{N}]^{2+}$  core in the designing of a molecule to target hypoxia was made by our group where we modified the -OH group of metronidazole to the corresponding xanthate by a simple procedure (Fig. 15.2) [15.55]. The  $^{99m}\text{TcN}$  complex could be prepared by incubating the ligand with the freshly prepared

$[^{99m}\text{Tc}\equiv\text{N}]^{2+}$  core for 30 min at room temperature. In vivo biodistribution studies carried out in Swiss mice bearing a fibrosarcoma tumour, indicated steady retention of activity in the tumour throughout the period of study of 3 h. Clearance of this complex was predominantly through the hepatobiliary route. The washout of the complex from the liver and blood was slow, which resulted in high background activity and poor tumour:blood ratios. These factors limit the utility of this complex.

Following this, Kong et al. reported an asymmetrical  $^{99m}\text{TcN}$  complex of metronidazole (Fig. 15.2) and a biphosphine ligand, PNP5 (N-ethoxyethyl-N,N-bis[2-(bis(3-methoxypropyl)phosphino)ethyl]-amine) [15.56]. As mentioned earlier, the  $[^{99m}\text{Tc}\equiv\text{N}]^{2+}$  core generally forms symmetrical  $^{99m}\text{TcNL}_2$  type complexes with bidentate ligands. However, with biphosphine ligands, asymmetrical complexes are formed. This asymmetric labelling approach is particularly useful for big molecules, such as fatty acids or peptides, where a  $^{99m}\text{TcNL}_2$  type complex may not be suitable (the resulting complex will be twice as big) for several reasons. Nevertheless, these ligands, when present in a complex, are sometimes very useful in vivo, as they contain ether groups which undergo hydrolysis in the liver, making the complex hydrophilic and, thus, excretion is faster. This helps in reducing background activity to a considerable extent, thereby improving the target:background ratio. Dejing et al. employed this strategy in their metronidazole derivative and the biodistribution clearly showed very fast excretion of the complex from the liver and other vital organs, resulting in better tumour:blood and tumour:muscle ratios compared with BMS194796 and BRU59-21. The biodistribution also showed uptake and slow clearance of activity from the tumour and warrants further investigation.

#### (b) Molecules labelled with the $[^{99m}\text{Tc}(\text{CO})_3(\text{H}_2\text{O})_3]^+$ core

The  $[^{99m}\text{Tc}(\text{CO})_3(\text{H}_2\text{O})]^+$  core (Fig. 15.2) is another addition to the list of novel technetium cores introduced relatively recently [15.57, 15.58]. The three substitutionally labile water molecules in the  $[^{99m}\text{Tc}(\text{CO})_3(\text{H}_2\text{O})_3]^+$  core facilitate the formation of stable complexes with tridentate ligands such as iminodiacetic acid, diethylene triamine, histidine, etc. [15.58] and, hence, target-specific molecules of interest are often modified to possess one of these ligating groups.

Attempts to explore the possibility of utilizing the  $[^{99m}\text{Tc}(\text{CO})_3(\text{H}_2\text{O})_3]^+$  core for designing molecules to target tumour hypoxia was initiated by our group. A 2-nitroimidazole iminodiacetic acid derivative [15.59] in which the iminodiacetic acid group was attached to 2-nitroimidazole by a two carbon methylene spacer was the first one to be reported in this category (Fig. 15.2). Excellent labelling yields could be achieved under low ligand concentrations by incubating the ligand and the  $^{99m}\text{Tc}(\text{CO})_3(\text{H}_2\text{O})_3]^+$  core for 30 min at room

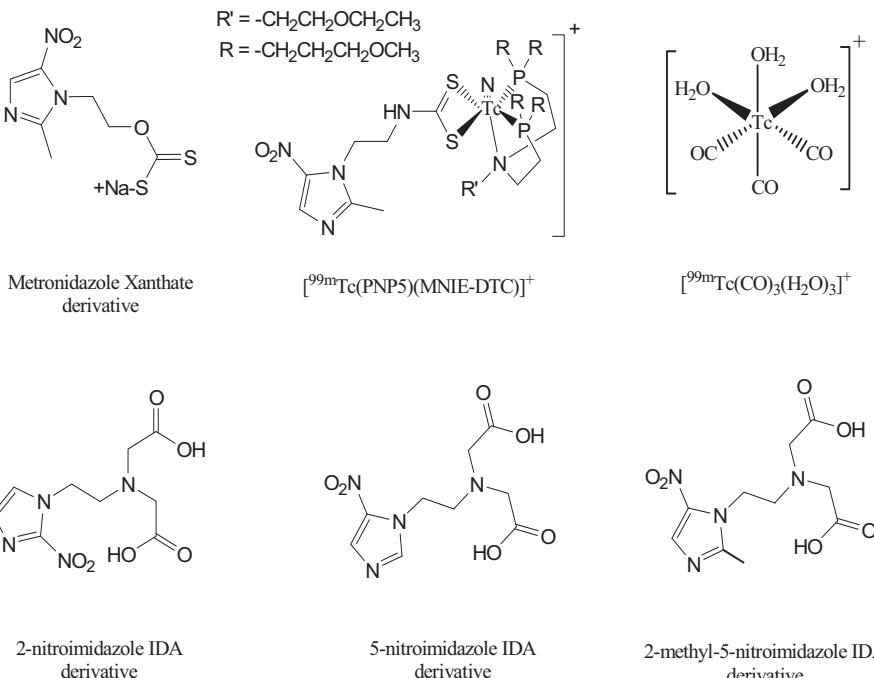


FIG. 15.2. Molecules labelled with novel cores of <sup>99m</sup>Tc studied for imaging tumour hypoxia.

temperature. Preliminary studies of this complex, in Swiss mice bearing a fibrosarcoma tumour, showed uptake and steady retention of activity in the tumour. Although the log  $P_{o/w}$  of this complex was  $-0.82$ , the clearance of injected activity from the body was predominantly through the hepatobiliary route, which was a matter of concern as this would lead to increased background activity and a poor target:background ratio, thereby posing difficulty in imaging hypoxic tissue in and around the abdominal region. Studies are ongoing to bring about a structural modification which could alleviate the problem.

As mentioned earlier, the mechanism of trapping nitroimidazole in hypoxic cells involves multiple reduction steps subsequent to the initial single electron reduction step. This initial step is crucial in deciding the specificity of the molecule to targeting hypoxic cells. Careful observation of the compilation of single electron reduction potential values of various nitroimidazoles by Wardman [15.60] reveals that the 2-nitroimidazoles are in the range of  $-250$  to  $-350$  mV (with respect to the standard hydrogen electrode), whereas the values for 5-nitroimidazoles range from  $-350$  to  $-450$  mV, and for 4-nitroimidazole are still further down. These values may increase or decrease depending upon the nature of the substituent in the nitroimidazole ring. The reduction potential of molecular

oxygen is  $-155$  mV in the same scale, which clearly explains the lack of accumulation of nitroimidazole based molecules in normoxic cells, and the preferential accumulation in hypoxic cells. This also explains why 2-nitroimidazole derivatives are being explored more than any other nitroimidazole derivatives. However, the single electron reduction potential is, probably, not the only factor that governs the retention of the molecules in hypoxic cells. There are reports of 4-nitroimidazole and 5-nitroimidazole derivatives showing uptake and retention in tumours similar to those of 2-nitroimidazole derivatives, suggesting that such molecules should not be left unexplored [15.49, 15.50, 15.61–15.63].

Recently, the potential of the unsubstituted 5-nitroimidazole derivative (Fig. 15.2) to target hypoxia has been explored by our group [15.64]. Although, there are several reports about labelled metronidazole [15.49, 15.61–15.63], a methyl-substituted 5-nitroimidazole, as a hypoxia targeting agent, has been studied for the first time owing to the unavailability of unsubstituted 5-nitroimidazole. This study will also reveal whether the methyl substitution in the nitroimidazole ring will result in any significant difference in the *in vivo* behaviour of the complex. The *in vivo* evaluation of the  $^{99m}\text{Tc}(\text{CO})_3$  labelled unsubstituted 5-nitroimidazole, in Swiss mice bearing a fibrosarcoma tumour, showed uptake and slow clearance of activity from the tumour, with a high tumour:muscle ratio. However, the results were not significantly different from the methyl substituted counterpart, 2-methyl-5-nitroimidazole, reported earlier (Fig. 15.2) [15.65].

#### 15.4. CONCLUSION

Realizing the negative role played by hypoxia in cancer management and treatment, and the logistical and economic problems associated with cyclotron based hypoxia agents, the need for a  $^{99m}\text{Tc}$  based molecule for qualitative and quantitative assessment of hypoxia is undoubtedly felt by the nuclear medicine community. Although several attempts have been made to realize this need, these have ended in limited success and no single  $^{99m}\text{Tc}$  based radiopharmaceutical has emerged as a successful candidate for imaging hypoxia. Unlike in the design of cyclotron based agents ( $^{18}\text{F}$ ,  $^{123}\text{I}$ , etc.), where the introduction of the radioactive isotope does not create a significant change in the properties of the targeting molecule, introduction of  $^{99m}\text{Tc}$  may require synthetic modifications of the target molecule to tag  $^{99m}\text{Tc}$ , resulting in the alteration of the original *in vivo* properties shown by the target molecule. In a way, this could be considered advantageous as the property of the complex can sometimes be fine tuned with such modification. Another major hurdle with developing  $^{99m}\text{Tc}$  based hypoxia targeting agents is the

lack of proper guidelines on defining the right combination of properties needed, such as lipophilicity, reduction potential, charge, etc., for a molecule to be a successful hypoxia targeting agent. The understanding of biochemical reactions in relation to cell oxygen content is the current guiding factor in designing hypoxia specific molecules for imaging. A systematic study of the effect of various parameters on the uptake, retention and pharmacokinetics of the complex *in vivo* may provide a path towards a successful hypoxia targeting agent.

## REFERENCES TO CHAPTER 15

- [15.1] HOCKEL, M., VAUPEL, P., Tumor hypoxia, definitions and current clinical, biologic, and molecular aspects, *J. Natl. Cancer Inst.* **93**(4) (2001) 266–276.
- [15.2] WIEBE, L.I., MACHULLA, H.J., “Hypoxia: An introduction”, *Imaging Hypoxia* (MACHULLA, H.J., Ed.), Kluwer Academic Publishers, The Netherlands (1999) 1–18.
- [15.3] VAUPEL, P., KALLINOWSKI, F., OKUNIEFF, P., Blood flow, oxygen and nutrient supply, and metabolic microenvironment of human tumors: a review, *Cancer Res.* **49** (1989) 6449–6465.
- [15.4] KROHN, K.A., LINK, J.M., MASON, R.P., Molecular imaging of hypoxia, *J. Nucl. Med.* **49** (2008) 129S–148S.
- [15.5] GRAY, L.H., CONGER, A.D., EBERT, M., HORNSEY, S., SCOTT, O.C., The concentration of oxygen dissolved in tissues at the time of irradiation as a factor in radiotherapy, *Br. J. Radiol.* **26** (1953) 638–648.
- [15.6] HALL, E.J., (Ed.), *Radiobiology for the Radiologist*, Lippincott, Philadelphia, PA (1994).
- [15.7] HILL, R.P., “Cellular basis of radiotherapy”, *The Basic Science of Oncology* (TANNOCK, I.F., HILL, R.P., Eds), McGraw-Hill, New York, NY (1992) 259–275.
- [15.8] BROWN, J.M., WILSON, W.R., Exploiting tumour hypoxia in cancer treatment, *Nat. Rev. Cancer* **4** (2004) 437–447.
- [15.9] WEBSTER, L., HODGKISS, R.J., WILSON, G.D., Cell cycle distribution of hypoxia and progression of hypoxic tumour cells *in vivo*, *Br. J. Cancer* **77** (1998) 227–234.
- [15.10] GRAEBER, T.G., et al., Hypoxia-mediated selection of cells with diminished apoptotic potential in solid tumors, *Nature* **379** (1996) 88–91.
- [15.11] YOUNG, S.D., MARSHALL, R.S., HILL, R.P., Hypoxia induces DNA overreplication and enhances metastatic potential of murine tumor cells, *Proc. Natl. Acad. Sci. USA* **85** (1988) 9533–9537.
- [15.12] REYNOLDS, T.Y., ROCKWELL, S., GLAZER, P.M., Genetic instability induced by the tumor environment induced by the tumour microenvironment, *Cancer Res.* **56**, (1996) 5754–5757.
- [15.13] HILL, R.P., Tumour progression: potential role of unstable genomic changes, *Cancer Metas. Rev.* **9** (1990) 137–147.

- [15.14] TEICHER, B.A., Hypoxia and drug resistance. *Cancer Metas. Rev.* **13** (1994) 139–168.
- [15.15] BINDRA, R.S., SCHAFFER, P.J., MENG, A. et al., down-regulation of Rad51 and decreased homologous recombination in hypoxic cancer cells, *Mol. Cell Biol.* **24** (2004) 8504–8518.
- [15.16] KOSHIJI, M., TO, K.K., HAMMER, S., et al., HIF-1 alpha induces genetic instability by transcriptionally downregulating MutSalpha expression, *Mol. Cell* **17** (2005) 793–803.
- [15.17] MAXWELL, P.H., Hypoxia-inducible factor as a physiological regulator, *Exp. Physiol.* **90** (2005) 791–797.
- [15.18] SEMENZA, G.L., Hydroxylation of HIF-1: oxygen sensing at the molecular level, *Physiology (Bethesda)* **19** (2004) 176–182.
- [15.19] STONE, H.B., BROWN, J.M., PHILIPS, T.L., SUTHERLAND, R.M., Oxygen in human tumors: correlations between methods of measurements and response to therapy. Summary of a workshop held November 19–20, at the national Cancer Institute, Bethesda, Maryland, *Radiat. Res.* **136** (1993) 422–434.
- [15.20] MUELLER-KLIESER, W., et al., Pathophysiological approaches to identifying tumor hypoxia in patients, *Radiother. Oncol.* **20**(Suppl.) (1991) 21–28.
- [15.21] CHAPMAN, J.D., Measurement of tumor hypoxia by invasive and non-invasive procedures: a review of recent clinical studies, *Radiother. Oncol.* **20**(Suppl.) (1991) 13–19.
- [15.22] CHAPMAN, J.D., ENGELHARDT, E.L., STOBBE, C.C., SCHNEIDER, R.F., HANKS, G.E., Measuring hypoxia and predicting tumor radioresistance with nuclear medicine assays, *Radiother. Oncol.* **46** (1998) 229–237.
- [15.23] CHAPMAN, J.D., Hypoxia sensitizers: implications for radiation therapy, *N. Engl. J. Med.* **301** (1979) 1429–1432.
- [15.24] KOH, W.J., et al., Imaging of hypoxia in human tumors with [F-18]fluoromisonidazole, *Int. J. Radiat. Oncol. Biol. Phys.* **22**(1) (1992) 199–212.
- [15.25] MARTIN, G.V., et al., Noninvasive detection of hypoxic myocardium using fluorine-18-fluoromisonidazole and positron emission tomography, *J. Nucl. Med.* **33**(12) (1992) 2202–2208.
- [15.26] MANNAN, R.H., et al., Radioiodinated 1-(5-iodo-5-deoxy-beta-D-arabinofuranosyl)-2-nitroimidazole (iodoazomycin arabinoside: IAZA): a novel marker of tissue hypoxia, *J. Nucl. Med.* **32**(9) (1991) 1764–1770.
- [15.27] PARLIAMENT, M.B., et al., Non-invasive assessment of human tumour hypoxia with 123I-iodoazomycin arabinoside: preliminary report of a clinical study, *Br. J. Cancer.* **65**(1) (1992) 90–95.
- [15.28] GROSHAR, D., et al., Imaging tumor hypoxia and tumor perfusion, *J. Nucl. Med.* **34**(6) (1993) 885–888.
- [15.29] NUNN, A.D., LINDER, K., STRAUSS, H.W., Nitroimidazoles and imaging hypoxia, *Eur. J. Nucl. Med.* **22** (1995) 265–280.

- [15.30] FUJIBAYASHI, Y., et al., Mitochondria-selective reduction of 62Cu-pyruvaldehyde bis(N4-methylthiosemicarbazone) (62Cu-PTSM) in the murine brain; a novel radiopharmaceutical for brain positron emission tomography (PET) imaging, *Biol. Pharm. Bull.* **16**(2) (1993) 146–149.
- [15.31] FUJIBAYASHI, Y., et al., Copper-62-ATSM: a new hypoxia imaging agent with high membrane permeability and low redox potential, *J. Nucl. Med.* **38** (1997) 1155–1160.
- [15.32] VAVERE, A.L., LEWIS, J.S., Cu-ATSM: a radiopharmaceutical for the PET imaging of hypoxia, *Dalton Trans.* **43** (2007) 4893–4902.
- [15.33] LEWIS, J.S., MCCARTHY, D.W., MCCARTHY, T.J., FUJIBAYASHI, Y., WELCH, M.J., Evaluation of <sup>64</sup>Cu-ATSM in vitro and in vivo in a hypoxic tumor model, *J. Nucl. Med.* **40** (1990) 177–183.
- [15.34] GRIGSBY, P.W., et al., Comparison of molecular markers of hypoxia and imaging with <sup>60</sup>Cu-ATSM in cancer of the uterine cervix, *Mol. Imaging Biol.* **9** (2007) 278–283.
- [15.35] RUMSEY, W.L., CYR, J.E., RAJU, N., NARRA, R.K., A novel [99m]Technetium-labeled nitroheterocycle capable of identification of hypoxia in heart, *Biochem. Biophys. Res. Commun.* **193**(3) (1993) 1239–1246.
- [15.36] BALLINGER, J.R., KEE, J.W., RAUTH, A.M., In vitro and in vivo evaluation of a Technetium-99m-labeled 2-nitroimidazole (BMS181321) as a marker of tumour hypoxia, *J. Nucl. Med.* **37** (1996) 1023–1031.
- [15.37] MELO, T., DUNCAN, J., BALLINGER, J.R., RAUTH, A.M., BRU59-21, a second generation <sup>99m</sup>Tc-labeled 2-nitroimidazole for imaging hypoxia in tumours, *J. Nucl. Med.* **41** (2000) 169–176.
- [15.38] ZHANG, X., et al., Studies of <sup>99m</sup>Tc-BnAO (HL-91): A non-nitroaromatic compound for hypoxic cell detection, *Int. J. Radiat. Oncol. Biol. Phys.* **42** (1998) 737–740.
- [15.39] HONESS, D.J., et al., Preclinical evaluation of the novel hypoxic marker <sup>99m</sup>Tc-HL-91 (Prognox) in murine and xenograft systems in vivo, *Int. J. Radiat. Oncol. Biol. Phys.* **42**(4) (1998) 731–735.
- [15.40] BRAUERS, G., ARCHER, C.M., BURKE, J.F., The chemical characterization of the tumor imaging agent 99mTc-HL91, *Eur. J. Nucl. Med.* **24** (1997) 943.
- [15.41] LINDER, K.E., et al., Synthesis, characterization, and *in vitro* evaluation of Nitroimidazole-BATO complexes: New technetium compounds designed for imaging hypoxic tissue, *Bioconjug. Chem.* **4** (1993) 326–333.
- [15.42] RAMALINGAM, K., et al., The synthesis and *in vitro* evaluation of a 99m-Technetium-nitroimidazole complex based on a bis(amine-phenol) ligand: comparison to BMS-181321, *J. Med. Chem.* **37**(24) (1994) 4155–4163.
- [15.43] ZHANG, Z., MANNAN, R.H., WIEBE, L.I., MCEWAN, A.J., “Development of a new technetium complex for hypoxia imaging: A technetium (V) amine nitrophenol complex”, *Technetium and Rhenium in Chemistry and Nuclear Medicine* (NICOLINI, M., BANDOLI, G., MASSI, U., Eds), Vol. 4, SGE Ditorialli, Padova (1995) 307–312.

- [15.44] ZHANG, Z., KUMAR, P., MANNAN, R.H., WIEBE, L.I., “Synthesis and evaluation of  $^{99m}\text{Tc}$ -1-[(diphenylphosphino/mercapto)acetylglycylglycyl-2-aminoethyl]-2-nitroimidazoles as markers of tissue hypoxia”, *Technetium and Rhenium in Chemistry and Nuclear Medicine* (NICOLINI M., BANDOLI G., MASSI U., Eds), Vol. 4, SGE Ditoriali, Padova (1999) 581–588.
- [15.45] SU, Z.F., et al., Synthesis and evaluation of two Technetium-99m-labeled peptidic 2-nitroimidazole for imaging hypoxia, *Bioconjug. Chem.* **10** (1999) 89–904.
- [15.46] SU, Z.F., BALLINGER, J.R., RAUTH, A.M., ABRAMS, D.N., BILLINGHURST, M.W., A novel amine-dioxime chelator for Technetium-99m: Synthesis and evaluation of 2-nitroimidazole-containing analogues as marker for hypoxia cells, *Bioconjug. Chem.* **11** (2000) 652–663.
- [15.47] MURUGESAN, S., et al., Technetium-99m-cyclam AK2123: A novel marker for tumour hypoxia, *Appl. Radiat. Isotop.* **54** (2001) 81–88.
- [15.48] KUMAR, P., et al., [ $^{99m}\text{Tc}$ ]Technetium labelled PnAo-azomycin glucuronides: a novel class of imaging markers of tissue hypoxia, *Appl. Radiat. Isotop.* **57**(5) (2002) 719–728.
- [15.49] DAS, T., et al.,  $^{99m}\text{Tc}$ -labeling studies of a modified metronidazole and its biodistribution in tumour bearing animal models, *Nucl. Med. Biol.* **30** (2003) 127–134.
- [15.50] CHU, T., et al., Synthesis and biological results of the technetium-99m-labeled 4-nitroimidazole for imaging tumour hypoxia, *Bioorg. Med. Chem. Lett.* **14** (2004) 747–749.
- [15.51] DUATTI, A., MARCHI, A., PASQUALINI, R., Formation of the  $\text{Tc}\equiv\text{N}$  multiple bond from the reaction of ammoniumpertechnetate with S-methyldithiocarbazate and its application to the preparation of technetium-99 in radiopharmaceuticals, *J. Chem. Soc. Dalton Trans.* (1990) 3729–3733.
- [15.52] PASQUALINI, R., COMAZZI, V., BELLANDE, E., DUATTI, A., MARCHI, A., A new efficient method for the preparation of  $^{99m}\text{Tc}$ -radiopharmaceuticals containing the  $\text{Tc}\equiv\text{N}$  multiple bond, *Appl. Radiat. Isotop.* **43** (1992) 1329–1333.
- [15.53] ALBERTO, R., SCHIBLI, R., EGLI, A., SCHUBIGER, A.P., A novel organometallic aqua complex of Technetium for the labeling of biomolecules: Synthesis of  $[^{99m}\text{Tc}(\text{OH}_2)_3(\text{CO})_3]^+$  from  $[^{99m}\text{TcO}_4]^-$  in aqueous solution and its reaction with a bifunctional ligand, *J. Am. Chem. Soc.* **120** (1998) 7987–7988.
- [15.54] PASQUALINI, R., et al., Bis(dithiocarbamato) nitrido technetium-99m radiopharmaceuticals: a class of neutral myocardial imaging agents, *J. Nucl. Med.* **35** (1994) 334–341.
- [15.55] MALLIA, M.B., et al., A novel  $[^{99m}\text{Tc}\equiv\text{N}]^{2+}$  complex of metronidazole xanthate as a potential agent for targeting hypoxia, *Bioorg. Med. Chem. Lett.* **15** (2005) 3398–3401.
- [15.56] KONG, D., LU, J., YE, S., WANG, X., Synthesis and biological evaluation of a novel asymmetrical  $^{99m}\text{Tc}$ -nitrido complex of metronidazole derivative, *J. Labelled Comp. Radiopharm.* **50** (2007) 1137–1142.
- [15.57] ALBERTO, R., ORTNER, K., WHEATLEY, N., SCHIBLI, R., SCHUBIGER, A.P., Synthesis and properties of Boranocarbonate: A convenient in situ CO source for the aqueous preparation of  $[^{99m}\text{Tc}(\text{OH}_2)_3(\text{CO})_3]^+$ , *J. Am. Chem. Soc.* **123** (2001) 3135–3136.

- [15.58] SCHIBLI, R., et al., Influence of the denticity of ligand systems on the in vitro and in vivo behavior of  $^{99m}\text{Tc}(\text{I})$ -tricarbonyl complexes: A hint for the future functionalization of biomolecules, *Bioconjug. Chem.* **11** (2000) 345–351.
- [15.59] MALLIA, M.B., et al., Comparing hypoxia-targeting potential of  $^{99m}\text{Tc}(\text{CO})_3$ -labeled 2-nitro and 4-nitroimidazole, *J. Labelled Comp. Radiopharm.* **51** (2008) 308–313.
- [15.60] WARDMAN, P., Reduction potentials of one-electron couples involving free radicals in aqueous solutions, *J. Phys. Chem. Ref. Data* **18**(4) (1989) 1664–1672.
- [15.61] JERABEK, P.A., PATRICK, T.B., KILBOURN, M.R., DISCHINO, D.D., WELCH, M.J., Synthesis and biodistribution of  $^{18}\text{F}$ -labeled fluoronitroimidazoles: potential in vivo markers of hypoxic tissue, *Int. J. Radiat. Appl. Instrum. [A]* **37**(7) (1986) 599–605.
- [15.62] YANG, D.J., et al., Noninvasive assessment of tumor hypoxia with  $^{99m}\text{Tc}$  labeled metronidazole, *Pharm. Res.* **16**(5) (1999) 743–750.
- [15.63] ITO, M., et al., PET and planar imaging of tumor hypoxia with labeled metronidazole, *Acad. Radiol.* **13**(5) (2006) 598–609.
- [15.64] MALLIA, M.B., et al., On the isolation and evaluation of a novel unsubstituted 5-nitroimidazole derivative as an agent to target tumor hypoxia, *Bioorg. Med. Chem. Lett.* **18**(19) (2008) 5233–5237.
- [15.65] MALLIA, M.B., SUBRAMANIAN, S., SARMA, H.D., VENKATESH, M., BANERJEE, S., Evaluation of  $^{99m}\text{Tc}(\text{CO})_3$  complex of 2-methyl-5-nitroimidazole as an agent for targeting tumor hypoxia, *Bioorg. Med. Chem.* **14**(23) (2006) 7666–7670.

## Chapter 16

# ROLE OF $^{99m}\text{Tc}$ IN THE DEVELOPMENT OF RHENIUM RADIOPHARMACEUTICALS

R. T. M. DE ROSALES, P. BLOWER

Division of Imaging Sciences, King's College London,  
London, United Kingdom

### Abstract

Due to the chemical analogy between rhenium and technetium, some potentially valuable therapeutic  $^{188}\text{Re}$  and  $^{186}\text{Re}$  radiopharmaceuticals have come about through prior experience with  $^{99m}\text{Tc}$ . These include the pentavalent Re(V)-DMSA complex and labelling methods for biomolecules such as cysteine containing peptide sequences and MAG3 for labelling with the Re(V)oxo core, and polyhistidine sequences for labelling with the Re(I)tricarbonyl core. However, emerging rhenium radiopharmaceuticals often show significant differences from their technetium counterparts in terms of preparation methods, and the structure, stability and biological behaviour of the products. Exceptions are the DMSA and tricarbonyl complexes which appear to be highly analogous in structure and oxidation state, if not in preparation. Many currently investigated rhenium radiopharmaceuticals are particulate in nature and in these instances technetium chemistry has little to contribute to their development. Despite the differences, the similarity between rhenium and technetium has been a useful guide in radiopharmaceutical development.

### 16.1. INTRODUCTION

Rhenium isotopes are very attractive radionuclides for therapy, and recently  $^{188}\text{Re}$ , in particular, has been the object of widespread research and development, largely because of the convenience and economy resulting from its availability in generator form. Rhenium is a chemical congener of technetium, and because of the similarity between Tc and Re, rhenium radiopharmaceuticals have been designed based on  $^{99m}\text{Tc}$  labelled tracer agents. This chapter addresses the questions of whether rhenium isotopes have, or are likely to have in the future, a substantial role in therapeutic nuclear medicine; and, if so, to what extent can the development and use of these isotopes be guided by the analogy between technetium and rhenium radiopharmaceuticals.

The future potential value of rhenium radiopharmaceuticals depends on the vigour of the field of targeted radionuclide therapy as a whole, and by the therapeutic efficacy of rhenium isotopes and the practicalities and costs of production and distribution, with respect to the competing isotopes. These aspects

are briefly summarized below, after which a review of the present status of research on  $^{186}\text{Re}$  and  $^{188}\text{Re}$  radiopharmaceuticals is presented, highlighting the analogy and contrast with the related  $^{99\text{m}}\text{Tc}$  counterparts.

## 16.2. RADIOLOGICAL PROPERTIES AND RADIOBIOLOGY

Rhenium-186 and  $^{188}\text{Re}$  offer suitable emission properties for targeted radionuclide therapy, and  $^{186}\text{Re}$  was identified early as a radionuclide for targeted radiotherapy (Table 16.1) [16.1]. The half-life of  $^{186}\text{Re}$  (about 4 d) is suited to delivery with labelled antibodies, while  $^{188}\text{Re}$  has a shorter half-life (17 h) at the lower limit of that which is considered useful for antibody mediated delivery. However, delivery with smaller molecules such as single chain antibodies, peptides and other small molecular forms is quite feasible as indicated in the examples discussed later. Taking into account the higher  $\beta$  energy and shorter half-life of  $^{188}\text{Re}$ , it is expected that, given optimal tumour size (see below), about 20% more  $^{188}\text{Re}$  radioactivity must be taken up per gram of tumour than  $^{186}\text{Re}$  to achieve the same tumour dose [16.2].

The moderate  $\beta$  energy (max. 1.08 MeV) of  $^{186}\text{Re}$  gives a range of about 5 mm in tissue, which is appropriate for macroscopic tumours and gives minimal irradiation of surrounding non-target tissue. The higher  $\beta$  energy of  $^{188}\text{Re}$  (max. 2.1 MeV) gives a higher total dose per disintegration and a range in tissue of about 11 mm, which is unsuitable for small tumours but is potentially very effective in large masses. Secondary electrons (Auger and conversion electrons) emitted by both radionuclides add to the radiation dose delivered within a very small radius (<1 cell diameter) [16.3, 16.4]. The different range in tissues means that the target:total body dose ratio is likely to be higher for  $^{186}\text{Re}$  than for  $^{188}\text{Re}$  [16.5]. Each radionuclide has an ‘optimal tumour size’ for which the probability of achieving a cure is maximal. For  $^{188}\text{Re}$ , this diameter is about 26 mm, while for  $^{186}\text{Re}$  it is estimated at 9 mm (based on computer modelling, not on a biological

TABLE 16.1. NUCLEAR PROPERTIES OF RHENIUM RADIONUCLIDES

	Half-life (h)	Max. $\beta$ energy (MeV)	Ave. $\beta$ energy (MeV)	Range in tissue (mm)	$\gamma$ energy (KeV)	Production
Re-186	90	1.07 (71%) 0.93 (21%)	0.36	5	137 (9%)	Re-185 + n (reactor)
Re-188	17	2.1	0.77	11	155 (15%)	W-188 decay (generator)

experiment). On this basis, it may be advantageous to use both radionuclides simultaneously in order to maximize the probability of sterilizing tumours of various sizes [16.2]. This possibility has not yet been investigated experimentally.

### 16.2.1. Production, availability and cost

Rhenium-186 is manufactured by neutron irradiation, in a nuclear reactor, of either natural rhenium or isotopically enriched  $^{185}\text{Re}$ . The moderate neutron flux required means that production is feasible at many locations worldwide. Natural rhenium (37.4%,  $^{185}\text{Re}$ ; 62.6%,  $^{187}\text{Re}$ ) gives a product heavily contaminated with  $^{188}\text{Re}$  (which is removed by decay) and  $^{186}\text{Re}$  has low specific activity. Where higher specific activity is desirable, enriched  $^{185}\text{Re}$  is required as the target for neutron irradiation. This minimizes  $^{188}\text{Re}$  contamination and residual non-radioactive ‘carrier’ rhenium ( $^{187}\text{Re}$ ). Even using enriched  $^{185}\text{Re}$ , the specific activity of the product is too low for the labelling of targeting molecules such as neuropeptides; common research reactors with a flux of  $10^{14} \text{ n}\cdot\text{cm}^{-2}\cdot\text{s}^{-1}$  give, at saturation (after 500 h of irradiation), about one atom of hot  $^{186}\text{Re}$  per 50 atoms of  $^{185}\text{Re}$ . Carrier-free  $^{186}\text{Re}$  can be produced by proton or deuteron bombardment of  $^{186}\text{W}$  in a cyclotron at high or moderate energies [16.6], but the practicality of this approach for manufacture on a clinical scale is uncertain. Another alternative to explore is the use of the Szilard–Chalmers reactions. Neutron capture by  $^{185}\text{Re}$ , initially gives a  $^{186}\text{Re}$  nucleus in a highly excited state. After prompt gamma emission, it experiences recoil which makes it leave the chemical environment. Further development may show that Szilard–Chalmers reactions offer a possibility to produce high specific activity within a very short time period and in reasonable activities.

The most useful route to  $^{188}\text{Re}$  is by decay of  $^{188}\text{W}$  (half-life = 60 d), by means of the  $^{188}\text{W}/^{188}\text{Re}$  generator system, which is analogous to the  $^{99}\text{Mo}/^{99m}\text{Tc}$  generator [16.7]. The decay product,  $^{188}\text{Re}$  is readily eluted with 0.9% (physiological) saline. However, the manufacture of the parent radionuclide  $^{188}\text{W}$  requires a double neutron capture reaction of  $^{186}\text{W}$  and, as a result, is relatively inefficient. The irradiation requires long periods at high neutron flux (e.g.  $3 \times 10^{14} \text{ n}\cdot\text{cm}^{-2}\cdot\text{s}^{-1}$  for 7 d) [16.8, 16.9]. Very few reactors worldwide (Oak Ridge, Dimitrigrad, Mol) can generate the necessary neutron flux for economic production on a clinical scale. The commitment of resources to the development of  $^{188}\text{Re}$  radiopharmaceuticals should, therefore, proceed with caution. While, at present, there is sufficient capacity, if one high flux reactor is decommissioned and not replaced, capacity will be severely compromised and may render the  $^{188}\text{Re}$  generator non-viable. Reactor ( $n, \gamma$ ) production may mitigate this problem, at the expense of reduced specific activity. A mixed radionuclide therapy using a mixture of  $^{186}\text{Re}$  and  $^{188}\text{Re}$  as obtained by using a natural Re target is another

option. However, the advantages of generator production in terms of distribution, day to day availability and economy of scale are lost by this approach.

The benefits of  $^{188}\text{Re}$  compared to reactor produced therapeutic radionuclides may be in terms of economy of scale if a large patient base can be served by a generator. If there are sufficient patient numbers within a few hours travelling distance, hundreds of patients could be treated during the lifetime of a 3 Ci generator. This would entail both increased patient numbers and indications, and coordinating the activities of several medical disciplines (e.g. oncology, rheumatology and cardiology; see applications below). The creation of a regional radiopharmacy serving many patients who are being managed by clinicians from different disciplines in many hospitals represents a major organizational challenge. It can only be achieved if the products are highly effective and superior to alternatives. Confidence in rhenium isotopes would be enhanced by demonstrating, through clinical and radiobiological studies, including characterization of the low energy Auger electron emissions, that  $^{188}\text{Re}$  has therapeutic properties as good as or better than alternatives such as  $^{90}\text{Y}$  which has been widely adopted commercially. These studies are proceeding very slowly and are at a very early stage.

### **16.2.2. Chemistry: complexity and versatility**

There is no doubt that the present status of rhenium bioconjugate chemistry is more complex than that of yttrium and the lanthanide radionuclides, and, in this respect, further development of rhenium bioconjugate chemistry is required. The complexity creates problems with product homogeneity and quality control, which are more pronounced than for competing radiometals such as  $^{90}\text{Y}$  and  $^{177}\text{Lu}$ . However, some good cores are available ( $\text{Re(V)-DMSA}$ ,  $\text{Re(CO)}_3$ ,  $\text{Re}=\text{N}$ ,  $\text{ReO(MAG3)}$ ) and, in principle, satisfactory new labelling methods and cores can be developed, and developed into kits, given more research. This may well be aided by directly focusing efforts on rhenium chemistry, rather than drawing on technetium chemistry for guidance.

### **16.2.3. Value of the imaging and treatment ‘matched pair’**

In principle, the idea of a ‘matched pair’ comprising a therapeutic radiopharmaceutical and an imaging analogue with identical biodistribution and pharmacokinetics is attractive, both at the research and development stage as well as in therapeutic practice. It would mean that dosimetry could be estimated in advance, thus helping with clinical decision making. In practice, truly matched pairs are rare, and relatively little use of the principle has been made in the past. However, attitudes are changing and methods to predict outcomes of all types of

therapy are becoming more important to avoid inappropriate use of debilitating and expensive treatments, and the matched pair principle may gain in importance. The matching of biodistribution between supposed ‘matched’ isotopes is often assumed rather than validated, and, hence, can be highly misleading. Indium-111 has been used as an imaging surrogate for  $^{90}\text{Y}$  but this has turned out to be ill advised if the purpose is to obtain a quantitative prediction, because the coordination chemistry of the two metals is not the same. Likewise, although technetium and rhenium share the same group in the periodic table and, indeed, many similarities in chemistry, they are not identical and careful validation of each pair is required. Examples are highlighted in the sections below. The ability to determine rhenium isotope dosimetry from technetium images is diminished in importance by the imageable gamma emissions of both  $^{186}\text{Re}$  and  $^{188}\text{Re}$  (Fig. 16.1). These emissions offer a further advantage of rhenium compared to  $^{90}\text{Y}$  and  $^{32}\text{P}$ , which have no imageable photons. Excellent images can be obtained with both  $^{188}\text{Re}$  and  $^{188}\text{Re}$ , yet, unlike  $^{131}\text{I}$ , the gamma emissions are not abundant enough to require isolation of the patient. Discussion of whether imageability is

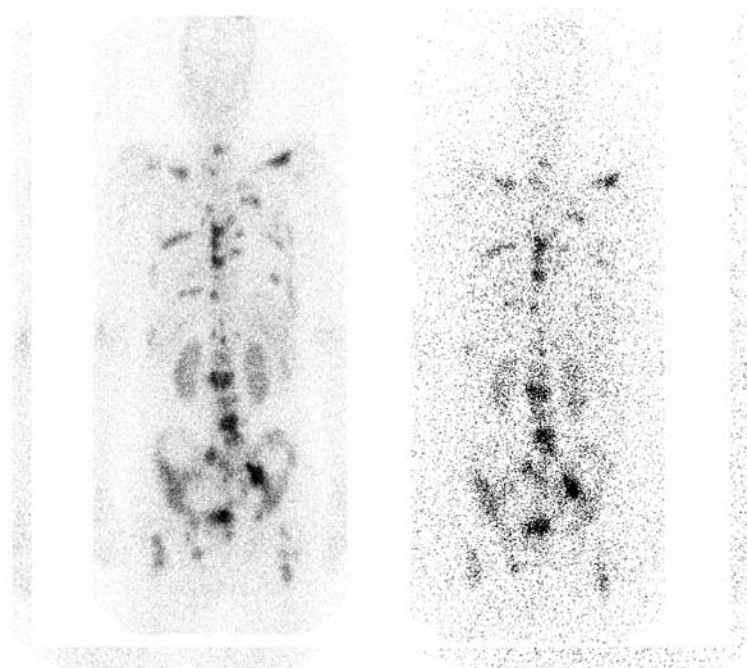


FIG. 16.1. Posterior scans of a patient with prostate cancer metastatic to bone, taken 24 h post-injection, using  $^{99\text{m}}\text{Tc(V)DMSA}$  (left) and  $^{188}\text{Re(V)DMSA}$  (right, with triple energy window scatter correction).

an important attribute of therapeutic radionuclides seems inconclusive: clinicians would like to be able to image but it is not clear that this property overrides, for example, the simpler chemistry of  $^{90}\text{Y}$  which, at present, is more widely used and accepted by commercial providers.

#### **16.2.4. Regulatory barriers**

A concern for the application of generator produced therapeutic radionuclides is that regulatory authorities may be cautious about approving in-house labelling of therapeutic radiopharmaceuticals. However, a precedent has been set for Zevalin, which is labelled at the point of use if the local radiopharmacy can meet the required standards. Another concern of regulators is the good manufacturing practice (GMP) status of the generator production and elution. Each generator will be used for several months, adding to the risk of degrading elution performance, radionuclidic impurities, and microbial and pyrogen contamination.

#### **16.2.5. The market and the competition**

The main competing therapeutic radioisotopes that have experienced the most clinical exploitation are  $^{131}\text{I}$ ,  $^{90}\text{Y}$  and, more recently,  $^{177}\text{Lu}$ . Iodine-131 is a medium energy  $\beta$  emitter that has been established for many years. Simple chemistry is available for biomolecule labelling with  $^{131}\text{I}$ . It is imageable and relatively inexpensive, but the gamma emissions are excessive and too high in energy for high quality imaging and require isolation of patients. Rhenium-186 has clear advantages in these respects, but its main disadvantage is low specific activity. Yttrium-90 is a high energy  $\beta$  emitter with a  $\beta$  emission profile similar to  $^{188}\text{Re}$ . It has found commercial acceptance more readily than  $^{188}\text{Re}$  despite its lack of imageable photon emissions, probably because of the relatively simple bioconjugate chemistry afforded by established chelators such as DOTA and DTPA derivatives, and because of fears over the reliability of supply of  $^{188}\text{W}$ . Lutetium-177 is a medium energy  $\beta$  emitter and, thus, a competitor for  $^{186}\text{Re}$ ; it too emits gamma photons but not enough to necessitate isolation of the patient. It shares the simple bioconjugate chemistry of  $^{90}\text{Y}$ , giving it a potential market advantage over  $^{186}\text{Re}$  and  $^{188}\text{Re}$ . Thus, so far, the advantages of generator availability and imageability of  $^{188}\text{Re}$  have been only potential ones and have not led to significant commercial exploitation. For therapeutic application on a commercial scale, these advantages appear to be insufficient. Better and simpler labelling chemistry is required and the indications for targeted radionuclide therapy must be increased, providing enough patient numbers to realize the economy of scale offered by a  $^{188}\text{Re}$  generator. Possibly the overriding factor that

limits commercial interest in therapeutic use of  $^{188}\text{Re}$ , is the limited number of locations able to produce the parent  $^{188}\text{W}$  and the consequent insecurity of supply.

## 16.3. REVIEW OF CURRENTLY INVESTIGATED RHENIUM RADIOPHARMACEUTICALS

The purpose of the following review is to provide an update on previous more detailed and thorough reviews of rhenium radiopharmaceuticals [16.10–16.12], and to highlight areas where the periodic relationship between technetium and rhenium has been an important factor, for better or worse, in the development process.

### 16.3.1. Bone palliation agents

Pain due to skeletal metastases is one of the principal factors limiting the quality of life of terminal cancer patients, and especially those with prostate and breast cancer. The mechanisms are not well understood [16.13]. To mitigate pain, hormone therapy and various chemotherapy modalities are used initially, but in refractory cases opioid analgesics are often required, with all the associated impairments in quality of life. An alternative is radiotherapy, which is unsuitable for widespread metastases because irradiation of critical organs cannot be avoided. In contrast, radionuclide therapy with agents that target bone mineral is an attractive alternative with relatively minor side effects.

The possibility that the radionuclide  $^{186}\text{Re}$  or  $^{188}\text{Re}$  could be selectively delivered to bone was indicated by the previous development of  $^{99\text{m}}\text{Tc}$  labelled diphosphonate agents, used for imaging bone metastases [16.14, 16.15]. In keeping with the theme of this chapter, it has undoubtedly been the success of bone imaging with  $^{99\text{m}}\text{Tc}$ -bisphosphonates that has driven development of  $^{186}\text{Re}$  and  $^{188}\text{Re}$  ‘analogues’ for treatment. The technetium agents accumulate in bone by adsorption to the surface of bone mineral (hydroxyapatite and/or its low density hydrated calcium phosphate precursor), probably with the diphosphonate molecule serving as a bridging ligand between the calcium and technetium ions, as shown in Fig. 16.2.

Several therapeutic bone targeting radiopharmaceuticals are under investigation, among which  $^{186}\text{Re}$ -HEDP (hydroxyethylidenediphosphonate) (Fig. 16.3), is currently the most studied [16.16–16.26]. The reported clinical experience indicates that  $^{186}\text{Re}$ -HEDP has a good efficacy: ca. 70–80% of patients report major pain relief and reduction of analgesic requirement, while ca. 20–25% experience total pain relief and are able to forego analgesics [16.27].

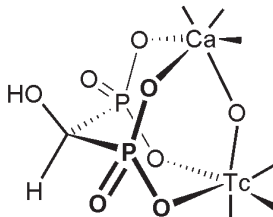


*FIG. 16.2. Proposed interaction between Tc-bisphosphonate and Re-bisphosphonate complexes, and calcium in bone mineral.*

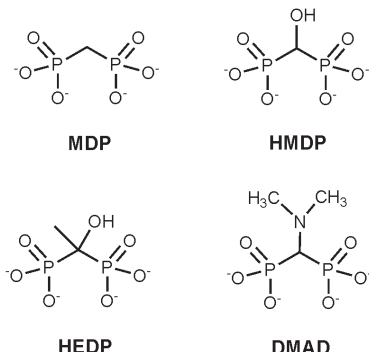


*FIG. 16.3. Some bisphosphonates evaluated for delivery of rhenium isotopes to bone metastases.*

These results are in line with other palliative bone targeting radiopharmaceuticals, such as  $^{89}\text{Sr}$  and  $^{153}\text{Sm}$  EDTMP. Interestingly, recent clinical trials strongly suggest that not only is there a palliative and consequently a quality of life effect, but there is also a clear clinical gain in terms of life expectancy, delayed onset of new metastases and pain, and reduction of bone metastases, especially at higher doses [16.22, 16.23]. It is possible that this may drive a future broadening of the use and purpose of these agents to include disease control as well as palliation.

The potential for use of  $^{188}\text{Re}$  in this application has attracted researchers, especially in less developed countries and south east Asia [16.28], because of its availability at a potentially very low cost. Several  $^{188}\text{Re}$  bone targeting radiopharmaceuticals have been developed, although none is commercially available or has regulatory approval. The most extensively evaluated (probably due to the analogy with commercially available  $^{186}\text{Re}$ -HEDP, see above) is  $^{188}\text{Re}$ -HEDP [16.12, 16.29–16.38]. Others have undergone preliminary evaluation in patients ( $^{188}\text{Re}$ -DMSA [16.39–16.45], which gives similar selectivity [16.41] to  $^{188}\text{Re}$ -HEDP, see below) or are in pre-clinical development, including other bisphosphonates (Fig. 16.3): MDP [16.30, 16.46–16.48], HDP

[16.30], SEDP [16.49] and aminobisphosphonates [16.12, 16.50–16.52], and phosphonate derivatives  $^{188}\text{Re}$ -CTMP [16.53], EDTMP, EDBMP [16.54] and NTMP [16.54]. The CTMP and EDTMP complexes show high lesion selectivity in animal studies [16.12, 16.47, 16.48, 16.54–16.57].

Rhenium-188-HEDP is undergoing clinical evaluation in several locations worldwide [16.12, 16.29, 16.31, 16.32, 16.35–16.38]. Early results suggest that its efficacy is similar to the more established agents labelled with  $^{89}\text{Sr}$ ,  $^{186}\text{Re}$  or  $^{153}\text{Sm}$ , but with the advantages that repeated doses not only enhance the benefit (including increased life expectancy and delayed disease progression as well as pain relief) but are economic to deliver [16.37], and that dosimetry can be calculated on the basis of imaged biodistribution. The short half-life and high energy  $\beta$  emission does not appear to be a significant disadvantage, whereas the prompt availability and low cost may be major advantages. Rhenium-188, therefore, represents a highly promising alternative, suitable for use in larger numbers of patients at an earlier stage of disease.

Despite the clinical promise of  $^{188}\text{Re}$ -HEDP, it is without doubt, as the other agents discussed above, far from an optimal radiopharmaceutical for delivery of radionuclide selectively to bone metastases. In particular, there is a need for a significantly improved lesion:background dose ratio. It may be argued that these deficiencies have arisen because of over reliance on the supposed analogy between technetium and rhenium. If we compare, using a  $^{99\text{m}}\text{Tc}$ -HDP bone scan (which shows exquisite selectivity for bone lesions) as a point of reference, it is apparent that  $^{188}\text{Re}$ -HEDP and the other established palliative bone agents have relatively low lesion:soft tissue and lesion:normal bone dose ratios, and slow clearance from soft tissue and normal bone. There is no a priori reason, however, why  $^{188}\text{Re}$  radiopharmaceuticals with selectivity equal to or better than  $^{99\text{m}}\text{Tc}$ -HDP and, hence, higher tumour doses and lower bone marrow and kidney doses than  $^{188}\text{Re}$ -HEDP, should not be achievable.

Known failings in the chemistry contribute to the sub-optimal targeting of  $^{188}\text{Re}$ -HEDP (and of the licensed commercially available  $^{186}\text{Re}$ -HEDP). It is clear from the available data that rhenium and technetium bisphosphonates are not directly analogous either chemically or biologically. The composition of the  $^{188}\text{Re}$  radiopharmaceutical is ill defined [16.58] and inhomogeneous (this is also true of  $^{188}\text{Re}$ -EDTMP [16.59]). In contrast to the  $^{99\text{m}}\text{Tc}$ -bisphosphonate complexes, if it is prepared without carrier perrhenate, no bone affinity is observed [16.30, 16.47, 16.51, 16.54, 16.60–16.63]. Indeed, if we examine the phosphonate and bisphosphonate containing complexes evaluated so far, it is clear that none are homogeneous, none of the structures are known and chromatography gives variable results. Thus, the preparations probably contain a variety of oligomeric species [16.58] with differing lesion selectivity and stability. There is also a rapid degradation to perrhenate *in vivo* [16.24],

manifested both in radiochromatographic results on blood and urine, and in visualization of the stomach on scans [16.25, 16.26]. To a large extent, the chemical deficiencies are predictable from a knowledge of rhenium chemistry. The bisphosphonate moiety is an outstanding bone targeting motif, but it is unreasonable to expect it also to form stable chelates with rhenium. According to Pearson's hard soft acid base principle (HSAB) [16.64], in oxidation states below VII, rhenium is best chelated by Lewis bases of soft or intermediate character (S or N) incorporating five membered chelate rings [16.10], whereas bisphosphonates are hard bases and form six membered chelates. Technetium-99m-bisphosphonates do not behave analogously and cannot be used for quantitative dose planning. Thus, clinical success with  $^{186}\text{Re}$  and  $^{188}\text{Re}$  bisphosphonates has been demonstrated despite chemical inadequacies, and this field, therefore, presents an opportunity for greatly enhanced targeting and efficacy by improving the rhenium chemistry.

In order to overcome these deficiencies, a recent promising rational approach is to separate the radionuclide site from the bone seeking molecule by conjugating bisphosphonates to known rhenium chelators. The main advantage of this design strategy is that it allows the control of the coordination mode (and also the kinetic and thermodynamic stability) of the metal and the whole complex by using known, well designed stable metal cores. At the same time, the bone seeking motif will bind to the bone mineral without interference from the

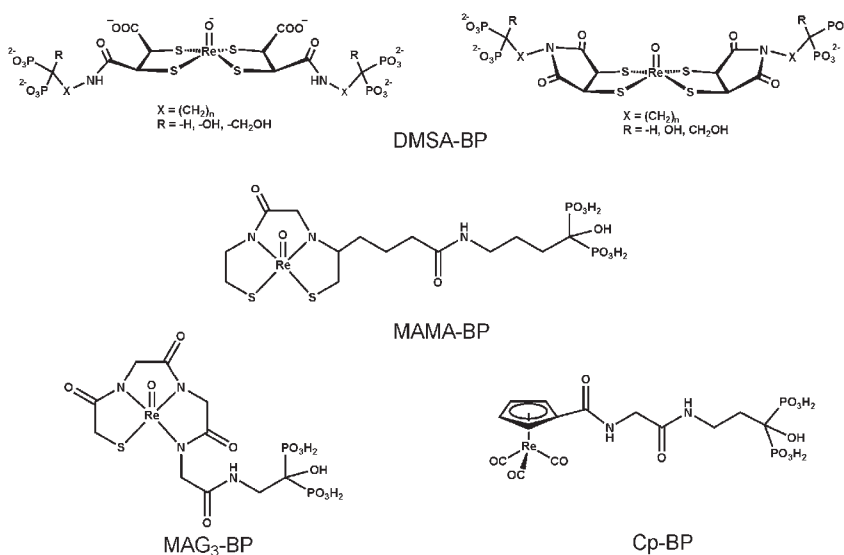


FIG. 16.4. Some examples of chelate–bisphosphonate (chelate-BP) conjugates of rhenium.

radionuclide complex (Fig. 16.4). Various rhenium binding groups are being evaluated including DMSA [16.65], cyclopentadienyl [16.66–16.70] and sulphur–nitrogen chelators MAMA [16.68, 16.70] and MAG3 [16.69]. In general, these bifunctional complexes show a higher plasma stability, bone accumulation and bone:blood ratio, and lower plasma protein binding when compared with  $^{186}\text{Re}$ -HEDP. Furthermore, it seems that these novel agents show a faster clearance from other soft tissues, including blood. Overall, this strategy seems to be highly promising for the development of improved radiopharmaceuticals for pain palliation and imaging of bone metastases. As a result of the use of better designed, more stable chelates in this new generation of radiopharmaceuticals, it can be expected that the biological behaviour of the technetium complexes will be more closely predictive of that of the rhenium analogues than is the case with the bisphosphonate complexes.

The pathway by which this stage has been reached reflects the advantages and pitfalls associated with the technetium–rhenium analogy. The initial development of rhenium bisphosphonates was driven by imaging success with technetium, but the differences in structure and biological behaviour were only appreciated later. Using properly designed chelators, differences in reactivity between technetium and rhenium can be suppressed while the structural similarities can be exploited fully.

### 16.3.2. $^{186}\text{Re}/^{188}\text{Re}(\text{V})\text{DMSA}$

DMSA (meso-2,3-dimercaptosuccinic acid) is a particularly favourable ligand that forms isomeric complexes with both rhenium(V) and technetium(V) ( $^{99\text{m}}\text{Tc}(\text{V})\text{DMSA}$ ), distinguished from the routinely used kidney imaging agent  $^{99\text{m}}\text{Tc}(\text{III})\text{DMSA}$  by the pentavalent technetium. Rhenium(V)DMSA is a prime example of a therapeutic agent designed on the basis of the supposed parallel with  $^{99\text{m}}\text{Tc}$ , despite the fact that at the time of its development the structure of the pentavalent  $^{99\text{m}}\text{Tc}$  complex was unknown. Technetium-99m(V)DMSA is clinically used as an imaging agent for medullary thyroid carcinoma and other tumours. As expected from the known structures of other technetium and rhenium oxo-bis-1,2-dithiolate complexes, the metal is coordinated by four thiolate donors and an apical oxo group [16.71–16.73], affording a mixture of three isomers as shown in Fig. 16.5 [16.44]. Although the structures are analogous, the differing preparative conditions required illustrate the different redox behaviour of rhenium and technetium. The  $^{188}\text{Re}/^{186}\text{Re}$  labelled complex of DMSA can be readily synthesized from the ‘kit’ vials used to prepare the renal agent  $^{99\text{m}}\text{Tc}$ -DMSA. In order to prevent the further reduction of Tc(V), the kit has to be modified for the production of Tc(V)DMSA. On the other hand, rhenium is harder to reduce; hence, the synthesis of the rhenium complex does not require

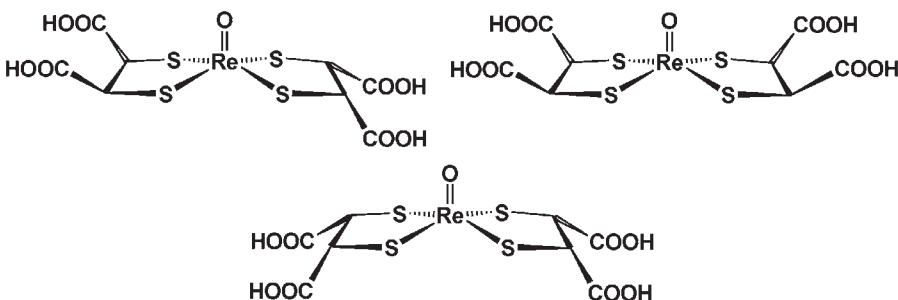
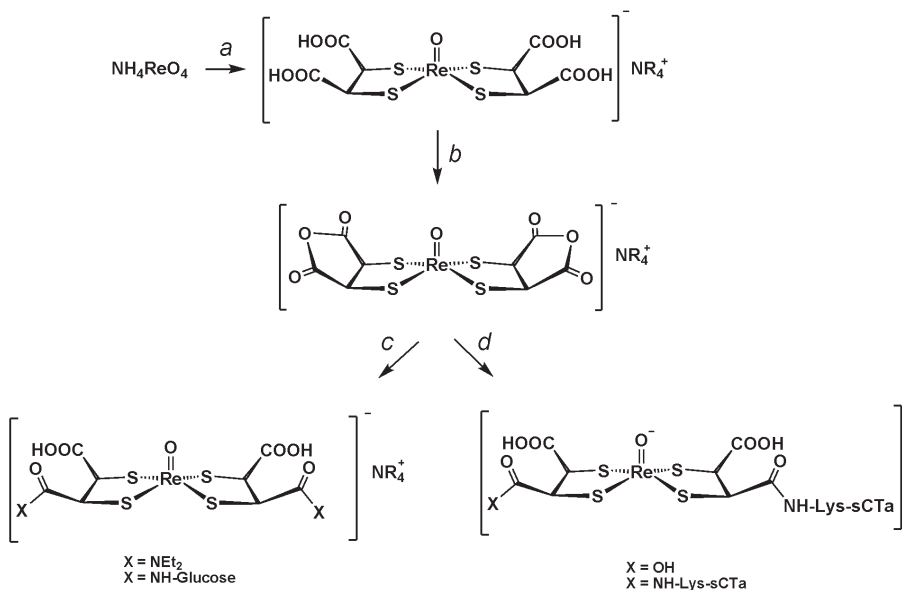


FIG. 16.5. Isomers of a pentavalent technetium/rhenium complex of meso-DMSA.

any modification. Simply adding  $^{186}\text{Re}$  or  $^{188}\text{Re}$  perrhenate and heating to 100°C for 30 min yields the radiochemically pure rhenium complex [16.39, 16.45]. Using a combination of high performance liquid chromatography (HPLC),  $^1\text{H-NMR}$  and X ray crystallography, the isomeric composition of the complex was elucidated, revealing that the syn-endo isomers and anti isomers are the most abundant [16.44]. These isomers are interconverted by acid catalysed ligand dissociation slowly, with a half-life in the order of weeks at physiological pH, although it is much faster *in vivo* for reasons that are not yet clear [16.74]. Milder methods have more recently been reported for synthesis of this radiopharmaceutical. It was shown that the simple addition of oxalate ions to the starting  $[^{188}\text{ReO}_4]^-$  allows  $^{188}\text{Re(V)DMSA}$  to be obtained in a physiological solution, at room temperature and in very high yield (>95%), using a small amount of  $\text{SnCl}_2$  (<0.2 mg) as a reducing agent, although details of the isomeric composition were not given [16.75]. Another improvement was recently reported, which not only shortens the time for its synthesis and purification (an important factor for potential clinical use) but also exclusively produces the syn-endo isomer [16.76]. Interestingly, a recent report has evaluated the organ uptake and kinetics of the individual isomers of  $^{188}\text{Re(V)DMSA}$  (see above) and found that there were only minor differences [16.74].

Like its technetium analogue,  $^{186/188}\text{Re(V)DMSA}$  shows selective uptake in tumour tissue in patients with medullary thyroid carcinoma [16.40]. Rhenium-188(V)DMSA is also taken up selectively in bone metastases in cancer patients, especially those with prostate carcinoma (Fig. 16.1) [16.41]. The complex is remarkably stable *in vivo*, as demonstrated by HPLC analyses of blood and urine from patients injected with the complex [16.41]. After 24 h, there is no evidence for decomposition/oxidation to perrhenate or any other chemical form. Technetium-99m(V)DMSA and  $^{186/188}\text{Re(V)DMSA}$  are structurally and biologically equivalent, and the former quantitatively predicts  $^{188}\text{Re(V)DMSA}$  biodistribution [16.42, 16.65].

The carboxylate groups of DMSA are not coordinated to the metal, allowing their use for conjugation with other molecules (e.g. biological targeting molecules) such as peptides or antibodies. For example, the Re(V)DMSA core was conjugated with one or two molecules of salmon calcitonin analogue peptide (sCTa) [16.76], a synthetic 32 amino acid peptide designed as a calcitonin receptor targeting agent. In order to conjugate with the peptide, the bis-anhydride of Re(V)DMSA was conveniently prepared by dehydration of the carboxylic acid groups with dicyclohexylcarbodiimide (Fig. 16.6). This has proven to be an efficient and mild method and represents a new route to bioconjugates of rhenium using the Re(V)DMSA core. Furthermore, because of the known stability and structural similarity of the rhenium and technetium complexes, the technetium and rhenium labelled peptides are expected to behave analogously. This approach has been developed further by the synthesis of tetradentate tetrathiolate chelators derived by linking two DMSA units [16.77, 16.78]. These chelators form highly stable complexes with rhenium and technetium.



*FIG. 16.6. Reaction scheme for the synthesis and conjugation of Re(V)DMSA to biomolecules. (a) Acetyl hydrazine,  $\text{HCl}$ , DMSA in acetonitrile or water followed by  $\text{NR}_4^+$  salt ( $R = \text{H, Et, Bu}$ ); (b) Dicyclohexylcarbodiimide (DCC) in acetonitrile or acetic anhydride; (c) Amine in acetonitrile; (d) Salmon calcitonin analogue (sCTa) in bicarbonate buffer.*

### 16.3.3. $^{186}\text{Re}/^{188}\text{Re}$ labelled antibodies

The ideal strategy for antibody labelling is to add the radioactive metal as the last step of production, to minimize the number of steps involving handling the radionuclide. This has been termed the ‘post-formed’ labelling approach. It may entail the ‘direct method’, whereby the metal is bound to thiol groups generated by reduction of native cystine disulphide bonds, or a pre-synthesized conjugate of the antibody with a specially designed chelator. Both have been applied with both rhenium and technetium, but the different kinetic reactivity of rhenium and technetium means that different conditions are required (harsher for rhenium, with potentially more damage to the antibody), and the labelled products may have different structures and in vivo stability properties. The alternative is to pre-form a chelator–radionuclide complex and to couple it with the antibody/peptide through functional groups such as amines and carboxylic acids (pre-formed chelate approach). This synthetic strategy has the advantage that it avoids exposing the antibody to the harsh conditions required for the chelator–radionuclide complex to form, but it usually requires a purification step. Although the conditions for labelling the chelator may differ between rhenium and technetium, once the chelates are formed, the reactivity differences are suppressed and structural similarities dominate, leading to analogous in vivo behaviour. An example is the coupling of pre-formed Tc-MAG3 or Re-MAG3 chelate to the amino groups of monoclonal antibodies (Fig. 16.7). Although the lengthy procedures needed have made this approach clinically impractical to date [16.79, 16.80], the technetium and rhenium derivatives show a similar pharmacokinetic behaviour and technetium could, thus, be used to predict the localization and dosimetry of the rhenium analogues in individual patients. The use of the pentavalent DMSA complex described above is a similar example [16.76].

The majority of biological and clinical evaluation of rhenium labelled antibodies has been done using the direct labelling method. Rhenium-188 labelled anti-CD20 antibody provides an example, representing a promising new alternative to the commercially available  $^{90}\text{Y}$ -anti-CD20 (Zevalin) for the treatment of non-Hodgkin’s lymphoma. Ferro-Flores et al. labelled anti-CD20 directly under mild conditions in high yield and high radiochemical purity (>97%) without the need of a purification step, by adding sodium perrhenate to a kit that contained lyophilized anti-CD20, anhydrous stannous chloride as the reducing agent and a large excess of sodium tartrate as the weakly competing ligand [16.81]. Investigations in normal mice showed no rhenium release from the complex, and in vitro binding studies proved the bioactivity of the labelled antibody. More recently, Stopar et al. labelled anti-CD20 with  $^{99\text{m}}\text{Tc}$  using UV light to induce reduction of the disulphide bonds [16.82, 16.83]. The resulting

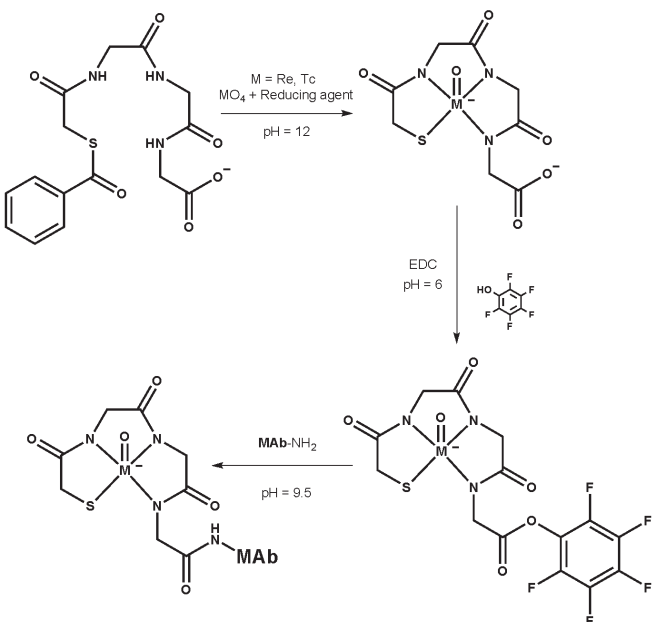


*FIG. 16.7. Reaction scheme for the synthesis and conjugation of Re-MAG to monoclonal antibodies (MAbs) [16.79, 16.80].*

$^{99\text{m}}\text{Tc}$ -anti-CD20 shows high radiochemical purity and yield, as well as the preserved ability to bind CD20. It is to be hoped that these Re and Tc labelled agents show analogous biodistribution properties, but previous experience is not encouraging in this respect. For example, Kotzerke et al. have explored the use of  $^{188}\text{Re}$ -anti-CD66 for targeted bone marrow irradiation of pre-stem cell transplantation leukaemia patients [16.84, 16.85]. The antibody was labelled by direct methods using tris-(2-carboxyethyl)phosphine to reduce the thiol groups and stannous chloride to reduce perrhenate at 37°C for 1 h [16.86]. Biodistribution studies with  $^{99\text{m}}\text{Tc}$ -anti-CD66 were performed prior to treatment with  $^{188}\text{Re}$ -anti-CD66, and some differences were found in their biokinetics, despite their supposed similarity. In particular, the rhenium conjugate showed a shorter biological half-life and lower bone marrow uptake [16.87]. These results are most likely due to poorer stability *in vivo* of  $^{188}\text{Re}$ -anti-CD66.

Direct labelling was also used to produce conjugates of the monoclonal antibody C595 with  $^{188}\text{Re}$ , to target bladder tumours after intravesical administration [16.88–16.92]. Again, a lack of stability was found for the  $^{188}\text{Re}$  labelled C595 antibody [16.88, 16.89]. Both technetium and rhenium C595 antibodies were labelled by standard direct methods, but about 50% of the  $^{188}\text{Re}$  was lost in the form of perrhenate after 22 h at room temperature [16.88].

Technetium-99m-C595, on the other hand, labelled by a similar method, shows higher stability and only minor dissociation after 24 h under the same conditions [16.89].

These stability issues could be rationalized in terms of the increased tendency of rhenium to oxidize to perrhenate, compared to technetium. Again, it is clear that the rhenium–technetium analogy should only be considered reliable when the metal core is in a well-defined and optimally designed, highly stable environment (kinetically and thermodynamically), preventing the oxidation of the metal as well as any ligand substitution events. This is not the case with native thiol groups of antibodies, any more than it is with bisphosphonates.

#### 16.3.4. $^{186/188}\text{Re}$ labelled peptides

Direct labelling methods are less applicable to peptides than antibodies because there is less likelihood of endogenous metal binding groups being present, and if they are present, there is a greater likelihood that labelling will interfere with receptor binding. Nevertheless, the approach has often been tried. An example is lanreotide, a disulphide containing cyclic octapeptide that binds to somatostatin receptors. It has been labelled with  $^{188}\text{Re}$  in the presence of HEDP as a ligand exchange partner [16.93]. The conjugate demonstrated tumour uptake but was highly lipophilic. Lanreotide has also been labelled using direct methods with  $^{99\text{m}}\text{Tc}$  in good yield and purity [16.94, 16.95], but the product is mainly excreted via the gastrointestinal tract. For efficient radionuclide therapy, low lipophilicity and fast renal excretion are highly desirable in order to minimize radiation toxicity. Lanreotide may also be labelled by bifunctional chelator methods [16.96]. It was efficiently conjugated with the pre-formed complex  $^{188}\text{Re}$ -MAG3 (Fig. 16.7). The resulting bioconjugate,  $^{188}\text{Re}$ -MAG3-lanreotide, showed lower lipophilicity than the conjugate made by direct methods [16.96] but its stability was also significantly lower, suggesting that MAG3 may not be the best chelating ligand for rhenium.

When the structures of peptides directly labelled with Re and Tc are probed in detail, it becomes apparent that there may be very major differences in structure. Labelling with technetium using water soluble phosphines as an efficient disulphide bond reducing agent gives peptide bound Tc(III) species with a coordinated phosphine (Fig. 16.8), whereas labelling with rhenium gave peptide-bound Re(V) oxo species with no phosphine bound. In both cases, the products were unstable and inhomogeneous, consisting of isomers of monomeric and dimeric species [16.97]. Thus, the direct labelling approach affords little control of the structure and homogeneity of the labelled products, and researchers must be alert to these defects in the direct labelling approach.

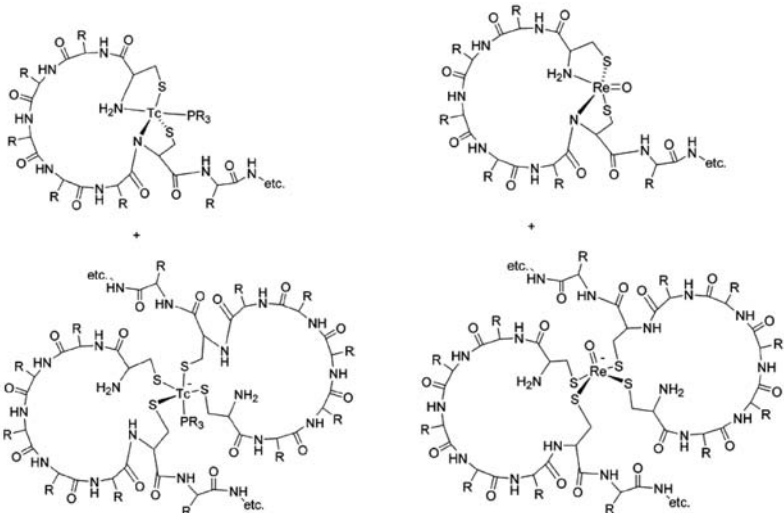
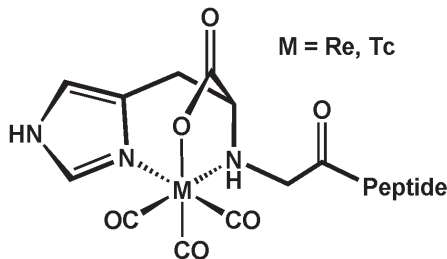


FIG. 16.8. Proposed structures of peptide conjugates with Tc and Re produced by use of water soluble phosphine reducing agents [16.97].

Other peptides such as  $\alpha$ -melanocyte stimulating hormone ( $\alpha$ -MSH), bombesin (BBN) and neuropeptides (NT) have also been labelled with  $^{188}\text{Re}$  and  $^{99\text{m}}\text{Tc}$ . Among them,  $^{188}\text{Re}/^{99\text{m}}\text{Tc}$ - $\alpha$ -MSH and  $^{188}\text{Re}$ -NT have shown high receptor binding affinity in tumour bearing mice and in vitro samples, respectively [16.98–16.103]. In vivo studies with  $^{188}\text{Re}/^{99\text{m}}\text{Tc}$ - $\alpha$ -MSH analogues in which the N termini contain the metal chelating CGCG tetrapeptide for metal coordination have shown that some may have potential as melanoma imaging agents [16.99]. The biodistribution in normal mice for Tc and Re agents was similar but there was a higher liver uptake of the  $^{99\text{m}}\text{Tc}$  analogue up to at least 4 h. The same technetium agent also showed some preferential melanoma tumour uptake. Unfortunately, the  $^{188}\text{Re}$  analogue was not evaluated with tumour bearing mice, so comparison of its tumour uptake with the Tc analogue is not possible [16.99]. In a later report, CCMSH (another  $\alpha$ -MSH analogue) was labelled with  $^{188}\text{Re}$ , using a direct method in which radiometal labelling induces peptide cyclization by thiolate binding. Its biodistribution and melanoma tumour targeting properties were similar to its technetium counterpart, including high kidney uptake [16.98, 16.104].

A direct in vivo comparison between technetium and rhenium was made with the radiolabelled NT analogue NT-XI [16.105], labelled using the ‘tricarbonyl’ method, with the tridentate chelator Na-histidinyl acetate at the N-terminus (Fig. 16.9), which offers a simple approach to form a stable and inert complex with the M(CO)<sub>3</sub> (M = Re, Tc) core [16.106–16.108]. The Re derivative



*FIG. 16.9. Supposed structure of the Tc/Re tricarbonyl adduct of Na-histidinyl acetate-linked peptide.*

was harder to synthesize, consistent with a more inert third row metal–carbonyl complex. Consequently, it required purification to separate the product from other uncharacterized by-products. This illustrates that methods for technetium are usually not directly transferable to rhenium, and that the harsher conditions required to directly or indirectly label a biomolecule with rhenium might generate unwanted by-products. Biodistribution studies in nude mice bearing an HT-29 tumour of NT-XI labelled with  $^{99m}\text{Tc}$  and  $^{188}\text{Re}$  were similar, although with  $^{188}\text{Re}$ -NT-XI, there was a higher spleen and liver uptake. Thus, despite the supposed structural similarity and stability of the rhenium and technetium tricarbonyl cores, it cannot yet be concluded with confidence that the respective labelled peptides have a quantitatively similar biodistribution.

### 16.3.5. Rhenium-188 colloids for liver therapy

Due to the high prevalence of hepatoma in some parts of the world (notably south-east Asia), an economic and readily available replacement for  $^{131}\text{I}$ -lipiodol has been a high profile target for development [16.109]. The high energy gamma radiation of  $^{131}\text{I}$  is a major disadvantage, requiring that patients stay isolated in a shielded room for several days [16.11, 16.12, 16.110–16.117].

Rhenium-188-lipiodol can be synthesized using  $^{188}\text{Re}$  [16.118], but the difficult and lengthy methods required have driven the search for new methods. One approach has been to prepare a  $^{188}\text{Re}$ -sulphur colloid that is lipophilic enough to form a suspension in lipiodol [16.117]. The  $^{188}\text{Re}$ -sulphur-lipiodol mixture showed good retention in the liver cancer of animal models. In another study,  $^{188}\text{Re}(\text{III})\text{-SSS-lipiodol}$  ( $\text{SSS} = (\text{S}_2\text{CPh})(\text{S}_3\text{CPh})_2$ ) was synthesized by dissolving the highly lipophilic complex  $^{188}\text{Re}(\text{III})\text{-SSS}$  in lipiodol [16.119]. The resulting material was synthesized in high yields and showed very weak urinary elimination. Furthermore, the biodistribution in healthy pigs was close to that of  $^{131}\text{I}$ -lipiodol in humans, and in vivo studies with hepatoma bearing rats have also shown promising results [16.115]. A similar rationale was used in the

development of  $^{188}\text{Re(V)}$ -HDD-lipiodol (HDD = 4-hexadecyl-1,2,9,9-tetramethyl-4,7-diaza-1,10-decanethiol) [16.113]. The long alkyl chains were introduced in the metal–chelate moiety to create good hydrophobic interactions with lipiodol. Rhenium-188(V)-HDD-lipiodol has been tested in patients, with promising preliminary results, but the labelling yields are low when compared with  $^{188}\text{Re(III)}$ -SSS-lipiodol, which may be a restricting factor for the synthesis of high therapeutic activities, and a significant urinary excretion has been observed [16.110, 16.111, 16.113]. A sharp improvement of this approach for labelling lipiodol was obtained through the introduction of the rhenium(V) nitrido bis(diethylthiocarbamate)complex  $^{188}\text{Re(V)}$ -N-DED<sub>C</sub> [16.120]. This compound can be prepared in very high yield using a lyophilized kit formulation, and exhibits a strong lipophilic character. It is, therefore, quantitatively extracted and tightly retained by lipiodol. The resulting  $^{188}\text{Re(V)}$ -N-DED<sub>C</sub>-lipiodol was investigated in a number of patients with hepatoma. The results showed that  $^{188}\text{Re(V)}$ -N-DED<sub>C</sub>-lipiodol is stable in vivo and is selectively accumulated in the tumour without any significant uptake in non-target tissues such as lungs, spleen and kidneys. This compound may, therefore, provide safe and effective therapy of unresectable hepatocellular carcinoma, either alone or in combination with transarterial chemoembolization [16.121].

#### 16.3.6. Other $^{186/188}\text{Re}$ colloids

Another area in which rhenium compounds have been applied is in radiation synovectomy, which is a potential alternative to surgical synovectomy for the treatment of rheumatoid arthritis. Radiation synovectomy is a procedure by which a  $\beta$  emitting radionuclide with enough tissue penetration, such as  $^{188}\text{Re}$ , is injected into the joint to reduce synovial inflammation and destroy the inflamed tissue. As colloidal particles are usually bigger than 100 nm, they tend to stay in closed compartments (such as the synovial space) and will not go into the blood stream. This characteristic has been the main driving force in the development of  $^{188}\text{Re}$  colloids for the treatment of rheumatoid arthritis. A  $^{188}\text{Re}$ -tin colloid has been evaluated in vivo and also seems to represent a strong candidate [16.122], and  $^{186/188}\text{Re}$ -sulphur colloids have also been widely explored [16.123–16.127].

#### 16.3.7. Rhenium-188 compounds in cardiovascular therapy

Percutaneous transluminal coronary angioplasty is one of the techniques used for the treatment of ischaemic heart disease. The goal of this method is to increase the diameter of the arteries, and hence the blood flow to the myocardium, by inflating a balloon in a stenosed coronary artery. One of the complications associated with this technique is recurrence of stenosis, which

affects almost 50% of the patients after angioplasty. To overcome this problem, it has been shown that irradiation may inhibit restenosis [16.128]. Consequently, if the balloon used for widening the stenosed artery is filled up with a solution of a radionuclide, the irradiation could be effectively and selectively applied to the affected zone. The rhenium containing molecules used for this have been designed for rapid renal excretion in the event of balloon rupture and consequent escape of radioactivity into the circulation, and well known technetium radiopharmaceuticals were the basis for this design. Rhenium-188 labelled DTPA or MAG3, both of which have technetium counterparts showing rapid renal excretion, have been used (although structural similarity between the rhenium and technetium DTPA complexes has not been experimentally confirmed) [16.129, 16.130]. Clinical trials with  $^{188}\text{Re}$ -DTPA filled balloons in more than 120 patients have shown a reduction of approximately 30% in restenosis rate [16.12]. As an alternative,  $^{188}\text{Re}$  labelled stents, prepared by plasma deposition of siloxan film containing chelating groups to bind  $^{188}\text{Re}$ , can also be applied for cardiovascular therapy [16.131]. However, the long term benefits of this technique are still unclear, and new techniques such as drug releasing stents are becoming more established [16.132].

#### 16.3.8. Radiobiology studies

The number of reported investigations of the effect of the various  $\beta$  emitting radionuclides incorporated within, or around, cells *in vitro* is very small at present. Most studies of efficacy have been done *in vivo*, with little control of radiation dose or microscopic distribution within tumours. There is a great need for comparative radiobiological investigation, comparing the rhenium isotopes with other important therapeutic radionuclides such as  $^{90}\text{Y}$ , with these radionuclides to compare their cellular toxicity quantitatively on a ‘per decay’ basis and in relation to the subcellular location of the radionuclides. A few studies have compared  $^{188}\text{Re}$  with  $^{131}\text{I}$  in Na/I symporter expressing cells and tumours [16.133, 16.134], and many computational microdosimetric modelling studies have been reported [16.4, 16.135], but there have been no direct experimental comparisons in cancer cell lines between  $^{90}\text{Y}$  and  $^{188}\text{Re}$ , which are the main high energy  $\beta$  emitters that can potentially be used in similar circumstances. This must be a high priority for the next years of research with  $\beta$  emitting radionuclides, including those of rhenium. The knowledge gained would be extremely valuable to guide selection of appropriate radionuclides for therapy.

## 16.4. SUMMARY

As a result of the chemical analogy between rhenium and technetium, some potentially valuable therapeutic  $^{188}\text{Re}$  and  $^{186}\text{Re}$  radiopharmaceuticals have come about because of prior experience with the  $^{99\text{m}}\text{Tc}$  analogue. These include the pentavalent Re(V)DMSA complex, which also led to the use of the exceptionally stable Re(V)DMSA complex core for biomolecule radiolabelling, and other labelling methods for biomolecules including cysteine containing peptide sequences and MAG3 for labelling with the Re(V)oxo core and polyhistidine sequences for labelling with the Re(I)tricarbonyl core. Nevertheless, this analogy must be pursued with great caution: the emerging rhenium radiopharmaceuticals in many cases, such as bisphosphonate complexes and antibodies and peptides labelled by direct methods, show significant differences from their technetium counterparts in terms of preparation methods and the structure and stability, and, hence, biological behaviour, of the products. The differences, in general, may be accounted for by assuming that rhenium is a little more ‘electron rich’ (leading to rhenium having lower redox potentials and, thus, being harder to reduce than technetium) than technetium in corresponding oxidation states. This can affect stability, structure and lipophilicity (and, hence, biodistribution) as well as redox potential. Exceptions are the DMSA and tricarbonyl complexes, which appear to be highly analogous in structure and oxidation state, if not in preparation. This has to be validated for each new radiopharmaceutical and cannot be assumed. Many rhenium radiopharmaceuticals currently being investigated are particulate in nature and, in these instances, technetium chemistry has little to contribute to their development. Despite the differences, the similarity between rhenium and technetium has been a useful guide in radiopharmaceutical development and, indeed, has often inspired, and sometimes guided, the therapeutic application of rhenium isotopes. Nevertheless, successful development of optimal rhenium radiopharmaceuticals will be aided by leaving behind the strategy of basing new rhenium chemistry on known technetium chemistry, and instead focusing on rhenium for its own sake.

## ACKNOWLEDGEMENTS

We thank the other contributors to this volume for interesting and valuable discussion that was of great value in the preparation of this chapter.

## REFERENCES TO CHAPTER 16

- [16.1] WESSELS, B.W., ROGUS, R.D., Radionuclide selection and model absorbed dose calculations for radiolabeled tumor associated antibodies, *Med. Phys.* **11** (1984) 638–645.
- [16.2] O'DONOGHUE, J.A., BARDIES, M., WHELDON, T.E., Relationships between tumor size and curability for uniformly targeted therapy with beta-emitting radionuclides, *J. Nucl. Med.* **36** (1995) 1902–1909.
- [16.3] SIMPKIN, D.J., MACKIE, T.R., EGS4 Monte Carlo determination of the beta dose kernel in water, *Med. Phys.* **17** (1990) 179–186.
- [16.4] UNAK, P., CETINKAYA, B., UNAK, I., Absorbed dose estimates at the cellular level for  $^{186}\text{Re}$  and  $^{188}\text{Re}$ , *Radiat. Phys. Chem.* **73** (2005) 137–146.
- [16.5] YORKE, E.D., BEAUMIER, P.L., WESSELS, B.W., FRITZBERG, A.R., MORGAN, A.C.J., Optimal antibody-radionuclide combinations for clinical radioimmunotherapy: a predictive model based on mouse pharmacokinetics, *Nucl. Med. Biol.* **18** (1991) 827.
- [16.6] SCHWARZBACH, R., BLÄUENSTEIN, P., JEGGE, J., SCHUBIGER, P.A., Is the production of  $^{186}\text{Re}$  with cyclotron irradiations an alternative to neutron activation in a reactor? *J. Labelled Comp. Radiopharm.* **37** (1995) 816.
- [16.7] KNAPP, F.F.J., The continuing role of radionuclide generator systems for nuclear medicine, *Eur. J. Nucl. Med.* **21** (1994) 1151–1165.
- [16.8] VANDERHEYDEN, J.-L., SU, F.-M., EHRHARDT, G.J., Soluble Irradiation Targets and Methods for the Production of Radiorhenium, U.S. Patent 5,053,186 (1991).
- [16.9] GRIFFITHS, G.L., et al., Evaluation of a  $^{188}\text{W}/^{188}\text{Re}$  generator system as a ready source of  $^{188}\text{Re}$  for use in radioimmunotherapy (RAIT), *Radioact. Radiochem.* **3** (1992) 33–37.
- [16.10] PRAKASH, S.D., BLOWER, P.J., Perspectives on Bioinorganic Chemistry (HAY, R., DILWORTH, J.R., NOLAN, K.B., Eds), Vol. 4, JAI Press, Connecticut (1999) 9–143.
- [16.11] LAMBERT, B., DE KLERK, J.M.H., Clinical applications of Re-188-labelled radiopharmaceuticals for radionuclide therapy, *Nucl. Med. Commun.* **27** (2006) 223–229.
- [16.12] JEONG, J.M., CHUNG, K.K., Therapy with Re-188-labeled radiopharmaceuticals: An overview of promising results from initial clinical trials, *Cancer Biother. Radiopharm.* **18** (2003) 707–717.
- [16.13] SERAFINI, A.N., Current status of systemic intravenous radiopharmaceuticals for the treatment of painful metastatic bone disease, *Int. J. Radiat. Oncol. Biol. Phys.* **30** (1994) 1187–1194.
- [16.14] MATHIEU, L., CHEVALIER, P., GALY, G., BERGER, M., Preparation of  $^{186}\text{Rhenium}$  labelled HEDP and its possible use in the treatment of osseous neoplasms, *Int. J. Appl. Radiat. Isotop.* **30** (1979) 725–727.
- [16.15] EISENHUT, M., Preparation of  $^{186}\text{Re}$ -perrhenate for nuclear medical purposes, *Int. J. Appl. Radiat. Isotop.* **33** (1982) 99–103.

- [16.16] MINUTOLI, F., et al., [Re-186]-HEDP in the palliation of painful bone metastases from cancers other than prostate and breast, *Q. J. Nucl. Med. Mol. Imaging* **50** (2006) 355–362.
- [16.17] O'SULLIVAN, J.M., et al., High activity rhenium-186 hydroxyethylidene diphosphonate (HEDP) with autologous peripheral blood stem cell (PBSC) transplant: A novel treatment strategy in hormone refractory prostate cancer metastatic to bone, *J. Clin. Oncol.* **22** (2004) 397S–397S.
- [16.18] LEONDI, A.H., et al., Palliative treatment of painful disseminated bone metastases with (186)rhenium-HEDP in patients with lung cancer, *Q. J. Nucl. Med. Mol. Imaging* **48** (2004) 211–219.
- [16.19] LAM, M., DE KLERK, J.M.H., VAN RIJK, P.P., <sup>186</sup>Re-HEDP for metastatic bone pain in breast cancer patients, *Eur. J. Nucl. Med. Mol. Imaging* **31** (2004) S162–S170.
- [16.20] BRENNER, W., et al., Bone uptake studies in rabbits before and after high-dose treatment with Sm-153-EDTMP or Re-186-HEDP, *J. Nucl. Med.* **44** (2003) 247–251.
- [16.21] DEKLERK, J.M.H., et al., Phase I study of rhenium-186-HEDP in patients with bone metastases originating from breast cancer, *J. Nucl. Med.* **37** (1996) 244–249.
- [16.22] O'SULLIVAN, J.M., et al., High activity Rhenium-186 HEDP with autologous peripheral blood stem cell rescue: a phase I study in progressive hormone refractory prostate cancer metastatic to bone, *Br. J. Cancer* **86** (2002) 1715–1720.
- [16.23] PALMEDO, H., et al., Remission of bone metastases after combined chemotherapy and radionuclide therapy with Re-186 HEDP, *Clin. Nucl. Med.* **23** (1998) 501–504.
- [16.24] DE KLERK, J.M.H., VAN DIJK, A., VAN HET SCHIP, A.D., ZONNENBERG, B.A., VAN RIJK, P.P., Pharmacokinetics of 186 Re after administration of 186 Re-HEDP to patients with bone metastases, *J. Nucl. Med.* **33** (1992) 646–651.
- [16.25] DE WINTER, F., BRANS, B., VAN DE WIELE, C., DIERCKX, R.A., Visualization of the stomach on rhenium-186 HEDP imaging after therapy for metastasized prostate carcinoma, *Clin. Nucl. Med.* **24** (1999) 898–899.
- [16.26] LIMOURIS, G.S., SKUKLA, S.K., Gastric uptake during Re-186 HEDP bone scintigraphy, *Anticancer Res.* **17** (1997) 1779–1781.
- [16.27] KRISHNAMURTHY, G.T., KRISHNAMURTHY, S., Radionuclides for metastatic bone pain palliation: a need for re-evaluation in the new millennium, *J. Nucl. Med.* **41** (2000) 688–691.
- [16.28] PANDIT-TASKAR, N., BATRAKI, M., DIVGI, C.R., Radiopharmaceutical therapy for palliation of bone pain from osseous metastases, *J. Nucl. Med.* **45** (2004) 1358–1365.
- [16.29] CHEN, S.L., et al., Treatment of metastatic bone pain with rhenium-188 hydroxyethylidene diphosphonate, *Med. Princ. Pract.* **10** (2001) 98–101.
- [16.30] HSIEH, B.T., et al., Comparison of various rhenium-188-labeled diphosphonates for the treatment of bone metastases, *Nucl. Med. Biol.* **26** (1999) 973–976.
- [16.31] LI, S.J., et al., Rhenium-188 HEDP to treat painful bone metastases, *Clin. Nucl. Med.* **26** (2001) 919–922.
- [16.32] LIEPE, K., et al., Rhenium-188-HEDP in the palliative treatment of bone metastases, *Cancer Biother. Radiopharm.* **15** (2000) 261–265.

- [16.33] LIEPE, K., KROPP, J., RUNGE, R., KOTZERKE, J., Therapeutic efficiency of rhenium-188-HEDP in human prostate cancer skeletal metastases, *Br. J. Cancer* **89** (2003) 625–629.
- [16.34] LIN, W.Y., et al., Rhenium-188 hydroxyethylidene diphosphonate: A new generator-produced radiotherapeutic drug of potential value for the treatment of bone metastases, *Eur. J. Nucl. Med.* **24** (1997) 590–595.
- [16.35] MAXON, H.R., et al., Rhenium-188(Sn)HEDP for treatment of osseous metastases, *J. Nucl. Med.* **39** (1998) 659–663.
- [16.36] PALMEDO, H., et al., Dose escalation study with rhenium-188 hydroxyethylidene diphosphonate in prostate cancer patients with osseous metastases, *Eur. J. Nucl. Med.* **27** (2000) 123–130.
- [16.37] PALMEDO, H., et al., Repeated bone-targeted therapy for hormone-refractory prostate carcinoma: Randomized phase II trial with the new, high-energy radiopharmaceutical rhenium-188 hydroxyethylidenediphosphonate, *J. Clin. Oncol.* **21** (2003) 2869–2875.
- [16.38] ZHANG, H., et al., Rhenium-188-HEDP therapy for the palliation of pain due to osseous metastases in lung cancer patients, *Cancer Biother. Radiopharm.* **18** (2003) 719–726.
- [16.39] BISUNADAN, M., BLOWER, P.J., CLARKE, S.E.M., SINGH, J., WENT, M.J., Synthesis and characterisation of [186Re]rhenium(V) dimercaptosuccinic acid: a possible tumour radiotherapy agent, *Appl. Radiat. Isotop.* **42** (1991) 167–171.
- [16.40] BLOWER, P.J., SINGH, J., CLARKE, S.E.M., BISUNADAN, M.M., WENT, M.J., Pentavalent rhenium-186 DMSA: a possible tumour therapy agent, *J. Nucl. Med.* **31** (1990) 768.
- [16.41] BLOWER, P.J., et al., Pentavalent rhenium-188 dimercaptosuccinic acid for targeted radiotherapy: synthesis and preliminary animal and human studies, *Eur. J. Nucl. Med.* **25** (1998) 613–621.
- [16.42] BLOWER, P.J., KETTLE, A.G., O'DOHERTY, M.J., COAKLEY, A.J., KNAPP, F.F., Quantitative prediction of Re-188(V)DMSA distribution from Tc-99m(V)DMSA scans for radio-nuclide therapy planning, *J. Nucl. Med.* **41** (2000) 1202.
- [16.43] KNAPP, F.F., et al., Reactor-produced radioisotopes from ORNL for bone palliation, *Appl. Radiat. Isotop.* **49** (1998) 309–315.
- [16.44] SINGH, J., POWELL, A.K., CLARKE, S.E.M., BLOWER, P.J., Crystal structure and isomerism of a tumour targetting radiopharmaceutical: [ReO(dmsa)2]<sup>-</sup>(H<sub>2</sub> dmsa = meso-2,3-dimercaptosuccinic acid), *J. Chem. Soc. Chem. Commun.* (1991) 1115–1117.
- [16.45] SINGH, J., et al., Studies on the preparation and isomeric composition of [186Re]- and [188Re]-pentavalent rhenium dimercaptosuccinic acid complex, *Nucl. Med. Commun.* **14** (1993) 197–203.
- [16.46] BOLZATI, C., et al., Efficient preparation and stabilization of Re-188-MDP under physiological conditions, *Eur. J. Nucl. Med.* **26** (1999) PS645.
- [16.47] FAINTUCH, B.L., FAINTUCH, S., MURAMOTO, E., Complexation of Re-188-phosphonates: in vitro and in vivo studies, *Radiochim. Acta* **91** (2003) 607–612.

- [16.48] MITTERHAUSER, M., et al., Binding studies of F-18-fluoride and polyphosphonates radiolabelled with In-111, Tc-99m, Sm-153, and Re-188 on bone compartments: a new model for the pre vivo evaluation of bone seekers? *Bone* **34** (2004) 835–844.
- [16.49] LISIC, E.C., et al., Synthesis of a new bisphosphonic acid ligand (SEDP) and preparation of a Re-188-(Sn)SEDP bone seeking radiotracer, *Nucl. Med. Biol.* **28** (2001) 419–424.
- [16.50] DE MURPHY, C.A., et al., Labelling of Re-ABP with Re-188 for bone pain palliation, *Appl. Radiat. Isotop.* **54** (2001) 435–442.
- [16.51] LI, Q.N., ZHANG, X.D., SHENG, R., LI, W.X., Preparation of (Re-188) Re-AEDP and its biodistribution studies, *Appl. Radiat. Isotop.* **53** (2000) 993–997.
- [16.52] ALYAFEI, S., et al., Biodistribution studies of the Re-186 complex of 3-amino-1-hydroxypropylidene-1,1-bisphosphonic acid in mice, *Nucl. Med. Commun.* **20** (1999) 551–557.
- [16.53] KOTHARI, K., et al., Re-186-1,4,8,11-tetraaza cyclotetradecyl-1,4,8,11-tetramethylene phosphonic acid: a novel agent for possible use in metastatic bone-pain palliation, *Nucl. Med. Biol.* **28** (2001) 709–717.
- [16.54] HASHIMOTO, K., Labelling of aminomethylenephosphonate derivatives with generator-produced Re-188, and a study of their stability, *Appl. Radiat. Isotop.* **51** (1999) 307–313.
- [16.55] OH, S.J., et al., Preparation and biological evaluation of Re-188-ethylenediamine-N,N,N',N'-tetrakis(methylene phosphoric acid) as a potential agent for bone pain palliation, *Nucl. Med. Commun.* **23** (2002) 75–81.
- [16.56] OH, S.J., MOON, D.H., WON, K.S., LEE, H.K., Effects of carrier on preparation and biodistribution of Re-188-EDTMP as a potential therapeutic bone agent, *J. Nucl. Med.* **42** (2001) 1097.
- [16.57] MITTERHAUSER, M., et al., Labelling of EDTMP (Multibone (R)) with In-111, Tc-99m and Re-188 using different carriers for “cross complexation”, *Appl. Radiat. Isotop.* **60** (2004) 653–658.
- [16.58] ELDER, R.C., et al., Studies of the structure and composition of rhenium-1,1-hydroxyethylidenediphosphonate (HEDP) analogues of the radiotherapeutic agent (ReHEDP)-Re-186, *Inorg. Chem.* **36** (1997) 3055–3063.
- [16.59] HASHIMOTO, K., MATSUOKA, H., Analysis of Re-188-EDTMP complexes by HPLC and ultrafiltration, *Radiochim. Acta* **92** (2004) 285–290.
- [16.60] CHUNG, Y.S., et al., Effect of carrier on labeling and biodistribution of Re-188-hydroxyethylidene diphosphonate (HEDP) in mice and rats, *J. Nucl. Med.* **39** (1998) 1037.
- [16.61] HASHIMOTO, K., Synthesis of a Re-188-HEDP complex using carrier-free Re-188 and study of its stability, *Appl. Radiat. Isotop.* **49** (1998) 351–356.
- [16.62] LIN, W.Y., et al., Effect of reaction conditions on preparations of Rhenium-188 hydroxyethylidene diphosphonate complexes, *Nucl. Med. Biol.* **26** (1999) 455–459.
- [16.63] VERDERA, E.S., et al., Rhenium-188-HEDP-kit formulation and quality control, *Radiochim. Acta* **79** (1997) 113–117.

- [16.64] PEARSON, R.G., Hard and soft acids and bases, *J. Am. Chem. Soc.* **85** (1963) 3533–3543.
- [16.65] BLOWER, P.J., KETTLE, A.G., O'DOHERTY, M.J., COAKLEY, A.J., KNAPP, F.F., Tc-99m(V)DMSA quantitatively predicts Re-188(V)DMSA distribution in patients with prostate cancer metastatic to bone, *Eur. J. Nucl. Med.* **27** (2000) 1405–1409.
- [16.66] UEHARA, T., et al., Re-186 chelate-conjugated bisphosphonate for the development of new radiopharmaceuticals for bones, *Nucl. Med. Biol.* **34** (2007) 79–87.
- [16.67] OGAWA, K., et al., Therapeutic effects of a (186) Re-complex-conjugated bisphosphonate for the palliation of metastatic bone pain in an animal model, *J. Nucl. Med.* **48** (2007) 122–127.
- [16.68] OGAWA, K., et al., Rhenium-186-monoaminemonoamidedithiol-conjugated bisphosphonate derivatives for bone pain palliation, *Nucl. Med. Biol.* **33** (2006) 513–520.
- [16.69] OGAWA, K., et al., Development of a rhenium-186-labeled MAG3-conjugated bisphosphonate for the palliation of metastatic bone pain based on the concept of bifunctional radiopharmaceuticals, *Bioconjug. Chem.* **16** (2005) 751–757.
- [16.70] OGAWA, K., et al., Design of a radiopharmaceutical for the palliation of painful bone metastases: rhenium-186-labeled bisphosphonate derivative, *J. Labelled Comp. Radiopharm.* **47** (2004) 753–761.
- [16.71] BLOWER, P.J., DILWORTH, J.R., HUTCHINSON, J.P., NICHOLSON, T., ZUBIETA, J., Rhenium complexes with di-thiolate and tri-thiolate ligands — the synthesis and X-ray crystal-structures of square pyramidal [Pph<sub>4</sub>][Re(Sch<sub>2</sub>ch<sub>2</sub>s)<sub>2</sub>] and [Nme<sub>4</sub>][Res(Sch<sub>2</sub>ch<sub>2</sub>s)<sub>2</sub>] and trigonal prismatic [Pph<sub>4</sub>][Re((Sch<sub>2</sub>)<sub>3</sub>ech<sub>3</sub>)<sub>2</sub>], *Dalton Trans.* (1986) 1339–1345.
- [16.72] DAVISON, A., et al., Preparation of oxobis(dithiolato) complexes of technetium(V) and rhenium(V), *Inorg. Chem.* **19** (1980) 1988–1992.
- [16.73] BLOWER, P.J., SINGH, J., CLARKE, S.E.M., The chemical identity of pentavalent technetium-99m-dimercaptosuccinic acid, *J. Nucl. Med.* **32** (1991) 845–849.
- [16.74] GUHLKE, S., et al., Re-188(V)-DMSA: in-vitro and in-vivo studies on the individual stereo isomers, *Radiochim. Acta* **92** (2004) 277–283.
- [16.75] BOLZATI, C., et al., An alternative approach to the preparation of (188)Re radiopharmaceuticals from generator-produced [(188)ReO(4)](-): efficient synthesis of (188)Re(V)-meso-2,3-dimercaptosuccinic acid, *Nucl. Med. Biol.* **27** (2000) 309–314.
- [16.76] CHOUDHRY, U., et al., New routes to bioconjugates of rhenium using the oxobis(dithiolato)rhenate(V) core, *Dalton Trans.* (2003) 311–317.
- [16.77] HEINRICH, T.K., KRAUS, W., PIETZSCH, H.J., SMUDA, C., SPIES, H., Novel rhenium chelate system derived from dimercaptosuccinic acid for the selective labeling of biomolecules, *Inorg. Chem.* **44** (2005) 9930–9937.
- [16.78] SEIFERT, S., et al., Preparation and biological characterization of isomeric 188Re(V) oxocomplexes with tetridentate S<sub>4</sub> ligands derived from meso-dimercaptosuccinic acid for labeling of biomolecules, *Bioconjug. Chem.* **17** (2006) 1601–1606.

- [16.79] VANGOG, F.B., et al., Monoclonal antibodies labeled with rhenium-186 using the MAG3 chelate: Relationship between the number of chelated groups and biodistribution characteristics, *J. Nucl. Med.* **37** (1996) 352–362.
- [16.80] VAN GOG, F.B., et al., Dose rhenium-186-labeling of monoclonal antibodies for clinical application - Pitfalls and solutions, *Cancer* **80** (1997) 2360–2370.
- [16.81] FERRO-FLORES, G., et al., An efficient, reproducible and fast preparation of Re-188-anti-CD20 for the treatment of non-Hodgkin's lymphoma, *Nucl. Med. Commun.* **26** (2005) 793–799.
- [16.82] STOPAR, T.G., MLINARIC-RASCAN, I., FETTICH, J., HOJKER, S., MATHER, S.J., Tc-99m-rituximab radiolabelled by photo-activation: a new non-Hodgkin's lymphoma imaging agent, *Eur. J. Nucl. Med. Mol. Imaging* **33** (2006) 53–59.
- [16.83] STALTERI, M.A., MATHER, S.J., Technetium-99m labelling of the anti-tumour antibody PR1A3 by photoactivation, *Eur. J. Nucl. Med.* **23** (1996) 178–187.
- [16.84] BUNJES, D., et al., Rhenium 188-labeled anti-CD66 (a, b, c, e) monoclonal antibody to intensify the conditioning regimen prior to stem cell transplantation for patients with high-risk acute myeloid leukemia or myelodysplastic syndrome: results of a phase I-II study, *Blood* **98** (2001) 565–572.
- [16.85] BUCHMANN, I., et al., Myeloablative radioimmunotherapy with Re-188-anti-CD66-antibody for conditioning of high-risk leukemia patients prior to stem cell transplantation: Biodistribution, biokinetics and immediate toxicities, *Cancer Biother. Radiopharm.* **17** (2002) 151–163.
- [16.86] SEITZ, U., et al., Preparation and evaluation of the rhenium-188-labelled anti-NCA antigen monoclonal antibody BW 250/183 for radioimmunotherapy of leukaemia, *Eur. J. Nucl. Med.* **26** (1999) 1265–1273.
- [16.87] KOTZERKE, J., et al., Radioimmunotherapy for the intensification of conditioning before stem cell transplantation: Differences in dosimetry and biokinetics of Re-188- and Tc-99m-labeled anti-NCA-95 MAbs, *J. Nucl. Med.* **41** (2000) 531–537.
- [16.88] MURRAY, A., et al., Production and characterization of Re-188-C595 antibody for radioimmunotherapy of transitional cell bladder cancer, *J. Nucl. Med.* **42** (2001) 726–732.
- [16.89] SIMMS, M.S., et al., Production and characterisation of a C595 antibody-Tc-99m conjugate for immunoscintigraphy of bladder cancer, *Urol. Res.* **29** (2001) 13–19.
- [16.90] HUGHES, O.D.M., et al., Preclinical evaluation of copper-67 labelled anti-MUC1 mucin antibody C595 for therapeutic use in bladder cancer, *Eur. J. Nucl. Med.* **24** (1997) 439–443.
- [16.91] KUNKLER, R.B., et al., Targeting of bladder-cancer with monoclonal-antibody Nrc48 - a possible approach for intravesical therapy, *Br. J. Urol.* **76** (1995) 81–86.
- [16.92] FRIER, M., Rhenium-188 and copper-67 radiopharmaceuticals for the treatment of bladder cancer, *Mini Rev. Med. Chem.* **4** (2004) 61–68.
- [16.93] DE MURPHY, C.A., et al., Uptake of Re-188-beta-naphthyl-peptide in cervical carcinoma tumours in athymic mice, *Nucl. Med. Biol.* **28** (2001) 319–326.
- [16.94] PERVEZ, S., MUSHTAQ, A., ARIF, M., Technetium-99m direct radiolabeling of Lanreotide: a somatostatin analog, *Appl. Radiat. Isotop.* **55** (2001) 647–651.

- [16.95] LAZNICEK, M., et al., Lanreotide labeled with  $^{99m}\text{Tc}$ : preparation, preclinical testing and comparison with  $(^{111}\text{In})\text{-DTPA-octreotide}$ , *Anticancer Res.* **22** 2125–2130.
- [16.96] FERRO-FLORES, G., et al., Peptide labeling using Re-188,Re-188-MAG(3) and Sm-153-H(1)ETA: A comparison on their in vitro lipophilicity, *J. Radioanal. Nucl. Chem.* **251** (2002) 7–13.
- [16.97] GREENLAND, W.E.P., BLOWER, P.J., Water-soluble phosphines for direct labeling of peptides with technetium and rhenium: Insights from electrospray mass spectrometry, *Bioconjug. Chem.* **16** (2005) 939–948.
- [16.98] MIAO, Y.B., et al., In vivo evaluation of  $(^{188}\text{Re})$ -labeled alpha-melanocyte stimulating hormone peptide analogs for melanoma therapy, *Int. J. Cancer* **101** (2002) 480–487.
- [16.99] CHEN, J.Q., GIBLIN, M.F., WANG, N.N., JURISSON, S.S., QUINN, T.P., In vivo evaluation of  $\text{Tc-99m}/\text{Re-188}$ -labeled linear alpha-melanocyte stimulating hormone analogs for specific melanoma targeting, *Nucl. Med. Biol.* **26** (1999) 687–693.
- [16.100] GIBLIN, M.F., JURISSON, S.S., QUINN, T.P., Synthesis and characterization of rhenium-complexed alpha-melanotropin analogs, *Bioconjug. Chem.* **8** (1997) 347–353.
- [16.101] SAWYER, T.K., et al., 4-Norleucine, 7-D-phenylalanine-alpha-melanocyte-stimulating hormone: A highly potent alpha-melanotropin with ultralong biological activity, *Proc. Natl. Acad. Sci. USA* **77** (1980) 5754–5758.
- [16.102] CODY, W.L., et al., Cyclic melanotropins .9. 7-D-phenylalanine analogs of the active-site sequence, *J. Med. Chem.* **28** (1985) 583–588.
- [16.103] GIBLIN, M.F., WANG, N., HOFFMAN, T.J., JURISSON, S.S., QUINN, T.P., Design and characterization of alpha-melanotropin peptide analogs cyclized through rhenium and technetium metal coordination, *Proc. Natl. Acad. Sci. USA* **95** (1998) 12814–12818.
- [16.104] CHEN, J.Q., CHENG, Z., HOFFMAN, T.J., JURISSON, S.S., QUINN, T.P., Melanoma-targeting properties of  $(^{99m}\text{Tc})$ -labeled cyclic alpha-melanocyte-stimulating hormone peptide analogues, *Cancer Res.* **60** (2000) 5649–5658.
- [16.105] BLAUENSTEIN, P., et al., Improving the tumor uptake of  $^{99m}\text{Tc}$ -labeled neuropeptides using stabilized peptide analogues, *Cancer Biother. Radiopharm.* **19**(2) (2004) 181–188.
- [16.106] REUBI, J.C., WASER, B., FRIESS, H., BUCHLER, M., LAISSUE, J., Neurotensin receptors: a new marker for human ductal pancreatic adenocarcinoma, *Gut* **42** (1998) 546–550.
- [16.107] BRUEHLMEIER, M., et al., Stabilization of neurotensin analogues: effect on peptide catabolism, biodistribution and tumor binding, *Nucl. Med. Biol.* **29** (2002) 321–327.
- [16.108] MAES, V., GARCIA-GARAYOA, E., BLAUENSTEIN, P., TOURWE, D., Novel  $^{99m}\text{Tc}$ -labeled neurotensin analogues with optimized biodistribution properties, *J. Med. Chem.* **49** (2006) 1833–1836.
- [16.109] PARK, C.H., SUH, J.H., YOO, H.S., Evaluation of intrahepatic I-131 ethiodol on patients with hepaticellular carcinoma, *Clin. Nucl. Med.* **11** (1986) 514.

- [16.110] LAMBERT, B., et al., Re-188-HDD/lipiodol therapy for hepatocellular carcinoma: an activity escalation study, *Eur. J. Nucl. Med. Mol. Imaging* **33** (2006) 344–352.
- [16.111] LAMBERT, B., et al., Re-188-HDD/lipiodol for treatment of hepatocellular carcinoma: A feasibility study in patients with advanced cirrhosis, *J. Nucl. Med.* **46** (2005) 1326–1332.
- [16.112] YOON, C.J., et al., Transcatheter arterial embolization with (188)Rhenium-HDD-labeled iodized oil in rabbit VX2 liver tumor, *J. Vasc. Interv. Radiol.* **15** (2004) 1121–1128.
- [16.113] SUNDRAM, F., CHAU, T.C.M., ONKHUDAI, P., BERNAL, P., PADHY, A.K., Preliminary results of transarterial rhenium-188 HDD lipiodol in the treatment of inoperable primary hepatocellular carcinoma, *Eur. J. Nucl. Med. Mol. Imaging* **31** (2004) 250–257.
- [16.114] LUO, T.Y., et al., Preparation and biodistribution of rhenium-188 ECD/lipiodol in rats following hepatic arterial injection, *Nucl. Med. Biol.* **31** (2004) 671–677.
- [16.115] GARIN, E., et al., Re-188-SSS lipiodol: radiolabelling and biodistribution following injection into the hepatic artery of rats bearing hepatoma, *Nucl. Med. Commun.* **25** (2004) 1007–1013.
- [16.116] BOSCHI, A., et al., A kit formulation for the preparation of Re-188-lipiodol: preclinical studies and preliminary therapeutic evaluation in patients with unresectable hepatocellular carcinoma, *Nucl. Med. Commun.* **25** (2004) 691–699.
- [16.117] KIM, Y.J., et al., Rhenium-188-sulfur colloid suspended in lipiodol: A capillary-blocking radiopharmaceutical for targeting liver cancer, *J. Nucl. Med.* **39** (1998) 235–235.
- [16.118] WANG, S.J., et al., Radiolabelling of lipiodol with generator-produced 188Re for hepatic tumour therapy, *Appl. Radiat. Isotop.* **1996** (1996) 13.
- [16.119] GARIN, E., et al., Development and biodistribution of 188Re-SSS lipiodol following injection into the hepatic artery of healthy pigs, *Eur. J. Nucl. Med. Mol. Imaging* **31** (2004) 542–546.
- [16.120] BOSCHI, A., BOLZATI, C., UCCELLI, L., DUATTI, A., High-yield synthesis of the terminal  $^{188}\text{Re} \equiv \text{N}$  multiple bond from generator-produced  $[^{188}\text{ReO}_4]^-$ , *Nucl. Med. Biol.* **30** (2003) 381–387.
- [16.121] BOSCHI, A., et al., A kit formulation for the preparation of Re-188-lipiodol: preclinical studies and preliminary therapeutic evaluation in patients with unresectable hepatocellular carcinoma, *Nucl. Med. Commun.* **25** (2003) 691–699.
- [16.122] SHIN, C.Y., et al., DA-7911, (188)rhenium-tin colloid, as a new therapeutic agent of rheumatoid arthritis, *Arch. Pharm. Res.* **26** (2003) 168–172.
- [16.123] LI, P.Y., et al., Applied radioactivity in radiation synovectomy with [Re-188]rhenium sulfide suspension, *Nucl. Med. Commun.* **27** (2006) 603–609.
- [16.124] YU, Y.B., et al., Preparation and stability of rhenium [Re-188] sulfide suspension with different particle size distributions, *J. Radioanal. Nucl. Chem.* **265** (2005) 395–398.
- [16.125] VAN DER ZANT, F.M., et al., Radiation synovectomy of the ankle with 75 MBq colloidal (186)rhenium-sulfide: Effect, leakage, and radiation considerations, *J. Rheumatol.* **31** (2004) 896–901.

- [16.126] LI, P., CHEN, G., ZHANG, H., SHEN, Z., Radiation synovectomy by Re-188-sulfide in haemophilic synovitis, *Haemophilia* **10** (2004) 422–427.
- [16.127] WANG, S.J., et al., Re-188 sulfur colloid as a radiation synovectomy agent, *Eur. J. Nucl. Med.* **22** (1995) 505–507.
- [16.128] WAKSMAN, R., SERRUYS, P.W., *Handbook of Vascular Brachytherapy*, Martin Dunitz, London (1998).
- [16.129] LEE, J., et al., Dosimetry of rhenium-188 diethylene triamine penta-acetic acid for endovascular intra-balloon brachytherapy after coronary angioplasty, *Eur. J. Nucl. Med.* **27** (2000) 76–82.
- [16.130] OH, S.J., et al., Automation of the synthesis of highly concentrated Re-188-MAG(3) for intracoronary radiation therapy, *Appl. Radiat. Isotop.* **54** (2001) 419–427.
- [16.131] AMOLS, H.I., et al., Dosimetric considerations for catheter-based beta and gamma emitters in the therapy of neointimal hyperplasia in human coronary arteries, *Int. J. Radiat. Oncol. Biol. Phys.* **36** (1996) 913–921.
- [16.132] BABAPULLE, M.N., JOSEPH, L., BELISLE, P., BROPHY, J.M., EISENBERG, M.J., A hierarchical Bayesian meta-analysis of randomised clinical trials of drug-eluting stents, *Lancet* **364** (2004) 583–591.
- [16.133] DADACHOVA, E., et al., Treatment with rhenium-188-perrhenate and iodine-131 of NIS-expressing mammary cancer in a mouse model remarkably inhibited tumor growth, *Nucl. Med. Biol.* **32** (2005) 695–700.
- [16.134] DADACHOVA, E., BOUZAHZAH, B., ZUCKIER, L.S., PESTELL, R.G., Rhenium-188 as an alternative to Iodine-131 for treatment of breast tumors expressing the sodium/iodide symporter (NIS), *Nucl. Med. Biol.* **29** (2002) 13–18.
- [16.135] BAO, A., et al., Theoretical study of the influence of a heterogeneous activity distribution on intratumoral absorbed dose distribution, *Med. Phys.* **32** (2005) 200–208.

## Chapter 17

# FUTURE TRENDS IN THE DEVELOPMENT OF TECHNETIUM RADIOPHARMACEUTICALS

R. ALBERTO

Institute of Inorganic Chemistry, University of Zurich,  
Zurich, Switzerland

### Abstract

Based on the current state of the art as described in the previous chapters of the book, possible future trends in  $^{99m}\text{Tc}$  radiopharmacy are discussed in the chapter. Since they are of fundamental interest, likely chemical developments based on the current cores and building blocks are presented at the beginning. Besides application in labelling, the importance of fundamental research towards novel cores is emphasized. Whereas labelling chemistry is general and does not necessarily relate to one class of molecules, targeting molecules are of course connected to targets and are, therefore, disease specific. Accordingly, the chapter attempts to identify new targets, targeting molecules and strategies as a base for reinforcing the perspectives of  $^{99m}\text{Tc}$  radiopharmacy in the future of nuclear medicine.

### 17.1. INTRODUCTION

To identify future trends in a field such as radiopharmacy and radiopharmaceutical chemistry is a difficult and sometimes dangerous task, since it represents the classical case of a multidimensional system with numerous variables and interlinkages. A thorough analysis of the current situation, written by the experts in the field, is available in the previous chapters and the discussion about future trends will be based on these. The authors summarize the state of the art with respect to different diseases and malfunctions for which  $^{99m}\text{Tc}$  could play a major role for improving diagnosis and, in the case of its higher homologue  $^{188/186}\text{Re}$ , in therapy. Nowadays, radiopharmacy with  $^{99m}\text{Tc}$  faces many problems and uncertainties, as it is experiencing ‘attacks’ from different competitors, and suffers, above all, from its relative unsuccessful attempts to provide the community with novel radiopharmaceuticals of comparable impact as Cardiolite® [17.1]. The question of whether commercial success is a must in our field is justified and is discussed in the context of future trends later in this text [17.2]. However, it is clear that for the development of chemistry and radiopharmacy (and, therefore, for future trends), an appropriate application in clinical routine is the ultimate ‘fuel’ for development in the corresponding science and is, therefore,

more or less the prerequisite. Commercialization and fundamental research are two faces of the same coin and the acquirement of basic knowledge is doubtless of the highest priority. However, much radiopharmaceutical research performed nowadays neither promises commercialization nor makes a real contribution to basic research, a situation which must change, and which should represent the future trend.

Besides not providing novel radiopharmaceuticals, some newly introduced radionuclides are enthusiastically assigned superiority over  $^{99m}\text{Tc}$ . Some of these radionuclides have been reviewed elsewhere [17.3]. Among them is  $^{68}\text{Ga}$ , which is available from a generator system. Gallium-68 is, however, considered to be the most expensive radionuclide for PET imaging [17.4]. Indium-111 has been used for a long time and has experienced a revival despite its comparably high price. We may argue that the chemistry of technetium is much broader than that of, for example, gallium and can be used for central nervous system (CNS) receptor targeting molecules and for peptides; however, when discussing future trends, we must be aware of the fact that for a given target, the most appropriate radionuclide is selected and not the one with the most interesting chemistry; hence, it does not have to be technetium.

Future trends are based on developed chemistry or expected developments towards new chemistry with respect to cores or the conjugation of building blocks to targeting molecules. The application of available labelling chemistry directly leads to the question about targets and targeting molecules, an issue which has been extensively discussed in the recent past on the occasion of conferences and symposia organized by, for example, the IAEA. One must be critically aware that contemporary labelling techniques and building blocks are still not ideal. Hence, fundamental chemistry is asked to make important contributions to the fields of labelling chemistry and biological studies. Due to this cross-linked situation, the discussion about future trends is subdivided into the respective individual steps and is supposed to stimulate thought and movement into new directions. It stands to reason that a breakthrough must be found within the next couple of years, otherwise the application of  $^{99m}\text{Tc}$  is likely to become extinct, not due to a lack of knowledge or more favourable properties of other radionuclides but simply because the competing methods will bypass  $^{99m}\text{Tc}$  based single photon emission computed tomography (SPECT) for convenience or commercial reasons.

## 17.2. CHEMISTRY

Basic technetium chemistry provides radiopharmaceutical research with building blocks, ligand conjugation and labelling methods. A number of these are reliably available and under intensive study. Nice biological results have been

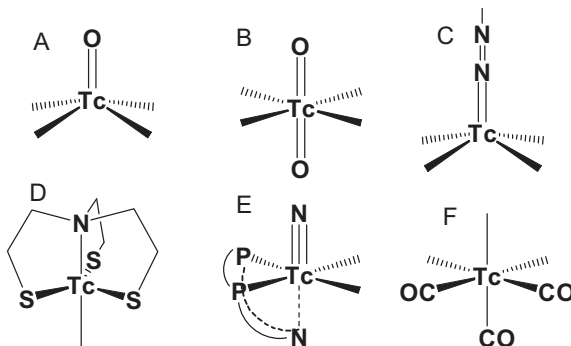


*FIG. 17.1.* Best explored labelling building blocks in radiopharmaceutical chemistry:  $[Tc=O]^{3+}$  (a),  $[O=Tc=O]^+$  (b),  $[Tc(hynic)]^{n+}$  (c),  $[Tc(III)(NS_3)]$  (d),  $[Tc\equiv N]^{2+}$  (e) and  $[Tc(CO)_3]^+$  (f).

obtained as well but no breakthrough has been achieved for various reasons. The most important building blocks are shown in Fig. 17.1.

Analysing an ideal situation would mean injecting the generator eluate into a vial, shaking, and having a quantitative labelling yield of the vector ready to administer, regardless of the targeting molecule's authenticity. Despite the nice building blocks at hand, technetium chemistry is still far from this goal. It is cold comfort that the same is true for most other radionuclides as well. Certainly, the hynic techniques come closest to these conditions but they still have the decisive disadvantage that the label is oddly characterized and that the technique is essentially restricted to peptides and antibodies [17.5]. For low targeting molecule concentrations, heating is still required. The same restrictions also apply for the Tc(V) approach with tetradentate mixed N,S,O ligands.

To compromise, let us allow heating for a limited time period. Besides the methods mentioned above, the new building blocks  $[Tc\equiv N]^{2+}$ , Tc(III) and  $[Tc(CO)_3]^+$  now come into play, all of which have the distinct advantage of being applicable to a broad variety of biomolecules [17.6]. Labelling in one single step, as required in the beginning, is essentially only possible for the last one, and for a limited selection of biomolecules and ligands. The former two building blocks still require a two step procedure. This brief discussion provides an overview about the development of technetium chemistry for the labelling of targeting molecules. Since future trends are the focus of this chapter, no more details will be given here and the reader should refer to Chapters 1 and 2.

Future trends in technetium chemistry have to consider two essential requirements, room temperature and a one pot reaction. Inspecting technetium chemistry reveals that the substitution inert  $[^{99m}TcO_4]^-$ , in principle, immediately

reacts with a variety of reducing agents, generating reactive species of lower oxidation states. Whereas the macroscopic level produces  $\text{TcO}_2\cdot\text{xH}_2\text{O}$  or similarly hydrated species in the absence of strong ligands, this is not necessarily the case for extremely diluted  $^{99m}\text{Tc}$ . Although the authenticities of these reactive species are unknown, they may be the origin for novel complexes, which can directly be used for labelling. The long known method of reducing  $[^{99m}\text{TcO}_4]^-$  in the presence of thiolato groups from, for example, reduced disulphide bonds in antibodies is such a model approach. Despite yielding undefined (and frequently unstable) species, the principle approach mirrors one possible way to go in the future, of course, with the objective of receiving well defined compounds.

Comparably, the search for complexes with intramolecular reactivity is an option for future chemistry. Technetium chemistry aiming at the development of new radiopharmaceuticals can be divided into two sections, building blocks or precursors which can be used for labelling of various biomolecules and completely stable substitution inert complexes. The chemically challenging strategy of producing compounds with metal induced but ligand centred reactivity is very common in other fields (such as catalysis) but has not been regarded as an option in radiopharmacy. There are very few examples of an exception to the rule [17.7]. Thus, instead of going towards new complexes or building blocks, why not aim for ligands that can quantitatively be coupled with functionalities on the biomolecule only when coordinated to the metal (the  $^{99m}\text{Tc}$ ).

A further trend related to technetium chemistry might be the study of solid phase based chemistry. Considering the fact that specific activity is one of the major issues in labelling techniques, it would be an incentive to produce no carrier added labelled biomolecules. This goal could principally be achieved if: (i) the labelling reaction is performed under close to stoichiometric conditions; (ii) the unlabelled biomolecule is not active at all; or (iii) the cold unlabelled biomolecule remains bound to a solid resin and is automatically removed from the solution.

Whereas the first approach is rather difficult to realize, some attempts for the second have been described in the literature. An example of the second approach is TRODAT for which the unlabelled CNS receptor ligand does not cross the blood–brain barrier (BBB), hence, labelling can easily be performed at high concentrations [17.8]. This is one of the very few exceptions but it includes the special case of BBB crossing agents and is certainly not generally applicable. TRODAT can be referred to as a ‘technetium essential radiopharmaceutical’, since the receptor ligand does not cross the BBB without technetium and, hence, is not active. The term ‘technetium essential radiopharmaceutical’ is usually used for perfusion agents rather than for targeting complexes but nevertheless describes the behaviour of TRODAT well. The third approach represents a wide

and open field of challenging and promising research. Not much has been done but since solid phase synthesis for the convenient removal of by-products or side products is applied in many other fields, why not also in radiopharmacy. A very limited number of papers appeared in the literature but none of them has been followed up further [17.9, 17.10]. Applying this technique in radiopharmaceutical chemistry too may represent one of the future trends in technetium chemistry.

Last but not least, the development of novel cores is a persistent challenge in radiopharmaceutical chemistry. As already emphasized, labelling techniques are not yet ideal. Problems with labelling and the characterization of labelled compounds can be optimized by following one of the three strategies outlined above, but the development of novel cores with different labelling reactivity is a current and a future trend. Novel technetium building blocks are not only important from a fundamental point of view but might also offer new opportunities in labelling which are not immediately obvious right now. Thus, continuous research on technetium chemistry is an important future trend which is currently suffering from a lack of adequate attention in the community.

### 17.3. TARGETS

Future trends in target assignments will govern the subsequent question about targeting molecules. It has been claimed that the failure to develop novel  $^{99m}\text{Tc}$  based radiopharmaceuticals is due to the selection of inappropriate targets or targeting molecules [17.11]. This opinion has to be refuted as the current targets are certainly those that have the most important impact on public health care and costs. Radioimaging and radiotherapeutic agents in oncology and cardiology, CNS receptor binding agents for assessing treatment response, and infection–inflammation, to name but a few, are still the most important targets [17.12–17.14]. All of these targets will continue to remain essential in radiopharmaceutical research.

The advent of molecular imaging will add new targets, or rather, new biochemical processes as targets to what is currently being investigated. Notably, the imaging of specific biochemical processes and gene expression, hence the term molecular imaging, represent important future trends which will challenge radiopharmaceutical researchers. Gene expression was reviewed in Chapter 8. Imaging of gene and nucleic acid based targets offers the opportunity to assess tumour cell proliferation [17.15, 17.16]. This could be helpful in the evaluation of tumour growth potential and the degree of malignancy, and could provide an early assessment of tumour treatment response. While some efforts in the direction of imaging proliferation have been made, most of these compounds

were not purine or pyrimidine based and, hence, did not directly relate to cell proliferation. Examples are [<sup>18</sup>F]FDG, which is an indicator for tumour proliferative activity but which is not a gene targeting agent [17.17]. The few purine or pyrimidine based compounds that have been developed were rather designed as probes for imaging Herpes virus type thymidine kinase expression and other reporter genes. One notable exception is an EC based guanine compound which shows potential for the evaluation of cell proliferation. Exploring gene expression is certainly a very valuable future trend in <sup>99m</sup>Tc based radiopharmacy but demands great skill in designing novel radiopharmaceuticals.

An equally important target in the future is the assessment of metabolic activity. This is essentially performed with [<sup>18</sup>F]FDG, not only in oncology. To complement or replace [<sup>18</sup>F]FDG with a corresponding <sup>99m</sup>Tc radiopharmaceutical is a persistent topic in the mind of many radiopharmaceutical scientists. Attempts towards achieving this objective have been published but have not yet been very successful [17.18, 17.19]. One of the main obstacles that has to be overcome is the highly selective GLUT1 transporter that does not tolerate large structural changes in its core structure, such as those caused by the introduction of a pendent metal complex. However, other means of cell entry are possible and other small molecules are, probably, equally important. Metabolic activity can, for instance, be correlated with the uptake of amino acids for which the respective transporter is much less selective. Consequently, labelling of amino acids might be more promising, and we could show that <sup>99m</sup>Tc labelled amino acids are still actively transported by the L type amino acid transporter LAT1 in vitro [17.20]. A further future trend will, thus, certainly be connected to the development of <sup>99m</sup>Tc labelled small molecules, the derivatization of which is not as difficult and, importantly, for which the cost is generally low. It should not be forgotten that labelling of small molecules provides important insight into structure–activity relationships, an indispensable basis for further drug discovery and development.

One of the most relevant problems in the clinic is hypoxia [17.21]. It is well established that most tumours have a considerable portion of hypoxic cells, which are known to be resistant to radiotherapy or chemotherapy. The assessment of hypoxia would help the physician to apply additional or alternative forms of treatment. Although hypoxia certainly represents an old target, it is of the utmost importance for health care to develop an agent which reliably allows the localization and quantification of hypoxic tumour tissue. All attempts in this direction have, so far, failed and only <sup>18</sup>F labelled compounds have shown limited applicability. The majority of compounds developed so far are active due to a nitroimidazole group which is reduced and trapped at the site of hypoxia. In contrast, in the copper complex Cu-ATSM, which is under evaluation, it is believed that the activity is metal centred, hence, the metal is reduced instead of

the ligand. To follow this methodology could represent a future trend in  $^{99m}\text{Tc}$  radiopharmacy. One option is the design and synthesis of complexes in which Tc is reduced instead of being a complex pendent organic functionality. Varying the ligand will allow fine tuning of the redox potential and, hence, of in vivo behaviour. Although hypoxia is a long standing target, new chemical approaches are required in order to develop a useful radiopharmaceutical agent in the near future.

Neurology probably has a comparable impact on human quality of life as oncology. An ageing population suffers more and more from neurodegenerative diseases such as Alzheimer's disease. Developing potent and cost efficient  $^{99m}\text{Tc}$  based radiopharmaceuticals is a long standing goal which has only had limited success despite the scientific challenge and its social importance. The only notable exception is [ $^{99m}\text{Tc}$ ]TRODAT, a dopamine transporter imaging agent which is used for the diagnosis of Parkinson's disease but which has not been introduced to the market (except in Taiwan), essentially for bureaucratic reasons [17.22]. Despite the useful properties of [ $^{99m}\text{Tc}$ ]TRODAT, different (market) forces have prevented its widespread utilization. The situation is different for Alzheimer's disease, since no imaging agents are available. Currently used drugs treat the symptoms but do not halt or reverse the disease [17.23]. Finding or developing more efficient drugs is problematic due to the slow development of Alzheimer's disease. Here, novel radiopharmaceuticals could intervene by rapidly quantifying progress or regression of amyloid plaques in the brain. Rather than being a diagnostic compound, amyloid plaque imaging agents could support the development of new therapeutic agents, thus, playing an important role in drug development and, at a later stage, in diagnosing the success or failure of a conventional therapy. A future trend in  $^{99m}\text{Tc}$  radiopharmaceutical chemistry should go in the direction of developing new agents for neurodegenerative diseases. The many failures of current research or the impossibility of market introduction might have discouraged many researchers but it, at least, remains a scientific challenge to develop a compound which passes the BBB to a large extent and binds to the corresponding receptors in sufficient amounts to allow imaging within a short time period and with a high target:background ratio.

It should not be overseen that diagnostic  $^{99m}\text{Tc}$  has a counterpart in therapeutic  $^{188/186}\text{Re}$ , the role and chemistry of which is reviewed in Chapter 10. The relevance of SPECT in a time of PET has been extensively discussed in general, with a focus on the future of  $^{99m}\text{Tc}$  in particular [17.1]. Whereas diagnosis with  $^{99m}\text{Tc}$  might or might not be replaced by PET or any other imaging modalities, therapy with radionuclides with concerted visualization remains an essentially unique option for  $\beta^-$ - $\gamma$  emitters such as  $^{188/186}\text{Re}$ . Therapy with radionuclides might not be of relevance for some of the current or future targets, such as neurology or cardiology as outlined above, but doubtless it will be of the

highest relevance for all targets in oncology. Since Tc and Re belong to the same triad, it is a long standing rule that the two can be considered as a ‘matched pair’, something which is not fully true, at least concerning complexes in the higher oxidation states [17.24]. Yet, any target which can be imaged with  $^{99m}\text{Tc}$  and for which a biologically stable  $^{188/186}\text{Re}$  analogue exists, is a subject for monitoring the success or failure of treatment. Comparable to the visualization of treatment progress in neurodegenerative diseases (where possible) with conventional pharmaceuticals, radiotherapy with  $^{188/186}\text{Re}$  can be followed with corresponding  $^{99m}\text{Tc}$  compounds. Hence, if current or future diagnostic targets are at the same time therapeutic targets, the role of  $^{99m}\text{Tc}$  will remain distinct. Hence, targets should be selected according to the criteria of complementarity between diagnosis and therapy.

Finally, to stay with radionuclide therapy, high LET radionuclides such as  $\alpha$  emitters and Auger electron emitters are shifting more and more into the focus of research. The therapeutic potential of  $\alpha$  emitters has been proven and studies with the Auger electron emitters  $^{111}\text{In}$  and  $^{125}\text{I}$  provide reasonable evidence for a potential therapeutic role [17.25]. Although having fewer emissions than  $^{111}\text{In}$ ,  $^{99m}\text{Tc}$  is also an Auger emitter and could, therefore, be applied in therapy, provided that it is possible to deliver it to the nucleus of a specific cell [17.26]. Hence, a further future target might be, in general, the cell nucleus or the DNA of malignant cells. It has been shown that  $^{99m}\text{Tc}$  can induce double strand breaks in DNA if the radionuclide is delivered in the intimate vicinity of DNA or can kill cells but the objective of delivering sufficient activity to the nucleus of specific cells remains a scientific challenge [17.27]. Regardless of how to design such a compound and in agreement with the philosophy of molecular imaging, it should be emphasized that the nucleus is an important future target but which was a ‘no go’ area until now [17.6]. If the dose delivered by  $^{99m}\text{Tc}$  to the nucleus is ever not lethal, the replacement of  $^{99m}\text{Tc}$  with  $^{188/186}\text{Re}$  might change this situation completely, provided that matched pair radiopharmaceuticals can be synthesized.

#### 17.4. TARGETING MOLECULES AND COMPLEXES

The list of targeting molecules used at present and in the past is broad and comprises all kinds of receptor binding agents. The strongest focus is probably on peptides. Peptides are followed to a lesser extent by antibodies or small molecules such as CNS receptor ligands, steroid hormones or metabolically active tracers, such as carbohydrates or amino acids. Comparably little research activity in the community focuses on antisense oligonucleotides for targeting oncogene mRNA expression to non-invasively measure the levels of specific mRNA [17.16]. In contrast to radiolabelled oligonucleotides, which tend to be

rapidly degraded *in vivo*, a new kind of targeting molecules emerging in the recent past are PNAs or PNA-peptides which represent important alternatives for cancer diagnosis via gene expression imaging [17.15]. PNA and PNA-peptides are not immediately degraded and provide comparable or sometimes better hybridization with the complementary target mRNA. A literature overview of the principles of function and the behaviour of PNA and PNA-peptides is provided in Chapter 8. The labelling of PNA and derivatives is not routine since the concentrations are usually very low and require very potent ligands and fast labelling kinetics [17.28]. However, PNAs and PNA-peptides are stable molecules and, in general, tolerate a broad range of synthetic conditions. Synthesis and conjugation of appropriate chelators is a challenging task, requiring advanced synthetic and analytical techniques. Remembering that molecular imaging of gene expression is one of the important targets in the future, underlines the relevance of PNA and derivatives as targeting molecules. More attention should be paid to the synthesis and study of the biological behaviour of such molecules.

Following the future target section, it becomes immediately obvious that small molecules represent an important class of future targeting molecules. The labelling of small molecules was the topic of a recent coordinated research project organized by the IAEA, the results of which were the subject of a recent book publication. As mentioned previously, PET radioimaging is dominated by [<sup>18</sup>F]FDG, a metabolic tracer of the utmost importance but which is expensive. To find a <sup>99m</sup>Tc substitute or complement for a metabolic tracer would have a strong impact in nuclear medicine, and future targeting molecules should be selected accordingly. It does not need to be emphasized that coordination chemistry is challenged by the very difficult task of combining a relatively bulky metal complex with a small tracer; however, it has been shown recently that such a combination may lead to a compound which is still recognized and transported by a trans-membrane protein. In this respect, future targeting molecules are carbohydrates, amino acids, purine or pyrimidine bases or nucleosides and nucleotides. They are all similar regarding the question of how to introduce a metal complex into the respective targeting molecule without affecting or abolishing the corresponding affinity and selectivity. One should keep in mind that intact functionality with respect to the transporters is not an indispensable must but that competitive inhibition of the corresponding transporter might be sufficient for imaging. Thus, the above mentioned small molecules represent important future targeting molecules, which merit being studied in more depth. The advantage is that they are, in general, cheap or very cheap and their chemistry relatively facile (with the exception of carbohydrates); their disadvantage is certainly finding a ‘starting point’. A starting point means a labelled targeting molecule which shows at least some affinity as a basis for

further structure–activity relationship optimization. This goal has not yet been achieved with glucose derivatives for instance.

Labelling of small molecules with  $^{99m}\text{Tc}$  is difficult for obvious reasons as already outlined. A strategy in the past was to use the integrated approach in which only complexation to  $^{99m}\text{Tc}$  creates a biologically active molecule. Using technetium as a structural building block for a receptor binding molecule is a difficult concept and requires rational design based on high level molecular modelling. The feasibility of this approach has, however, been shown very recently with cold ruthenium complexes bound to protein kinase inhibitors based on staurosporin [17.29]. Similar approaches should also be possible with  $^{99m}\text{Tc}$  to generate de novo targeting molecules. It stands to reason that such a procedure is at the high end of radiopharmaceutical chemistry as far as design and synthesis are concerned.

To follow up on the future targets as mentioned in the previous section, the importance of finding new targeting molecules for the cell nucleus shall be touched on briefly. Nuclear targeting agents, if not peptide based, are often strongly fluorescent and are well known in molecular biology. In molecular biology, the visualization of processes or cell compartments is crucial and corresponding fluorescent probes are very well known and developed. This is especially true for staining DNA. Many agents exist which allow visualization of DNA with very high selectivity. The combination of corresponding small DNA targeting molecules with  $^{99m}\text{Tc}$  complexes is very attractive, since molecular imaging can be performed with very high resolution. The radioactivity allows absolute quantification about how much is taken up into the cell, whereas the fluorescence allows highly resolved localization of the compounds [17.30]. Such data gives access to a more targeted delivery of the radiopharmaceuticals and a clearer picture about their functionality. Thus, an important kind of future targeting molecules will be luminescent agents due to the possibility of merging two different types of electromagnetic radiation, light and  $\gamma$  rays.

In conclusion, the proper selection of current or future targeting molecules is not always straightforward and depends on many uncertainties and variable parameters. The selection of the target to be studied confines the kind of targeting molecules, whereas the selection of the targeting molecule determines the target. Both targets and targeting molecules, on the other hand, depend on market demands and limitations imposed by the market. For a selected targeting molecule, various labelling methods are usually possible and it is wise but time consuming and difficult to compare them. New targeting molecules might emerge from aspects of biological or medicinal chemistry that are not immediately obvious, and a thorough study of fields other than traditional radiopharmacy might offer rational molecular opportunities which are not conceivable but are identified from an unexpected field of research. Besides following traditional

methods, it is, therefore, very important to have a broad view of the field in order to identify novel candidates for targeted imaging.

## REFERENCES TO CHAPTER 17

- [17.1] JANSEN, F.P., VANDERHEYDEN, J.L., The future of SPECT in a time of PET, *Nucl. Med. Biol.* **34** (2007) 733–735.
- [17.2] PIESLOR, P.C., Barriers to achieving commercial success for diagnostic and therapeutic radiopharmaceuticals, *Nucl. Med. Biol.* **34** (2007) 737–742.
- [17.3] LIU, S., The role of coordination chemistry in the development of target-specific radiopharmaceuticals, *Chem. Soc. Rev.* **33** (2004) 445–461.
- [17.4] WELCH, M.J., MCCARTHY, T.J., The potential role of generator-produced radiopharmaceuticals in clinical PET, *J. Nucl. Med.* **41** (2000) 315–317.
- [17.5] DECRISTOFORO, C., MATHER, S.J., <sup>99m</sup>-technetium-labelled peptide-HYNIC conjugates: Effects of lipophilicity and stability on biodistribution, *Nucl. Med. Biol.* **26** (1999) 389–396.
- [17.6] BLOWER, P., Towards molecular imaging and treatment of disease with radionuclides: the role of inorganic chemistry, *Dalton Trans.* (2006) 1705–1711.
- [17.7] WANG, W.W., SPINGLER, B., ALBERTO, R., Reactivity of 2-pyridine-aldehyde and 2-acetyl-pyridine coordinated to [Re(CO)(3)](+) with alcohols and amines: Metal mediated Schiff base formation and dimerization, *Inorg. Chim. Acta* **355** (2003) 386–393.
- [17.8] KUNG, H.F., Development of Tc-99m labeled tropanes: TRODAT-1, as a dopamine transporter imaging agent, *Nucl. Med. Biol.* **28** (2001) 505–508.
- [17.9] MUNDWILER, S., CANDREIA, L., HAFLIGER, P., ORTNER, K., ALBERTO, R., Preparation of no-carrier-added technetium-99m complexes via metal-assisted cleavage from a solid phase, *Bioconjug. Chem.* **15** (2004) 195–202.
- [17.10] DUNN-DUFAULT, R., POLLAK, A., FITZGERALD, J., THORNBACK, J.R., BALLINGER, J.R., A solid-phase technique for preparation of no-carrier-added technetium-99m radiopharmaceuticals: Application to the streptavidin/biotin system, *Nucl. Med. Biol.* **27** (2000) 803–807.
- [17.11] WELCH, M., [Tc(CO)(3)](+) chemistry: a promising new concept for SPET? *Eur. J. Nucl. Med. Mol. Imaging* **30** (2003) 1302–1304.
- [17.12] YANG, D.J., KIM, E.E., INOUE, T., Targeted molecular imaging in oncology, *Ann. Nucl. Med.* **20** (2006) 1–11.
- [17.13] OKARVI, S.M., Peptide-based radiopharmaceuticals: Future tools for diagnostic imaging of cancers and other diseases (Vol. 24, p. 357, 2004), *Med. Res. Rev.* **24** (2004) 685–686.
- [17.14] WEINER, R.E., THAKUR, M.L., Radiolabeled peptides in the diagnosis and therapy of oncological diseases, *Appl. Radiat. Isotop.* **57** (2002) 749–763.
- [17.15] WICKSTROM, E., et al., Oncogene mRNA imaging with Tc-99m-chelator-PNA-peptides, *Russ. Chem. Bull.* **51** (2002) 1083–1099.

- [17.16] TIAN, X.B., et al., Imaging oncogene expression, *Ann. NY. Acad. Sci.* **1002** (2003) 165–188.
- [17.17] OKADA, J., et al., Positron emission tomography using fluorine-18-fluorodeoxyglucose in malignant-lymphoma — a comparison with proliferative activity, *J. Nucl. Med.* **33** (1992) 325–329.
- [17.18] YANG, D.J., et al., Imaging with Tc-99m ECDG targeted at the multifunctional glucose transport system: Feasibility study with rodents, *Radiology* **226** (2003) 465–473.
- [17.19] SCHIBLI, R., et al., Synthesis and in vitro characterization of organometallic rhenium and technetium glucose complexes against glut 1 and hexokinase, *Bioconjug. Chem.* **16** (2005) 105–112.
- [17.20] KIM, Y.S., HE, Z.J., HSIEH, W.Y., LIU, S., A novel ternary ligand system useful for preparation of cationic Tc-99m-diazenido complexes and Tc-99m-labeling of small biomolecules, *Bioconjug. Chem.* **17** (2006) 473–484.
- [17.21] SONG, H.C., et al., Prognostication of recovery in patients with acute ischemic stroke through the use of brain SPECT with technetium-99m-labeled metronidazole, *Stroke* **34** (2003) 982–986.
- [17.22] KUNG, H.F., KUNG, M.P., WEY, S.P., LIN, K.J., YEN, T.C., Clinical acceptance of a molecular imaging agent: a long march with [Tc-99m]TRODAT, *Nucl. Med. Biol.* **34** (2007) 787–789.
- [17.23] MATHIS, C.A., LOPRESTI, B.J., KLUNK, W.E., Impact of amyloid imaging on drug development in Alzheimer’s disease, *Nucl. Med. Biol.* **34** (2007) 809–822.
- [17.24] ALBERTO, R., ABRAM, U., Nuclear Chemistry (VERTES, A., NAGY, S., KLENCSAR, Z., Eds), Kluwer Academic Publishers, Dordrecht (2003) 211–256.
- [17.25] O’DONOGHUE, J.A., WHELDON, T.E., Targeted radiotherapy using Auger electron emitters, *Phys. Med. Biol.* **41** (1996) 1973–1992.
- [17.26] PEDRAZA-LOPEZ, M., FERRO-FLORES, G., MENDIOLA-CRUZ, T., MORALES-RAMIREZ, P., Assessment of radiation-induced DNA damage caused by the incorporation of Tc-99m-radiopharmaceuticals in murine lymphocytes using single cell gel electrophoresis, *Mutat. Res. Gen. Tox. En.* **465** (2000) 139–144.
- [17.27] HAEFLIGER, P., et al., Induction of DNA-double-strand breaks by Auger electrons from 99mTc complexes with DNA-binding ligands, *ChemBioChem* **6** (2005) 414–421.
- [17.28] THAKUR, M.L., et al., Tc-99m-PNA-peptide: Imaging oncogene expression in breast lesions, *J. Nucl. Med.* **43** (2002) 124P–124P.
- [17.29] MEGGERS, E., Exploring biologically relevant chemical space with metal complexes, *Curr. Opin. Chem. Biol.* **11** (2007) 287–292.
- [17.30] STEPHENSON, K.A., et al., Bridging the gap between in vitro and in vivo imaging: Isostructural Re and Tc-99m complexes for correlating fluorescence and radioimaging studies, *J. Am. Chem. Soc.* **126** (2004) 8598–8599.

## CONTRIBUTORS TO DRAFTING AND REVIEW

Akizawa, H.	Graduate School of Pharmaceutical Sciences, Chiba University, Japan
Alberto, R.	University of Zürich, Institute of Inorganic Chemistry, Switzerland
Arano, Y.	Graduate School of Pharmaceutical Sciences, Japan
Banerjee, S.	Bhabha Atomic Research Centre, India
Blower, P.	Division of Imaging Sciences, King's College London, United Kingdom
Decristoforo, C.	Clinical Department of Nuclear Medicine, Medical University Innsbruck, Austria
Di Domenico, G.	Department of Physics, University of Ferrara, Italy
Duatti, A.	Laboratory of Nuclear Medicine, University of Ferrara, Italy
Ferro-Flores, G.	Instituto Nacional de Investigaciones Nucleares, Departamento de Materiales Radiactivos, Mexico
Kuge, Y.	Department of Patho-functional Bioanalysis, Graduate School of Pharmaceutical Sciences, Kyoto University, Japan
Liu, S.	School of Health Sciences, Purdue University, United States of America
Mallya, M.	Bhabha Atomic Research Centre, Mumbai, India
Martin De Rosales, R.S.	Division of Imaging Sciences, King's College London, United Kingdom
Mindt, T.L.	Center for Radiopharmaceutical Sciences, Paul Scherrer Institute, Switzerland
Ogawa, K.	Division of Tracer Kinetics, Advanced Science Research Center, Kanazawa University, Japan

Pietzsch, H-J.	Institute of Radiopharmacy, Forschungszentrum Dresden-Rossendorf, Germany
Pillai, M.R.A.	International Atomic Energy Agency
Pirmettis, I.	Institute of Radioisotopes, National Centre for Scientific Research “Demokritos”, Greece
Schibli, R.	Center for Radiopharmaceutical Sciences, Paul Scherrer Institute, Switzerland
Struthers, H.	Center for Radiopharmaceutical Sciences, Paul Scherrer Institute, Switzerland
Uehara, T.	Graduate School of Pharmaceutical Sciences, Chiba University, Japan
Venkatesh, M.	Bhabha Atomic Research Centre, Mumbai, India
Welling, M.M.	Leiden University Medical Center, Department of Radiology, Netherlands
Wiebe, L.I.	Cross Cancer Institute, University of Alberta, Canada
Zavattini, G.	Department of Physics, University of Ferrara, Italy

### **Technical Meeting**

Vienna, Austria: 10–14 November 2006

### **Consultants Meeting**

Vienna, Austria: 21–25 July 2008



**IAEA**

International Atomic Energy Agency

No. 21, July 2006

# Where to order IAEA publications

**In the following countries** IAEA publications may be purchased from the sources listed below, or from major local booksellers. Payment may be made in local currency or with UNESCO coupons.

## Australia

DA Information Services, 648 Whitehorse Road, Mitcham Victoria 3132  
Telephone: +61 3 9210 7777 • Fax: +61 3 9210 7788  
Email: service@dadirect.com.au • Web site: <http://www.dadirect.com.au>

## Belgium

Jean de Lannoy, avenue du Roi 202, B-1190 Brussels  
Telephone: +32 2 538 43 08 • Fax: +32 2 538 08 41  
Email: [jean.de.lannoy@infoboard.be](mailto:jean.de.lannoy@infoboard.be) • Web site: <http://www.jean-de-lannoy.be>

## Canada

Bernan Associates, 4611-F Assembly Drive, Lanham, MD 20706-4391, USA  
Telephone: 1-800-865-3457 • Fax: 1-800-865-3450  
Email: [order@bernan.com](mailto:order@bernan.com) • Web site: <http://www.bernan.com>

Renouf Publishing Company Ltd., 1-5369 Canotek Rd., Ottawa, Ontario, K1J 9J3  
Telephone: +613 745 2665 • Fax: +613 745 7660  
Email: [order.dept@renoufbooks.com](mailto:order.dept@renoufbooks.com) • Web site: <http://www.renoufbooks.com>

## China

IAEA Publications in Chinese: China Nuclear Energy Industry Corporation, Translation Section, P.O. Box 2103, Beijing

## Czech Republic

Suweco CZ, S.R.O. Klecakova 347, 180 21 Praha 9  
Telephone: +420 26603 5364 • Fax: +420 28482 1646  
Email: [nakup@suweco.cz](mailto:nakup@suweco.cz) • Web site: <http://www.suweco.cz>

## Finland

Akateeminen Kirjakauppa, PL 128 (Keskuskatu 1), FIN-00101 Helsinki  
Telephone: +358 9 121 41 • Fax: +358 9 121 4450  
Email: [akatilaus@akateeminen.com](mailto:akatilaus@akateeminen.com) • Web site: <http://www.akateeminen.com>

## France

Form-Edit, 5, rue Janssen, P.O. Box 25, F-75921 Paris Cedex 19  
Telephone: +33 1 42 01 49 49 • Fax: +33 1 42 01 90 90 • Email: [formedit@formedit.fr](mailto:formedit@formedit.fr)

Lavoisier SAS, 14 rue de Provigny, 94236 Cachan Cedex  
Telephone: + 33 1 47 40 67 00 • Fax +33 1 47 40 67 02  
Email: [livres@lavoisier.fr](mailto:livres@lavoisier.fr) • Web site: <http://www.lavoisier.fr>

## Germany

UNO-Verlag, Vertriebs- und Verlags GmbH, August-Bebel-Allee 6, D-53175 Bonn  
Telephone: +49 02 28 949 02-0 • Fax: +49 02 28 949 02-22  
Email: [info@uno-verlag.de](mailto:info@uno-verlag.de) • Web site: <http://www.uno-verlag.de>

## Hungary

Librotrade Ltd., Book Import, P.O. Box 126, H-1656 Budapest  
Telephone: +36 1 257 7777 • Fax: +36 1 257 7472 • Email: [books@librotrade.hu](mailto:books@librotrade.hu)

## India

Allied Publishers Group, 1st Floor, Dubash House, 15, J. N. Heredia Marg, Ballard Estate, Mumbai 400 001,  
Telephone: +91 22 22617926/27 • Fax: +91 22 22617928  
Email: [alliedpl@vsnl.com](mailto:alliedpl@vsnl.com) • Web site: <http://www.alliedpublishers.com>

Bookwell, 24/4800, Ansari Road, Darya Ganj, New Delhi 110002  
Telephone: +91 11 23268786, +91 11 23257264 • Fax: +91 11 23281315  
Email: [bookwell@vsnl.net](mailto:bookwell@vsnl.net) • Web site: <http://www.bookwellindia.com>

## Italy

Libreria Scientifica Dott. Lucio di Biasio "AEIOU", Via Coronelli 6, I-20146 Milan  
Telephone: +39 02 48 95 45 52 or 48 95 45 62 • Fax: +39 02 48 95 45 48

## Japan

Maruzen Company, Ltd., 13-6 Nihonbashi, 3 chome, Chuo-ku, Tokyo 103-0027  
Telephone: +81 3 3275 8582 • Fax: +81 3 3275 9072  
Email: [journal@maruzen.co.jp](mailto:journal@maruzen.co.jp) • Web site: <http://www.maruzen.co.jp>

**Korea, Republic of**

KINS Inc., Information Business Dept. Samho Bldg. 2nd Floor, 275-1 Yang Jae-dong SeoCho-G, Seoul 137-130  
Telephone: +02 589 1740 • Fax: +02 589 1746  
Email: sj8142@kins.co.kr • Web site: <http://www.kins.co.kr>

**Netherlands**

Martinus Nijhoff International, Koraalrood 50, P.O. Box 1853, 2700 CZ Zoetermeer  
Telephone: +31 793 684 400 • Fax: +31 793 615 698 • Email: [info@nijhoff.nl](mailto:info@nijhoff.nl) • Web site: <http://www.nijhoff.nl>

Swets and Zeitlinger b.v., P.O. Box 830, 2160 SZ Lisse

Telephone: +31 252 435 111 • Fax: +31 252 415 888 • Email: [infoho@swets.nl](mailto:infoho@swets.nl) • Web site: <http://www.swets.nl>

**New Zealand**

DA Information Services, 648 Whitehorse Road, MITCHAM 3132, Australia  
Telephone: +61 3 9210 7777 • Fax: +61 3 9210 7788  
Email: [service@dadirect.com.au](mailto:service@dadirect.com.au) • Web site: <http://www.dadirect.com.au>

**Slovenia**

Cankarjeva Zalozba d.d., Kopitarjeva 2, SI-1512 Ljubljana  
Telephone: +386 1 432 31 44 • Fax: +386 1 230 14 35  
Email: [import.books@cankarjeva-z.si](mailto:import.books@cankarjeva-z.si) • Web site: <http://www.cankarjeva-z.si/uvoz>

**Spain**

Díaz de Santos, S.A., c/ Juan Bravo, 3A, E-28006 Madrid  
Telephone: +34 91 781 94 80 • Fax: +34 91 575 55 63 • Email: [compras@diazdesantos.es](mailto:compras@diazdesantos.es)  
[carmela@diazdesantos.es](mailto:carmela@diazdesantos.es) • [barcelona@diazdesantos.es](mailto:barcelona@diazdesantos.es) • [julio@diazdesantos.es](mailto:julio@diazdesantos.es)  
Web site: <http://www.diazdesantos.es>

**United Kingdom**

The Stationery Office Ltd, International Sales Agency, PO Box 29, Norwich, NR3 1 GN  
Telephone (orders): +44 870 600 5552 • (enquiries): +44 207 873 8372 • Fax: +44 207 873 8203  
Email (orders): [book.orders@tso.co.uk](mailto:book.orders@tso.co.uk) • (enquiries): [book.enquiries@tso.co.uk](mailto:book.enquiries@tso.co.uk) • Web site: <http://www.tso.co.uk>

On-line orders:

DELTA Int. Book Wholesalers Ltd., 39 Alexandra Road, Addlestone, Surrey, KT15 2PQ  
Email: [info@profbooks.com](mailto:info@profbooks.com) • Web site: <http://www.profbooks.com>

Books on the Environment:

Earthprint Ltd., P.O. Box 119, Stevenage SG1 4TP  
Telephone: +44 1438748111 • Fax: +44 1438748844  
Email: [orders@earthprint.com](mailto:orders@earthprint.com) • Web site: <http://www.earthprint.com>

**United Nations (UN)**

Dept. I004, Room DC2-0853, First Avenue at 46th Street, New York, N.Y. 10017, USA  
Telephone: +800 253-9646 or +212 963-8302 • Fax: +212 963-3489  
Email: [publications@un.org](mailto:publications@un.org) • Web site: <http://www.un.org>

**United States of America**

Bernan Associates, 4611-F Assembly Drive, Lanham, MD 20706-4391  
Telephone: 1-800-865-3457 • Fax: 1-800-865-3450  
Email: [order@bernan.com](mailto:order@bernan.com) • Web site: <http://www.bernan.com>

Renouf Publishing Company Ltd., 812 Proctor Ave., Ogdensburg, NY, 13669  
Telephone: +888 551 7470 (toll-free) • Fax: +888 568 8546 (toll-free)  
Email: [order.dept@renoufbooks.com](mailto:order.dept@renoufbooks.com) • Web site: <http://www.renoufbooks.com>

**Orders and requests for information** may also be addressed directly to:

**Sales and Promotion Unit, International Atomic Energy Agency**

Vienna International Centre, PO Box 100, 1400 Vienna, Austria  
Telephone: +43 1 2600 22529 (or 22530) • Fax: +43 1 2600 29302  
Email: [sales.publications@iaea.org](mailto:sales.publications@iaea.org) • Web site: <http://www.iaea.org/books>

**CYCLOTRON PRODUCED RADIONUCLIDES:  
GUIDELINES FOR SETTING UP A FACILITY**

**Technical Reports Series No. 471**

STI/DOC/010/471 (213 pp.; 2009)

ISBN 978-92-0-103109-9

Price: €45.00

**THERAPEUTIC RADIONUCLIDE GENERATORS:**

**<sup>90</sup>SR/<sup>90</sup>Y AND <sup>188</sup>W/<sup>188</sup>RE GENERATORS**

**Technical Reports Series No. 470**

STI/DOC/010/470 (233 pp.; 2009)

ISBN 978-92-0-111408-2

Price: €45.00

**CYCLOTRON PRODUCED RADIONUCLIDES:**

**PHYSICAL CHARACTERISTICS AND PRODUCTION METHODS**

**Technical Reports Series No. 468**

STI/DOC/010/468 (279 pp.; 2009)

ISBN 978-92-0-106908-5

Price: €52.00

**TECHNETIUM RADIOPHARMACEUTICALS:**

**MANUFACTURE OF KITS**

**Technical Reports Series No. 466**

STI/DOC/010/466 (202 pp.; 2008)

ISBN 978-92-0-100408-6

Price: €50.00

**CYCLOTRON PRODUCED RADIONUCLIDES:**

**PRINCIPLES AND PRACTICE**

**Technical Reports Series No. 465**

STI/DOC/010/465 (230 pp.; 2008)

ISBN 978-92-0-100208-2

Price: €45.00

**COMPARATIVE EVALUATION OF THERAPEUTIC  
RADIOPHARMACEUTICALS**

**Technical Reports Series No. 458**

STI/DOC/010/458 (310 pp.; 2007)

ISBN 92-0-115106-3

Price: €56.00

**LABELLING OF SMALL BIOMOLECULES  
USING NOVEL TECHNETIUM-99M CORES**

**Technical Reports Series No. 459**

STI/DOC/010/459 (312 pp.; 2007)

ISBN 92-0-101607-7

Price: €70.00

**TRENDS IN RADIOPHARMACEUTICALS (2 volumes)**

STI/PUB/1294 (Vol. 1: 408 pp.; Vol. 2: 464 pp.; 2007)

ISBN 92-0-101707-3

Price: €120.00

This publication provides a broad overview of the current status and future prospects of technetium-99m ( $^{99m}\text{Tc}$ ) radiopharmaceuticals, including a description of the most advanced chemical techniques for labelling biomolecules and synthesizing suitable multifunctional ligands. It also reviews the most recent applications of  $^{99m}\text{Tc}$  agents for monitoring different biological processes. Various subfields of clinical relevance are identified where  $^{99m}\text{Tc}$  radiopharmaceuticals will continue to have a significant impact on nuclear medicine, such as cardiology, oncology, neurology, infection/inflammation, and gene expression.